INDIAN AGRICULTURAL
RESEARCH INSTITUTE, NEW DELHI.

12749

I.A. R. I. 6.
MGIPC—S4—10 AR—21-6-49—1,000.

PROCEEDINGS

OF THE

ROYAL SOCIETY OF LONDON

SERIES A. MATHEMATICAL AND PHYSICAL SCIENCES

VOL 179

12749
IARI

LONDON
Printed and published for the Royal Society
By the Cambridge University Press
Bentley House, N.W.1

27 February 1942

PRINTED IN GREAT BRITAIN BY
WALTER LEWIS, M.A.
AT THE CAMBRIDGE UNIVERSITY PRESS

CONTENTS

SERIES A VOL 179

No. A 976. 29 August 1941

PAGE

Anomalous reflexions in X-ray patterns. By G. D. Preston 1

An experimental study of diffuse X-ray reflexion by single crystals. By K. Lonsdale and H. Smith. (Plates 1–28) 8

The diffuse spots in X-ray photographs. By Sir William H. Bragg, F.R.S. 51

Diffraction of monochromatic X-rays by crystals at high temperatures. By Sir W. Lawrence Bragg, F.R.S. 61

Diffuse reflexions of X-rays by crystals. By C. G. Darwin, F.R.S. . . 65

Diffuse reflexions of X-rays by crystals. By G. I. Finch, F.R.S. . . 67

The effect of thermal vibrations on the scattering of X-rays. By M. Born, F.R.S. and K. Sarginson 69

The diffuse spots in X-ray crystal photographs. By Sir William Bragg, F.R.S. (Plate 29) 94

No. A 977. 10 October 1941

The low-temperature properties of gaseous helium. II. By R. A. Buckingham, J. Hamilton and H. S. W. Massey, F.R.S. . . . 103

The scattering of neutrons by deuterons and the nature of nuclear forces. By R. A. Buckingham and H. S. W. Massey, F.R.S. 123

The behaviour of visual purple at low temperature. By E. E. Broda and C. F. Goodeve, F.R.S. 151

The velocity of diffusion in a mixed gas; the second approximation. By S. Chapman, F.R.S. and T. G. Cowling 159

The polymerization of olefines induced by free radicals. By C. J. Danby and C. N. Hinshelwood, F.R.S. 169

PAGE

The vapour-pressure curve. By K. Fuchs 194

The absorption spectra of the cyclic dienes in the vacuum ultra-violet. By W. C. Price and A. D. Walsh. (Plates 30, 31) 201

On the heat of sublimation of carbon and on some absorption bands of three mesomeric hydrocarbons. By G. J. Kynch and W. G. Penny 214

No. A 978. 23 January 1942

Anniversary Address by Sir Henry Dale, C.B.E. 233

On Laplace's differential equations for the tides. By J. Proudman, F.R.S. 261

Reflexion and scattering of X-rays with change of frequency. I. Theoretical. By Sir C. Venkata Raman, F.R.S. (Plates 32, 33) . . 289

Reflexion and scattering of X-rays with change of frequency. II. Experimental. By Sir C. Venkata Raman, F.R.S. 302

Extra reflexions from the two types of diamond. By K. Lonsdale (Plates 34–39) 315

Diffuse scattering of X-rays by crystals. The Faxén-Waller theory and the surfaces of isodiffusion for cubic crystals. By H. A. Jahn . . 320

Statistical mechanics of binary systems. By K. Fuchs 340

Penetrating cosmic-ray showers. By L. Jánossy. (Plate 40) . . . 361

No. A 979. 27 February 1942

The summation of infinite harmonic series. By F. Soddy, F.R.S. . . 377

The stone-iron meteorites called pallasites: A synthetic study of their structure and probable mode of formation. By Lord Rayleigh, F.R.S. (Plates 41, 42) 386

Interaction between adsorbed substances of simple constitution and insoluble monolayers. II. By K. G. A. Pankhurst 393

Structure and thermal properties associated with some hydrogen bonds in crystals. IV. Isotope effects in some acid phosphates. By A. R. Ubbelohde and I. Woodward. (Plate 43) 399

The statistical mechanics of many component gases. By K. Fuchs . 408

PAGE

Pressure dependence of the equilibrium constant of ammonia. By K. Fuchs 433

The spectra of chilled hydrocarbon flames. By A. G. Gaydon. (Plates 44, 45) 439

A stress-strain curve for the atomic lattice of mild steel, and the physical significance of the yield point of a metal. By S. L. Smith and W. A. Wood. (Plate 46) 450

An elementary theory of thermal diffusion. By R. Fürth . . . 461

The role of hydrogen bonds in condensed monolayers. By A. E. Alexander 470

A proposed general structure for condensed monomolecular films. By A. E. Alexander 486

Supersonic dispersion in gases. The vibrational activation of the acetaldehyde molecule. By E. A. Alexander and J. D. Lambert 499

Index 513

DIFFUSE REFLEXIONS OF X-RAYS BY CRYSTALS

A discussion, held at a meeting of the Royal Society on 6 February 1941. The original communications have been recast by the authors in a form suitable for publication. A further paper on this subject by Sir William Bragg is appended.

Anomalous reflexions in X-ray patterns

By G. D. Preston, M.A.
National Physical Laboratory

(*Received* 11 *March* 1941)

The presence on X-ray diffraction patterns of anomalous reflexions, that is to say, reflexions which cannot be accounted for by the simple theory of diffraction, is almost a commonplace. Many of these effects are no doubt to be ascribed to imperfections in the specimen, strains, etc., but even after these have been taken into account there remain streaks and spots for which there is no satisfactory explanation. The observation of effects of the type considered here is by no means novel; Friedrich (1913) recorded them as radial streaks running through the Laue spots in a photograph of KCl. The extra spots are generally very weak compared with the normal Laue reflexions and indeed may not be observed at all unless the photographs are somewhat over-exposed. They are most easily observed on Laue photographs taken with a tube emitting a characteristic radiation such as the *K* radiation of Cu or Ag, and their study will be greatly facilitated by the use of powerful sources of monochromatic radiation.

My own interest in background reflexions arose in the first place from a study of an age-hardening alloy of aluminium with 4 % of copper (Preston, 1938). Laue photographs of single crystals of this alloy aged at room temperature showed a number of streaks which changed in intensity as the hardening process continued. When the Laue photograph was taken with radiation from a copper or silver target, so that there was an intense beam of K characteristic radiation superimposed on the white radiation, there appeared on some of the streaks spots caused by the characteristic radiation. All these effects could be explained by the segregation of the relatively heavy copper atoms in very small groups of the form of thin plates on the (100) planes of the aluminium matrix. At room temperature the hardening process reaches a final state in about four days, but even when photographs were taken within 1 hr. of quenching the crystal, there were some traces of background reflexions present. It was important to ascertain whether these weak reflexions were due to some segregation taking place during the quench and the time of photographing the crystal or whether they were characteristic of the solid solution. To settle the question a Laue photograph was taken with the crystal at a temperature of 500° C, so that all the copper atoms should be in solution and no anomalous reflexions should be observed. All the effects which had been ascribed to the hardening process did in fact disappear from the high temperature photograph, but some new spots appeared. Further investigation showed that these were present on Laue photographs of single crystals of pure aluminium, and were therefore not due to the presence of copper in the alloy. At elevated temperatures the diffuse background was much more intense than at room temperature. In fact these diffuse spots are so weak at room temperature that with an aluminium crystal and copper radiation prolonged exposure is necessary for their detection. Using radiation from a silver target and a 'Fluorazure' screen, they can be recorded in 10–15 min. (Preston, 1939).

The general appearance of the background on Laue photographs taken with radiation from a silver target is shown in the photographs reproduced in the paper already referred to.

The fact that this background of diffuse spots becomes so much more intense as the temperature is raised and that the increase and decrease could be repeated by raising and lowering the temperature, showed that these reflexions were connected in some way with the temperature of the crystal and were not to be ascribed to any mechanical strain or imperfection caused by changing the temperature. It was therefore natural to seek an explanation of their presence in the disturbing influence of the Debye thermal spectrum on the regular arrangement of the atoms in the crystal. The only theory of the effect of temperature on X-ray reflexions with which I was acquainted in 1938 when these experiments were done was that due to Darwin and Debye. In these investigations attention was confined to the normal reflexions and the way in which their intensity diminished with rise of temperature as a result of thermal agitation of the atoms. The background was not considered and the theory did not indicate that energy would be scattered in other than the normal directions. Nevertheless, it seems clear that if the normal reflexions diminish in intensity, i.e. less energy is scattered in these directions, then since the scattering power of each atom remains unchanged with rise of temperature, some energy must appear in other directions and will form a background to the normal reflexions. At a later date Faxén (1923) developed a theory of the effect of temperature on X-ray reflexion which led him to the belief that the streaks observed by Friedrich in a Laue photograph of KCl were due to the thermal vibrations of the lattice. The theory is exceedingly complex—so much so that Faxén did not predict any general background such as that observed. It is probable that Faxén's theory does in fact contain all the information required to analyse the pictures but it is not in a readily available form for comparison with experiment, with the exception of one approximate formula to which I will refer later.

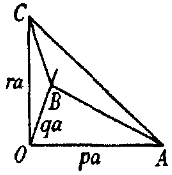

FIGURE 1*a*

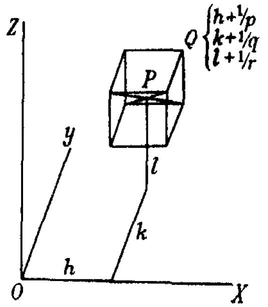

FIGURE 1*b*

FIGURE 1*a*. The direction of the wave front ABC is defined by the numbers p, q, r, its intercepts on the crystal axes.

FIGURE 1*b*. In reciprocal space the wave is represented by a point such as Q associated with each normal spectrum P.

It is not difficult to see that the existence of a wave-like disturbance of the geometrically regular atomic pattern will produce some sort of background scattering. It is, however, by no means so easy to see that this background will have a number of maxima such as are observed. The simplest way of describing the effect of a disturbance is by means of reciprocal space. The normal spectra are represented in figure 1*b* by the points $P(h, k, l)$ in reciprocal space, h, k, l being integers. If a plane wave travels along the h axis with wave-length pa, say, ($p > 2$), then two extra spectra appear associated with each point h, k, l represented by the points

$(h \pm 1/p, k, l)$ in reciprocal space. In general it will require three numbers p, q, r to define the direction of propagation of a plane wave, figure 1*a*, just as it requires three integers to specify the 'order' of the diffraction spectrum of a three-dimensional grating. This gives rise to eight 'ghosts' associated with each integral point (h, k, l) at the eight points, such as Q, figure 1*b*, $(h \pm 1/p, k \pm 1/q, l \pm 1/r)$ when positive and negative signs are distributed among the three numbers p, q, r. A reflexion will be recorded from one of these points if, and only if, it lies on the sphere of reflexion so that Bragg's law is satisfied, but for a fictitious plane with non-integral indices. The intensity associated with these new reflexions is determined by the amplitude of the wave and the calculation of this is the most difficult part of the theory, depending on the propagation of elastic waves in the crystal. The photographs show very clearly that the background intensity is by no means uniform but, in the cases examined, is much greater near the normal reflexion, that is for large p, q, r or long waves.

So far the explanation of the background is not difficult; but the theory of Faxén which takes account of all the waves which can be transmitted through the crystal becomes exceedingly complex. So much so that the implications of his investigations have lain concealed in a mass of mathematical symbolism for over fifteen years. For this reason it seemed to be worth while attempting to give a simpler picture of the sort of imperfection of the crystal which would account for the observed effects. As a result of an analysis of the photograph of aluminium, I was led to suggest that the spots could be accounted for by the diffraction pattern of a small group of atoms in close packed array. This picture is not to be taken in any way as an exact representation of the state of the crystal but rather as a substitute for a very complex state of affairs. Sir William Bragg has recently examined the spectrum of diffuse spots of KCl and has shown that even when the incident beam is inclined to the cube edge the pattern can be, at any rate approximately, explained by diffraction of a simple cube of eight neighbouring atoms. The case of NaCl also falls into line as the accompanying diagram (figure 2) shows. Here the dotted lines and circle are minima of intensity and correspond very closely with the faint background of the photograph (figure 3) taken with silver target. The full circle represents a region of maximum intensity and there is a recrudescence of anomalous spots in this region. There seems to be no doubt that this idea of diffraction by small groups of atoms does give an approximately correct account of the observed maxima. Moreover, it seems natural to suppose that any atom if displaced will carry its neighbours to some extent with it, so that on this ground the idea is plausible. Nevertheless, it must not be taken as anything more than a first approximation to the complete theory of Faxén.

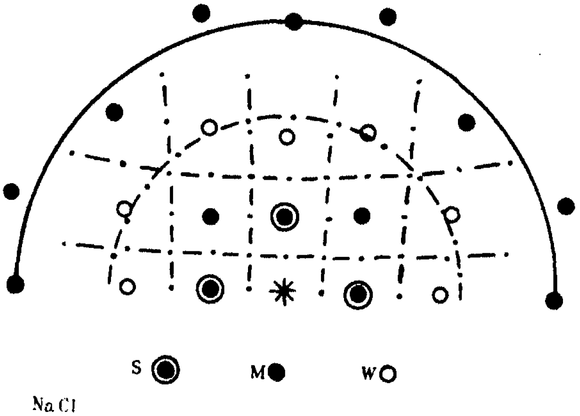

FIGURE 2. Minima of intensity are to be expected along the dotted lines and circle: maxima at the centre and near the full circle, cf. figure 3.

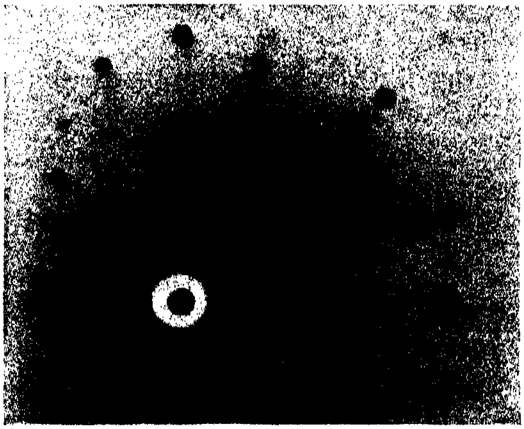

FIGURE 3. Sodium chloride at 300° C.

I have alluded above to an approximate formula given by Faxén which defines the position of one of the anomalous spots with reference to the angles which the incident and diffracted rays make with the nearest crystal plane. Denoting these angles by θ and ϕ, the formula is

$$d \sin(\theta+\phi) = \lambda \cos \phi$$

or

$$d(\sin\theta + \cos\theta \tan\phi) = \lambda,$$

where d is the spacing of the crystal plane (h, k, l) near the temperature spot. It is only quite recently, in the course of a discussion with Dr Lonsdale, that I have realized that the analysis which I have given of the pattern produced by aluminium confirms this formula. The matter may be put quite simply thus: in figure 4, O is the origin of reciprocal space, C the centre of the sphere of reflexion radius $1/\lambda$, P is the crystal plane (h, k, l) of spacing d so that $OP = 1/d$, Q is the point representing the temperature spot. In my original analysis I showed that the observed spot fell on the line PC provided PQ were not too large. If now CN is the normal to OP, then the glancing angles of incidence θ and of diffraction ϕ are as shown and the formula of Faxén follows at once. It will be observed that when θ is equal to ϕ the formula reduces to Bragg's law, and it has in fact been put forward in several quarters as a modification of Bragg's law. At the time when I was engaged on the study of the pattern of aluminium I was aware of the existence of this formula of Faxén's, but I was not prepared to admit any necessity for abandoning a law which I believed could not be modified in any circumstances. Although the experiments I have described do in fact confirm the accuracy of Faxén's formula, I still think that it is of little use to attempt to describe the observed maxima in the form of a modification of Bragg's law. In the particular case illustrated in the figure when Q lies on the line PC the angles θ, ϕ are very simply related to the spacing d and wave-length λ. But if Q lies elsewhere, the relation will become much more complex. In general there does not appear to be any necessity for Q to be coplanar with O, C and P. The attempt to represent the temperature spots by means of a modified Bragg's law is the outcome of an attitude of mind which regards these spots as abnormal reflexions from the crystal plane P. This seems to me to be a mistaken view and I much prefer to think of these spots as normal re-

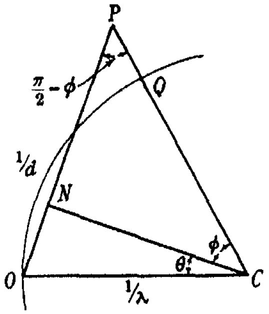

FIGURE 4. Geometrical interpretation of Faxén's rule.

flexions from the fictitious plane Q, the indices of which are not integers. We are primarily concerned with the determination of the intensity of reflexion associated with every point in reciprocal space; the intensity maxima are naturally of great importance but their relation to the integral points is of secondary importance. We should therefore be prepared to admit fractional values of h, k, l and to regard the d of Bragg's law as a *function of the three continuously variable numbers* h, k, l.

The author's work described above has been carried out as part of the research programme of the National Physical Laboratory, and this paper is published by permission of the Director of the Laboratory.

REFERENCES

Faxén 1923 *Z. Phys.* **17**, 266.
Friedrich 1913 *Phys. Z.* **14**, 1082.
Preston 1938 *Proc. Roy. Soc.* A, **167**, 526.
Preston 1939 *Proc. Roy. Soc.* A, **172**, 116.

An experimental study of diffuse X-ray reflexion by single crystals

By K. Lonsdale and H. Smith
Royal Institution

(*Received* 4 *March* 1941)

[Plates 1–28]

A historical introduction outlines the development of experimental and theoretical interest in the diffuse diffraction of X-rays by single crystals. The present experimental study, illustrated by numerous photographs, has consisted in taking Laue, oscillation and rotation photographs, in many different orientations, of inorganic and organic crystals belonging to various systems, using Cu, Mo and Ag radiations, unfiltered, filtered or monochromatized. Rules are laid down for the indexing of diffuse spots and for the determination of the conditions under which such spots appear. Attention is drawn to the presence of non-radial streaks and to the difference in origin of these and of the more usual radial streaks. The relations of the intensity, shape, size, position and persistence of the diffuse spots to the nature, structure, perfection, orientation and temperature of the crystal examined, to the radiation used and to the conditions of photography, are considered in some detail. The use of diffuse spot patterns as a subsidiary method of crystal structure determination is emphasized. It is pointed out that in reciprocal space each reflecting lattice point is surrounded by a region of diffuse scattering, whose physical significance is open to various theoretical interpretations. These diffusely reflecting regions are not, in general, spherical, but are extended along reciprocal lattice planes and axes.

INTRODUCTION

Well-exposed X-ray photographs of stationary single crystals frequently show, in addition to the usual clearly defined Laue spots,* a fainter background pattern of diffuse streaks and spots. When the applied voltage is below that required to excite the X-radiation characteristic of the anti-cathode used, the incident X-ray beam is composed either wholly or in considerable part of continuous radiation. The diffuse pattern then consists mainly of radial streaks running through the strongest Laue spots. Such an effect was first observed by Friedrich (1913). If, however, the incident beam contains a high proportion of characteristic X-radiation, the diffuse pattern may show non-radial streaks and spots which do not apparently correspond in position to the Bragg reflexions from any planes of the stationary crystal. Such diffuse spots have frequently been observed, but it is only in the last two or three years that any serious attempt has been made to study them.

---

* In the following discussion the term 'Laue' reflexion will be reserved for the selective reflexion of X-rays of a wave-length not characteristic of the anti-cathode used, the 'Bragg' reflexion being the selective reflexion of characteristic X-rays.

Using tungsten radiation, Wadlund (1938) observed a diffuse background pattern of streaks and spots on Laue photographs of rocksalt and sylvine, but failed to obtain it with mica, fluorite, gypsum or calcite. Preston (1939) made a more precise investigation showing that (1) the diffuse spot pattern persisted when monochromatized (Ag) radiation was used, although the Laue spots of course disappeared and (2) that the intensity of the diffuse spots was greatly enhanced by raising the temperature of the crystals used (Al, NaCl, MgO, each in several different settings). Preston could find no diffuse spots on Laue photographs of diamond, using Ag radiation, though the background scattering gave the impression of not being of uniform intensity, and at 500° C four faint diffuse streaks were visible on a photograph taken with the incident beam parallel to [110].

Independently, and in advance of Preston's investigation, a comprehensive and fundamental experimental study of the diffusion of X-rays by crystals, using ionization spectrometer methods, was carried out by Jean Laval (1938, 1939*a*, *b*; Mauguin and Laval 1939). Laval's memoir appears to have been almost completely overlooked, so a short résumé may not be out of place. As he pointed out, the Debye theory (1914) indicates that the diffusing power of a crystal should be independent of its orientation. Brillouin (1922), taking into account the longitudinal vibrations due to thermal agitation in a crystal, came to a somewhat different conclusion. He summarized the total X-ray scattering by a single crystal as follows:

(1) Bragg spots.
(2) Intense scattering around the central spot.
(3) Diffuse scattering around each Bragg spot.
(4) Light general scattering in every direction.

Faxén (1923) and, more completely, Waller (1923, 1925) worked out a theory of diffuse scattering which took into account not only longitudinal, but transverse, thermal vibrations and in which the diffuse scattering in any direction depended not only upon the orientation of the crystal but upon its various elastic constants. Faxén referred to the streaks observed by Friedrich and suggested that an attempt should be made to correlate these streaks with the temperature of the crystal.

A number of experimenters attempted to test the validity of these various theories and concluded that Debye's theory was correct (Coven 1932; Jauncey and Pennell 1933; Harvey, Williams and Jauncey 1934; and other papers). Laval (1939*b*), in a critical examination of their methods, showed that their experimental conditions were too restricted for a proper conclusion to be reached, and undertook a more complete experimental research using monochromatized Cu and Mo radiations, with single crystals of sylvine, rocksalt, aluminium, calcite and diamond, and a powdered specimen of silver. He varied the orientation of the single crystals and measured their absolute 'diffusing power' in various directions, over a wide range, and also measured the variation of 'diffusing power' with change of temperature from 289° to 665° A. [The 'diffusing power' of a crystal element, mass dm, is defined by $P = \frac{1}{\varpi}\frac{di}{I\,dm\,d\omega}$, where ϖ is the diffusing power of a free electron placed in the same beam, I the intensity of the incident beam, di the intensity of radiation diffused in a solid angle $d\omega$ in the given direction.] Laval found that, as Brillouin, Faxén and Waller had predicted, each Bragg reflexion is surrounded by a region of strong diffusion, within which the intensity decreases rapidly as the direction of diffusion departs from that of selective reflexion. There is also a feeble general scattering in every direction. He measured the shape and extent of the regions of strong diffusion and the variations of intensity within those regions, for various Bragg reflexions, expressing his results in terms of the reciprocal lattice. He found that, of all the diffuse regions studied, that surrounding the diamond (111) reflexion was the smallest in extent, while the difference in intensity between the strong diffusion accompanying the Bragg reflexion and the weak background diffusion was also less for diamond than for any of the other crystals studied, considering only planes of equal structure factor. It was, of course, impossible for him to study the diffuse scattering within those regions where selective reflexion occurred, but subject to this limitation he came to the conclusion that the maxima of diffuse reflexion decreased more slowly with increasing order of reflexion than those of the corresponding Bragg reflexions. On the other hand, he found no appreciable difference between the strong diffusion of Mo $K\alpha$ and of Cu $K\alpha$ radiations. Temperature experiments were carried out using Mo $K\alpha$ radiation and a single crystal of sylvine; the maximum diffusing power and the extent of the region of strong diffusion were both found to increase markedly with rise of temperature, more especially for low order reflexions, while the weak general diffusion also increased in absolute intensity as the temperature rose. Laval finally concludes: 'La diffusion forte a son origine surtout dans l'agitation ther-

mique des atomes. Ses domaines s'accroissent lorsque la température s'élève; ils sont beaucoup plus étendus pour la sylvine où l'agitation thermique est forte, que pour la diamant où l'agitation thermique est faible. On peut espérer que la topographie des domaines de la diffusion forte apportera des renseignements précis sur la distribution de l'énergie entre les diverses ondes élastiques qui constituent l'agitation thermique.'

It has been pointed out by Zachariasen (1940), in the course of a new derivation of the intensity expression for the coherent scattering of X-rays by a small crystal, that although the diffuse scattering maxima will coincide with the Bragg maxima when monochromatic radiation is used, there are conditions in which the maxima will be separated. These conditions, which are frequently fulfilled in the taking of a normal Laue photograph, are that the incident beam used should contain both characteristic and continuous or 'white' radiation, and that the stationary single crystal should only be near to, and not actually in, the Bragg reflecting position appropriate to the characteristic wave-length and to the plane under consideration. A preliminary experimental study of such 'separated maxima' has been carried out by Siegel and Zachariasen (1940) who, using a rock-salt crystal and Cu $K\alpha$ radiation (filtered but not monochromatized), have studied the peak intensities and half-widths of the diffuse maxima for various degrees of separation, by means of photometered recordings of photographic plates.

More recently, Sir C. V. Raman and his collaborators have published Laue photographs of diamond, $NaNO_3$, NaCl and $CaCO_3$ showing a number of these diffuse maxima, together with tables showing the relation between angles of incidence and of scattering for selected maxima (Raman and Nilakantan 1940 *a*, *b*, *c*; Raman and Nath 1940 *a*, *b*). Raman and Nilakantan consider that the 'modified' (diffuse) reflexions are due to pulsations in the crystal lattice having the characteristic infra-red frequencies, which are excited by the incident X-ray beam and which in turn cause periodic variations in the structure-amplitude of the crystal spacings and therefore result in reflexions of the X-rays with change of frequency. They conclude therefore that 'the modified reflection is a quantum effect and is not primarily a thermal phenomenon, though for low lattice frequencies or at high temperatures it may be thermally influenced'. They included among their experiments a temperature study of $NaNO_3$, the X-ray beam being perpendicular to one cleavage face and temperature varied between 25° and 275° C. They found, as Preston had already observed for Al, NaCl and MgO, that the intensity of the diffuse spots is very greatly increased, while the Laue spots are much fainter in the high temperature photographs than in those taken at room temperatures. Kracek, Posnjak and Hendricks (1931) had found that, above 180° C, the rise of temperature affects very unequally the intensity of the Bragg (powder) reflexions due to different planes, some being practically wiped out at 250° C. Raman and Nilakantan observed that, for just those planes, a room temperature photograph showed intense Laue spots unaccompanied by any diffuse satellites, while a photograph taken at 275° C showed a great diminution in intensity of the Laue spots (which in fact had practically disappeared) and the appearance of strong diffuse spots in their immediate neighbourhood.

Raman and Nilakantan also pointed out the resemblance between the diffuse pattern observed for an oblique setting of the NaCl crystal and the layer-line diagram of an oscillating or rotating crystal.

During the course of an investigation of the age-hardening of alloys, Guinier (1938) and Preston (1938) independently found well-marked diffuse streaks and spots on Laue photographs, which could clearly be interpreted as 'cross-grating' effects due to the segregation of one metal into thin sheets within the alloy. [See also Calvet, Jacquet and Guinier 1938, 1939; Preston 1940; Barrett and Geisler 1940; Ewald 1940.] Sir William Bragg has suggested that the diffuse spot patterns of sylvine and other crystals may be due to simple three-dimensional diffraction by very small groups of atoms, orientated alike but scattering independently (Bragg 1940); such X-ray diffraction would not, of course, be subject to the usual Bragg condition $n\lambda = 2d \sin \theta$.

It is not proposed in the following paper to make any comparison between the various theories put forward, but rather to supply or to emphasize those detailed experimental facts without which no theory can be properly considered.

AIMS OF PRESENT RESEARCH

During the course of X-ray investigations covering the past eighteen years, many isolated instances of weak diffuse spots have been observed on Laue photographs taken by various workers (Knaggs, Lonsdale, Müller and Ubbelohde 1940) in this laboratory; but they were usually regarded as evidence of crystal imperfection, since they could not be given any direct interpretation from a structural point of view. More recently, however, Laue photographs of benzil were found to possess such a beautiful and intricate background pattern (plate 3*a*), even with a relatively moderate exposure, that a more extensive investigation was undertaken in order to determine:

(1) Exactly what conditions are needed for the production of diffuse spots on Laue photographs; why, for instance, some substances show them while others do not; why some wave-lengths seem more favourable for their production than others; why they are more easily obtained in some crystal orientations than in others; whether they are in any way related to the imperfection or surface conditions of the crystals.

(2) Under what conditions the spots are accompanied by streaks, radial or non-radial.

(3) How the positions, size, shape and intensity of the diffuse spots are related to the structure and orientation of the crystal for any particular wave-length of incident X-rays.

(4) Whether the study of diffuse patterns can be used as a subsidiary method of crystal structure determination, and what is their relation to the various physical properties of the crystal, including its temperature.

EXPERIMENTAL DETAILS

The following experiments, of which a preliminary account has already been published (Lonsdale, Knaggs and Smith 1940), were mainly carried out on the medium (5 kW.) X-ray tube (Clay 1934) at the Davy-Faraday laboratory, using Cu, Ag and Mo anticathodes; the tube was operated at 34 kV (for the copper anticathode) with an output of 140 mA, and exposures varied from 0·5 to 5 min. for oscillation photographs, from 2 to 15 min. for rotation photographs, from 5 to 30 min. for Laue photographs. Ilfex double-coated blue base X-ray film was used throughout, and given 5 min. development at 18° C. Room temperature varied from 20° to 30° C. A few photographs were also taken on the 50 kW X-ray tube (Muller and Clay 1939) with copper anticathode, and some on a small experimental 0·5 kW tube with Mo anticathode. No methods of intensification were used.

The crystals chosen for investigation were all small single specimens, rather larger than would normally be used for structure determination. It was found that crystals obtained by cleavage were sometimes distorted and gave misshapen Laue spots; every effort was therefore made to grow or to choose crystals of a suitable size, but a certain amount of distortion due to cleavage, bending or fracture could not always be avoided. Except for the low temperature experiments, the crystals were mounted on fine glass fibres on arcs, and as far as possible were so placed that the incident X-rays did not strike either adhesive or glass fibre; this meant, of course, that the crystal could not, in general, be wholly bathed in the incident beam, which was cylindrical and slightly divergent. The arcs carrying the crystal were used with a Müller spectrometer, the film being contained in a plate-holder placed, usually, at right angles to the incident X-ray beam (though a few photographs were taken with the plate-holder parallel to a main crystal face, and not perpendicular to the beam). The crystal to film distance was varied from 3 to 8 cm., but was usually 3·5 or 4 cm., as experiment showed that for the substances examined, these were the distances at which most diffuse spots were recorded on the films. No attempt was made to calibrate the spectrometer and to measure these distances exactly, because the crystals used were all substances whose unit cell dimensions were well known and for purposes of accurate measurement it would therefore be preferable in any particular case to obtain the crystal to film distance from the evidence of the Laue spots themselves.

Comparison of Laue and oscillation photographs

It had been noticed that, using a copper anticathode, diffuse spot patterns were more readily obtained with organic than with inorganic compounds. A quick survey was made of those organic crystals whose structures had either been determined or were undergoing investigation in the laboratory, and detailed preliminary studies were made of α-resorcinol, an orthorhombic crystal whose structure has been determined by Robertson (1936), of benzil, a hexagonal crystal studied by Knaggs and Lonsdale (1939), and of sorbic acid, a monoclinic crystal whose structure has been investigated by Lonsdale, Robertson and Woodward (1941).

α-*Resorcinol. ortho*-$C_6H_4(OH)_2$

The crystals, which were selected from among those used by Robertson, grow in the form of stout needles parallel to the *c* crystallographic axis. The structure is fairly dense, since the hydrogen bonds draw the molecules closer together than the normal van der Waals distance, and it is relatively isotropic. There is no definite cleavage and the crystals are not easily distorted; they give excellent Laue photographs in any orientation. The crystal was first set with the needle axis vertical and the X-ray beam (unfiltered Cu radiation) parallel to the (100) plane. Laue photographs were taken in this position and at 10° intervals of rotation about the [001] axis, until the incident beam was parallel to the (010) plane. Over a limited range photographs were also taken at 1° intervals. Plates 1*a* and 2*b* show two typical photographs. The most noticeable features of the diffuse scattering are the dense halo surrounding the central spot, to which further reference will be made later, and the well-marked 'layer lines' of diffuse spots. So striking was the arrangement of the diffuse spots in layer lines similar to those occurring on oscillation photographs that it seemed natural to take and compare an oscillation photograph having the 'Laue' position as the centre of the oscillation. It was found that, in fact, a short-exposure oscillation photograph (plate 1*b*) taken with the crystal oscillating through 7½° on each side of the 'Laue' position, gave Bragg spots many of which were practically coincident in position with many of the diffuse spots observed in the corresponding Laue photograph (plate 1*a*). A third photograph, in which the oscillation photograph was superimposed on the Laue photograph (plate 2*a*), shows how closely the positions of Bragg and diffuse spots agree.

This indicates that the diffuse spots may be considered as due to the reflexion of the incident beam by 'planes' which are within a few degrees of the reflecting positions characteristic of ordinary crystal planes and whose spacings are equal, or nearly equal, to those of the normal crystal planes.

Laue photographs are particularly sensitive to mis-setting, and change rapidly in appearance for slight changes of crystal orientation, but the diffuse spot pattern changes much more slowly in successive photographs at slightly different angles. This is easily comprehensible when the similarity of the diffuse spot pattern to the oscillation pattern is taken into account, since the 15° oscillation photograph taken, for instance, with the incident beam at 20° to [010], will differ very little from that taken, say, at 17° or 23° to [010].

A further point of resemblance is that the shape of the diffuse spots is, in general, similar to that of the oscillation spots and quite unlike that of the Laue spots.

Benzil. $C_6H_5.CO.CO.C_6H_5$

Benzil forms good undistorted crystals in the form of hexagonal prisms bounded by $\{10\bar{1}0\}$ planes, which give excellent Laue photographs with Cu or Mo radiation. The structure of benzil has not been fully determined, but it is known that the crystals are built up of skew molecules grouped round a hexagonal alternating axis in such a way that the benzene rings are more nearly parallel than perpendicular to the axis.

The hexagonal pattern obtained when a well-exposed Laue photograph is taken with the incident Cu radiation parallel to the [0001] axis (plate 3*a*) is strongly reminiscent of a benzene ring, and suggests that there may be some connexion between these diffuse patterns and those observed by

Charlesby, Finch and Williams (1939) on electron diffraction photographs of aromatic substances. An analogy would only be possible, however, if the benzene rings of the benzil molecule were normal or nearly normal to the [0001] axis, which they certainly are not. [A better compound on which to compare X-ray and electron diffraction diffuse patterns would have been anthracene, but the Laue photographs of anthracene all revealed so much distortion of the crystals that this compound was felt to be unsuitable for present study.] Photographs taken in directions more nearly normal to the benzene rings (plates 9 and 10 *a* and *b*) showed no trace of trigonal or hexagonal symmetry.

A Laue photograph taken with the X-ray beam at about 7° to the [0001] axis, and the [11$\bar{2}$0] axis only approximately vertical (plate 3*b*), had lost all hexagonal symmetry as far as the Laue spots were concerned. The diffuse pattern, however, still showed approximate hexagonal alternating symmetry. A photograph taken with the crystal oscillating through 7½° on each side of this Laue position (plate 4*a*) showed Bragg spots corresponding in position with many of the diffuse spots of the Laue photograph. This oscillation photograph had only a one-minute exposure to Cu radiation filtered through 0·0008 in. Ni foil; an otherwise identical photograph given ten times this exposure (plate 4*b*) shows a strong diffuse background similar to that found on the Laue photograph but accompanied by much stronger radial streaks.

It is clear, from Laval's experiments and from the present study, that every type of X-ray photograph, Laue, oscillation, rotation, powder, etc., may *if sufficiently exposed* show a diffuse background picture, characteristic of the crystal in its particular setting. If Bragg reflexions are possible, the diffuse scattering will occur as a background to the Bragg reflexions (whether spots as in rotation photographs, lines or rings as in powder photographs). If Bragg reflexions are not possible, the diffuse background spots will still occur provided that the planes giving the corresponding Bragg reflexions are only a few degrees mis-set. In Laue photographs the *indices* of the plane corresponding to any particular diffuse spot can be determined, with reasonable certainty, by treating the diffuse spot pattern as though it were an oscillation photograph covering some 10° or 15° on each side of the stationary position of the crystal (the oscillations must, of course, be considered as taking place in every direction, and not only about a vertical axis); the *true position* of the plane having those indices can then be determined by reference to its Laue reflexion.

In this way the Laue photograph of benzil shown in plate 3*a* has been interpreted, and the indices of all spots, both Laue and diffuse, are given in figure 1. It will be seen that there are a number of diffuse reflexions corresponding to planes which are actually parallel to the incident beam. This is true also of the photographs published by Preston (1939) and by Raman and Nilakantan (1940); and indeed, as the latter point out, it is even possible for the angles of incidence and of diffuse reflexion to be of opposite sign.

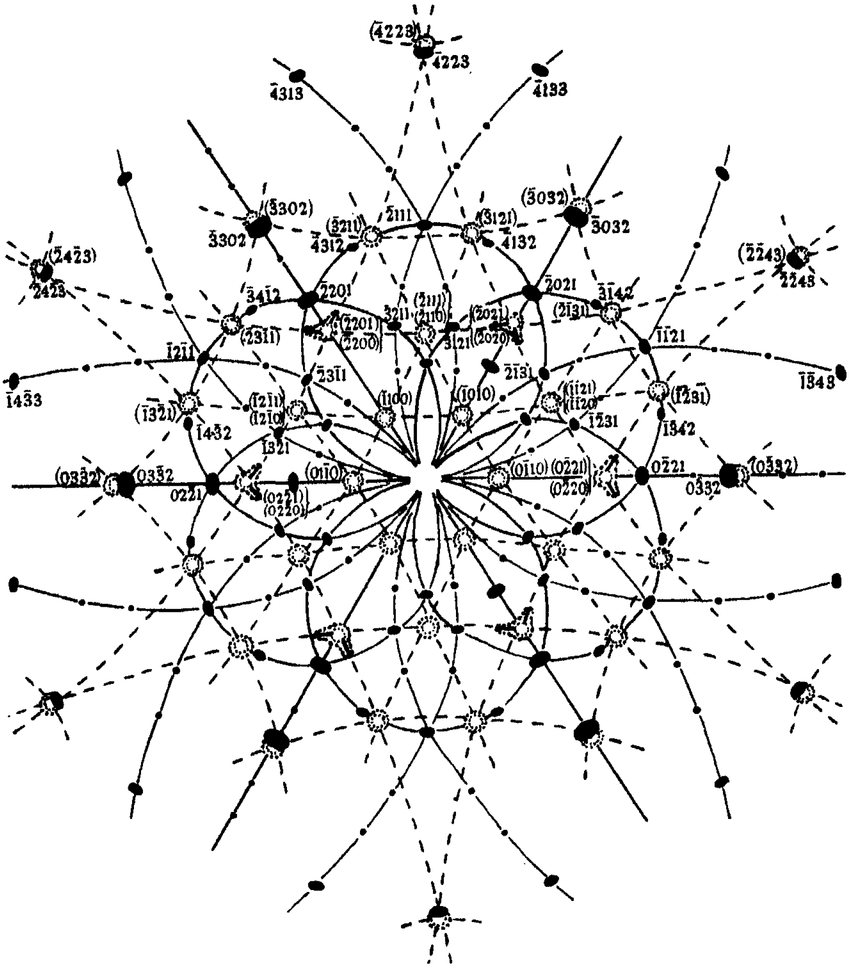

FIGURE 1. Benzil: Laue photograph with X-rays along [0001] axis: diffuse spots, shown in outline only, given by Cu $K\alpha$ radiation. Indices of diffuse spots in brackets.

In symmetrical photographs and in many other cases, apparently, the diffuse spot and its corresponding Laue spot are along the same radius vector, but this does not always seem to be true, and exceptions will be indicated later.

Sorbic acid. $CH_3.CH:CH.CH:CH.COOH$

Sorbic acid forms monoclinic crystals in the form of prisms elongated on the *b* axis. The structure will be described later in some detail. Laue photographs have been taken with filtered Cu radiation at 10° intervals with the [010] axis vertical and the grouping of the diffuse spots into layer lines is most striking (plates 5*a*, 11, 12, 23*a*). A [010] rotation photograph is shown for comparison (plate 5*b*). In this case the vertical crystallographic axis is short (4·03 A) and there is well-marked separation of the layer lines. Photographs taken with the long *c* axis (15·83 A) vertical show, on a suitably orientated Laue photograph, well-marked *rows* of diffuse spots corresponding to outstanding reflexions in the [001] rotation photograph, the layer lines being in this case closer together and therefore less obviously defined (plate 6 *a* and *b*).

Other compounds

In order to make sure that the relation between the diffuse spot pattern and that of the corresponding oscillation diagram is a perfectly general one, applying to X-radiation of any wave-length and to crystals of any kind, organic or inorganic, photographs have been taken of

(1) Several other organic compounds, using Cu radiation, filtered and unfiltered.

(2) Benzil, using Mo radiation (by Dr I. E. Knaggs).

(3) Sylvine, KCl; complete sets of Laue and oscillation photographs with cube axis vertical, using Mo radiation (by Dr I. E. Knaggs).

(4) Sylvine; complete sets of Laue and rotation photographs with cube axis and [011] axis vertical, using Ag radiation.

(5) Rocksalt, NaCl; complete sets of Laue and rotation photographs with cube axis vertical, using Ag radiation.

(6) $NaNO_3$, $CaCO_3$, quartz in various orientations, using Ag, Mo and Cu radiations.

(7) Diamond; Laue and rotation photographs in various orientations, using Cu and Mo radiations.

Further reference will be made later to many of these experiments, but the following deductions have been made from a preliminary survey of the results:

I. The relation between the diffuse spot pattern on a Laue photograph and the oscillation photograph taken with the Laue position as centre of the oscillation is quite general; it applies both to organic and to inorganic compounds; to crystals of any system and to all the different kinds of X-radiation used (Cu, Mo, Ag; $K\alpha$ and $K\beta$).

II. The same conditions, to a certain extent, govern the appearance of a diffuse spot diagram as govern the appearance of the corresponding oscillation photograph. If the wave-length of the radiation used is such that very few spots would appear on an oscillation photograph, then a Laue photograph taken with the crystal stationary at the centre of the oscillation range would also show very few diffuse spots, though it might show radial streaks corresponding to the diffuse scattering of general radiation of other wave-lengths. Since Cu radiation is, in general, most suitable for the examination of organic crystals, together with a crystal to film distance of about 3·5–4 cm., Laue photographs of organic crystals will show most diffuse spots when taken with Cu radiation at that distance. The strongest Bragg reflexions from organic crystals are nearly always those of spacing greater than 2 A, and with Cu radiation these are well placed on the film; the lower symmetry of the crystals also ensures that, whatever the crystal orientation, some planes will nearly always be near to a reflecting position. On the other hand, simple inorganic compounds such as KCl, NaCl, $NaNO_3$, $CaCO_3$, SiO_2, crystallizing in the cubic or hexagonal system, have relatively few planes which reflect Cu radiation with appreciable intensity within the range of a quarter-plate size film (3 cm. being the nearest possible distance of approach to a crystal set on arcs), and a shorter wave-length is much more suitable both for rotation or oscillation photographs and for the production of diffuse spot patterns.

This, perhaps, can best be illustrated by examples.

TABLE 1

crystal to film distance (cm.)	3	3·5	4	5	6
sin θ (min.)	0·05	0·04	0·04	0·03	0·02
sin θ (max.)	0·54	0·51	0·48	0·44	0·40

In table 1 are given the limiting observable values of $\lambda/2d$ (sin θ, where 2θ is the angle of deflexion) for quarter-plate size films at various crystal to film distances. Table 2 shows the indices of the principal Bragg reflexions from NaCl, together with their intensities (Brill, Grimm, Hermann and Peters 1939) including all reflexions above 1 % of the maximum observed, and the observable values of $\lambda/2d$ corresponding to Cr, Cu, Mo and Ag $K\alpha$ radiations. Table 3 gives the corresponding data for α-resorcinol, except that in this case only (*hk*0) reflexions are included, since otherwise the list would be much too long. Table 4 gives similar data for diamond.

Table 2. NaCl

		sin θ			
hkl	intensity	Cr	Cu	Mo	Ag
111	5·5	0·35	0·23	0·11	0·08
200	100	0·41	0·27	0·12	0·10
220	44	0·57	0·38	0·18	0·13
222	28	—	0·47	0·22	0·17
400	18	—	0·54	0·25	0·20
420	11	—	0·61	0·28	0·22
422	9	—	—	0·30	0·23
440	4·5	—	—	0·35	0·28
442	3·5	—	—	0·38	0·30
600	3·5	—	—	0·38	0·30
620	3	—	—	0·40	0·31
622	3	—	—	0·42	0·33
444	2	—	—	0·43	0·34
640	1·5	—	—	0·45	0·36
642	1·5	—	—	0·47	0·37
800	1	—	—	0·50	0·40

It will be seen that for NaCl, which is typical of many inorganic crystals, either Mo or Ag radiation gives values of sin θ which would be readily observable on a film set at 3–5 cm. from the crystal, although either Cu or, worse still, Cr radiation would give only a few spots towards the outside of the picture.

On the other hand, for α-resorcinol Cu is the most suitable radiation with which to obtain an even distribution of spots. With either Mo or Ag radiation the strongest spots would be very close to the central spot and there would be no spots observable towards the outside of the film. The number of diffuse spots observable in the case of α-resorcinol will also clearly be much larger than that from NaCl; in fact, all those reflexions whose indices are given in table 3 will occur only on the zero layer line in '[001] axis vertical' photographs.

Diamond is rather an interesting case; it is clear from table 4 that Mo or Ag radiation should give a great many more characteristic reflexions than Cu. In fact, Cu radiation will only give the {111} reflexions, as can readily be proved by rotation photographs. Yet all successful experiments so far reported for diamond have been made using Cu radiation, while previous attempts to obtain diffuse spots with Ag radiation have been unsuccessful. This is due to the fact that only symmetrical settings of

TABLE 3. α-RESORCINOL: (*hk*0)

		sin θ			
*hk*0	intensity	Cr	Cu	Mo	Ag
110	1	0·16	0·11	0·05	0·04
200	7	0·21	0·14	0·07	0·05
020	1	0·24	0·16	0·07	0·06
210	100	0·24	0·16	0·07	0·06
120	52	0·26	0·17	0·08	0·06
220	79	0·32	0·22	0·10	0·08
130	2	0·38	0·25	0·12	0·09
320	3	0·40	0·27	0·12	0·10
230	1·5	0·42	0·28	0·13	0·10
400	5	0·43	0·29	0·13	0·10
410	8	0·45	0·30	0·14	0·11
040	5	0·48	0·32	0·15	0·12
330	12	0·48	0·32	0·15	0·12
140	1	0·49	0·33	0·15	0·12
420	7	0·50	0·33	0·15	0·12
240	2·5	0·52	0·35	0·16	0·13
510	2	—	0·37	0·17	0·13
430	1·5	—	0·38	0·18	0·14
440	3	—	0·43	0·20	0·16
600	2	—	0·44	0·20	0·16
610	8	—	0·44	0·21	0·16
620	1·5	—	0·46	0·21	0·17
060	1·5	—	0·48	0·22	0·17
540	1	—	0·49	0·23	0·18
160	1	—	0·49	0·23	0·18
710	3	—	0·52	0·24	0·19
640	1	—	—	0·25	0·20
170	2·5	—	—	0·26	0·20
800	1·5	—	—	0·27	0·21
470	1·5	—	—	0·29	0·23
660	3	—	—	0·30	0·24
580	1	—	—	0·34	0·27
390	1·5	—	—	0·35	0·27

TABLE 4. DIAMOND

		sin θ			
hkl	intensity	Cr	Cu	Mo	Ag
111	100	0·55	0·37	0·17	0·13
022	46	—	0·61	0·28	0·22
311	17	—	—	0·33	0·26
400	21·5	—	—	0·40	0·31
133	9·5	—	—	0·43	0·34
422	11	—	—	0·49	0·38
333	5·5	—	—	0·52	0·41
511	5·5	—	—	0·52	0·41
044	9	—	—	—	0·44

diamond have been investigated. It so happens that when the incident beam is normal to a (111) plane, three other {111} planes are nearly in a reflecting position for Cu radiation, and these give diffuse spots on a Laue photograph taken in that setting. Such a Laue photograph taken with Mo or Ag radiation would show no diffuse spots, only perhaps white radiation streaks through the {111} Laue spots. In order to obtain diffuse spots the crystal must be turned into those particular orientations in which the planes indicated in table 4 are either in or near the position of selective reflexion of Mo or Ag reflexion. This has been confirmed experimentally.

It seems almost certain that every crystal will give diffuse spots when both conditions are fulfilled, namely, that the radiation chosen gives values of sin θ, for Bragg reflexions of appreciable intensity, within the observable range on the film, and that the crystal setting should be such that planes giving those Bragg reflexions should be at or near to the correct angle of incidence for selective reflexion. In any particular case the best conditions can be determined either by trial, or for crystals of known structure, by calculation. It may safely be said that if, with a given radiation and crystal to film distance, a good rotation picture is obtained, then there will be crystal orientations which will give a good diffuse spot picture.

It should be added, however, that an exposure time sufficient to give a good Laue picture is not usually sufficient to show the diffuse spots as well; the exposures must be greatly increased for the production of good diffuse spot patterns. Only the fact that extremely powerful sources of X-radiation were being used accounts for the short exposure times given in this paper. In general, therefore, choice of radiation and crystal setting should be made first by calculation, if possible.

MONOCHROMATIC PHOTOGRAPHS

In the above discussion it has been tacitly assumed, in comparing diffuse with Bragg reflexions, that the diffuse spots are due to scattering of the *characteristic* radiation. This was, of course, proved both by Laval and by Preston, for the inorganic compounds and elements they investigated. It is also indicated, as Raman and Nilakantan have pointed out, by the fact that pairs of diffuse spots, obviously due to $K\alpha$ and $K\beta$ components, are frequently observed, the $K\beta$ spots being removable by the use of a suitable filter. Our experiments with different radiations also show that the positions of the diffuse spots shift in accordance with what would be expected for characteristic reflexion when the X-radiation used is changed from Cu to Mo or from Mo to Ag (plate 7*a* and *b*). The most satisfactory test, however, is provided by using monochromatized radiation; this has been carried out for benzil, sorbic acid and diamond using Cu $K\alpha$ radiation, and for sylvine using Ag $K\alpha$ radiation. A further advantage of using monochromatized radiation is that it has been possible to find out whether the diffuse streaks and the diffuse halo surrounding the central spot are due to white or to characteristic radiation.

In order to obtain a good Laue photograph continuous radiation covering as large as possible a range of wave-lengths is usually employed. [It was very noticeable, for instance, that the 50 kW tube, for which hexa-phase rectification was employed, gave far fewer Laue spots than the 5 kW tube, which had bi-phase rectification, since it followed that the latter was running at less than the critical voltage for characteristic emission for a considerable part of the exposure time, while the former maintained a constant applied voltage to within a few per cent.] When the incident beam contains a high proportion of characteristic radiation, it may happen that some crystal planes will be in a position to reflect it and these will then give exceptionally strong spots on a Laue photograph, but they will be relatively few. A Laue photograph taken with strictly monochromatized radiation will usually, therefore, show few or no spots due to selective reflexion. If there are any, they will be easily recognizable because of the sharpness of their definition.

The method of obtaining monochromatic Laue photographs was, first, to set the crystal in position using an unfiltered beam, and then to monochromatize the beam by reflexion from the cleavage plane of a large crystal of urea nitrate (Lonsdale 1941). Considerable difficulties were experienced owing to the fact that after monochromatization the direction of the incident beam relative to the crystal had frequently changed slightly, so that the crystal setting was no longer perfect. The presence of a few Laue spots on the photograph was therefore an advantage, as it enabled any such imperfection of setting to be detected at once. Fortunately, however, our previous experiments showed that the diffuse picture would not be affected by slight mis-setting, but it was naturally avoided as much as possible.

Benzil. Plate 8*a* shows the appearance of the Laue photograph of benzil taken with ordinary Cu radiation, when the incident beam is along the [0001] axis, and $\{10\bar{1}0\}$ faces are vertical; the corresponding monochromatic (Cu $K\alpha$) photograph, plate 8*b*, was given 2 hr. exposure as compared with 10 min. for the ordinary photograph. It shows a few sharp Laue spots, not quite symmetrically placed. It also shows a beautifully symmetrical pattern of diffuse spots and streaks. The most remarkable features of this pattern are:

(1) That no *radial* streaks are present (except traces towards the outside of the film).

(2) That the diffuse spots are partly joined by *non-radial* streaks of considerable intensity which follow the direction of the main [$11\bar{2}0$] 'layer lines'. Through the strongest spots there are traces of layer line streaks corresponding to the [$40\bar{4}0$] periodicity.

(3) The innermost of these streaks are very fine and at their points of intersection there are very small, but still diffuse, spots.

(4) No diffuse halo appears around the central spot, although the background intensity does not appear to be absolutely uniform.

The diffuse pattern is thus clearly proved to be due to characteristic radiation, as far as spots and non-radial streaks are concerned. The same diffuse pattern is of course visible in the background of plate 8*a*.

In plates 9*a* and *b*, 10*a* and *b*, are seen ordinary and monochromatic Laue photographs of benzil with the X-rays normal to the [0001] axis. It was thought possible that in these photographs traces of diffuse circles might occur, corresponding to the strong hyperbolic streaks on the photographs taken with the beam along [0001], but nothing of the kind was found. The streaks are much more fragmentary than before and there are roughly triangular patches of diffuse scattering, some accompanied and others unaccompanied by clearly defined diffuse spots.

Sorbic acid. The photographs of sorbic acid (plate 11 *a* and *b*) also show incipient streaks. The diffuse spot corresponding to the strong ($40\bar{2}$) Bragg reflexion, in particular, is accompanied by diagonal streaks giving it the appearance of a cross. The ordinary photograph shows an intense diffuse halo around the central spot, but in the monochromatic photograph this has almost completely disappeared.

Diamond. This disappearance of the diffuse halo is also characteristic of the monochromatic photographs of diamond which, in fact, are singularly blank, since they show nothing but the $\{111\}$ diffuse spots and (in suitable orientations) their accompanying non-radial streamers. The statement of Raman and Nilakantan, that the most intense region of the halo owes its origin to the monochromatic $K\alpha$ and $K\beta$ radiations of the copper anticathode, is therefore not confirmed.

Sylvine. Monochromatic photographs of sylvine taken with Ag $K\alpha$ radiation show that there are weak non-radial streaks connecting the diffuse spots. Similar streaks also occur on Preston's monochromatic photographs of aluminium, and on photographs of sylvine taken with ordinary radiation (plate 7*b*).

Origin of radial streaks

The disappearance of the majority of radial streaks from monochromatic photographs shows that they are almost always due to white radiation. There is no reason, of course, why some radial streaks due to characteristic radiation should not occur in special circumstances; indeed, traces of such streaks do occur towards the outside of the benzil [0001] monochromatic photograph (plate 8*b*), apparently emanating from alternate ($3\bar{3}02$) diffuse spots (compare figure 1). In most of the monochromatic photographs, however, radial streaks are conspicuous only by their absence.

On ordinary Laue photographs of undistorted crystals, the radial streaks are due to *diffuse* reflexion of white radiation; on oscillation or rotation photographs (and on Laue photographs of distorted crystals) the radial streaks are due to *selective* reflexion of white radiation, with, of course, the appropriate diffuse background. They are only straight lines in the neighbourhood of the central spot; extended, they trace out the 'α constant curves' (Bernal 1926) often seen on rotation photographs taken with a beam containing a good deal of white radiation (plates 5*b*, 6*b* and 20*b*).

Change of crystal to film distance

It has been mentioned previously that photographs taken at a crystal to film distance of 3·5 or 4 cm. usually give the best diffuse pictures within a reasonable exposure time. In order to find out whether the sizes of the diffuse spots change with distance in the same proportion as those of the Laue spots, Laue photographs have been taken at different distances with the same setting of various crystals. Two of these are shown in plates 12*a* and *b*; the 6 cm. photograph was given four times the exposure of the 3 cm. photograph. It will be seen that, owing to the divergence of the incident beam, both Laue and diffuse spots have increased in size on the film taken at the greater distance. There is no measurable difference in the rate of increase with distance for the two types of spot. This result was common to all such photographs taken.

Effect of condition of crystal surface

In order to determine whether the condition of the crystal surface affected the diffuse pattern, successive Laue photographs were taken of a crystal of α-resorcinol (water soluble), first dry and then sprayed gently with water until at last it was almost completely dissolved. For some of the photographs the crystal surface was actually covered with a drop of water. No change in the diffuse pattern could be detected, it became neither weaker nor stronger, and the crystal continued to give an excellent Laue photograph even when it was practically eaten away.

Nor was there any noticeable change in the diffuse pattern when a freshly cleaved surface was used, although such cleaved specimens were frequently found to be rather distorted, giving bad Laue spots. Occasionally the diffuse spots from cleaved or fractured crystals were found to have an intense and rather sharply defined core, not usually at the centre of the spot, even when the Laue pattern appeared to be undistorted. This effect may be seen on plates 12*b* and 18*a*, and was observed by Wadlund (1938) on his photographs of NaCl and KCl. That this core is also due to characteristic radiation is proved by the fact that it persists when the incident beam is monochromatized.

INTENSITY OF THE DIFFUSE SPOTS

No attempt has been made at this stage to obtain a quantitative estimate of the diffuse spot intensities, particularly as these are known to be affected by several different factors. The two principal factors at room temperature are:

(1) That the intensity of a diffuse spot is related to the absolute intensity of the corresponding Bragg reflexion (in particular there are no diffuse spots corresponding to Bragg reflexions either far from the observable region of the sphere of reflexion, or 'forbidden' by the space-group).

(2) That it is dependent on the degree of misorientation involved, that is, on the angular separation between the diffuse spot and its corresponding Laue spot, or alternately, on the angle through which the crystal must be turned in order to obtain the selective Bragg reflexion corresponding to the diffuse spot in question (subsequently referred to as the 'angle of mis-setting').

Factor (1) may be observed in a number of different ways. For instance, plate 6*a* and *b* show that the diffuse spots correspond to the *strongest* of the reflexions seen on the rotation photograph. In Laue photographs showing diffuse spots corresponding to different orders of the same plane (plate 2*b*) the relative intensities of the diffuse spots approximate roughly to the known relative intensities of the Bragg reflexions, *as long as the diffuse spots compared are equidistant from the corresponding Laue reflexion.* Laval states that a comparison of five even orders of reflexion from the sylvine cube face shows that whereas the Bragg reflecting power falls off in the ratio 100:20:7:3:1, the maxima of the diffuse scattering curves corresponding to a mis-setting of 2°·5 decrease more slowly, in the ratio 42:21:14:9:6. Any rigorous comparison, however, must involve integrated intensity measurements, with monochromatized radiation if possible, for a *complete range* of crystal mis-setting. Even then, the results would be incomplete, since for the angle of selective reflexion and for a small range of angles about this value the diffuse scattering simply forms a background to the Bragg reflexion and is therefore included in any measurements that are made of intensity of the latter.

The fact that many spots are accompanied by monochromatic streaks must also make intensity measurements difficult and uncertain in those cases. Experiments show that this includes not only such an interesting case as the diffuse reflexions of Cu radiation corresponding to the {111} planes of diamond, but also those from KCl, Al and various organic compounds.

The absolute maximum peak intensity of diffuse scattering cannot be measured, as it coincides with that of the Bragg reflexion; the maximum peak intensity for any particular angle of mis-setting greater than that included under the Bragg reflexion could be measured by ionization or photometer methods. This has been done by Laval (1939 *a*, *b*) and by Siegel and Zachariasen (1940), both of whom find that there is a rapid falling off of intensity as the angle of mis-setting increases. Plates 13 and 14 show this in rather a striking way. The diffuse spot is that corresponding to the (002) cleavage plane of urea nitrate. In the first strip the X-rays are parallel to the cleavage plane; a diffuse spot may be seen on each side of the central spot. Then as the angle of incidence increases, the (00*l*) Laue spot moves outwards towards the position of the diffuse spot and the intensity of the latter increases until the diffuse and Laue spots coincide, after which the diffuse spot intensity decreases as the Laue spot moves away towards the edge of the film. The actual series of photographs includes several for which the Laue spot has gone beyond the edge of the film and the diffuse spot is still just visible, though not reproducible. The range of angles of incidence is from 0° to over 30° in this series; the Bragg angle is 14°·1. On the opposite side of the central spot in the films corresponding to orientations of 17°·7, 18°·7 and 19°·6 may be seen a very small diffuse spot, evidently corresponding to a much less intense Bragg reflexion. This diffuse spot fades out very quickly, and is a good contrast to the persistent, intense (002) spot.

As Raman and Nilakantan have pointed out, it frequently happens that the $K\beta$ diffuse spot is actually more intense than the $K\alpha$, because it is nearer to the corresponding Laue reflexion; its angle of mis-setting is less. This may be seen in plates 2*b*, 7*b* and 24*a*. Except in the case of diamond (plate 24*a*) and sylvine (plates 7*b*, 26, etc.), the observed $K\beta$ diffuse spots are always much *smaller* than the $K\alpha$ (plates 1*a*, 2*b*, 6*a*, 20*a* and 21*d*).

LOW-TEMPERATURE EXPERIMENTS

Laval, Preston, and Raman and Nilakantan found a great enhancement of the intensity of many of the diffuse spots when the crystal temperature was raised. Organic crystals, in general, melt at relatively low temperatures; a test experiment showed that even a rise of temperature of 50° C was sufficient to give a marked increase of intensity in the case of the diffuse spots of benzil (m.p. 95° C). The next step was to try the effect of lowering the temperature. The experimental technique, which was very simple, was similar to that described by us (Lonsdale and Smith 1939) for the investigation of crystal structure at liquid air temperatures.

The crystal was set with cellulose solution on a glass or metal rod, and enclosed in a thin cellophane tube, the whole being set on a pair of arcs with cellulose solution, and adjusted to the orientation required. A photograph having been taken at room temperature, a fine stream of liquid air was allowed to impinge directly on the cellophane-covered crystal all the time a second photograph was being taken. No ice formed on the crystal during the experiment, and although no attempt was made to measure the temperature attained, it seems probable that this was at least as low as that of liquid air. When the crystal had warmed up again, a third photograph was taken at room temperature. Sometimes a fourth and a fifth photograph were taken at liquid air and room temperatures again. The exposures were made as nearly as possible the same, but a further check was sometimes made by taking a room temperature photograph at considerably less than the exposure given to the corresponding low temperature photograph (see plate 17 *a* and *b*). Photographs were also taken of the cellophane tube alone (plate 15*a*), of cellophane + liquid air stream (plate 15*b*) and of liquid air stream alone. All the photographs taken at low temperatures showed rings due to the cellophane and liquid air stream; these were of varying intensity, because sometimes the cellophane tube was vertical and the liquid air streamed over it continuously; at other times the cellophane tube was inclined and the liquid air stream impinged on it and was sprayed off in such a way as to give no clear reflecting jet.

The substances photographed in this way were α-resorcinol,* benzil (plate 16 *a* and *b*), sorbic acid (plate 17 *a* and *b*), KCl, $NaNO_3$ (plate 18*a* and *b*) and diamond (plate 19 *a* and *b*). In all cases except diamond the diffuse spot pattern is practically non-existent at liquid air temperatures. The Laue pattern, on the other hand, shows many more spots and has a much clearer background. *In every case the changes are completely reversible* and can be repeated as often as desired. The Laue spots remain consistently sharp at all temperatures. The few diffuse spots which do not completely disappear are much sharper at low than at room temperatures (plates 16*b* and 18*b*).

The {111} diffuse spots of diamond (all orientations) show only a slight diminution of intensity at low temperatures, but it should be noted that the lowering of temperature involved (some 200°) is relatively small compared with the characteristic temperature of diamond (2340°).

SHAPE AND SIZE OF THE DIFFUSE SPOTS

No intensity measurements giving only peak values can be considered satisfactory, since the size and shape of individual spots vary enormously. Sometimes the diffuse spots are approximately circular, in which case estimates of the size given by 'half-maximum-intensity' or 'half-width' measurements would have some meaning; but more often they are not circular. Frequently, as has been mentioned in the discussion on α-resorcinol, the diffuse spots are quite different in shape from the Laue spots; a close examination of the diffuse spot group seen in plate 20*a* shows this clearly. The crystal used was a small lath of urea oxalate obtained by cleavage and set with the long axis vertical. The cleavage plane $(20\bar{1})$, to which corresponds the prominent diffuse spot on the film (seen accompanied by a smaller $K\beta$ component), is parallel to the thin faces of the lath; the main faces are {010} planes. The rotation photograph (plate 20*b*) shows, as might be expected, Bragg spots whose length is parallel to the 'row lines'; the diffuse spots are similar in shape to the Bragg spots although different in size; by contrast, many of the Laue spots slope sharply; in the original film the $(20\bar{1})$ Laue spot can be seen sloping between the $K\alpha$ and $K\beta$ diffuse spots.

The (220) and (330) diffuse spots of α-resorcinol (plate 2*b*) appear to be slightly concave towards the (*hh*0) Laue spot accompanying them, and definitely appear to increase in size as the angle of mis-setting increases.

---

* Note: photographs reproduced in *Nature* 1941, **147**, 469.

In three photographs of sorbic acid (plate 16 *a*, *b* and *c*) taken at 5° intervals it will also be seen that the diffuse spots on the outer films are longer than the corresponding diffuse spot on the central film, for which the crystal was more nearly in the position for Bragg reflexion. On the other hand, the size of the urea nitrate (002) diffuse spot (plates 13 and 14) does not appreciably change with change of crystal orientation. It sometimes appears that spots occurring at larger angles of deviation are larger than those occurring at smaller angles, but this is by no means a general rule. For instance, the (002) diffuse spot of hexamethylbenzene (plate 21 *e*) is smaller than the (001) diffuse spot (plate 21*d*). Moreover, as Laval's measurements and Preston's photographs show very clearly, at elevated temperatures the inner spots increase remarkably in size, whereas the outer spots are comparatively unchanged in this respect and are much smaller.

Relation of shape and size to crystal structure

Many experiments agree in showing that both shape and size of the diffuse spots are closely related to the crystal structure. *Layer structures* always give Laue photographs showing, for suitable orientations, one outstanding oval diffuse spot which corresponds to the layer plane (Lonsdale 1941). Plate 21*d* shows such a Laue photograph of hexamethylbenzene, a triclinic crystal in which all the atoms lie practically in the (001) planes (Lonsdale 1929; Brockway and Robertson 1939). Laue photographs taken with the (001) plane inclined at various angles to the vertical show that the maximum length of the diffuse spot is always parallel to the layers of atoms. Urea nitrate (plates 13, 14 and 22*a*), monoclinic, with all the atoms in or very near to the (002) plane, and urea oxalate (plate 20*a*), with all the atoms in or near to the $(20\bar{1})$ plane, each show the same prominent type of spot; large, oval, intense and persistent over a wide range of angles of incidence.

Chain structures give diffuse spots of a completely different type. They are fine, needle-like, with only a small intense core in orientations not far from the correct setting for Bragg reflexion. The length of the spot is roughly perpendicular to the length of the chains. Such diffuse spots have been observed on Laue photographs of single crystals of long chain compounds, where they are so sharp as to be barely distinguishable from genuine Laue spots. They are most clearly seen, however, on certain Laue photographs of sorbic acid (Lonsdale, Robertson and Woodward 1941).

Sorbic acid is a monoclinic crystal, the unit cell of which contains eight $CH_3.CH:CH.CH:CH.COOH$ molecules, linked in pairs by hydrogen bonds about the symmetry centres of the crystal. The long chain axes of the molecules lie in or near to the (010) plane and are inclined at a small angle to the *a* axis in the obtuse angle β. The molecules are plane (lath-shaped) and the atoms lie in or near to the $\{11\bar{3}\}$ crystal planes. The results, which are given by the usual X-ray, optical and magnetic methods, are most interesting when considered in relation to the diffuse spot patterns. It is found that the diffuse spots observed may be divided into two main classes (except for a few spots which are intermediate in shape), one set corresponding to the 'layer' type, the other to the 'chain' type (plates 5*a*, 11, 12, 21 *a*, *b* and *c* and 23 *a* and *b*). In the Laue photograph taken with the incident beam along [010] (plate 23*b*) the shapes of the diffuse spots in various positions directly indicate the direction of the molecule length in that particular projection. The correspondence between spot and structure is shown in figure 2.

It is clear that in the case of compounds whose crystals, though perhaps composed of complicated molecules, possess a well-defined chain or layer structure (or both, as in sorbic acid), the study of diffuse spot pictures can supply a most useful secondary method of structure determination. It is particularly useful as a quick method of detecting layer structures, even when a rotation photograph reveals nothing outstanding (compare plate 21 *a* and *b*). A *very well exposed* rotation (Weissenberg, etc.) photograph of a layer structure, however, always shows that the Bragg spot corresponding to the layer plane has an intense diffuse background.

Shape of diffuse spots from diamond

When Cu radiation is used, the diffuse spots from the {111} planes of diamond are particularly interesting as regards shape. The crystal used (kindly given by Professor Gordon) was a perfect octahedron, edge lengths about 1 mm. With an incident beam normal, or nearly normal, to a (111) face, photographs similar to those already published by Raman and Nilakantan (1940*b*) have been obtained. That is to say, the $K\alpha$ and $K\beta$ diffuse spots are small, nearly circular, and accompanied when near to the (111) Laue spot by fine streaks directed away from the Laue spot, and either towards or away from the other two {111} diffuse spots (plate 24*a*). When, however, the crystal is set with a [110] axis vertical and the vertical {111} planes making angles of nearly $-21^\circ{\cdot}9$ and $+48^\circ{\cdot}6$ respectively with the incident beam, so that, in effect, diffuse scattering takes place from *the other side* of the (111) plane ($21^\circ{\cdot}9$ being the Bragg angle), then the diffuse spot is of an entirely different shape (Jahn and Lonsdale 1941). For various angles of mis-setting it consists of three small spots grouped triangularly about a more diffuse centre. The radial apex of the triangle always points away from the Laue spot and as the angle of mis-setting increases the three spots separate without increasing individually in size (plates 24*b* and 25*b*). One rather extraordinary result of this (easily observed, but not reproducible) is that for angles of scattering less than twice the angle of incidence the $K\beta$ group of spots is larger than the $K\alpha$ group. When the crystal is properly set for selective Cu $K\alpha$ reflexion, the $K\alpha$ diffuse spot forms an apparently circular background to the Bragg spot, while the $K\beta$ diffuse spot forms a weak triangular group nearer, of course, to the undeviated beam (plate 25*a*).

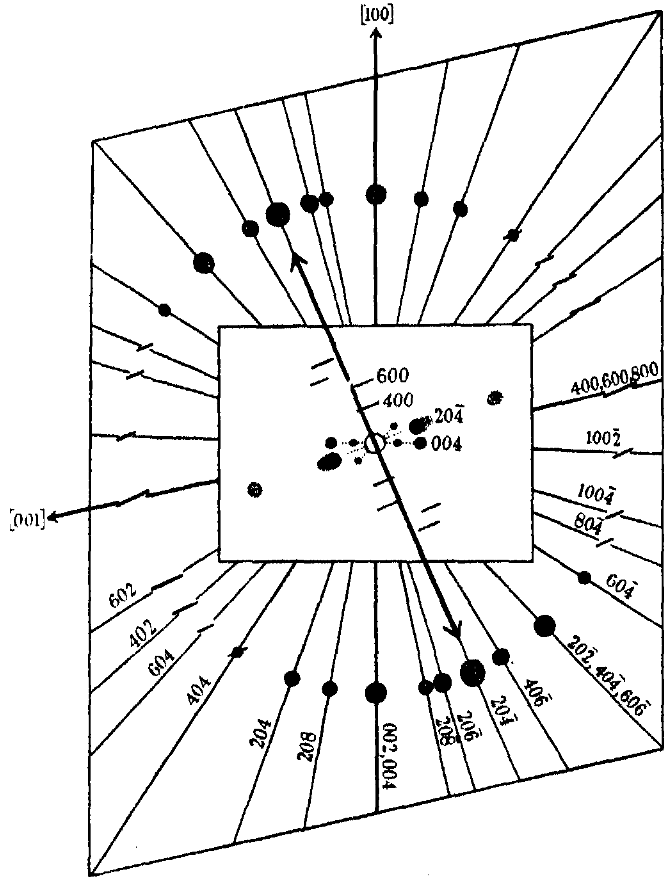

FIGURE 2. Sorbic acid: [010] projection, showing direction of length of molecular chain relative to planes giving broad -●- and fine -/- diffuse spots. Inset is actual appearance of diffuse spots on the corresponding Laue photograph (plate 23*b*).

In other positions of the (111) plane, as for instance when one edge is horizontal, the diffuse spot is asymmetric in shape.

Monochromatic photographs prove that the compound diffuse spot and the circular spot with streamers are both due entirely to scattering of the Cu $K\alpha$ radiation.

Preliminary calculations indicate that it is possible to explain the different shapes of these diamond (111) diffuse spots by means of an extension of Waller's theory, taking particular values of the elastic constants (Jahn and Lonsdale 1941).

Photographs taken using Mo radiation and appropriate crystal settings show diffuse spots corresponding to the (111) (022) (311) (400) planes. None of these have either streaks or structure similar to those obtained for (111) with Cu radiation. They are small, circular, and fade out more rapidly as the angle of mis-setting increases than those of any other crystal examined. It will be shown in a later section that if the positions of the diffuse spots and streaks are plotted on a reciprocal lattice net, the reason for the difference in behaviour with Cu and Mo radiation becomes apparent.

POSITION OF THE DIFFUSE SPOTS

Relation between angles of incidence and of deflexion

It has been made clear by the similarity between diffuse spot and oscillation photographs that the positions of the diffuse spots are nearly those of the corresponding Bragg spots. The words 'nearly' and 'approximately' have been used deliberately, because the correspondence is not always exact. It is exact when the orientation of the crystal is such that selective reflexion takes place. The diffuse spot then forms a background to the Bragg spot. In this position θ, the angle of incidence; $\theta+\phi$, the total angle of deflexion; and θ_B, the Bragg angle, are related as follows: $2\theta=\theta+\phi=2\theta_B$. As has been seen (plates 13 and 14) the angle $\theta+\phi$ changes very little even when θ varies by over 30°, and $\theta+\phi$ is always *nearly* equal to $2\theta_B$; but the small differences involved depend on the nature of the crystal and its orientation and are therefore very important.

Faxén deduced that a formula of the type $a(\sin\theta+\tan\phi\cos\theta)=\lambda$ would give the relation between the incident and diffusely scattered beams in the simplest case of a cubic crystal, lattice constant a, for which spherical symmetry of the elastic constants is assumed. Zachariasen (1940) deduced the same formula, in the form $[1+\lambda\tau_{\text{min.}}]\,k_m=B_H+k_0$ (the original paper should be consulted for the meanings of these terms), which for small values of $(\theta-\theta_B)$ reduces to $\theta+\phi\approx 2\theta_B+2(\theta-\theta_B)\sin^2\theta_B$; and Raman and

Nilakantan found empirically that the same formula (expressed in the form $d \sin(\theta+\phi) = \lambda \cos\phi$) holds approximately for diamond, when the incident Cu radiation is nearly normal to a (111) face (cf. plate 24*a*) and three $\{111\}$ diffuse spots are observed for various angles of incidence within a range of about 4°. More recently still, Jauncey (1941) has deduced the same formula, in yet another form, for angles of incidence not far from the Bragg angle, on the assumption (Bragg 1940) that the diffuse spots are due to simple diffraction by very small groups of atoms.

For $NaNO_3$, $CaCO_3$ and NaCl, Raman and Nilakantan state that a symmetrical formula $2d \sin \frac{1}{2}(\theta+\phi) = \lambda$ (which implies that $\theta+\phi$ is independent of crystal orientation) suits the results of diffuse spot measurements better than the Faxén formula. In fact, however, neither the symmetrical nor the unsymmetrical formula is really satisfactory for any of the crystals examined, and Raman and Nath (1940*b*) have recently suggested a more general formula, $2d \sin\psi . \sin(I+\epsilon) = n\lambda \sin I$, where I, in terms of their theory, is the inclination of the 'phase-waves of the lattice vibration' to *the static crystal planes under consideration, 2ψ is the angle of deflexion* (that is, $\theta+\phi$ in the previous notation), and ϵ is the inclination of the 'static' to the 'dynamic stratifications'. If the plane of incidence (plane containing the incident beam and the normal to the undisturbed crystal plane) contains also the diffusely reflected beam, then $\epsilon = \frac{1}{2}(\phi-\theta)$ and the equation becomes

$$2d \sin \tfrac{1}{2}(\phi+\theta) \sin (I + \tfrac{1}{2}(\phi-\theta)) = n\lambda \sin I.$$

Taking $I = \frac{1}{2}\pi - \phi$, this formula reduces to Faxén's original formula $d \sin(\phi+\theta) = n\lambda \cos\phi$; $I = \frac{1}{2}\pi - \frac{1}{2}(\phi-\theta)$ gives the symmetrical formula $2d \sin \frac{1}{2}(\phi+\theta) = n\lambda$. Raman and Nilakantan (1941) suggest that for rock-salt $I = \frac{1}{2}\pi$ and for diamond $I = 55 \pm 1°$ (half the tetrahedral angle). These results will be examined more critically in a later section.

Measurements of the photographs taken in the course of the present study are too numerous to be given in detail. Certain general results may however be mentioned. One of the most noticeable features of diffuse spot photographs of organic crystals is that the diffuse spot tends to be displaced from the Bragg position *towards* the Laue spot corresponding to it. In other words, $\theta+\phi \gtreqless 2\theta_B$ according as $\theta \gtreqless \theta_B$. This may be seen on the three photographs of sorbic acid (plate 21 *a*, *b* and *c*) showing the displacements of the (604) Laue and diffuse spots as the crystal is rotated by 5° at a time. The diffuse spot positions in this case agree well with Faxén's formula. The photograph of benzil in plate 3*b*, where the crystal is set so that the incident beam makes an angle of about 7° with the hexagonal axis, shows that the layer line diffuse streaks, with the spots lying on them, are also displaced in the same sense. That the relationship between θ and ϕ cannot always be expressed in terms of a single formula over a wide range of values of θ, is shown by measurements on the set of diffuse spots illustrated in plates 13 and 14. In table 5 is given the value of the (002) spacing of urea nitrate (to which this set of diffuse spots corresponds) deduced from various modifications of the general formula, as follows:

TABLE 5

				calculated (002) spacing			
θ	$\theta+\phi$	ϕ	$\theta-\phi$	(1)	(2)	(3)	(4)
0°	27° 38′	27° 38′	−27° 38′	3·32	2·94	$3{\cdot}22_5$	3·13
4° 0′	27° 51′	23° 51′	−19° 51′	3·25	$3{\cdot}01_5$	3·20	3·15
5° 0′	27° 51′	22° 51′	−17° 51′	3·24	3·04	3·20	3·16
5° 56′	27° 51′	21° 55′	−15° 59′	3·23	$3{\cdot}05_5$	3·20	$3{\cdot}16_5$
7° 7′	27° 45′	20° 38′	−13° 31′	3·23	3·09	3·21	$3{\cdot}18_5$
8° 2′	28° 5′	20° 3′	−12° 1′	$3{\cdot}18_5$	3·07	3·17	$3{\cdot}15_5$
8° 55′	27° 58′	19° 3′	−10° 8′	$3{\cdot}19_5$	3·10	3·18	3·17
9° 58′	28° 5′	18° 7′	− 8° 9′	3·18	$3{\cdot}10_5$	3·17	3·16
11° 2′	28° 5′	17° 3′	− 6° 1′	$3{\cdot}17_5$	3·13	3·17	$3{\cdot}16_5$
12° 7′	28° 5′	15° 58′	− 3° 51′	$3{\cdot}17_5$	3·14	3·17	3·17
13° 7′	28° 12′	15° 5′	− 1° 58′	3·16	3·15	3·16	3·16
14° 6′	*28° 12′*	*14° 6′*	*0°*	*3·16*	*3·16*	*3·16*	*3·16*
14° 32′	28° 12′	13° 40′	0° 52′	3·16	3·17	3·16	3·16
15° 35′	28° 25′	12° 50′	2° 45′	$3{\cdot}13_5$	$3{\cdot}15_5$	$3{\cdot}13_5$	$3{\cdot}13_5$
16° 39′	28° 25′	11° 46′	4° 53′	3·14	$3{\cdot}16_5$	$3{\cdot}13_5$	$3{\cdot}13_5$
17° 41′	28° 32′	10° 51′	6° 50′	3·13	3·16	$3{\cdot}12_5$	3·12
18° 40′	28° 38′	9° 58′	8° 42′	$3{\cdot}12_5$	$3{\cdot}16_5$	$3{\cdot}11_5$	$3{\cdot}10_5$
19° 36′	28° 38′	9° 2′	10° 34′	3·13	3·17	$3{\cdot}11_5$	3·10
20° 36′	28° 38′	8° 2′	12° 34′	$3{\cdot}13_5$	3·18	$3{\cdot}11_5$	$3{\cdot}09_5$
21° 28′	28° 46′	7° 18′	14° 10′	$3{\cdot}12_5$	$3{\cdot}17_5$	3·10	$3{\cdot}07_5$
22° 39′	28° 51′	6° 12′	16° 27′	3·12	3·17	3·09	3·06
24° 30′	29° 4′	4° 34′	19° 56′	$3{\cdot}11_5$	3·16	3·07	3·02
26° 23′	29° 18′	2° 55′	23° 28′	$3{\cdot}10_5$	3·14	3·04	2·98
28° 27′	29° 25′	0° 58′	27° 29′	3·12	$3{\cdot}13_5$	3·03	2·94
30° 25′	29° 30′	−0° 55′	31° 20′	$3{\cdot}14_5$	3·13	3·03	2·92

(1) $I=\frac{1}{2}\pi$. $\quad d=\dfrac{\lambda}{2\sin\frac{1}{2}(\theta+\phi)\,.\cos\frac{1}{2}(\theta-\phi)}$.

(2) $I=\frac{1}{2}\pi-\phi$. $\quad d=\dfrac{\lambda\cos\phi}{\sin(\theta+\phi)}$ (Faxén's formula).

(3) $I=\frac{1}{2}\pi-\frac{1}{2}(\phi-\theta)$. $\quad d=\dfrac{\lambda}{2\sin\frac{1}{2}(\theta+\phi)}$
(Raman's symmetrical formula).

(4) $I=\frac{1}{2}\pi-\frac{1}{2}(\phi-\theta)$. $\quad d=\dfrac{\lambda\cos\frac{1}{2}(\theta-\phi)}{2\sin\frac{1}{2}(\theta+\phi)}$.

Other values of I have been tested, but these are sufficient to show the general trend of the results.

It will be seen that for values of θ from about $0° \rightarrow 15°$, (4) gives the best agreement, whereas for values of θ from $15° \rightarrow 30°$, (2) agrees best. No constant value of I can be found which gives good agreement over the whole range of θ. For a small range of angles near to the Bragg angle, 14° 6′, there is little to choose between all the values tested.

One factor that makes measurements a little uncertain is the difficulty of determining the exact position of the origin on oblique Laue photographs, since the undeflected beam cannot usually be allowed to mark the film for fear of fogging. This point will be referred to later.

Direction of diffuse scattering relative to plane of incidence

In some previous work it has been assumed or asserted that the diffusely scattered beam lies in the plane of incidence; in other words, that the incident beam, the diffusely scattered characteristic beam and the corresponding selectively reflected 'white' beam are coplanar. This is not always the case, but as deviations are only observable when the Laue and diffuse spots are well separated, measurements are most difficult to make.

On plate 28 *a* and *b* it is quite clear that the streak extending from the central spot to the ($h00$) Laue spot is a curved one, and that the diffuse spots corresponding to the 2nd, 4th, 6th and 8th order reflexions lie on this curve, and not on the straight line joining the Laue spot to the trace of the undeviated incident beam. This curve apparently corresponds to the direction along which the Laue spot moves as the crystal is rotated about a [$\bar{1}10$] vertical axis, as may clearly be seen on successive photographs taken at 5° intervals (plates 26, 27 and 28 give a selection of these). It appears to be, in fact, one of the 'α constant curves, given in Chart III of Bernal's paper (1926) on 'The interpretation of X-ray, single crystal, rotation photographs', which may be seen traced out by the white radiation streaks on rotation photographs taken with an X-ray beam containing a considerable amount of continuous radiation (cf. plates 5*b*, 6*b* and 20*b*).

When the X-rays are normal to a (001) face, [$\bar{1}10$] axis vertical (as in plate 26*a*) the ($h00$) planes are parallel to the incident beam and the corresponding plane of incidence (plane containing the incident beam and the [100] axis) is inclined at 45° to the vertical. The diffuse spots corresponding to the (200) (400) Bragg reflexions then lie exactly along 45° diagonals on the X-ray film. As the crystal rotates through an angle ω, the inclination of the plane of incidence to the vertical decreases to ψ', where

$$\sin(45^\circ - \psi') = \sin^2 \tfrac{1}{2}\omega/\sqrt{(1 - \tfrac{1}{2}\sin^2 \omega)}.$$

This change of inclination is very slow at first ($\omega = 30^\circ$ gives $45^\circ - \psi' = 4^\circ{\cdot}1$; $\omega = 35^\circ$ gives $5^\circ{\cdot}7$). The angle of incidence θ after a rotation ω is given by $\sin\theta = \frac{1}{\sqrt{2}}\sin\omega$ and hence the positions of the ($h00$) Laue spot and the corresponding value or values of λ may be calculated for any value of ω, by means of the relations $r = D\tan 2\theta$, $\psi = \psi'$, $n\lambda = 2d\sin\theta$, where r, ψ are the angular co-ordinates of the Laue spot on a plane film at distance D from the crystal, relative to the central spot and vertical axis. The fact that the values of ψ corresponding to the *diffuse* spots for any particular value of ω are not the same as that of the Laue spot, but lie between ψ' and 45° must mean that, as the crystal rotates, the diffuse spot moves nearly in the small arc of a circle, since the total angle of scattering $(\theta + \phi)$ remains approximately constant. This small circular movement is, however, *less* than it would be if the diffuse reflexion remained always in the plane of incidence.

The movement is very apparent in the case of the diffuse spots corresponding to ($\bar{1}10$), the horizontal plane. When $\omega = 0$ or 90°, these diffuse reflexions lie just above and below the central disk in the vertical plane of incidence. As ω increases from 0° to 45°, the diffuse spots move out of the vertical plane, the displacement being clearly seen in plates 27 and 28. A similar displacement is seen on plate 7 in the case of the (200) and (400) diffuse spots corresponding to the (100) horizontal plane. In neither case, however, is there any question of a tilting of the plane of incidence, which remains always vertical.

That the diffuse spots do not always lie on the 'α constant' curves is at once apparent from a consideration of such Laue spots as ($\bar{2}21$) and the corresponding ($\bar{4}42$) diffuse spot. The ($\bar{2}21$) plane of incidence is initially vertical, but as ω increases, its inclination ψ to the vertical increases from 0° to a maximum value of $19^\circ{\cdot}5$. For very small values of ω, however, ψ is also small and the α constant curve is nearly horizontal. The ($\bar{4}42$) diffuse spot is initially in the plane of incidence, $(\theta + \phi)$ being considerably less than 2θ, and it appears to move with and remain in the plane of incidence as the Laue spot traverses the α constant curve. When $\omega = 60^\circ$ it is still just observable, $(\theta + \phi) \gg 2\theta$. In this case the values of ψ are apparently the same for both Laue and corresponding diffuse spots. That discrepancies in ψ do frequently occur (even when exact measurements would be very difficult to make) is apparent from the fact that early attempts to locate the true centre of the Laue photograph by finding the point of intersection of straight lines drawn through corresponding Laue and diffuse spots seemed, in many cases of oblique setting, to be almost impossible, because such lines had no common point of intersection.

Future measurements on any series of diffuse spots should give not only r but also ψ, preferably for various initial orientations of the plane of incidence, as well as for different angles of mis-setting. The fact that the $(\bar{2}20)$ diffuse spots, for instance, move out of the vertical plane of incidence as the crystal setting (plates 27 and 28) becomes more oblique, indicates that the 'modified plane' responsible for these diffuse spots *moves with the crystal*, that is, that its direction bears a fairly definite relation to the crystal framework. This important result would be entirely overlooked in measurements giving only the angles of incidence and total deflexion.

REPRESENTATION OF RESULTS IN RECIPROCAL SPACE

Most of the workers in this field have expressed their results, whether experimental or theoretical, in terms of reciprocal space. The convenience of this must be apparent when the similarity of diffuse spot and oscillation photographs is considered, since the interpretation of oscillation and rotation photographs is greatly facilitated by the use of reciprocal lattice methods (Bernal 1926). According to the usual theory, selective (Bragg) reflexion takes place, during the oscillation or rotation of the crystal, just as each reciprocal lattice point P coincides with the sphere of reflexion (figure 3). The Bragg condition $\lambda = 2d \sin \theta_B$ is then fulfilled.

When the positions of the diffuse reflexions are plotted in reciprocal space, it is found that the strongest of these reflexions correspond to points which are not far from strongly reflecting reciprocal lattice points. As the angle of mis-setting $(\theta - \theta_B)$ increases, the point of diffuse reflexion moves away from its corresponding reciprocal lattice point, and the reflexion decreases in intensity.

The general formula which was given by Raman and Nath (putting $n = 1$ for simplicity),

$$2d \sin \psi \sin (I + \epsilon) = \lambda \sin I, \qquad \text{(i)}$$

is readily deduced from a reciprocal lattice diagram, ψ, I and ϵ being definite angles in reciprocal space (figure 4). O is the reciprocal lattice origin, P a reciprocal lattice point (corresponding to an infinite set of crystal planes of spacing d), CO the direction of the incident beam, CD that of the diffusely reflected beam ($CO = CD = 1/\lambda$), D being the point of diffuse reflexion. D, which lies on the sphere of reflexion, is not necessarily in the plane COP. If CN is the perpendicular from C to OP, the angle OCN is θ, the angle of incidence. The angle OCD is 2ψ, the angle of total deflexion. Then in the triangle OCD,

$$OD = \frac{2\sin\psi}{\lambda}.$$

In the triangle OPD,
$$OD = \frac{\frac{1}{d}\sin I}{\sin(\pi - (I+\epsilon))}.$$

Hence
$$\frac{2}{\lambda}\sin\psi = \frac{\sin I}{d\sin(I+\epsilon)},$$

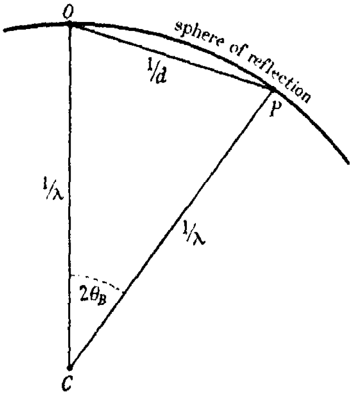

FIGURE 3

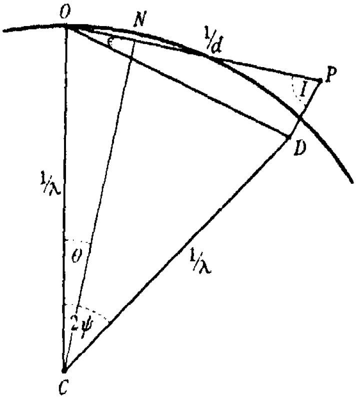

FIGURE 4

where I is defined as the angle OPD, and ϵ as the angle POD. These two angles are sufficient to determine D uniquely. It may easily be proved also that

$$\cos\epsilon = \sin\theta\sin\psi + \cos\theta\cos\psi\cos\delta, \qquad \text{(ii)}$$

where δ is the (measurable) angle between the plane of incidence COP and the plane of diffuse reflexion COD. If $\delta = 0$,

$$\epsilon = \psi - \theta = \tfrac{1}{2}(\phi - \theta).$$

It should be clearly recognized that the general formula (i), proved above, is *a purely geometrical relationship in reciprocal space*, connecting

O, C, P and D. It involves no other assumptions than that P is a point distant $1/d$ from O, and that O and D lie on the sphere, radius $1/\lambda$, whose centre is C. *It is quite independent of the particular physical interpretation given to the point D, or to the angles ψ, I or ϵ.* Any theory which involves the existence of a cloud of diffusely reflecting points around each or any reciprocal lattice point will give the diffuse spot positions in terms of this general formula. Such diffusely reflecting points may result from the existence of harmonic vibrations in the crystal (either due to thermal motions as in the Faxén-Waller theory, or to quantum excitation as in the Raman theory), or from the limiting of the crystal size so that the sets of crystal planes are not of infinite extent (Laue and Riewe 1936; Preston 1939; Ewald 1940; Bragg 1940; Jauncey 1941). It seems probable that measurements of diffuse spot positions alone will not give material for a decisive choice to be made between the different theories put forward, unless one theory can be shown to account, correctly and uniquely, for the variations in position over a wide range of substances, crystal orientations and crystal planes.

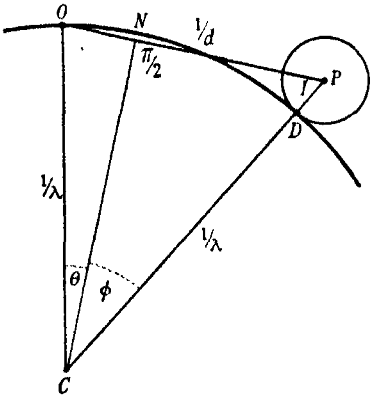

FIGURE 5

It would be simplest to assume, as Preston does, that there is a *spherical* distribution of the diffusely reflecting points around each reciprocal lattice point P, and that diffuse reflexion reaches its maximum intensity when D lies on the straight line CP (cf. Zachariasen 1940), or in other words, when CO and CDP are coplanar and $I = \frac{1}{2}\pi - \phi$ (figure 5). In that case

$$d \sin(\theta + \phi) = \lambda \cos \phi.$$

The experimental results, however, show that although this formula applies in certain cases, yet in general, and over a wide range of values of θ, it does not apply. In particular, it does not hold for KCl, which may reasonably be taken as a simple cubic crystal. On the other hand, even preliminary measurements can usefully indicate the general distribution of diffuse scattering power in reciprocal space.

In figures 6 and 7 are shown the observed diffuse reflexions from KCl of Mo and Ag radiations respectively, plotted on reciprocal lattice nets, the data being obtained from the zero layer lines of Laue photographs taken with a [001] axis vertical, for which the angle of incidence to a cube face was varied by small angular intervals over the whole range of 360°. Allowance being made for inaccuracies of measurement (due chiefly to uncertainty as to the exact position of the origin on successive photographs), it is clear that the points of diffuse reflexion tend to congregate in the neighbourhood of reciprocal lattice axes, being most dense near to reciprocal lattice points. Only certain axes are favoured, however; no diffuse

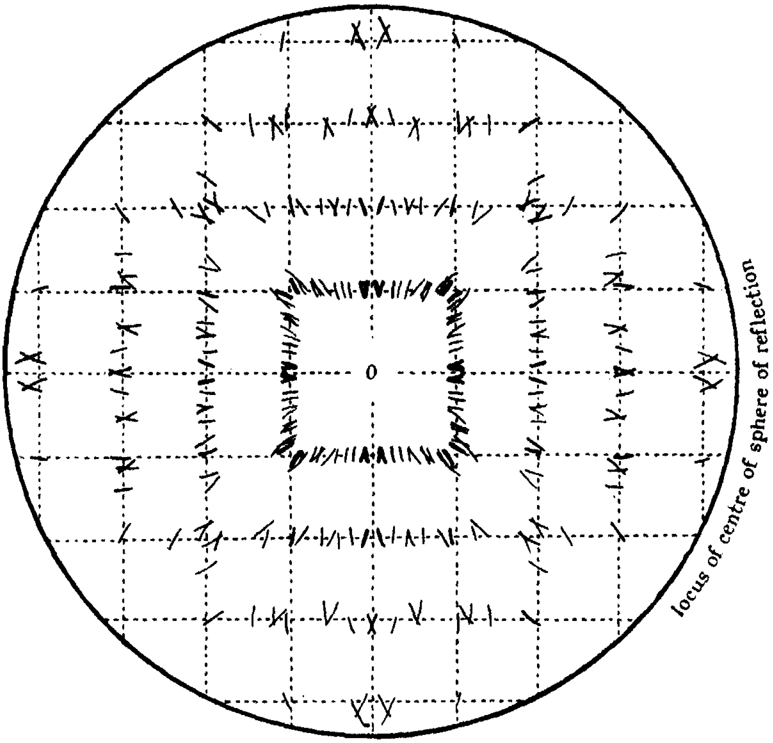

FIGURE 6. KCl; Mo $K\alpha$; reciprocal net showing positions of diffuse spots on central layer line of Laue photographs taken with cube axis of crystal vertical. Each spot is shown as an arc of the appropriate sphere of reflection.

reflexion takes place at points in reciprocal space which would correspond to a considerable variation in *spacing* of real crystal planes.

These results are confirmed by a study of diffuse reflexions not in the zero layer line and also of those on Laue photographs taken with the [110] axis vertical (figure 8). In particular, the movements of the plane of deflexion relative to the plane of incidence are significant, in that the effect in reciprocal space of non-coincidence of these planes is always such as to bring the point of diffuse reflexion nearer to a reciprocal lattice axis. The existence of the faint diffuse streaks connecting strong diffuse spots is also interesting in this connexion, because such streaks, plotted in reciprocal space, are found always to correspond to reflexion along or near to reciprocal lattice axes. Diffuse *radial* streaks would correspond to reciprocal lattice axes passing through the origin O, that is, to large variations of crystal spacing in real space. As our monochromatic photographs

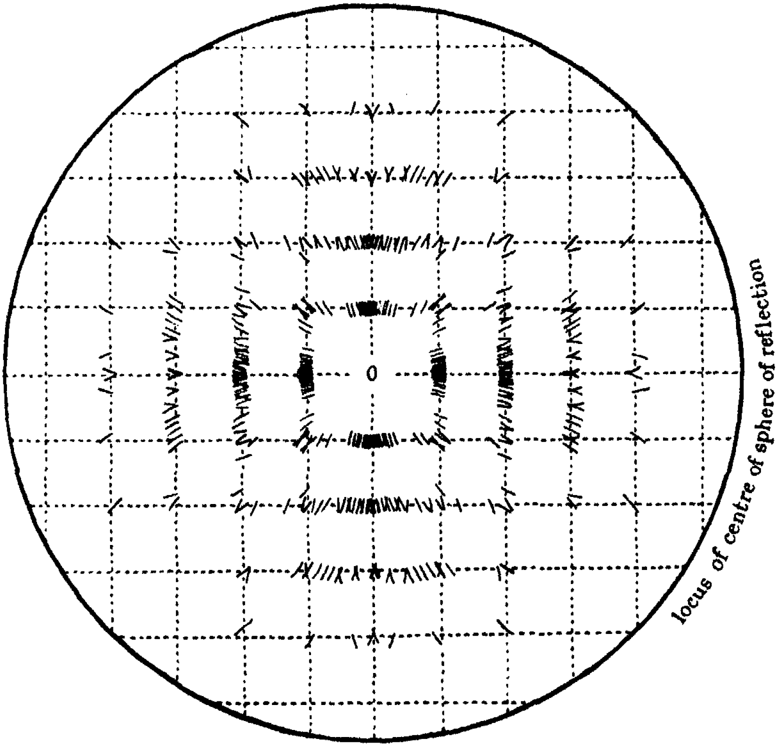

FIGURE 7. KCl; Ag $K\alpha$; reciprocal net showing positions of diffuse spots on central layer line of Laue photographs taken with cube axis of crystal vertical.

showed, such streaks do not, in general, occur. Indeed, even the marked preference of the diffusely reflecting points for the neighbourhood of reciprocal lattice axes appears to be modified by a tendency to avoid much variation of crystal spacing.

This is also apparent in Raman and Nilakantan's measurements on rocksalt. These workers have suggested that $I = \frac{1}{2}\pi$ gives quite good agreement with their data. This is approximately the case, at least for diffuse spots corresponding to the (400) plane, but in fact $I = \frac{1}{2}\pi - \epsilon$ gives much better agreement with their data for (200) and (220), while $I = \frac{1}{2}\pi - \frac{1}{2}\epsilon$ gives the best agreement for (400). In each case the effect is to reduce the change of spacing that would otherwise be involved.*

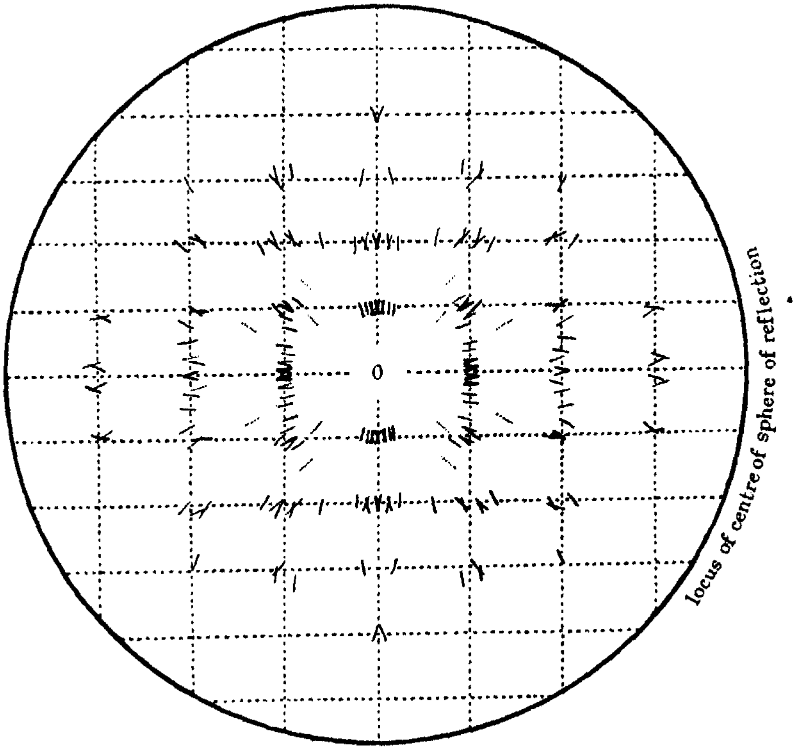

FIGURE 8. KCl; Ag $K\alpha$; reciprocal net showing positions of diffuse spots on contra layer line of Laue photographs taken with [110] axis of crystal vertical.

The fact that the diffuse streaks in the (0001) Laue photographs of benzil are in the positions of layer lines in rotation photographs, that is,

---

[*] There is, in general, however, a *small* change of spacing, as is shown both by their own data, and by the more recent investigation of Jauncey and Baltzer (1940).

that they correspond to the main crystal *periodicities*, means that in reciprocal space these streaks are given by unusually strong diffuse reflexion from reciprocal lattice planes or axes which happen to be roughly tangential to the sphere of reflexion in that particular crystal orientation. Similar considerations apply to the fragmentary streaks and patches of diffuse scattering found in other orientations. This is easily verified by plotting their positions on the appropriate reciprocal lattice nets.

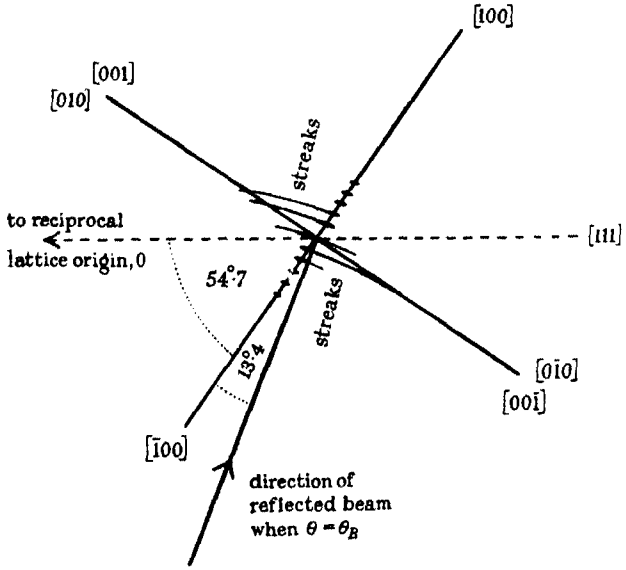

FIGURE 9. [010], [001] are at ±45° to plane of [100] and [111].

The diffuse reflexions of Cu radiation from diamond $\{111\}$ planes are most interesting in this connexion. Raman and Nilakantan (1941) found that although the Faxén formula fitted their measurements (on diffuse spots similar to those shown in plate 24*a*) fairly well, an even better agreement resulted from the substitution of $I = 54^\circ\cdot 7$ in the general formula. This result, which agrees with our own measurements on spots of this type, shows that for diamond also the points of diffuse reflexion lie mainly along reciprocal lattice axes, in this case along [100] directions. The same result is obtained very quickly by plotting the experimental data on a reciprocal lattice net. It is found, moreover, that the diffuse streaks observed on Laue photographs where the (111) diffuse spot is very near to its Laue spot, correspond to diffuse reflexion along [010] and [001] directions in reciprocal space which are nearly tangential to the sphere of reflexion (figure 9).

When, however, the direction of the incident beam is such that the diffusely reflected beam is almost equally inclined to the [100], [010] and [001] directions in reciprocal space (figure 10), a triangular group of three diffuse spots results (plate 24*b* and 25 *a* and *b*). Two of the spots in each group form striking examples of non-coincidence of the planes of incidence and deflexion. The maximum observed value of δ was 11°·8. All three spots in each group are relatively sharp (showing that the diffusely reflecting regions in reciprocal space are confined closely to the neighbourhood of the [100], [010] and [001] directions, figure 11), *especially* when the angle of incidence differs considerably from the Bragg angle (plate 25*b*). In contrast to this, the diffuse centre of the triangle, which fairly closely obeys Faxén's formula, becomes relatively much weaker and more diffuse as the Laue and diffuse spots separate, that is, as the angle of mis-setting increases.

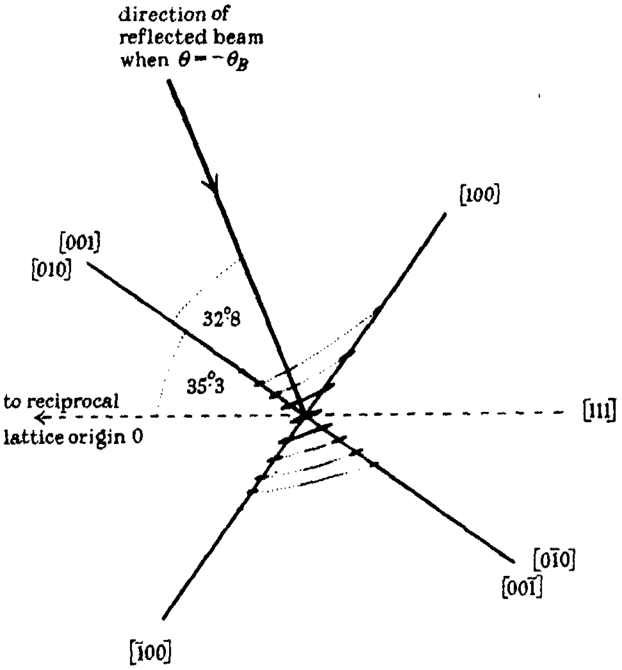
direction of reflected beam when $\theta = -\theta_B$
[100]
[001]
[010]
32°8
35°3
to reciprocal lattice origin 0
[111]
[0$\bar{1}$0]
[00$\bar{1}$]
[$\bar{1}$00]

FIGURE 10. [010], [001] are at 45° to plane of [100] and [111].

When Mo radiation is used instead of Cu, the scale of the reciprocal net is considerably reduced relative to the sphere of reflexion. More diffuse reflexions are observed, but any structure that these might possess is swallowed up within the inevitable size of the spots themselves (due to the width of the X-ray beam and the size of the crystal).

A more detailed account of the measurements of the diamond diffuse spots and of their significance will be given in a subsequent publication.

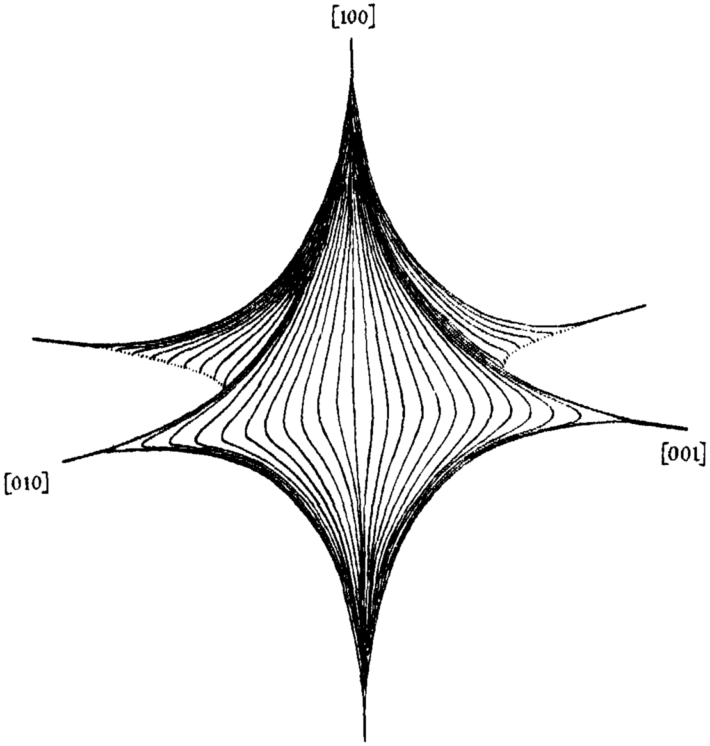

FIGURE 11. Approximate distribution of diffuse reflecting power about (111) reciprocal lattice point of diamond.

It is perhaps worth mentioning, however, that in terms of *any* wave theory, the fact that diffusely reflecting regions in reciprocal space are confined to, or extended along, certain directions implies that in real space the atoms or molecules tend to remain strictly in phase with each other along those directions; whereas in the 'finite crystal' theory the intensity spikes are normal to the boundary planes (Laue and Riewe 1936).

CONCLUSION

The main facts that emerge from this study may be summed up as follows.

1. The diffuse spots sometimes found on Laue photographs lie very nearly or sometimes exactly in the positions of Bragg reflexions from crystal planes which are not necessarily, however, quite at their proper reflecting angle. The indices of the corresponding Bragg reflexion can be found by treating the diffuse spot picture as though it were an oscillation photograph taken about the Laue position as centre of oscillation. This is a general fact applying to inorganic and organic crystals of any system, and to all wave-lengths of X-radiation used.

2. Conversely, a diffuse spot picture will only be found under conditions in which Bragg spots would be obtained on an oscillation photograph if the crystal, instead of being held stationary, were allowed to oscillate through a small angle about any direction normal to the incident beam. This involves relationships between wave-length, crystal structure and orientation, size and distance of photographic film, which are readily determined.

3. Such diffuse spot patterns may not only be seen on Laue photographs, where the diffuse spot and its corresponding Laue spot are, in general, well separated, but also on oscillation, rotation, Weissenberg and powder photographs, where the diffuse spots form a background to the selective Bragg reflexions. They may also, of course, be observed and measured by ionization spectrometer methods.

4. In general, a much longer exposure is necessary in order to produce the diffuse background picture than to obtain a normally satisfactory Laue or rotation photograph.

5. That the diffuse spots are due to diffraction of *characteristic* X-rays may be proved by using a monochromatized beam (Laval 1939; Preston 1939).

6. The diffuse halo surrounding the central spot on ordinary Laue or rotation photographs does not appear on monochromatic Laue photographs, even when the diffuse spot pattern on the latter is stronger than that on the former, showing the exposure to be more than equivalent.

7. The radial streaks on ordinary Laue photographs are almost always due to diffuse reflexion of *white* radiation. The radial streaks on oscillation or rotation photographs are due to selective reflexion of white radiation, but must also have a diffuse background.

8. Monochromatic Laue photographs sometimes show non-radial diffuse streaks, some well defined and some fragmentary; also triangular patches

of diffuse scattering and other anomalies which have, as yet, received no theoretical attention.

9. The *diffuse spot pattern is not apparently affected by the condition of the crystal surface or by crystal imperfection*, except that sometimes diffuse spots show an *intense and sharply defined core* which may be due to distortion, as it is only found for cleaved or fractured crystals.

10. The intensity of a diffuse spot is related to the absolute intensity of the corresponding Bragg reflexion; it depends also very markedly on the angle of incidence θ (angle between the incident beam and the set of planes giving the corresponding Bragg reflexion), reaching a maximum when $\theta = \theta_B$.

11. A most important factor affecting intensity is the crystal temperature. At elevated temperatures (experiments extend up to 500° C) some diffuse spots increase enormously both in intensity and in size (Laval 1939, and others), and non-radial streaks appear which were not previously visible (Preston 1939). Other diffuse spots, however, are not so strongly affected. Planes which show a big increase in diffuse spot intensity show a corresponding decrease in the Laue or Bragg spot intensity. Conversely, at liquid air temperatures the diffuse spot pattern almost completely disappears, the Laue spots become more profuse and the general background clearer. These effects are reversible.

12. The shapes and sizes of the diffuse spots vary considerably. Very frequently they are not circular or even elliptical. They are more closely *related to the shape of the corresponding Bragg spots than to those of the Laue spots.* They are definitely and obviously related to the structure and nature of the crystal planes to which they correspond. 'Layer' planes and planes perpendicular to 'chain' directions give rise to diffuse spots which are very different in several respects. This indicates that diffuse spot patterns may give valuable subsidiary help in structure determination, and also points to a relation between the physical properties of a set of crystal planes and the character of the corresponding diffuse reflexion.

13. The shapes of the diffuse spots from diamond $\{111\}$ planes, using Cu radiation, are different from those of any other substance yet examined, and provide valuable data for theoretical investigation.

14. The diffuse spots, although occurring nearly in the positions where the corresponding Bragg spots would be, may deviate from those positions by small amounts. The total angle of deflexion may be slightly more or less than twice the Bragg angle, and the plane of diffuse scattering may be inclined at a small angle to the 'plane of incidence'.

15. These facts may be visualized most easily by considering the rela-

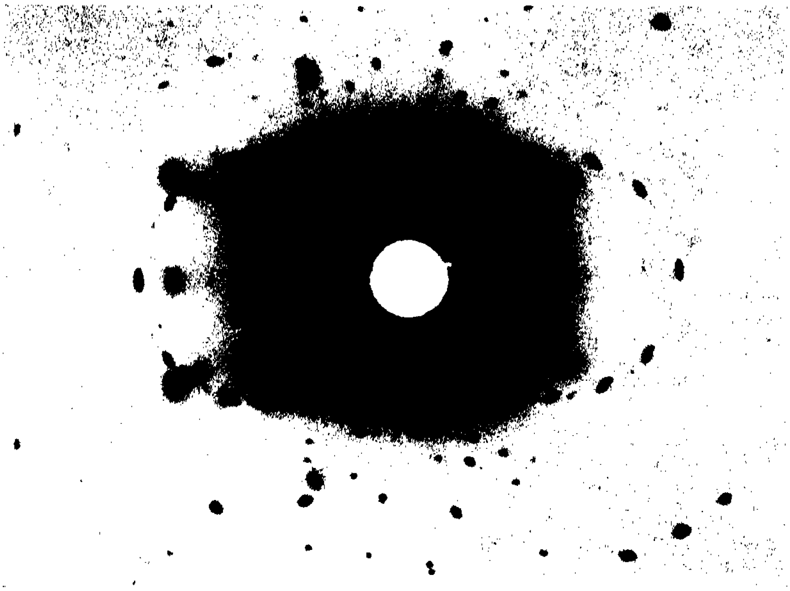

(*a*)

α-Resorcinol: [001] vertical: 4 cm.; unfiltered Cu radiation at 21°·3 to [010]. Note arrangement of diffuse spots in layer lines, and intense central halo.

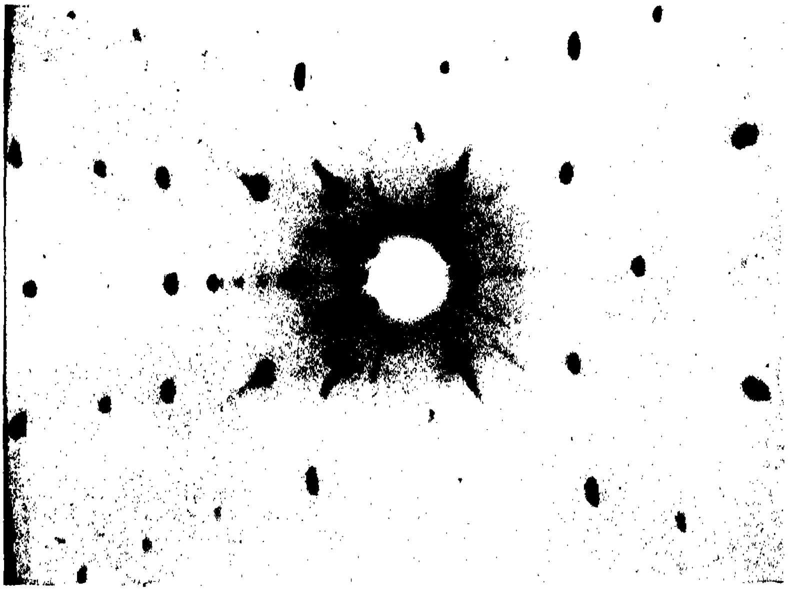

(*b*)

α-Resorcinol: filtered Cu radiation: oscillation 7°·5 each side of Laue position given above. 2 min. exposure, cf. 20 min. Laue exposure.

(*Facing p.* 48)

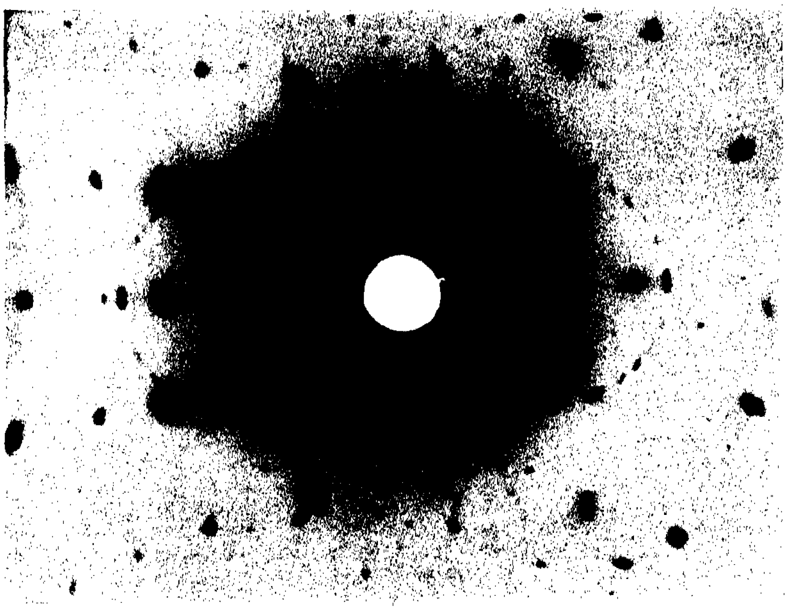

(*a*)

α-Resorcinol: filtered Cu radiation; position as in plate 1 *a* and *b*. Oscillation (2 min.) superposed on Laue (20 min.) photograph.

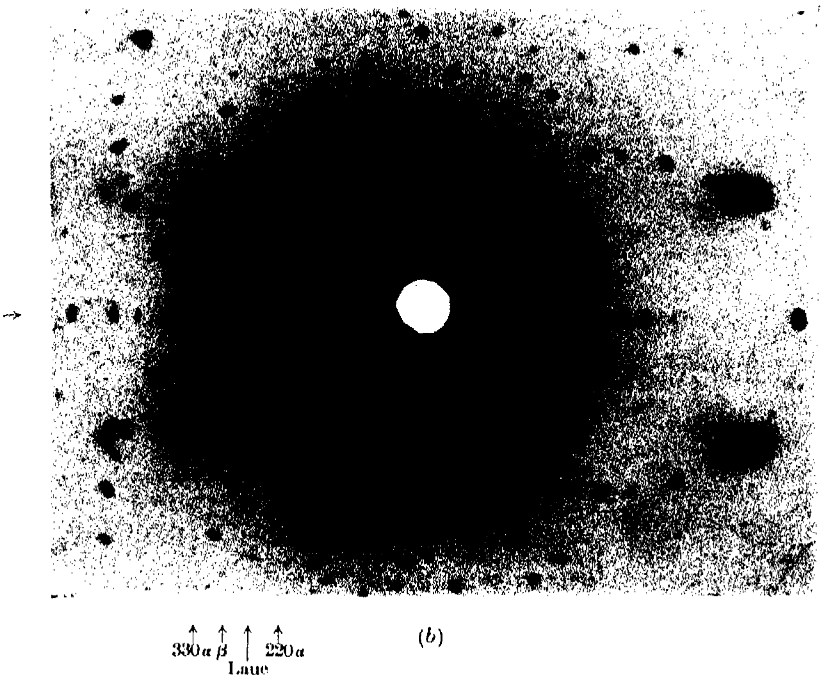

(*b*)

α-Resorcinol: {001} vertical: 4 cm.; unfiltered Cu radiation at 25°·9 to [010]. Note relative intensity, size, shape of 220α, 330α and β diffuse spots on either side of *hh*0 Laue spot.

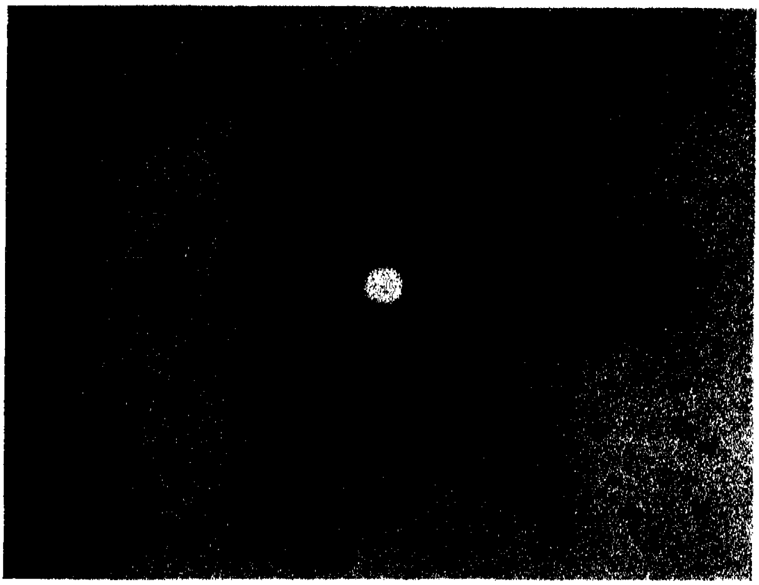

(*a*)

Benzil: [11$\bar{2}$0] vertical: 4 cm.: unfiltered Cu radiation along [0001]; 10 min. exposure. Note alternating hexagonal symmetry of both Laue and diffuse patterns (cf. figure 1).

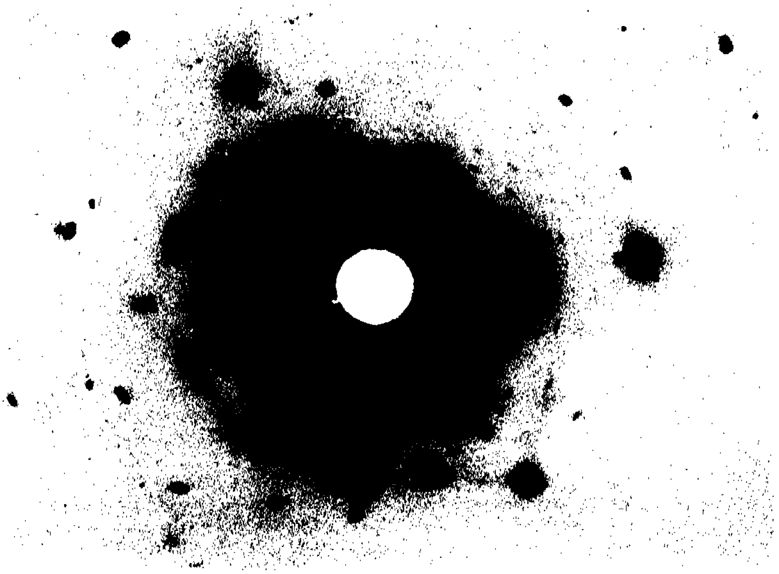

(*b*)

Benzil: filtered Cu radiation at about 7° from [0001]. Note loss of symmetry of Laue pattern, although diffuse pattern still shows approximate hexagonal alternating symmetry.

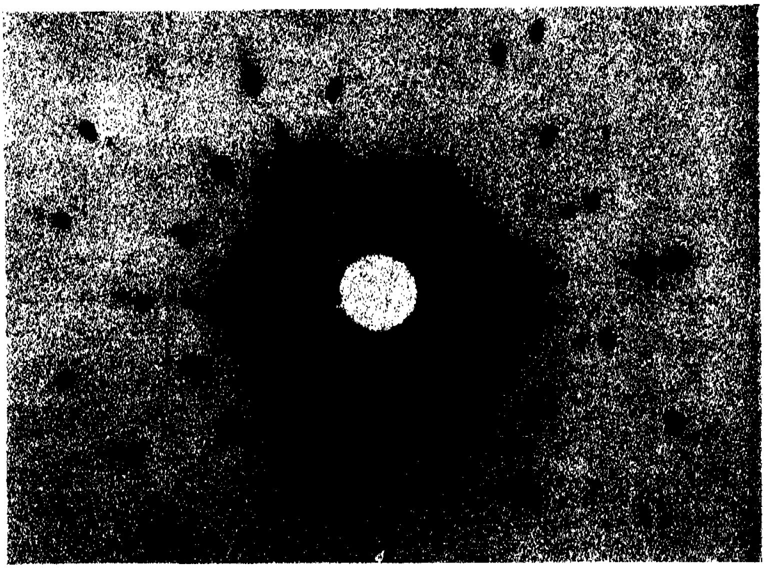

(*a*)

Benzil: 4 cm.; filtered Cu radiation: oscillation 7°·5 on each side of Laue position in plate 3*b*; 1 min. exposure. Note weak background pattern.

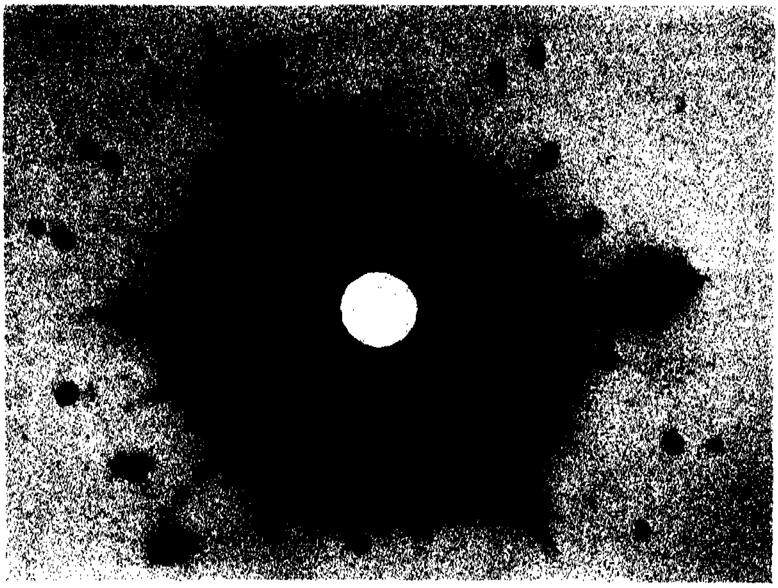

(*b*)

Benzil: same as (*a*), but exposure 10 min. Note strong background pattern and intense radial streaks.

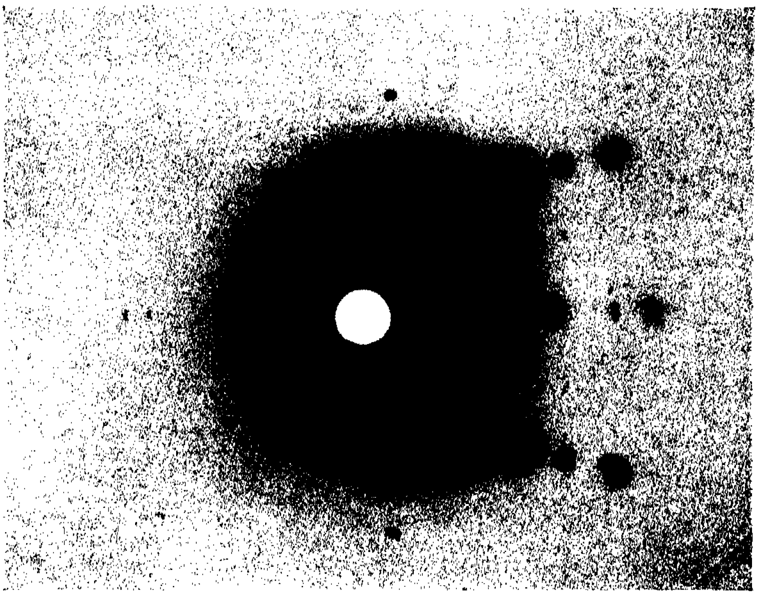

(*a*)

Sorbic acid: [010] vertical: 4 cm.; filtered Cu radiation at 70°·6 to [001] in obtuse β. Note arrangement of diffuse spots in layer lines and compare 5*b*.

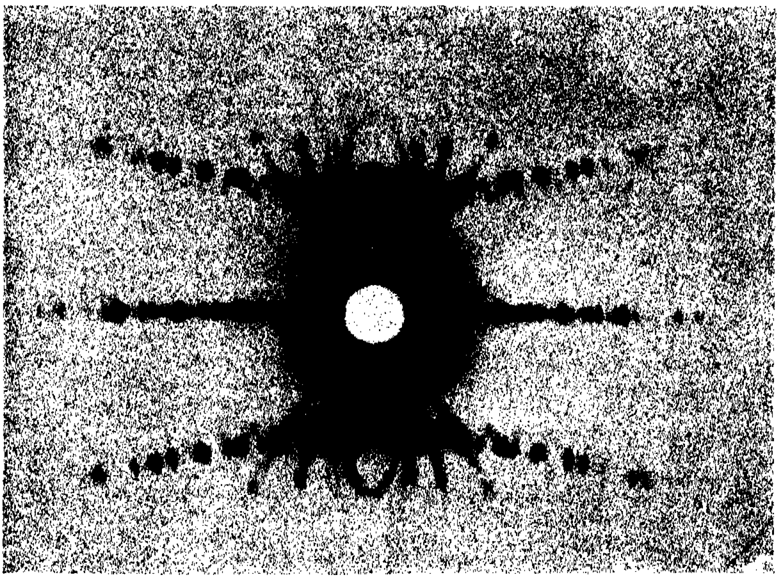

(*b*)

Sorbic acid: [010] vertical: 4 cm.; rotation using unfiltered Cu radiation. Shows layer lines corresponding to 4·03 A periodicity, and also strong 'α constant' curves due to white radiation.

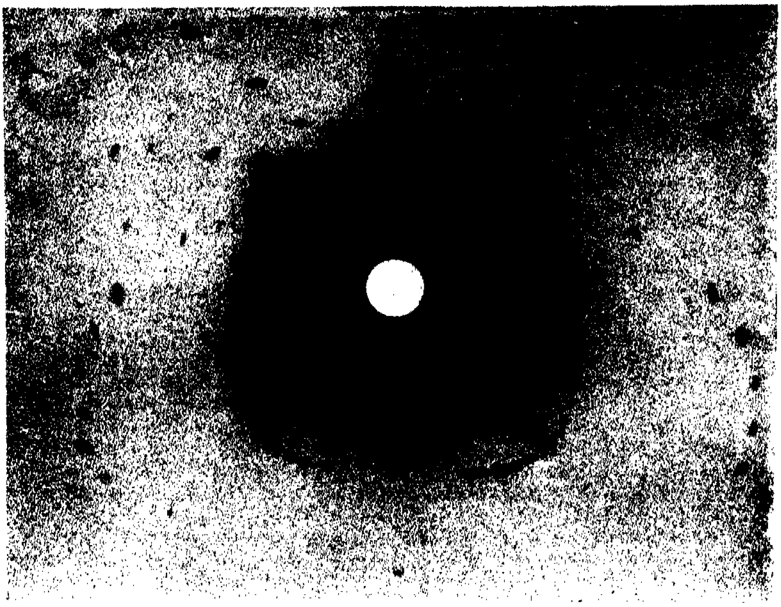

(*a*)

Sorbic acid: [001] vertical: 4 cm.; unfiltered Cu radiation nearly along [110]. Shows strong diffuse spots corresponding with strong spots on rotation photograph below.

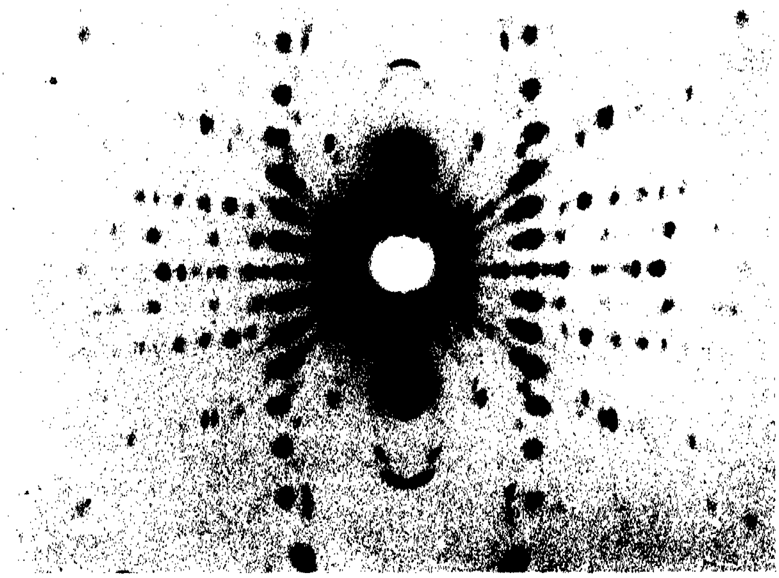

(*b*)

Sorbic acid: [001] vertical: 4 cm.; rotation using unfiltered Cu radiation: 1 min. exposure. Layer lines close together corresponding to 15·83 A periodicity. Note strong spots on (11*l*) row line, and compare with 6*a*.

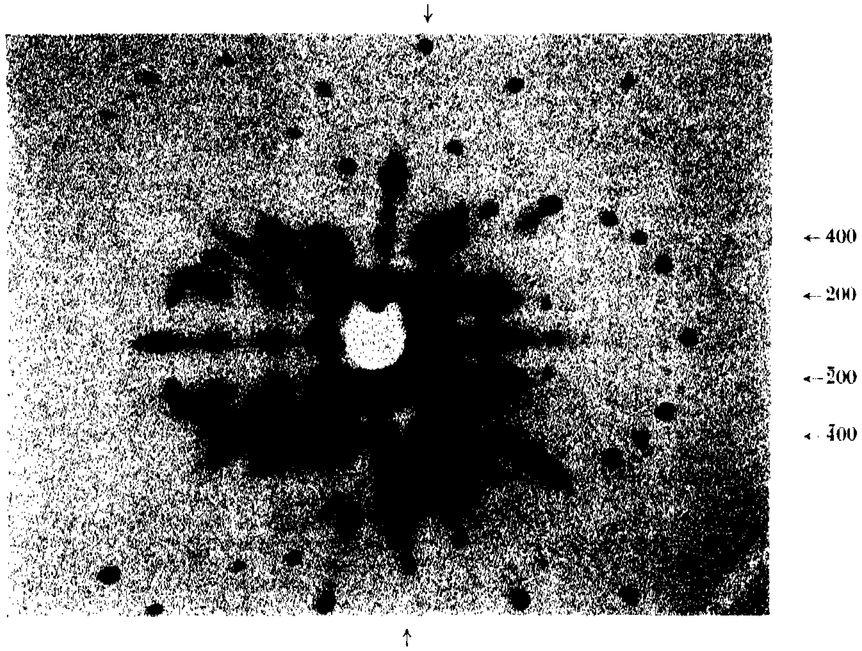

(*a*)

Sylvine: [100] vertical: ~3·5 cm.; unfiltered Ag radiation at 20° at [010] axis. Note displacement of diffuse 200, 400 spots out of vertical plane of incidence.

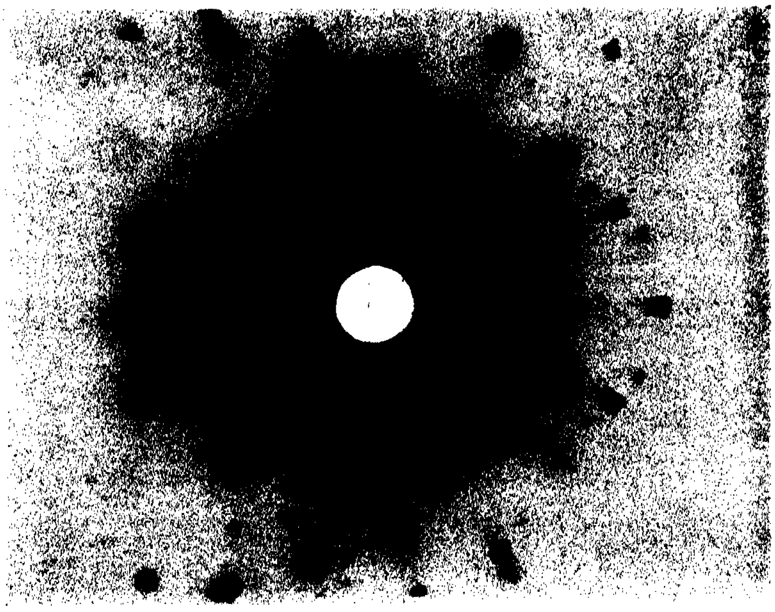

(*b*)

Sylvine: [100] vertical: ~3·5 cm.; unfiltered Mo radiation at 20° to [010] axis. Note that while the Laue pattern is relatively unaltered, the diffuse pattern has expanded compared with that due to Ag radiation.

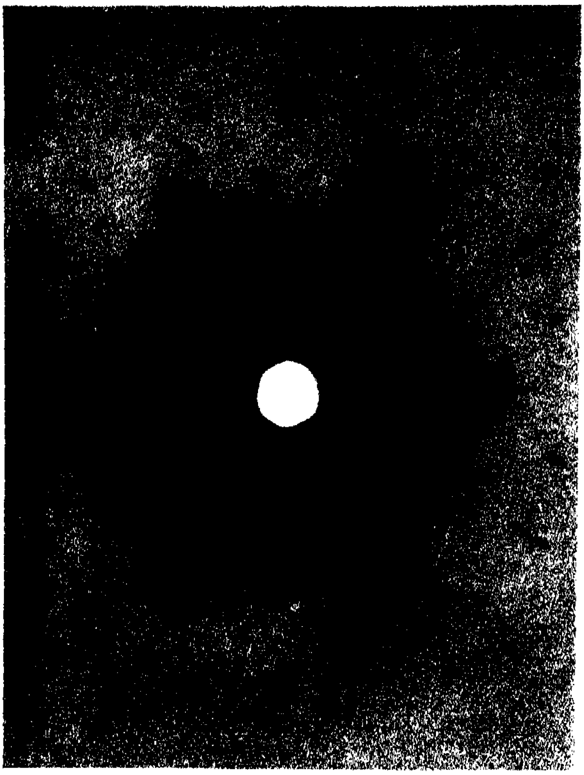

(*a*)

Benzil: [1120] vertical: 3·5 cm.; unfiltered Cu radiation along [0001]; 10 min. exposure. Note background diffuse pattern, especially near central spot.

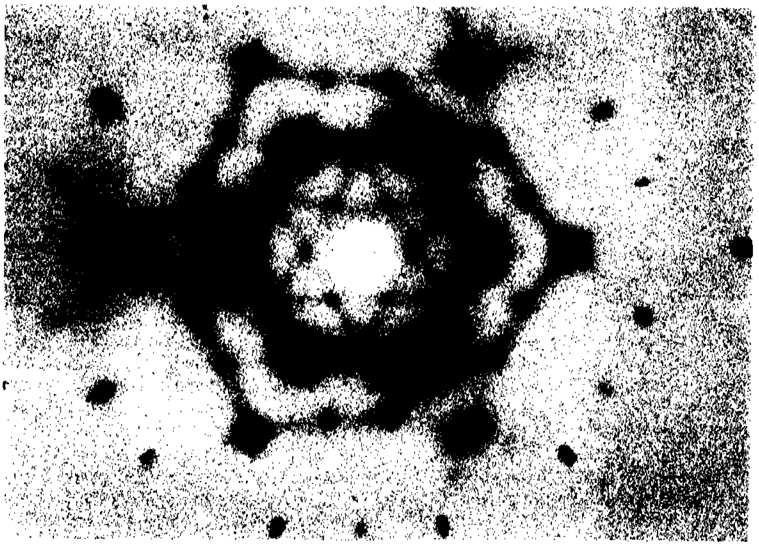

(*b*)

Benzil: [1120] vertical: 3·5 cm.; monochromatized Cu *Kα* radiation very nearly along [0001]; 2 hr. exposure. Note disappearance of radial streaks near to central spot and general cleanness of background in that region. Non-radial streaks correspond to [1120] and [40$\bar{4}$0] periodicities.

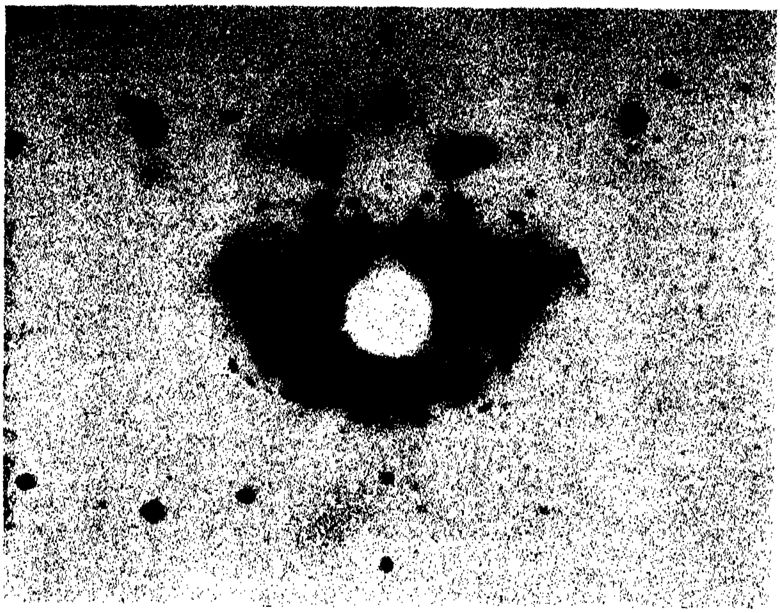

(*a*)

Benzil: [0001] vertical: 3·5 cm.; filtered Cu radiation along [1010]; 10 min. exposure.

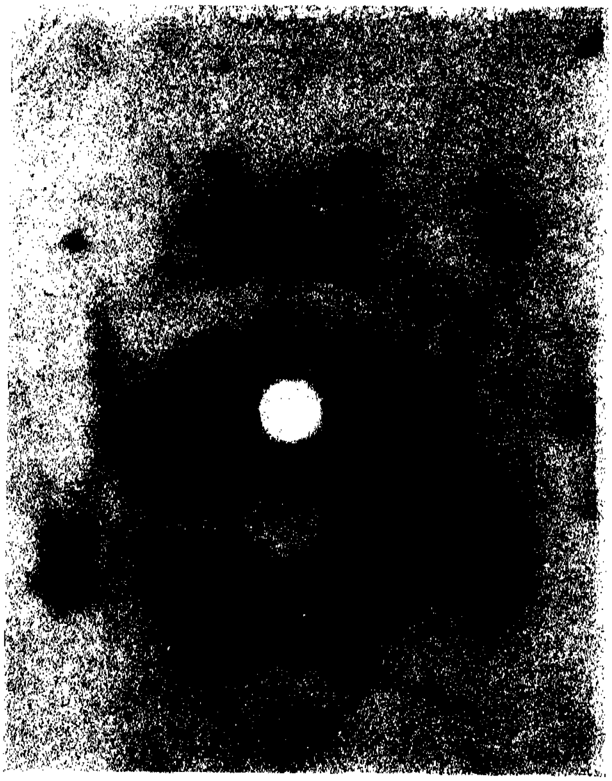

(*b*)

Benzil: [0001] vertical: 3·5 cm.; monochromatized Cu $K\alpha$ radiation along $[10\bar{1}0]$: 1 hr. exposure. Note patches of diffuse radiation and partial streaks.

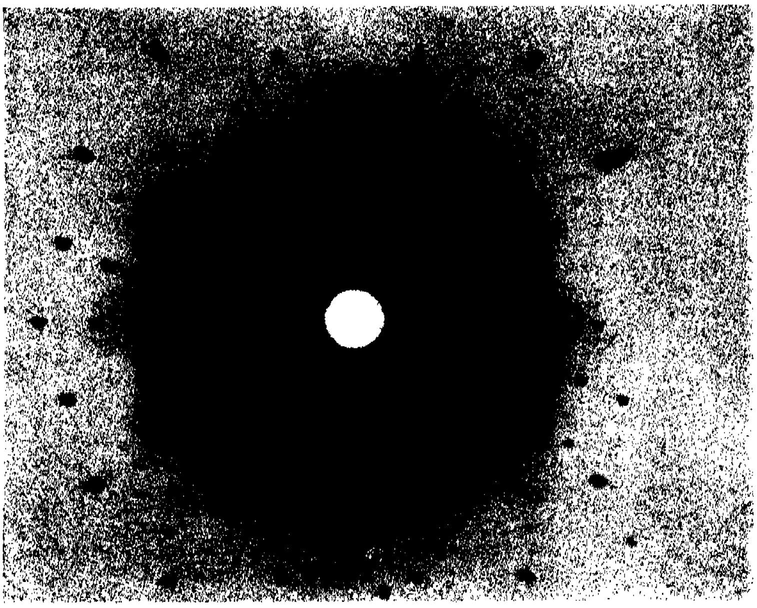

(*a*)

Benzil: [0001] vertical: 3·5 cm.; unfiltered Cu radiation along [1120]; 10 min. exposure.

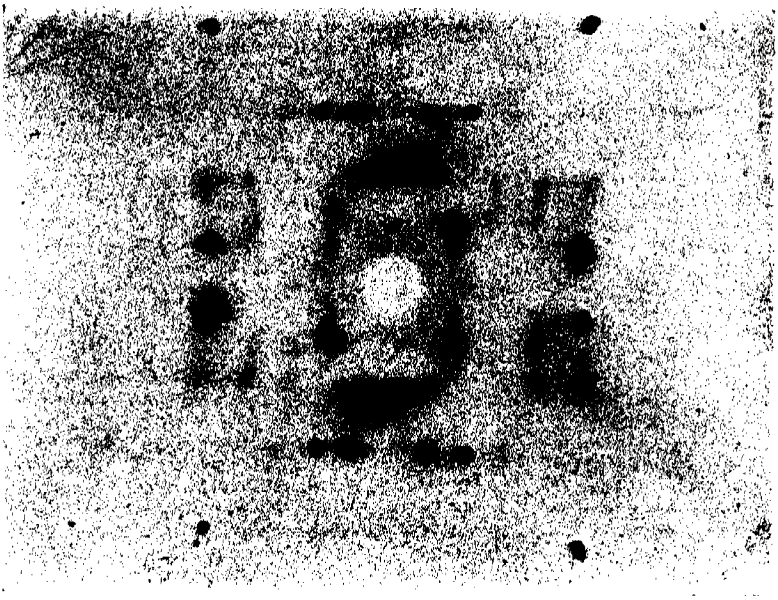

(*b*)

Benzil: [0001] vertical: 3·5 cm.; monochromatized Cu *Kα* radiation along [1120]; 1½ hr. exposure.

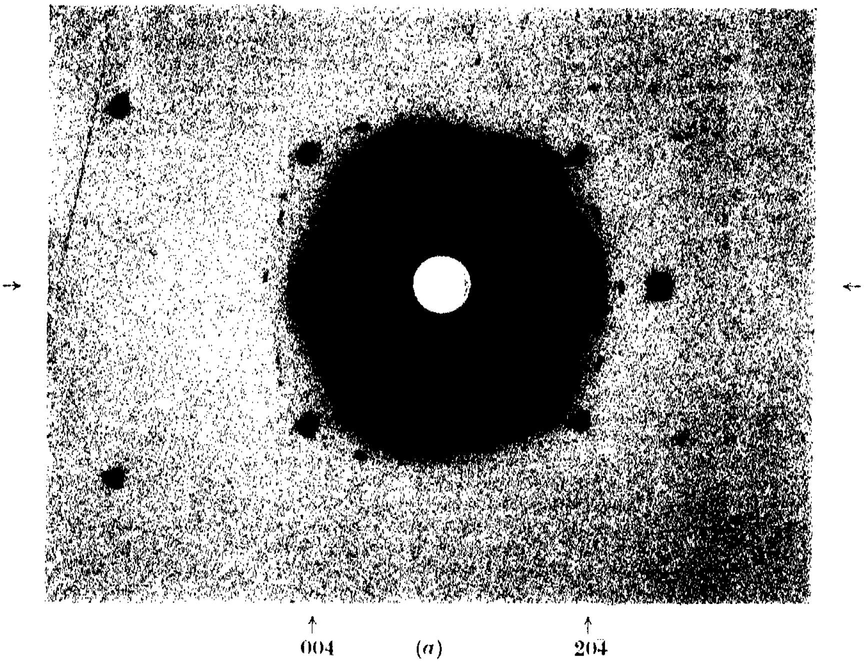

(*a*)

Sorbic acid: [010] vertical: 4 cm.; filtered Cu radiation nearly normal to (100); 10 min. exposure. Note streaks through $20\bar{4}$ diffuse spot.

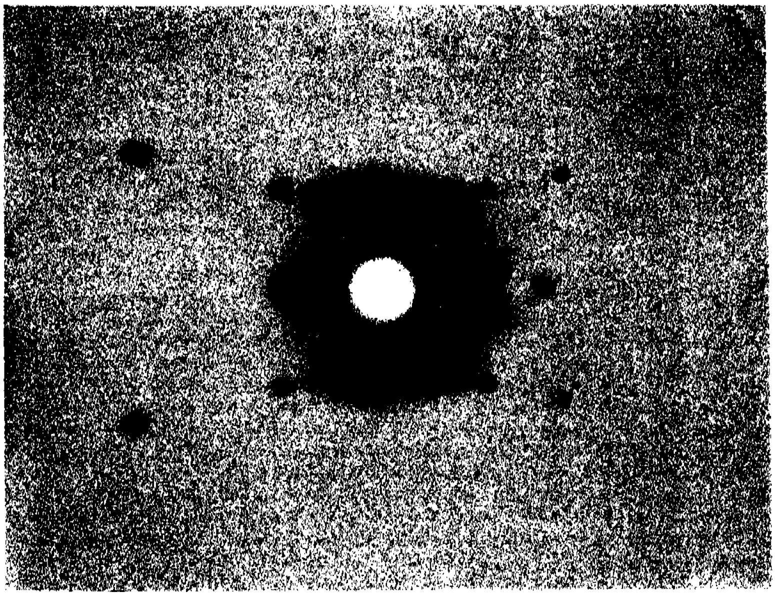

(*b*)

Sorbic acid: [010] **vertical: 3** cm.; monochromatized Cu *Kα* radiation nearly normal to (100); 2 hr. exposure. Note almost complete disappearance of diffuse scattering in neighbourhood of central spot.

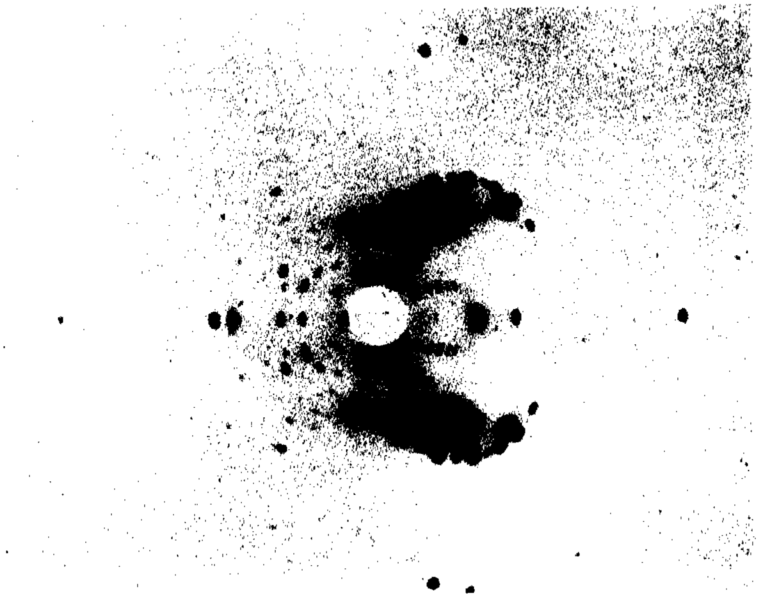

(*a*)

Sorbic acid: filtered Cu radiation: 3 cm.

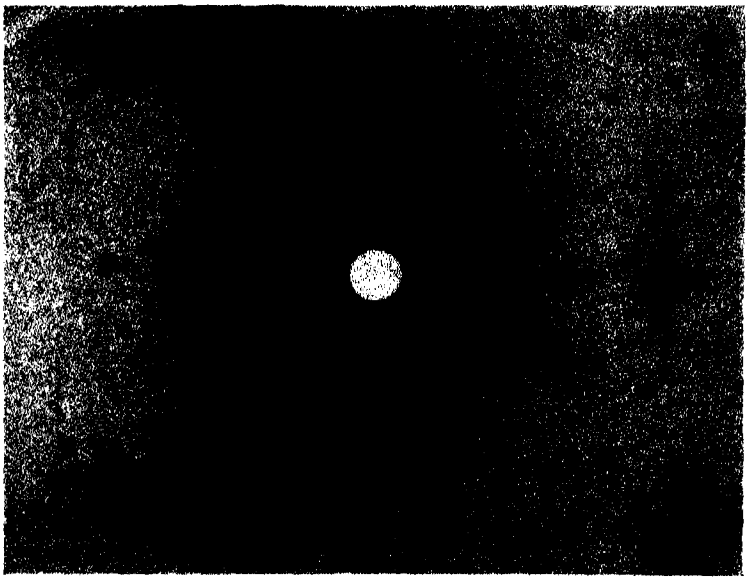

(*b*)

Sorbic acid: filtered Cu radiation: 6 cm. Same setting as 12*a*; exposure 4 times as long. Note increase of size of both Laue and diffuse spots.

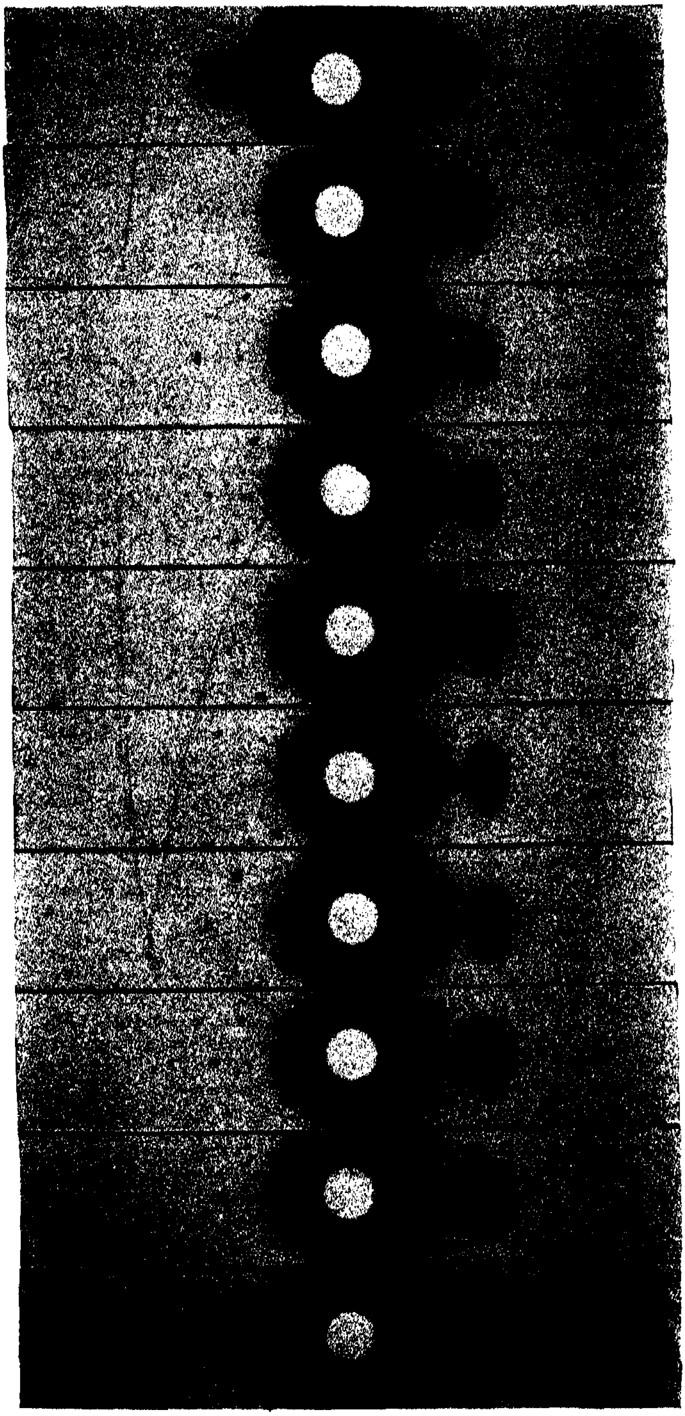
0°
4·0
5·0
5·9
8·1
10·0
11·0
12·1
13·1
14·1

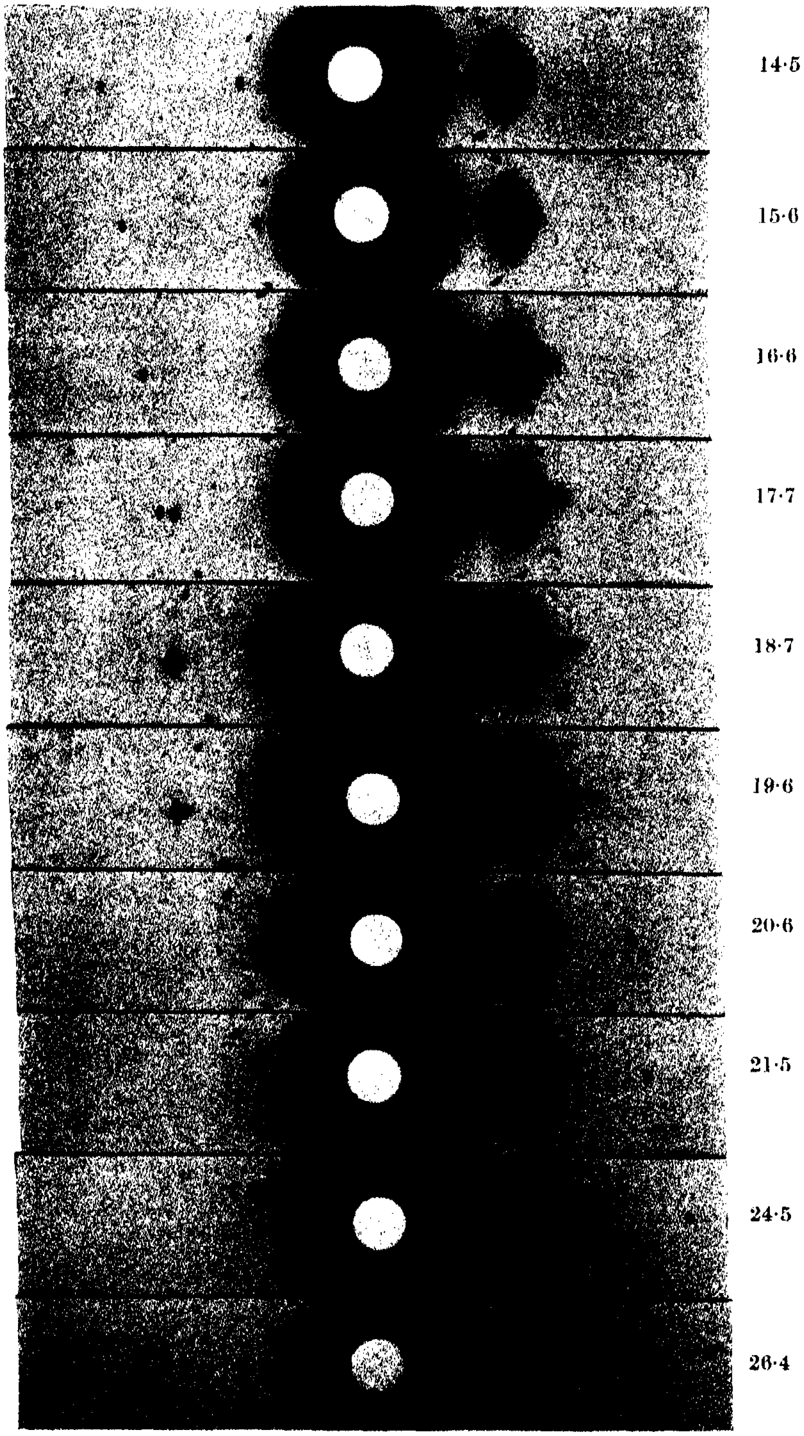
14·5
15·6
16·6
17·7
18·7
19·6
20·6
21·5
24·5
26·4

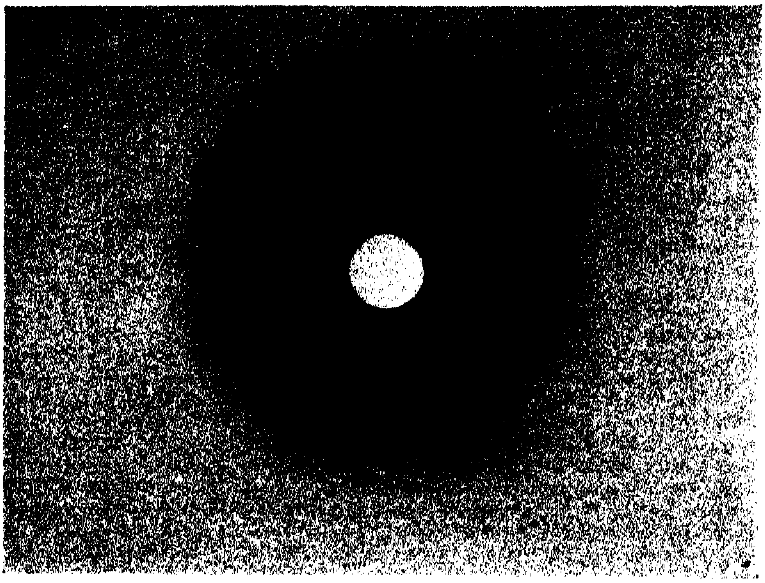

(*a*)

Empty cellophane tube: unfiltered Cu radiation: 4 cm.

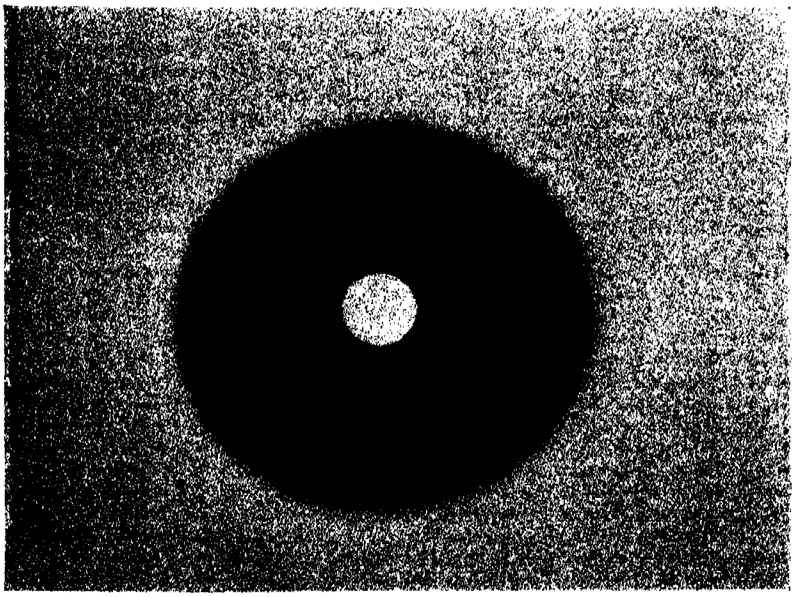

(*b*)

Liquid air streaming over empty cellophane tube: unfiltered Cu radiation: 4 cm.

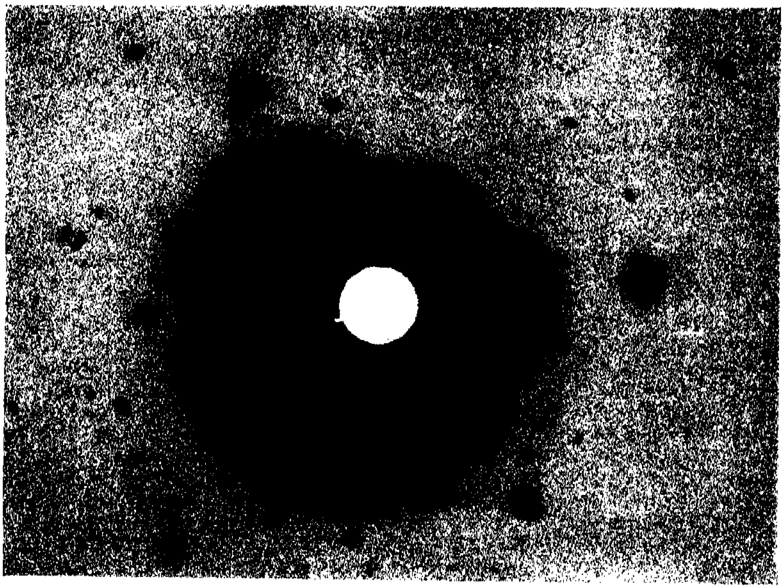

(*a*)

Benzil: filtered Cu radiation at about 7° to [0001]: 4 cm.; room temperature; photographs taken before and after liquid air experiment are identical.

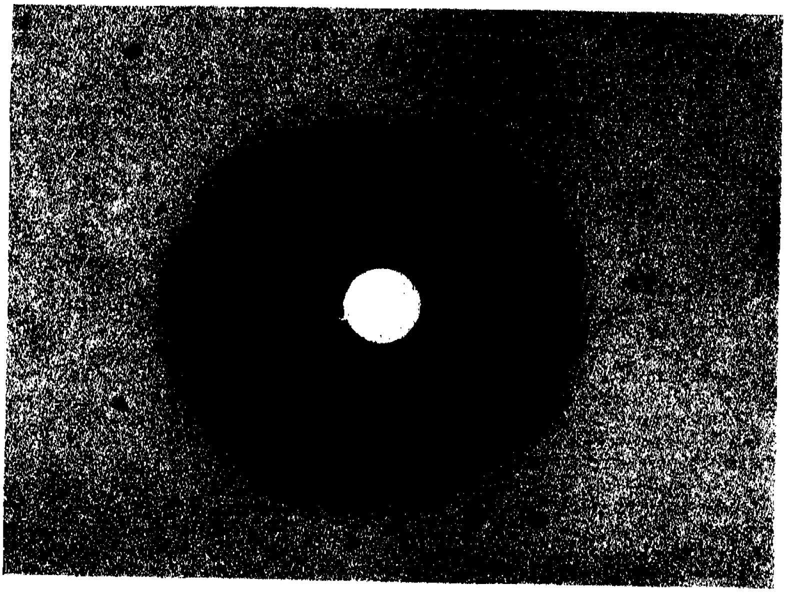

(*b*)

Benzil: same exposure and setting at liquid air temperature, ~ −180° C. Only a trace of the strongest diffuse spots remains; many more Laue spots visible.

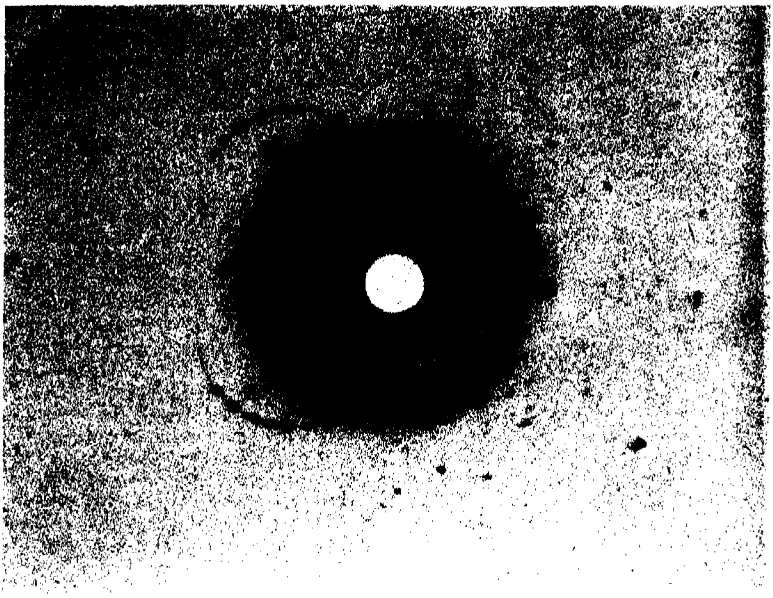

(*a*)

Sorbic acid: filtered Cu radiation; 3·2 cm.; 17½ min. exposure at liquid air temperature. Only a trace of diffuse spots present.

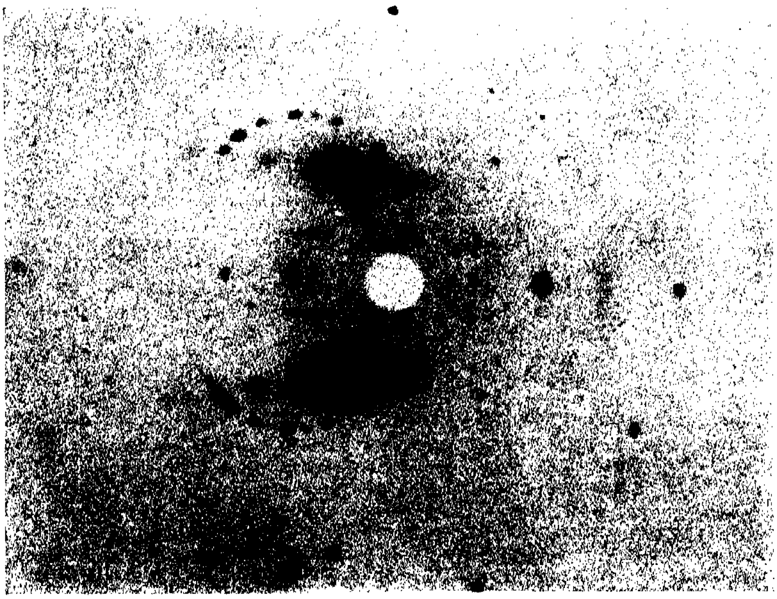

(*b*)

Sorbic acid: setting as above; filtered Cu radiation; 3·2 cm.; 10 min. exposure at room temperature. Many diffuse spots visible, but Laue pattern not so good as at low temperature.

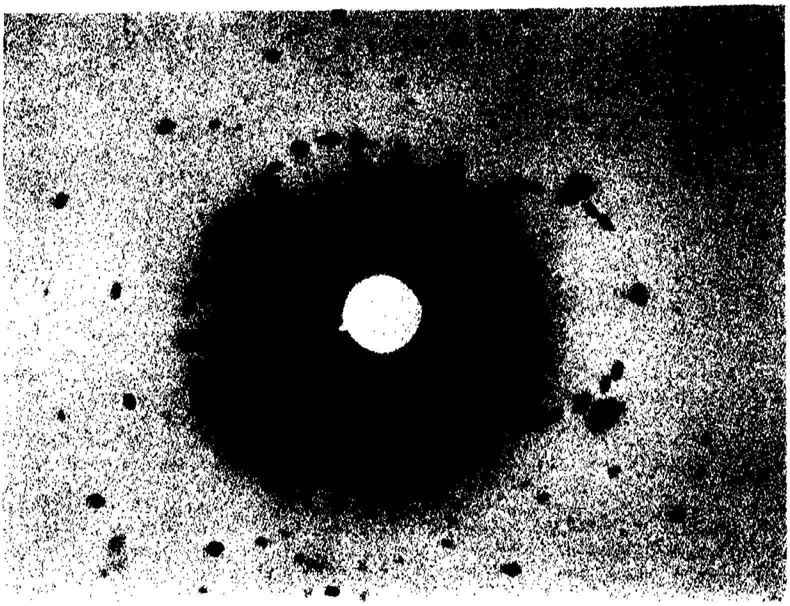

(*a*)

$NaNO_3$: filtered Cu radiation nearly normal to cleavage plane: 4 cm.; 10 min. exposure at 25° C. Photographs before and after liquid air experiment were identical.

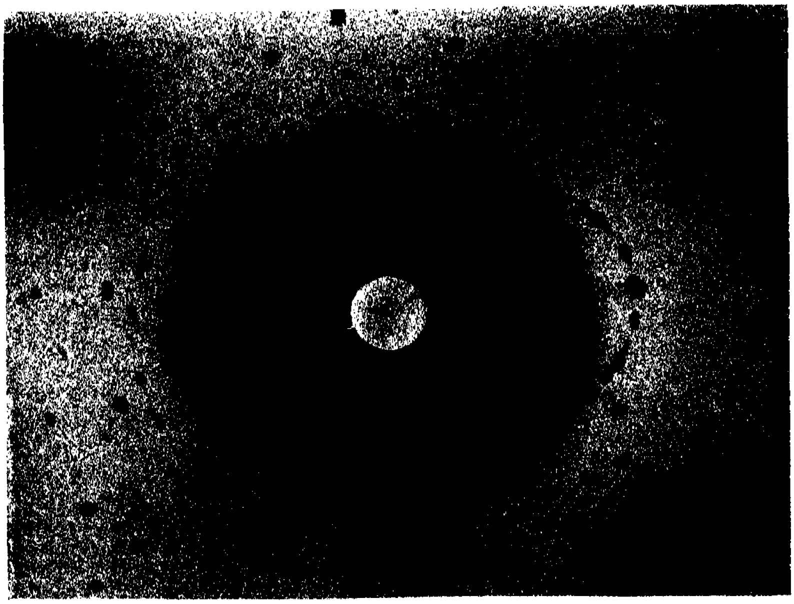

(*b*)

$NaNO_3$: same setting and exposure as above, but at liquid air temperature, $\sim -180°$ C. Laue pattern much improved, but only a trace of diffuse spots or streaks remains.

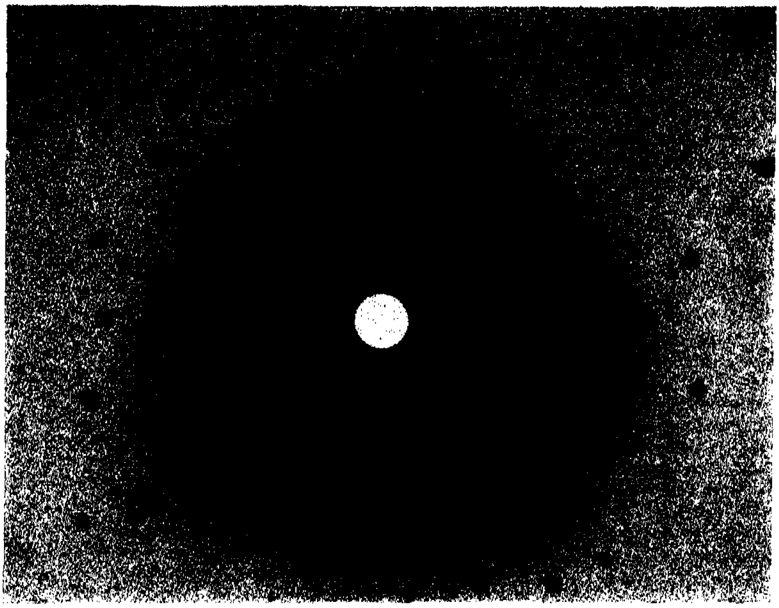

(*a*)

Diamond: [110] vertical; 3·5 cm.; filtered Cu radiation, giving triangular group of 111 diffuse spots, at room temperature. Photographs before and after liquid air experimental identical.

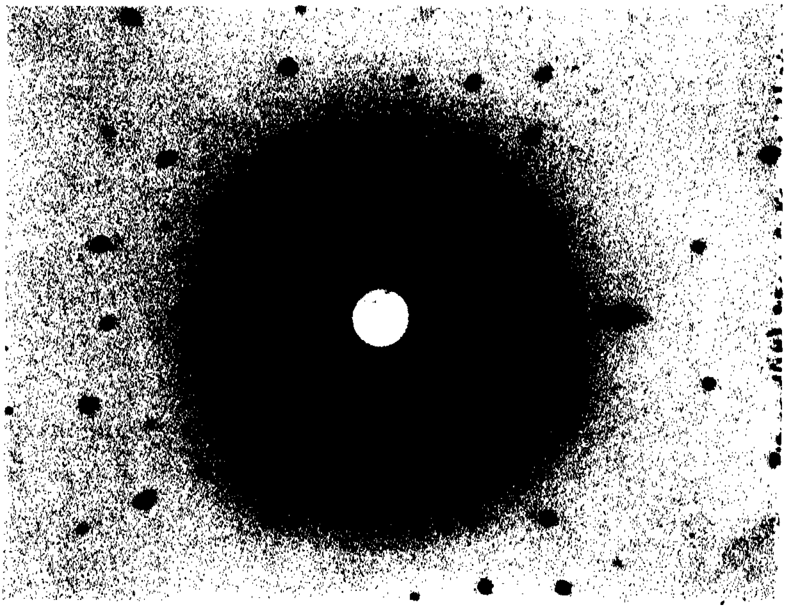

(*b*)

Diamond: same setting and exposure as above, at liquid air temperature. Very little change either in Laue pattern or in intensity of diffuse group. The latter appears to be slightly diminished.

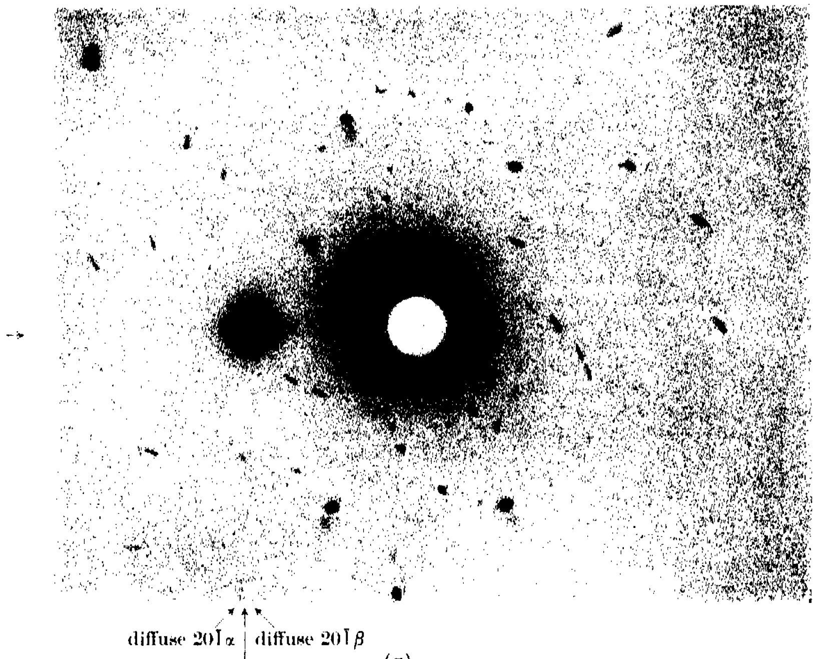

(*a*)

Urea oxalate: (010) (201) planes vertical: unfiltered Cu radiation at 14°·1 to [010]. Sharply sloping 20$\bar{1}$ Laue spot lies between corresponding diffuse spots due to Cu $K\alpha$ and β radiations respectively.

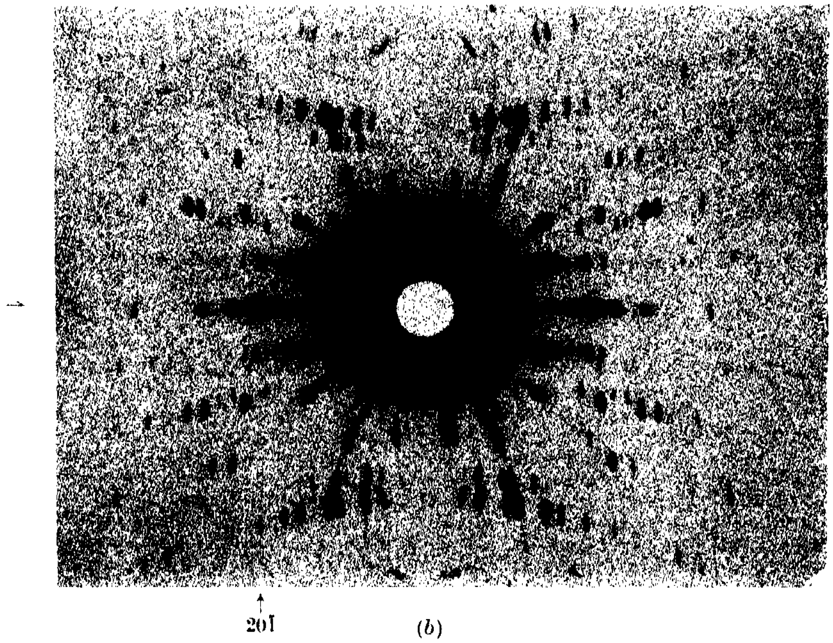

(*b*)

Urea oxalate: (010) (20$\bar{1}$) planes vertical: rotation, using unfiltered Cu radiation, about needle axis of crystal. Compare shape of spots with those in Laue photograph above.

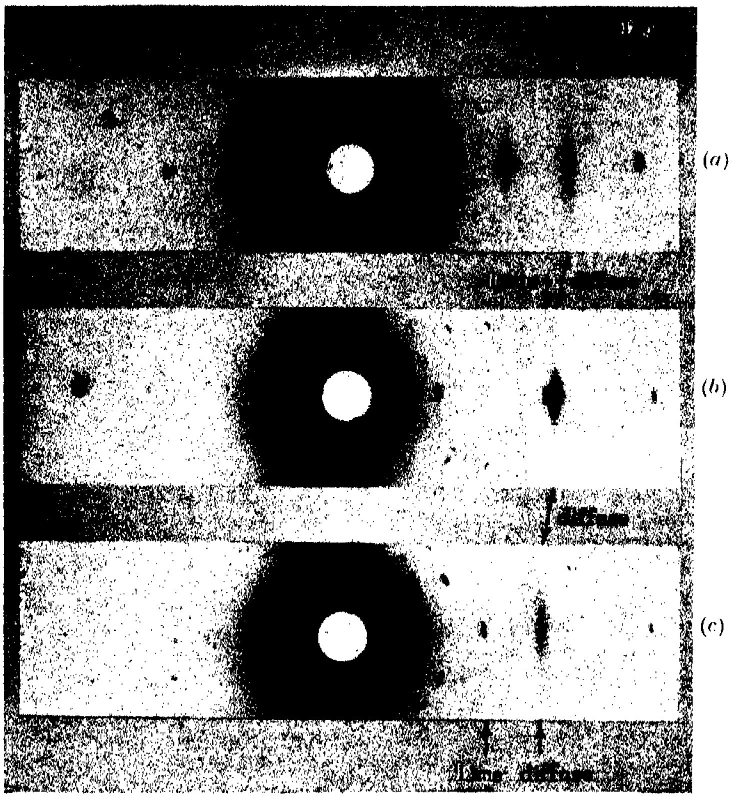

Sorbic acid: showing changes in position, intensity and shape of $60\bar{4}$ diffuse spot as angle of incidence changes.

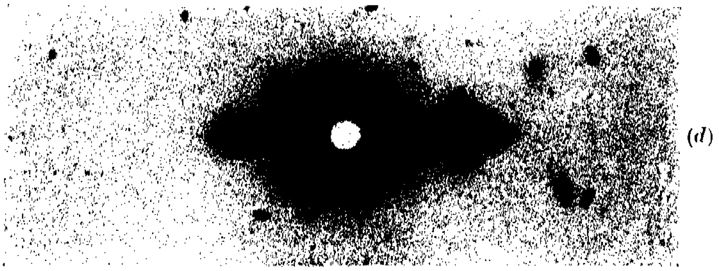

Hexamethylbenzene: [010] vertical; 4 cm.; unfiltered Cu radiation; showing intense diffuse spot corresponding to layer plane (001); small angle of missetting.

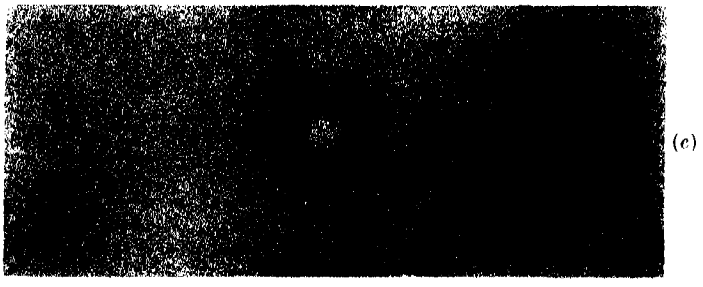

Hexamethylbenzene: [010] vertical; 4 cm.; unfiltered Cu radiation; showing strong 002 diffuse spot at a small angle of missetting and very weak 001 diffuse spot at a large angle of missetting, both to right of central spot.

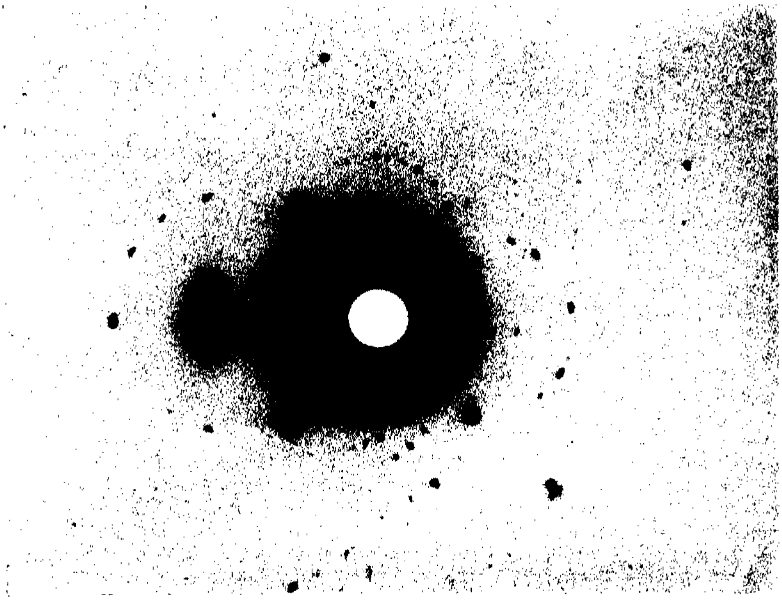

(*a*)

Urea nitrate: filtered Cu radiation; showing how diffuse spot corresponding to (002) layer plane stands out, even for a large angle of missetting. Other diffuse spots, nearer to their appropriate Laue spots, are much smaller.

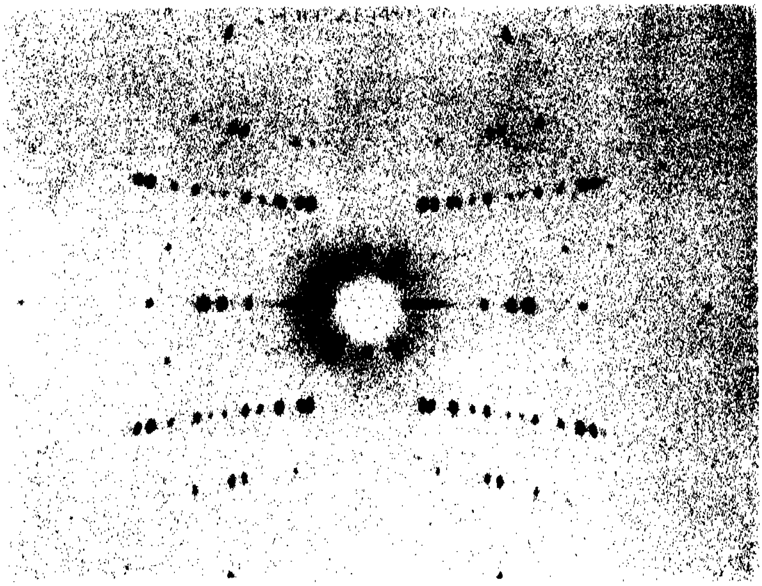

(*b*)

Urea nitrate: filtered Cu radiation; [100] rotation, corresponding to Laue photograph above. No outstanding reflexion from layer plane for moderate exposure.

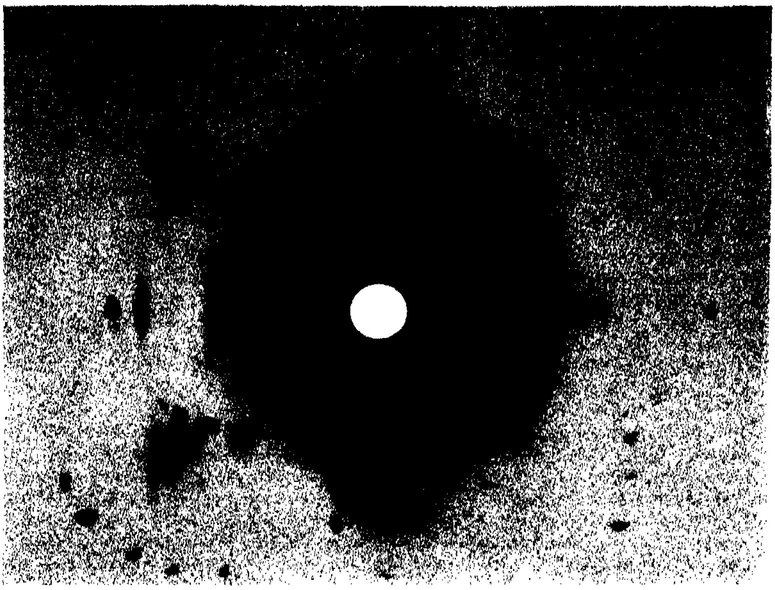

(*a*)

Sorbic acid: [010] vertical; 4 cm.; unfiltered Cu radiation at 20°·6 to [001] in obtuse β. Note the two types of diffuse spot; intense and broad on the one hand, comparatively weak and elongated on the other.

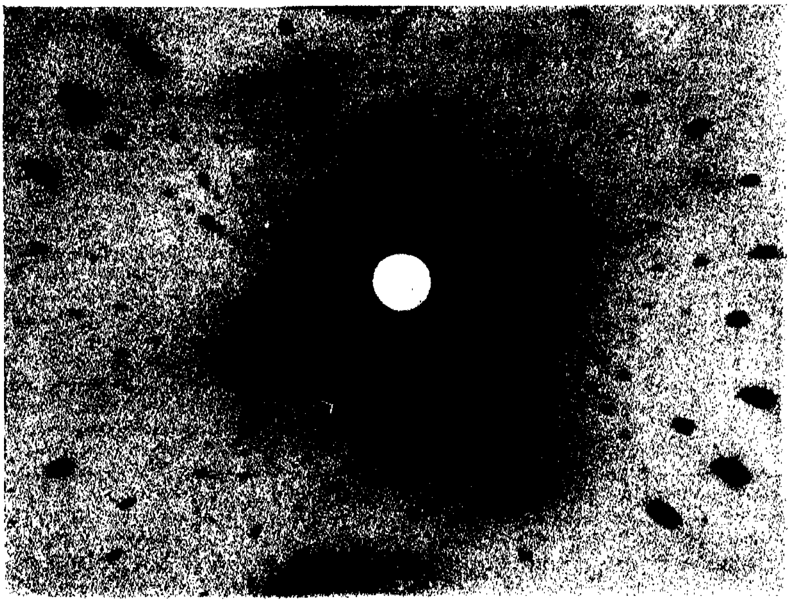

(*b*)

Sorbic acid: [100] vertical; 4 cm.; filtered Cu radiation along [010] axis. Projected length of molecule lies parallel to plane ($20\bar{4}$), giving very intense $20\bar{4}$ diffuse spots. Lengths of streaky spots are perpendicular to this direction (cf. figure 2).

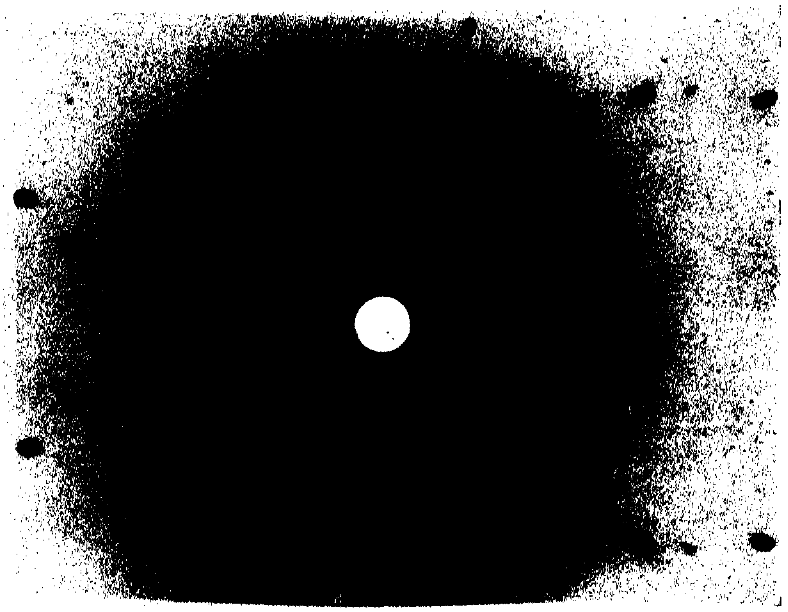

(*a*)

Diamond: $[\bar{1}10]$ vertical; 3·2 cm.; unfiltered Cu radiation nearly normal to a (111) plane. Note nearly circular diffuse spots accompanied by streamers; also relative sizes of Cu $K\alpha$ and β diffuse spots.

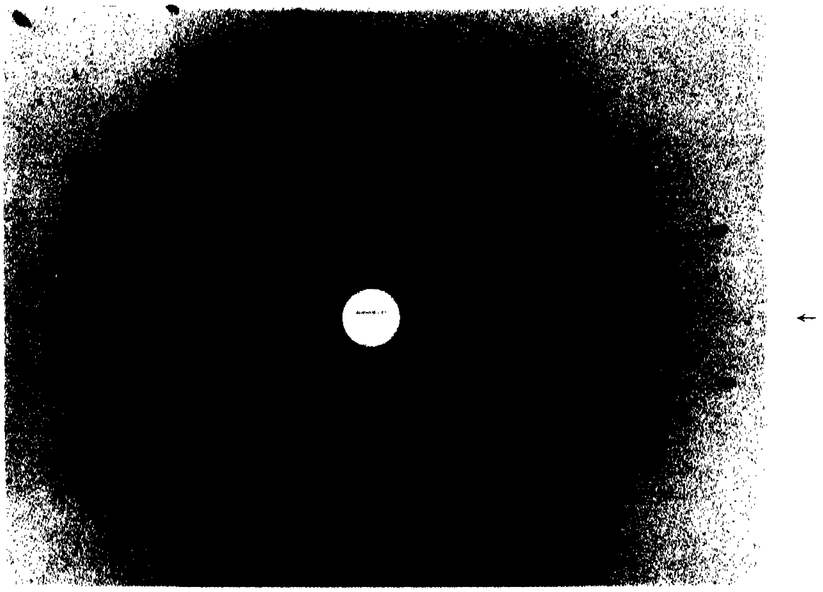

(*b*)

Diamond: $[\bar{1}10]$ vertical; 2·97 cm.; unfiltered Cu radiation at −23°·75 and +46°·75 to {111} planes. Note triangular group of diffuse spots with apex away from 111 Laue spot; compare plate 19.

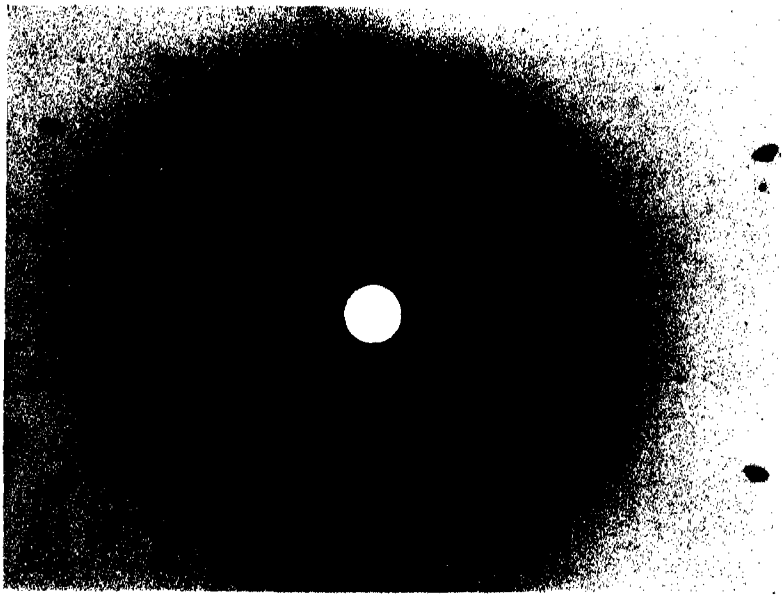

(*a*)

Diamond: [110] vertical; 2·97 cm.; unfiltered Cu radiation at −21°·9 and +48°·6 to {111} planes. Diffuse Cu $K\alpha$ spot coincides with Laue spot; weak triangular group of β diffuse spots clearly visible on original film.

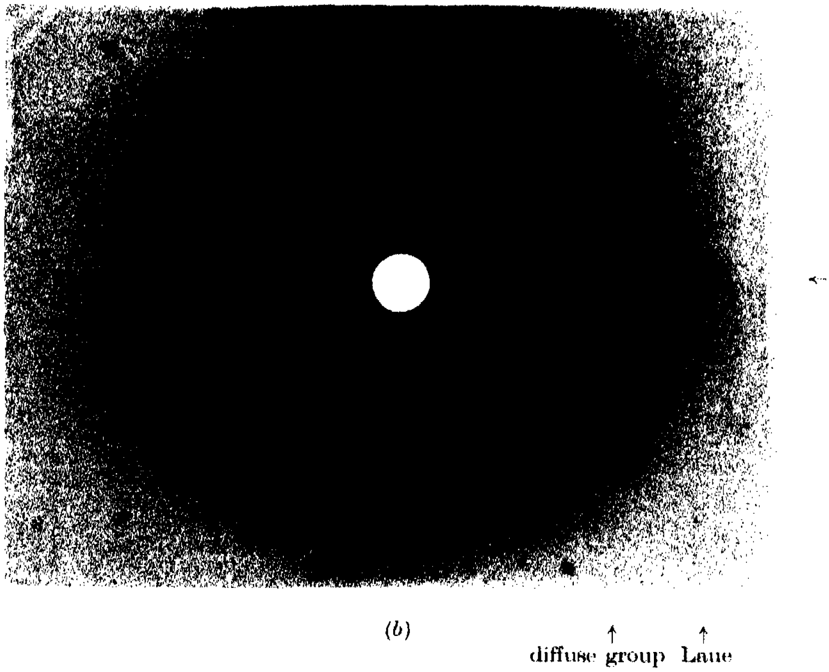

(*b*)

Diamond: [$\bar{1}$10] vertical; 3·03 cm.; unfiltered Cu radiation at −26°·8 and +43°·7 to {111} planes. Note wide separation of components of Cu $K\alpha$ diffuse group, and sharpness of definition of the three outer spots.

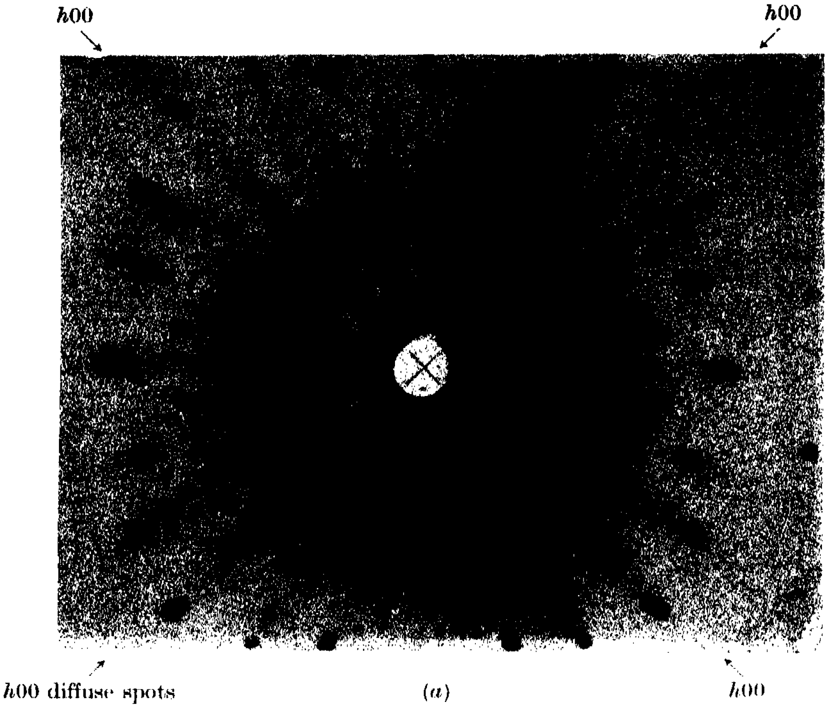

(*a*)

Sylvine: [110] vertical; ~3·5 cm.; unfiltered Ag radiation along [001]. Diffuse spots corresponding to {200} {400} {620} along diagonals, and to {220} {221} along vertical.

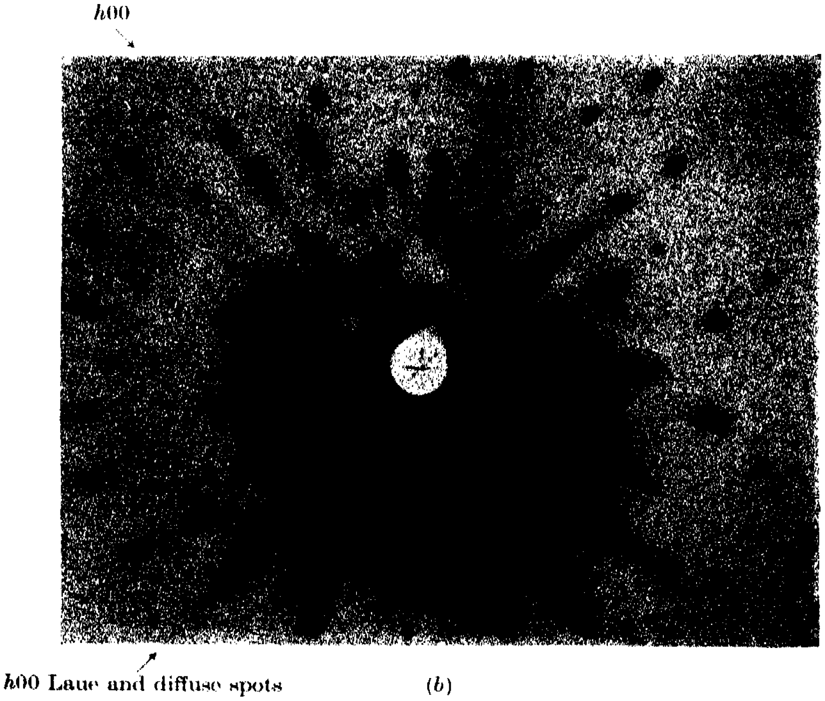

(*b*)

Sylvine: [$\bar{1}$10] vertical; ~3·5 cm.; unfiltered Ag radiation at 15° to [001].

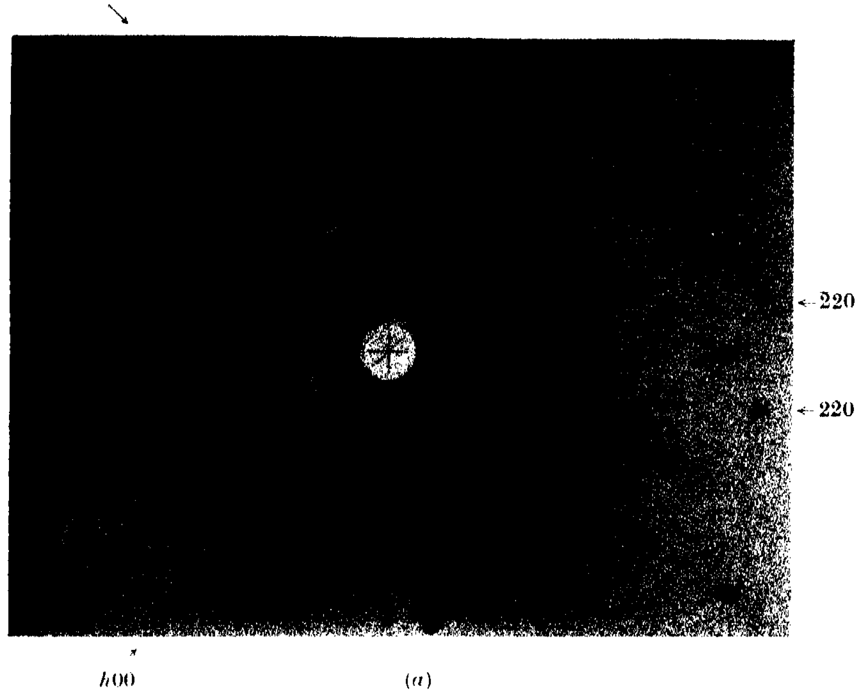

(*a*)

Sylvine: [$\bar{1}$10] vertical: ~3·5 cm.; unfiltered Ag radiation at 20° to [001]. Note displacement of 220 diffuse spots out of vertical plane of incidence.

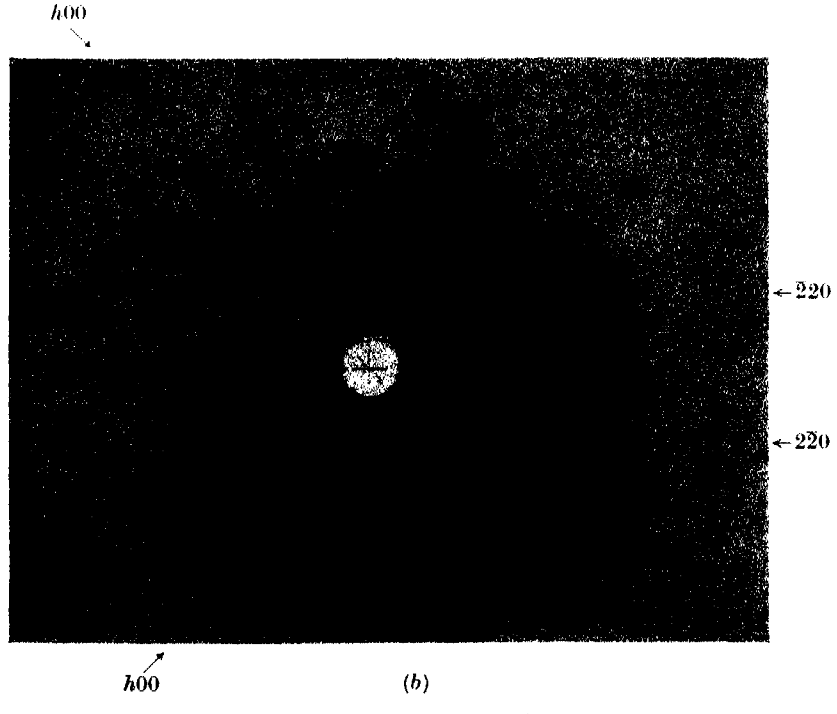

(*b*)

Sylvine: [$\bar{1}$10] vertical; ~3·5 cm.; unfiltered Ag radiation at 25° to [001]. Diffuse spots corresponding to 200, 400, 600 reflexions seen on diagonal streaks, together with *h*00 Laue spots.

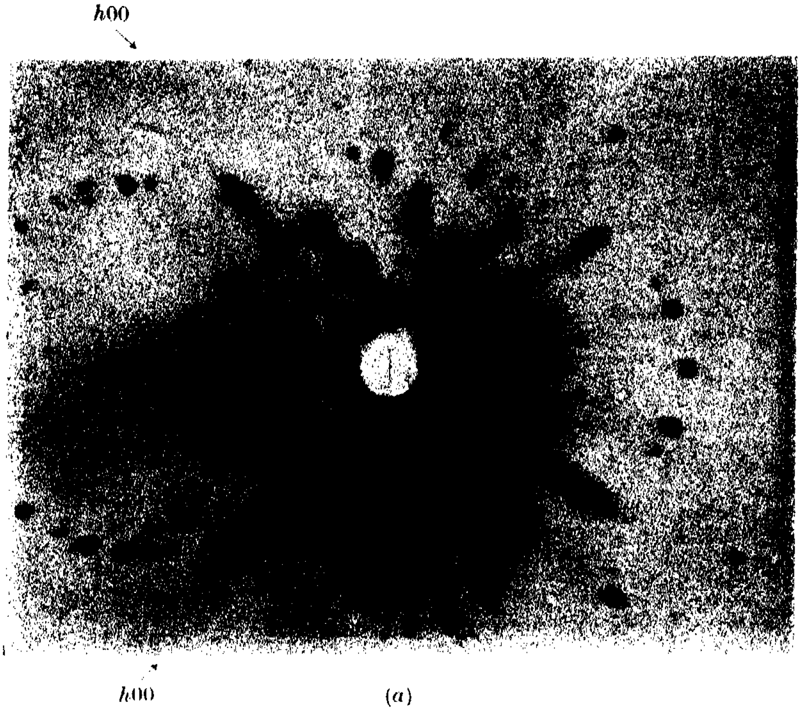

(*a*)

Sylvine: $[\bar{1}10]$ vertical; ~3·5 cm.; unfiltered Ag radiation at 30° to [001]. Note curvature of the streak on which the 200, 400, 600, 800 diffuse spots lie.

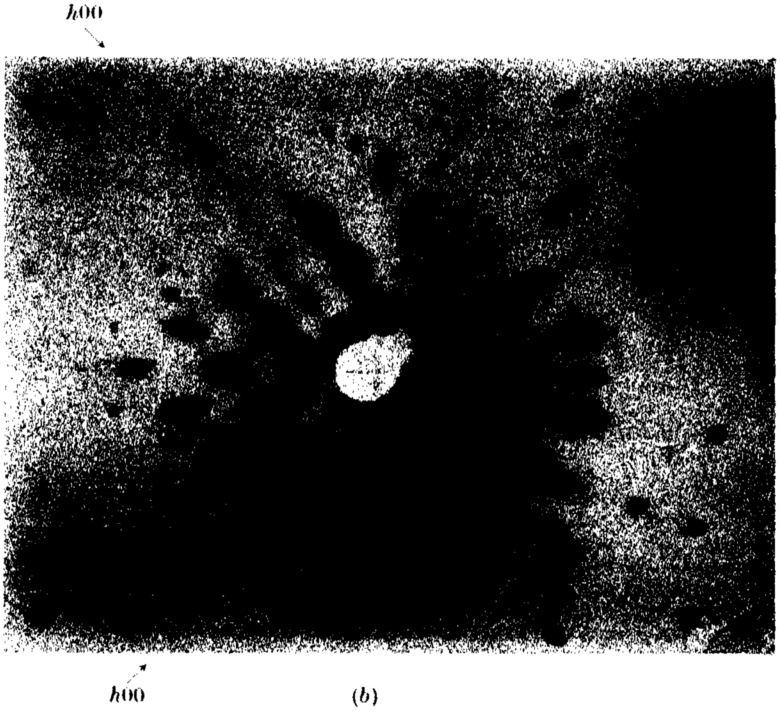

(*b*)

Sylvine: $[\bar{1}10]$ vertical; ~3·5 cm.; unfiltered Ag radiation at 35° to [001]. Curvature of streak connecting 200. 400, 600, 800 diffuse spots is even more marked.

tion of diffuse to Bragg reflexions *in reciprocal space.* The diffuse reflexions correspond to points in reciprocal space, on the sphere of reflexion, which are not far from (relatively strongly reflecting) reciprocal lattice points. Thus each such reciprocal lattice point (corresponding to an infinite set of crystal planes) may be regarded as being surrounded by a cloud of reflecting points, whose physical significance is open to various interpretations. Future experiments must involve a detailed exploration of such diffusely reflecting regions, which are certainly not, in general, spherical, being extended along reciprocal lattice planes and axes. The non-radial streaks correspond to reflexion in the near neighbourhood of reciprocal lattice planes or axes, and the non-existence of monochromatic radial streaks (except for large angles of deflexion) is readily understood, since these would correspond to reflexions near to the reciprocal lattice origin, that is, to relatively large spacings.

We are indebted to the Managers of the Royal Institution for laboratory facilities and especially to Sir William Bragg for the keen interest he has taken in this research. We have derived much help from conversations with our fellow-workers in the laboratory and we are particularly grateful to Dr I. E. Knaggs for handing over to us the material indicated in the text as being her work.

REFERENCES

Barrett and Geisler 1940 *J. Appl. Phys.* **11**, 733.
Bernal 1926 *Proc. Roy. Soc.* A, **113**, 117.
Bragg 1940 *Nature, Lond.*, **146**, 509.
Brill, Grimm, Hermann and Peters 1939 *Ann. Phys., Lpz.*, **34**, 393.
Brillouin 1922 *Ann. Phys., Paris*, **17**, 88.
Brockway and Robertson 1939 *J. Chem. Soc.* p. 1324.
Calvet, Jacquet and Guinier 1938 *C.R. Acad. Sci., Paris*, **206**, 1972.
Calvet, Jacquet and Guinier 1939 *J. Inst. Met.* **6**, 177.
Charlesby, Finch and Williams 1939 *Proc. Phys. Soc.* **51**, 479.
Clay 1934 *Proc. Phys. Soc.* **46**, 703.
Coven 1932 *Phys. Rev.* **41**, 422.
Debye 1914 *Ann. Phys., Lpz.*, **43**, 49.
Ewald 1940 *Proc. Phys. Soc.* **52**, 167.
Faxén 1923 *Z. Phys.* **17**, 266.
Friedrich 1913 *Phys. Z.* **14**, 1082.
Guinier 1938 *C.R. Acad. Sci., Paris*, **206**, 1641; *Nature, Lond.*, **142**, 569.
Harvey, Williams and Jauncey 1934 *Phys. Rev.* **46**, 365.
Jahn and Lonsdale 1941 *Nature, Lond.*, **147**, 88.
Jauncey 1941 *Nature, Lond.*, **147**, 146.
Jauncey and Baltzer 1940 *Phys. Rev.* **58**, 1116.
Jauncey and Pennell 1933 *Phys. Rev.* **43**, 505; **44**, 138.

Knaggs and Lonsdale 1939 *Nature, Lond.*, **143**, 1023.
Knaggs, Lonsdale, Muller and Ubbelohde 1940 *Nature, Lond.*, **145**, 820.
Kracek, Posnjak and Hendricks 1931 *J. Amer. Chem. Soc.* **53**, 3339.
Laue and Riewe 1936 *Z. Kristallogr.* **95**, 408.
Laval 1938 *C.R. Acad. Sci., Paris*, **207**, 169.
Laval 1939*a* *C.R. Acad. Sci., Paris*, **208**, 1512.
Laval 1939*b* *Bull. Soc. franç. Minér.* **62**, 137.
Lonsdale 1929 *Proc. Roy. Soc.* A, **123**, 494; *Trans. Faraday Soc.* **25**, 352.
Lonsdale 1941 *Proc. Roy. Soc.* A, **177**, 272.
Lonsdale, Knaggs and Smith 1940 *Nature, Lond.*, **146**, 332.
Lonsdale, Robertson and Woodward 1941 *Proc. Roy. Soc.* A (in the Press).
Lonsdale and Smith 1939 *Phil. Mag.* **28**, 614.
Mauguin and Laval 1939 *C.R. Acad. Sci., Paris*, **208**, 1446.
Muller and Clay 1939 *J. Inst. Elect. Engrs*, **84**, 261.
Preston 1938 *Nature, Lond.*, **142**, 570.
Preston 1939 *Nature, Lond.*, **143**, 76; *Proc. Roy. Soc.* A, **172**, 116.
Preston 1940 *Proc. Phys. Soc.* **52**, 77.
Raman and Nath 1940*a* *Proc. Indian Acad. Sci.* **12**, 83.
Raman and Nath 1940*b* *Proc. Indian Acad. Sci.* **12**, 427.
Raman and Nilakantan 1940*a* *Nature, Lond.*, **145**, 667, 860; **146**, 523, 686; *Curr. Sci.* **9**, 165.
Raman and Nilakantan 1940*b* *Proc. Indian Acad. Sci.* **11**, 379, 389, 398.
Raman and Nilakantan 1940*c* *Proc. Indian Acad. Sci.* **12**, 141.
Raman and Nilakantan 1941 *Nature, Lond.*, **147**, 118.
Robertson 1936 *Proc. Roy. Soc.* A, **157**, 79.
Siegel and Zachariasen 1940 *Phys. Rev.* **57**, 795.
Wadlund 1938 *Phys. Rev.* **53**, 843.
Waller 1923 *Z. Phys.* **17**, 398.
Waller 1925 Dissertation: Theoretische Studien zur Interferenz- und Dispersionstheorie der Rontgenstrahlen. *Uppsala Univ. Årsskr.*
Zachariasen 1940 *Phys. Rev.* **57**, 597; *Nature, Lond.*, **145**, 1019.

The diffuse spots in X-ray photographs

By Sir William H. Bragg, F.R.S.

(*Received* 2 *April* 1941)

A crystal consisting, as it does, of some molecular combination repeated as a unit at regular intervals in three directions in space can act as a three-dimensional diffraction grating. When monochromatic rays fall upon it, the scattered rays form a diffraction pattern, which can be derived by calculation from the diffraction formula. The pattern of 'diffuse spots' now under discussion agrees very closely, in fact within the errors of experiment so far made, with this calculated result. Either the conditions in the crystal which give rise to the diffuse spots are those which allow the diffraction pattern to be observed or they simulate them.

This diffraction pattern differs from the diffraction effects so widely used in recent years in the examination of crystal structure. The Laue pattern of spots is not a true diffraction pattern because every spot in it is due to a different wave-length. In the examination of a crystal by an *ionization* spectrometer or in the oscillation photograph, the different spots are not observed simultaneously. In a true diffraction pattern all the spots or lines are due to monochromatic rays and are observed at one and the same time.

The general expression for the relative intensity of the ray diffracted in different directions is

$$\Sigma m_1 m_2 \cos {}_1\phi_2 \frac{\sin^2 p\phi_a/2}{\sin^2 \phi_a/2} \cdot \frac{\sin^2 q\phi_b/2}{\sin^2 \phi_b/2} \cdot \frac{\sin^2 r\phi_c/2}{\sin^2 \phi_c/2},$$

in which formula the symbols have the following meanings:

The unit of the crystal contains various atoms which may have different powers of scattering. The relative amplitudes of the waves scattered by them are denoted by m_1, m_2, ... The waves scattered by any two, m_1, m_2, differ in phase by an amount ${}_1\phi_2$, which is equal to

$$\frac{2\pi}{\lambda}\{(h-h')(x-x')+(k-k')(y-y')+(l-l')(z-z')\},$$

where λ is the wave-length; (x, y, z) and (x', y', z') are the coordinates of m_1 and m_2; (h', k', l') and (h, k, l) are the direction cosines of the incident and the diffracted rays. In the summation each m is multiplied in turn by every other m including itself. The quantities ϕ_a, ϕ_b and ϕ_c are the phase differences due to a single repetition in each of the three standard directions. The numbers of the repetitions are p, q and r respectively.

The thermal movements of the atoms do not affect the geometry of the diffraction pattern as described by the formula, except in so far as they cause changes in the dimensions of the crystal. They may affect the intensities of various parts. This is also true of the observed diffuse spot pattern. In the same way the intensities but not the geometry may be affected by the summation factor in the formula and by the scattering factors of the atoms.

Nor does the formula take any account of absorption or of secondary scattering within the crystal. Under the usual conditions of observation, these effects are so large that the formula is useless. The reason is that when p, q and r are large numbers, the intensity of the diffracted ray is too small to be observed unless the denominators of the three fractions in the formula are all zero, or very nearly zero: unless, in other words, the changes of phase due to the three principal repetitions are all multiples of π at the same time. This can only happen by accident, since two variables determine the direction of the diffracted ray, and there are three equations to be satisfied. Complete satisfaction can be obtained only by freedom to move the crystal at the same time, or to alter the wave-length; hence the usual condition $n\lambda = 2d\sin\theta$. Monochromatic rays do not give a Laue pattern. When the three denominators are all very close to zero simultaneously, the intensity of the diffracted ray is proportional to $p^2.q^2.r^2$; all the units then act together. This is very large compared to what happens in the rest of the diffraction field: absorption and secondary scattering become great, and vary with minute changes of crystal position. Complicated calculations are then required. The problem was attacked by Darwin in the early days of crystal analysis and has been the subject of much investigation.

If however there were groups of atoms in the crystal, for which p, q and r were so small that the contrast between the intensities of the maxima in the pattern and the general intensity of the background was not so excessive, the true diffraction diagram might be observed. The groups must act independently. They must be in slight disarray with the crystal as a whole, and with the larger groups which the crystal contains. Changes of orientation of a few degrees would make very little change in the positions of the spots in the pattern, so that effects would be additive. It would therefore be possible to conceive of the formation of the true pattern, provided that the groups were small and sufficiently numerous. This was the fundamental idea in Preston's paper (*Proc. Roy. Soc.* A, **172**, 116). It has also been described by v. Laue (*Ann. Phys., Lpz.*, **26**, 55 (1936) and **29**, 211 (1937)), and also by Ewald, *Proc. Phys. Soc.* **52**, 167 (1939).

This hypothetical case agrees so closely in many respects with the actual that, even if there is no more than a parallelism, it is worthy of careful examination. Examples in the form of figures are given below; the crystals being potassium chloride, calcite and diamond.

Certain general characteristics are to be observed in these examples and others provided by Lonsdale and Smith in the preceding paper. All these can be derived from the formula.

(1) The diffuse spot diagram is due to monochromatic rays. Diffuse spots are in general much weaker than Laue spots.

(2) Diffuse spots are found where the product of the three denominators of the formula is a minimum. The expression for the intensity is then in general a maximum. Small movements of the crystal such as rotations through 5 or 10° make little change in the pattern.

(3) Rotation of the crystal may bring all three denominators to zero at the same time. The corresponding diffuse spot then becomes a Laue spot. In an actual experiment the latter moves into the place of the former. The wave-length of the Laue spot changes during the movement, the wave-length of the diffuse spot does not. Hence arises the close connexion between the diffuse spot pattern and the oscillation pattern which Mrs Lonsdale has shown to exist.

(4) If the Laue spot is strong, so also in general is the diffuse spot into which it moves: they are affected alike by the first factor in the formula.

(5) Other correlations between theory and experiment are shown in detail in the illustrative diagrams.

POTASSIUM CHLORIDE (figures 1 and 2)

The first figure represents the diffraction pattern due to Mo rays of wave-length 0·71 A acting on a crystal of KCl. The crystal is placed at an angle of 20° away from the symmetrical position as shown in the smaller figure (figure 2). (See Lonsdale and Smith's plate 7*b*.)

In this case the direction cosines of the incident ray are taken to be (0, 0, 1) and of the diffracted ray (h, k, l). The crystal is rotated through 20° about the axis of y. The phase differences of the principal repetitions are therefore

$$\frac{2\pi a}{\lambda}\{h\cos\theta-(l-1)\sin\theta\};\quad \frac{2\pi ak}{\lambda};\quad \frac{2\pi a}{\lambda}\{h\sin\theta+(l-1)\cos\theta\},$$

where a has the value 3·14. The atoms of K and Cl are taken to be of equal value. The sines of the halves of these angles are the denominators in the general formula. The intensity of the diffracted ray is great when the denominators are small. When values of h and k are found which make the denominators separately equal to zero, three sets of curves are obtained. The equations used are

$$a\{h\cos\theta-(l-1)\sin\theta\}=M(\lambda);\quad ak=M(\lambda);\quad a\{h\sin\theta+(l-1)\cos\theta\}=M(\lambda),$$

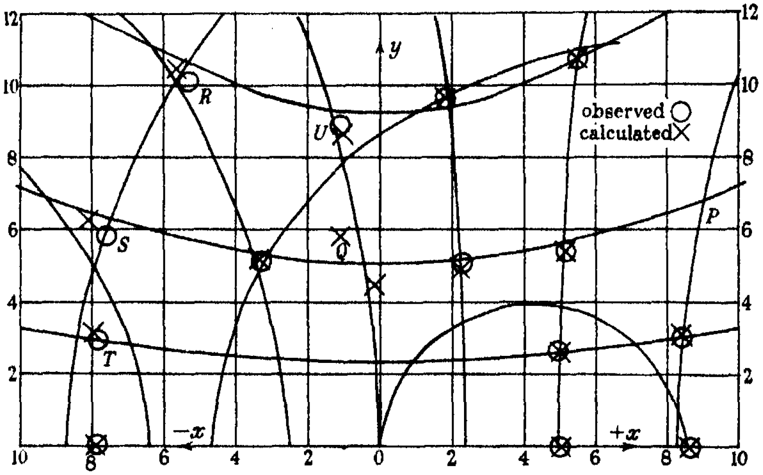

FIGURE 1. Diffuse spots of potassium chloride: $\lambda = 0{\cdot}71$. Crystal to photographic plate, 10 cm. See figure 2.

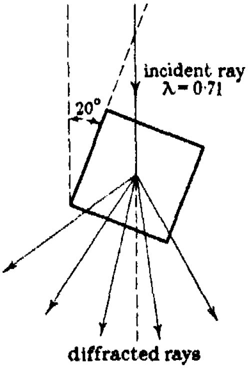

FIGURE 2

where M is any integer, $\theta = 20°$, $\lambda = 0{\cdot}71$. The results can be shown either as (h, k) curves, as in the succeeding diagrams for calcite and diamond, or can be translated into (x, y) curves by the relation $x = Dh/l$, $y = Dk/l$, where D is the distance from the crystal to the photographic plate. The (x, y) curves then show lines of maximum intensity referred to coordinate axes in the photograph. This has been done in figure 1.

The positions of the observed diffuse spots are marked by circles. It will be observed that they lie in general close to the intersections of the lines which in the (x, y) curves are hyperbolae and in the (h, k) curves of this case would be lines parallel to the axes. It seems that the third set of curves, ellipses in the (x, y) diagram (figure 1), have in general little effect on the position of the spots. The reason is that in the diagram the first two sets of curves lie much closer together than the third, and the intensity varies more rapidly from one curve of a series to the next. Calculation shows that this is the right explanation; crosses in the diagram show where the calculated values of the maxima are found: the agreement with observation is close. For the purpose of this calculation p, q and r are all taken to be equal to 2; but the choice of values is unimportant when it is merely a question of finding the positions of maxima.

The third set of curves has sometimes a considerable effect. For example, there is no spot at P because P lies in phase exactly half way between two maximum curves of the third set. It is to be remembered that the intensity is the product of certain factors, not the square of the sum of certain terms. If one of the factors is zero the product is zero, and this is the case at P. At other points, such as R, S, T and U, the peak position clearly depends on all three of the curves of maximum intensity. At Q there is a confused effect in the actual photograph; there are two calculated maxima as shown, and in the photograph a very diffuse effect covers the two. This point lies close to the same zero curve that passes through P.

DIAMOND (figures 3 and 4, 5 and 6)

Figure 3 represents the case when the direction of the incident rays coincides with the trigonal axis AO in figure 4. The three principal displacements are along the edges of the tetrahedron, viz. AB, AC and AD. The axes of coordinates being as shown in figure 4, the coordinates of $ABCD$ are, in Ångström units,

	x	y	z
A	0	0	2·053
B	$\overline{1{\cdot}257}$	$\overline{0{\cdot}726}$	0
C	1·257	$\overline{0{\cdot}726}$	0
D	0	1·452	0

and the (h, k) curves of figure 3 are drawn from the equations

$$1{\cdot}257h + 0{\cdot}726k + 2{\cdot}053(l-1) = M(1{\cdot}54),$$
$$\overline{1{\cdot}257}h + 0{\cdot}726k + 2{\cdot}053(l-1) = M(1{\cdot}54),$$
$$\overline{1{\cdot}452}k + 2{\cdot}053(l-1) = M(1{\cdot}54),$$

where $M(1{\cdot}54)$ stands for some multiple of 1·54, the wave-length of Cu_α radiation. For the three ellipses passing through O the multiple is zero. Portions of three larger ellipses are shown for which the multiple is unity.

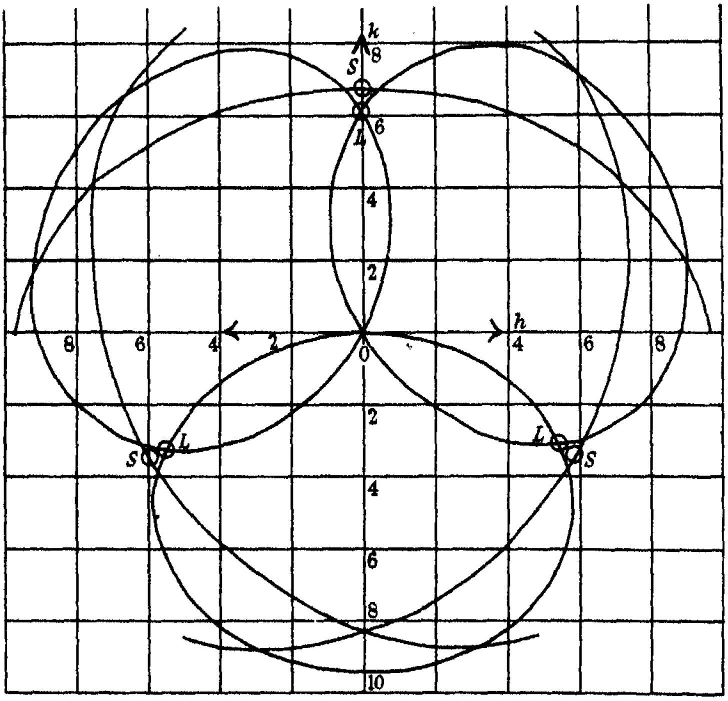

FIGURE 3. Diamond: (h, k) diagram. Incident ray normal to cleavage force. h and k are expressed in tenths.

It will be observed that the cases where members of three sets of curves approximate to each other are in this case very few; only three are included in the figure, at points marked L. The reason is that λ is large and the principal displacements are small. Original photographs are shown in Lonsdale and Smith, plates 24 and 25.

It may serve to make the problem clearer if it is pointed out that any point on the upper complete ellipse on the left of figure 3 defines the direction of a diffracted ray which is in the same phase whether it comes from A or B; and correspondingly for the right-hand ellipse and the points A and C.

At L, where the ellipses meet, the value of k, ($h = 0$), is such that the diffracted ray is in the same phase whether it comes from A, B, or C: it is usual to speak of it as reflected in the plane ABC. The other ellipse that passes close to L defines the values of (h, k) for which rays from A and D differ in length of path by 1·54 A. The ellipses change in form and position when the crystal is moved. The inner ellipses have no relation to wave-length; but the outer ellipses have. There is one wave-length for which the outer ellipse will pass through L: and as this is included in the white radiation, a Laue spot appears at L, as indicated in figure 4. The diffuse spot is farther out as shown.

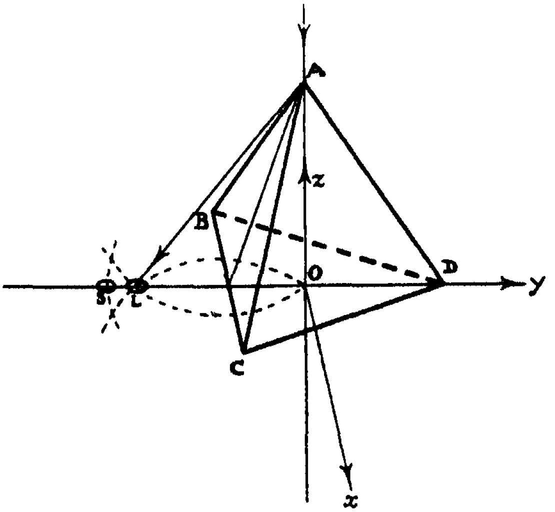

FIGURE 4

The curves of figure 5 refer to a case when the diamond is rotated about BC (figure 4) through an angle of 43° in the direction Oy to Oz. The curvilinear triangle formed where $h = 0$ and $k = 0{\cdot}7$ approximately by portions of three ellipses is then larger than in figure 3. Mrs Lonsdale shows that in this case the diffuse spot breaks up into a set of three spots: when these are plotted upon the diagram (figure 5), they appear at the middle points of the sides as shown. By changing the amount of tilt about BC, the triangle formed by the three curves in figure 5 can be reversed so that its apex now points towards the origin as in figure 6. A photograph due to Mrs Lonsdale shows that in this case the triangular spot is also reversed. There is clearly a connexion between the set of triangular spots in the photographs and the small triangle shown in the diagrams (figures 5 and 6). The three last factors of the general equation are at their maxima along the three sides of the triangle; minima and other subsidiary maxima occur in lines parallel to the sides, the periodicity depending on the size of the group. The intensity at any point depends on the product of three factors, and it may easily be that the intensity is great at the middle points of the sides and small at the corners. Possibly an explanation is to be found *in some such consideration of the diffraction effect.*

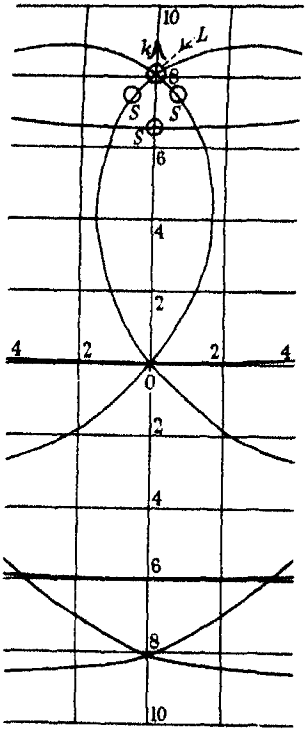

Figure 5. Diamond rotated. Compare with figures 3 and 6.

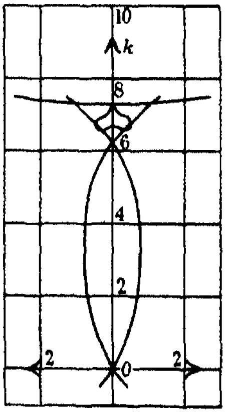

Figure 6

Calcite (figures 7 and 8)

Calcite presents a problem more complicated than those of potassium chloride and diamond. Potassium chloride is structurally simple, and the intermolecular distances of diamond are so small that there are very few spots in the diagram. But calcite is monoclinic and its repeat distances are much larger than those of diamond. The diffraction pattern is therefore much less simple than in the other two cases. The photographs obtained by Raman and by Lonsdale show a number of interesting features.

It is convenient to consider those in which the X-rays have been normal to a cleavage plane. In figure 7 the corners of the rhomb are *A*, *B*, *C*, *D* and their inverses A', B', C', D'. AA' is the trigonal axis. The centres of the faces meeting at A are E, F, G; and the inverses of these are E', F', G'. The axes are chosen as shown in the figure; the X-rays travel along the z axis which is perpendicular to the cleavage face $ABD'C$. Supposing the rhomb to contain four molecules of $CaCO_3$, the dimensions are $BC = 9{\cdot}94$ A, $AD' = 8{\cdot}06$ A, $AD = 6{\cdot}28$ A, and the angle between GG' and the axis of z is 19°.

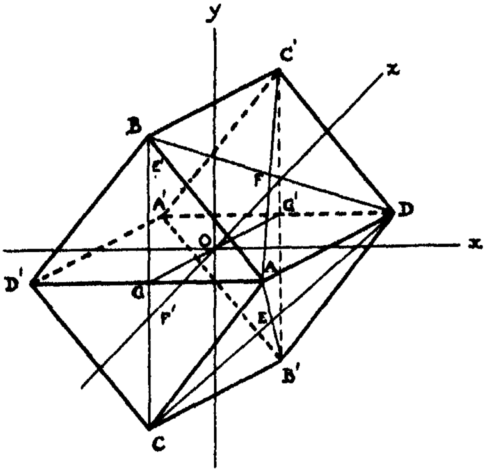

FIGURE 7. The calcite rhomb.

The true unit cell contains two molecules; its translations are AE', AF', AG'. The corresponding equations are

$$5{\cdot}005h \pm 2{\cdot}485k - 3{\cdot}030(l-1) = M(\lambda),$$

$$1{\cdot}950h - 6{\cdot}060(l-1) = M(\lambda), \text{ integral multiple of } \lambda.$$

These are plotted as the firm curved lines in the (h, k) diagram of figure 8, the wave-length being 0·71 A. It will be observed that at points marked a, b, c, d, e, f, g, h, curves of the three series come near to coincidence. Strong diffuse spots are found at these points, as is to be expected on the simple diffraction hypothesis. Their positions are marked on the figure. As these positions are oddly placed, the coincidence is the more satisfactory.

A number of other points of less intensity, some of them very faint and difficult to place, are found in the photograph. These do not all lie on the diagram of firm lines. All of these, with the exception of one or two which are due to β rays, and one or two which are clearly spurious, since they only appear on some of the plates, have been transferred to the diagram.

It is a striking fact that nearly all of them lie on a network which is in fact the diffraction pattern for the translations *AB*, *AC*, and *AD*, as if the 4 molecule cell were really the unit cell. The diagram is shown in dotted lines; it is calculated from the equations

$$4{\cdot}030h \pm 4{\cdot}97k = M(\lambda),$$

$$2{\cdot}080h + 6{\cdot}060(l-1) = M(\lambda).$$

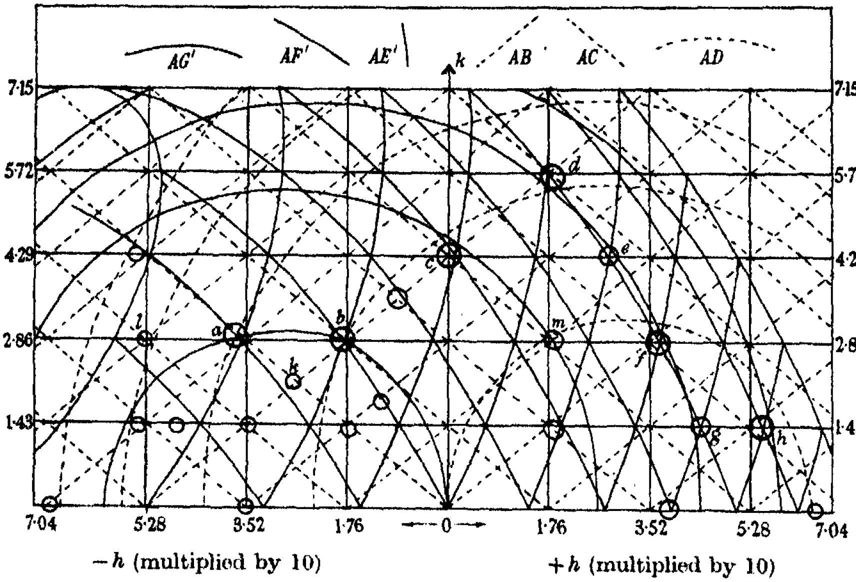

FIGURE 8

Most of the strong spots lie on this diagram also, as they should do; but not all of them because it does not always follow that if the diffracted pencil from *A* is in phase with the diffracted pencils from *E'*, *F'* and *G'*, it is also in phase with pencils from *B*, *C* and *D*. Such, for example, are the points marked *e* and *g*. On the other hand, the less intense points marked *k*, *l*, *m* belong to the diagram of the cleavage rhomb. The most direct explanation of this unexpected result could be that the four molecules of this rhomb differ from each other in some way; further experiment is required. One or two faint spots remain to be accounted for.

The short portions of lines which are placed above the main diagram in figure 8 show the meanings of the various lines in the figure. Thus the dotted line marked *AB* denotes that the dotted lines sloping the same way in the figure are the loci of all points giving values of *h* and *k* for which the pencils diffracted at *A* and *B* are in the same phase.

Diffraction of monochromatic X-rays by crystals at high temperatures

By Sir W. Lawrence Bragg, F.R.S.

(*Received* 10 *March* 1941)

The diffuse spots which appear in the diffraction pattern of a crystal at high temperatures, to which Preston (1939) and Laval (1939) have drawn attention, have the following characteristics:

(*a*) When the initial radiation is monochromatic, or has a strong monochromatic component, the spots appear in positions where rays scattered from neighbouring elements of the fundamental lattice reinforce each other.

(*b*) A crystal irradiated with white radiation containing a monochromatic component gives at the same time sharp Laue spots and diffuse spots. If a rotation photograph is taken with monochromatic radiation, the usual sharp spots appear, together with the diffuse diffraction.

(*c*) As the crystal is heated, the diffuse spots increase in strength and the sharp spots become fainter.

The positions of the diffuse spots can be explained by supposing that the crystal is broken up into a number of small approximately parallel elements. When monochromatic rays fall on an extended perfect crystal, the three conditions for diffraction must be rigorously obeyed if a diffracted beam is to be observed, and the beam is sharply defined. For a very small crystal, only a few atoms wide in each direction, diffraction is strong in any direction for which the three conditions are approximately obeyed, and the diffracted beam is diffuse. Since the form of the diffuse pattern resembles that which would be observed if the crystal consisted of numerous small parallel elements which diffract independently, Preston and W. H. Bragg have used this analogy as a basis for analysing it.

This cannot, however, be the complete explanation. If the crystal were so broken up by the heat waves, the Laue spots and spots of the rotation photograph would also be diffuse. This is not the case; they are as sharp at high temperatures as at low, though diminished in intensity. It might be postulated that part of the crystal remains unchanged and gives the sharp spots, while another part breaks down to give the diffuse spots. Such a supposition is not as attractive an explanation of the simultaneous production of sharp and diffuse spots by the one crystal structure. The essential feature of the first way of explaining the spots is the supposition *that the elements into which the crystal is broken down scatter independently*; the essential feature of the alternative explanation is that it takes into account the phase relationships between waves scattered by the atoms throughout the crystal, which remains a single structure though distorted by the heat waves.

It is convenient to deal with the reciprocal lattice and express the experimental results in terms of it (see 'conclusion' in Laval's paper). One example shown by Preston is that of silver $K\alpha$ (0·56 A) radiation incident upon a heated aluminium crystal in a direction parallel to a cube axis. Aluminium has a face-centred cubic lattice with $a = 4{\cdot}09$ A at 500° C. The reciprocal lattice is body-centred cubic, the side of the cube being $2/a$, as illustrated in figure 1. The points of the lattice (200), (400), (111), (311), etc. have hkl all odd or all even. These points represent Fourier elements of the distribution of electron density in the aluminium crystal, and are weighted so as to be proportional to the amplitudes of these elements. At the same time they represent the possible X-ray reflexions by the crystal. The construction for testing whether the conditions of diffraction are satisfied is to draw the familiar 'sphere of reflexion' shown in the figure, which has a radius of $1/\lambda$. If this sphere passes through a point of the lattice, there is a corresponding diffracted beam.

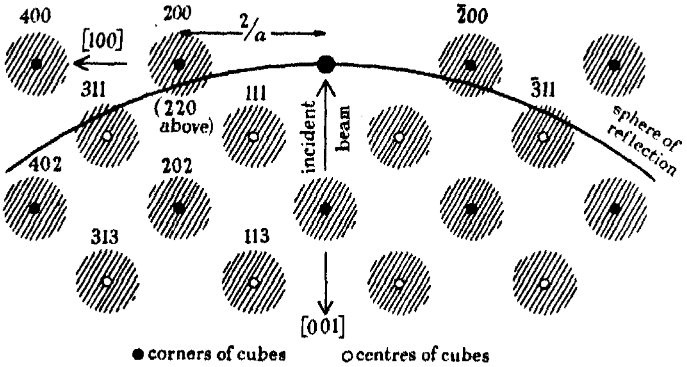

FIGURE 1

The diffuse spots at high temperatures appear when the sphere of reflexion passes near points of the reciprocal lattice; this is merely an alternative way of saying that they appear where the three conditions for diffraction are approximately but not necessarily rigorously obeyed. At the same time, if the crystal is rotated, a sharp spot appears when the sphere cuts a point of the reciprocal lattice. As Laval has shown, the whole phenomenon can be expressed by saying that the reciprocal lattice of the hot crystal consists of points, surrounded by clouds which are strongest near the points and weak between them. For instance, aluminium as shown by Preston gives diffuse spots corresponding to the section of these clouds by the sphere near (200) and (311). Laval has made a close study of the forms of the clouds around the points (002), (004) and (006) in the reciprocal lattice of sylvine.

The perfect crystal at zero temperature has a reciprocal lattice consisting of points alone. If the crystal is slightly distorted at a given instant by a heat wave whose wave-number is n, any Fourier component of wave-number N is split up into a main component of wave-number N and a pair of 'ghosts' of wave-numbers $N+n$, $N-n$. N and n are combined vectorially. The whole series of heat waves combines with each point of the reciprocal lattice and surrounds it with a cloud of ghost points, each of which represents a Fourier coefficient of the crystal structure. All such points lying on the sphere of reflexion give rise to corresponding diffracted beams.

Since all possible heat vibrations of a simple lattice reciprocate into points which fill uniformly one unit cell of the reciprocal lattice, the combinations of these vibrations with the Fourier elements of the crystal uniformly fill the whole reciprocal lattice. Monochromatic radiation is therefore scattered in all directions by the hot crystal. Three points are to be noted:

(*a*) If there is equipartition of energy amongst the heat vibrations and the elasticity is constant for all wave-numbers, and if the amplitude of the vibrations is very small, the ghost points are to be weighted equally. This follows from the consideration that the amplitude of the diffracted ghost is proportional to the amplitude of density variation caused by the heat wave, and this again is proportional to the energy of the lattice. Under such conditions the scattering would be uniform and no diffuse spots would appear.

(*b*) The amplitude is proportional to the scattering F factor of the unit of the cell at each point. If therefore the unit of pattern is a rigid complex, such as an organic molecule, its F will be a factor modifying the scattered background and its character will be imprinted upon it.

(*c*) At high temperatures the average amplitude of vibration of the points of the crystal lattice is an appreciable fraction of the distance between neighbouring points. When this is so, the reflected spectra become weaker especially in the higher orders (Debye effect). The longer heat waves are mainly responsible for the amplitude of vibration. Hence the energy of each spectrum is reduced at high temperatures by passing into the energy of the ghosts, and, as the longer heat waves produce the greatest effect, it passes mainly into the ghosts which are nearest to each lattice point. Since the cloud is therefore most dense round each lattice point, one gets a stronger diffraction at high temperatures in directions corresponding to regions where the sphere of reflexion passes near the lattice point. The diffuse spots diffracted by the hot crystal originate in this way.

The above treatment is only a qualitative version of the quantitative treatment by Debye and Waller. It is given to support the view that it is more direct to treat the effect as due to the modulation of the whole crystal by the heat waves, than as due to a breaking down of the crystal into elements by the heat waves. The essential point is that the former treatment accounts for both sharp and diffuse spots, whereas the latter cannot account for the sharp spots which appear at all temperatures.

REFERENCES

Laval 1939 *Bull. Soc. Franç. Minér.* **62**, 137.
Preston 1939 *Proc. Roy. Soc.* A, **172**, 116.

Diffuse reflexions of X-rays by crystals

By C. G. Darwin, F.R.S.

(*Received 5 March 1941*)

The straightforward method of attack on the problem of the diffuse spots found by Preston consists in applying to them the work of Faxén and Waller, or some such process. Such a method is purely inductive and would give all the information which can be extracted rigorously from the experiments. The method should certainly be worked out, as it might throw light on that very interesting subject, the short-wave limit of the Debye elastic waves. But Preston and Sir William Bragg have proposed an alternative analysis in which the atoms are supposed to stick together in small nearly rigid groups, and these groups are then displaced relative to one another through distances which impair the phase relations of the waves scattered by them. So far this description has only been qualitative, but if it should be verified quantitatively it would suggest a different way of regarding the whole subject, and it is to this that I wish to draw attention. It can best be done by analogy from a different subject.

The prediction of the tides of a harbour is done by harmonic analysis. Astronomy provides a set of natural frequencies, and the height of water as a function of the time is analysed into the sum of harmonic terms in these frequencies, with experimentally determined amplitudes and phases. Such an analysis gives a complete prediction of the future height at any time, but it does not always give the best description of what is happening. For example we might apply the analysis to an estuary which dried out completely at half tide, and the method would still be applicable, yielding the lower half of the curve as a flat level, but the examination of the table of amplitudes and phases would in no way suggest this constancy of level for half the time. The method of harmonic analysis, though perfect and complete, may become uninformative.

It seems possible that the same might be true of the harmonic analysis of the elastic waves in the crystal, but there is an important difference because with the tides we know both amplitude and phase but in the crystal only the amplitude, and the method of X-rays is incompetent to give any information about the relative phases of the various elastic waves. If the pure inductive analysis were carried to completion, it might be found that, by equipping each wave with an appropriate phase, the combined waves yielded groups of atoms of the type proposed by Bragg. If the phases cannot be so chosen, then we may be sure that Bragg's description will break down in some respect. If they can, there is still no *proof* of the correctness of his analysis, but it becomes a possibility well worth exploring, since it gives a very different picture of crystalline structure from that usually adopted in atomic theories of the solid state. It might for example be interesting to examine whether there would be any difference in such phenomena as elasticity or the plastic yielding of metals when the typical strain displacements are regarded not as continuously variable from each atom to its neighbour, but as though the crystal broke up into small blocks each composed of a few atoms nearly rigidly tied together, with the strain imposed on the block as a whole.

An objection may be felt against the suggestion in that it would seem, at first sight, that it would kill the ordinary Laue spots, but this certainly calls for careful examination. Without closer analysis it is not evident that the partial disorder of the small groups must remove so much of the long-range order as to spoil the Laue spots; only a thorough analysis of the relative intensities of the two types of spot could clear this up. The situation may be summarized by saying that the method of Preston and Bragg is certainly a convenient half-way house giving the positions of the diffuse spots. If that is all it is, then it will break down by failure to give correctly the intensities or positions of some such spots, but if it is successful in giving them all, including the intensities of the ordinary Laue spots, then it becomes an important contribution to our ideas of crystal structure. It must remain a matter for trial whether the analysis should be made by building on the inductive process of Faxén, or whether a new start based on the small groups of atoms themselves would be more profitable.

Diffuse reflexions of X-rays by crystals

By G. I. Finch, F.R.S.

(*Received* 26 *February* 1941)

In 1937 Dr H. Wilman and I (Finch and Wilman 1937) first drew attention to a new effect consisting in the occurrence of broad bands or areas of blackening in electron diffraction transmission patterns obtained from crystals of organic compounds such as long-chain hydrocarbons and polycyclic aromatic compounds. We found that the position of these diffuse areas corresponded to the arrangement and separation of the carbon atoms in the molecules.

Subsequently, in collaboration with Dr A. Charlesby (1939), we were able to show that this diffuse-area pattern appeared to be due to molecules which, though orientated with respect to the beam in accordance with the crystal orientation, nevertheless bore no definite phase relationship to each other, and this pattern thus resembled that of a gaseous stream of orientated molecules. We found that this lack of phase relationship could be explained on the assumption that, due to thermal agitation, the individual molecules were displaced from their mean position in a random fashion, there being no connexion between the displacement of adjacent molecules. The expression for the diffracted beam intensity can be written

$$I = (A^2+B^2)\frac{\sin^2 M_1 h\pi}{\sin^2 h\pi}\,\frac{\sin^2 M_2 k\pi}{\sin^2 k\pi}\,\frac{\sin^2 M_3 l\pi}{\sin^2 l\pi}\,(\overline{\cos\phi})^2 + N\sum_p (A_p^2+B_p^2)(1-\overline{\cos^2\phi}),$$

where A^2+B^2 is the structure factor for the complete unit cell, whereas $A_p^2+B_p^2$ is the structure factor for each independently moving group or molecule. ϕ is the phase angle introduced by the motion of each molecule from its mean position and hence depends on the direction of the emergent and incident beams, as well as on the amplitude of motion. The factor $(\overline{\cos\phi})^2$ is a thermal factor, decreasing the spot intensity at increasing distances from the central spot. On the other hand, $1-\overline{\cos^2\phi}$ increases with the distance. The pattern thus consists of a spot pattern modified by a thermal factor, and also of a diffuse area pattern corresponding to the orientation of the individual molecules in the crystal, the latter part of the pattern being such that the intensity near the central spot is very small, but increases to a finite limit on receding away from the central spot.

The calculation of the quantity $(\overline{\cos\phi})^2$ was carried out with certain assumptions (restoring force proportional to displacement, molecules vibrating independently and using Maxwell-Boltzmann statistics) and leads to the value

$$(\overline{\cos\phi})^2 = \exp\left(-\frac{16\pi^2\sin^2\theta}{\lambda^2}\frac{kT}{f}\right)$$

similar to that obtained by Debye in his initial work on strongly bound lattices. A different type of distribution law would not, however, alter the above conclusions.

For true Bragg spots h, k and l must all be integers, and the resultant intensity of the spots will be proportional to the square, N^2, of the number of unit cells. In certain cases (e.g. electron diffraction transmission patterns) not all three indices will be simultaneously integral, and the spot intensity will depend on the number N of unit cells to a power between 1 and 2. The diffuse pattern intensity will however be accurately proportional to N. The ratio of the intensity of spot and diffuse area patterns increases with increasing number of unit cells, and thus with increasing crystal thickness the diffuse area effect will become less clear. This presumably accounts for the fact that the diffuse area pattern has not so far been obtained with X-rays. Nevertheless it is felt that, subject to suitable preparation of specimens, they should be observable.

From a comparison between the patterns found by X-rays and electron diffraction the following factors emerge.

(*a*) In electron diffraction the diffuse pattern is directly associated with the orientation of the individual molecules. This does not appear to be the case with the X-ray pattern.

(*b*) Both effects depend on imperfections produced in the crystal lattice by thermal agitation. Depending on the strength of the intermolecular forces the real physical units (molecules or blocks) of the structure will either move as virtually independent groups, or else as strongly coupled groups with strong mutual interaction. Where a diffuse pattern of molecular origin appears intermolecular forces must be slight. Where the diffuse pattern on the other hand does not appear to be related to the orientation and structure of the molecules the inter-unit forces must be more appreciable.

REFERENCES

Charlesby 1939 *Proc. Phys. Soc.* **51**, 479.
Finch and Wilman 1937 *Ergebn. exakt. Naturw.* **16**, 375.

The effect of thermal vibrations on the scattering of X-rays

By M. Born, F.R.S. and Kathleen Sarginson
University of Edinburgh

(*Received* 4 *March* 1941)

The structures discovered recently in the background of Laue photographs show a striking dependence on temperature. After discussing theories suggested by Raman and Nilakantan, and by Preston and Bragg, it is assumed that there can be no other explanation of this phenomenon than the effect of thermal vibrations, as first discussed by Debye. Although there is an extended literature on this subject, it seemed worth while to reconsider the problem. Formulae are derived representing the Laue spots and the background for any crystal as function of its structure and of temperature. These formulae are simplified by applying them to the case of the three cubic Bravais lattices; for the body centred lattices one obtains an expression for the position of the spots which is identical with that given by Bragg, but with an additional law expressing the dependence of intensity on temperature. Approximate formulae are developed for all three cubic Bravais lattices which describe the position, shape, and intensity of the 'extra spots' in the vicinity of Laue spots.

INTRODUCTION

The general background of luminosity on Laue photographs is not structureless, as the theory of Debye (1914) predicts, but consists of more or less well-defined spots and streamers (Friedrich 1913; Wadlund 1938; Preston 1939; Raman and Nilakantan 1940, 1941; Lonsdale *et al.* 1940, 1941). These 'extra spots' differ from the Laue spots chiefly by the fact that they are not bound on definite positions of the crystal relative to the incident (monochromatic) beam, but exist for a continuous range of angles, though with decreasing intensity for increasing distance from the Laue spots. A conspicuous feature of the spots is the decrease of intensity with lowering temperature.

It is this latter fact which indicates very strongly that the mechanism responsible for these extra spots must be the temperature movement of the atoms in the crystal, as considered in Debye's paper. There exist a number of publications (Brillouin 1922; Faxén 1923; Waller 1923, 1928; Waller and James 1927; James, Waller and Hartree 1928; Jauncey and Harvey 1931; Woo 1932; Ott 1935; Manguin and Laval 1939; Zachariasen 1940) which contain corrections and improvements of Debye's theory; some of them (Faxén, Waller, Zachariasen) derive the existence of maxima in the scattered radiation. Raman rejects these theories as inconsistent with his observations (although he uses a formula identical with that of Faxén, for representing the extra spots of diamond) and suggests another hypothesis, namely, that the extra spots are due to a modulation of the lattice vibrations excited by the transfer of energy of momentum from the incident X-rays to the crystal. A third type of explanation, first suggested by Preston (1939), was recently developed by Sir William Bragg (1940) into a definite formula which represents the position of the extra spots for KCl fairly well. The assumption is that small groups of atoms produce their own diffraction patterns, apart from the Laue spots due to the crystal as a whole; a group of eight particles in the corners of a cube lead to the successful formula.

None of these theories seemed to us completely satisfactory. To begin with the last one (Preston-Bragg), the assumption of very small groups of particles scattering independently from the rest is hardly reconcilable with other well-established knowledge about crystal lattices. Further, KCl is face-centred cubic, and neither the first neighbours (of the other kind) nor the second neighbours (of the same kind) form a cube. Lastly, the strong dependency of the intensity of the spots on temperature cannot be explained by such a simple model.

Nevertheless, Bragg's formula for the position of the spots seems to fit the observations so well that one would expect it to be the result of a more satisfactory theory based on the temperature movement. It is one of our aims to show that this is the case.

Concerning Raman's hypothesis, the only possible interpretation seems to be that the extra spots are due to an ordinary Raman effect enhanced by interference. Raman scattering has already been considered in the paper of Ott, quoted above, where it is shown that it has no observable effect. As this theory is very complicated, we have reconsidered the question from the standpoint of Placzek's (1934) quasi-classical theory and found that the change of polarizability due to atomic vibrations gives additional terms to the direct vibrational (Debye) effect, but with a small intensity, namely, in the ratio of Raman scattering to Rayleigh scattering (or of the square of the ratio of total polarizability to its alteration induced by the thermal vibrations). It is a secondary effect hardly observable. We have also considered the effect of electronic excitation waves (Ehrenfest 1929; Frenkel 1931; Peierls 1932) on scattering and found it much too small.

There remains only the vibrational theory. In spite of the considerable number of publications devoted to it, we have reconsidered the problem because none of them reveals clearly the simple fundamental character of the 'background' scattering, the maxima of which are observed as 'extra spots'. The majority of the publications are repetitions of Debye's classical treatment with some modifications and improvements. A few (Waller, Ott) are careful quantum-mechanical investigations, but not suitable for the discussion of the present problem because of too general assumptions and consequently too great complication. Ott considers simultaneously electronic and atomic excitation levels; but it is well known from Placzek's theory of the Raman effect (quoted above) that this is not necessary even in the optical region, and of course even less so in the X-ray region where the photons are extremely large compared with the acoustical quanta.

For the purpose of describing the influence of thermal motion on scattering, one can replace the electronic action by a simple factor; but one has to use quantum mechanics for the calculation of the influence of the vibrations for obtaining the dependence on temperature in the correct form.

We shall derive the law of scattering for any atomic system with a degree of accuracy sufficient for our purpose, and apply it to the case of an arbitrary crystal lattice. The expression for the background scattering is then simplified for cubic lattices of the Bravais type. Debye's approximation of the lattice vibrations by the spectrum of a continuous medium is of little use for the background scattering, as it depends explicitly on the real acoustical spectrum, the frequency being a periodic function of the wave numbers. For sake of simplification, we neglect the vector character of the elastic waves and assume that the interatomic forces are acting only between first neighbours. In this way, we obtain a scattering law which represents the position of the maxima by a formula similar to that of Bragg, but gives also the dependence on temperature. In the vicinity of the Laue spots the position, shape and intensity of the extra spots can be described with the help of developments with respect to powers of the angular deviation of the crystal from its Laue position. In the present paper we give only the lowest terms of developments; in this approximation the intensity of the maxima turns out to change in a symmetric way if the spots are moved through the Laue spot by rotating the crystal. Experimentally a distinct asymmetry of intensity is observed. Therefore, the next approximation must be calculated. This and other improvements will be treated in a following publication.

1. Scattering of X-rays by an atomic system

We consider a system of N atoms, which in equilibrium have the position vectors $\mathbf{r}_k$ ($k = 1, 2, \ldots, N$) and are displaced by thermal motion to $\mathbf{r}_k + \mathbf{u}_k$, where the displacements $|\mathbf{u}_k|$ are considered as small.

Let the wave vectors of the incident and scattered beam of X-rays be

$$\mathbf{K} = \frac{2\pi}{\lambda}\mathbf{s}, \quad \mathbf{K}' = \frac{2\pi}{\lambda}\mathbf{s}', \quad |\mathbf{s}| = |\mathbf{s}'| = 1, \tag{1·1}$$

where λ is the wave-length which is assumed to be practically unchanged by the scattering. Nevertheless, the small changes of frequency due to the interaction of the light wave with the atom cannot be completely neglected, as they are responsible for the incoherence of the different components.

We distinguish the different quantum states of the atomic vibrations by a quantum number n which stands symbolically for a whole set of quantum numbers to be defined presently. The system has, on account of the thermal motion, a certain probability W_n to be in the state n. Under the action of the incident light wave it makes transitions to all possible other states n' (lower and higher ones as well) emitting a radiation, the intensity of which is proportional $|\mathscr{M}(n, n')|^2$, where $\mathscr{M}$ is the electric moment. This depends on the amplitude of the incident wave, properly retarded; for a crystal, small compared with the distance r to the observer, we can write, following Placzek,

$$\mathscr{M} = \sum_k \alpha_k \mathscr{E}_0 e^{i(\mathbf{K}-\mathbf{K}')\cdot(\mathbf{r}_k+\mathbf{u}_k)},$$

omitting all effects of the vector character of the light wave. α_k is the polarizability of the atom k which is in general a function of the positions $\mathbf{r}_k$ and displacements $\mathbf{u}_k$ of the other atoms. We assume it independent of the $\mathbf{u}_k$, which means neglecting the Raman effect. α_k can be calculated with the help of the well-known dispersion formula of quantum theory where it is expressed in terms of the energy states and matrix elements of the polarizabilities of the atoms. We assume this calculation as performed and write

$$\alpha_k = \alpha_0 f_k,$$

where α_0 is the polarizability due to a free electron and f_k the atomic scattering factor. If we define

$$f = \sum_k f_k e^{i(\mathbf{K}-\mathbf{K}')\cdot(\mathbf{r}_k+\mathbf{u}_k)}, \tag{1·2}$$

and denote by $\mathcal{I} = \mathcal{E}_0^2$ the incident intensity, the scattered intensity for the transition $n \rightarrow n'$ can be written

$$\mathcal{I}_{nn'} = \mathcal{I}_0 C \,|\, f(n, n') \,|^2, \tag{1·3}$$

where $f(n, n')$ is the matrix element of f for this transition and

$$C = \left(\frac{e^2}{mc^2}\frac{1}{r}\right)^2 \frac{1 + \cos^2\vartheta}{2} \tag{1·4}$$

is the scattering power of a free electron (Thomson factor).

All these induced emissions correspond to slightly different frequencies $\omega \pm \omega(n, n')$ and are therefore incoherent. We neglect $\omega(n, n')$ as small compared with the X-ray frequency ω; but we take account of the incoherency by forming the total intensity

$$\mathcal{I} = \mathcal{I}_0 C \sum_n \sum_{n'} |\, f(n, n') \,|^2 \, W_n. \tag{1·5}$$

We describe the quantum state of the vibrating system with the help of normal co-ordinates ξ_j, introduced by the linear transformation

$$\mathbf{u}_k = \frac{1}{\sqrt{m_k}} \sum_j \mathbf{e}_k^j \xi_j, \quad \xi_j = \sum_k \sqrt{m_k}(\mathbf{e}_k^j \cdot \mathbf{u}_k), \quad (j = 1, 2, \ldots, 3N), \tag{1·6}$$

where $\mathbf{e}_k^j$ is the vector belonging to the proper frequency ω_j, normalized in such a way that

$$\sum_k \mathbf{e}_k^j \cdot \mathbf{e}_k^{j'} = \delta_{jj'}, \quad \sum_j e_{kx}^j \cdot e_{k'y}^j = \delta_{kk'} \delta_{xy}. \tag{1·7}$$

The Hamiltonian becomes

$$\mathcal{H} = \tfrac{1}{2} \sum_j (p_j^2 + \omega_j^2 \xi_j^2); \tag{1·8}$$

where p_j is the conjugate momentum to ξ_j. The wave function of the whole system is a product of (normalized) wave functions of the oscillator

$$\psi(n, \xi) = \psi(n_1, \xi_1)\, \psi(n_2, \xi_2) \ldots, \tag{1·9}$$

the number of factors being $3N - 6$ (for $N > 2$); the symbol n replaces the set of single quantum numbers n_1, n_2, ..., describing the states of the independent oscillators.

Since the ψ are real (Hermitean functions), we have

$$f(n, n') = \int \psi(n, \xi) f \psi(n', \xi)\, d\xi = f(n', n); \tag{1·10}$$

hence $$\sum_{n'} |\, f(n, n') \,|^2 = \sum_{n'} f(n, n') f^*(n', n) = |\, f \,|^2(n, n),$$

the diagonal element of the matrix $|f|^2$, and (1·5) becomes

$$\mathscr{I} = \mathscr{I}_0 C \sum_n |f|^2(n,n)\, W_n. \tag{1·11}$$

We introduce the ξ_j in (1·2) and obtain

$$f = \sum_k A_k e^{i\sum_j \mathscr{L}_k^j \xi_j}, \tag{1·12}$$

with $$A_k = f_k e^{i(\mathbf{K}-\mathbf{K}').\mathbf{r}_k}, \quad \mathscr{L}_k^j = \frac{1}{\sqrt{m_k}}(\mathbf{K}-\mathbf{K}').\mathbf{e}_k^j; \tag{1·13}$$

thus $$|f|^2 = \sum_{kk'} A_k A_{k'}^* e^{i\sum_j (\mathscr{L}_k^j - \mathscr{L}_{k'}^j)\xi_j}. \tag{1·14}$$

The intensity (1·11) now becomes

$$\mathscr{I} = \mathscr{I}_0 C \sum_n W_n \sum_{kk'} A_k A_{k'}^* \int \psi^2(n,\xi)\, e^{i\sum_j (\mathscr{L}_k^j - \mathscr{L}_{k'}^j)\xi_j} d\xi. \tag{1·15}$$

Most of the previous papers (quoted in the Introduction) treat this integral by developing the exponential function in a power series

$$1 + i\sum_j (\mathscr{L}_k^j - \mathscr{L}_{k'}^j)\xi_j + \dots$$

and integrating term by term. The term linear in ξ_j vanishes, the next one gives the factors $\overline{\xi_j^2} = \xi_j^2(n,n) = \int \psi^2(n,\xi)\,\xi_j^2\, d\xi$. Now since the potential energy of the oscillator $\frac{1}{2}\omega_j \overline{\xi_j^2} = \frac{1}{2}kT$ is finite, $\overline{\xi_j^2}$ becomes very large for small ω_j. This fact prohibits the application of such an approximation method to crystals, for the frequencies of the acoustic branch approach zero for long waves. It is therefore unavoidable to evaluate the integral correctly, and this has been done by Ott; a new derivation is given in the Appendix. In order to apply Ott's formula, we write (1·15)

$$\mathscr{I} = \mathscr{I}_0 C \sum_{kk'} A_k A_{k'}^* \prod_j \operatorname{mean}\left(e^{i(\mathscr{L}_k^j - \mathscr{L}_{k'}^j)\xi_j}\right),$$

where $$\operatorname{mean}(e^{i\mu\xi}) = \sum_n W_n \int \psi^2(n,\xi)\, e^{i\mu\xi}\, d\xi = \sum_n W_n (e^{i\mu\xi})_{nn}$$

$$= e^{-\frac{1}{4}(\mu^2\hbar/\omega)\coth\frac{1}{2}\beta},$$

according to (A. 11). Hence we obtain

$$\mathscr{I} = \mathscr{I}_0 C \sum_{kk'} A_k A_{k'}^* e^{-\mathscr{U}_{kk'}}, \tag{1·16}$$

where $$\mathscr{U}_{kk'} = \sum_j \hbar(\mathscr{L}_k^j - \mathscr{L}_{k'}^j)^2 \frac{\coth\frac{1}{2}\beta_j}{4\omega_j}, \quad \beta_j = \frac{\hbar\omega_j}{kT}. \tag{1·17}$$

The temperature function appearing here (and in the following sections) is directly related to the averaged energy of the linear oscillator:

$$\bar{\epsilon} = \hbar\omega\left(\frac{1}{2}+\frac{1}{e^{\beta}-1}\right) = \tfrac{1}{2}\hbar\omega\coth\tfrac{1}{2}\beta, \quad \beta = \frac{\hbar\omega}{kT}. \tag{1·18}$$

The formula (1·16) represents correctly the temperature influence on the scattering of molecules. Although this problem is interesting by itself, we shall not enter into a discussion here, but proceed to the treatment of crystals. One remark only has to be made. The centre of the system must be considered as fixed so that zero vibrations (translations) are excluded. This is physically evident and necessary in order to avoid infinite terms in (1·17), as $\dfrac{\coth\frac{1}{2}\beta}{\omega}\to\infty$ if $\omega\to 0$.

2. SCATTERING OF X-RAYS BY A CRYSTAL LATTICE

Let $\mathbf{a}_1$, $\mathbf{a}_2$, $\mathbf{a}_3$ be the basis vectors of the lattice, $\mathbf{b}_1$, $\mathbf{b}_2$, $\mathbf{b}_3$ those of the reciprocal lattice.

The cell contains several atoms $k = 0, 1, 2, \ldots$ with the position vectors $\mathbf{r}_k$.

An arbitrary lattice point has the position vector

$$\mathbf{r}_k^l = \mathbf{r}_k + l_1\mathbf{a}_1 + l_2\mathbf{a}_2 + l_3\mathbf{a}_3. \tag{2·1}$$

We consider a piece of the crystal similar in shape to the cell, containing $n^3 = N$ cells, and use the cyclic boundary conditions (Born 1923).

Let the second order terms of the potential energy be

$$\mathscr{U}_2 = \tfrac{1}{2}\sum_{klx}\sum_{k'l'y}\begin{bmatrix} l-l' \\ kk' \\ xy \end{bmatrix} u_{kx}^l u_{k'y}^{l'}; \tag{2·2}$$

here the coefficients satisfy

$$\begin{bmatrix} l \\ kk' \\ xy \end{bmatrix} = \begin{bmatrix} -l \\ k'k \\ yx \end{bmatrix}, \quad \sum_{kl}\begin{bmatrix} l \\ kk' \\ xy \end{bmatrix} = 0, \tag{2·3}$$

since $\mathscr{U}_2$ must vanish for equal displacements of all particles. The equations for small vibrations

$$-\omega^2 m_k u_{kx}^l + \sum_{k'l'y}\begin{bmatrix} l-l' \\ kk' \\ xy \end{bmatrix} u_{k'y}^{l'} = 0 \tag{2·4}$$

can be solved by the plane waves

$$\mathbf{u}^l_k = \mathbf{e}^j_k(q)\frac{e^{i(lq)}}{\sqrt{N}}, \tag{2·5}$$

$$(lq) = l_1q_1+l_2q_2+l_3q_3, \quad q_\alpha = \frac{2\pi}{n}\kappa_\alpha, \quad \kappa_1, \kappa_2, \kappa_3 \text{ integers}, \quad -\tfrac{1}{2}n \leqslant \kappa_\alpha \leqslant \tfrac{1}{2}n,$$

if $\mathbf{e}^j_k(q)$ satisfy the linear equations

$$m_k\,\omega_j^2(q)\,e^j_{kx}(q) - \sum_{k'y}\begin{bmatrix}kk'\\xy\\q\end{bmatrix}e^j_{k'y}(q) = 0, \tag{2·6}$$

where

$$\begin{bmatrix}kk'\\xy\\q\end{bmatrix} = \sum_l\begin{bmatrix}l\\kk'\\xy\end{bmatrix}e^{-i(lq)}. \tag{2·7}$$

The characteristic equation of (2·6) determines the proper frequencies $\omega_j(q)$. The $\mathbf{e}^j_k(q)$ are normalized according to

$$\sum_k \mathbf{e}^j_k(q)\,.\,\mathbf{e}^{*j'}_k(q) = \delta_{jj'}, \quad \sum_j e^j_{kx}(q)\,e^{*j}_{k'y}(q) = \delta_{kk'}\delta_{xy}. \tag{2·8}$$

We introduce *complex normal co-ordinates* by

$$\mathbf{u}^l_k = \frac{1}{\sqrt{m_k}}\sum_{jq}\mathbf{e}^j_k(q)\frac{e^{i(lq)}}{\sqrt{N}}\,\xi_j(q), \quad \xi_j(q) = \sum_{kl}\sqrt{m_k}\frac{e^{-i(lq)}}{\sqrt{N}}\,\mathbf{e}^j_k(q)\,.\,\mathbf{u}^l_k. \tag{2·9}$$

Then (2·2) goes over in

$$\mathscr{U}_2 = \tfrac{1}{2}\sum_{jq}\omega_j^2(q)\,|\,\xi_j(q)\,|^2. \tag{2·10}$$

The complex variables $\xi_j(q)$ are not ordinary normal co-ordinates to which wave mechanics can be applied. They are not quite independent; for as (2·3) and (2·7) show, one has

$$\begin{bmatrix}k'k\\yx\\q\end{bmatrix} = \begin{bmatrix}kk'\\xy\\q\end{bmatrix}^* = \begin{bmatrix}kk'\\xy\\-q\end{bmatrix}; \tag{2·11}$$

hence

$$e^j_k(q)^* = e^j_k(-q), \tag{2·12}$$

and

$$\xi_j(q)^* = \xi_j(-q). \tag{2·13}$$

In order to obtain real and independent normal co-ordinates, we split ξ_j in real and imaginary parts, adding a factor $1/\sqrt{2}$:

$$\xi_j(q) = \frac{1}{\sqrt{2}}\{\eta_j(q)+i\zeta_j(q)\}. \tag{2·14}$$

From (2·12) one has

$$\eta_j(-q) = \eta_j(q), \quad \zeta_j(-q) = -\zeta_j(q). \tag{2·15}$$

Now we can choose the $\eta_j(q)$, $\zeta_j(q)$ arbitrary for just half of the points of the total fundamental domain, $-\pi \leqslant q_\alpha \leqslant \pi$ $(-\frac{1}{2}n \leqslant \kappa_\alpha \leqslant \frac{1}{2}n)$, for instance

$$-\pi \leqslant q_1 \leqslant \pi, \quad -\pi \leqslant q_2 \leqslant \pi, \quad 0 \leqslant q_3 \leqslant \pi. \tag{2·16}$$

The total number of independent co-ordinates $\eta_j(q)$, $\zeta_j(q)$ is then again $n^3 = N$ for each branch j, as (2·10) goes over in

$$\mathscr{U}_2 = \tfrac{1}{2}\sum_{jq} \omega_j^2(q)\,\tfrac{1}{2}\{\eta_j^2(q) + \zeta_j^2(q)\} = \tfrac{1}{2}\sum_{jq}{}' \,\omega_j^2(q)\,\{\eta_j^2(q) + \zeta_j^2(q)\}, \tag{2·17}$$

where the accent at the summation sign means that the sum is to be extended over half the q-space, as defined by (2·16).

The pair of variables $\eta_j(q)$, $\zeta_j(q)$ is degenerate; but as we are not interested in the removal of this degeneracy by higher approximations, we need not pay attention to it and can form the total wave function as a product

$$\psi(n, \xi) = \prod_{jq}{}' \phi(n_j(q), \eta_j(q))\,\chi(\bar{n}_j(q), \zeta_j(q)), \tag{2·18}$$

where $n_j(q)$ and $\bar{n}_j(q)$ are independent quantum numbers and the accent at the product has the same meaning as at the sum above in (2·17): restriction to half the q-space (2·16).

We form now the function f, (1·2), for the crystal; it can be written

$$f = \sum_{kl} f_k e^{i(\mathbf{K}-\mathbf{K}')(l_1\mathbf{a}_1 + l_2\mathbf{a}_2 + l_3\mathbf{a}_3)}\, e^{i(\mathbf{K}-\mathbf{K}')\mathbf{r}_k}\, e^{i(\mathbf{K}-\mathbf{K}')\mathbf{u}_k^l}, \tag{2·19}$$

or, introducing the normal co-ordinates (2·9) and using the abbreviations

$$\left.\begin{aligned} Q_1 &= (\mathbf{K}'-\mathbf{K})\,.\,\mathbf{a}_1, \quad Q_2 = (\mathbf{K}'-\mathbf{K})\,.\,\mathbf{a}_2, \quad Q_3 = (\mathbf{K}'-\mathbf{K})\,.\,\mathbf{a}_3,\\ A_k &= f_k e^{i(\mathbf{K}-\mathbf{K}')\mathbf{r}_k},\\ \mathscr{L}_k^j(q) &= \frac{1}{\sqrt{m_k}}(\mathbf{K}-\mathbf{K}')\,.\,\mathbf{e}_k^j(q) \end{aligned}\right\} \tag{2·20}$$

and

$$(lQ) = l_1Q_1 + l_2Q_2 + l_3Q_3, \tag{2·21}$$

$$f = \sum_k A_k \sum_l e^{-i(l\,.\,Q)}\, e^{i\sum_j\sum_q \mathscr{L}_k^j(q)\xi_j(q)e^{i(l\,.\,q)}/\sqrt{N}}. \tag{2·22}$$

Thus

$$|f|^2 = \sum_{kk'} A_k A_{k'}^* \sum_{ll'} e^{-i(l-l'\,.\,Q)} \prod_{jq} e^{i\mathscr{Z}_{kk'}^{ll'j}(q)} \tag{2·23}$$

with

$$\mathscr{Z}_{kk'}^{ll'j}(q) = \frac{1}{\sqrt{N}}\{\mathscr{L}_k^j(q)\,e^{i(l\,.\,q)}\,\xi_j(q) - \mathscr{L}_{k'}^{*j}(q)\,e^{-i(l'.\,q)}\,\xi_j^*(q)\}. \tag{2·24}$$

We have now to replace the complex normal co-ordinates by the real ones, $\eta_j(q)$, $\zeta_j(q)$, as defined by (2·14). As these are only independent for half the q-space, as for instance defined by (2·16), we must replace the product $\prod\limits_q$ in (2·23) by $\prod\limits_q{}'$.

Now since $\mathscr{X}(-q) = \mathscr{X}^*(q)$, we have

$$\prod_q e^{i\mathscr{X}(q)} = \prod_q e^{\frac{1}{2}i[\mathscr{X}(q)+\mathscr{X}^*(q)]} = \prod_q{}' e^{i[\mathscr{X}(q)+\mathscr{X}^*(q)]}. \tag{2·25}$$

Omitting for the moment the indices j, q and combining k, l into k, we write for abbreviation

$$\frac{1}{\sqrt{N}}\mathscr{L}^j_k(q)\,e^{i(l\cdot q)} = \mathscr{L}_k. \tag{2·26}$$

Then $$\mathscr{X}_{kk'} = \mathscr{L}_k\xi - \mathscr{L}^*_{k'}\xi^* = \frac{1}{\sqrt{2}}(\mathscr{L}_k - \mathscr{L}^*_{k'})\,\eta + \frac{i}{\sqrt{2}}(\mathscr{L}_k + \mathscr{L}^*_{k'})\,\zeta;$$

hence $$\mathscr{X}_{kk'} + \mathscr{X}^*_{kk'} = \mathscr{M}_{kk'}\eta + \mathscr{N}_{kk'}\zeta,$$

with $$\left.\begin{aligned}\mathscr{M}_{kk'} &= \frac{1}{\sqrt{2}}\{(\mathscr{L}_k + \mathscr{L}^*_k) - (\mathscr{L}_{k'} + \mathscr{L}^*_{k'})\},\\ \mathscr{N}_{kk'} &= \frac{i}{\sqrt{2}}\{(\mathscr{L}_k - \mathscr{L}^*_k) - (\mathscr{L}_{k'} - \mathscr{L}^*_{k'})\},\end{aligned}\right\} \tag{2·27}$$

and the product (2·25) becomes

$$\prod_q{}' e^{i\mathscr{M}_{kk'}(q)\,\eta}\,e^{i\mathscr{N}_{kk'}(q)\,\zeta}.$$

We can now form the weighted average of the (diagonal) matrix element of each factor independently with the help of Ott's formula (see Appendix). If we add the omitted indices, we obtain

$$\prod_{qj}{}' e^{-\{\mathscr{M}^j_{kk'}(q)^2+\mathscr{N}^j_{kk'}(q)^2\}\,\hbar\coth\frac{1}{2}\beta_j(q)/4\omega_j(q)}, \quad \beta_j(q) = \frac{\hbar\omega_j(q)}{kT}. \tag{2·28}$$

From (2·27) we get easily

$$\mathscr{V}_{kk'} = \tfrac{1}{2}(\mathscr{M}^2_{kk'} + \mathscr{N}^2_{kk'}) = |\mathscr{L}_k|^2 + |\mathscr{L}_{k'}|^2 - (\mathscr{L}_k\mathscr{L}^*_{k'} + \mathscr{L}^*_k\mathscr{L}_{k'}),$$

or, restoring the omitted indices

$$\begin{aligned}\mathscr{V}^{l-l'}_{kk'}(jq) = \frac{1}{N}\{|\mathscr{L}^j_k(q)|^2 + |\mathscr{L}^j_{k'}(q)|^2 \\ -[\mathscr{L}^j_k(q)\,\mathscr{L}^{*j}_{k'}(q)\,e^{i(l-l'\cdot q)} + \mathscr{L}^{*j}_k(q)\,\mathscr{L}^j_{k'}(q)\,e^{-i(l-l'\cdot q)}]\}.\end{aligned} \tag{2·29}$$

Now this is a real and even function of q. We can therefore extend the product in (2·28) over the whole q-space if we add a factor $\frac{1}{2}$ in the exponent. Hence our product becomes

$$\prod_{qj} e^{-\mathscr{V}^{l-l'}_{kk'}(jq)\,\frac{1}{2}[\hbar/\omega_j(q)]\coth\frac{1}{2}\beta_j(q)} = e^{-\mathscr{V}^{l-l'}_{kk'}}, \tag{2·30}$$

where

$$\mathscr{V}^{l-l'}_{kk'} = \sum_{jq} \mathscr{V}^{l-l'}_{kk'}(j,q)\frac{\hbar}{4\omega_j(q)}\coth\frac{\beta_j(q)}{2}. \tag{2·31}$$

We replace the summation over q by an integration

$$\sum_q \ldots = \frac{N}{(2\pi)^3}\int_{-\pi}^{+\pi} d\bar{q}\,\ldots,$$

$$d\bar{q} = dq_1 dq_2 dq_3.$$

Substituting (2·28), we obtain

$$\mathscr{V}^{l-l'}_{kk'} = \mathscr{U}_k + \mathscr{U}_{k'} - \mathscr{U}^{l-l'}_{kk'}, \tag{2·32}$$

where

$$\left.\begin{aligned} \mathscr{U}_k &= \frac{1}{(2\pi)^3}\sum_j \int_{-\pi}^{\pi} d\bar{q}\,|\mathscr{L}^j_k(q)|^2 \frac{\hbar}{4\omega_j(q)}\coth\frac{\beta_j(q)}{2},\\ \mathscr{U}^{l-l'}_{kk'} &= \frac{1}{(2\pi)^3}\sum_j \int_{-\pi}^{\pi} d\bar{q}[\mathscr{L}^j_k(q)\,\mathscr{L}^{*j}_{k'}(q)\,e^{i(l-l'.q)} + \mathscr{L}^{*j}_k(q)\,\mathscr{L}^j_{k'}(q)\,e^{-i(l-l'.q)}]\\ &\qquad\qquad\qquad\qquad\qquad\qquad\qquad\qquad \times\frac{\hbar}{4\omega_j(q)}\coth\frac{\beta_j(q)}{2}. \end{aligned}\right\} \tag{2·33}$$

The product (2·30) becomes

$$e^{-(\mathscr{U}_k+\mathscr{U}_{k'})}\,.\,e^{\mathscr{U}^{l-l'}_{kk'}}. \tag{2·34}$$

So we obtain

$$\sum_n W_n\,|\,f\,|^2(n,n) = \sum_{kk'} A_k\,A^*_{k'}\,e^{-(\mathscr{U}_k+\mathscr{U}_{k'})}\sum_{ll'} e^{-i(l-l'.Q)}\,e^{\mathscr{U}^{l-l'}_{kk'}}. \tag{2·35}$$

Now the quantities $\mathscr{U}$ can be considered as small; the correct order of magnitude will be determined later, and here the remark may suffice that as $\mathscr{L}^j_k$ is proportional to λ^{-1}, the $\mathscr{U}$ are proportional to λ^{-2} and therefore small for sufficiently soft X-rays.

Hence we develop the last factor and obtain for the double sum over l, l'

$$\sum_{ll'} e^{-i(l-l'.Q)}\{1 + \mathscr{U}^{l-l'}_{kk'} + \ldots\}. \tag{2·36}$$

Now

$$\sum_{ll'} e^{-i(l-l'.Q)} = |\sum_l e^{-i(lQ)}|^2 = (2\pi)^3 N \prod_{\alpha=1}^{3}\left(\frac{\sin\frac{1}{2}nQ}{2\pi n\sin\frac{1}{2}Q}\right)^2 = (2\pi)^3 N\delta_n(Q), \tag{2·37}$$

where $\delta_n(Q)$ is the well-known intensity factor of Laue which for $n \to \infty$

approximates a periodic Dirac function (period 2π for each Q_α). We shall assume that the crystal is big enough to replace $\delta_n(Q)$ by $\delta(Q)$. Then

$$\begin{aligned}\sum_{ll'} e^{-i(l-l'.Q)}\,\mathscr{U}^{l-l'}_{kk'}\\ &= N\sum_j \int_{-\pi}^{+\pi} d\bar{q}\,[\mathscr{L}^j_k \mathscr{L}^{*j}_{k'}\,\delta(q-Q)+\mathscr{L}^{*j}_k \mathscr{L}^j_{k'}\,\delta(q+Q)]\,\frac{\hbar}{4\omega_j}\coth\frac{\beta_j}{2}\\ &= N\sum_j [\mathscr{L}^j_k(Q)\,\mathscr{L}^{*j}_{k'}(Q)+\mathscr{L}^{*j}_k(-Q)\,\mathscr{L}^j_{k'}(-Q)]\,\frac{\hbar}{4\omega_j(Q)}\coth\frac{\beta_j(Q)}{2}\\ &= N\sum_j \mathscr{L}^j_k(Q)\,\mathscr{L}^{*j}_{k'}(Q)\,\frac{\hbar}{2\omega_j(Q)}\coth\frac{\beta_j(Q)}{2}. \qquad (2{\cdot}38)\end{aligned}$$

We write the result $$\mathscr{I} = \mathscr{I}_L+\mathscr{I}_B, \qquad (2{\cdot}39)$$

where $\mathscr{I}_L$ represents the Laue scattering and $\mathscr{I}_B$ the background scattering. In $\mathscr{I}_L$ we can replace $Q_\alpha = (\mathbf{K}'-\mathbf{K})\,.\,\mathbf{a}_\alpha$ in the factor of $\delta(Q)$ by $2\pi\kappa_\alpha$; from $(\mathbf{K}'-\mathbf{K})\,.\,\mathbf{a}_\alpha = 2\pi\kappa_\alpha$ there follows $\mathbf{K}'-\mathbf{K} = 2\pi b_\kappa$, where

$$\mathbf{b}_\kappa = \kappa_1\mathbf{b}_1+\kappa_2\mathbf{b}_2+\kappa_3\mathbf{b}_3$$

is the point in the reciprocal lattice representing the Laue spot κ. So we obtain

$$\begin{aligned}\mathscr{I}_L &= \mathscr{I}_0 CN(2\pi)^3\,\delta(Q)\sum_{kk'} A_k A^*_{k'}\,e^{-(\mathscr{U}_k+\mathscr{U}_{k'})}\\ &= \mathscr{I}_0 CN(2\pi)^3\,\delta(Q)\sum_{kk'} g_k g_{k'}\cos\left[2\pi\mathbf{b}_\kappa\,.\,(\mathbf{r}_k-\mathbf{r}_{k'})\right]. \qquad (2{\cdot}40)\end{aligned}$$

For the background scattering we obtain

$$\begin{aligned}\mathscr{I}_B &= \mathscr{I}_0 CN\sum_{kk'} A_k A^*_{k'}[\mathscr{B}_{kk'}(Q)-i\mathscr{C}_{kk'}(Q)]\,e^{-(\mathscr{U}_k+\mathscr{U}_{k'})}\\ &= \mathscr{I}_0 CN\sum_{kk'} g_k g_{k'}\left\{\mathscr{B}_{kk'}(Q)\cos\left[\frac{2\pi}{\lambda}(\mathbf{s}'-\mathbf{s})\,.\,(\mathbf{r}_k-\mathbf{r}_{k'})\right]\right.\\ &\qquad\left.+\mathscr{C}_{kk'}(Q)\sin\left[\frac{2\pi}{\lambda}(\mathbf{s}'-\mathbf{s})\,.\,(\mathbf{r}_k-\mathbf{r}_{k'})\right]\right\}, \qquad (2{\cdot}41)\end{aligned}$$

where

$$\left.\begin{aligned}\mathscr{B}_{kk'}(q) = \mathscr{B}_{k'k}(q) &= \sum_j \{\mathscr{L}^j_k(q)\,\mathscr{L}^{*j}_{k'}(q)+\mathscr{L}^{*j}_k(q)\,\mathscr{L}^j_{k'}(q)\}\,\frac{\hbar}{4\omega_j(q)}\coth\frac{\beta_j(q)}{2},\\ \mathscr{C}_{kk'}(q) = -\mathscr{C}_{k'k}(q) &= i\sum_j \{\mathscr{L}^j_k(q)\,\mathscr{L}^{*}_{k'}(q)-\mathscr{L}^{*j}_k(q)\,\mathscr{L}^j_{k'}(q)\}\,\frac{\hbar}{4\omega_j(q)}\coth\frac{\beta_j(q)}{2},\end{aligned}\right\} \qquad (2{\cdot}42)$$

$$\mathscr{U}_k = \frac{1}{2}\int_{-\pi}^{\pi}\mathscr{B}_{kk}(q)\,\frac{d\bar{q}}{(2\pi)^3}, \qquad (2{\cdot}43)$$

$$g_k = f_k e^{-\mathscr{U}_k}. \qquad (2{\cdot}44)$$

The temperature influences the scattering in two rather different ways: it changes the atomic structure factor f_k into g_k, and it produces a continuous background of the Laue spots.

We introduce now dimensionless quantities. We have

$$\mathscr{L}^j_k(q) = \frac{2\pi}{\lambda\sqrt{m_k}}(\mathbf{s}-\mathbf{s}') \,.\, \mathbf{e}^j_k(q).$$

Let ω_0 be the maximum frequency of the vibrational spectrum, and

$$w_j(q) = \frac{\omega_j(q)}{\omega_0}, \quad \Theta = \frac{\hbar\omega_0}{k}, \quad \beta_j(q) = \frac{\Theta}{T} w_j(q). \tag{2·45}$$

Then we have

$$\mathscr{B}_{kk'}(q,\xi) = \frac{b}{\Theta\lambda^2\sqrt{(\mu_k\mu_{k'})}}((\mathbf{s}-\mathbf{s}')\,\mathscr{F}^{kk'}(q,\xi)\,(\mathbf{s}-\mathbf{s}')), \quad \xi = \frac{\Theta}{T}, \tag{2·46}$$

where μ_k is the atomic weight, b a numerical constant, and the bracket indicates the quadratic form with the coefficient matrix

$$\mathscr{F}^{kk'}_{xy}(q,\xi) = \sum_j [e^j_{kx}(q)\, e^{*j}_{k'y}(q) + e^{*j}_{kx}(q)\, e^j_{k'y}(q)]\,\frac{\coth[\xi w_j(q)]}{2w_j(q)}. \tag{2·47}$$

Similarly, the coefficient $\mathscr{C}_{kk'}(q,\xi)$ is expressed by a quadratic form of $\mathbf{s}-\mathbf{s}'$ with coefficients $\mathscr{G}^{kk'}_{xy}(q,\xi)$ which are obtained from (2·47) in changing the + sign in the bracket into a − sign.

The constant b is given by (m_{H} mass of the hydrogen atom)

$$b = \frac{h^2}{2m_{\mathrm{H}}k} = 957^\circ\,\mathrm{K}\,(\mathrm{A})^2, \tag{2·48}$$

if in (2·46) λ is measured in $\mathrm{A} = 10^{-8}$ cm. From (2·43) we get

$$\mathscr{U}_k\left(\frac{\Theta}{T}\right) = \frac{b}{\Theta\lambda^2\mu_k}\left((\mathbf{s}-\mathbf{s}')\,\mathscr{F}^k\left(\frac{\Theta}{T}\right)(\mathbf{s}-\mathbf{s}')\right), \tag{2·49}$$

with

$$\mathscr{F}^k_{xy}(\xi) = \frac{1}{2}\int_{-\pi}^{\pi} \mathscr{F}^{kk}_{xy}(q,\xi)\,\frac{d\bar{q}}{(2\pi)^3}. \tag{2·50}$$

The validity of our calculation depends on the question whether the development (2·36) is admissible, and this again on the question whether $\mathscr{B}_{kk'}$, $\mathscr{C}_{kk'}$ are small. (2·46) shows that this is the case if Θ is high (hard material), λ is large (soft X-rays) and the μ_k are large (heavy atoms); furthermore if $\coth[\Theta/T\, w_j(Q)]/w_j(Q)$ is small. The latter condition excludes the immediate neighbourhood of a Laue spot ($Q_\alpha = 2\pi\kappa_\alpha$, $w(Q) = 0$) and very high temperatures ($\Theta/T \ll 1$). If these conditions are not satisfied, higher terms of the development must be considered.

We wish here to emphasize the importance of the observation of the background scattering as it depends explicitly on the elastic frequency spectrum $\{e_k^j(q), \omega_j(q)\}$. All other properties of crystals which depend on temperature, as, for instance, specific heat, thermal expansion, etc., are integrals over this spectrum and are therefore very little sensitive to the more delicate features of it; to this class of quantities belongs also the exponent $\mathscr{U}_k$ of the modified structure factor. Just as the Laue scattering allows to determine the geometry of the lattice, the background scattering supplies in principle the means to check the dynamical theory of lattice vibrations. While for the integral properties Debye's approximation is sufficient for all but the most accurate measurements, it is useless for the explanation of the background effect; for it consists in replacing the periodic functions $\omega_j(q)$ by the aperiodic $c_j q$, a process by which the most essential feature of the effect, its appearance in the neighbourhood of each Laue spot, is destroyed. We have therefore to look out for different methods in order to simplify and discuss the general formulae. This will be done in the following section.

Here we add a few remarks about the exponent $\mathscr{U}_k$. As it is an integral, one can use the Debye approximation for the three acoustical branches. Let us consider a cubic lattice and assume that no optical branches exist (simple lattice), then the index k can be dropped and $j = 1, 2, 3$ only. We replace the three frequencies $\omega_j(q)$ by one mean quantity cq (c mean velocity of sound).

From (2·42) we get

$$\mathscr{B}(q) = \frac{\hbar}{4cq}\coth\left(\frac{cq\hbar}{2kT}\right)\sum_{j=1}^{3} |\mathscr{L}^j(q)|^2.$$

On account of the cubic symmetry and the normalization (2·8) we have

$$|\mathscr{L}^j(q)|^2 = \frac{2\pi}{\lambda}(\mathbf{s}'-\mathbf{s})^2 = \frac{2\pi}{\lambda}2(1-\cos\vartheta),$$

where ϑ is the angle of deflexion.

Now we replace $N\,d\bar{q}/(2\pi)^3$ by $3N\,x^2\,dx/x_m^3$, where

$$x = \frac{c\hbar}{kT}q, \quad x_m = \frac{\Theta}{T}, \quad \Theta = \frac{c\hbar}{k}q_m;$$

then
$$N\int\frac{d\bar{q}}{(2\pi)^3} = \frac{3N}{x_m^3}\int_0^{x_m} x^2\,dx = N$$

is the number of vibrations in *one* branch. From (2·43) we obtain

$$\mathscr{U} = \frac{3}{4\pi^2}(1-\cos\vartheta)\frac{h^2}{mk\Theta}\left(\frac{2\pi}{\lambda}\right)^2 \Psi(x), \tag{2·51}$$

where

$$\left.\begin{aligned} \Psi(x) &= \frac{1}{x^2}\int_0^x \xi\,\tfrac{1}{2}\coth\tfrac{1}{2}\xi\,d\xi = \frac{1}{4}+\frac{1}{x}\Phi(x),\\ \Phi(x) &= \frac{1}{x}\int_0^x \frac{\xi\,d\xi}{e^{\xi}-1}. \end{aligned}\right\} \tag{2·52}$$

$\Phi(x)$ is the function tabulated by Debye. We have written (2·51) in such a form that it can readily be compared with Debye's formula (56″), p. 83 of his paper quoted above. $-\mathscr{U}$ coincides completely with Debye's exponent M; but as the intensity depends on the products of the form factors g_k, the effect of one kind of particles is given by $f^2 = g^2e^{-2\mathscr{U}}$; hence our exponent is in fact $2M$. The absence of this factor 2 is a mistake in Debye's paper, due to a wrong definition of the normal co-ordinates, and was corrected by Waller (1928). The agreement of our result with that of Waller is a check on the computations.

3. BACKGROUND SCATTERING FOR CUBIC BRAVAIS LATTICES

We apply our general formulae to the three Bravais types of cubic lattices (*s* simple, *f* face centred, *b* body centred). It is well known that there exists a cell for each of these which contains one particle only. Hence all sums over k can be omitted. For further simplification we replace the three branches of elastic vector waves approximately by one scalar wave; then the tensor (2·47) has to be replaced by the scalar

$$\mathscr{F}(q,\xi) = \frac{1}{3}\frac{\coth[\xi w(q)]}{w(q)}, \tag{3·1}$$

and we have the simplified intensity formula (2·41)

$$\mathscr{I}_B = \mathscr{I}_0 CN g^2 \mathscr{B}(Q, \Theta/T), \tag{3·2}$$

with (2·46)

$$\mathscr{B}(q,\xi) = \frac{2b(1-\cos\vartheta)}{\Theta\lambda^2\mu}\mathscr{F}(q,\xi) = \frac{2b(1-\cos\vartheta)}{3\Theta\lambda^2\mu}\frac{\coth[\xi w(q)]}{w(q)}. \tag{3·3}$$

It is convenient to refer the lattice vectors not to the smallest (rhombic) cell, but to the cubic cell given by the vectors

$$\mathbf{a}_1 = (a,0,0), \quad \mathbf{a}_2 = (0,a,0), \quad \mathbf{a}_3 = (0,0,a). \tag{3·4}$$

An arbitrary lattice point is given by $l_1\mathbf{a}_1 + l_2\mathbf{a}_2 + l_3\mathbf{a}_3$, where l_1, l_2, l_3 are in the three cases restricted in the following way:

$$\left.\begin{array}{ll} s: & l_1, l_2, l_3 \text{ any integer;} \\ f: & l_1, l_2, l_3 \text{ all even, or one even and two odd;} \\ b: & l_1, l_2, l_3 \text{ all even, or all odd.} \end{array}\right\} \tag{3·5}$$

a is not the distance of next neighbours, except in case s; if this distance is called r_0, one has

$$s{:}\ r_0 = a, \quad f{:}\ r_0 = a\surd 2, \quad b{:}\ r_0 = a\surd 3. \tag{3·6}$$

The three quantities Q_1, Q_2, Q_3 become rectangular components of the vector

$$\mathbf{Q} = \sigma(\mathbf{s}' - \mathbf{s}), \quad \sigma = \frac{2\pi a}{\lambda}. \tag{3·7}$$

The frequency is a periodic function of the q_α, given by, say,

$$\omega^2(q) = -\sum_l \Phi_l e^{i(lq)} = -\sum_l \Phi_l \cos(lq); \tag{3·8}$$

as ω must vanish for $q_\alpha = 0$ (translations), we have

$$\sum_l \Phi_l = 0, \tag{3·9}$$

and we can therefore write

$$\omega^2(q) = 2\sum_l \Phi_l \sin^2\frac{(lq)}{2}. \tag{3·10}$$

We introduce now the last simplification that only the first neighbours contribute appreciably to (3·10). Then we have

$$\begin{aligned} s{:}\quad \omega^2 &= 4\Phi_1\left(\sin^2\frac{q_1}{2} + \sin^2\frac{q_2}{2} + \sin^2\frac{q_3}{2}\right) \\ &= 2\Phi_1\{3 - [\cos q_1 + \cos q_2 + \cos q_3]\}, \\ f{:}\quad \omega_2 &= 4\Phi_1\left(\sin^2\frac{q_2+q_3}{2} + \sin^2\frac{q_3+q_1}{2} + \sin^2\frac{q_1+q_2}{2} + \sin^2\frac{q_2-q_3}{2} + \sin^2\frac{q_3-q_1}{2} + \sin^2\frac{q_1-q_2}{2}\right) \\ &= 2\Phi_1\{6 - [\cos(q_2+q_3) + \cos(q_3+q_1) + \cos(q_1+q_2) \\ &\qquad + \cos(q_2-q_3) + \cos(q_3-q_1) + \cos(q_1+q_2)]\} \\ b{:}\quad \omega^2 &= 4\Phi_1\left(\sin^2\frac{q_1+q_2+q_3}{2} + \sin^2\frac{-q_1+q_2+q_3}{2} + \sin^2\frac{q_1-q_2+q_3}{2} + \sin^2\frac{q_1+q_2-q_3}{2}\right) \\ &= 2\Phi_1\{4 - [\cos(q_1+q_2+q_3) + \cos(-q_1+q_2+q_3) + \cos(q_1-q_2+q_3) + \cos(q_1+q_2-q_3)]\}. \end{aligned}$$

These three expressions can be combined into

$$\omega = \omega_0 w(q), \quad w^2(q) = \tfrac{1}{2}\{1-f(q)\}, \quad \omega_0^2 = 2\nu\Phi_1, \tag{3·11}$$

where ω_0 is the maximum frequency and ν the number of first neighbours; we have

$$\left.\begin{aligned} s&: \ \nu = 6, \quad f = \tfrac{1}{3}(\cos q_1 + \cos q_2 + \cos q_3), \\ f&: \ \nu = 12, \quad f = \tfrac{1}{3}(\cos q_2 \cos q_3 + \cos q_3 \cos q_1 + \cos q_1 \cos q_2), \\ b&: \ \nu = 8, \quad f = \cos q_1 \cos q_2 \cos q_3. \end{aligned}\right\} \tag{3·12}$$

The function $(2/3w)\coth(\xi w)$ is monotonously decreasing. Hence there is a maximum of intensity where $w(Q)$ has a minimum or $f(Q)$ a maximum.

$f(Q)$ has absolute maxima of magnitude 1 at the Laue spots

$$Q_\alpha = 2\pi\kappa_\alpha \quad (\kappa_\alpha \text{ integer}). \tag{3·13}$$

For a given direction of the incident beam these three conditions can only be satisfied for certain positions of the crystal. But if this position is changed the intensity distribution $\mathcal{J}_B$ will still have maxima given by the maxima of $f(Q)$, and it is these which we suggest to represent the extra spots.

We take the direction of the incident beam as x-axis, $\mathbf{s}(1, 0, 0)$, and assume the crystal rotating around the y-axis, coinciding with its $\mathbf{a}_2$ vector, through an angle ϕ; then

$$\mathbf{a}_1(a\cos\phi, 0, a\sin\phi), \quad \mathbf{a}_2(0, a, 0), \quad \mathbf{a}_3(-a\sin\phi, 0, a\cos\phi). \tag{3·14}$$

Let ξ, η, ζ be the components of $\mathbf{s}'$,

$$\xi^2 + \eta^2 + \zeta^2 = 1; \tag{3·15}$$

then we have

$$\left.\begin{aligned} Q_1 &= \sigma\{(\xi-1)\cos\phi + \zeta\sin\phi\}, \\ Q_2 &= \sigma\eta, \\ Q_3 &= \sigma\{-(\xi-1)\sin\phi + \zeta\cos\phi\}. \end{aligned}\right\} \tag{3·16}$$

If these expressions are substituted in (3·12*b*), one has precisely Bragg's formula mentioned in the Introduction; indeed, the first neighbours in a body-centred lattice form a cube. Bragg has shown by numerical calculations that this function of η, ζ (being given by (3·16)), which he takes to be the intensity itself, has maxima which coincide fairly well with the observed spots for KCl.

We shall not follow this direct but cumbersome way but develop a method for describing the position, shape and intensity of the spots by analytical development valid in the vicinity of a Laue spot.

4. BACKGROUND MAXIMA IN THE VICINITY OF LAUE SPOTS

A Laue spot is defined by three integers, κ_1, κ_2, κ_3, which determine the Q_α by (3·13). Substituting this in (3·16), one has with (3·15) four equations for ξ, η, ζ and ϕ which by elementary calculation lead to the following solution:

$$\left.\begin{aligned} \xi_\kappa &= 1-\frac{1}{2}\left(\frac{\lambda}{a}\right)^2\kappa^2, \quad \kappa^2 = \kappa_1^2+\kappa_2^2+\kappa_3^2, \\ \eta_\kappa &= \frac{\lambda}{a}\kappa_2, \\ \zeta_\kappa &= \frac{\lambda}{a}\sqrt{\left[(\kappa^2-\kappa_2^2)-\frac{1}{4}\left(\frac{\lambda}{a}\right)^2\kappa^4\right]}, \\ \cos\phi_\kappa &= \frac{1}{\kappa^2-\kappa_2^2}\left\{\kappa_3\sqrt{\left[(\kappa^2-\kappa_2^2)-\frac{1}{4}\left(\frac{\lambda}{a}\right)^2\kappa^4\right]}-\frac{1}{2}\frac{\lambda}{a}\kappa_1\kappa^2\right\}. \end{aligned}\right\} \tag{4·1}$$

For these arguments we have

$$f_\kappa = 1, \quad w_\kappa = 0. \tag{4·2}$$

We now develop w^2 or f in a power series with respect to the positions relative to the Laue spot

$$\eta-\eta_\kappa = \bar{\eta}, \quad \zeta-\zeta_\kappa = \bar{\zeta}, \quad \phi-\phi_\kappa = \bar{\phi}. \tag{4·3}$$

The linear terms in this development vanish; for one has, for instance,

$$\frac{\partial f}{\partial \eta} = \sum_{\alpha=1}^{3}\frac{\partial f}{\partial Q_\alpha}\frac{\partial Q_\alpha}{\partial \eta}; \tag{4·4}$$

but from (3·12)

$$\left.\begin{aligned} s&: \quad \frac{\partial f}{\partial q_1} = -\tfrac{1}{3}\sin q_1, \ldots, \\ f&: \quad \frac{\partial f}{\partial q_1} = -\tfrac{1}{3}\sin q_1(\cos q_2+\cos q_3), \ldots, \\ b&: \quad \frac{\partial f}{\partial q_1} = -\sin q_1 \cos q_2 \cos q_3, \ldots \end{aligned}\right\} \tag{4·5}$$

and these vanish for $q_\alpha = Q_\alpha = 2\pi\kappa_\alpha$.

Hence the development of f begins with the quadratic terms:

$$f = 1+\tfrac{1}{2}\{a_{11}\bar{\eta}^2+2a_{12}\bar{\eta}\bar{\zeta}+a_{22}\bar{\zeta}^2-2a\bar{\eta}\bar{\phi}-2b\bar{\zeta}\bar{\phi}-c\bar{\phi}^2\}+\ldots, \tag{4·6}$$

where

$$\left.\begin{aligned} a_{11} &= \left(\frac{\partial^2 f}{\partial \eta^2}\right)_\kappa, \quad a_{22} = \left(\frac{\partial^2 f}{\partial \zeta^2}\right)_\kappa, \quad a_{12} = \left(\frac{\partial^2 f}{\partial \eta\,\partial \zeta}\right)_\kappa, \\ a &= -\left(\frac{\partial^2 f}{\partial \eta\,\partial \phi}\right)_\kappa, \quad b = -\left(\frac{\partial^2 f}{\partial \zeta\,\partial \phi}\right)_\kappa, \quad c = -\left(\frac{\partial^2 f}{\partial \phi^2}\right)_\kappa. \end{aligned}\right\} \tag{4·7}$$

We have to determine the extremum of f as function of $\bar{\eta}$, $\bar{\zeta}$ for a given $\bar{\phi}$; it is given by the two equations

$$\left.\begin{aligned} \frac{\partial f}{\partial \bar{\eta}} &= a_{11}\bar{\eta}+a_{12}\bar{\zeta}-a\bar{\phi}+\ldots = 0, \\ \frac{\partial f}{\partial \bar{\zeta}} &= a_{12}\bar{\eta}+a_{22}\bar{\zeta}-b\bar{\phi}+\ldots = 0. \end{aligned}\right\} \tag{4·8}$$

From these we obtain $\bar{\eta}$, $\bar{\zeta}$ as functions of $\bar{\phi}$, namely

$$\bar{\eta}_0 = \frac{aa_{22}-ba_{12}}{a_{11}a_{22}-a_{12}^2}\bar{\phi}+\ldots, \quad \bar{\zeta}_0 = \frac{-aa_{12}+ba_{11}}{a_{11}a_{22}-a_{12}^2}\bar{\phi}+\ldots. \tag{4·9}$$

Since from (4·8) it follows by multiplication with $\bar{\eta}_0, \bar{\zeta}_0$ and addition that

$$a_{11}\bar{\eta}_0^2+2a_{12}\bar{\eta}_0\bar{\zeta}_0+a_{22}\bar{\zeta}_0^2-a\bar{\phi}\bar{\eta}_0-b\bar{\phi}\bar{\zeta}_0+\ldots = 0, \tag{4·10}$$

the extremal value of f is

$$f_0 = 1-\tfrac{1}{2}(a\bar{\eta}_0+b\bar{\zeta}_0+c\bar{\phi})\bar{\phi}+\ldots, \tag{4·11}$$

and f can be written in the form

$$f = f_0+\tfrac{1}{2}\{a_{11}(\bar{\eta}-\bar{\eta}_0)^2+2a_{12}(\bar{\eta}-\bar{\eta}_0)(\bar{\zeta}-\bar{\zeta}_0)+a_{22}(\bar{\zeta}-\bar{\zeta}_0)^2\}+\ldots. \tag{4·12}$$

We shall perform the calculations with the degree of accuracy of the terms written out. We shall verify that we have to do with a maximum which, according to (4·9), moves through the Laue spot ($\bar{\phi} = 0$) if the crystal is rotated. This is exactly what the observations of the extra spots show.

We have now to calculate the derivatives (4·7).

Since $(\partial f/\partial q_\alpha)_\kappa = 0$, we have

$$\left.\begin{aligned} \left(\frac{\partial^2 f}{\partial \eta^2}\right)_\kappa &= \sum_{\alpha\beta}\left(\frac{\partial^2 f}{\partial q_\alpha \partial q_\beta}\right)_\kappa \left(\frac{\partial Q_\alpha}{\partial \eta}\right)_\kappa \left(\frac{\partial Q_\beta}{\partial \eta}\right)_\kappa, \ldots, \\ \left(\frac{\partial^2 f}{\partial \eta \partial \zeta}\right)_\kappa &= \sum_{\alpha\beta}\left(\frac{\partial^2 f}{\partial q_\alpha \partial q_\beta}\right)_\kappa \left(\frac{\partial Q_\alpha}{\partial \eta}\right)_\kappa \left(\frac{\partial Q_\beta}{\partial \zeta}\right)_\kappa, \ldots. \end{aligned}\right\} \tag{4·13}$$

But from (4·5) it follows easily that

$$\left(\frac{\partial^2 f}{\partial q_\alpha^2}\right)_\kappa = -\gamma, \quad \left(\frac{\partial^2 f}{\partial q_\alpha \partial q_\beta}\right)_\kappa = 0, \tag{4·14}$$

where γ is constant, different for the three lattices

$$s\colon\ \gamma = \tfrac{1}{3}, \quad f\colon\ \gamma = \tfrac{1}{3}, \quad b\colon\ \gamma = 1. \tag{4·15}$$

Hence (4·13) reduces to

$$\left.\begin{aligned}\left(\frac{\partial^2 f}{\partial\eta^2}\right)_\kappa &= -\gamma\left\{\left(\frac{\partial Q_1}{\partial\eta}\right)^2+\left(\frac{\partial Q_2}{\partial\eta}\right)^2+\left(\frac{\partial Q_3}{\partial\eta}\right)^2\right\}, \ldots,\\ \left(\frac{\partial^2 f}{\partial\eta\,\partial\zeta}\right)_\kappa &= -\gamma\left\{\frac{\partial Q_1}{\partial\eta}\frac{\partial Q_1}{\partial\zeta}+\frac{\partial Q_2}{\partial\eta}\frac{\partial Q_2}{\partial\zeta}+\frac{\partial Q_3}{\partial\eta}\frac{\partial Q_3}{\partial\zeta}\right\}, \ldots.\end{aligned}\right\} \tag{4·16}$$

These operations can be easily performed on (3·16). The result is

$$\left.\begin{aligned}a_{11} &= -\gamma\sigma^2\left(1+\frac{\eta_\kappa^2}{\xi_\kappa^2}\right), & a &= -\gamma\sigma^2\frac{\eta_\kappa\zeta_\kappa}{\xi_\kappa},\\ a_{22} &= -\gamma\sigma^2\left(1+\frac{\zeta_\kappa^2}{\xi_\kappa^2}\right), & b &= -\gamma\sigma^2\left(\xi_\kappa-1+\frac{\zeta_\kappa^2}{\xi_\kappa}\right),\\ a_{12} &= -\gamma\sigma^2\frac{\eta_\kappa\zeta_\kappa}{\xi_\kappa^2}, & c &= \gamma\sigma^2\{(\xi_\kappa-1)^2+\zeta_\kappa^2\}.\end{aligned}\right\} \tag{4·17}$$

Then by a simple calculation one finds from (4·9)

$$\left.\begin{aligned}\bar{\eta}_0 &= \eta_\kappa\zeta_\kappa\bar{\phi},\\ \bar{\zeta}_0 &= (\zeta_\kappa^2+\xi_\kappa-1)\bar{\phi} = (\xi_\kappa-\xi_\kappa^2-\eta_\kappa^2)\bar{\phi},\end{aligned}\right\} \tag{4·18}$$

$$w_0^2 = \tfrac{1}{2}(1-f_0) = \frac{\gamma\sigma^2}{4}\zeta_\kappa^2\bar{\phi}^2 = \frac{\gamma}{4}\left(\frac{2\pi a}{\lambda}\right)^2\zeta_\kappa^2\bar{\phi}^2. \tag{4·19}$$

Here the coefficient γ has the values (4·15). w^2 can be written in the form

$$w^2-w_0^2 = \frac{\gamma}{4}\left(\frac{2\pi a}{\lambda}\right)^2\left\{(\bar{\eta}-\bar{\eta}_0)^2+(\bar{\zeta}-\bar{\zeta}_0)^2+\left[\frac{\eta_\kappa}{\xi_\kappa}(\bar{\eta}-\bar{\eta}_0)+\frac{\zeta_\kappa}{\xi_\kappa}(\bar{\zeta}-\bar{\zeta}_0)\right]^2\right\}. \tag{4·20}$$

The curves of constant w are ellipses with $\bar{\eta}_0$, ζ_0 as centre and the principal axes

$$\frac{\lambda}{2\pi a}2\sqrt{\frac{w^2-w_0^2}{\gamma}}, \quad \xi_\kappa\frac{\lambda}{2\pi a}2\sqrt{\frac{w^2-w_0^2}{\gamma}}; \tag{4·21}$$

the minor axis is inclined at an angle

$$\psi = \tan^{-1}\zeta_\kappa/\eta_\kappa \tag{4·22}$$

into the η-axis, that is, the meridian passing through the Laue spot.

The displacement of the maximum against the Laue spot can be better described by using polar co-ordinates. If we put

$$\eta_\kappa = \rho_\kappa\cos\alpha_\kappa, \quad \zeta_\kappa = \rho_\kappa\sin\alpha_\kappa, \quad \xi_\kappa = \sqrt{(1-\rho_\kappa^2)}, \tag{4·23}$$

we obtain from (4·18)

$$\left.\begin{aligned}\bar\eta_0 &= \tfrac{1}{2}\rho_\kappa^2 \sin 2\alpha_\kappa \,.\, \bar\phi,\\ \bar\zeta_0 &= (\beta_\kappa - \tfrac{1}{2}\rho_\kappa^2 \cos 2\alpha_\kappa)\bar\phi, \quad \beta_\kappa = \sqrt{(1-\rho_\kappa^2)} - 1 + \tfrac{1}{2}\rho_\kappa^2.\end{aligned}\right\} \qquad (4{\cdot}24)$$

If we consider a set of Laue spots on a circle around the incident beam (ρ_κ = const.), the displacement vector describes also a circle with radius $\frac{1}{2}\rho_\kappa^2\bar\phi$ and double 'angular velocity', the centre of which is displaced by $\beta_\kappa\bar\phi$; but β_κ is extremely small for small ρ_κ (of the 4th order).

Although the quantities η, ξ, which are the co-ordinates in a plane normal to the Laue ray, are the natural variables for this problem, there are other quantities used in the literature. One obtains a simple law for the angle χ between the Laue ray $(\xi_\kappa, \eta_\kappa, \zeta_\kappa)$ and the extra ray $(\xi_\kappa + \bar\xi_0, \eta_\kappa + \bar\eta_0, \zeta_\kappa + \bar\zeta_0)$. As the square sums of these two sets of direction cosines are both equal to unity, one obtains

$$2(\xi_\kappa\bar\xi_0 + \eta_\kappa\bar\eta_0 + \zeta_\kappa\bar\zeta_0) = -(\bar\xi_0^2 + \bar\eta_0^2 + \bar\zeta_0^2).$$

On the other hand

$$\begin{aligned}\cos\chi = 1 - \tfrac{1}{2}\chi^2 + \ldots &= \xi_\kappa(\xi_\kappa + \bar\xi_0) + \eta_\kappa(\eta_\kappa + \bar\eta_0) + \zeta_\kappa(\zeta_\kappa + \bar\zeta_0)\\ &= 1 - \tfrac{1}{2}(\bar\xi_0^2 + \bar\eta_0^2 + \bar\zeta_0^2);\end{aligned}$$

hence

$$\chi^2 = \bar\xi_0^2 + \bar\eta_0^2 + \bar\zeta_0^2 + \ldots.$$

Here $\bar\xi$ has to be expressed in terms of $\bar\eta$, $\bar\zeta$, where it is sufficient to use the first order approximation

$$\bar\xi = -\frac{1}{\xi_\kappa}(\eta_\kappa\bar\eta_0 + \zeta_\kappa\bar\zeta_0).$$

Hence

$$\begin{aligned}\chi^2 &= \frac{1}{\xi_\kappa^2}(\eta_\kappa\bar\eta_0 + \zeta_\kappa\bar\zeta_0)^2 + \bar\eta_0^2 + \bar\zeta_0^2\\ &= \frac{1}{\xi_\kappa^2}\{\bar\eta_0^2 + \bar\zeta_0^2 - (\bar\eta_0\zeta_\kappa - \bar\zeta_0\eta_\kappa)^2\}.\end{aligned}$$

By introducing here the expressions (4·18) for $\bar\eta_0$, $\bar\zeta_0$, one obtains after some reduction the simple result

$$\chi^2 = (1-\xi_\kappa)^2\bar\phi^2,$$

or with $\xi_\kappa = \cos\vartheta$,

$$\chi = (1-\xi_\kappa)\bar\phi = 2\sin^2\frac{\vartheta}{2}\bar\phi. \qquad (4{\cdot}25)$$

This formula has been derived by many authors (Faxén 1923; Raman and Nilakantan 1940; Jauncey 1941; Preston 1941; Lonsdale 1941). It is, just as our general formulae (4·18), of a purely geometrical character and gives little information about the physical mechanism; it is furthermore incomplete and has to be supplemented by another formula expressing the azimuthal displacement, such as (4·24). The physical assumptions are contained in our expression for the intensity of the scattered light.

The total intensity of a spot is obtained by integrating the expression (3·2) over all η, ζ. But one has to remember that this expression (3·2) holds only for directions of the scattered beam which are not too near to that of a Laue spot. Therefore the following formulae are valid only, if the centre of the spot has a certain minimum distance from the Laue spot, or $\bar{\phi} > \phi_{\text{min.}}$; on the other hand, our geometrical formulae hold only for small $\bar{\phi}$, that is for $\bar{\phi} < \phi_{\text{max.}}$. The following formulae hold therefore only in a limited region $\phi_{\text{min.}} < \bar{\phi} < \phi_{\text{max.}}$; the lower limit is given by the condition that the total intensity of the extra spot is still smaller than that of the Laue spot, and the upper limit by the condition that the relative change of the frequency $\omega(Q)$ is small.

The area of an ellipse of constant w is

$$4\pi\left(\frac{\lambda}{2\pi a}\right)^2\frac{w^2-w_0^2}{\gamma}\,|\,\xi_\kappa\,|;$$

hence the total intensity of an extra spot

$$\mathfrak{J}=\left(\frac{\lambda}{2\pi a}\right)^2\frac{8\pi}{\gamma}\,|\,\xi_\kappa\,|\int_{w_0}^{1}\mathcal{J}_B\,w\,dw,$$

where $\mathcal{J}_B$ is given by (3·2), (3·3), so that

$$\mathfrak{J}=\mathcal{J}_0CNg^2\frac{2b(1-\cos\vartheta)}{3\Theta\lambda^2\mu}\left(\frac{\lambda}{2\pi a}\right)^2\frac{8\pi}{\gamma}\,|\,\xi_\kappa\,|\int_{w_0}^{1}\coth\left(\frac{\Theta}{T}w\right)dw,$$

or

$$\mathfrak{J}=\mathcal{J}_0CNg^2\frac{2b(1-\cos\vartheta)}{3\Theta\lambda^2\mu}\left(\frac{\lambda}{2\pi a}\right)^2\frac{8\pi}{\gamma}\,|\,\xi_\kappa\,|\,\frac{T}{\Theta}\log\frac{\sinh\Theta/T}{\sinh\Theta w_0/T};\qquad(4\cdot26)$$

with (4·19)

$$w_0=\frac{\sqrt{\gamma}}{2}\frac{2\pi a}{\lambda}\,|\,\zeta_a\bar{\phi}\,|;\quad \phi_{\text{min.}}<\bar{\phi}<\phi_{\text{max.}}.\qquad(4\cdot27)$$

The formula shows the dependence on temperature (which besides from explicit appearance is also contained in $g^2 = e^{-2\mathcal{U}(T)}$, where $\mathcal{U}(T)$ is approximately given by (2·51)). The formula shows moreover how the total intensity of the extra spot depends on wave-length λ, atomic weight μ, atomic distance a, characteristic temperature Θ, position of the Laue spot relative to the axis of rotation ζ_κ, and the angle of rotation $\bar{\phi}$.

All these predictions of the theory ought to be compared with the experiments, apart from the positions of the spot. We have not sufficient material to do this ourselves, and we hope that the experimentalists will do it.

There is, however, one conspicuous feature of the observations which the theory in the present stage of approximation fails to account for, namely, the asymmetry of intensity produced by the rotation of the crystal. As our formulae are even in ζ_κ and $\bar{\phi}$ they predict a symmetric behaviour of the spots on both sides of the axis of rotation and for rotations on opposite directions. Therefore, it is necessary to develop the next approximation with respect to $\bar{\phi}$. This and other improvements will be made in a following paper.

APPENDIX

We prove the formula of Ott used several times in the text by a method which is much simpler as the analytical calculations of Ott himself, namely with the help of Dirac's density matrix. Let $\psi_1(\xi)$, $\psi_2(\xi)$, ... be any orthogonal normalized complete system of functions; let us denote the Hamiltonian of any system by $\hbar\omega\mathscr{H}(p,q)$, where $\hbar\omega$ is a constant energy and $\mathscr{H}$ dimensionless. Then the density matrix is

$$\rho(q,q'\,|\,\beta) = \sum_n \psi_n^*(q')\,e^{-\beta\mathscr{H}}\,\psi_n(q), \quad \beta = \frac{\hbar\omega}{kT}. \tag{A. 1}$$

It satisfies evidently the 'Bloch equation'

$$\frac{\partial\rho}{\partial\beta} = -\mathscr{H}\rho \tag{A. 2}$$

and is characterized as that solution for which

$$\rho(q,q'\,|\,0) = \sum_n \psi_n^*(q')\,\psi_n(q) = \delta(q-q'). \tag{A. 3}$$

Now we consider a linear oscillator with the amplitude ξ; put $\xi = q\sqrt{(\hbar/\omega)}$, then

$$\mathscr{H} = \frac{1}{\omega\hbar}\left(-\hbar^2\frac{\partial^2}{\partial\xi^2} - \omega^2\xi^2\right) = -\frac{\partial^2}{\partial q^2} + q^2 \tag{A. 4}$$

has the eigenvalues $n+\frac{1}{2}$. The differential equation (A. 2),

$$\frac{\partial\rho}{\partial\beta} = \frac{\partial^2\rho}{\partial q^2} - q^2\rho,$$

has the solution (Mehler formula) satisfying (A. 3)

$$\rho(q,q'\,|\,\beta) = \frac{1}{\sqrt{(2\pi \sinh \beta)}}\, e^{-\frac{1}{4}\{(q+q')^2 \tanh \frac{1}{2}\beta + (q-q')^2 \coth \frac{1}{2}\beta\}}, \tag{A. 5}$$

as can be directly verified by forming the derivatives.

The problem is to determine the thermal average of the function $e^{i\mu\xi}$, where μ is a constant:

$$\text{mean}\,(e^{i\mu\xi}) = \text{mean}\,(e^{i\mu q\sqrt{(\hbar/\omega)}}) = \sum_n W_n (e^{i\mu q\sqrt{(\hbar/\omega)}})_{nn}, \tag{A. 6}$$

where
$$(e^{i\mu q\sqrt{(\hbar/\omega)}})_{nn} = \int_{-\infty}^{\infty} \psi_n(q)\, e^{i\mu q\sqrt{(\hbar/\omega)}}\, \psi_n(q)\, dq, \tag{A. 7}$$

$\psi_n(q)$ being the (real) eigenfunction of the oscillator, Hamiltonian $\mathscr{H}_1$ (A. 4), and W_n the probability to find the oscillator, in the state n, namely

$$W_n = \frac{e^{-\beta E_n}}{\sum\limits_{n=0}^{\infty} e^{-\beta E_n}}, \quad E_n = n + \tfrac{1}{2}. \tag{A. 8}$$

Since for eigenfunctions ψ_n of $\mathscr{H}$ (A. 1) can be written

$$\rho(q,q'\,|\,\beta) = \sum_n \psi_n^*(q)\, e^{-\beta E_n}\, \psi_n(q),$$

we obtain for (A. 6) with (A. 7) and (A. 8)

$$\text{mean}\,(e^{i\mu\xi}) = \frac{\int_{-\infty}^{\infty} e^{i\mu q\sqrt{(\hbar/\omega)}}\, \rho(q,q\,|\,\beta)\, dq}{\int_{-\infty}^{\infty} \rho(q,q\,|\,\beta)\, dq}, \tag{A. 9}$$

where according to (A. 5)

$$\rho(q,q\,|\,\beta) = \frac{e^{-q^2 \tanh \frac{1}{2}\beta}}{\sqrt{(2\pi \sinh \beta)}}. \tag{A. 10}$$

Substituting this in (A. 9), one obtains by elementary calculation,

$$\text{mean}\,(e^{i\mu\xi}) = e^{-\frac{1}{4}(\mu^2\hbar/\omega) \coth \frac{1}{2}\beta}. \tag{A. 11}$$

This is Ott's formula which can also be written in terms of the mean oscillator energy

$$\text{mean}\,(e^{i\mu\xi}) = e^{-\frac{1}{2}\mu^2 \bar{\epsilon}/\omega^2}, \quad \bar{\epsilon} = \hbar\omega\left(\frac{1}{2} + \frac{1}{e^\beta - 1}\right). \tag{A. 12}$$

References

Born, M. 1923 *Atomtheorie des Festen Zustandes*. Teubner, Leipzig.
Bragg, Sir W. H. 1940 *Nature, Lond.*, **146**, 509.
Brillouin, L. 1922 *Ann. Phys., Paris*, **17**, 88.
Debye, P. 1914 *Ann. Phys., Paris*, **43**, 49.
Ehrenfest, P. 1929 *Gedenkbuch für Kamerlingh Onnes*, p. 362.
Faxén, H. 1923 *Z. Phys.* **17**, 266.
Frenkel, I. 1931 *Phys. Rev.* **37**, 17, 1276.
Friedrich, W. 1913 *Phys. Z.* **14**, 1082.
Jahn, H. A. and Lonsdale, K. 1941 *Nature, Lond.*, **147**, 88.
James, R. W., Waller, I. and Hartree, D. R. 1928 *Proc. Roy. Soc.* A, **118**, 334.
Jauncey, G. E. M. 1941 *Nature, Lond.*, **147**, 146.
Jauncey, G. E. M. and Harvey, G. G. 1931 *Phys. Rev.* **37**, 1203.
Lonsdale, K. 1941 *Nature, Lond.*, **147**, 481.
Lonsdale, K., Knaggs, I. E. and Smith, H. 1940 *Nature, Lond.*, **146**, 332.
Manguin, C. and Laval T. 1939 *C.R. Acad. Sci., Paris*, **208**, 1446, 1512.
Ott, H. 1935 *Ann. Phys., Paris*, **23**, 169.
Peierls, R. 1932 *Ann. Phys., Paris*, (4) B, p. 905.
Placzek, G. 1934 *Handbuch der Radiologie*, VI, **2**, 209.
Preston, G. D. 1939 *Proc. Roy. Soc.* A, **172**, 116.
Preston, G. D. 1941 *Nature, Lond.*, **147**, 358, 467.
Raman, Sir C. V. and Nagendra Nath, N. S. 1940 *Proc. Indian Acad. Sci.* **12**, 83.
Raman, Sir C. V. and Nilakantan, P. 1940*a* *Nature, Lond.*, **145**, 667.
Raman, Sir C. V. and Nilakantan, P. 1940*b* *Curr. Sci.* **9**, 165.
Raman, Sir C. V. and Nilakantan, P. 1940*c* *Proc. Indian Acad. Sci.* **11**, 379, 389, 398.
Raman, Sir C. V. and Nilakantan, P. 1941 *Nature, Lond.*, **147**, 118.
Siegel, S. S. and Zachariasen, W. H. 1940 *Phys. Rev.* **57**, 795.
Wadlund, A. P. R. 1938 *Phys. Rev.* **53**, 873.
Waller, I. 1923 *Z. Phys.* **17**, 398.
Waller, I. 1928 *Z. Phys.* **51**, 213.
Waller, I. and James, R. W. 1927 *Proc. Roy. Soc.* A, **117**, 214.
Woo, Y. H. 1932 *Phys. Rev.* **38**, 1; **41**, 21.
Zachariasen, W. H. 1940 *Phys. Rev.* **57**, 597.

The diffuse spots in X-ray crystal photographs

By Sir William Bragg, O.M., F.R.S.

(*Received* 20 *June* 1941)

[Plate 29.]

The results of these experiments and of those in a previous paper (Bragg 1941) may be summed up in the statement that the positions and forms of the diffuse spots, so far as they have been observed, correspond closely to the geometry of the true diffraction patterns of the crystal, as calculated from first principles. The reverse is partly true: the calculated pattern shows places where diffuse spots might have been found and are not, but this does not negative the value of the correspondence that is observed. The question then arises: Why is it possible to use the diffraction formula to such effect? The formula would be applicable if there were in the crystal a sufficient number of small crystalline groups acting with some independence of each other. Any other explanation must describe a condition which simulates the effects of small groups so far as these effects have been observed.

The geometry of the pattern of diffuse spots which is observed under certain conditions in X-ray crystal photographs can be derived immediately from the fundamental principles of wave interference. I have given examples in a previous paper (Bragg 1941) in which the calculated patterns for sylvine, diamond, and calcite were shown to correspond with observations within experimental error. In what follows the diamond pattern is discussed in greater detail. The photographs used in illustration are due to Lonsdale and Smith.

The method of calculation has been described in the paper already referred to, but, as the procedure is so direct, it is convenient to begin from first principles in this case also.

In figure 1*a*, A represents a corner of the face-centred cube lattice of diamond; D', D'', D''' are the neighbouring cube corners; B, C, D are the middle points of the neighbouring cube faces; and $ABCD$ is a regular tetrahedron. The length of AO, the perpendicular from A on BCD is 2·053 A. This perpendicular is part of one of the four trigonal axes.

The figure represents the disposition of the crystal towards the incident ray (Cu$K\alpha$, $\lambda = 1{\cdot}54$) in a particular experiment. The point O being taken as origin, the axis of z is taken to be the direction of the incident ray, pointing upwards in the figure. The axis of x is parallel to BC. The trigonal axis AO makes an angle of 2° with the axis of z: in the drawing the angle is made somewhat larger in order to avoid confusion of lines.

The co-ordinates of various points in the lattice of which figure 1*a* shows a portion can be calculated. For instance, the co-ordinates of A are 0·000, 0·072, 2·052, and those of B are 1·257, $\bar{0}{\cdot}\overline{726}$, 0·025. The differences of co-ordinates are therefore $\bar{1}{\cdot}\overline{257}$, 0·798, 2·027.

The direction cosines of the incident ray are 0, 0, 1. Those of the scattered rays being taken to be h, k, l, the ray scattered by A gains on the ray scattered by B by a length equal to $h \times \bar{1}{\cdot}\overline{257} + k \times 0{\cdot}798 + (l-1) \times 2{\cdot}027$. This direction can be represented by (h, k); and an (h, k) curve can be plotted which shows all the values of (h, k) for which the gain or loss is of any given amount.

Thus in figure 1 the curve marked AB gives all the values of (h, k) for which there is neither gain nor loss. A may be said to be in zero phase with B in respect to this particular direction. The curve marked $AB\bar{\lambda}$ shows those values of (h, k) for which A loses a wave-length on B. In this direction A may be said to be in negative primary phase to B. Various curves of this kind are shown; all lie within the circle $h^2+k^2 = 1$.

The AB and AC curves meet at $h = 0$, $k = 0{\cdot}675$. At this point A, B and C are all in zero phase with each other and therefore with all other points in the plane ABC, and this for all values of λ. If the rays are not monochromatic, they will generally include one of such a wave-length that the curves $AD\bar{\lambda}$, $AD'\bar{\lambda}$, $AD''\bar{\lambda}$ and $AD'''\lambda$ for that particular value of λ will all pass through this same point; unlike the AB or AC or similar curves, these curves change position if λ is altered. At this point there is a Laue spot because all the scattering points of the crystal are there in phase with each other.

In the region of the diagram close by this Laue spot there is an approach to uniformity of phase with respect to $\lambda = 1{\cdot}54$ A, and a diffuse spot is found there. The position of its maximum intensity can be calculated with accuracy in some cases at least, e.g. in the sylvine calculations (loc. cit.). In this particular case the diffuse spot has horn-like attachments, shown in the accompanying photograph (plate 29 A) by Lonsdale and Smith. They are found to correspond in position to overlapping portions of $AD'\bar{\lambda}$ and AB curves on the one side and $AD''\bar{\lambda}$, AC curves on the other. To make this more obvious the values of (h, k) given by figure 1 have been used to calculate the relevant portions of the figure that should appear on the photographic film. The values of the co-ordinates of various points are

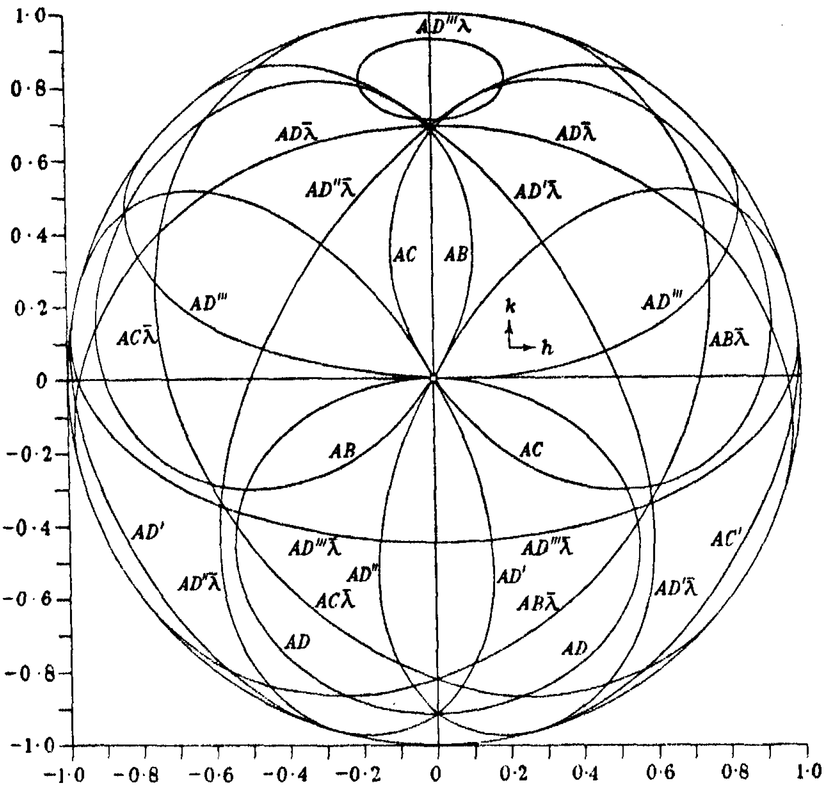

Figure 1

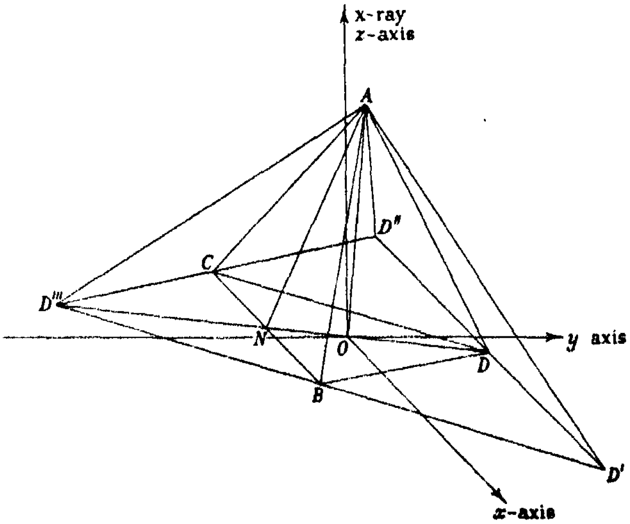

Figure 1a

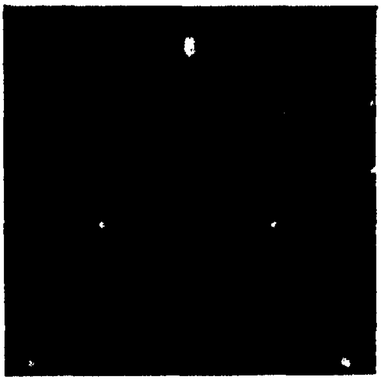

(A)

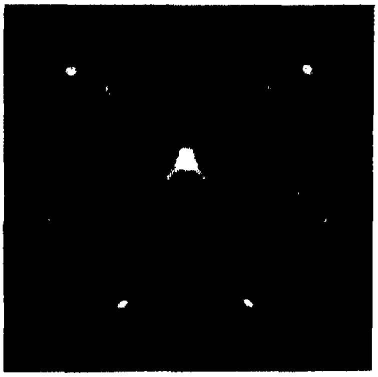

(B)

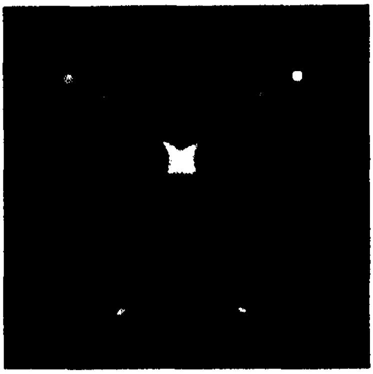

(C)

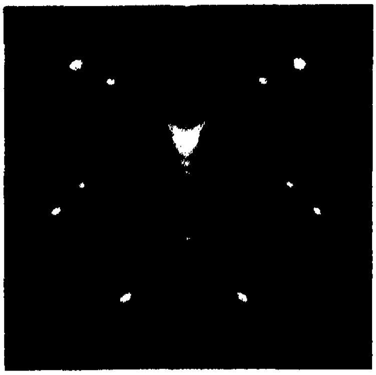

(D)

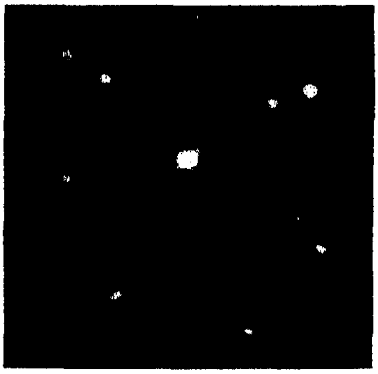

(E)

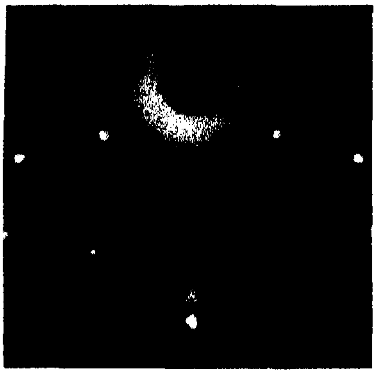

(F)

(*Facing p.* 96)

calculated from the equation $x = Dh/l$; $y = Dk/l$, where D is the distance from crystal to film. The result is shown in figure 1*b* which is to be compared with the photograph. The centre of the black spot in the photograph corresponds to the point O in figure 1*b*. The spot with horns is at the top of the photograph. Spots associated with the faces *ABD*, and *ACD* are at the bottom corners: in figure 1*b* they are indicated by small circles.

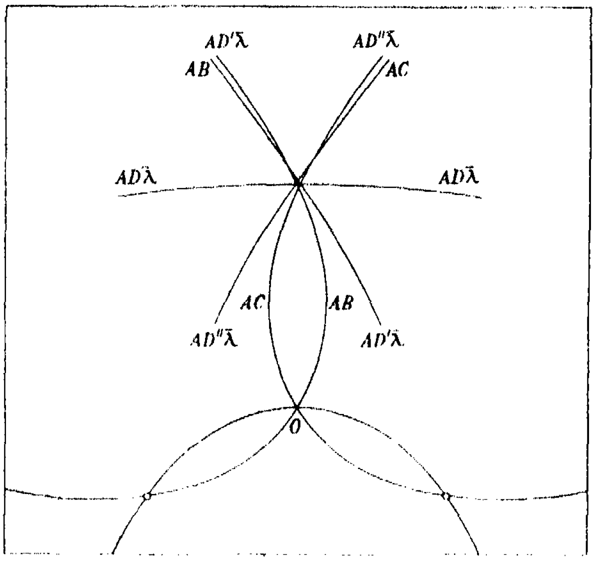

FIGURE 1*b*

The correspondence is further illustrated by a comparison of the photographs (plate 29 B, C, D) due to Lonsdale and Smith with the drawings of figure 2. In these the effect is due to Fe radiation for which $\lambda = 1{\cdot}935$ A. The film is in this case perpendicular to the diffracted ray. Otherwise the conditions are the same as those of figure 1. The form of the horns changes remarkably when the angle of incidence is carried through a very small range which includes the correct angle of incidence for the Fe ray. In the photographs the angles of incidence are 28° 51′, 28° 3′ and 27° 21′. In the first of the series the horns point downwards, but on the other side of the characteristic angle their direction is reversed. The accompanying figures show corresponding changes in the relative dispositions of the curves. In figure 2*a* the *AB* and $AD'\lambda$ (or *AC* and $AD''\lambda$) curves intersect below the Laue spot. In 2*b* they all meet in the one spot and there is close coincidence for some distance above it. In 2*c* the coincidence is disappearing.

Lonsdale and Smith have taken other photographs in which the crystal is rotated about that trigonal axis which is normal to the plane *ABC*. The angle of incidence remains the same during the rotation, but the pattern of Laue spots and diffuse spots changes, becoming of course asymmetric. In particular the horns disappear, one of them much in advance of the other (plate 29 E). Correspondingly the calculated pattern shows that the coincidences of curves which have been associated with the horns disappear in the same order. In figure 3 it is to be observed that only one of the coincidences remains.

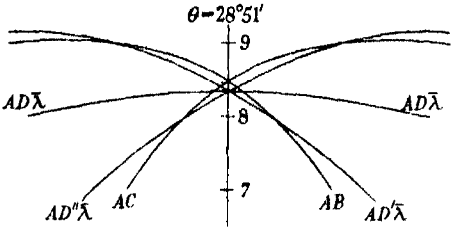

Figure 2*a*

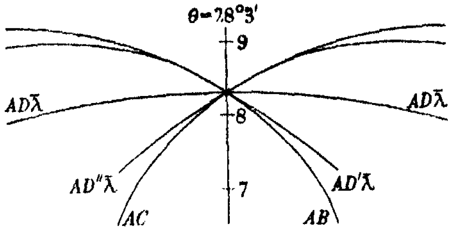

Figure 2*b*

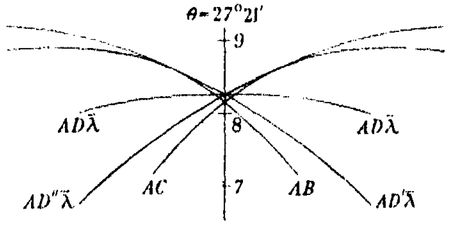

Figure 2*c*

There are other points of intersection or near intersection in figure 1 besides that of the assemblage in the neighbourhood of $h = 0$, $k = 0{\cdot}7$.

as slightly inaccurate, since the 1935 and 1939 measurements near the helium boiling-point are in good agreement. Keesom and Walstra give a smoothing function of the form

$$B = a - b/T$$

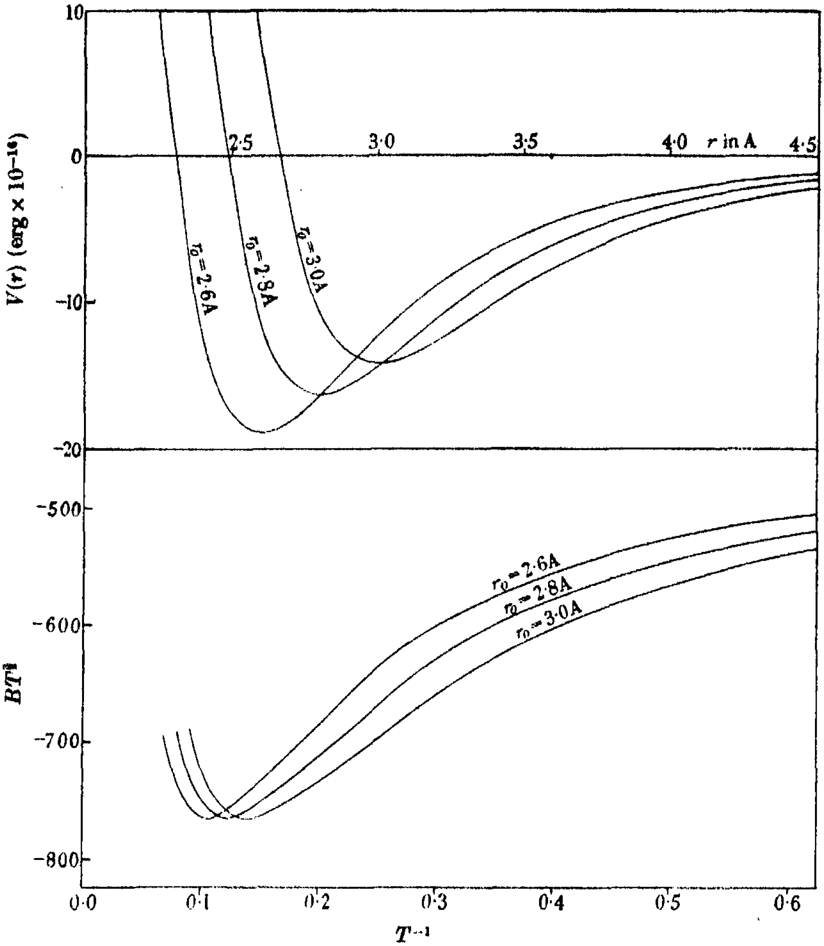

FIGURE 2. The upper figure shows three related potentials of form A: $r_0 = 2{\cdot}6$, $2{\cdot}8$, $3{\cdot}0$ A and $\epsilon r_0^2 = 127{\cdot}4 \times 10^{-16}$ erg A^2. The lower figure shows the corresponding curves for $BT^{\frac{1}{2}}$ as a function of $1/T$.

(with a, b equal to 11·07, 367·2 respectively if B is in c.c./g.mol.), and we shall accept this as the best empirical representation of B in this region. It is shown in figure 1 as the curve KW.

Before proceeding to a more detailed discussion of the experimental data it is desirable to call attention to a few general facts about the theoretical results, to illustrate the importance of the potential constants r_0 and ϵr_0^3. The dependence of $BT^{\frac{1}{2}}$ upon ϵr_0^3 is well shown by figure 1, for if we regard the curves in relation to the T scale they correspond to potentials with the same r_0 but differing ϵr_0^3, neglecting the slight differences which exist in the $f(\sigma)$ functions. At any chosen temperature the values of $BT^{\frac{1}{2}}$ for the five potentials, when plotted against the corresponding values of ϵr_0^3, give quite a smooth curve, suitable for interpolation. Similarly table 4, in which the potentials are given in order of increasing ϵr_0^3, shows that in general the viscosity increases with ϵr_0^3 as one would expect.

The effect of varying the constant r_0 of the potential whilst keeping ϵr_0^3 unchanged can be shown by an application of the relations (19) and (20) which were deduced at the end of the last section. Thus in figure 2 three potentials are shown, each having the same value of ϵr_0^3 as the potential A but with r_0 equal to 2·6, 2·8 and 3·0 respectively; below are the corresponding curves for $BT^{\frac{1}{2}}$ plotted as a function of $1/T$. The variable $1/T$ has been chosen this time to bring out the close relation between the forms of $BT^{\frac{1}{2}}$ and the potential. We see how in this range of temperature $BT^{\frac{1}{2}}$ depends almost entirely on the magnitude of the attractive potential. Figures 1 and 2 indicate the difference in the roles played by r_0 and ϵr_0^3, for whereas the depth of the minimum in $BT^{\frac{1}{2}}$ is more or less determined by ϵr_0^3, the position of the minimum depends mainly on r_0.

Similar families of curves might be drawn for $\eta T^{-\frac{1}{2}}$, but as the minimum is absent the relationship with the potential is not so obvious.

4. COMPARISON OF THEORETICAL AND EXPERIMENTAL RESULTS

As mentioned already, only two viscosity measurements come within our range of calculation, and these have been given in table 4. Other measurements have been made at 15° K and above, but even the calculation at 15° would require δ_L to be determined for values of q^2 at least as far as 100. The extent of the data for the second virial coefficient can be seen from figure 1, in which are shown the results of four sets of measurements. Of these, two fall within our range, namely the three points due to Keesom and Kraak (1935), and the five by Keesom and Walstra (1939). The later measurements appear to be the more satisfactory, as four of the points lie on a line roughly parallel to the theoretical curves, and Keesom and Walstra state that the fifth, at 2·05° K, may be in error by as much as 10 %. To be more precise it is only the earlier results at 2·6 and 3·1° K that one is tempted to regard interpolated at the other points by linear interpolation of η. Underneath are the values of q_0^2 corresponding to 2, 3 and 5° K; $q_0^2(BM)$ refers specifically to BM, and $q_0^2(S)$ to the other five potentials. Although de Boer and Michels did not calculate the viscosity from their potential it was easily done from data published in their paper.

TABLE 4. VISCOSITY COEFFICIENTS

Values of $\eta T^{-\frac{1}{2}}$ (η in 10^{-6} c.g.s. units)

T° K	S'	A	BM	S	B	C	exp.
1·64	—	—	—	—	—	—	2·60
2·0	1·54	1·61	1·65	1·83	1·92	2·14	(2·30)
3·0	1·37	1·37	1·39	1·52	1·59	1·74	(1·77)
4·23	—	—	—	—	—	—	1·46
5·0	1·14	1·12	—	1·18	1·25	1·33	(1·33)

T° K	$q_0^2(S)$	$q_0^2(BM)$	q^2(max.)
2·0	1·44	1·37	4·0
3·0	2·16	2·06	4·6
5·0	3·60	3·43	6·0

It is necessary to explain the values denoted by q^2(max.) in the above table. They represent the values of q^2 at which the integrand $Q'_\eta q^4 e^{-(q/q_0)^2}$ *in formula (16) has its maximum value;* they vary a little of course for the different potentials, but the figures given are fairly representative. The peak in the integrand is well defined, and the function falls off quite steeply on either side. It is instructive to make a comparison with the function $\Delta\, e^{-(q/q_0)^2}$, which forms the integrand in the formula for $BT^{\frac{1}{2}}$. This is most often a function without a well-defined peak, and its value when q is zero is 0 or 1 according to the behaviour of δ_0. It is, however, possible to define a value of q^2 at which $\Delta\, e^{-(q/q_0)^2}$ begins to fall sharply, either because of the exponential or because Δ is changing rapidly from positive to negative, which occurs when q^2 is about 15 to 20. For instance, when q_0^2 is 3·6 the fall occurs when q^2 is about 3·0; when q_0^2 is 7·2 (about 10° K) there is a well-defined peak centred about 3·9. Comparing these with the values of q^2(max.) in table 4 we see that the range of q^2 most effective in determining $\eta(T)$, at say 2° K, affects $B(T)$ most strongly at a much higher temperature, between 5 and 10° K or even higher. For this reason the values of η and B at the same temperature are far from comparable as regards the influence of the interatomic potential. More could be added on this point, especially on the relative contributions of δ_0, δ_2, etc., but we hope that its bearing on the interpretation of experimental data is clear enough.

verging as q increases, whereas the steeper barrier associated with S' is shown by a more negative value of δ_0. As q decreases the differences in the negative parts of the potentials soon dominate the phase constants.

From the constants in table 3 were derived the functions Δ and Q'_η for the various potentials.* A good deal of interpolation among the δ_L's was necessary, particularly as Q'_η is not a very smooth function, and also some extrapolation in estimating the contributions of δ_8, δ_{10}, etc., for the higher values of q. However, the much more extensive table of phases available for S' was a useful guide in making the extrapolation for the other potentials, and the Δ and Q'_η functions are not likely to be seriously in error, even for the highest value of q. The values of $BT^{\frac{1}{2}}$ and $\eta T^{-\frac{1}{2}}$ should be much less affected by any error in extrapolation owing to the exponential term in the integrands.

The results of the calculations for the second virial coefficient are shown in the lower half of figure 1, where the full curves represent $BT^{\frac{1}{2}}$ as a function of q_0^2 for the potentials S', A, BM, S and C. The BM curve is taken from the paper of de Boer and Michels (1939*b*); that for S' has been revised at one or two points since it was first given in I and it is now more regular. A temperature scale has been added, based upon the relation (12) between q_0 and T with r_0 equal to 2·945. This is applicable to all the curves except BM, for which r_0 is equal to 2·874A and therefore the numbers on the T scale should be increased in the ratio $(2{\cdot}945)^2 : (2{\cdot}874)^2$. The BM curve ceases at about 7° K; S, A and C continue to 11° K and S' to beyond 20° K. It must be added that the C curve is only approximate, having been estimated by comparing the values of Δ for S and C.

In calculating $BT^{\frac{1}{2}}$, consideration had to be given to the possible existence of discrete states. An indication of this is given by the behaviour of δ_0 as q tends to zero; the fact that δ_0 tends to zero for S, B and C shows the absence of any discrete state for these potentials, but for S' and A it appears to tend to π, which would correspond to one such state when L is zero. In fact, for these two potentials an energy level was found, the values of q_1^2 being 0·043 and 0·003 for S' and A respectively. For S' the extra term (15) contributes about 12 % of $BT^{\frac{1}{2}}$ at 1° K and 1·3 % at 7° K; the corresponding figures for A are 1 % and 0·1 %. It is not certain whether BM has any discrete state, but q_1^2 would certainly be so small as to be negligible.

We turn now to the viscosity. The values of $\eta T^{-\frac{1}{2}}$ at 2, 3 and 5° K, as calculated for the various potentials, are shown in table 4; also the two experimental results of van Itterbeek and Keesom (1938), with values

---

* In order to save space, tables of Δ and Q'_η have been omitted, but they will be made available to anyone who wishes to consult them.

Buckingham and Sullivan 1938). In several cases checks were obtained by using both methods, with satisfactory results.

TABLE 3. PHASE CONSTANTS

		potentials				
L	q	S'	A	S	B	C
0	0·056	**2·797**	**2·332**	**0·439**	**0·255**	**0·067**
	0·279	1·910	**1·433**	**0·866**	**0·683**	**0·248**
	0·558	**1·230**	**0·988**	**0·683**	**0·580**	**0·231**
	1·116	0·40	**0·322**	**0·149**	**0·095**	**−0·128**
	1·673	**−0·262**	**−0·271**	**−0·395**	**−0·426**	**−0·592**
	2·789	−1·37	(−1·33)	**−1·411**	(−1·45)	(−1·57)
	3·718	−2·22	−2·17	−2·22	−2·24	−2·32
	4·958	−3·27	−3·22	−3·26	−3·265	−3·31
	6·135	−4·36	−4·15	−4·17	−4·18	−4·21
2	0·558	0·007	(0·01)	(0·008)	(0·008)	(0·007)
	1·116	**0·164**	**0·131**	**0·110**	**0·098**	**0·071**
	1·673	0·43	**0·429**	**0·345**	**0·312**	**0·216**
	2·232	**0·655**	**0·562**	**0·449**	**0·415**	**0·283**
	2·789	**0·435**	**0·435**	**0·334**	**0·308**	**0·185**
	3·718	−0·06	**−0·036**	**−0·112**	**−0·127**	**−0·222**
	4·958	−0·92	−0·84	−0·90	−0·915	−0·97
	6·135	(−1·75)	−1·645	−1·66	−1·69	−1·73
4	1·673	0·01	**0·019**	**0·018**	(0·017)	**0·012**
	2·789	**0·199**	0·19	0·16	**0·135**	**0·100**
	3·718	0·41	**0·370**	**0·313**	(0·28)	(0·20)
	4·958	0·26	0·315	0·21	0·195	0·09
	6·135	−0·20	−0·13	−0·17	−0·19	−0·24
6	3·718	**0·103**	—	**0·064**	—	—
	4·958	0·20	0·20	0·18	0·15	0·09
	6·135	0·31	0·30	0·27	0·19	0·16

Note. Values in heavy type were obtained by numerical integration of the wave equation; those in ordinary type by mechanical integration. Values in brackets are interpolated.

The phases for S' are taken from paper I. The calculations for S, A, B and C were considerably simplified by the fact that all four potentials were chosen to be identical within the zero of $V(r)$. The functions F_L in this region are therefore the same for all of them, and need to be evaluated once only. As it is a process of trial and error to find the proper function which remains finite as the origin is approached, much labour was avoided by this device. The outward integration was carried out separately for each potential, usually from the first point of inflexion, at which each function was properly joined to the common solution.

The effect of the common potential barrier is most noticeable in the δ_0 phases when q is equal to 6·135. There it is clear that the δ_0 curves are conwhere

$$Q'_\eta = 8\pi \sum_L \frac{2}{2L+3}\left\{\frac{2L^3+3L^2-L-1}{2L-1}\sin^2\delta_L \right.$$
$$\left. -(L+2)(L+1)\cos(\delta_L-\delta_{L+2})\sin\delta_L\sin\delta_{L+2}\right\}. \quad (17)$$

Q'_η is the viscosity cross-section in units of $(r_0/q)^2$. ϵ is a quantity small compared with unity and will be neglected. The sum over L is again for even values only.

These results may be summed up very concisely by stating that

$$\left.\begin{aligned} B(T)\,T^{\frac{3}{2}} &= F(q_0^2, r_0^2 V),\\ \eta(T)\,T^{-\frac{1}{2}} &= G(q_0^2, r_0^2 V),\end{aligned}\right\} \quad (18)$$

with the same interpretation on the second variable as in (11). It is now clear that when $BT^{\frac{3}{2}}$ and $\eta T^{-\frac{1}{2}}$ have been found as functions of T for one potential V, they have in fact been found for a family of such potentials. Thus, let us consider another potential V' obtained from V by changing r_0 to r'_0 and ϵ to $\epsilon(r_0/r'_0)^2$, and suppose that at the same time the temperature scale is changed to T', where

$$r_0^2 T = (r'_0)^2\, T'. \quad (19)$$

As a result $q'_0 = q_0$ and $(r'_0)^2 V' = r_0^2 V$, and therefore the functions F and G are the same for both potentials. Indeed $BT^{\frac{3}{2}}$ for the potential V' is obtained from the corresponding function for V merely by a change in the temperature scale, applying the relation

$$B(T')\,(T')^{\frac{3}{2}} = B(T)\,T^{\frac{3}{2}}. \quad (20)$$

Similarly, for $\eta T^{-\frac{1}{2}}$. These relations are most useful in interpreting the results of calculations, and we shall return to them shortly.

3. Numerical results

We are now in a position to present the results of the calculations which have been made. The first and most arduous stage of the work is the derivation of the phase constants δ_L, and table 3 contains those phases which have been obtained directly by solution of equation (9) for the potentials S', A, S, B and C, details of which have already been given. A large proportion of the phases were evaluated by numerical integration of the wave equation, more particularly those for the smaller q values, and the remainder by mechanical integration using a differential analyser (Massey, Wylie, This solution is zero at the origin and behaves asymptotically like

$$\sin(q\sigma + \delta_L),$$

δ_L being a constant. It is clear from (9) that δ_L, besides being a function of L, depends upon q_0^2 and the form of $r_0^2 V(\sigma)$; in fact we may write symbolically

$$\delta_L = \delta_L(q^2, r_0^2 V), \tag{11}$$

remembering that when we are dealing with potentials which all have the same form $f(\sigma)$, the second variable reduces to ϵr_0^2.

The temperature may be introduced most naturally by defining a quantity q_0 such that*

$$q_0^2 = (4\pi^2 M r_0^2/h^2)\,\kappa T. \tag{12}$$

The quantities $BT^{\frac{3}{2}}$ and $\eta T^{-\frac{1}{2}}$ are expressible in terms of q_0 and the constants δ_L. Thus for the second virial coefficient, on the assumption that helium atoms obey Einstein-Bose statistics, we have

$$B(T)\,T^{\frac{3}{2}} = -\frac{h^3 N}{(\pi M\kappa)^{\frac{3}{2}}}\left[\tfrac{1}{16} + (1/q_0^2)\int_0^\infty \Delta e^{-(q/q_0)^2}\,dq^2\right], \tag{13}$$

where

$$\Delta = (1/\pi)\sum_L (2L+1)\,\delta_L. \tag{14}$$

The sum over L, for these statistics, is restricted to even values of L. This formula is complete if no discrete energy states exist, otherwise further terms must be added. Thus, if (9) has a proper solution when $L = 0$ and q^2 has the negative proper value $-q_1^2$—corresponding to a polarization molecule with zero angular momentum—the term to be added to the right-hand side of (13) is

$$-\frac{h^3 N}{(\pi M\kappa)^{\frac{3}{2}}}\,(e^{(q_1/q_0)^2} - 1). \tag{15}$$

Turning to the viscosity, we have

$$\eta T^{-\frac{1}{2}} = \frac{5\pi(\pi M\kappa)^{\frac{1}{2}}}{4h^2}\,q_0^6(1+\epsilon)\Big/\int_0^\infty Q'_\eta\, q^4\, e^{-(q/q_0)^2}\,dq^2, \tag{16}$$

---

* This is equivalent to measuring energies in terms of the temperature unit κT, a natural procedure when dealing with temperature-dependent properties. In the formulae which follow, (13) and (16), it would be logical to express the integrals with $(q/q_0)^2$, i.e. $E/\kappa T$ as variable. For purposes of computation this is indeed very convenient, but one finds that the dependence of $B(T)$ and $\eta(T)$ on the potential constants is more easily demonstrated when q^2 is kept as the variable. Incidentally, q is r_0 times the parameter k which is more often used.

forward by Margenau, and are essentially theoretical. The earlier one (SM) was a modification of the Slater-Kirkwood potential which included not only an r^{-8} term, as in (2), but also a term in r^{-10}; this has been allowed for in making an estimate of β. In M the unusually large value of β is partly due to the fact that it has been artificially increased to allow for a small exponential term, negative in sign, which should otherwise be included. It is a coincidence that this agrees with the value given for SM. The value 1·39 for c was deduced by Margenau from the observed spectrum of 'f' values, modified to give the correct polarizability. The potential HER was derived by Hirschfelder, Ewell and Roebuck from the second virial and Joule-Thomson coefficients at relatively high temperatures; the classical formula for $B(T)$ was used, with an approximate correction for quantum effects. For comparison an earlier potential due to Lennard-Jones is included, also based upon experimental data for $B(T)$ but for which the classical formula was used without correction.

Although we have carried out detailed calculations for the six potentials S, S', BM, A, B, C sufficient for the purpose in hand, it must be emphasized that the conclusions arrived at about the values of ϵr_0^3 and c are not yet satisfactory, because of the inadequacy and lack of self-consistency of the experimental data. However, the theoretical results, and the technique evolved, will be immediately applicable when further sufficient observations of $B(T)$ and $\eta(T)$ are completed.

2. THE FORMULAE FOR $B(T)$ AND $\eta(T)$

The method of calculating $B(T)$ and $\eta(T)$ has been described in I, and therefore we shall merely restate the formulae as briefly as possible in a slightly different form more suitable to the present purpose. The wave function representing the collision of two helium atoms, each of mass M and with relative kinetic energy E, can be reduced to the sum

$$\psi = \sum_L F_L(\sigma)\, P_L(\cos\theta), \tag{8}$$

where $\sigma F_L(\sigma)$ is the finite solution of the equation

$$\frac{d^2}{d\sigma^2}(\sigma F_L) + \left\{q^2 - \frac{4\pi^2 M r_0^2}{h^2}\, V(\sigma) - \frac{L(L+1)}{\sigma^2}\right\}(\sigma F_L) = 0, \tag{9}$$

in which $V(\sigma)$ is the interatomic potential in reduced co-ordinates, and

$$q^2 = (4\pi^2 M r_0^2/h^2)\, E. \tag{10}$$

An indication of the differences in form between the chosen potentials is given in table 2, which includes some numerical values of $-f(\sigma)$ for the three forms (1*a*), (2*a*) and (3*a*), for values of σ between 0·7 and 1·6. The parameters α, β and s have been chosen so that the forms correspond very closely to those of the potentials *S*, *A* and *BM* respectively. As a matter of interest values have been included for the Morse potential, for which

$$f(\sigma) = -e^{-\alpha(\sigma-1)} + 2e^{-\frac{1}{2}\alpha(\sigma-1)}.$$

TABLE 2. POTENTIAL FORMS: $-f(\sigma)$

σ	(1*a*)	(2*a*)	(3*a*)	Morse
0·7	30·6	40·8	55·2	42·2
0·8	5·04	5·29	6·92	7·27
0·9	−0·301	−0·274	−0·224	−0·071
1·0	−1·0	−1·0	−1·0	−1·0
1·2	−0·550	−0·540	−0·558	−0·453
1·4	−0·235	−0·226	−0·248	−0·130
1·6	−0·107	−0·101	−0·116	−0·035
α (or s)	13·5	13·5	12·0	13·5
β	—	0·20	—	—

It is interesting to find that between 1·0 and 0·7 the form (3*a*) with σ^{-12} rises more steeply than either of those with an exponential. The difference might hardly show itself in low-temperature calculations, but if the potential constants were being derived from high temperature data there would be a tendency for a difference in form to be compensated for by a small difference, perhaps 1 or 2 %, in r_0. To illustrate the effect of decreasing r_0 slightly, we find that the *BM* potential, which contains σ^{-12}, does not rise above *S* until r has reached 2·3 A, or σ is approximately 0·79, and this in spite of a value of ϵ 12 % larger.

In the other direction the form with σ^{-12} falls off more slowly than either (1*a*) or (2*a*), and this is a difference which becomes significant at a low temperature. It means that if the three forms were associated with the same potential constants, the values of $B(T)$ calculated from them would be increasingly negative in the order (2), (1), (3), as a consequence of the increasing attractive potential. Again such differences could be compensated for by slight changes in the potential constants, as in fact we have tried to do above by a slight modification of ϵr_0^3. The Morse potential with the same α of course falls off more rapidly than any of the others.

The opportunity has been taken to include in table 1 the details of several other potentials which have been suggested by various authors, but which are not used explicitly in these calculations. *SM* and *M* have both been put chosen potentials as closely as possible over the range of most interest. This we do by defining a standard form $f^*(\sigma)$, and fitting each potential $\epsilon f(\sigma)$ to one having this form by a suitable choice of ϵ^* to be associated with $f^*(\sigma)$. A simple criterion for ϵ^* which seems adequate is that the areas under the potentials $\epsilon f(\sigma)$ and $\epsilon^* f^*(\sigma)$ should be equal between suitable limits of σ, say 1·0 and 1·4, which include the most effective part of the attractive field. Then if r_0 is the same for both potentials, they may be regarded as practically equivalent as far as the derivation of low-temperature properties is concerned. It will be shown later that this equivalence partially persists even when r_0 is not the same for the two potentials, provided that a change of r_0 for either potential is accompanied by a change of ϵ or ϵ^* which keeps ϵr_0^2 or $\epsilon^* r_0^2$ invariant.

The result of introducing these 'equivalent potentials' is that with each potential in table 1 is associated a value of $\epsilon^* r_0^2$, which may differ from the value of ϵr_0^2, and the magnitude of this difference shows how significant is the departure of the form of the potential from $f^*(\sigma)$, which provides the basis of comparison. Another way of looking at the matter is to say that, whereas the values of ϵr_0^2 in the table constitute a satisfactory scale by which to compare the attractive part of the potentials if the differences in form between them can be neglected, the values of $\epsilon^* r_0^2$ give, as it were, a modified scale which compensates for the variations in form.

It is convenient to take as the standard form $f^*(\sigma)$ that which is common to the potentials A, B and C, with α and β equal to 13·54 and 0·193 respectively. The other constants for the potentials equivalent to those we propose to use are given on the right of table 1, and it will be seen that the differences between ϵr_0^2 and $\epsilon^* r_0^2$ are small compared with the variations among the potentials themselves. This shows that the differences in form are certainly secondary to the differences existing between the potential constants. Further evidence on this point will be given in the last section.

In addition to $\epsilon^* r_0^2$ the van der Waals constant c^* has been included in the table, this being derived using the relation, easily derived from (6), that

$$c^*/r_0^4 = \epsilon^* r_0^2/0{\cdot}6358. \tag{7}$$

In calculating c^* it has been assumed that in all cases r_0 has the arbitrary value 2·943 A. It should be noted that the values of c or c' given in table 1, being the actual coefficients of r^{-6} regardless of the value of β, are not strictly comparable and therefore not suitable for purposes of interpolation. The values of c^*, however, based on constant values of β and r_0, can be used for interpolation, though we prefer to use $\epsilon^* r_0^2$, with precisely the same results.

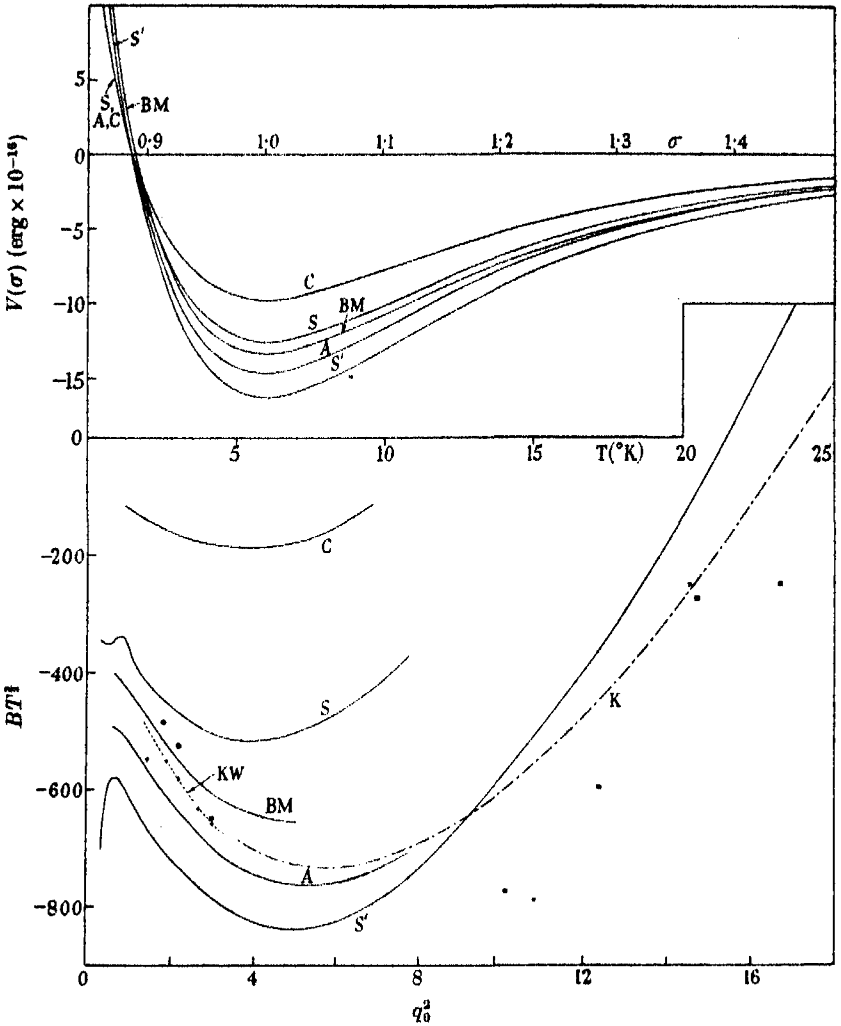

FIGURE 1. (Upper figure.) Helium potentials in reduced co-ordinates, $\sigma = r/2{\cdot}945$. The *BM* potential is modified by changing r_0 from 2·874 to 2·945 and ϵ from 14·04 to 13·37, ϵr_0^6 being unchanged. (Lower figure.) Second virial coefficient. Full curves represent results calculated from potentials shown above, assuming Bose-Einstein statistics. Experimental points: × Holborn and Otto (1926). ☐ Nijhoff, Iliin and Keesom (1928). ⊙ Keesom and Kraak (1935). + Keesom and Walstra (1939). ···· Keesom and Walstra's smoothing function. -·-·- Keyes's smoothing function.

all of the form (2*a*) beyond the point at which $V(r)$ is zero, this point being the same as in S and S'; within the zero the continuation of each is assumed to be the function S. Thus A, B, C have effectively the same values of α and r_0 as S and S' (the trivial differences arise from the slight shift in the minimum due to the β term), but differ in the values of ϵ beyond the zero. β has been fixed somewhat arbitrarily at 0·193; though smaller than some theoretical estimates, it probably represents a reasonable average value. This choice of potential greatly simplifies the numerical work, and as the departure from a consistent form occurs only in the repulsive region it is not likely that the conclusions from low-temperature calculations will be appreciably affected. Finally, the potential BM is the one derived by de Boer and Michels (1939*a*) from gas data above 50° K; it is a potential of form (3*a*) with s equal to 12. The potentials S', A, BM, S and C are depicted, as functions of σ, in the upper half of figure 1; B is not shown, but it lies close to S, though slightly above at distances beyond the minimum.

TABLE 1. HELIUM POTENTIALS

potential		α	β	r_0 in A	ϵ 10^{-16} erg	ϵr_0^2 10^{-32} erg cm.^{2}	c or c' 10^{-60} erg cm.^{6}	equivalent potentials of form (2a) with $\alpha = 13{\cdot}54$, $\beta = 0{\cdot}193$, $r_0 = 2{\cdot}943$ A	
								$\epsilon^* r_0^2$	c^*
S'	(1)	13·56	—	2·947	16·34	142·0	1·92	143·9	1·70
A	(2)	13·54	0·193	2·943	14·69	127·2	1·50	127·2	1·50
BM	(3)	(12)	—	2·874	14·04	116·0	1·58	119·0	1·39
S	(1)	13·56	—	2·947	12·58	109·3	1·48	110·8	1·31
B	(2)	13·54	0·193	2·943	12·24	106·0	1·25	106·0	1·25
C	(2)	13·54	0·193	2·943	9·80	84·9	1·00	84·9	1·00
other potentials:									
SM	(2′)	12·73	(0·338)	2·768	21·20	162·5	1·48	—	—
M	(2)	12·90	0·338	2·805	19·01	149·6	1·39	150·9	1·78
HER	(3)	(12)	—	2·885	13·19	109·8	1·522	111·3	1·32
LJ	(3)	(12)	—	2·915	10·12	86·0	1·24	87·1	1·03

S	Slater (1928).	HER	Hirschfelder, Ewell and Roebuck (1938*a*).
LJ	Lennard-Jones (1931).	BM	de Boer and Michels (1939*a*).
SM	Margenau (1931).	M	Margenau (1939).

From table 1 it will be seen that these six potentials cover a wide range of values of ϵr_0^2, and are at intervals which make interpolation of results derived from them quite practicable, assuming that the small differences of form have a negligible influence. In order to show that these differences are indeed a factor of secondary importance it is helpful to introduce a set of potentials which all have the same form, but otherwise represent our accurately, as it can be regarded as introducing a second-order term in the van der Waals force. This means that the form function can be considered as fixed, to a sufficient degree of approximation, from values of α and β derived from theory and experiment in previous investigations, and our efforts are then directed to the accurate determination of ϵ and r_0. In this way the factors in the interaction to which low-temperature phenomena are sensitive are separated out. If ϵ and r_0 can be determined from low-temperature data, then observations at high temperatures can be used to fix α more precisely.

In this paper we are concerned only with the low-temperature part of this programme. For reasons which will be clearer later it is convenient to choose as the two independent constants to be determined, not ϵ and r_0, but ϵr_0^2 and r_0. Ideally, the procedure in determining these constants would be to calculate $B(T)$ and $\eta(T)$ for a number of suitably chosen potentials, all of which have the same form, approximately correct, but differ in the values of ϵr_0^2 and r_0. Comparison with an adequate range of experimental results should then suffice to fix the best values of the constants. It would only be necessary, in fact, to make detailed calculations for potentials with an arbitrarily fixed value of r_0, as results for other values of r_0 can be derived by dimensional arguments.

Two modifications of this procedure were found to be necessary to meet difficulties introduced by scarcity of experimental data, and the amount of work involved in a very thorough investigation. First, although the low-temperature data make it possible to pick out very precisely the value of ϵr_0^2 for the potential giving the best agreement with experiment, it is much more difficult to assign close limits to the value of r_0 itself. It is necessary to fall back on the van der Waals constant c, which satisfies the relation

$$c/r_0^4 = \epsilon r_0^2/\{1-6/\alpha+\beta(1-8/\alpha)\}. \qquad (6)$$

As c is known within fairly close limits from theoretical and other investigations, it is possible to deduce r_0 by means of (6) once ϵr_0^2 is known. It may be noted in passing that c does depend somewhat on the form parameters α and β; also that when α, β are fixed, c/r_0^4 is simply proportional to ϵr_0^2. The second point is that, in order to reduce the quantity of numerical work required and to make as much use as possible of previous work, the potentials used do not exactly satisfy the condition of having the same form.

The properties of the potentials chosen, six in number, are summarized in table 1. The potential denoted by S, which is the well-known Slater-Kirkwood potential, has the same form as S', which was used in paper I and has a value of ϵ 30 % greater than S. The three potentials A, B, C are

A third expression which has often been used is

$$V(r) = b'r^{-s} - c'r^{-6}, \tag{3}$$

where the exponent s is usually put equal to 12. This can be modified like (1) by the addition of another term.

There is another and more useful way of writing these functions which is based upon the position and depth of the potential minimum. Suppose the minimum of $V(r)$ occurs when r is equal to r_0, and $V(r_0)$ is equal to $-\epsilon$. Then if r is expressed in units of r_0,

$$V(r) = -\epsilon f(\sigma), \tag{4}$$

in which $\sigma = r/r_0$, and $f(\sigma)$ is a function of σ which has the following forms for the potentials (1), (2) and (3) respectively:

$$f(\sigma) = \{-6e^{-\alpha(\sigma-1)} + \alpha\sigma^{-6}\}/(\alpha - 6), \tag{1a}$$

$$f(\sigma) = \left\{-\frac{1}{\alpha}(6+8\beta)\, e^{-\alpha(\sigma-1)} + \frac{1}{\sigma^6}(1+\beta/\sigma^2)\right\}\Big/\{1-6/\alpha+\beta(1-8/\alpha)\}, \tag{2a}$$

$$f(\sigma) = (-6\sigma^{-s} + s\sigma^{-6})/(s-6), \tag{3a}$$

in which $$\alpha = ar_0 \quad \text{and} \quad \beta = d/cr_0^2. \tag{5}$$

It will be convenient to refer to f as the 'form of the potential', and to the constants which occur in f as the 'form parameters'. By contrast the physical quantities r_0 and ϵ will be called the 'potential constants'. It will be seen that (1 *a*) and (3 *a*) both contain one form parameter, respectively α and s, whereas (2 *a*) contains two, viz. α and β. The formulae show that α and s are alike in function, and they are also alike in magnitude; thus as mentioned already s is usually put equal to 12, and for most simple non-polar molecules α certainly lies between 12·5 and 14. As for β, there is evidence that for gases other than helium its value is fairly constant and close to 0·150, but for helium itself theoretical calculations suggest a larger value, even as large as 0·250. Some typical $f(\sigma)$ functions are given in table 2, which will be discussed later.

The separation of the interaction into a form function involving two parameters α and β, and scale factors for energy (ϵ) and nuclear separation (r_0) is especially convenient for our purpose, which is to use the available experimental data about the virial coefficient and viscosity of helium gas at very low temperature—below 10° K—to obtain information about the helium-helium interaction. These low-temperature phenomena are not very sensitive to the form of the repulsive part of the interaction, and therefore to the value assumed for α. Neither need the value of β be specified at all

The upper limit of temperature which has been considered is much less than in the previous paper, being 11° K for the second virial coefficient, denoted by $B(T)$, and 5° K for the viscosity coefficient $\eta(T)$. This was found to be adequate to give decisive information about the attractive part of the potential, provided that the experimental observations are sufficiently numerous. Actually the data at present available are limited to eight observations for $B(T)$ between 2 and 4·3° K, and two for $\eta(T)$ at 1·64 and 4·23° K, though of course results at higher temperature give indirect assistance. We should say at once that the virial coefficients lead to conclusions in marked contradiction to those indicated by the viscosity coefficients, but as the observations are so scanty, especially for the viscosity, it is not yet necessary to assume that the theory which has been applied is insufficient. The exact position will be made clear later.

We shall begin by discussing the helium potential, and follow this with a brief statement of the formulae used for $B(T)$ and $\eta(T)$, the results of the calculations and an analysis of them.

1. THE HELIUM POTENTIAL AND LOW-TEMPERATURE PHENOMENA

Several ways of representing the interatomic potential by an analytical function have been suggested at various times, and one which is particularly well known in connexion with helium is that having the form

$$V(r) = be^{-ar} - c'r^{-6}. \tag{1}$$

Here the negative term has the form indicated theoretically for the leading term of the van der Waals energy, and the energy of the short-range repulsion is represented empirically by the exponential. r is the distance between nuclei. A modification of (1), which has further advantages and forms the basis of the present work, includes the second van der Waals term; thus

$$V(r) = be^{-ar} - cr^{-6} - dr^{-8}. \tag{2}$$

Theoretical estimates of all the constants a, b, c and d have been made, and we may mention the following:

$a = 4{\cdot}6\ \text{A}^{-1}$ (Slater 1928),
$b = 770 \times 10^{-12}$ erg (Slater 1928),
$c = 1{\cdot}37 \times 10^{-12}$ erg A^6 (Baber and Hassé 1937),
$d = 2{\cdot}4 - 3{\cdot}0 \times 10^{-12}$ erg A^8 (Page 1938; Margenau 1939).

The low-temperature properties of gaseous helium. II.

By R. A. Buckingham, Ph.D., *Exhibition of 1851 Senior Student*,
J. Hamilton, M.Sc., *Queen's University, Belfast*
and H. S. W. Massey, F.R.S., *University College, London*

(*Received 6 November* 1940)

Some earlier calculations of the second virial and viscosity coefficients of gaseous helium have been extended, using as before the exact quantum formulae. A brief discussion of the atomic interaction, which is expressed in the form

$$V(\sigma) = -\epsilon f(\sigma),$$

where $\sigma = r/r_0$, r_0 is the atomic separation when V is a minimum, and $f(1) = 1$, is followed by the results of the new calculations and their interpretation. Several interactions, with widely varying values of ϵr_0^2, have been employed, and inferences about the actual interaction are made by interpolating the available experimental data, a method particularly suitable for interpreting future results. The results of some calculations by de Boer and Michels have been incorporated. It is found that the present data for the second virial coefficient, between 2 and 4·3° K, indicate for ϵr_0^2 a value about 122×10^{-16} erg A^2. Though the separate determination of r_0 and ϵ is not likely to be very precise unless calculations are extended to temperatures much beyond the present limit (11° K), the assumption of a probable value for the first van der Waals coefficient leads to the values

$$r_0 = 2{\cdot}93\ \text{A}, \quad \epsilon = 14{\cdot}2 \times 10^{-16}\ \text{erg}.$$

The influence of possible variations in the function $f(\sigma)$ are discussed and shown to be of secondary importance, and these results are based on a reasonable form for $f(\sigma)$ with two parameters.

Comparisons are also made with two viscosity measurements below 5° K, but the inferences from these are not at all in agreement with the evidence from the equation of state.

In an earlier paper (Massey and Buckingham 1938, later referred to as I) the results were given of some calculations of properties of gaseous helium at temperatures below 30° K; in particular, the second virial coefficient, which defines the equation of state at low densities, and the viscosity coefficient. The hope was that a comparison of theoretical and experimental results might lead to further information about the potential of the helium-helium interaction, and as the preliminary investigation showed this to be likely, the calculations have since been considerably extended. We intend in this paper to describe the more recent work, and to discuss its bearing on the helium potential.

former arrangement the local figure is reversed when the crystal is rotated about *BC* through the position of perfect reflexion (Lonsdale and Smith 1941; Bragg 1941). The curvilinear triangle points in the opposite direction, but the spots are still found at the centres of the sides.

REFERENCES

Bragg, Sir W. 1941 *Proc. Roy. Soc.* **179**, 51.
Lonsdale and Smith 1941 *Proc. Roy. Soc.* **179**, 8.

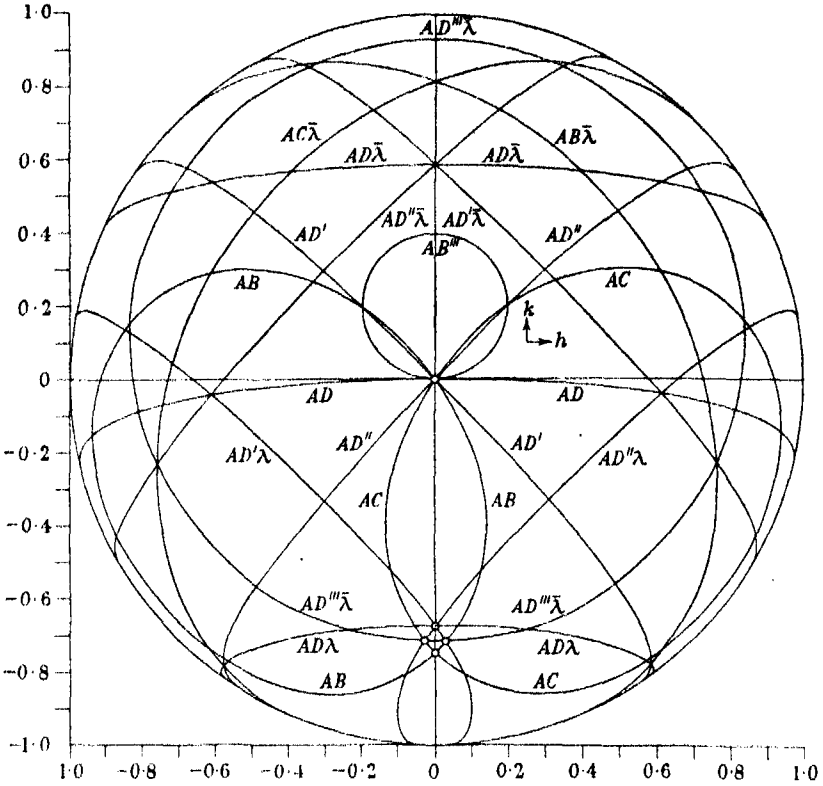

FIGURE 4

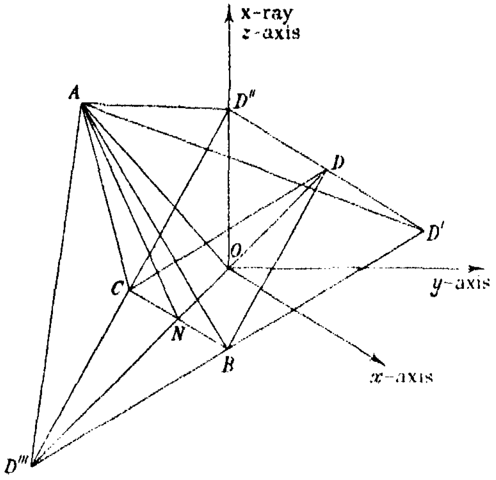

FIGURE 4*a*

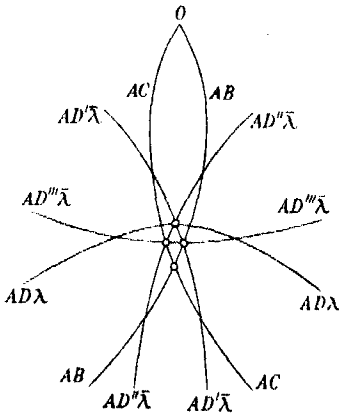

FIGURE 4*b*

There is a triple point of intersection of the curves drawn in the figure at $h = 0$, $k = \bar{0}\cdot\overline{915}$. This does not imply a general agreement in phase of all the centres in the crystal, but only that all the centres in any one plane parallel to $AD'D''$ are in zero phase with each other. The AD curve must pass through the intersection of the AD' and AD'' curves because D lies in the plane $AD'D''$. At $h = \pm 0\cdot 58$, $h = \bar{0}\cdot\overline{30}$ there are Laue points; and there are diffuse spots close by. At the diffuse spot A is very nearly in negative primary phase with C, D'' and D''', and not far from being in zero phase with B and D. That is to say the conditions are nearly right for reflexion of the Cu ray by the set of planes parallel to ABD.

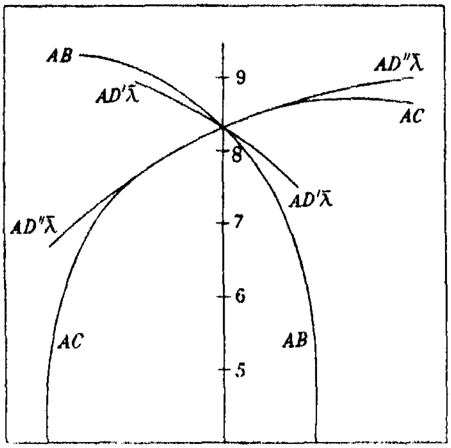

Figure 3

The (h, k) diagram changes in an interesting way if the crystal is rotated about BC from the position shown in figure 1*a* to that of figure 4*a*. The reflexions from the cleavage plane now face the other way. The ellipses in figure 4 have changed their positions and the whole diagram has a different appearance. Especially the small curvilinear triangle formed by the AB, AC and $AD\lambda$ ellipses, now at the bottom of the diagram, is crossed by the $AD'\bar{\lambda}$, $AD''\bar{\lambda}$ and $AD'''\bar{\lambda}$ curves in a different way. The coincidences along stretches of the curves have disappeared. These last three curves cross the sides of the curvilinear triangle at high angles of intersection.

Correspondingly, it has been found that in this arrangement of the experiment there are no horns: there are triangular arrangements of well-defined spots (plate 29 F). These are found to agree, within experimental error, with the positions of intersection just referred to. Also as in the

The curve K is another empirical function suggested by Keyes* as a suitable representation of all the available data between 2° K and about 650° K. The function chosen for this purpose has the form

$$BT^{\frac{1}{2}} = a - b/T^{\frac{1}{2}} - c/T,$$

for which it happens that the constants can be conveniently determined by a least squares method; the numerical values of a, b, c are 65·98, 296·5, 124·9 respectively. The low temperature end of the curve is based mainly on the data between 2 and 4·3° K, and in this region the curve lies close to KW. Over the chief range of observation, about 60–500° K, the representation is quite good, but in the intermediate range a few points lie some distance from Keyes's curve, notably those in the neighbourhood of 15° K. Another point at 23·2° K, due to Nijhoff, is considerably off the line, but it is also scarcely compatible with the two measurements near 20° K. How much of this discrepancy is due to inflexibility in Keyes's function and how much to experimental error it is hard to determine on such limited evidence, though we may note that it is much easier to reconcile the theoretical results with K than for instance with a curve passing near the points roundabout 15° K. Only further experiment will decide whether a preference for Keyes's function on such grounds would be justified.

This short discussion of the present results of experiment leads at once to a comparison with the theoretical curves, and the inferences which can be drawn about the constants of the helium potential. From these meagre experimental results it is not possible to reach any definite conclusions about the values of both ϵ and r_0, but it will be seen below that reliable data will determine ϵr_0^2 within close limits without necessarily giving much idea of the values of the constants separately. Whether low temperature data can determine r_0 precisely is doubtful, because the flat minimum in the $BT^{\frac{1}{2}}$ curve does not discriminate very well between different values of r_0. The discussion which follows deals mainly with the second virial coefficient, but as we rely almost entirely on the KW curve, the conclusions depend upon the validity of this curve. Actually these are not inconsistent with what one would expect on other grounds, and with the help of a theoretical value for the van der Waals constant c, quite reasonable values of r_0 and ϵ are derived. However, the measured values of the viscosity coefficient suggest quite different results.

In figure 1 the experimental $BT^{\frac{1}{2}}$ points are based on the T scale at the top of the diagram, and this, as described earlier, is drawn on the supposition that r_0 is 2·945 A. As we have as yet no reason to prefer one value of r_0 to another, this choice is clearly quite arbitrary and we may at will extend or contract the T scale, with the consequent displacement of the experimental points relative to the theoretical curves. Thus, as q_0^2 is proportional to $r_0^2 T$, an extension of the T scale would correspond to a larger value of r_0 and a contraction to a smaller value; in the first case the KW curve would be brought closer to BM, in the second to A. We could indeed find values of r_0 which would bring KW into partial agreement with either of these two curves, but it would not be a very sensible procedure as it means forcing the observed data to conform to a potential with a preconceived value of ϵr_0^2, nor does it give a good fit. It is more reasonable to begin by assuming various r_0, and finding for each the value of ϵr_0^2 most likely to accord with KW, by interpolating between the potentials S', A, BM and S.

---

* We are indebted to Professor Keyes for the details of this function, which at the time of writing have not been published, and one of us (R. A. B.) has also had the benefit of discussion with him about it.

The method of interpolation is quite simple. First a series of KW curves are plotted as in figure 1 on different temperature scales corresponding to the chosen values of r_0; then for any suitable value of q_0^2, $BT^{\frac{1}{2}}$ can be plotted against ϵr_0^2 (using the data in table 1), and the value of ϵr_0^2 appropriate to each KW curve read off. Alternatively we may use the 'modified ϵr_0^2 scale' by plotting $BT^{\frac{1}{2}}$ against $\epsilon^* r_0^2$. The values of c^* and $\epsilon^* r_0^2$ derived by interpolating on this scale should contain a rough correction for differences in $f(\sigma)$.

The results of following out this procedure are shown in the table below, which contains, first, the interpolated values of ϵr_0^2 obtained from the actual ϵr_0^2 values for the potentials involved, and secondly the values of c^* and ϵr_0^{2*} derived from the alternative procedure. The values are mean values, as each interpolation was repeated for five values of T, viz. 2·65° K, 4·24° K and three intermediate temperatures. This is roughly the range on which the KW curve is based. As an indication of the amount of variation the ϵr_0^2 for r_0 equal to 2·8 is the mean of five values between 121·6 and 123·8, the trend being for ϵr_0^2 to increase as T increases. It will be noticed that as r_0 rises from 2·7 to 3·0 A the change in ϵr_0^2 is really quite small, especially in comparison with the diversity of values displayed in table 1; moreover the differences between ϵr_0^2 and $\epsilon^* r_0^2$ are slight. On the other hand the rise in c^* is considerable, mainly because of the r_0^4 factor.

r_0	2·7	2·8	2·9	3·0	A
mean int. ϵr_0^2	125·3	123·0	121·1	119·5	10^{-16} erg A^2
,, c^*	1·050	1·196	1·359	1·538	10^{-12} erg A^6
,, $\epsilon^* r_0^2$	125·6	123·7	122·2	120·7	10^{-16} erg A^2

The position now is that some additional information must be forthcoming if ϵ and r_0 are to be determined separately. An obvious solution of the difficulty would be to assume that c^* may be given the value $1{\cdot}39 \times 10^{-12}$ which was found by Margenau for the first van der Waals coefficient. It is indeed unlikely that c^* should deviate far from this value, and as a result fairly close limits are placed upon r_0. The following table shows how the potential constants vary if r_0 is between 2·90 and 2·96 A:

r_0	$\epsilon^* r_0^2$	ϵ^*	c^*
2·90	122·2	14·53	1·359
2·93	121·7	14·18	1·411
2·96	121·3	13·84	1·465

This gives a clear indication that $\epsilon^* r_0^2$ is close to 122×10^{-16} erg A^2, and r_0 is 2·93 A or slightly less. The corresponding value of ϵ^* is slightly greater than for de Boer and Michels's potential.

It is unfortunate that we have not precise experimental evidence about the position and depth of the minimum in $BT^{\frac{1}{2}}$, as that would provide a direct method of estimating ϵr_0^2. The depth of the minimum, it has already been pointed out, depends essentially upon ϵr_0^2, small variations in $f(\sigma)$ being neglected. Moreover the theoretical data is sufficient to allow an interpolation similar to that already made at points inside the minimum. Whether the position of the minimum can be found experimentally with enough accuracy to do more than confirm an estimate of r_0 obtained on other grounds is rather doubtful. In fact, to fix r_0 at all precisely it is probably necessary to consider $B(T)$ at the Boyle point and higher temperatures, unless, as we have done above, one makes use of external evidence for the value of c.

The only guide we have as to the minimum is Keyes's curve, which gives -733 for the minimum value of $BT^{\frac{1}{2}}$; from this we should infer by interpolation that $\epsilon^* r_0^2$ is about 124·0. Conversely, if $\epsilon^* r_0^2$ is 122·0 the corresponding minimum is -710. This is quite good agreement, but without knowing what uncertainty attaches to Keyes's function in this region it is difficult to add any other comment. As a further example we may take the potential M, and judging by the values of c^* and ϵr_0^2 it seems unlikely that it would lead to a minimum value for $BT^{\frac{1}{2}}$ of less than -850; within the minimum the $BT^{\frac{1}{2}}$ curve probably lies slightly below that for S'. This suggests that the attractive part of the potential is exaggerated.

It may be unreasonable to expect exact agreement in the values of $\epsilon^* r_0^2$ deduced from $BT^{\frac{1}{2}}$ at the minimum and from observations at lower temperatures; for instance it would not be so if the form A which has been adopted were seriously in error. We may recall the similarity in the curves for the potential $V(r)$ and for $BT^{\frac{1}{2}}$, shown in figure 2. If, as T decreases, the experimental curve for $BT^{\frac{1}{2}}$ rises more steeply than the theoretical one which gives the correct minimum value, then the fault may be that the form $f(\sigma)$ does not tend to zero rapidly enough. This would show itself in a tendency for the interpolated $\epsilon^* r_0^2$ to decrease steadily with decreasing temperature of observation. It is doubtful whether the present experimental curve is accurate enough for any tendency of this sort to be considered significant.

This completes the analysis of the results for the second virial coefficient, and if the discussion has been rather detailed it is not because any air of finality surrounds the numerical results but rather that the procedure is one which is easily applied to fresh experimental data as it comes to hand. With regard to the viscosity an exactly similar procedure can be followed if the data is available, but at present we need only draw attention to the fact that the best agreement between theory and experiment appears to be given by potential C of table 1. A glance at figure 1 shows that this is hopelessly at variance with the evidence from $B(T)$. For consistency the observed $\eta(T)$ values should lie between those for potentials A and BM. It may be noted that the magnitude of δ_2 has a considerable influence on the calculated $\eta(T)$ near 3° K, as in the region where δ_0 is small or zero the main contribution to Q'_η comes from δ_2. As δ_2 increases, so does Q'_η and in consequence $\eta(T)$ becomes smaller.

Between 15 and 30° K good agreement with experiment was obtained in I, using the potential S'. The position is clearly very unsatisfactory, and there is need of further experiments, particularly between 2 and 15° K.

REFERENCES

Baber, T. B. and Hassé, H. R. 1937 *Proc. Camb. Phil. Soc.* **33**, 253.
de Boer, J. and Michels, A. 1939*a* *Physica*, **5**, 945.
de Boer, J. and Michels, A. 1939*b* *Physica*, **6**, 409.
Hirschfelder, J. O., Ewell, R. B. and Roebuck, J. R. 1938 *J. Chem. Phys.* **6**, 205.
Holborn, L. and Otto, J. 1926 *Z. Phys.* **38**, 359.
Keesom, W. H. and Kraak, H. H. 1935 *Physica*, **2**, 37.
Keesom, W. H. and Walstra, W. K. 1939 *Physica*, **6**, 1146.
van Itterbeck, A. and Keeson, W. H. 1938 *Physica*, **5**, 257.
Lennard-Jones, J. E. 1931 *Proc. Phys. Soc.* **43**, 461.
Margenau, H. 1931 *Phys. Rev.* **38**, 747.
Margenau, H. 1939 *Phys. Rev.* **56**, 1000.
Massey, H. S. W. and Buckingham, R. A. 1938 *Proc. Roy. Soc.* A, **168**, 378; **169**, 205.
Massey, H. S. W., Wylie, J., Buckingham, R. A. and Sullivan, R. 1938 *Proc. R. Irish Acad.* **45**, 1.
Nijhoff, G. P., Iliin, B. and Keesom, W. H. 1928 *Commun. Phys. Lab. Univ. Leiden*, no. 188*c*.
Page, C. H. 1938 *Phys. Rev.* **53**, 426.
Slater, J. C. 1928 *Phys. Rev.* **32**, 349.

The scattering of neutrons by deuterons and the nature of nuclear forces

By R. A. Buckingham, Ph.D.* and H. S. W. Massey, F.R.S.
University College, London

(*Received* 21 *March* 1941)

The theory of the scattering of neutrons by deuterons has been worked out for neutrons with energy in the range 0–11·5 MV. It is assumed that the interaction energy of all fundamental particles is the same, and calculations have been carried out assuming three types of such interaction—an ordinary unsaturated force, an exchange force of Majorana-Heisenberg type, and a 'mixed' exchange force involved all exchange operators. The space-dependent part of the interaction is taken to be of the form $Ae^{-2r/a}$, with the constants A and a as determined by Present and Rarita from a study of the binding energies and collision properties of the light nuclei. To obtain differential equations for the functions describing the relative motion of neutron and deuteron Wheeler's method of resonating group structure was employed. The resulting integro-differential equations, which include exchange of particles as well as exchange forces, were solved numerically. An exact solution of the deuteron internal wave equation for the exponential interaction was used throughout.

Results for the total elastic cross-section, calculated with exchange forces, agree well with the observed values, but ordinary forces give, for 2·2 MV neutrons, a cross-section 1·5 times too large. The calculated angular distribution, in relative co-ordinates, is very much more uniform for exchange forces than for ordinary forces. For 2·2 MV neutrons this difference is so marked as to be easily detectable by experiment, and it is deduced that the measurements by Barschall and Kanner of the angular distribution for such neutrons are compatible only with the assumption of exchange forces. It is pointed out that the result that ordinary forces lead to a much less uniform angular distribution is likely to be a general one, independent of the detailed accuracy of the theory.

The experimental investigation of neutron and proton collisions offers at first sight the simplest and most direct method of examining the nature of nuclear forces. The angular distribution of protons projected by impact of neutrons certainly depends very markedly on the nature of the forces acting, provided the energy of the neutron is sufficiently large for those colliding particles with one quantized unit of relative angular momentum to pass sufficiently close to affect each other appreciably. Unfortunately, this energy is somewhat larger than that of the only convenient source of neutrons, homogeneous in velocity, at present available. These are the neutrons of energy 2·2 MV resulting from the reaction

---

* Exhibition of 1851 Senior Research Student.

$$D + D \rightarrow He^3 + n^0.$$

A detailed discussion of the elastic collisions of these neutrons with protons has been given in a previous paper (Massey and Buckingham 1937), and the effects specific to the nature of the forces were found to be so small as to be almost beyond the limit of experimental detection (Dee and Gilbert 1937).

In view of this it is important to consider the possibility of arriving, from other collision experiments, at some more definite decision as to the nature of the fundamental nuclear forces. Experiments on the scattering of high-energy protons (15 MV) in hydrogen would give decisive information, but these also are as yet impracticable. The next type of collision, in order of simplicity, is that of neutrons with deuterons and, from the experimental point of view, this has much to recommend it. Thus, because of its low binding energy, a deuteron is a comparatively large structure and neutrons of 2·2 MV energy, possessing one unit of quantized angular momentum relative to the centre of mass of the deuteron, pass sufficiently close to its structure to interact quite strongly. An angular distribution of projected deuterons departing markedly from the form characteristic of collisions in which *s* state interactions are alone involved should therefore easily be observed. This is what is required, for the nature of the nuclear forces should be most apparent in *p*-state interactions, as for neutron-proton collisions. On the other hand, it is not possible to develop the theory of neutron-deuteron collisions to the same degree of accuracy as that for neutron-proton impacts, and some uncertainty must always attach to its predictions. In this paper we calculate the angular distributions and effective cross-sections for elastic collisions between neutrons of 2·2 MV energy and deuterons at rest, with as high degree of accuracy as is possible in dealing with the three-body problem. Theoretical values have been obtained using fundamental interactions of ordinary and of exchange types, so the possibility of distinguishing between these types by collision experiment can be thoroughly examined.

The method and a large number of the numerical tables required in the calculation can be made use of to deal with the closely similar problem of the collisions between protons and deuterons and it is hoped to extend the work to this case when circumstances permit.

1. THE FUNDAMENTAL LAWS OF FORCE

We assume that the interaction of a neutron and proton is the same as that between two neutrons and can be represented, for particles 1 and 2, by

$$\mathscr{V}(r_{12}) = (mM_{12} + hH_{12} + bM_{12}H_{12} + w)\,V(r_{12}), \tag{1}$$

where $V(r_{12})$ is a function of $r_{12} = |\mathbf{r}_1 - \mathbf{r}_2|$ only, M_{12} is the Majorana operator interchanging the positions but not the spin co-ordinates of the two particles and H_{12} the Heisenberg operator interchanging both positions and spins. m, h, w and b are pure numbers subject always to the condition $m + h + w + b = 1$. Further, if x is the ratio of the magnitude of the interaction between particles with opposite and with same spin respectively, we have

$$m - h + w - b = x. \tag{2}$$

The value of x may be determined from the known energies of the bound ^{3}S and virtual ^{1}S states of the deuteron and is usually taken to be 0·6 (Motz and Schwinger 1940).

This still leaves two of the constants undefined and we consider three special cases in detail:

I. *Ordinary force type*: $m = 0$, $h = 0$, $w = \frac{1}{2}(1+x)$, $b = \frac{1}{2}(1-x)$. This is an unsaturated type of force, a combination of an ordinary force and a spin dependent type. The choice of constants agrees with available experimental material concerning the deuteron and its validity cannot be precluded by arguments based on the necessity for saturation in heavy nuclei until it can be shown that multibody forces or other phenomena are not effective in this respect.

II. *Majorana-Heisenberg force*: $w = 0$, $b = 0$, $m = \frac{1}{2}(1+x)$, $h = \frac{1}{2}(1-x)$. This is a saturated exchange force of the type originally suggested and is the exchange analogue of I.

III. *General interaction*: m, h, w, b all finite. To fix completely all constants they were chosen so that, in the differential equations of relative motion of neutron and deuteron, no ordinary force appears. This requires $h = 2w$, $m = 2b$, giving

$$m = 2b = \tfrac{1}{3}(1+3x), \quad h = 2w = \tfrac{1}{3}(1-3x).$$

It remains to fix the potential function $V(r_{12})$. This was chosen to be of the form

$$V(r) = Ae^{-2r/a}, \tag{3}$$

with $\quad a = 1{\cdot}73 \times 10^{-13}\,\text{cm.}, \quad A = 242mc^2.$

The constants are those found by Present and Rarita (1937) to give the best representation of the binding forces of the light nuclei consistent with the observed scattering of neutrons and of protons by protons.

Recent developments of meson field theory (Fröhlich, Heitler and Kemmer 1938) have suggested that the best form for $V(r)$ is

$$V(r) = r^{-1}Be^{-\lambda r},$$

and the discovery of the quadripole moment of the deuteron (Rabi, Ramsey and Zacharias 1939) has shown that the potential energy cannot be regarded as exactly spherically symmetrical. However, the departure from this symmetry is not very marked, and its influence on the scattering phenomena will probably not be large except at such high energies that states with two units of quantized angular momentum become effective. We have therefore continued with the forms (2) and (3) with which the work was commenced before the development of meson theory.

2. General theory

The most suitable method for dealing with the collision problem is that of resonating group structure introduced by Wheeler (1937) and we follow this throughout.

Two somewhat different modes of treatment may be used, depending on whether or not the concept of isotopic spin is introduced to distinguish the identity of the particles. If it is employed, an interchange of two particles involves an interchange of all three sets of co-ordinates (position, spin and isotopic spin), and the complete wave function must be antisymmetric for interchange of any two of the three particles concerned. Alternatively the two neutrons are treated as particles distinct from the proton, only two sets of co-ordinates are involved in an interchange and the complete wave function must be antisymmetric in the co-ordinates of the two neutrons only. We use both methods and they are not found to produce substantially different results. The two cases will now be discussed separately.

Case (*a*). *Isotopic spin included.* We distinguish the particles by the numbers 1, 2, 3. The two spin functions for particle 1, say, are denoted by $\alpha(1)$, $\beta(1)$ respectively, and the two isotopic spin functions for the same particle by $a(1)$, $b(1)$, the first corresponding to the state in which particle 1 is a proton, the second to that in which it is a neutron.

A wave function representing a group structure (in the sense used by Wheeler (1937)) in which particles 1, 2 form a deuteron (in its ground state) can be written in the form

$$w(12,3) = \phi(\overline{12},3)\,\sigma(\overline{12},3)\,\rho(\widetilde{12},3), \tag{4}$$

if we assume separability of spin and isotopic spin co-ordinates. Here $\phi(\overline{12},3)$ is a function of position, symmetrical (as indicated by the —) in the particles 1, 2, $\sigma(\overline{12},3)$ is the spin function also symmetrical in the particles 1, 2, and $\rho(\widetilde{12},3)$ is the isotopic spin function antisymmetrical with regard to the same two particles. Given this, it is now possible to construct a properly antisymmetric complete wave function for the three-particle system in the form

$$\Psi(123) = w(12,3)+w(23,1)+w(31,2), \tag{5}$$

which we adopt as the basis of our theory. It is next necessary to examine how the function w is to be determined.

Since we are dealing with a system in which the two particles bound in a deuteron have opposite isotopic spins, we write

$$\rho(\widetilde{12},3) = 2^{-\frac{1}{2}}\{a(1)\,b(2)-a(2)\,b(1)\}\,b(3). \tag{6}$$

The total spin quantum number s of the system may be $\frac{3}{2}$ or $\frac{1}{2}$ according as the spin of the third particle is the same or opposite to that of each particle comprising the deuteron. We therefore have

$$\sigma(\overline{12},3) = \alpha(1)\,\alpha(2)\,\alpha(3), \quad \text{quartet state}, \quad (s=\tfrac{3}{2}), \tag{7}$$

$$= \alpha(1)\,\alpha(2)\,\beta(3), \quad \text{doublet state}, \quad (s=\tfrac{1}{2}). \tag{8}$$

For $\phi(\overline{12},3)$ we now make the approximation of supposing the presence of the third particle to be ineffective in polarizing the deuteron pair so that we may write

$$\phi(\overline{12},3) = \chi(12)\,F(12,-3), \tag{9}$$

where $\chi(12)$ is the unperturbed deuteron wave function for the relative motion of particles 1 and 2 in the ground state and $F(12,-3)$ is a function of the position of the third particle relative to the centre of mass of the other two.

In this way we are left with one unknown function which may be used to describe the scattering. For, if we obtain a solution for F which has the asymptotic form of a plane wave of unit amplitude and the corresponding scattered wave (in the relative co-ordinates), the square of the amplitude of this scattered wave gives the required intensity of elastic scattering. To derive the differential equation for F under the assumptions (5), (6) and (7), (8), (9) we proceed as follows.

The function Ψ must satisfy the wave equation

$$[T+\mathscr{V}(12)+\mathscr{V}(23)+\mathscr{V}(31)]\,\Psi = (E_n+E_d)\,\Psi, \tag{10}$$

where E_d is the energy of the ground state of the deuteron ($-2{\cdot}2$ MV), E_n that of the motion of the incident neutron relative to the deuteron ($\frac{2}{3}$ of that of the neutron in the 'laboratory' system in which the deuteron is initially at rest), and the functions $\mathscr{V}$ are of the form (1). T is the operator representing the kinetic energy of the motion, that of the centre of mass of the whole system having been separated out. It may be written in the form

$$-\frac{h^2}{8\pi^2 M}[2\nabla_{12}^2+\tfrac{3}{2}\nabla_{12,3}^2], \tag{11}$$

or in either of the two alternative forms differing from (11) only by cyclic interchange of the variables. M is here the mass of a neutron or proton, and ∇_{12}^2, $\nabla_{12,3}^2$ are Laplacian operators in the relative co-ordinates of particles 1 and 2 and of particle 3 relative to the centre of mass of the other two, respectively.

Substituting the form (5) for Ψ, performing the exchange operations included in the functions $\mathscr{V}$, multiplying both sides by $\sigma(\overline{12},3)\,\rho(\overline{12},3)$ and summing over the spin and isotopic spin co-ordinates, gives the equations:

Doublet:

$$\begin{aligned}[T-E_d-E_n+V(12)+(w-\tfrac{1}{2}h)\{V(13)+V(23)\}]\,\phi(\overline{12},3)&\\ =(\tfrac{1}{2}b-m)\{V(13)\,\phi(\overline{23},1)+V(23)\,\phi(\overline{13},2)\}.&\end{aligned} \tag{12}$$

Quartet:

$$\begin{aligned}&[T-E_d-E_n+V(12)+(w+b)\,V(23)+(w+b-m-h)\,V(13)]\,\phi(\overline{12},3)\\ &\quad=[T-E_d-E_n+V(23)+(w+b)\,V(12)+(w+b-m-h)\,V(13)]\,\phi(\overline{23},1)\\ &\qquad+(m+h)\{V(12)-V(23)\}\,\phi(\overline{31},2).\end{aligned} \tag{13}$$

For the doublet state it is now a simple matter to derive the differential equation for $F(12,-3)$. It is first convenient to introduce a more explicit notation for the various co-ordinates. The position vectors to the various particles from a fixed origin will be denoted by $\mathbf{r}_1$, $\mathbf{r}_2$, $\mathbf{r}_3$. Then we write

$$\mathbf{R}=\mathbf{r}_1-\mathbf{r}_2,\quad \mathbf{r}=\tfrac{1}{2}(\mathbf{r}_1+\mathbf{r}_2)-\mathbf{r}_3.$$

We note also the relations

$$\mathbf{r}_2-\mathbf{r}_3=\mathbf{r}-\tfrac{1}{2}\mathbf{R},\quad \mathbf{r}_1-\mathbf{r}_3=\mathbf{r}+\tfrac{1}{2}\mathbf{R},$$

$$\mathbf{r}_1-\tfrac{1}{2}(\mathbf{r}_2+\mathbf{r}_3)=\tfrac{1}{2}\mathbf{r}+\tfrac{3}{4}\mathbf{R},\quad \mathbf{r}_2-\tfrac{1}{2}(\mathbf{r}_1+\mathbf{r}_3)=\tfrac{1}{2}\mathbf{r}-\tfrac{3}{4}\mathbf{R}.$$

Substituting the form (9) for ϕ in (12) and using the fact that

$$\left[-\frac{h^2}{4\pi^2 M}\nabla_R^2+V(R)\right]\chi(R)=E_d\,\chi(R), \tag{14}$$

gives

$$\begin{aligned}\left[\frac{3h^2}{16\pi^2 M}\nabla_r^2+E_n-(w-\tfrac{1}{2}h)\{V(|\mathbf{r}+\tfrac{1}{2}\mathbf{R}|)+V(|\mathbf{r}-\tfrac{1}{2}\mathbf{R}|)\}\right]F(\mathbf{r})\,\chi(R)\\ =(m-\tfrac{1}{2}b)\{V(|\mathbf{r}+\tfrac{1}{2}\mathbf{R}|)\,\chi(|\mathbf{r}-\tfrac{1}{2}\mathbf{R}|)\,F(-\tfrac{1}{2}\mathbf{r}-\tfrac{3}{4}\mathbf{R})\\ +V(|\mathbf{r}-\tfrac{1}{2}\mathbf{R}|)\,\chi(|\mathbf{r}+\tfrac{1}{2}\mathbf{R}|)\,F(-\tfrac{1}{2}\mathbf{r}+\tfrac{3}{4}\mathbf{R})\}.\end{aligned} \tag{15}$$

Multiplying both sides of (14) by $\chi(R)$ and integrating over **R** space gives finally

$$(\nabla^2+k^2)\,F(\mathbf{r})=(2w-h)\,U(\mathbf{r})\,F(r)+(2m-b)\int Q(\mathbf{r},\mathbf{r}')\,F(\mathbf{r}')\,d\mathbf{r}', \tag{16}$$

where $k^2=\dfrac{16\pi^2 M}{3h^2}E_n,$

$$U=\frac{16\pi^2 M}{3h^2}\int|\chi(R)|^2\,V(|\mathbf{r}+\tfrac{1}{2}\mathbf{R}|)\,d\mathbf{R}, \tag{17}$$

$$Q=\frac{16\pi^2 M}{3h^2}(\tfrac{4}{3})^3\,\chi(u)\,V(t)\,\chi(v), \tag{18}$$

$$u=\tfrac{2}{3}|2\mathbf{r}'+\mathbf{r}|,\quad v=\tfrac{2}{3}|\mathbf{r}'+2\mathbf{r}|,\quad t=\tfrac{2}{3}|\mathbf{r}-\mathbf{r}'|,$$

and we have changed the variable of integration from **R** to $\mathbf{r}'=-\tfrac{1}{2}\mathbf{r}-\tfrac{3}{4}\mathbf{R}$.

A similar integro-differential equation may now be obtained for the quartet case but is more complicated owing to the presence of terms involving T on the right-hand side of (13). When we carry out the same operations as those which led to the derivation of (16) from (12) we obtain, on the right-hand side, a term

$$\int\chi(R)\,T\chi(|\mathbf{r}-\tfrac{1}{2}\mathbf{R}|)\,F(-\tfrac{1}{2}\mathbf{r}-\tfrac{3}{4}\mathbf{R})\,d\mathbf{R}, \tag{19}$$

which may be thrown into the same form as the right-hand side of (16) in the following way.

Taking $$T=-\frac{h^2}{8\pi^2 M}[2\nabla_{23}^2+\tfrac{3}{2}\nabla_{23,1}^2], \tag{20}$$

then

$$\begin{aligned}\frac{16\pi^2 M}{3h^2}\int \chi(12)\, T\chi(23)\, F(23,-1)\, d\mathbf{R} \\ &= -\frac{4}{3}\int \chi(12)\,\{\nabla^2_{23}\,\chi(23)\}\, F(23,-1)\, d\mathbf{R} \\ &\quad -\int \chi(12)\,\chi(23)\,\{\nabla^2_{23,1}\, F(23,-1)\, d\mathbf{R}, \\ &= \frac{16\pi^2 M}{3h^2}\int \chi(12)\,\{E_d - V(23)\}\,\chi(23)\, F(23,-1)\, d\mathbf{R} \\ &\quad -\int \{\nabla^2_{23,1}\,\chi(12)\,\chi(23)\}\, F(23,-1)\, d\mathbf{R}, \end{aligned} \tag{21}$$

where we have transformed the first integral by use of (14) and the second by Green's theorem.

Changing the variable of integration to $\mathbf{r}'$, as in (16), the right-hand terms become

$$\left(\frac{4}{3}\right)^3 \left[\int \left\{\frac{16\pi^2 M}{3h^2}\,\chi(u)\,(E_d - V(v))\,\chi(v) - \nabla^2_{r'}\,\chi(u)\,\chi(v)\right\} F(\mathbf{r}')\, d\mathbf{r}'\right]. \tag{22}$$

Now

$$\begin{aligned}\nabla^2_{r'}\{\chi(u)\,\chi(v)\} &= \frac{16}{9}\,\chi(v)\,\frac{d^2}{u\,du^2}(u\chi(u)) + \frac{4}{9}\,\chi(u)\,\frac{d^2}{v\,dv^2}(v\chi(v)) \\ &\quad + \frac{16}{9}\,\frac{d\chi(u)}{du}\,\frac{d\chi(v)}{dv}\,\frac{\mathbf{u}\,.\,\mathbf{v}}{uv}, \\ &= \frac{16\pi^2 M}{h^2}\,[\chi(u)\,\chi(v)\,\{-5E_d + V(v) + 4V(u)\}] \\ &\quad + \frac{16}{9}\,\chi'(u)\,\chi'(v)\,\frac{\mathbf{u}\,.\,\mathbf{v}}{uv}, \end{aligned} \tag{23}$$

for the functions χ satisfy the deuteron wave equation (14). Hence

$$\begin{aligned}&\int \chi(R)\, T\chi(|\,\mathbf{r} - \tfrac{1}{2}\mathbf{R}\,|)\, F(-\tfrac{1}{2}\mathbf{r} - \tfrac{3}{4}\mathbf{R})\, d\mathbf{R} \\ &\quad = \left(\frac{4}{3}\right)^4 \int \left[\{2E_d - V(u) - V(v)\}\,\chi(u)\,\chi(v) - \frac{h^2}{4\pi^2 M}\,\frac{\mathbf{u}\,.\,\mathbf{v}}{uv}\,\chi'(u)\,\chi'(v)\right] F(\mathbf{r}')\, d\mathbf{r}'. \end{aligned} \tag{24}$$

Using this result we find, for the quartet case,

$$(\nabla^2+k^2)\,F(\mathbf{r}) = (2w+2b-m-h)\,U(r)\,F(\mathbf{r})$$
$$+\int\left\{(2m+2h-w-b)\,Q(\mathbf{r},\mathbf{r}')+P(\mathbf{r},\mathbf{r}')+\left(\frac{E_n}{E_d}-\frac{5}{3}\right)N(\mathbf{r},\mathbf{r}')\right\}F(\mathbf{r}')\,d\mathbf{r}', \tag{25}$$

where

$$P = \frac{16\pi^2 M}{9h^2}\left(\frac{4}{3}\right)^3\left[\chi(u)\{V(u)+V(v)\}\chi(v)+\frac{h^2}{\pi^2 M}\chi'(u)\frac{\mathbf{u}\,.\,\mathbf{v}}{uv}\chi'(v)\right], \tag{26}$$

$$N = \frac{16\pi^2 M}{3h^2}\left(\frac{4}{3}\right)^3 E_d\,\chi(u)\,\chi(v). \tag{27}$$

Case (*b*). *Neutron and proton treated as distinct particles.* We now no longer include the isotopic spin co-ordinates so, distinguishing the neutrons by the numerals 1 and 2, the appropriate wave functions for the two cases are:

Doublet:

$$\Psi = 12^{-\frac{1}{2}}[\{\alpha(1)\,\alpha(2)\,\beta(3)+\alpha(1)\,\beta(2)\,\alpha(3)-2\beta(1)\,\alpha(2)\,\alpha(3)\}\,\phi(23,1)$$
$$-\{\alpha(2)\,\alpha(1)\,\beta(3)+\alpha(2)\,\beta(1)\,\alpha(3)-2\beta(2)\,\alpha(1)\,\alpha(3)\}\,\phi(13,2)]. \tag{28}$$

Quartet:

$$\Psi = 2^{-\frac{1}{2}}\alpha(1)\,\alpha(2)\,\alpha(3)\,[\phi(23,1)-\phi(13,2)]. \tag{29}$$

Proceeding exactly as before, we find the following equations:

Doublet:

$$(\nabla^2+k^2)\,F(\mathbf{r}) = (2w-b+\tfrac{1}{2}m-h)\,U(r)\,F(\mathbf{r})+\int\left\{(2m-h+\tfrac{1}{2}w-b)\,Q(\mathbf{r},\mathbf{r}')\right.$$
$$\left.-\tfrac{1}{2}P(\mathbf{r},\mathbf{r}')-\frac{1}{2}\left(\frac{E_n}{E_d}-\frac{5}{3}\right)N(\mathbf{r},\mathbf{r}')\right\}F(\mathbf{r}')\,d\mathbf{r}'. \tag{30}$$

Quartet:

As for case (*a*) (25).

Summary of equations obtained. For each case considered the integro-differential equation derived for the function F can be written in the form

$$(\nabla^2+k^2)\,F(\mathbf{r}) = \alpha U(r)\,F(\mathbf{r})$$
$$+\int\left[\beta Q(\mathbf{r},\mathbf{r}')+\gamma\left\{P(\mathbf{r},\mathbf{r}')+\left(\frac{E_n}{E_d}-\frac{5}{3}\right)N(\mathbf{r},\mathbf{r}')\right\}\right]F(\mathbf{r}')\,d\mathbf{r}'. \tag{31}$$

It is convenient to summarize the values taken by α, β, γ for the quartet and the two doublet cases (doublet (*a*) including isotopic spin, doublet (*b*) treating neutrons and protons as distinct), for the three types of force considered. This is done in table 1.

TABLE 1

nuclear force assumed	total spin of colliding systems	α	β	γ
I	quartet	2	-1	1
	doublet (*a*)	$1+x$	$-\frac{1}{2}(1-x)$	0
	(*b*)	$\frac{1}{2}(1+3x)$	$-\frac{1}{4}(1-3x)$	$-\frac{1}{2}$
II	quartet	-1	2	1
	doublet (*a*)	$-\frac{1}{2}(1-x)$	$1+x$	0
	(*b*)	$-\frac{1}{4}(1-3x)$	$\frac{1}{2}(1+3x)$	$-\frac{1}{2}$
III	quartet	0	1	1
	doublet (*a*)	0	$\frac{1}{2}(1+3x)$	0
	(*b*)	0	$\frac{1}{4}(1+9x)$	$-\frac{1}{2}$
as used by	quartet	$-\frac{1}{3}x$	$1+\frac{1}{3}x$	1
Wheeler (1937)	doublet (*b*)	$\frac{2}{3}x$	$\frac{1}{4}(1+\frac{10}{3}x)$	$-\frac{1}{2}$

x is the ratio of the force between two nuclear particles when their spins are anti-parallel to that when they are parallel.

In this table we have also included the values of α, β, γ which arise when the interactions between the fundamental particles are those assumed by Wheeler (1937).

It will be noted that the constants satisfy the condition that, if the 'potential' terms

$$U(r)\,F(\mathbf{r}),\quad \int Q(\mathbf{r},\mathbf{r}')\,F(\mathbf{r}')\,d\mathbf{r}',$$

$$\frac{2}{3x-1}\int\left\{P(\mathbf{r},\mathbf{r}')+\left(\frac{E_n}{E_d}-\frac{5}{3}\right)N(\mathbf{r},\mathbf{r}')\right\}F(\mathbf{r}')\,d\mathbf{r}',$$

were all equivalent, then all the equations would be the same.

Calculation of the scattering. To determine the scattering we seek a solution of the equation (31) which has the asymptotic form

$$F \sim e^{ikz}+r^{-1}g(\theta)\,e^{ikr}.$$

Then, distinguishing doublet and quartet cases by indices D, Q respectively, we have, for the intensity of elastic scattering per unit solid angle about θ,

$$I(\theta) = \tfrac{1}{3}\{2\,|\,g^Q(\theta)\,|^2+|\,g^D(\theta)\,|^2\}, \tag{32}$$

and for the total elastic cross-section

$$Q = \int_0^\pi I(\theta)\sin\theta\,d\theta. \tag{33}$$

Here θ is the relative angular co-ordinate. To obtain the angular distribution of projected deuterons in the system of co-ordinates in which the deuteron is initially at rest ('laboratory' system) we write, if Θ is the angle the direction of projection makes with that of the incident neutron,

$$J(\Theta) = 4I(2\Theta)\cos\Theta. \tag{34}$$

$J(\Theta)$ is the required distribution function per unit solid angle in this system.

To evaluate $g^Q(\theta), g^D(\theta)$ we expand the functions F, Q, P, N in harmonics, so that

$$rF(\mathbf{r}) = \sum_l f_l(r)\,P_l(\cos\theta),$$

$$\left.\begin{matrix} Q(\mathbf{r},\mathbf{r}') \\ P(\mathbf{r},\mathbf{r}') \\ N(\mathbf{r},\mathbf{r}') \end{matrix}\right\} = \sum \frac{(2s+1)}{4\pi rr'} P_s(\cos\vartheta) \left\{\begin{matrix} q_s(r,r') \\ p_s(r,r'), \\ n_s(r,r') \end{matrix}\right.$$

where

$$\left.\begin{matrix} q_s(r,r') \\ p_s(r,r') \\ n_s(r,r') \end{matrix}\right\} = 2\pi rr' \int_0^\pi P_s(\cos\vartheta)\sin\vartheta\,d\vartheta \left\{\begin{matrix} Q(\mathbf{r},\mathbf{r}') \\ P(\mathbf{r},\mathbf{r}') \\ N(\mathbf{r},\mathbf{r}') \end{matrix}\right.$$

and

$$\cos\vartheta = \frac{\mathbf{r}\,.\,\mathbf{r}'}{rr'}. \tag{35}$$

We then have, using the orthogonal property of the harmonics,

$$\frac{d^2f_l}{dr^2} + \left\{k^2 - \frac{l(l+1)}{r^2}\right\} f_l = \alpha U f_l + \int \left[\beta q_l + \gamma\left\{p_l + \left(\frac{E_n}{E_d} - \frac{5}{3}\right) n_l\right\}\right] f_l(r')\,dr'. \tag{36}$$

The right-hand side of this equation vanishes as $r \to 0$ so the asymptotic form of the solution can be written

$$f_l \sim \sin(kr - \tfrac{1}{2}l\pi + \delta_l). \tag{37}$$

It then follows in the usual way (Mott and Massey 1933) that

$$g(\theta) = \frac{1}{2ik}\sum(2l+1)\,(e^{2i\delta_l} - 1)\,P_l(\cos\theta). \tag{38}$$

The problem is then one of determining the phases δ_l by numerical integration of the equation (36) for the various cases which arise. For our purposes it is only necessary to consider the cases with $l = 0, 1$ as higher order phases are negligible except at neutron energies beyond 10 MV.

3. NUMERICAL CALCULATIONS

Calculation of potential function and kernels. The functions U, q_l, p_l, n_l all involve the solution χ of the deuteron wave equation (14). Using the function (3) for V, χ may be found in terms of Bessel functions (Massey and Mohr 1935) and the normalized solution for the ground state is given by

$$r\chi = nJ_{0\cdot4}\left\{\left(\frac{4\pi^2 MAa^2}{h^2}\right)^{\frac{1}{2}} e^{-r/a}\right\}, \tag{39}$$

with $n = 0\cdot7084$, A and a as in (3).

This function was tabulated at suitable intervals by using the series expansion to calculate the Bessel function at various points and then interpolating. Its form is illustrated in figure 1. For large r

$$\chi \sim 0\cdot9389 r^{-1} e^{-0\cdot2312r}, \tag{40}$$

a result made use of in calculating q_l, p_l, n_l for large r, r'. These numerical values are given with 10^{-13} cm. as unit of length, and this unit will be used henceforward.

To calculate U we now have, using (3) and (17),

$$\frac{3h^2}{16\pi^2 M}U(r) = \tfrac{1}{2}An^2\int_0^\infty\int_{-1}^1 r'^2\{\chi(r')\}^2 \exp\left\{-\frac{2}{a}(r^2+\tfrac{1}{4}r'^2-rr'x)^{\frac{1}{2}}\right\}dr'dx,$$

$$= \frac{Aan^2}{2r}\int_0^\infty r'^2\{\chi(r')\}^2\{G(r\sim\tfrac{1}{2}r')-G(r+\tfrac{1}{2}r')\}\,dr', \tag{41}$$

where

$$G(y) = e^{-2y/a}(y+\tfrac{1}{2}a). \tag{42}$$

Using the tabulated values of χ, U was evaluated for various r by numerical integration. The resulting function is illustrated in figure 1.

The evaluation of the kernels q_0, q_1; p_0, p_1; n_0, n_1 was also carried out by numerical methods. At various suitably chosen points in the r, r' plane the integrals (35) were evaluated numerically either by Shovelton's or Gregory's method. Intermediate values were obtained by interpolation along lines in the rr' plane parallel to the main diagonal (through the origin), to the r, r' axes and in other directions, care being taken that interpolation in different directions gave the same results. Over 750 numerical integrations were necessary to obtain sufficient points adequately to determine the kernels but the work was greatly reduced by being made as systematic as possible.

Contour lines illustrating the magnitudes of the various kernels are given in figure 2. It will be seen that of the kernels for l equal to 0, p_0 and n_0 have considerably greater range than q_0. For small values of r, r', p_0 and q_0 are comparable and n_0 much less, whereas for large r, r', q_0 is negligible and p_0 and n_0 comparable. However, p_0 and n_0 are always combined with opposite signs (equation (36)), and as n_0 has the larger factor it is the dominant term at large distances. q_1 is so small everywhere as to be effectively negligible, and the main contribution for small r, r' arises from p_1 in those cases when α and γ are not zero. It will be noted also that, while the diagonal values of p_1 have the same sign as n_1, for certain other values of r, r', p_1 changes sign.

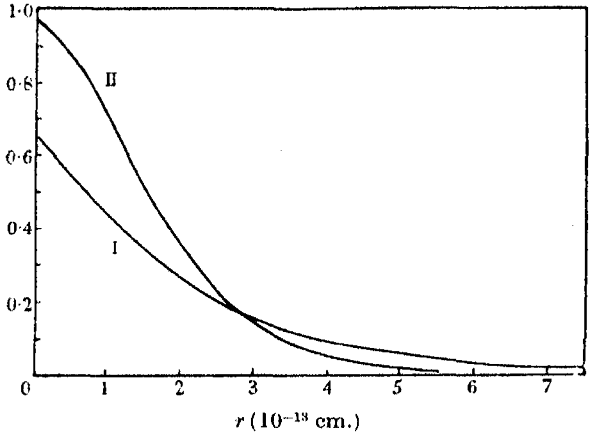

FIGURE 1. Normalized deuteron ground state wave function. Curve (I), $\chi(r)$ normalized and curve (II) 'ordinary' potential $U(r)$, as $\frac{16\pi^2 M}{3h^2}U(r)$ in 10^{26} cm.^{2}, occurring in interaction with a deuteron.

Solution of the equations. The procedure adopted depended largely on the particular case concerned. For $l = 1$ methods based on the usual perturbation theory quickly gave the desired results, but for $l = 0$ other methods had to be employed so we discuss the different cases separately.

$l = 0$. *Doublet* (a). *Mixed exchange forces.* For this case, which is especially simple as $\alpha = 0$, use was made of an approximate analytical expression for the only kernel concerned in the form

$$q_0(r, r') = -\mu rr'e^{-b(r+r')}, \tag{43}$$

with $\mu = 6{\cdot}56, \quad b = 1{\cdot}25.$

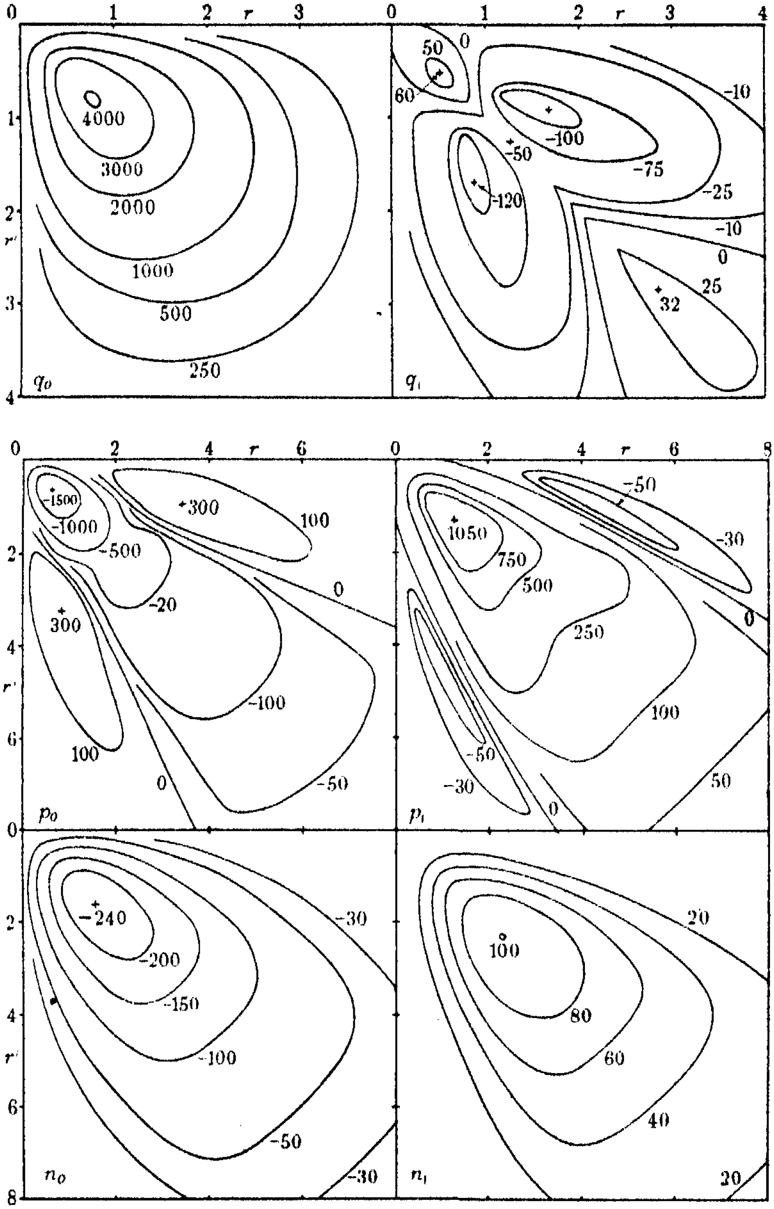

FIGURE 2. Contour representatives of the kernels q_0, q_1; p_0, p_1; n_0, n_1. r, r' are given in units of 10^{-13} cm., and the numbers attached to the contours represent units of 10^{61} cm.$^{-5}$.

Using this expression for q_0 the equation (36) can be solved to give

$$f_0 = \sin(kr+\delta_0) - \sin\delta_0\{1+(b^2+k^2)\,r/2b\}\,e^{-br}, \tag{44}$$

where

$$\cot\delta_0 = \{4b^3(b^2+k^2)^4+\mu(-5b^6+15b^4k^2+5b^2k^4+k^6)\}/(16kb^5\mu). \tag{45}$$

Equation (44) provides at once a very satisfactory approximation to the doublet wave function, which can be improved by a simple iteration process. The function f^0 is inserted in the integral on the right-hand side of (36), which then becomes a second order differential equation, soluble by the usual numerical methods. Suppose the solution with the same initial gradient as f^0 is f^1: a repetition of the process with f^1 in place of f^0 gives a further approximation to the exact solution which is rapidly attained with sufficient accuracy after two or three such approximations. For doublet equations the final solution invariably lies between f^0 and f^1 and the convergence is therefore quite stable.

In particular this method has been applied when k is equal to 0·075 and 0·50. A knowledge of the differences between the values of δ_0 given by (44) and those finally obtained for these values of k—differences which do not exceed 0·10 radian—makes it easy to apply a rough correction to the approximate results given by (44) for intermediate values of k.

Other doublet states. For all doublet states other than the one just considered, the equations are complicated either by the presence of a term in $U(r)\,f_0(r)$, or by a kernel which is not uniformly negative or positive. It is not then possible to obtain a good approximation by the simple method used above. However, when $l = 0$ the doublet solutions do not differ very much among themselves, and it is sufficient to take the solution for the doublet (a) state, with type III forces, as the basis of an iterative process to find a more accurate solution for any other doublet equation. This presents no numerical difficulty.

In a few cases detailed calculations have been made to derive δ_0; in particular, the doublet (a) phases for type I forces and k equal to 0·075 and 0·50, and also the doublet (b) phase for type III forces and k equal to 0·20. These phases appear to be slightly larger than the doublet (a) δ_0's for type III forces and the corresponding value of k.

Quartet state, Mixed exchange forces. Considerable difficulty was met here at the outset. Because of the p_0 and the n_0 terms the kernel is not uniformly negative as in the doublet equation first considered; it is indeed large and negative for small values of r and r', but later changes sign and the positive tail is appreciable out to distances of $8-12\times10^{-13}$ cm.

Some preliminary investigations disclosed that the solution differs very markedly from those for the corresponding doublet states, which were therefore valueless as a first approximation. Moreover, it turns out to be large in the region where the kernel is positive, and the product $g(r, r')f(r')$ then has the effect of a repulsive field which is more than sufficient to counterbalance any attraction at the shorter distances. An instability is thereby introduced which makes solution by iteration difficult and slowly convergent.

An insight into the behaviour of the solution for kernels of this type was obtained by representing the kernel by the approximate form

$$-\mu rr'(e^{-\alpha(r+r')}-\gamma e^{-\beta(r+r')}), \quad \alpha>\beta$$

and examining the resulting solution which is expressible in analytical terms. If we give to α, β, μ values of the order necessary to make the representation reasonable, leaving the fourth parameter γ variable, then $\tan\delta_0$ can be written as

$$K(\gamma-\gamma_0)/(\gamma-\gamma_1),$$

where K, γ_0, γ_1 are new constants depending on k as well as α, β, μ. The change in the phase δ_0 as γ increases from zero is quite remarkable, mainly because γ_0 and γ_1 are in general very nearly equal. Thus, assuming that $\gamma_0<\gamma_1$, we see that, when γ is zero or small, δ_0 is very close to $\tan^{-1}K$, an angle which in general lies between 0 and $\pi/2$, if μ is positive. In the other limit when $\gamma\gg\gamma_1$, $\tan\delta_0$ is again nearly equal to K, but δ_0 is less than its initial value by π. This is because δ_0 must vary continuously as γ increases, and as γ increases to γ_0, δ_0 falls to zero and subsequently takes on negative values, the final value being between $-\frac{1}{2}\pi$ and $-\pi$. A similar change occurs when $\gamma_0>\gamma_1$, but the initial value of δ_0 is between $\frac{1}{2}\pi$ and π, and the final between 0 and $-\frac{1}{2}\pi$. Moreover it is clear that when $\gamma_1\sim\gamma_0$ is small compared with either γ_0 or γ_1, the change from the positive value of $\tan^{-1}K$ to the negative takes place very rapidly, and except in the neighbourhood of γ_0 and γ_1, δ_0 is close to one or other of the two 'steady' values differing by π.

Now although in the case of the quartet equation the kernel cannot be represented very satisfactorily by an expression as simple as (45), yet it appears that, for equations of the type we have been considering, there do exist two stable forms of solution which differ in phase approximately by π, and which correspond to the doublet and quartet functions. Thus the doublet solution has a positive δ_0, corresponding to a kernel for which γ is small or zero, whereas the quartet has a negative δ_0 such as would follow from a kernel with γ greater than either γ_0 or γ_1. In both instances in which the phase δ_0^Q has been determined with precision for type III forces, when

k is 0·2 and 0·5, the difference $\delta_0^D - \delta_0^Q$ is very close to π, as it should be if this interpretation is correct. The marked difference in the forms of the two solutions for k equal to 0·2 is clearly seen in figure 3.

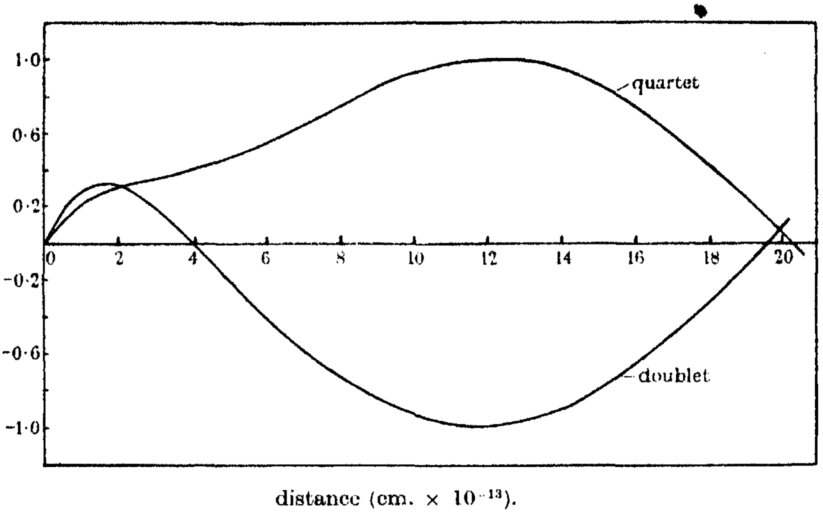

FIGURE 3. Functions $rf_0(r)$ for radial motion of neutrons of 1·85 MV energy relative to deuterons at rest, with zero relative angular momentum and each possibility of total spin. Exchange forces of mixed type have been assumed in deriving the functions, which are normalized to unit amplitude at infinity.

It is now evident that one must proceed from an initial approximation of the right type in solving the quartet equation. In general, when faced with a kernel of the 'quartet type', it is not possible to decide at once whether the solution is one with positive δ_0 or with negative δ_0. Not much assistance is to be gained by using the analytical solution obtained from (45), because the crudity of the approximation to the exact kernel leads to some ambiguity in allotting a value to γ. This is rather serious if, as in the case of our quartet equation, the indicated value of γ is in the region of γ_0 and γ_1; then a relatively small error of judgment in fixing γ may lead to an initial solution with quite the wrong characteristics, and the subsequent iteration process will converge very slowly, if at all.

Although the details of the methods finally adopted for solving the quartet equation will be reserved for a later paper, we shall describe briefly one practicable method which was actually used. In this the equation (36) is first replaced by

$$\frac{d^2f}{dr^2}+k^2f=\int_0^{R_0}\left\{q_0+p_0+\left(\frac{E_n}{E_d}-\frac{5}{3}\right)n_0\right\}f(r')\,dr', \tag{46}$$

the infinite range of integration being curtailed to one which is finite. If R_0 is not too large, say of order 4–6, it is possible to solve (46) in the range from 0 to R_0 by replacing it by a set of finite difference equations, which may be solved to give a function f^0 zero at the origin and defined at a number of equidistant points up to R_0. Numerical integration of (46) can then be applied to extend this function to R_1 ($> R_0$). Next the function f^0 is used as a first approximation in solving the equation

$$\frac{d^2f}{dr^2}+k^2f=\int_0^{R_1}\left\{q_0+p_0+\left(\frac{E_n}{E_d}-\frac{5}{3}\right)n_0\right\}f(r')\,dr'. \tag{47}$$

f^0 is introduced into the integral and an iterative process used to determine a consistent solution of (47), say f^1. This is again extended by numerical integration to R_2, and the process repeated until further increase in the upper limit to the integral produces no appreciable change in the solution.

Provided that $R_0, R_1, R_2, \ldots$ are suitably chosen this process gives a steady convergence to the exact solution required. If R_0 is taken to be not greater than about 4 it is apparent from figure 3 that the function f^0 may not be very different whether the final solution is one with positive or negative δ_0. However, when the part of the kernel between R_0 and R_1 (about 6) is introduced in the course of solving (47), the main modification to f^0 is in the region R_0-R_1, and this gives the first indication of the final form of the solution, according as whether f^1 tends to lie above or below f^0 in this range. Further extensions of the range show more and more conclusively which type of solution is the proper one. Unlike the doublet case the convergence is such that the functions $f^0, f^1, f^2, \ldots$ form a sequence which tends to the final solution from one side only, and the convergence is in general slower than for the doublet. However, as usual in such processes, some experience allows the work involved to be much curtailed, since the final solution can be anticipated in some degree.

As already mentioned δ_0^Q has been determined precisely for k equal to 0·2 and 0·5, assuming mixed exchange forces. The rough rule which has been discovered, that the difference $\delta_0^D-\delta_0^Q$ is nearly equal to π, enables δ_0^Q to be estimated with almost equal precision for any other value of k for which δ_0^D is known.

Other quartet states. The method outlined above for the solution of the quartet equation in the particular case of mixed exchange forces, is equally applicable for other types of force, when terms in $U(r)$ may be present in the equation for $f(r)$. One such case has been worked out in detail, assuming ordinary forces (type I) and k equal to 0·2, and the value of δ_0^Q, though still negative, is somewhat smaller in magnitude than the corresponding phase assuming mixed exchange forces. It seems reasonable to assume the difference between δ_0^D and δ_0^Q for other types of force does not depart very far from π, hence rough estimates of δ_0^Q for other values of k can be made as before.

$l = 1$. *Forces of type III.* These are characterized by having $\alpha = 0$: the initial approximation for f_1 used to calculate the kernels on the right-hand side of (36) was then the plane wave

$$f_1^0 = \cos kr - \frac{\sin kr}{kr}.$$

The approximate value of δ_1, say δ_1^0, is then given by

$$\delta_1^0 = k^{-1}\iint f_1^0(r)\left[\beta q_1+\gamma\left\{p_1+\left(\frac{E_n}{E_d}-\frac{5}{3}\right)n_1\right\}\right]f_1^0(r')\,dr\,dr'.$$

It was verified by accurate solution of the equations by iteration, carried out for $k = 0{\cdot}2$ and $0{\cdot}5$, that the value of δ_1^0 is itself quite a good approximation and this was used to obtain results for other cases.

Forces of type I. Here the initial approximation f_1^0 used for f_1 is the proper solution of the equation

$$\frac{d^2f_1^0}{dr^2}+\left(k^2-\frac{2}{r^2}-\alpha U\right)f_1^0 = 0.$$

Normalizing this solution to have the asymptotic form

$$f_1^0 \sim \sin\left(kr - \tfrac{1}{2}\pi + \delta_1^0\right),$$

the first approximation to δ_1 is given by

$$\delta_1^1 = \delta_1^0 + k^{-1}\iint f_1^0(r)\left[\beta q_1+\gamma\left\{p_1+\left(\frac{E_n}{E_d}-\frac{5}{3}\right)n_1\right\}\right]f_1^0(r')\,dr\,dr'.$$

Accurate solution of the equations by iteration for $k = 0{\cdot}2$ and $k = 0{\cdot}5$ showed that this is a good initial approximation capable of use for other cases.

Forces of type II. For the quartet cases these offered a more difficult problem but the case $k = 0{\cdot}2$ was solved by a trial and error procedure. The doublet states can be dealt with in the same way as for type I forces.

Numerical values of the phases. In table 2 the values of δ_0 and δ_1 are given for several values of k and several types of force, including ordinary forces (type I), Majorana-Heisenberg exchange forces (type II), mixed exchange forces (type III), and the forces assumed by Wheeler (1937). In the table the values obtained by exact numerical solution of the differential equations, as described in the present section, are in heavy type. Those δ_1 phases derived by use of the perturbation methods described in the same section, which were found to yield results in agreement with the more accurate methods when both were tried, are indicated by enclosing brackets. The remaining δ_0 phases, in ordinary type, have been estimated by noting certain regularities of behaviour between the phases accurately calculated and relating these with expectations based on the approximate kernel (43). Of these the principal one, to which attention has already been drawn, is the close proximity of the difference $\delta_0^D - \delta_0^Q$ to π. Use can also be made of the fact that δ_0^D is slightly greater for the doublet (b) state than for the doublet (a), and slightly greater for ordinary forces than for exchange forces.

TABLE 2. PHASES IN SCATTERING OF NEUTRONS BY DEUTERONS

k	total spin	type of force	I (ordinary)	II (M-H exchange)	III ('mixed' exchange)	Wheeler
0·075	quartet	δ_0	—	−0·39	−0·390	—
	doublet (a)	δ_0	**2·79**	2·78	**2·782**	—
0·20	quartet	δ_0	**−0·750**	−0·92	**−0·922**	−0·92
		δ_1	**0·57**	**0·17**	**0·25**	0·24
	doublet (a)	δ_0	2·32	2·27	2·273	2·27
		δ_1	**0·16**	(0·00)	(0·00)	(0·00)
	doublet (b)	δ_0	2·4	2·36	**2·36**	2·36
		δ_1	(−0·01)	(−0·10)	(−0·11)	(−0·09)
0·40	quartet	δ_0	−1·38	−1·61	−1·61	−1·61
		δ_1	(1·05)	—	(0·54)	(0·50)
	doublet (a)	δ_0	1·70	1·60	1·605	1·60
		δ_1	**0·73**	**−0·03**	(0·00)	—
	doublet (b)	δ_0	1·8	1·72	1·72	1·72
		δ_1	(0·43)	(−0·21)	(−0·27)	(−0·14)
0·50	quartet	δ_0	−1·63	−1·88	**−1·879**	−1·88
		δ_1	**1·22**	—	**0·45**	(0·39)
	doublet (a)	δ_0	**1·46**	1·34	**1·337**	1·34
		δ_1	**0·92**	**−0·05**	0·02	—
	doublet (b)	δ_0	1·58	1·46	1·46	1·46
		δ_1	(0·50)	(−0·15)	(−0·23)	(−0·07)

All phases in heavy type have been obtained by precise methods of integrating the differential equations. The δ_1 phases in brackets were derived by perturbation methods. For type III forces the doublet (a) δ_0's for k equal to 0·2 and 0·4 were derived from the analytical approximation (45), with correction for the error in the kernel; all other δ_0's in ordinary type have been estimated by empirical rules relating the phases for different states and different types of force.

† *Note added in proof*, 11 *August* 1941. Since these results were obtained, the accuracy of the numerical evaluation of the kernels has been increased in the course of an extension of the work to proton-deuteron collisions. As a result it appears that the quartet δ_0, δ_1 phases as given in table 2 are slightly too small in absolute magnitude. The differences are unimportant, particularly for the lower energies.

No detailed calculations of δ_0 for exchange forces of type II, or those assumed by Wheeler, have been made, but it is probable that they are nearly the same as for the other forces. In fact it has been assumed throughout that the phases are the same as for the mixed exchange forces. A rough check has been carried out for $k = 0{\cdot}2$ by using for the kernels the values they have for the type III forces, and then carrying out the integration of the differential equation with the constants α, β, γ appropriate to a type II force. It was found that the resulting solution is not very different from that for the type III force, so partially confirming our assumption.

4. COMPARISON WITH EXPERIMENT

Angular distribution. It will be noticed immediately that for all neutrons in the wide energy range considered (0·25 to 11·5 MV), the δ_1 phases calculated on the assumption of exchange forces, of either type, are much smaller than the corresponding ones for ordinary forces. Also the quartet δ_1 phases, which have the same sign for all types of force, are generally larger than the corresponding doublet phases. As the δ_0 phases are practically independent of the type of force assumed it follows that the general form of the angular distribution can be expected to be rather similar for all types of force, but to exhibit a much wider variation for ordinary forces. This is clearly revealed in the angular distributions calculated for neutrons of 1·85 MV ($k = 0{\cdot}2$) and 11·5 MV ($k = 0{\cdot}5$) energy, assuming the three types of force, and illustrated in figure 4.

At the lower energy, backward scattering ($\theta > 90°$) is stronger than forward but the reverse is true at the higher energy. The transition from one kind of distribution to the other occurs at the energy such that δ_0^Q passes through the value $-\frac{1}{2}\pi$, and for which δ_0^D is very close to $\frac{1}{2}\pi$ as $\delta_0^Q \simeq \delta_0^D - \pi$.

The general conclusion that exchange forces lead to more uniform scattering is independent of the inclusion or otherwise of isotopic spin (thus differences between doublet (*a*) and doublet (*b*) do not appreciably affect the weighted mean cross-section), and of the type of exchange force assumed. It is therefore probable that an experimental investigation of the scattered intensity at neutron energies of 2 MV or higher would provide very valuable evidence about the nature of nuclear forces. At present the only evidence of this kind is given by the preliminary experiments of Kruger, Shoupp, Watson and Stallmann (1938) and the recent investigations of Barschall and Kanner (1940), all using D-D neutrons. The results obtained by the two groups of workers do not agree, as Barschall and Kanner find that the angular distribution (in relative co-ordinates) is nearly uniform over the angular range investigated (70–120°), but the other workers find a distribution far from uniform.

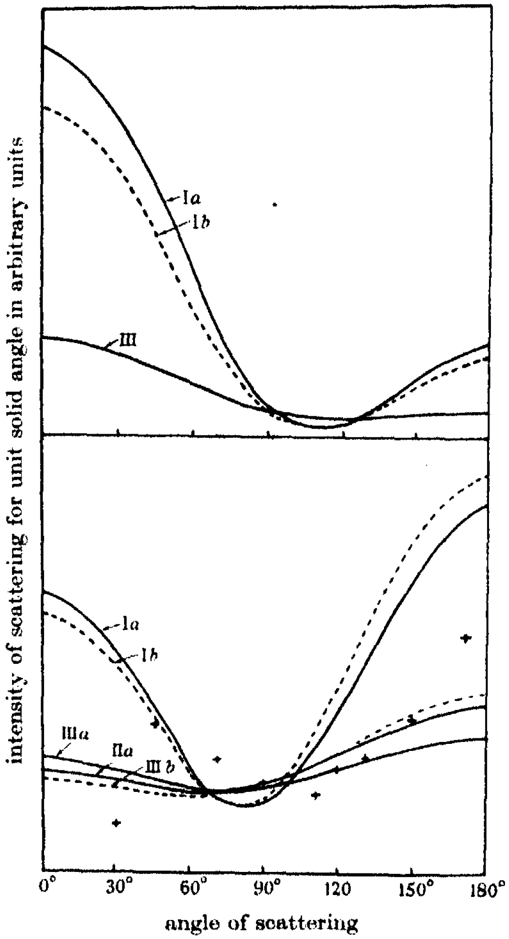

FIGURE 4. Calculated angular distributions (in relative co-ordinates) for collisions of neutrons with deuterons, assuming various types of nuclear force; curves I, ordinary forces; curves II, Majorana-Heisenberg exchange forces; curves III, mixed exchange forces; *a*, calculated assuming isotopic spins; *b*, treating neutron and proton as distinct; +, observed points obtained by Kruger and others (1938), adjusted to agree at 90° with III. Upper curves: $k = 0{\cdot}5$, neutron energy = 11·5 MV. Lower curves: $k = 0{\cdot}2$, neutron energy = 1·85 MV.

Referring to figure 4 we see that, assuming the more recent work, that of Barschall and Kanner, to be correct, there is strong evidence in favour of the reality of exchange forces. Thus both types of forces II and III give only a small variation in scattered intensity over the 70–120° range, whereas ordinary forces give an extreme variation of at least 2 : 1 in this range. On the other hand the results of Kruger, Shoupp, Watson and Stallmann included in figure 4 also, do not agree with any of the calculated distributions. In view of this unsatisfactory position it is very desirable that further experimental results be obtained.

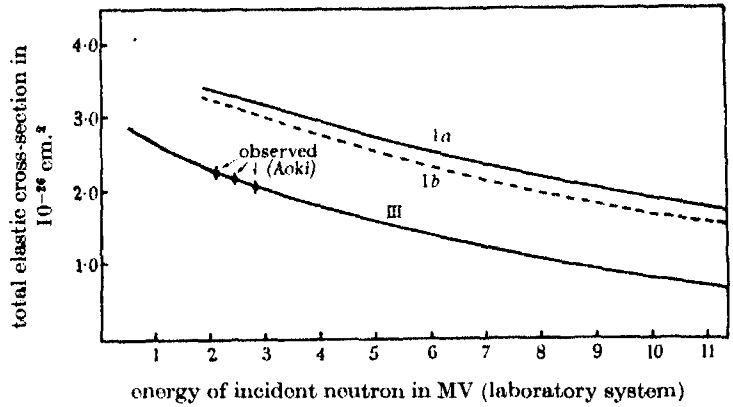

FIGURE 5. Calculated total elastic cross-sections for collisions of neutrons with deuterons. I*a*, assuming ordinary forces and isotopic spins; I*b*, assuming ordinary forces, but different identities for neutron and proton; III, assuming mixed exchange forces, with or without introducing isotopic spin. ♦, observed cross-sections with range of experimental error (Aoki 1939). At neutron energies below 1·85 MV the shape of the curves I has not been determined, but must tend to near equality with III at the zero energy limit.

Total elastic cross-section. The total cross-sections Q_0, calculated by substitution of the phases given in table 2 into the formula (38), are illustrated in figure 5 as functions of the neutron energy. At low energies, to the accuracy of our calculations, there is little difference between the values derived from the various types of force, as in this range δ_0 alone is important. At higher energies, when δ_1 becomes appreciable, the cross-section calculated on the assumption of ordinary forces is larger than those derived from exchange forces owing to the more rapid rise of δ_1 in the former case. As we have not calculated δ_1 for type I forces for neutron energies below 1·85 MV the shape of the cross-section curve for this case is not known for such energies. However, as it tends to near equality with the corresponding curve for exchange forces as $k \rightarrow 0$, it is highly probable that it must exhibit a maximum at some energy between 0 and 1·85 MV.

On the scale of figure 5 the difference between the curves for forces of type III, calculated with and without the assumption of isotopic spin, is inappreciable. For forces of type II the cross-section, at energies beyond 1 MV or so, is less than for forces of type III but, as we have not calculated δ_1^Q phases for $k = 0{\cdot}4$ and $k = 0{\cdot}5$ for this case, it is not possible to include an appropriate curve in figure 5. However, for neutrons of energy 1·85 MV we find that forces of type II give a cross-section of $2{\cdot}10_5 \times 10^{-24}$ cm.^{2} (assuming isotopic spin) and of $2{\cdot}07 \times 10^{-24}$ cm.^{2} (assuming separate identity for neutron and proton).

For D-D neutrons, Q_0 has recently been measured by Aoki (1939): by using neutrons emitted in various directions relative to the deuterons incident in the D-D reaction he obtained values of Q_0 for neutrons of three different energies, 2·1, 2·4 and 2·8 MV. His results, included in figure 5, agree very well with the values calculated for exchange forces, but are considerably smaller than those calculated assuming ordinary forces of type I. Again we have evidence tending to favour exchange forces.

The most recent observed value of Q_0 for thermal neutrons is that of Carroll and Dunning (unpublished but quoted by Motz and Schwinger 1940), who find Q_0 to be $5{\cdot}7 \times 10^{-24}$ cm.^{2}, without allowance for the effect of molecular binding. As allowance for this requires the inclusion of a reduction factor of between 1·5 and 2·0, there appears to be good agreement with the value of $3{\cdot}3 \times 10^{-24}$ cm.^{2} which is obtained by a short extrapolation of our results to zero energy and which is independent of the nature of the forces (see also figure 6).

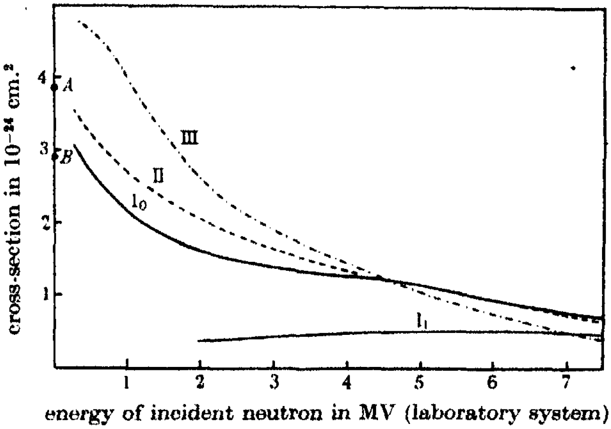

FIGURE 6. Calculated zero order elastic cross-sections for collisions of neutrons with deuterons assuming mixed exchange forces with different ranges. I_0 with range $1{\cdot}73 \times 10^{-13}$ cm.; II, with range $2{\cdot}16 \times 10^{-13}$ cm.; III, with range $3{\cdot}24 \times 10^{-13}$ cm.; I_1, the first order cross-section, assuming a range of $1{\cdot}73 \times 10^{-13}$ cm. Observed low velocity limit of Q_0 lies between points A and B.

Variation of range of fundamental interaction. The effect of an alteration of the range a of the fundamental interaction (3) on the total cross-section Q_0 can be approximately determined as follows. If the deuteron wave function χ can be easily calculated for a particular value of a it is not difficult to find the quantities μ, α which make the approximate kernel (43) a good representation of the actual q_0 kernel for this case. All that is necessary is to use χ to calculate by numerical integration a few of the diagonal elements of the kernel matrix, and then to adjust μ and α to give the best fit at these points. By using (45) a good approximation to the δ_0^D phase may quickly be obtained, and it is reasonable to expect that δ_0^Q will again be nearly equal to $\delta_0^D - \pi$. The derivation of Q_0, when δ_1 is small, follows at once. Further simplification is introduced by choosing values of a for which $(4\pi^2M/a^2h^2)^{\frac{1}{2}}$ is $\frac{1}{2}$ and $\frac{3}{4}$, for then, in accordance with (39), χ can be obtained quickly from tables of $J_{\frac{1}{2}}(x)$ and $J_{\frac{3}{4}}(x)$ respectively.

In this way we have found the following values of μ, α for these values of a, in addition to 1·73:

$(4\pi^2M/a^2h^2)^{\frac{1}{2}}$	a	μ	α
0·40	1·73	−6·56	1·25
0·50	2·162	−3·225	1·05
0·75	3·244	−0·90	0·76

The cross-sections Q_0 derived from these constants for the increased values of a are illustrated in figure 6. At the lower neutron energies ($< 1{\cdot}5$ MV) the total elastic cross-section Q_0 is effectively equal to the zero order cross-section Q_0^0, and in this range the cross-section is greater the greater the interaction range a. It will be seen that the low velocity limit of the cross-section for the range $1{\cdot}73 \times 10^{-13}$ cm., used in our detailed calculation, falls within the limits obtained in the recent experiments quoted by Motz and Schwinger (1940). The experimental uncertainty is due to the correction for molecular binding being known only to lie between 1·5 and 2·0. The other ranges appear to give too large values at the low velocity limit.

At the higher energies the order of the Q_0^0 for different a changes over, but in this region Q_0^1, the contribution from δ_1, becomes important, as will be seen from figure 6. Since Q_0^1 at its maximum is certainly of the same order as a^2, its effect may well be to preserve the same order in the Q_0's at high energies as at low.

5. COMPARISON WITH PREVIOUS THEORETICAL RESULTS

Although no estimates of δ_1 phases for neutron-deuteron collisions have been published previously, a number of calculations of zero order phases have been carried out under various assumptions.

Schiff (1937) used an approximate method to calculate the low velocity limit of the cross-section Q_0, assuming forces of type II and for the particle interaction:

$$V(r) = A\{e^{-4r/a} - 2e^{-2r/a}\}, \tag{48}$$

with 36 MV for A, $2{\cdot}69 \times 10^{-13}$ cm. for a, and for x (in (2)) the value 0·4. He used an exponential approximation for $\chi(r)$ and found Q_0 to be $6{\cdot}11 \times 10^{-24}$ cm.^{2}, which is 2–3 times too big. As it is difficult to estimate the accuracy of his approximation owing to the use of a co-ordinate system unusual in collision problems, it is likely that much of the discrepancy can be traced to the inaccuracy of the method used.

Ochiai (1937) used a method somewhat similar to that of Schiff but embodying the relative co-ordinate system 'natural' for collision problems; he also assumed forces of type II but with

$$V(r) = Ae^{-r^2/a^2}, \tag{49}$$

and 30·3 MV for A, $2{\cdot}69 \times 10^{-13}$ cm. for a, 0·58 for x. Using a similar approximation for χ he evaluated δ_0^D and δ_0^Q for neutrons of 0, 0·5 and 1·0 MV energy, and the values he gives for δ_0^D agree very well with ours. Thus for these energies he finds that $\pi - \delta_0^D$ is equal to $4{\cdot}14k$, 0·420 and 0·576 respectively, whereas our results are approximately $4{\cdot}4k$, 0·481 and 0·66. For δ_0^Q he obtains phases greater than ours by π, i.e. his δ_0^D and δ_0^Q are nearly equal, whereas our δ_0^D phases are greater than the δ_0^Q's by about π. This difference has no effect on the scattered amplitudes.

Flügge (1938) derived the equations (12), (13) and carried out numerical calculations of δ_0^D. He assumed an exchange force of type III with x equal to 0·5, and a function $V(r)$ of the same form as did Ochiai, but with 28·1 MV for A and $2{\cdot}81 \times 10^{-13}$ cm. for a. Representing χ approximately by a function also of the form (49) he solved the equation (12) by an ingenious method. His results for δ_0^D agree very closely with ours; thus for neutrons of 2·1 MV energy he obtains δ_0^D equal to 2·1 radians, which is to be compared with our result of 2·22 for the same energy. For some reason Flügge erroneously assumed that quartet zero order scattering is forbidden by the Pauli Principle and made no attempt to determine δ_0^Q.

Finally, Motz and Schwinger (1940) have calculated the low energy limit of Q_0 for exchange forces of types II and III. They have taken $V(r)$ to be of the form (49), with 36 MV for A and $2{\cdot}24 \times 10^{-13}$ cm. for a; for the type II forces the quantity x has the value 0·6, but for type III they assume that $m = 2{\cdot}13$, $h = -1{\cdot}78$, $b = -1{\cdot}35$ and $w = 2{\cdot}00$. Motz and Schwinger set up equations to calculate the scattering by a method which introduces exchange effects in a different way to the method of resonating group structure, and they obtain equations for the functions $F^Q(\mathbf{r})$, $F^D(\mathbf{r})$ which differ from ours in the omission of the terms involving the kernel N and also the contribution to the kernel P arising from $\chi'(u)$. For the type II forces they find a limiting cross-section of $4{\cdot}57 \times 10^{-24}$ cm.^{2} and, for type III, $6{\cdot}91 \times 10^{-24}$ cm.^{2}, both these values being considerably larger than that observed (see figure 6).

It is important to decide how far our theoretical results are reliable in view of the complexity of the problem. The omission of the kernel N as made by Motz and Schwinger does not seem justified, as has been remarked by Wheeler (1937), and any method based on the variation principle certainly includes it. The kernel N and the terms in P containing χ' arise from the necessity for satisfying certain orthogonality conditions which are not satisfied in a method such as that used by Motz and Schwinger. A similar situation arises in the theory of electron scattering with inclusion of exchange, as first pointed out by Feenberg (1932) and discussed by Mott and Massey (1933, p. 153). It is of interest, however, to examine how the δ_1 phases would be modified if Motz and Schwinger's equations were assumed. We may do this by using in place of our kernel P the kernel

$$P' = \frac{16\pi^2 M}{9h^2} (\tfrac{4}{3})^3 \chi(u) \{V(u) + V(v)\} \chi(v),$$

the numerical values of which can be derived from our calculations of P by omitting the terms involving χ'. The general effect of this, together with the omission of the kernel N, is to change the sign of the contribution of the exchange forces to δ_1. Moreover the contributions from P' are usually greater in absolute magnitude than those from $P + (E_n/E_d - 5/3)N$. It appears from an approximate numerical integration that the δ_1 phases for ordinary forces remain considerably larger in absolute magnitude than the corresponding ones for exchange forces, though in all cases, apart from doublet (a), the phases are changed in sign. As the absolute sizes of the various phases appear to be practically the same as for our calculations it follows that Motz and Schwinger's equations would lead to the same general conclusions as those used in our investigation, but the derived angular distributions would be the approximate mirror images of those we have found. This assumes that to the first approximation the δ_0 phases given by the Motz-Schwinger equations will differ only by the addition of π to our δ_0^Q phases, a result which follows from the discussion in § 2. However, the numerical results given by Motz and Schwinger for the low velocity limit of Q_0 do not agree with this, and, until it can be decided whether the discrepancy is due to the interaction $\mathscr{V}$ assumed by them, it must remain uncertain how far the δ_0

phases will be modified by the omission of N and the substitution of P' for P. It remains true, however, that the angular distributions on the assumption of ordinary forces will show more variation than those derived from exchange forces, whatever their detailed shape.

A possible source of inaccuracy in our calculations, as in the work of all other authors on the subject, arises from the neglect of the polarization of the deuteron by the incident neutron. It is difficult to estimate the effect of this, although Ochiai (1937) has obtained some evidence that, at least for the δ_0 phases, it is unimportant. The fact that we obtain good agreement with observed total elastic cross-sections over the range from 0 to 2 MV seems to confirm this.

The agreement of our results with those of Ochiai and Flügge, where they are comparable, suggests that the δ_0 phases are not very sensitive to the shape assumed for the potential function $V(r)$, but this is less likely to be true for the δ_1 phases. The general differences between ordinary and exchange forces will probably persist, however. It is clear that more experimental information is urgently required as there is some prospect of deciding at the same time the validity of our theory and the reality of exchange forces.

We are indebted to the Government Grant Committee of the Royal Society for receipt of a grant which enabled us to employ the very skilled professional services of the Scientific Computing Service to carry out many of the complex arithmetical operations involved in solving the integro-differential equations for the quartet functions. It is a pleasure to acknowledge the special interest, far in excess of professional requirements, which Dr Comrie and Dr Hartley of the S.C.S. have taken in the work. Finally, one of us (R.A.B.) wishes to thank the Royal Commissioners of the Exhibition of 1851 for the award of a Senior Studentship during the period in which these calculations were carried out.

REFERENCES

Aoki, H. 1939 *Proc. Phys.-Math. Soc. Japan*, **21**, 232.
Barschall, H. H. and Kanner, M. H. 1940 *Phys. Rev.* **58**, 590.
Dee, P. I. and Gilbert, C. W. 1937 *Proc. Roy. Soc.* A, **163**, 265.
Feenberg, E. 1932 *Phys. Rev.* **40**, 40.
Flügge, S. 1938 *Z. Phys.* **108**, 545.
Fröhlich, H., Heitler, W. and Kemmer, N. 1938 *Proc. Roy. Soc.* A, **166**, 154.
Kruger, P. G., Shoupp, W. E., Watson, R. E. and Stallmann, F. W. 1938 *Phys. Rev.* **53**, 1014.
Massey, H. S. W. and Buckingham, R. A. 1937 *Proc. Roy. Soc.* A, **163**, 281.

Massey, H. S. W. and Mohr, C. B. O. 1935 *Proc. Roy. Soc.* A, **148**, 206.
Mott, N. F. and Massey, H. S. W. 1933 *Theory of atomic collisions*. Oxford: Clarendon Press.
Motz, L. and Schwinger, J. 1940 *Phys. Rev.* **58**, 26.
Ochiai, K. 1937 *Phys. Rev.* **52**, 1221.
Present, R. and Rarita, W. 1937 *Phys. Rev.* **51**, 788.
Rabi, I. I., Ramsey, N. F. and Zacharias, J. R. 1939 *Phys. Rev.* **55**, 318.
Schiff, L. I. 1937 *Phys. Rev.* **52**, 149.
Wheeler, J. A. 1937 *Phys. Rev.* **52**, 1083.

The behaviour of visual purple at low temperature

By E. E. Broda and C. F. Goodeve, F.R.S.

The Sir W. Ramsay and Ralph Forster Laboratories of Chemistry,
University College, London

(*Received* 21 *April* 1941)

Visual purple is soluble and stable in a mixture of glycerol and water (3:1). At room temperature the spectrum of such a solution is identical with that of the aqueous solution. At −73° C the peak of the absorption curve is higher and narrower than at room temperature, and it is shifted towards longer waves.

The product of photodecomposition at −73° C has a spectrum independent of pH and is at low temperatures thermostable and photostable, but at room temperature it decomposes thermally to indicator yellow. The primary product appears to be identical with transient orange.

The quantum yields of the photoreaction at low and at room temperature are of the same order.

Introduction

Numerous studies have been devoted in recent years to the absorption spectrum and photochemical kinetics of visual purple, the chromoprotein contained in the 'rods' of the retinae of vertebrates. In this paper are described experimental studies at low temperatures up to the point where they were interrupted by the war.

Previous to this work only aqueous solutions of visual purple have been prepared and consequently no solutions could be investigated below 0° C. It has now been found possible, however, to extend the range for experiments on visual purple solutions by the use of a solvent consisting of 75 % glycerol and 25 % water by volume. Such solutions assume glass-like consistency at the temperature of solid CO_2 and remain perfectly homogeneous and brilliantly clear. Even at liquid-air temperatures no crystallization occurs, although a great number of minute cracks due to the contraction of the mass scatter the light and prevent spectroscopic investigations.

While small amounts of any other organic solvent soluble in water to some extent, e.g. alcohol, ether and chloroform, bleach aqueous solutions of visual purple and produce 'indicator yellow', even large quantities of glycerol do not harm the chromoprotein. The peculiar toleration of visual purple for glycerol recalls results obtained with 'serum protein' (Spiro 1903). The stability of aqueous solutions of this protein against denaturation was decreased by the addition of univalent alcohols, especially of higher molecular weight, but was increased by polyvalent alcohols, e.g. glycerol, mannitol, glucose, galactose and lactose.

THE ABSORPTION SPECTRUM

Experiments were carried out to determine whether visual purple belongs to the wide class of coloured organic substances, the absorption curves of which sharpen on reduction of temperature.

Experimental

The spectroscopic determinations were carried out in a room illuminated with ruby light with a Hilger Spekker photometer. The light beams were produced by an iron spark, and filtered through an acid quinine sulphate solution in order to eliminate ultra-violet and violet light. Hypersensitive panchromatic Ilford plates were employed, and the use of a strong metol developer facilitated short exposures. No appreciable decomposition of visual purple occurred during the spectrographic determinations.

The visual purple solutions were prepared from frogs' eyes as described by Lythgoe (1937). Enough glycerol and water were added to the buffered solutions to obtain a mixture containing 75 % glycerol and to fill the all-glass optical cell 5 cm. long and 2·7 cm. wide. The optical density of the solution so obtained at 500 mμ was of the order 0·2 cm.$^{-1}$. The cell was fixed into a rubber-lined brass box lagged outside with asbestos. The box served to hold the mixture of solid carbon dioxide and alcohol, thus keeping the temperature in the cell at −73° C. Two holes facing the cell ends were drilled into the walls of the box so that the light beam could pass; the diameter of the holes was slightly less than that of the cell. One of the two walls provided with holes was detachable and could be screwed to the rest of the box, after the cell was fitted in, in order to hold the cell firmly in position. The rubber lining on both holed walls of the box acted as washers.

In order to prevent condensation of water vapour on the faces of the cell, glass cylinders closed with small plates of optical glass were fixed with tap grease coaxially to each end of the cell and supported by joining them to the metal box with apiezon grease. The optical glass plates were sealed to the cylinders with apiezon, and heated electrically by means of wire spirals wound around the cylinders. The cylinders were kept evacuated during experiments. In this way all glass faces remained perfectly clear. The comparison beam passed through a cell containing solvent only. It was not cooled, but preliminary tests showed that the zero of the spectrophotometer was maintained when the cell in the box, filled with pure solvent, was cooled.

Mist was formed near the cold box, but a powerful fan operating towards the light beams dispersed it and prevented interference with the beams.

Results

The first measurements showed that the spectrum of visual purple in glycerol-water solution at room temperature is identical with that of a twin solution diluted with water to the same strength. Furthermore, it was found that the spectrum remains unaltered by cooling the solution down to −73° with exclusion of light and warming up again to room temperature.

In figure 1 the spectrum of a solution (pH 6·0) at room temperature (curve 1) is compared with that at −73° (curve 2). Curve 1 comprises densities both in water and in glycerol-water. The influence of thermal contraction, which is very nearly 10 %, was eliminated by subtracting 10 % from the density values obtained at the low temperature.

Curve 2 is not only narrower and higher than curve 1, but the peak is at about 515 mμ instead of at 505 mμ. A similar shift in the position of an absorption peak on cooling was observed with solutions of diphenyl-polyenes (Hausser, Kuhn and Seitz 1935) and of β-carotene (Bowden 1934). On the other hand, solutions of porphyrins and related compounds, including oxyhaemoglobin, show a shift in the opposite direction (Hartridge 1921; Hellström 1931; Conant and Kamerling 1931). It is remarkable that the spectra of the compounds with the shift to shorter waves are of one particular type; they all show sharp maxima and steep thresholds. The meaning of the difference in the shape of the bands has been discussed by Arnold and Kistiakowsky (1932) and by Goodeve (1939).

It is uncertain whether the peak of curve 2 is as smooth as shown in figure 1, as the iron spark in this region is not very rich in lines.

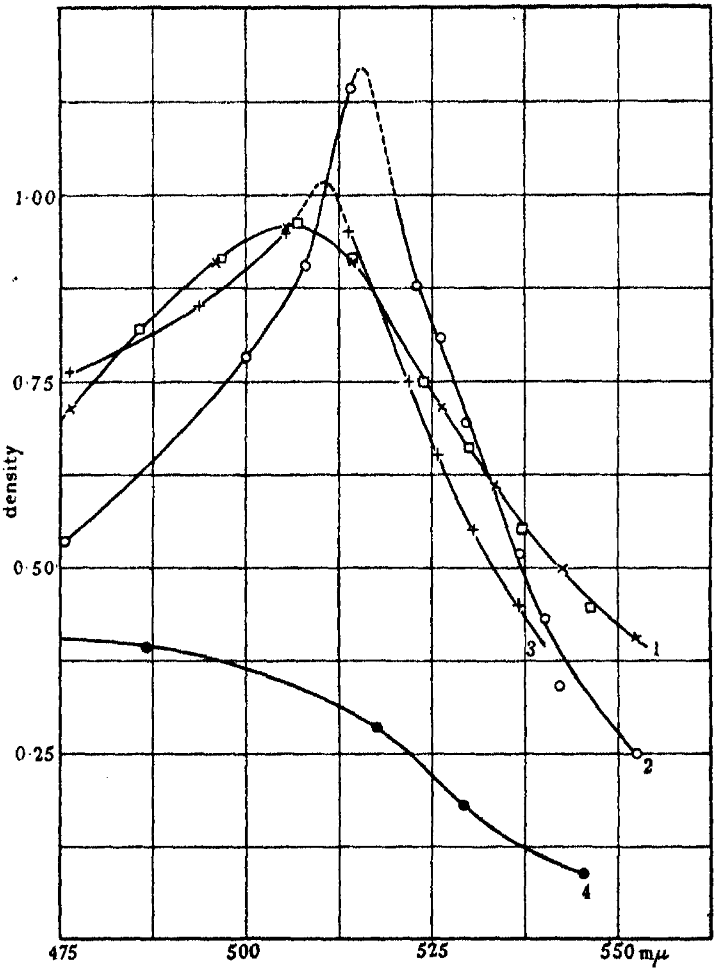

FIGURE 1. The absorption spectra of visual purple and its products (pH 6·0). Curve 1, visual purple at room temperature in water × × ×, in glycerol-water □ □ □. Curve 2, visual purple at −73°. Curve 3, primary decomposition product at −73°. Curve 4, secondary decomposition product at room temperature.

INTERMEDIATE PRODUCTS OF BLEACHING

The photodecomposition of visual purple at room temperature proceeds in several stages (Dartnall 1936; Lythgoe 1937; Wald 1937; Lythgoe and Quilliam 1938*a*, *b*). The primary product ('transient orange') is photostable, but undergoes a thermal change, which at room temperature is rapid enough to make its detection difficult. The spectrum of transient orange is independent of pH and the intensity of its light absorption is not much below that of visual purple (at their respective maxima). The thermal change leads to a yellow compound, the absorption spectrum of which changes with pH, and which, therefore, has been termed 'indicator yellow'. It is possible that water takes part in one or both of these reactions (Lythgoe and Quilliam 1938*a*).

Lythgoe (1937) has shown that the orange colour of a freshly bleached solution of visual purple is stable over a period of minutes, if it is kept near 0° C. The frozen retina as well as frozen solutions of visual purple are more or less photostable, and no transient orange is produced (Kühne 1879; Garten 1906; Dartnall, Goodeve and Lythgoe 1938); but, as under these conditions crystalline water must have separated from the protein, these observations have no bearing on the reaction mechanism proceeding in aqueous solution.

Procedure

To determine the intermediate reaction products at low temperature the cell was illuminated with white light by means of a 4 W lamp fixed in the optical axis of the cell at a distance of 8·5 cm. from the centre of the cell at the opposite end from the spark. The spectrum was taken before and at intervals during the illumination, with interruption of the latter. At the end of each experiment the cell was warmed up to room temperature, and the spectrum taken again.

Results

On irradiation at low temperature the spectrum smoothly changed from that of curve 2 to that of curve 3, figure 1, indicating that a chemical change had occurred. The primary product did not undergo further change after 2 hr. in the dark or on continued illumination. Figure 2 shows how the change on illumination at low temperature comes to an end. When, however, the primary product was warmed up to room temperature in the light or in the dark, it was destroyed very quickly and gave way to a secondary (final) decomposition product represented by curve 4, figure 1 and by curves 4 and 5, figure 2.

In figure 3 the absorption spectra of visual purple solutions (from different preparations) at 73° C are shown for pH 6·0 and 9·0 and also of the primary and secondary decomposition products at these two pH values. This pH range is the one in which the greatest effects of pH on the final product of visual purple occur (Lythgoe 1937). Results are given for the range 510–550 mμ, which is near enough to the maximum of the primary product, but where there is little influence of the 'yellow impurities' always present in visual purple solutions (Lythgoe 1937) and accurate comparison between different solutions is possible. As the concentration of visual purple solutions

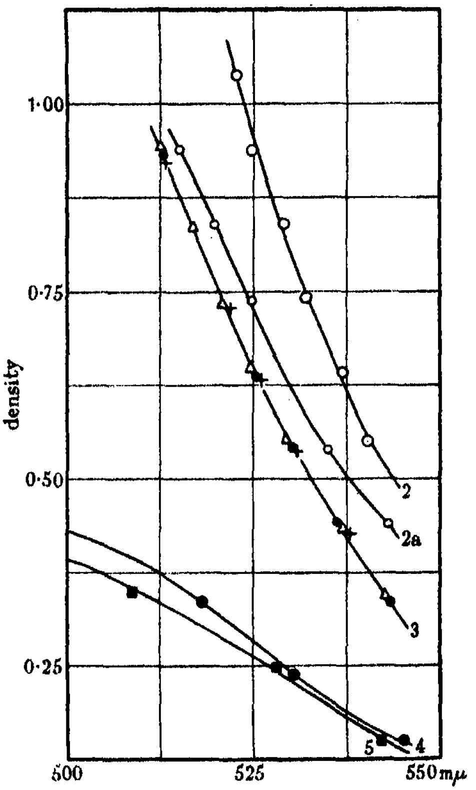

FIGURE 2

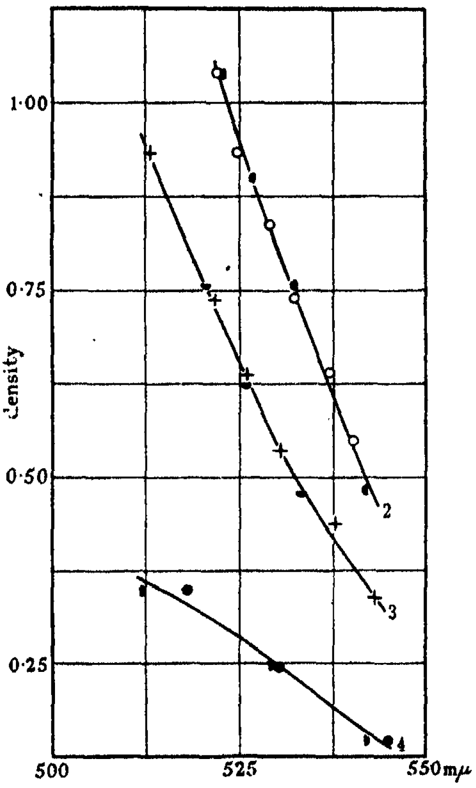

FIGURE 3

FIGURE 2. The changes of absorption in the region 510–550 mμ shown in greater detail than in figure 1. Curve 2, before illumination. Curve 2*a*, after illumination for 3 min. Curves 3, 12 min. △ △ △; 72 min. ● ● ●; and 87 min. + + +. Curve 4, after warming up to room temperature in the dark. Curve 5, 8 hr. later.

FIGURE 3. Comparison of solutions of different pH (−73°). The results for the two solutions are brought to a common basis by superimposing the curves of the unilluminated solutions at 527 mμ. Curve 2, before illumination, ○ ○ ○ pH 6·0, ◖ ◖ ◖ pH 9·0. Curve 3, after illumination, + + + pH 6·0, ▾ ▾ ▾ pH 9·0. Curve 4, after warming up, ● ● ● pH 6·0, ◗ ◗ ◗ pH 9·0.

cannot be determined otherwise than through their optical densities, all density values of one solution had to be recalculated so that the densities of the unbleached solutions agreed at one wave-length. As will be seen from figure 3 no appreciable difference is found between the two solutions. The maximum of the absorption band of the secondary (final) reaction product (not shown in the figure) which is in any case well below 500 mμ, was however shifted to shorter waves at pH 9·0.

Discussion

A comparison of the behaviour of the primary and final reaction products of visual purple at low temperature with the corresponding products at or near room temperature, i.e. transient orange and indicator yellow respectively, shows sufficient resemblance to make it unnecessary to postulate the presence of any new species. The primary product at low temperature is photostable and has a spectrum which is independent of pH, both characteristics of transient orange. Furthermore, the maximum of its absorption curve is on the shorter wave-length side of that of visual purple (at the same temperature) and is nearly as high as the latter.

Likewise, the shape of the curve of the *final* reaction product in the low temperature work and the effect of pH on it show that this substance is indicator yellow.

The difference between the maximum at room temperature and that at -73° C is much greater with transient orange, about 30 mμ, than with visual purple, about 10 mμ; consequently, the difference in hue between illuminated and unilluminated solutions at low temperature is small and when at first a test tube containing cooled solution was exposed to daylight, and the colour examined with the naked eye, it was erroneously believed that no change at all had taken place and that visual purple is photostable at low temperature.

The stability of transient orange in cooled glycerol opens up possibilities for its closer study. It would be particularly interesting to decide whether the loosening of the chromophore-protein bond occurring on bleaching (Wald 1937) is due to the primary or to the secondary reaction, and, thus, to elucidate the nature of the transition transient orange → indicator yellow. As was first shown by Wald, indicator yellow can be extracted from its aqueous solution with organic solvents and separated from the protein. Attempts made here to extract at low temperature transient orange from glycerol-water with ethyl ether were unsuccessful. Extraction from this extremely viscous liquid, however, meets with great experimental difficulties; attempts to extract night blue from cooled glycerol-water with ether, and vice versa, were equally unsuccessful.

RATES OF REACTION

Procedure

The quantum yield of the primary reaction at low temperature was estimated by comparing the velocity of the photoreaction with the velocity in the same experimental arrangement and with the same light source at room temperature. At low temperature the progress of the reaction was measured through the percentage of primary reaction product produced. At room temperature, owing to the instability of the primary reaction product, the progress of the reaction had to be measured by determining the optical density of the illuminated solution after the dark changes had come to an end, i.e. after the transient orange was completely decomposed.

Results

It was first found that by exposing visual purple solutions in water and glycerol-water to daylight in a test tube that, at least at room temperature, both bleach at an equal rate. Although accurate measurements in glycerol-water could only be completed at low temperature (figure 2) it emerged clearly from preliminary tests that the velocity of the primary reaction is about of the same order as at room temperature. The quantum yield is not far from unity over the range 20–60° C (Dartnall, Goodeve and Lythgoe 1938) and from the above it follows that it is also of the order of unity over the wider range of temperature from − 73° C.

The secondary (thermal) reaction, on the other hand, has a considerable temperature coefficient at room temperature (Lythgoe 1937; Lythgoe and Quilliam 1938 *a*, *b*) and is immeasurably slow at − 73° C.

Our sincere thanks are due to the late Dr R. J. Lythgoe for his interest and help, to Professor A. J. Allmand, F.R.S., for his kind hospitality at King's College, London, to Miss S. J. Hooper for the preparation of visual purple, and to the Rockefeller Foundation for a financial grant.

REFERENCES

Arnold, L. B. jr. and Kistiakowsky, G. B. 1932 *J. Amer. Chem. Soc.* **54**, 1713.
Bowden, F. P. See Twyman, F. and Alsopp, C. B. 1934 *The practice of spectrophotometry*, plate IV. London.
Conant, J. B. and Kamerling, S. E. 1931 *J. Amer. Chem. Soc.* **53**, 3522.
Dartnall, H. J. A. 1936 Ph.D. Thesis.
Dartnall, H. J. A., Goodeve, C. F. and Lythgoe, R. J. 1938 *Proc. Roy. Soc.* A, **164**, 216.
Garten, S. 1906 *v. Graefes Arch. Ophthal.* **63**, 112.

Goodeve, C. F. 1939 *Nature, Lond.*, **143**, 1007.
Hartridge, H. 1921 *J. Physiol.* **54**, *Proc.* cxxviii.
Hausser, K. W., Kuhn, R. and Seitz, G. 1935 *Z. phys. Chem.* B, **29**, 391.
Hellström, H. 1931 *Z. phys. Chem.* B, **12**, 353.
Kühne, W. 1879 In Hermann's *Handbuch der Physiologie*, **3**, Part I, 284.
Lythgoe, R. J. 1937 *J. Physiol.* **89**, 331.
Lythgoe, R. J. and Quilliam, J. P. 1938*a* *J. Physiol.* **93**, 24.
Lythgoe, R. J. and Quilliam, J. P. 1938*b* *J. Physiol.* **94**, 399.
Spiro, K. 1903 *Beitr. Chem. Physiol. Path.* **4**, 300.
Wald, G. 1937 *J. Gen. Physiol.* **21**, 795.

The velocity of diffusion in a mixed gas; the second approximation

By S. Chapman, F.R.S., *Imperial College, London*
and T. G. Cowling, *The University, Manchester*

(*Received* 22 *April* 1941)

The general equation of diffusion in a mixed gas in non-uniform motion, in the presence of forces imparting differential accelerations to the two constituents, and of gradients of composition, pressure, and temperature, has been carried to a second approximation. This adds nine new terms to the expression for the velocity of diffusion, and each term involves as a factor a new 'second order' diffusion coefficient. All the new terms depend on the gradients of the mean motion of the gas, and vanish if this is uniform. One of the new terms is proportional to the space gradient of the tensor that expresses the rate of distortion of the gas; two other terms include parts involving the second space differential coefficients of the mean motion. The other portions of the two latter terms, and the remaining six terms, depend on products of the velocity gradients and the factors that appear in the first-order diffusion equation, namely the gradients of composition, pressure, and temperature, and the relative accelerations of the two types of molecule.

The expressions for the nine new diffusion coefficients are extremely complicated, and have been evaluated only approximately.

The new terms in the velocity of diffusion are with one exception negligible compared with the first-order terms, at pressures above 10^{-6} atm., except possibly in shock waves where the mean velocity of the gas alters by an appreciable fraction in a distance equal to the mean free path.

The excepted term is the one which depends on the gradient of the rate-of-distortion tensor; in certain circumstances this is comparable with, though smaller than, the first-order pressure-diffusion term. It materially reduces the rate of diffusion in a stream of mixed gas flowing under pressure along a fine capillary tube.

1. INTRODUCTION

In the mathematical theory of non-uniform gases (cf. Chapman and Cowling 1939), successive approximations to the velocity-distribution function f are sought. The first approximation, $f^{(0)}$, has the same form as Maxwell's velocity distribution function for a uniform gas; later approximations to f add successive further terms $f^{(1)}, f^{(2)}, \ldots$.

The first additional term, $f^{(1)}$, in the case of a simple gas, has two parts, one proportional to certain combinations of the gradients of the velocity components, the other proportional to the temperature gradient; these terms lead to the usual expressions for the viscous stresses in a non-uniformly moving gas, and for thermal conduction in a gas whose temperature is non-uniform. In the case of a mixed gas, $f^{(1)}$ includes similar terms, and also others which are proportional to the gradients of concentration and pressure, and to the external forces acting on the molecules; the additional terms modify the equation of thermal conduction, and all the terms except those depending on the velocity gradients lead to corresponding terms in the equation of diffusion.

The second additional term, $f^{(2)}$, is much more complicated than $f^{(1)}$. Burnett (1935) has determined $f^{(2)}$ completely, for a simple gas; partial expressions had previously been given by Maxwell (1867), Enskog (1917), and Lennard-Jones (1923). A simplified approximate derivation of $f^{(2)}$ for a simple gas is given in Chapter 15 of our book.

The expression for $f^{(2)}$ for a mixed gas has not hitherto been determined. As in the case of a simple gas, it contributes terms which supplement those given by $f^{(1)}$ for the stress-system and the heat-conduction. The coefficients will be even more complicated than those of viscosity and conduction, given by $f^{(1)}$; in the present state of theory and experiment on gases, it does not seem worth while to evaluate them. However, $f^{(2)}$ also includes terms that enter into the expression for the velocity of diffusion, and we have recently considered in what way the ordinary equation of diffusion is modified thereby. This work is briefly described here; we use the relatively simple approximate method which was applied to the case of a simple gas in Chapter 15 of our book. With one exception (cf. § 2 (2)) we also use the same notation (cf. § 5) as in that book, to which we refer for numerous details (section or page references being given).

2. THE GENERAL EQUATIONS

We write
$$\left.\begin{aligned} f_1^{(1)} &= A_1'\boldsymbol{C}_1\cdot\frac{\partial T}{\partial \boldsymbol{r}}+D_1'\boldsymbol{C}_1\cdot\boldsymbol{d}_{12}+B_1'\overset{\circ}{\boldsymbol{C}_1\boldsymbol{C}_1}:\mathrm{e},\\ f_1^{(1)} &= A_2'\boldsymbol{C}_2\cdot\frac{\partial T}{\partial \boldsymbol{r}}+D_2'\boldsymbol{C}_2\cdot\boldsymbol{d}_{12}+B_2'\overset{\circ}{\boldsymbol{C}_2\boldsymbol{C}_2}:\mathrm{e},\end{aligned}\right\} \tag{1}$$

(cf. 15·1 (3)), wherein, departing from the notation of our book (p. 19),

$$\mathrm{e}=\frac{\partial}{\partial \boldsymbol{r}}\boldsymbol{c}_0, \tag{2}$$

namely the velocity-gradient tensor, instead of the symmetrical part of this tensor. The suffixes 1 and 2 refer to the two constituents of the mixture. We also write

$$f_1^{(2)}=f_1^{(0)}\Phi_1^{(2)},\quad f_2^{(2)}=f_2^{(0)}\Phi_2^{(2)}. \tag{3}$$

The ordinary equation of diffusion is derived from $f^{(1)}$ (p. 144). An additional velocity of diffusion, $\overline{\boldsymbol{C}}_1^{(2)}-\overline{\boldsymbol{C}}_2^{(2)}$, is derived from $f^{(2)}$, where (cf. p. 142)

$$\begin{aligned}\overline{\boldsymbol{C}}_1^{(2)}-\overline{\boldsymbol{C}}_2^{(2)} &= \frac{1}{n_1}\int f_1^{(2)}\boldsymbol{C}_1\,d\boldsymbol{c}_1-\frac{1}{n_2}\int f_2^{(2)}\boldsymbol{C}_2\,d\boldsymbol{c}_2\\ &= \frac{1}{n_1}\int f_1^{(0)}\Phi_1^{(2)}\boldsymbol{C}_1\,d\boldsymbol{c}_1-\frac{1}{n_2}\int f_2^{(0)}\Phi_2^{(2)}\boldsymbol{C}_2\,d\boldsymbol{c}_2\\ &= \int \Phi_1^{(2)}\{n_1^2 I_1(\boldsymbol{D}_1)+n_1n_2I_{12}(\boldsymbol{D}_1+\boldsymbol{D}_2)\}\,d\boldsymbol{c}_1\\ &\qquad+\int \Phi_2^{(2)}\{n_2^2 I_2(\boldsymbol{D}_2)+n_1n_2I_{21}(\boldsymbol{D}_1+\boldsymbol{D}_2)\}\,d\boldsymbol{c}_2\\ &= n_1n_2\{\Phi^{(2)},\boldsymbol{D}\}\\ &= \int \boldsymbol{D}_1\{n_1^2 I_1(\Phi_1^{(2)})+n_1n_2I_{12}(\Phi_1^{(2)}+\Phi_2^{(2)})\}\,d\boldsymbol{c}_1\\ &\qquad+\int \boldsymbol{D}_2\{n_2^2 I_2(\Phi_2^{(2)})+n_1n_2I_{21}(\Phi_1^{(2)}+\Phi_2^{(2)})\}\,d\boldsymbol{c}_2\\ &= -\int \boldsymbol{D}_1\{\mathscr{D}_1^{(2)}+J_1(f_1^{(1)}f^{(1)})+J_{12}(f_1^{(1)}f_2^{(1)})\}\,d\boldsymbol{c}_1\\ &\qquad-\int \boldsymbol{D}_2\{\mathscr{D}_2^{(2)}+J_2(f_2^{(1)}f^{(1)})+J_{21}(f_1^{(1)}f_2^{(1)})\}\,d\boldsymbol{c}_2\end{aligned} \tag{4}$$

(see pp. 141 (5), 86, 136 (5), 137).

Since $\boldsymbol{D} = \boldsymbol{C}\,D(C)$, the only terms in the curly brackets which make non-zero contributions to the last two integrals are those of odd degree in $\boldsymbol{C}$.

The terms of odd degree in $\mathscr{D}_1^{(2)}$ are as follows (see pp. 138 (3, 7), 139, 261):

$$
\begin{aligned}
&-f_1^{(0)}\frac{m_1}{k\rho T}\boldsymbol{C}_1\frac{\partial}{\partial\boldsymbol{r}}:\mathsf{p}^{(1)}-\tfrac{2}{3}\Delta\left(T\frac{\partial A_1'}{\partial T}+C_1^2\frac{\partial A_1'}{\partial C_1^2}\right)\boldsymbol{C}_1\cdot\frac{\partial T}{\partial\boldsymbol{r}}\\
&-\tfrac{2}{3}\Delta\left(T\frac{\partial D_1'}{\partial T}+C_1^2\frac{\partial D_1'}{\partial C_1^2}\right)\boldsymbol{C}_1\cdot\boldsymbol{d}_{12}+A_1'\boldsymbol{C}_1\cdot\left\{\frac{D_0}{Dt}\left(\frac{\partial T}{\partial\boldsymbol{r}}\right)-\mathsf{e}\cdot\frac{\partial T}{\partial\boldsymbol{r}}\right\}\\
&+D_1'\boldsymbol{C}_1\cdot\left\{\frac{D_0}{Dt}(\boldsymbol{d}_{12})-\mathsf{e}\cdot\boldsymbol{d}_{12}\right\}+\left(\boldsymbol{C}_1\cdot\frac{\partial T}{\partial\boldsymbol{r}}\right)(\boldsymbol{C}_1\boldsymbol{C}_1:\overset{\circ}{\mathsf{e}})\left(\frac{\partial B_1'}{\partial T}-\frac{\partial A'}{\partial C_1^2}\right)\\
&+\left\{\left(\boldsymbol{C}_1\cdot\frac{\partial n_{10}}{\partial\boldsymbol{r}}\right)(\boldsymbol{C}_1\boldsymbol{C}_1:\overset{\circ}{\mathsf{e}})\left(\frac{n^2}{n_2}\frac{\partial B_1'}{\partial n_1}+\frac{2p}{\rho_1}\frac{\partial B_1'}{\partial C_1^2}\right)+\frac{2p}{\rho_1}B_1'\frac{\partial n_{10}}{\partial\boldsymbol{r}}\boldsymbol{C}_1:\overset{\underset{=}{\circ}}{\mathsf{e}}\right\}\\
&-\left\{(\boldsymbol{C}_1\cdot\boldsymbol{d}_{12})(\boldsymbol{C}_1\boldsymbol{C}_1:\overset{\circ}{\mathsf{e}})\left(\frac{2p}{\rho_1}\frac{\partial B_1'}{\partial C_1^2}+2\frac{\partial D_1'}{\partial C_1^2}\right)+\frac{2p}{\rho_1}B_1'\boldsymbol{d}_{12}\boldsymbol{C}_1:\overset{\underset{=}{\circ}}{\mathsf{e}}\right\}\\
&+\frac{2}{m_1 n}\frac{\partial p}{\partial\boldsymbol{r}}\cdot\left\{\boldsymbol{C}_1\frac{\partial B_1}{\partial C_1^2}(\boldsymbol{C}_1\boldsymbol{C}_1:\overset{\circ}{\mathsf{e}})+B_1'\boldsymbol{C}_1\cdot\overset{\underset{=}{\circ}}{\mathsf{e}}\right\}+B_1'\boldsymbol{C}_1\cdot\frac{\partial}{\partial\boldsymbol{r}}(\boldsymbol{C}_1\boldsymbol{C}_1:\overset{\circ}{\mathsf{e}}).
\end{aligned}
\tag{5}
$$

The terms of odd degree in $\mathscr{D}_2^{(2)}$ are obtained by changing the suffix 1 in (5) into 2, save that the seventh and eighth terms become

$$
\begin{aligned}
&\left(\boldsymbol{C}_2\cdot\frac{\partial n_{10}}{\partial\boldsymbol{r}}\right)(\boldsymbol{C}_2\boldsymbol{C}_2:\overset{\circ}{\mathsf{e}})\left(\frac{n^2}{n_2}\frac{\partial B_1'}{\partial n_1}-\frac{2p}{\rho_2}\frac{\partial B_1'}{\partial C_2^2}\right)-\frac{2p}{\rho_2}B_2'\frac{\partial n_{10}}{\partial\boldsymbol{r}}\boldsymbol{C}_2\cdot\overset{\underset{=}{\circ}}{\mathsf{e}}\\
&\qquad+(\boldsymbol{C}_2\cdot\boldsymbol{d}_{12})(\boldsymbol{C}_2\boldsymbol{C}_2:\overset{\circ}{\mathsf{e}})\left(\frac{2p}{\rho_2}\frac{\partial B_2'}{\partial C_2^2}-2\frac{\partial D_2'}{\partial C_2^2}\right)+\frac{2p}{\rho_2}B_2'\boldsymbol{d}_{12}\boldsymbol{C}_2:\overset{\underset{=}{\circ}}{\mathsf{e}}.
\end{aligned}
\tag{6}
$$

The terms of odd degree in $J_1(f_1^{(1)}f^{(1)})+J_{12}(f_1^{(1)}f_2^{(1)})$ are

$$
\begin{aligned}
&J_1\left\{\left(A_1'\boldsymbol{C}_1\cdot\frac{\partial T}{\partial\boldsymbol{r}}+D_1'\boldsymbol{C}_1\cdot\boldsymbol{d}_{12}\right)B'\boldsymbol{C}\boldsymbol{C}:\overset{\circ}{\mathsf{e}}\right\}\\
&\qquad+J_1\left\{B_1'\boldsymbol{C}_1\boldsymbol{C}_1:\overset{\circ}{\mathsf{e}}\left(A'\boldsymbol{C}\cdot\frac{\partial T}{\partial\boldsymbol{r}}+D'\boldsymbol{C}\cdot\boldsymbol{d}_{12}\right)\right\}\\
&\qquad+J_{12}\left\{\left(A_1'\boldsymbol{C}_1\cdot\frac{\partial T}{\partial\boldsymbol{r}}+D_1'\boldsymbol{C}_1\cdot\boldsymbol{d}_{12}\right)B_2'\boldsymbol{C}_2\boldsymbol{C}_2:\overset{\circ}{\mathsf{e}}\right\}\\
&\qquad+J_{12}\left\{B_1'\boldsymbol{C}_1\boldsymbol{C}_1:\overset{\circ}{\mathsf{e}}\left(A_2'\boldsymbol{C}_2\cdot\frac{\partial T}{\partial\boldsymbol{r}}+D_2'\boldsymbol{C}_2\cdot\boldsymbol{d}_{12}\right)\right\}.
\end{aligned}
\tag{7}
$$

3. THE NINE NEW DIFFUSION TERMS

The terms in $\mathscr{D}^{(2)}$ which involve the factor $\mathsf{p}^{(1)}$ do not contribute to the diffusion velocity, by virtue of 8·31 (9) (*loc. cit.*). The other terms in $\mathscr{D}^{(2)} + J^{(2)}$ contribute the following nine parts to the diffusion-velocity:

$$\left.\begin{array}{ll}
(a) & D_a A \dfrac{\partial T}{\partial \boldsymbol{r}}, \\[2ex]
(b) & D_b A \boldsymbol{d}_{12}, \\[2ex]
(c) & D_c \left\{\dfrac{D_0}{Dt}\left(\dfrac{\partial T}{\partial \boldsymbol{r}}\right) - \mathsf{e}\cdot\dfrac{\partial T}{\partial \boldsymbol{r}}\right\}, \\[2ex]
(d) & D_d \left\{\dfrac{D_0}{Dt}(\boldsymbol{d}_{12}) - \mathsf{e}\cdot\boldsymbol{d}_{12}\right\}, \\[2ex]
(e) & D_e \dfrac{\partial T}{\partial \boldsymbol{r}}\cdot\overset{\circ}{\overline{\mathsf{e}}}, \\[2ex]
(f) & D_f \dfrac{\partial n_{10}}{\partial \boldsymbol{r}}\cdot\overset{\circ}{\overline{\mathsf{e}}}, \\[2ex]
(g) & D_g \boldsymbol{d}_{12}\cdot\overset{\circ}{\overline{\mathsf{e}}}, \\[2ex]
(h) & D_h \dfrac{\partial p}{\partial \boldsymbol{r}}\cdot\overset{\circ}{\overline{\mathsf{e}}}, \\[2ex]
(i) & D_i \dfrac{\partial}{\partial \boldsymbol{r}}\cdot\overset{\circ}{\overline{\mathsf{e}}}.
\end{array}\right\} \qquad (8)$$

The factors D_a, D_b, ... in these terms may be called 'second order diffusion coefficients'. Each term in (5), after the first, corresponds to one term in (8), the order of corresponding terms in the two expressions being the same. The terms of (7) contribute to D_c and D_g alone.

4. APPROXIMATE EVALUATION OF THE SECOND ORDER DIFFUSION COEFFICIENTS

The functions A', B', D' and $\boldsymbol{D}$ occurring in the integrals giving the diffusion coefficients are considered in Chapter 8 of our book. They are expressible as infinite series: the formulae for successive terms in these series rapidly increase in complexity, and usually only the first one or two terms are considered; fortunately the series converge rapidly, so that results numerically accurate within a few per cent can thus be obtained.

We have evaluated the second-order diffusion coefficients using one-term approximations to B', D' and $\boldsymbol{D}$, and two-term approximations to A'. A high order of accuracy is not to be expected, but the order of magnitude is all that is required for most purposes. The details of the calculations will not be given.

Our approximate expressions are as follows:

(*a*) $$D_a = \frac{2}{3}\frac{n^2 m_1 m_2}{p\rho}\frac{D_{12}}{n_{10}n_{20}}\left(\frac{7D_T}{2T}-\frac{\partial D_T}{\partial T}\right),$$

(*b*) $$D_b = \frac{2}{3}\frac{n^2 m_1 m_2}{p\rho}\frac{D_{12}}{n_{10}n_{20}}\left(\frac{7}{2}D_{12}-T\frac{\partial D_{12}}{\partial T}\right),$$

(*c*) $$D_c = \frac{n^2 m_1 m_2}{p\rho}\frac{D_{12}}{n_{10}n_{20}}\frac{D_T}{T},$$

(*d*) $$D_d = \frac{n^2 m_1 m_2}{p\rho}\frac{D_{12}^2}{n_{10}n_{20}}.$$

(*e*) The coefficient D_e can be divided into three parts, D_e', D_e'', and D_e''', corresponding respectively to the parts of the sixth term of (5) involving $\partial B'/\partial T$ and $\partial A'/\partial C^2$, and to the contribution from $J^{(2)}$. We find

$$D_e'' = \frac{2}{T}\frac{n^2 m_1 m_2}{p\rho}\frac{D_{12}D_T}{n_{10}n_{20}}.$$

The approximation to D_e' is complicated, but when the molecules 1 and 2 are of nearly equal mass, and have identical fields of force, it is of the form

$$D_e' = \frac{4-3A}{2+3A}\frac{n(m_2-m_1)}{p\rho}D_{12}\left(\tfrac{7}{2}\mu - T\frac{\partial \mu}{\partial T}\right),$$

where A is a number which depends on the law of intermolecular force; for molecules whose interaction is proportional to $r^{-\nu}$, it is tabulated on p. 172 of our book.

The calculation of D_e''', like that of the J-term D_g''' in D_g, is more complicated than that of the terms arising from $\mathscr{D}^{(2)}$ (cf. Chapter 15 of our book), but its order of magnitude can be inferred without an exact calculation; for Maxwellian molecules D_e''' vanishes, and in general it is comparable with D_e'', which has the same property.

(*f*) We similarly divide D_f into parts D_f', D_f'', the first corresponding to the part of the seventh term of (5) involving $\partial B_1'/\partial n_1$, and the second to the rest of this term. If the molecules are mechanically similar,

$$D_f' = \frac{2D_{12}\mu}{n_{10}n_{20}p},$$

and in more general cases this equation will give the order of magnitude of D_f'. For mechanically similar molecules D_f'' vanishes to this degree of approximation, and in more general cases it will be a numerical multiple of $\mu D_T/p$; the numerical factor will depend on the concentration ratio.

(g) We divide D_g into parts D_g', D_g'', D_g''', the first two corresponding to the parts of the eighth term of (5) which involve D_1' and B_1' respectively, and the third arising from $J^{(2)}$. We find

$$D_g' = 2\frac{n^2m_1m_2}{p\rho}\frac{D_{12}^2}{n_{10}n_{20}},$$

which differs from D_d only by a numerical factor: D_g'' and D_g''' are likewise similar to D_f'' (in fact $D_g'' = -D_f''$).

(h) The coefficient D_h vanishes to our degree of approximation; it is in general a numerical multiple of $\mu D_T/p^2$; the numerical factor varies with the concentration ratio.

(i) The magnitude of the coefficient D_i will be similar to that of D_e'; for molecules of nearly equal mass and identical fields of force

$$D_i = \frac{4-3A}{2+3A}\frac{n(m_2-m_1)}{p\rho}D_{12}\mu.$$

5. Discussion of the second-order diffusion terms

The new terms in the diffusion equation involve Δ, defined by

$$\Delta = \frac{\partial}{\partial \mathbf{r}}.\mathbf{c}_0 = \frac{\partial u_0}{\partial x}+\frac{\partial v_0}{\partial y}+\frac{\partial w_0}{\partial z},$$

and $\mathbf{d}_{12}$, defined (p. 140) by

$$\mathbf{d}_{12} = \frac{\partial n_{10}}{\partial \mathbf{r}}+\frac{n_1n_2(m_2-m_1)}{n\rho}\frac{\partial \log p}{\partial \mathbf{r}}-\frac{\rho_1\rho_2}{p\rho}(\mathbf{F}_1-\mathbf{F}_2) = -\mathbf{d}_{21};$$

also (p. 138)

$$\frac{D_0}{Dt}\left(\frac{\partial T}{\partial \mathbf{r}}\right) = -\frac{2}{3}\frac{\partial(T\Delta)}{\partial \mathbf{r}} - \mathsf{e}\cdot\frac{\partial T}{\partial \mathbf{r}},$$

$$\frac{D_0}{Dt}(\boldsymbol{d}_{12}) = -\mathsf{e}\cdot\boldsymbol{d}_{12} - \frac{5}{3}\frac{n_1 n_2(m_2-m_1)}{n\rho}\frac{\partial\Delta}{\partial \mathbf{r}} - \frac{\rho_1\rho_2}{p\rho}\left\{\mathsf{e}\cdot(\boldsymbol{F}_1-\boldsymbol{F}_2)+\tfrac{2}{3}\Delta(\boldsymbol{F}_1-\boldsymbol{F}_2)\right\}.$$

Consequently all the new terms depend on the velocity-gradient, and vanish if the mass-velocity $\boldsymbol{c}_0$ is uniform. This makes the corresponding diffusion velocities difficult to observe, since the presence of turbulence, even to a slight degree, is sufficient to mask diffusion. The terms (*c*) and (*d*) involve $\frac{\partial\Delta}{\partial \mathbf{r}}$, and (i) involves $\frac{\partial}{\partial \mathbf{r}}\cdot\overset{\stackrel{\circ}{=}}{\mathsf{e}}$, both of which are combinations of the second space derivatives; otherwise, the terms involve only products of the first space derivatives of $\boldsymbol{c}_0$, multiplied by $\boldsymbol{F}_1-\boldsymbol{F}_2$ or by the first space derivatives of T, n_{10} or p. We proceed to compare the terms with the first-order terms in the diffusion velocity, derived from $f^{(1)}$.

The term (*a*) may be compared with the thermal diffusion term in the ordinary equation of diffusion, which is

$$-\frac{D_T}{n_{10}n_{20}T}\frac{\partial T}{\partial \mathbf{r}};$$

the ratio of (*a*) to this term is of order

$$\frac{n^2 m_1 m_2}{p\rho}\Delta D_{12}.$$

If $\bar{m}$, $\bar{C}$, l denote respectively the mean molecular mass and speed, and the mean free path, then $\rho = n\bar{m}$, and p and D_{12} are respectively of order $n\bar{m}\bar{C}^2$ and $l\bar{C}$. Hence the ratio is of order $l\Delta/\bar{C}$, and therefore the term (*a*) is comparable with the ordinary thermal diffusion term only if Δ is so large that the mean velocity of the gas alters by an appreciable fraction of the velocity of sound in a distance equal to the mean free path (p. 271). Hence, except possibly in shock waves, the term (*a*) can be neglected at pressures above 10^{-6} atm. Diffusion in a shock wave is, in any case, not important for the separation it produces; but it may have an effect on the propagation of the wave, like viscosity and thermal conduction.

The other second-order (or $f^{(2)}$) diffusion terms which do not involve second-order space-derivatives of $\boldsymbol{c}_0$ are likewise negligible compared with analogous first-order (or $f^{(1)}$) terms, save in similar extreme conditions.

The importance of the terms involving second-order derivatives of $\mathbf{c}_0$ can conveniently be estimated by considering a simple particular case.

6. DIFFUSION IN THE NON-UNIFORM RECTILINEAR MOTION OF A MIXED GAS

Consider a mixed gas in non-uniform but purely rectilinear motion; let the direction of the motion be that of the z-axis, so that $\mathbf{c}_0$ has only one non-zero component, w_0. We suppose that w_0 is a function of x and y, so that viscous forces operate; the motion therefore requires a pressure gradient in the z-direction. If, as we shall suppose, the temperature is uniform, this implies a z-gradient of ρ, and also, in order that the equation of continuity may be fulfilled, of w_0. There being no motion in the x and y directions, the pressure does not depend on x and y (if we ignore the weight of the gas). Thus the Cartesian components of $\frac{\partial \Delta}{\partial \mathbf{r}}$ and $\frac{\partial}{\partial \mathbf{r}}.\overset{\circ}{\overline{\overline{\mathrm{e}}}}$ are respectively

$$\frac{\partial^2 w_0}{\partial x \partial z}, \quad \frac{\partial^2 w_0}{\partial y \partial z}, \quad \frac{\partial^2 w_0}{\partial z^2}$$

and

$$\frac{1}{6}\frac{\partial^2 w_0}{\partial x \partial z}, \quad \frac{1}{6}\frac{\partial^2 w_0}{\partial y \partial z}, \quad \tfrac{1}{2}\nabla^2 w_0 + \frac{1}{6}\frac{\partial^2 w_0}{\partial z^2}.$$

Since $w_0 \rho$ or $w_0 p$ is independent of z, and p is independent of x and y,

$$\frac{\partial^2 w_0}{\partial x \partial z} = -\frac{\partial w_0}{\partial x}\frac{\partial \log p}{\partial z}, \quad \frac{\partial^2 w_0}{\partial y \partial z} = -\frac{\partial w_0}{\partial y}\frac{\partial \log p}{\partial z},$$

and the velocities of diffusion corresponding to these terms are negligible under normal conditions, involving, like the terms considered earlier, products of derivatives of c_0 and p. Similarly, $\partial^2 w_0/\partial z^2$ is the sum of a negligible product of derivatives and

$$-\frac{w_0}{p}\frac{\partial^2 p}{\partial z^2}.$$

Again, if the motion is steady, the z-equation of motion is

$$\rho w_0 \frac{\partial w_0}{\partial z} = -\frac{\partial p}{\partial z} + \mu \nabla^2 w_0 + \tfrac{1}{3}\mu \frac{\partial^2 w_0}{\partial x^2}.$$

Hence the last component of $\partial/\partial\mathbf{r}\,.\,\overset{\circ}{\overline{\mathbf{e}}}$ is

$$\frac{1}{2\mu}\left(\frac{\partial p}{\partial z}+\rho w_0\frac{\partial w_0}{\partial z}\right)=\frac{1}{2\mu}\left(1-\frac{\rho w_0^2}{p}\right)\frac{\partial p}{\partial z}$$

$$=\frac{1}{2\mu}\frac{\partial p}{\partial z}$$

approximately, since $w_0/\bar{C}$ is in general small. The ratio to this of $-\frac{w_0}{p}\frac{\partial^2 p}{\partial z^2}$ is of order $lw_0\frac{\partial^2 p}{\partial z^2}\Big/\bar{C}\frac{\partial p}{\partial z}$, which is in general small; hence, since the coefficients are of the same order, the diffusion velocity arising from the $\partial\Delta/\partial\mathbf{r}$ terms is in general small compared with that arising from the z-component of $\partial/\partial\mathbf{r}\,.\,\overset{\circ}{\overline{\mathbf{e}}}$. The latter is

$$\frac{D_t}{2\mu}\frac{\partial p}{\partial z}=\frac{2-\frac{3}{2}A}{2+3A}\,\frac{n(m_2-m_1)}{p\rho}\,D_{12}\frac{\partial p}{\partial z}.$$

In the circumstances of this problem, the only term in the *first* order diffusion velocity is that depending on the pressure gradient, namely (p. 244),

$$-\frac{n(m_2-m_1)}{p\rho}\,D_{12}\frac{\partial p}{\partial z}.$$

The second order term is of opposite sign to this, and its magnitude is smaller in the ratio $(2-\frac{3}{2}A)/(2+3A)$. This ratio is less than unity, but is not small, so that the second order term in this case makes a significant contribution to the diffusion velocity. This, however, is because in the present problem $\partial p/\partial z$ is itself proportional to μ, for given velocity gradients, so that the first order pressure diffusion term depends on a product of D_{12} and μ. The diffusion is important only if $\partial \log p/\partial z$ is of the same order as $\partial n_{10}/\partial z$ in ordinary diffusion experiments, i.e. in flow in very fine capillary tubes, or at very low pressures.

The likelihood of a significant second-order contribution to the pressure diffusion term in these circumstances was indicated to us by Professor R. Peierls, and it was in consequence of this that we undertook the present investigation. The factor $(2-\frac{3}{2}A)/(2+3A)$ is $\frac{7}{16}$ or 0·437 for rigid elastic spherical molecules; for Maxwellian molecules, interacting according to the inverse fifth power of the distance, it is 0·345. These values are only approximations, which in any case refer only to a gas mixture in which the molecular masses are nearly equal and the molecular interactions all follow the same distance law. For this case the numerical factors are probably correct within 10 or 15 %; hence the second approximation reduces the ordinary pressure diffusion by between $\frac{1}{3}$ and $\frac{1}{2}$ its magnitude. When the two molecular masses are very different, the value of the numerical ratio of the $f^{(2)}$ to the $f^{(1)}$ term may be very different from (and perhaps less than) that for the case of nearly similar molecules, here considered.

REFERENCES

Burnett, D. 1935 *Proc. Lond. Math. Soc.* **40**, 382.
Chapman, S. and Cowling, T. G. 1939 *The mathematical theory of non-uniform gases.* Camb. Univ. Press.
Enskog, D. 1917 Upsala Dissertation.
Lennard-Jones, J. E. 1923 *Phil. Trans.* A, **223**, 1.
Maxwell, J. C. 1867 *Phil. Trans.* **157**, 49.

The polymerization of olefines induced by free radicals

By C. J. Danby and C. N. Hinshelwood, F.R.S.

(*Received* 6 *June* 1941)

The rate of photolysis of the simple aldehydes at 300° is in general reduced by ethylene, propylene or *iso*-butylene, and many molecules of the olefine may undergo an induced polymerization for each quantum of light absorbed by the aldehyde. A similar polymerization is induced by photolysis of ketones. The kinetics of these interdependent processes have been investigated by combining pressure measurements with chemical analysis at each stage, the rates of olefine polymerization and of aldehyde photolysis being independently determined.

The experimental results accord with a mechanism in which large radicals are built up by the successive addition of olefine molecules to the primary radicals from the photolysis of the aldehyde or ketone. When the polymer radicals contain approximately three olefine molecules they undergo one of two alternative processes, either breaking down by regeneration of a methyl radical which begins a new polymerization chain, or giving inactive products. The former 'transfer process' explains how the chain length of the reaction may be large, yet the molecular weight of the product comparatively small. Certain differences between acetaldehyde and propionic aldehyde are explained by the fact that the ethyl radicals from the latter may regenerate in the course of the reaction cycle methyl radicals of slightly greater reactivity.

A quantitative comparison of the various reactions shows that on ascending the series of alkyl radicals their reactivity towards both aldehydes and olefines diminishes only slowly. On ascending the olefine series, however, the rate of polymerization rapidly decreases. This depends not upon a lowered efficiency of reaction of the primary radicals with the olefines, but rather upon a greater tendency of the more complex polymer radicals to be transformed into products which do not continue the reaction cycle.

The polymerization of ethylene may be induced in a variety of ways: for example, by excited mercury (Olson and Meyers 1926), or by free radicals from the thermal decomposition of metal alkyls (Taylor and Jones 1930), or of azomethane (Rice and Sickmann 1935). In the present work the polymerization of the lower olefines induced by free radicals produced photochemically from aldehydes and ketones has been studied. The aldehyde-olefine system is particularly suitable for an investigation of the polymerization mechanism, since not only is the rate of formation of the reaction-inducing radicals determinable, but also information about their subsequent fate can be obtained by measuring the effect of the olefine on the photolysis of the aldehyde.

EXPERIMENTAL METHOD

The method of investigation was in general to expose mixtures of aldehyde or ketone and olefine to ultra-violet light. In the absence of light, or of aldehyde or ketone, the olefine is unchanged, but when photolysis occurs the olefine is polymerized. The rates of photolysis and of polymerization were independently measured. In the presence of sufficient olefine the aldehyde photolysis takes place with a drop in pressure due to the induced polymerization. After a known time the pressure change in the reaction was measured and the partial pressure of unchanged aldehyde determined by chemical analysis. The amount decomposed gave the initial rate of photolysis (ρ). The rate of olefine polymerization (σ) was obtained by adding this value to the observed pressure change during the same time. The pressure increase at any early stage of the acetaldehyde photolysis corresponds exactly to the amount of aldehyde decomposed, as measured by analysis (Danby 1940).

Reactions were carried out at 300° in a cylindrical silica vessel of about 150 c.c. capacity provided with plane parallel windows and supported in a horizontal electric furnace also with quartz windows. It was connected to a capillary mercury manometer, to reservoirs containing the various reactants and was evacuated by the usual system of pumps. Provision was made for the collection and analysis of gas samples. Temperatures were measured by a mercury thermometer calibrated against a Pt/Pt-Rh thermocouple and potentiometer. The light source was a Hanovia mercury lamp which was focused on the reaction vessel by a spherical silica flask of water. The intensity was frequently checked by measurement of the rate of photolysis of pure acetaldehyde and was found to be almost constant. The aldehydes and ketones were purified by fractionation, the olefines by distillation between traps cooled in liquid air, only the middle fractions being taken. To avoid possible obscuring of the windows of the reaction vessel by high molecular weight products only initial rates of reaction were measured.

The analysis for aldehyde, by which the reaction was to a great extent followed, was based on the method of Friedemann, Cotonio and Shaffer (1927), which depends on the fact that while the aldehyde-bisulphite compound is not attacked by iodine in neutral or acid solution, it is rapidly decomposed if the solution is alkaline. To estimate the partial pressure of aldehyde in the reaction vessel at any instant its contents were shared with a large evacuated gas pipette attached to the apparatus by a ground joint. The aldehyde in the pipette was absorbed in excess N/10 sodium bisulphite solution and the excess bisulphite removed by titration with iodine. The solution was then made alkaline by addition of about 1 g. of solid sodium bicarbonate and titrated with N/100 iodine. This estimates the bisulphite which was in combination with the aldehyde. With a knowledge of the volumes of pipette, reaction vessel and dead-space the partial pressure of aldehyde in the reaction vessel at the moment of taking the sample can be calculated. This method has been found to give excellent results with propionic and *n*-butyric aldehydes as well as with acetaldehyde.

Analyses of the gaseous products were made with a Bone and Wheeler apparatus, the samples being passed through a coil cooled to − 15° to remove any unchanged aldehyde or condensable hydrocarbons. Higher olefines were estimated by absorption in 85 % sulphuric acid, which will remove all except ethylene (Davis and Schuler 1930). The latter was absorbed in saturated mercuric acetate solution, and carbon monoxide in ammoniacal cuprous chloride. The average carbon chain length of the saturated hydrocarbon fraction was determined by combustion.

Reaction rates are expressed throughout in terms of millimetres of gas reacting in 7 min.

CHARACTERISTICS OF THE INDUCED POLYMERIZATION

Experimental observations can be accounted for by assuming that the photolysis of acetaldehyde at about 300° takes place essentially by reactions (1), (2) and (3) of the scheme below (p. 173) (Leermakers 1934; Mitchell and Hinshelwood 1937). The chain length at 200 mm. is about 150 for a moderate light intensity. On prolonged photolysis there is a pressure increase of almost 100 %. Since the chains are long the amount of ethane is negligible, the product consisting almost entirely of methane and carbon monoxide.

In general the rate of photolysis of aldehyde is reduced by olefines. As the latter do not absorb light of the wave-length employed, this inhibition must be due to the removal—by reaction with olefine—of a chain-carrying radical of the aldehyde photolysis. Polymerization evidently then occurs by the successive addition of olefine molecules to the new radical thereby formed, as in reactions (4), (5), (5′), ..., (5*) below (p. 173). Since the rate of ethylene polymerization is comparable with that of the acetaldehyde photolysis, which has a considerable chain length, it follows that the induced polymerization must also have long chains. But the product is of low molecular weight. All the ethylene molecules which polymerize in one reaction chain cannot therefore grow on to the initiating radical, and there must be a 'Chain Transfer' process such as reaction (6). Conclusive evidence that such a step occurs in the ethylene polymerization induced by photolysis of acetone is given later.

If polymerization took place solely by means of reactions (4)–(6), then the rate of photolysis of aldehyde would not be reduced by olefines, because each methyl radical removed in reaction (4) is subsequently regenerated in reaction (6). The observed inhibition must be due to an additional chain-ending process such as:

$$R_n = \text{chain ended}, \qquad (a)$$

or

$$R_n + \mathrm{CH_3} = \text{chain ended}. \qquad (b)$$

Unimolecular and bimolecular chain-ending processes are most easily distinguished at high olefine pressures where the inhibition of the aldehyde photolysis is large. The polymerization rate, σ, according to (b) can be shown to be proportional to the root of the olefine pressure, and according to (a) independent of it. With propylene and iso-butylene σ is found experimentally to be independent of olefine pressure—which suggests chain-ending by (a). With ethylene σ falls off at higher pressures, but no experiments could be made at high enough pressures to find out whether or not it eventually becomes independent of pressure. However, since the unimolecular process is favoured with the higher olefines, and since in any case a bimolecular chain-ending step is already represented by reaction (3), reaction (*a*) will be assumed to be the additional chain-ending step (7). It presumably involves the isomerization of the radical to a form which, for steric or other reasons, is relatively inactive to the olefine. Its ultimate fate will then have little effect on the kinetics of the main reaction.

The assumed mechanism is therefore:

$$\begin{array}{llllr}
\mathrm{CH_3CHO} + h\nu & & = \mathrm{CH_3} + \mathrm{CHO} & k_1, & (1)\\
\mathrm{CH_3} & + \mathrm{CH_3CHO} & = \mathrm{CH_3} + \mathrm{CH_4} + \mathrm{CO} & k_2, & (2)\\
\mathrm{CH_3} & + \mathrm{CH_3} & = \mathrm{C_2H_6} & k_3, & (3)\\
\mathrm{CH_3} & + \mathrm{C_2H_4} & = R_1 & k_4, & (4)\\
R_1 & + \mathrm{C_2H_4} & = R_2 & k_5, & (5)\\
R_2 & + \mathrm{C_2H_4} & = R_3 & k_5', & (5')\\
\cdots\cdots & \cdots\cdots & \cdots\cdots & & \\
R_{n-1} & + \mathrm{C_2H_4} & = R_n & k_5^*, & (5^*)\\
R_n & & = \text{olefine} + \mathrm{CH_3} & k_6, & (6)\\
R_n & & = \text{chain ended} & k_7. & (7)
\end{array}$$

For a stationary state with respect to the concentration of radicals:

$$d[\mathrm{CH_3}]/dt = k_1 I_{\mathrm{abs.}} - k_3[\mathrm{CH_3}]^2 - k_4[\mathrm{CH_3}][\mathrm{C_2H_4}] + k_6[R_n] = 0, \qquad (\mathrm{I})$$

$$d[R_1]/dt = k_4[\mathrm{CH_3}][\mathrm{C_2H_4}] - k_5[R_1][\mathrm{C_2H_4}] = 0, \qquad (\mathrm{II}a)$$

$$\cdots\cdots\cdots\cdots\cdots\cdots\cdots\cdots\cdots\cdots\cdots\cdots$$

$$d[R_n]/dt = k_5^*[R_{n-1}][\mathrm{C_2H_4}] - k_6[R_n] - k_7[R_n] = 0, \qquad (\mathrm{II}n)$$

$$-d[\mathrm{CH_3CHO}]/dt = k_1 I_{\mathrm{abs.}} + k_2[\mathrm{CH_3}][\mathrm{CH_3CHO}], \qquad (\mathrm{III})$$

$$-d[\mathrm{C_2H_4}]/dt = k_4[\mathrm{CH_3}][\mathrm{C_2H_4}] + k_5[R_1][\mathrm{C_2H_4}] + \ldots + k_5^*[R_{n-1}][\mathrm{C_2H_4}]. \qquad (\mathrm{IV})$$

From these equations it follows that

$$k_3[\mathrm{CH_3}]^2 + k_4\beta[\mathrm{CH_3}][\mathrm{C_2H_4}] - k_1 I_{\mathrm{abs.}} = 0,$$

whence
$$[\mathrm{CH_3}] = \frac{-k_4\beta[\mathrm{C_2H_4}] + \{(k_4\beta[\mathrm{C_2H_4}])^2 + 4k_1k_3I_{\mathrm{abs.}}\}^{\frac{1}{2}}}{2k_3},$$

where
$$\beta = 1 - \frac{k_6}{k_6 + k_7}.$$

As long as the chain length of the aldehyde photolysis is considerable, i.e. provided relatively little is decomposed by reaction (I), the rate of aldehyde decomposition will be

$$\rho = k_2[\mathrm{CH_3CHO}]\left\{\frac{-k_4\beta[\mathrm{C_2H_4}]+\{(k_4\beta[\mathrm{C_2H_4}])^2+4k_1k_3I_{\mathrm{abs.}}\}^{\frac{1}{2}}}{2k_3}\right\}. \tag{V}$$

If the initiating radicals grow by the addition of n ethylene molecules, giving R_n, and if the intermediate radicals suffer no alternative fate, then the velocity constants of the reactions (5), (5′), …, (5*) do not appear in the equations for the stationary state. Reaction (4) could therefore be written in the form

$$\mathrm{CH_3}+n\mathrm{C_2H_4} = R_n,$$

and reactions (5), (5′), …, etc. omitted. (This does not in any sense imply a polymolecular reaction.)

The rate of ethylene polymerization will be

$$\begin{aligned}\sigma &= nk_4[\mathrm{CH_3}][\mathrm{C_2H_4}]\\ &= nk_4[\mathrm{C_2H_4}]\left\{\frac{-k_4\beta[\mathrm{C_2H_4}]+\{(k_4\beta[\mathrm{C_2H_4}])^2+4k_1k_3I_{\mathrm{abs.}}\}^{\frac{1}{2}}}{2k_3}\right\}.\end{aligned} \tag{VI}$$

If ρ_0 is the rate of acetaldehyde photolysis in the absence of ethylene, then:

$$\rho_0 = k_2\left(\frac{k_1}{k_3}I_{\mathrm{abs.}}\right)^{\frac{1}{2}}[\mathrm{CH_3CHO}],$$

whence $$I_{\mathrm{abs.}} = \frac{\rho_0^2k_3}{k_1k_2^2[\mathrm{CH_3CHO}]^2}.$$

Substituting this value for $I_{\mathrm{abs.}}$ in equations (V) and (VI) for ρ and σ:

$$\rho = k_2[\mathrm{CH_3CHO}]\left\{\frac{-k_4\beta[\mathrm{C_2H_4}]+\left((k_4\beta[\mathrm{C_2H_4}])^2+4\dfrac{k_3^2\rho_0^2}{k_2^2[\mathrm{CH_3CHO}]^2}\right)^{\frac{1}{2}}}{2k_3}\right\}, \tag{VII}$$

$$\sigma = nk_4[\mathrm{C_2H_4}]\left\{\frac{-k_4\beta[\mathrm{C_2H_4}]+\left((k_4\beta[\mathrm{C_2H_4}])^2+4\dfrac{k_3^2\rho_0^2}{k_2^2[\mathrm{CH_3CHO}]^2}\right)^{\frac{1}{2}}}{2k_3}\right\}. \tag{VIII}$$

With $$\frac{k_2k_4\beta}{2k_3} = C, \quad \text{and} \quad \frac{k_4^2\beta}{k_3} = K:$$

$$\rho = C[\mathrm{CH_3CHO}]\left[\left\{[\mathrm{C_2H_4}]^2+\frac{\rho_0^2}{C^2[\mathrm{CH_3CHO}]^2}\right\}^{\frac{1}{2}}-[\mathrm{C_2H_4}]\right] \tag{IX}$$

and $$\sigma = \tfrac{1}{2}nK[\mathrm{C_2H_4}]\left[\left\{[\mathrm{C_2H_4}]^2+\frac{\rho_0^2}{C^2[\mathrm{CH_3CHO}]^2}\right\}^{\frac{1}{2}}-[\mathrm{C_2H_4}]\right]. \tag{X}$$

POLYMERIZATION OF OLEFINES PHOTOSENSITIZED BY ACETALDEHYDE

Experimental results for the inhibition of the acetaldehyde photolysis by ethylene and for the induced ethylene polymerization are given in table 1 and figure 1. In these experiments the initial acetaldehyde pressure was constant, and the ethylene pressure was varied. Values of the constant C may be obtained by substituting the values of the acetaldehyde and ethylene pressures, the value of ρ_0 and the corresponding values of ρ in equation (IX). For an initial acetaldehyde pressure of 50 mm., corresponding to $\rho_0 = 17\cdot0$, the mean value of C is $7\cdot8 \times 10^{-4}$. Calculated values of ρ are compared with those observed in table 2, and are plotted as a continuous line in figure 1. The results of similar experiments with the ethylene pressure constant and the acetaldehyde pressure varied are given in table 3. The value of C obtained from these results is identical with that found from those in table 1.

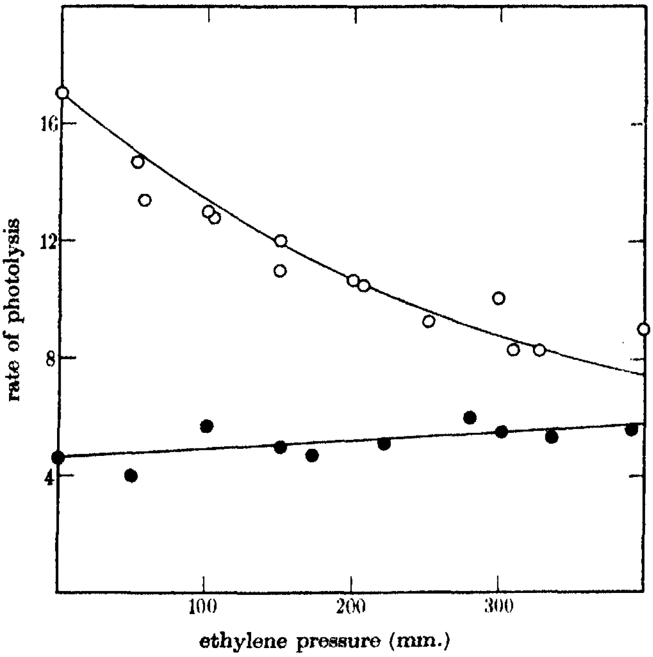

FIGURE 1. Inhibition of the photolysis of acetaldehyde and propionic aldehyde by ethylene. ○ acetaldehyde, ● propionic aldehyde. For acetaldehyde the line drawn is that calculated from equation (IX) with $C = 7\cdot8 \times 10^{-4}$.

TABLE 1. PHOTOLYSIS OF 50 MM. ACETALDEHYDE IN THE PRESENCE OF ETHYLENE, AND THE INDUCED POLYMERIZATION OF THE LATTER

ethylene pressure (mm.)	acetaldehyde photolysis rate	ethylene polymerization rate
0	17·0	—
53	14·7	7·2
57	13·4	7·8
100	13·0	14·0
105	12·8	11·2
150	11·0	15·8
150	12·0	15·6
200	10·7	20·2
207	10·5	19·5
252	9·3	22·2
300	10·1	24·1
310	8·3	25·0
329	8·3	26·5
400	9·0	30·0

TABLE 2. RATES OF PHOTOLYSIS OF 50 MM. ACETALDEHYDE IN THE PRESENCE OF ETHYLENE. $C = 7{\cdot}8 \times 10^{-4}$

ethylene pressure (mm.)	$\rho_{\text{obs.}}$	$\rho_{\text{calc.}}$
0	17·0	17·0
100	13·0	13·5
200	10·7	10·7
300	10·1	8·9
400	9·0	7·5

TABLE 3. RATES OF PHOTOLYSIS OF ACETALDEHYDE IN PRESENCE OF 300 MM. ETHYLENE

acetaldehyde pressure (mm.)	ρ_0	$\rho_{\text{obs.}}$	$\rho_{\text{calc.}}$
20	5·2	2·5	2·3
30	9·1	4·2	4·4
40	13·2	6·7	6·8
50	17·0	9·1	9·1

From equation (X), with the value of C already determined, the results given in tables 4 and 5 are calculated.

TABLE 4. RATE OF ETHYLENE POLYMERIZATION WITH 50 MM. ACETALDEHYDE AND VARIABLE ETHYLENE PRESSURE. $\frac{1}{2}nK = 3{\cdot}42 \times 10^{-4}$

ethylene pressure (mm.)	$\sigma_{\text{obs.}}$	$\sigma_{\text{calc.}}$
100	14·0	12·2
200	20·2	19·6
300	24·1	24·1
400	30·0	26·9

TABLE 5. RATE OF ETHYLENE POLYMERIZATION WITH 300 MM. ETHYLENE AND VARIABLE ACETALDEHYDE PRESSURES. $\frac{1}{2}nK = 2{\cdot}88 \times 10^{-4}$

acetaldehyde pressure (mm.)	$\sigma_{\text{obs.}}$	$\sigma_{\text{calc.}}$
20	12·9	12·9
30	16·3	16·3
40	19·6	18·8
50	22·5	20·5

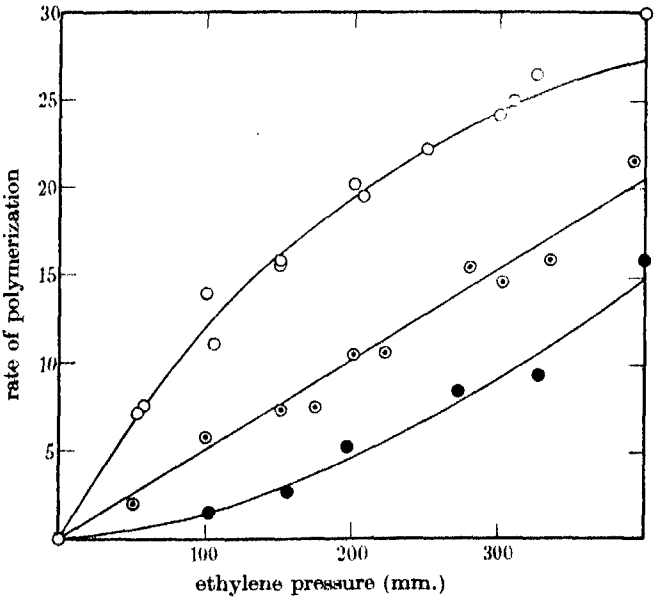

FIGURE 2. The polymerization of ethylene induced by photolysis of acetaldehyde, propionic aldehyde and *n*-butyric aldehyde. ○ acetaldehyde, ⊙ propionic aldehyde, ● *n*-butyric aldehyde. For acetaldehyde the line drawn is that calculated from equation (X) with $C = 7{\cdot}8 \times 10^{-4}$ and $\frac{1}{2}nK = 3{\cdot}4 \times 10^{-4}$.

Similar experiments were made with propylene and *iso*-butylene (tables 6 and 7, figures 3 and 4).

TABLE 6. INHIBITION OF THE ACETALDEHYDE PHOTOLYSIS BY PROPYLENE, AND THE INDUCED POLYMERIZATION OF THE LATTER. ACETALDEHYDE PRESSURE 50 MM.

propylene pressure (mm.)	acetaldehyde photolysis rate	propylene polymerization rate
0	17·0	—
15	9·3	0·1
25	7·3	0·3
42	6·5	2·3
61	5·0	2·0
81	5·0	3·1
106	4·7	2·9
145	5·2	4·7
191	4·6	4·6
203	4·6	4·6
250	3·5	4·2
302	3·4	4·4
352	2·6	3·9
413	3·3	4·6

The best agreement with these experimental results is given with $C = 8{\cdot}4 \times 10^{-3}$ and $\frac{1}{2}nK = 5{\cdot}2 \times 10^{-3}$, in equations (IX) and (X).

TABLE 7. INHIBITION OF THE PHOTOLYSIS OF 50 MM. ACETALDEHYDE BY *ISO*-BUTYLENE, AND THE INDUCED POLYMERIZATION OF THE LATTER

iso-butylene pressure (mm.)	acetaldehyde photolysis rate	*iso*-butylene polymerization rate
0	17·0	—
5	(10·8)	(0·5)
10	8·5	1·4
20	6·0	1·7
25	6·2	1·7
35	5·0	1·6
50	3·5	1·6
80	(2·5)	(1·6)

(Values in brackets are interpolated)

The best agreement with these experimental results is given with $C = 1{\cdot}72 \times 10^{-2}$, and $\frac{1}{2}nK = 1{\cdot}05 \times 10^{-2}$.

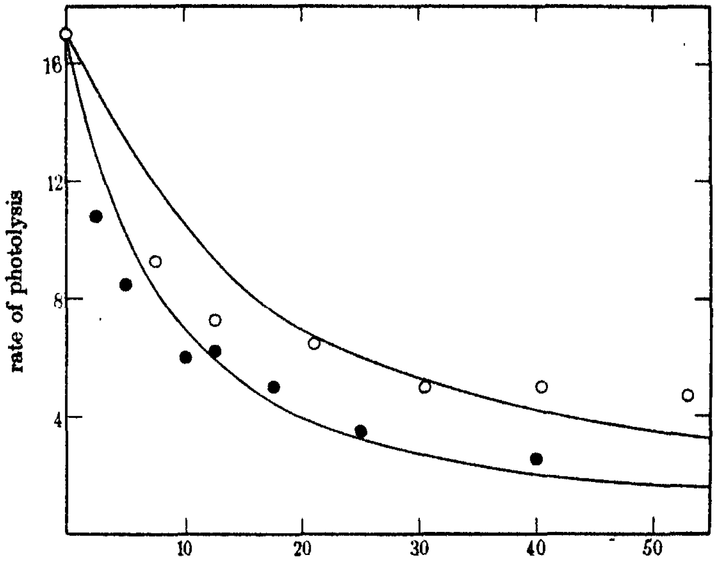

FIGURE 3. The inhibition of the photolysis of acetaldehyde by propylene and *iso*-butylene. ○ propylene, ● *iso*-butylene. The line for propylene is calculated from equation (IX) with $C = 8{\cdot}4 \times 10^{-3}$, that for *iso*-butylene with $C = 1{\cdot}72 \times 10^{-3}$.

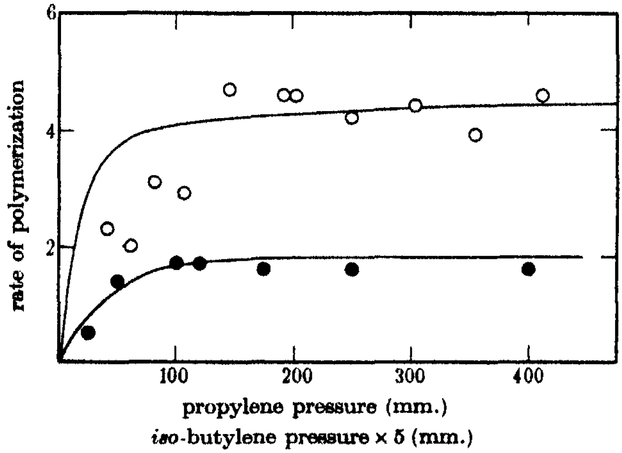

FIGURE 4. Polymerization of propylene and *iso*-butylene induced by acetaldehyde photolysis. ○ propylene, ● *iso*-butylene. The line for propylene is calculated from equation (X) with $C = 8{\cdot}4 \times 10^{-3}$ and $\frac{1}{2}nK = 5{\cdot}2 \times 10^{-3}$, that for *iso*-butylene with $C = 1{\cdot}72 \times 10^{-3}$ and $\frac{1}{2}nK = 1{\cdot}05 \times 10^{-3}$.

With *iso*-butylene the inhibition is greater than with either ethylene or propylene, and the polymerization less, becoming independent of the olefine above a comparatively small pressure. The values for σ were taken from the smoothed curves for the acetaldehyde photolysis rate and of the observed pressure change, the individual values being somewhat erratic.

MOLECULAR WEIGHT OF THE PRODUCTS

The factor n, which is the number of olefine molecules in the final polymer, appears in the equations for σ, and must now be evaluated. Measurement of the vapour pressure-temperature relations of the condensed reaction product from acetaldehyde and ethylene showed that, while it was not homogeneous, yet the molecular weights were distributed over a comparatively small range. Hence no great error is introduced by assuming a singular value for n. On prolonged irradiation (30–40 hr.), though considerable unchanged ethylene is found by analysis, the observed pressure decrease of the ethylene is slightly greater than 50 %. The average molecular weight of the polymer is therefore substantially higher than that corresponding to butylene. This is confirmed by the fact that at room temperature and pressure a fraction of the gaseous products condenses out. On account of this condensation the proportions found by gas analysis will not correspond to the partial pressures in the reaction vessel. They can, however, be brought into relation with them by using the carbon monoxide as a reference gas. 50 mm. acetaldehyde on complete photolysis will give 49·2 mm. of carbon monoxide. The percentage of carbon monoxide found by analysis must therefore correspond to this pressure. The partial pressures of the products of reaction calculated in this way are given in table 8.

TABLE 8. MEAN OF TEN ANALYSES OF THE PRODUCTS (UNCONDENSED AT −15°) OF PROLONGED PHOTOLYSIS OF 50 MM. ACETALDEHYDE IN PRESENCE OF 300 MM. ETHYLENE

	percentage	pressure (mm.)
carbon monoxide	27·5	49·2
ethylene	25·6	45·8
higher olefines	19·6	35·1
saturated hydrocarbons	27·0	48·4

The fate of the initial 300 mm. of ethylene can now be determined. The mean carbon chain length of the saturated hydrocarbon fraction was found by combustion to be 1·98 units. This fraction should consist of methane from reaction (2), together with a small proportion of ethane from the chain-ending reaction (3). However, higher paraffins could be produced by interaction of the larger radicals and aldehyde by reactions of the type:

$$C_3H_7 + CH_3CHO = C_3H_8 + CO + CH_3, \qquad (2')$$

and a relatively small proportion would raise the apparent molecular weight to the value observed. Ethylene must have entered into the composition of this fraction, the raising of the apparent molecular weight depending only on the amount of it which has reacted in this way, and not on the particular molecular species in which it appears. For the purposes of calculation this paraffin fraction can be taken to be a mixture of equal amounts of methane and propane. Then $\frac{1}{2}(48{\cdot}4) = 24{\cdot}2$ mm. of ethylene will have entered into its composition. Deducting this and the 45·8 mm. of unchanged ethylene found by analysis from the initial 300 mm. of ethylene leaves 230 mm. which has polymerized. Taking the gaseous higher olefine fraction to be butylene, 70·2 mm. of ethylene will have been required to form the 35·1 mm. found, leaving 159·8 mm. in the form of condensed liquid products. Initially there were 350 mm. of reactants. The average pressure decrease on prolonged reaction was 120 mm., leaving 230 mm. of products. Of this 45·8 mm. are ethylene, 35·1 mm. gaseous olefines other than ethylene, and 98·5 mm. carbon monoxide and paraffins from the aldehyde photolysis. This leaves 51·1 mm. for the higher products which condense out on cooling. Coming from 159·8 mm. of ethylene, the average ethylene content per molecule of this fraction must hence be 3·12. In the polymerization of ethylene under the present conditions therefore, $n = 3$. With propylene and *iso*-butylene, where there is much less polymerization, n will be taken to be 2.

EFFECT OF OXYGEN ON THE REACTION

Traces of oxygen are known to have a considerable effect on many polymerization processes. The effect of oxygen on the acetaldehyde photosensitized polymerization of ethylene is shown in table 9. At 300° the

TABLE 9. EFFECT OF OXYGEN ON THE POLYMERIZATION OF ETHYLENE INDUCED BY ACETALDEHYDE PHOTOLYSIS. 50 MM. ACETALDEHYDE, 300 MM. ETHYLENE

air added (mm.)	observed polymerization rate	reduction in rate (%)
0	14·8	0
10	13·0	12·2
30	11·6	21·6

acetaldehyde might be oxidized at once by air. 30 mm. of air contain about 6 mm. of oxygen and would be capable of oxidizing 12 mm. of aldehyde. This would be a reduction of 24 % in the aldehyde available to induce polymerization. The observed reduction in polymerization by this amount of air is 21 %. The effect of oxygen on the reaction is hence small, and can entirely be attributed to the oxidation of part of the acetaldehyde.

POLYMERIZATION PHOTOSENSITIZED BY PROPIONIC AND *n*-BUTYRIC ALDEHYDES

Propionic aldehyde photolyses in ultra-violet light by a chain process similar to that occurring with acetaldehyde, at about one-third the rate (Mitchell and Hinshelwood 1937). This photolysis is apparently uninhibited by ethylene, though the latter is polymerized. The rate of polymerization is proportional to the ethylene pressure up to at least 600 mm. (table 10, figures 1 and 2). This contrast with acetaldehyde could be explained by the assumption that with propionic aldehyde all the growing polymer radicals regenerate the initial radical, none suffering chain termination by reaction (7). This would mean that $\beta = 0$, so that in equation (VII) for the aldehyde photolysis rate,

TABLE 10. PHOTOLYSIS OF 50 MM. PROPIONIC ALDEHYDE IN THE PRESENCE OF ETHYLENE, AND THE INDUCED POLYMERIZATION OF THE LATTER

ethylene pressure (mm.)	propionic aldehyde photolysis rate	ethylene polymerization rate
0	4·6	—
50	4·0	2·0
100	5·7	5·7
151	5·0	7·2
172	4·7	7·5
200	6·0	10·6
222	5·1	10·7
280	6·0	15·5
302	5·5	14·7
337	5·3	15·9
391	5·6	21·7
565	6·0	30·0

$$\rho = \rho_0,$$

and in equation (VIII) for the polymerization rate,

$$\sigma = \frac{nk_4\rho_0}{k_2[\text{EtCHO}]}[\text{C}_2\text{H}_4].$$

as observed. This assumption, however, demands that the chain-ending process (7), shown to be important with acetaldehyde, should play no part in the propionic aldehyde reaction, which is unlikely. A more probable explanation is that the large radicals R_n regenerate, not ethyl, but methyl radicals in reaction (6), and that the latter are somewhat more reactive than the primary ethyl radicals. The inhibition due to reaction (7) might then be masked, and could even be converted into a slight acceleration, as indeed is observed with butyric aldehyde and ethylene (table 11). Further evidence that the lack of inhibition with propionic aldehyde and ethylene is due to the balancing of two effects is afforded by the fact that propylene does cause slight inhibition (table 12).

TABLE 11. POLYMERIZATION OF ETHYLENE PHOTOSENSITIZED BY 50 MM. *n*-BUTYRIC ALDEHYDE

ethylene pressure (mm.)	*n*-butyric aldehyde photolysis rate	ethylene polymerization rate
0	3·0	—
101	3·0	1·5
156	3·1	2·6
198	3·0	5·1
276	3·4	8·4
328	4·1	9·4
400	3·5	15·8
426	4·3	13·1
487	4·0	23·5

TABLE 12. POLYMERIZATION OF PROPYLENE PHOTOSENSITIZED BY 50 MM. PROPIONIC ALDEHYDE

propylene pressure (mm.)	propionic aldehyde photolysis rate	propylene polymerization rate
0	4·6	—
63	4·0	2·2
125	3·7	2·9
151	3·8	3·0
201	3·5	3·0
250	3·2	3·2
326	2·8	3·7
363	2·8	4·2
406	2·5	4·1

Agreement with these experimental results is obtained with $C = 1{\cdot}29 \times 10^{-4}$ and $\frac{1}{2}nK = 2{\cdot}96 \times 10^{-5}$ in equations (IX) and (X).

Taken together these various results suggest that absorption of ethyl radicals by the olefine is in fact being followed by the regeneration of slightly more reactive methyl radicals.

MECHANISM WITH ETHYL RADICALS REGENERATING METHYL RADICALS

The following typical mechanism may now be considered:

$$\begin{array}{llll}
\mathrm{EtCHO} + h\nu & = \mathrm{Et} + \mathrm{CHO} & k_1, & (1) \\
\mathrm{Et} + \mathrm{EtCHO} & = \mathrm{Et} + \mathrm{CO} + \mathrm{C_2H_6} & k_2', & (2') \\
2\mathrm{Et} & = \text{chain ended} & k_3', & (3') \\
\mathrm{Et} + n\mathrm{C_2H_4} & = R_n' & k_4', & (4') \\
R_n' & = \text{olefine} + \mathrm{CH_3} & k_6', & (6') \\
R_n' & = \text{chain ended} & k_7', & (7') \\
\mathrm{CH_3} + \mathrm{EtCHO} & = \mathrm{CH_3} + \mathrm{CO} + \mathrm{C_2H_6} & k_2, & (2) \\
\mathrm{CH_3} + \mathrm{Et} & = \text{chain ended} & k_3, & (3) \\
\mathrm{CH_3} + n\mathrm{C_2H_4} & = R_n & k_4, & (4) \\
R_n & = \text{olefine} + \mathrm{CH_3} & k_6, & (6) \\
R_n & = \text{chain ended} & k_7. & (7)
\end{array}$$

This mechanism leads to the following stationary state equations:

$$\begin{array}{lll}
d[\mathrm{Et}]/dt = k_1 I_{\mathrm{abs.}} - k_3'[\mathrm{Et}]^2 - k_4'[\mathrm{Et}][\mathrm{C_2H_4}] - k_3[\mathrm{CH_3}][\mathrm{Et}] & = 0, & (\mathrm{XI}) \\
d[\mathrm{CH_3}]/dt = k_6'[R_n'] - k_4'[\mathrm{CH_3}][\mathrm{C_2H_4}] - k_3[\mathrm{CH_3}][\mathrm{Et}] + k_6[R_n] & = 0, & (\mathrm{XII}) \\
d[R_n']/dt = k_4'[\mathrm{Et}][\mathrm{C_2H_4}] - (k_6' + k_7')[R_n'] & = 0, & (\mathrm{XIII}) \\
d[R_n]/dt = k_4[\mathrm{CH_3}][\mathrm{C_2H_4}] - (k_6 + k_7)[R_n] & = 0. & (\mathrm{XIV})
\end{array}$$

The problem can be simplified by considering only the condition that with small additions of ethylene there shall be neither acceleration nor inhibition of the rate of the propionic aldehyde photolysis, and proceeding by successive approximation. Considering [Et] the loss of ethyl radicals by combination with methyl radicals may first be neglected compared with their removal by mutual recombination—provided that the ethylene concentration, and hence the methyl concentration, is small. Neglecting the term $k_3[\mathrm{CH_3}][\mathrm{Et}]$ in equation (XI), therefore,

$$[\mathrm{Et}] = \frac{-k_4'[\mathrm{C_2H_4}] + 2(k_1 k_3' I_{\mathrm{abs.}})^{\frac{1}{2}} \left\{1 + \dfrac{(k_4'[\mathrm{C_2H_4}])^2}{8k_1 k_3' I_{\mathrm{abs.}}}\right\}^{\frac{1}{2}}}{2k_3'}.$$

As the $[C_2H_4]$ approaches zero, this approximates to

$$[\mathrm{Et}] = \frac{-k_4'[C_2H_4] + 2(k_1 k_3' I_{\mathrm{abs.}})^{\frac{1}{2}}}{2k_3'}$$

$$= \left(\frac{k_1 I_{\mathrm{abs.}}}{k_3'}\right)^{\frac{1}{2}} - \frac{k_4'[C_2H_4]}{2k_3'}. \qquad \text{(XV)}$$

From equation (XII), substitution of the values of $[R_n']$ and $[R_n]$ from equations (XIII) and (XIV), of the value for [Et] from equation (XV), and putting $k_6/(k_6+k_7) = (1-\beta)$, gives $[CH_3]$. When $[C_2H_4]$ is small, terms involving $[C_2H_4]^2$ may be neglected; then

$$[CH_3] = \frac{(1-\beta)\, k_4'[C_2H_4] \left\{\frac{k_1 I_{\mathrm{abs.}}}{k_3'}\right\}^{\frac{1}{2}}}{k_3\left\{\frac{k_1 I_{\mathrm{abs.}}}{k_3'}\right\}^{\frac{1}{2}} - \frac{k_3 k_4'[C_2H_4]}{2k_3'} - \{(1-\beta)\, k_4 - k_4'\}\, [C_2H_4]}.$$

As $[C_2H_4]$ approaches zero, this reduces to

$$[CH_3] = \frac{(1-\beta)\, k_4'[C_2H_4]}{k_3}.$$

This approximate value for $[CH_3]$ may now be reintroduced into equation (XI) in the term previously neglected and a more accurate value for [Et] obtained:

$$[\mathrm{Et}] = \left\{\frac{k_1 I_{\mathrm{abs.}}}{k_3'}\right\}^{\frac{1}{2}} - \frac{k_4'[C_2H_4]}{2k_3'} - \frac{(1-\beta)\, k_4'[C_2H_4]}{2k_3'}.$$

Calling the concentration of propionic aldehyde $[A]$:

$$-d[A]/dt = k_2'[A]\,[\mathrm{Et}] + k_2[A]\,[CH_3],$$

$$\frac{1}{[A]}\frac{d[A]}{dt} = k_2'.\frac{k_1 I_{\mathrm{abs.}}}{k_3'} - \frac{k_4'[C_2H_4]}{2k_3'} - \frac{(1-\beta)\, k_4'[C_2H_4]}{2k_3'} + \frac{k_2 k_4'[C_2H_4]\,(1-\beta)}{k_3},$$

$$\frac{1}{[A]}\frac{d\rho}{d[C_2H_4]} = \frac{k_2 k_4'(1-\beta)}{k_3} - \frac{k_2' k_4'}{2k_3'} - \frac{k_2' k_4'(1-\beta)}{2k_3'}. \qquad \text{(XVI)}$$

From equation (IX), if the ethylene pressure is small,

$$\frac{1}{[A]}\frac{d\rho}{d[C_2H_4]} = -C.$$

Expressing the slope of the aldehyde inhibition curve in terms of an 'apparent' value of β, we may write

$$C = \frac{k_2' k_4' \beta_{\mathrm{apparent}}}{2k_3'}.$$

If these values are inserted in equation (XVI), and it is assumed that the recombination rate of ethyl with methyl does not differ significantly from that of two ethyl radicals (i.e. that $k_3 = k_3'$), then

$$\frac{k_2'}{k_2} = \frac{2(1-\beta)}{2-\beta-\beta_{\text{apparent}}}. \qquad \text{(XVII}a\text{)}$$

For the aldehyde photolysis rate to be unchanged by increasing ethylene concentration (i.e. for there to be no inhibition by ethylene as found with propionic aldehyde), β_{apparent} must be zero. This gives

$$\frac{k_2'}{k_2} = \frac{1-\beta}{1-\frac{1}{2}\beta}. \qquad \text{(XVII}b\text{)}$$

If β has a value similar to that for the acetaldehyde-ethylene reaction, namely, 0·06, then $k_2'/k_2 = 0{\cdot}97$. Therefore if most of the ethyl radicals originally reacting with ethylene in reaction (4′) are replaced in reaction (6′) by methyl radicals which are about 3 % more active, then an inhibition of the same magnitude as that found with acetaldehyde and ethylene could be compensated.

The results with propionic aldehyde and propylene, assuming the true value of β to be the same as that found with acetaldehyde and propylene, give $k_2'/k_2 = 0{\cdot}85$. The agreement of the two values for the ratio is not very good but the assumption of equal β values can only be roughly true. In any case the results show that the reactivities of methyl and ethyl radicals are not very different. Alternatively, but less probably, it could be assumed that $k_2' = k_2$; β would then have to be zero, i.e. k_7 would be zero.

The results for acetaldehyde above are expressed in terms of the constants C and K, the ratio $K/2C$ giving the ratio k_4/k_2. This latter ratio may be obtained directly for propionic aldehyde. From equations (VII) and (VIII)

$$\frac{\rho}{\sigma} = \frac{k_2[\text{EtCHO}]}{nk_4[\text{C}_2\text{H}_4]},$$

giving k_4/k_2. Strictly ρ and σ are of the form given only at low ethylene pressures where replacement of ethyl by methyl is small. With propionic aldehyde the ratio is obviously constant even at high ethylene pressures, since ρ is constant and σ varies linearly with ethylene pressure on account of the balancing of effects described above.

DISCUSSION

The inhibition of the acetaldehyde photolysis by ethylene is relatively slight, that by the two higher olefines considerable. The polymerization rate of ethylene increases only a little less than linearly with pressure; that of propylene and *iso*-butylene is almost independent of pressure except when this is low. With propionic aldehyde and ethylene there is no inhibition of the photolysis, and the polymerization rate is strictly linear with ethylene pressure. These facts are interconnected. When there is no inhibition of the photolysis the stationary concentration of radicals is unchanged by the olefine, which competes for them with the aldehyde to an extent proportional to its own pressure. When, on the other hand, inhibition is large, nearly all the radicals are removed by the olefine. The aldehyde then becomes simply a primary source of radicals, the normal radical removal process being negligible in comparison with the new chain-ending step introduced by the olefine, which is now the controlling factor. If this step is of the first order, the rate of polymerization must become independent of olefine concentration.

In equations (IX) and (X),

$$\frac{k_2 k_4 \beta}{2k_3} = C \quad \text{and} \quad \frac{k_4^2 \beta}{k_3} = K,$$

whence

$$\frac{K}{2C} = \frac{k_4}{k_2}$$

(K being found from the experimental values of $\frac{1}{2}nK$, and n), and

$$\beta = \frac{4k_3 C^2}{k_2^2 K}.$$

From equation (V), when $[C_2H_4] \rightarrow 0$,

$$\rho_0 = k_2 \left\{\frac{k_1 I_{\text{abs.}}}{k_3}\right\}^{\frac{1}{2}} [CH_3CHO].$$

Therefore

$$\beta = \frac{4C^2 k_1 I_{\text{abs.}} [CH_3CHO]^2}{K\rho_0^2}. \qquad \text{(XVIII)}$$

For pure acetaldehyde

$$\text{chain length} = \phi_0 = \frac{\text{total rate}}{\text{rate of primary process}} = \frac{\rho_0}{k_1 I_{\text{abs.}}},$$

or

$$k_1 I_{\text{abs.}} = \frac{\rho_0}{\phi_0},$$

where ρ_0 and ϕ_0 are respectively the rate and chain length for the photolysis of 50 mm. of pure acetaldehyde. The value of ϕ_0 at 300° is 28 units by extrapolation from the results of Mitchell and Hinshelwood (1937), allowance being made for the difference in light intensity. Substitution in equation

(XVIII) gives β, from which the ratio k_7/k_6 is obtained. From the known values of C and of $\frac{1}{2}nK$, with $n = 3$ for ethylene and $n = 2$ for the other olefines, the values for the ratios given in table 13 are obtained. As shown above, effects due to the regeneration of methyl radicals from ethyl radicals can be formally expressed in terms of an apparent value of β, which, where applicable, is included in the table.

TABLE 13

aldehyde	olefine	k_4/k_2	$\beta_{\text{app.}}$	β	k_7/k_6	k'_2/k_2
acetaldehyde	ethylene	0·14	—	0·06	0·06	—
acetaldehyde	propylene	0·31	—	0·29	0·41	—
acetaldehyde	*iso*-butylene	0·31	—	0·59	1·44	—
propionic aldehyde	ethylene	0·17	0·00	(0·06)	—	(0·97)
propionic aldehyde	propylene	0·115	0·04	(0·29)	—	(0·85)

Defining the chain length in the polymerization reaction as

$$\phi_{\text{polym.}} = \frac{\text{number of } C_2H_4 \text{ molecules polymerized}}{\text{number of initiating radicals } (= \text{number of quanta absorbed})},$$

then

$$\phi_{\text{polym.}} = \frac{\text{observed ethylene polymerization rate}}{\rho_0/\phi_0} = \frac{\sigma\phi_0}{\rho_0}. \tag{XIX}$$

Similarly, the chain length of the acetaldehyde photolysis in the presence of ethylene is

$$\phi_{\text{aldehyde}} = \frac{\text{observed photolysis rate in presence of ethylene}}{\rho_0/\phi_0} = \frac{\rho\phi_0}{\rho_0}. \tag{XX}$$

The values for the chain lengths of the two reactions obtained from equations (XIX) and (XX) are given in table 14.

TABLE 14. CHAIN LENGTH OF THE ACETALDEHYDE PHOTOLYSIS IN THE PRESENCE OF ETHYLENE, AND OF THE INDUCED POLYMERIZATION REACTION. 50 MM. ACETALDEHYDE HAS $\rho_0 = 17{\cdot}0$, $\phi_0 = 28$

ethylene pressure	$\rho_{\text{obs.}}$	$\sigma_{\text{obs.}}$	chain lengths	
			CH_3CHO	C_2H_4
0	17·0	—	28	—
100	12·5	14·0	20	23
200	10·8	19·5	18	32
300	9·8	24·0	16	39
400	8·9	28·3	14	48

Under the same conditions of incident light intensity, temperature and pressure, the ratio of the rates of photolysis of acetaldehyde and propionic aldehyde is 3·48, and the ratio of the amounts of light absorbed by equal pressures of the two aldehydes, determined by the use of a photoelectric photometer, is 1·26. The ratio of the quantum efficiencies of photolysis is therefore

$$\frac{\phi(\text{acetaldehyde})}{\phi(\text{propionic aldehyde})} = 3{\cdot}48 \times 1{\cdot}26 = 4{\cdot}38.$$

Taking ϕ(acetaldehyde) = 28, gives ϕ(propionic aldehyde) = 6·4. This is the overall quantum efficiency. The results of Mitchell and Hinshelwood (1937) show that in the primary process for each quantum absorbed by propionic aldehyde, 0·49 molecules react, of which only 0·22 are able to react with nitric oxide, i.e. are free radicals, and 0·51 quanta are degraded as heat. If α is the number of reaction cycles arising from one initial radical,

$$0{\cdot}22\alpha + 0{\cdot}27 = \text{overall quantum yield} = 6{\cdot}4,$$

or

$$\alpha = \text{real chain length} = 28.$$

This value is the same as that for the acetaldehyde photolysis. The experimental conditions used by Mitchell and Hinshelwood differed, however, in several important respects from those in the present work, the light being monochromatic (3135 A), and of much lower intensity. The results therefore cannot be strictly applied, but they do show that there is no very marked difference in the reactivity of methyl and ethyl radicals with aldehydes.

If the number of initiating radicals with propionic aldehyde is taken, as with acetaldehyde, to be equal to the number of quanta absorbed, then from equation (XIX) $\phi_{\text{polym.}} = 6{\cdot}9$ with 100 mm. ethylene. If, however, the value 0·22 for the number of radicals produced by propionic aldehyde per quantum is applicable under these conditions, then $\phi_{\text{polym.}}$ at 100 mm. is 31·4. The corresponding value for the acetaldehyde induced reaction is 22. Owing to the doubt about the applicability of the value 0·22, it can only be said that the polymerization chain length is several times the quantum efficiency and reaches a value comparable with that for the acetaldehyde induced polymerization.

Polymerization photosensitized by ketones

The polymerization of ethylene is also induced by the photolysis of dimethyl and diethyl ketones. These photolyses yield free radicals, though, in contrast with aldehydes, no reaction chains are propagated (Leermakers 1934).

The rate of photolysis of the ketones under the conditions employed was so small that it could be assumed to be unaffected by the ethylene. Analyses for ketone were therefore not necessary, the polymerization rate being obtained directly from the observed rate of pressure change with a small correction for the ketone decomposition. The experimental results for the polymerization of ethylene by dimethyl and diethyl ketones are given in table 15 and are plotted in figure 5. The light absorptions of the ketones

TABLE 15. POLYMERIZATION OF ETHYLENE INDUCED BY PHOTOLYSIS OF DIMETHYL AND DIETHYL KETONES

25 mm. dimethyl ketone photolysis rate 0·5		50 mm. dimethyl ketone photolysis rate 0·7		25 mm. diethyl ketone photolysis rate 0·4	
ethylene pressure	polymerization rate	ethylene pressure	polymerization rate	ethylene pressure	polymerization rate
111	4·0	106	5·6	66	1·6
200	7·5	131	6·2	94	2·5
300	10·7	213	10·0	102	2·0
395	14·6	300	14·5	120	3·3
600	22·5	328	15·2	155	3·8
		565	27·0	203	6·0
				251	7·0
				292	9·5
				300	9·5
				390	14·0

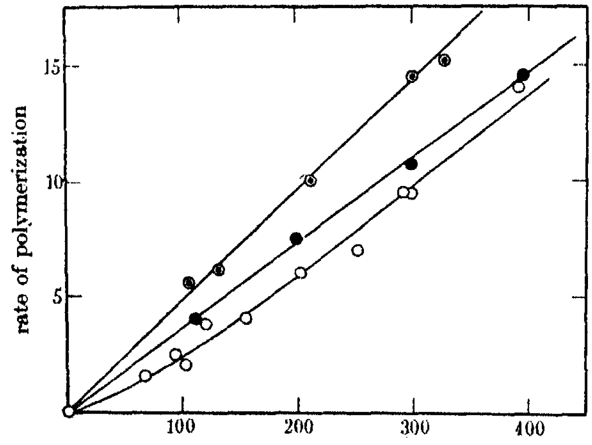

FIGURE 5. Polymerization of ethylene induced by photolysis of dimethyl and diethyl ketones. ⊙ 50 mm. dimethyl ketone, ● 25 mm. dimethyl ketone, ○ 25 mm. diethyl ketone.

and of acetaldehyde are compared in table 16. Comparison of the rates of polymerization of 300 mm. of ethylene photosensitized by 50 mm. of acetaldehyde and by 50 mm. of dimethyl ketone respectively, making allowance for the slightly different light absorptions in the two cases, gives a ratio of 24·1 : 15·8. Though the ketone photolysis takes place without chains, the polymerization induced by it occurs at almost three-quarters of the rate of the acetaldehyde induced reaction, which has a chain length of between 20 and 30 units. The polymerization process itself must therefore have a considerable chain length. This conclusively confirms the existence of a 'chain transfer' step in the reaction mechanism.

TABLE 16. LIGHT ABSORPTIONS OF DIMETHYL AND DIETHYL KETONES COMPARED WITH ACETALDEHYDE

	absorption (arbitrary units)
50 mm. acetaldehyde	9·9
25 mm. dimethyl ketone	5·1
50 mm. dimethyl ketone	8·4
25 mm. diethyl ketone	5·8

The rate of the ketone-induced polymerization is proportional to the ethylene pressure up to the highest pressures investigated. The mechanism must be similar to that of the aldehyde-induced reactions, except for the different primary process and the absence of a chain reaction in the ketone itself. The kinetics of the induced polymerization should therefore be the same. The expression for the rate of the ketone-induced polymerization reduces to

$$\sigma = nk_4[C_2H_4]\sqrt{\frac{k_1 I_{\text{abs.}}}{k_3}}, \tag{XXI}$$

when β is zero or the olefine pressure small. According to this equation σ will be proportional to the olefine pressure, as observed. The rate of the aldehyde-induced polymerization falls below the linear value at higher olefine pressures, but over the same range of polymerization rates, up to the highest observed with dimethyl ketone, it also obeys equation (XXI).

Comparison of the rates of ethylene polymerization by acetaldehyde, dimethyl and diethyl ketones affords an opportunity of estimating their relative efficiency as sources of radicals. With 50 mm. of acetaldehyde and 400 mm. of ethylene the polymerization rate is 30·0 units with a light absorption of 9·9 units. The corresponding rate with dimethyl ketone is 19·1 with light absorption 8·4 units. Corrected to the same light absorption the ratio of the rates is 0·69. If the quantum efficiency of radical production for acetaldehyde is unity (Mitchell and Hinshelwood 1937), the above result suggests that only 69 % of the dimethyl ketone gives rise to free radicals in the primary process.

Photolysis of diethyl ketone gives ethyl radicals. As with propionic aldehyde, the possibility arises of a mechanism in which the absorption of these ethyl radicals by olefine is being followed by the regeneration of methyl radicals at the end of the polymerization cycle. The complex expression for the polymerization rate derived from such a mechanism can be shown to approximate, at high olefine pressures (where the methyl radical concentration will greatly exceed that of ethyl), to that obtained for dimethyl ketone (equation (XXI)). At low olefine pressures, where there is only little conversion of ethyl to methyl radicals, σ is still given by equation (XXI), with the velocity constant for the reaction of ethyl with olefine, (k_4'), in place of k_4. The slope of the curve of σ against $[C_2H_4]$ for diethyl ketone does indeed seem to be smaller at the lowest olefine pressures, which is in agreement with the mechanism above, but the experimental results at such low ethylene pressures are unreliable.

At the higher ethylene pressures the rates of polymerization by the two ketones are almost equal. This would indicate equal reactivities of ethyl and methyl were it not for the possibility of an almost complete replacement of ethyl by methyl in the course of the reaction cycle.

GENERAL CONCLUSIONS REGARDING REACTIVITIES

From the quantitative comparison of the various reactions the following conclusions may be drawn:

(1) There is no marked diminution in the reactivity of the alkyl radicals as the series is ascended. This is shown by the facts that (*a*) in the photolysis the true chain lengths for acetaldehyde and propionic aldehyde are comparable; (*b*) propionic aldehyde is attacked by methyl radicals regenerated in the ethylene polymerization only a little more readily than by ethyl radicals; and (*c*) there is only limited variation in the ratio k_4/k_2 in the different reactions. Like the aldehydes therefore, the olefines must be attacked about equally easily by the different alkyl radicals. This conclusion is consistent with the experiments on the polymerization of ethylene induced by ketone photolysis.

(2) The polymerization rate diminishes rapidly in the series ethylene, propylene, *iso*-butylene. This is not due to a decreasing ease of reaction between radical and olefine, for the higher olefines inhibit the aldehyde

photolysis strongly, which shows that they absorb alkyl radicals very effectively. Their failure to give rapid polymerization must hence depend on high values of β, which is a measure of the tendency of the growing polymer radical to be converted into products unable to propagate the chain process.

(3) The failure of the growing polymer to incorporate more than about three molecules of ethylene must be attributed more to the increasing tendency of the larger radicals to decompose than to a decrease in their rate of reaction with ethylene. Thus the limiting factor, both with the rapid reaction of ethylene and with the slower reactions of the higher olefines, is the decomposition of the growing radical when it exceeds a critical size, either to give a methyl radical which continues the chain, or to give products which are inactive.

As both types of reaction are probably unimolecular, it is understandable that they should occur more readily as the number of degrees of freedom in the radical increases.

REFERENCES

Danby 1940 *Nature, Lond.*, **145**, 940.
Davis and Schuler 1930 *J. Amer. Chem. Soc.* **52**, 721.
Friedemann, Cotonio and Shaffer 1927 *J. Biol. Chem.* **73**, 342.
Leermakers 1934 *J. Amer. Chem. Soc.* **56**, 1537.
Mitchell and Hinshelwood 1937 *Proc. Roy. Soc.* A, **159**, 32.
Olson and Meyers 1926 *J. Amer. Chem. Soc.* **48**, 389.
Rice and Sickmann 1935 *J. Amer. Chem. Soc.* **57**, 1384.
Taylor and Jones 1930 *J. Amer. Chem. Soc.* **52**, 1111.

The vapour-pressure curve

By Klaus Fuchs

The University of Edinburgh

(*Communicated by M. Born, F.R.S.—Received* 12 *March* 1941)

By an extension of Mayer's theory of condensation, exact equations are derived for the vapour pressure and the condensation volume of the gas in terms of the virial coefficients on the one hand and the free energy of the condensed phase on the other. The formula for the vapour pressure reduces in first approximation to Stern's vapour-pressure equation.

1. Introduction

Mayer, together with several collaborators, developed a few years ago a very powerful method of dealing with the thermodynamical properties of gases (Mayer 1937; Mayer and Ackermann 1937; Mayer and Harrison 1938). A rigorous treatment of Mayer's theory has been given by Born and myself (1938).

The central idea of Mayer's method is this: If we evaluate the partition function correctly, taking into account all configurations of the particles possible in a given volume, then any phase change must follow automatically from the partition function. If, in particular, the phase change is associated with a change of volume, the pressure must automatically be constant between the volumes of the two phases.

The partition function then is a non-analytic function of the volume. It has singularities for those volumes where a phase change takes place. Mayer used this property of the partition function in order to obtain a theoretical description of the phenomenon of condensation. If we develop the partition function in a power series of the reciprocal volume, this series diverges for the condensation volume. Beyond this volume the pressure remains constant. The lower terms of the series give the properties of the gas and they can in principle be evaluated, if the forces between the particles are known.

The condensation volume and pressure, on the other hand, are determined by the asymptotic value of the higher coefficients in this series. These are of such a complicated nature that a direct evaluation is impossible.

If the condensed phase is a solid, the partition function can be evaluated by different means. We can then reverse the problem. Instead of evaluating the partition function in terms of the coefficients of the power series, we may evaluate the asymptotic value of the coefficients in terms of the partition function. If this can be done, the condensation volume and vapour pressure can be expressed in terms of the lower coefficients of the expansion on the one hand, and the partition function of the condensed state on the other.

I shall show that this actually can be done. The resulting equation for the vapour pressure gives in first approximation the vapour-pressure equation of Stern.

2. THE EXPANSION OF THE PARTITION FUNCTION

It will be necessary to repeat some equations of Mayer's theory, since we have to inquire whether they can be applied to the condensed phase.

The notation of Born and myself (1938, in the following quoted as I) will be used. We defined the F-functions (I, 3·1)

$$F(N-m, N, vb) = \sum_{\substack{m_l \\ \Sigma l m_l = N-m}} \prod_{l} \frac{(Nvb_l)^{m_l}}{m_l!}. \tag{2·1}$$

If v is the volume per particle, N the number of particles and b_l the 'cluster integrals' (I, 1·6), then the partition function of the system is given by (I, 1·1 and I, 3·2)

$$Q^{(N)} = \left(\frac{2\pi mkT}{h^2}\right)^{3N/2} \frac{Q_\tau^{(N)}}{N!}, \quad \frac{Q_\tau^{(N)}}{N!} = F(N, N, vb). \tag{2·2}$$

We then formed the H-functions (I, 5·1)

$$H_\lambda^m(x, vb) = \sum_{N=1}^{\infty} \frac{F(N-m, N, vb)}{N^\lambda} x^N. \tag{2·3}$$

By the theorem of Cauchy Hadamard the asymptotic value of $Q_\tau^{(N)}/N!$ can be expressed by the radius of convergence X of the series H_λ^0 (in I we used r, R for x, X; the change of notation is introduced in order to avoid confusion with the gas constant R)

$$\frac{1}{X} = \lim_{N\to\infty} F(N, N, vb)^{1/N} = \lim_{N\to\infty} \left(\frac{Q_\tau^{(N)}}{N!}\right)^{1/N}. \tag{2·4}$$

The H-functions are closely connected with the G-functions (I, 3·3)

$$G_\lambda(z, vb) = \sum_{l=1}^{\infty} e l^\lambda v b_l z^l = vG_\lambda(z, b). \tag{2·5}$$

The connexion is given by the theorems (I, 5·2, 5·11 and 5·12)

$$H_0^m(x, vb) = \frac{z^m}{1 - G_1(z, vb)} - \delta(m, 0), \tag{2·6}$$

$$H_1^m(x, vb) = \begin{cases} G_0(z, vb) & m = 0, \\ z^m/m & m > 0, \end{cases} \tag{2·7}$$

where the variables x and z are connected by the equation

$$x = ze^{-G_0(z, vb)}. \tag{2·8}$$

In I we distinguished two regions. In the region of the gaseous phase, we defined Z as the root of the equation

$$G_1(Z, vb) = 1. \tag{2·9}$$

From (2·6) it follows that for this value of z, H_0^0 diverges and with (2·8), (2·4), (2·2) we found the partition function and free energy A

$$\begin{aligned} \frac{-A}{kT} &= \ln Q = N\{G_0(Z) - \ln Z - \ln v_k\}, \quad v_k = \left(\frac{\hbar^2}{2\pi mkT}\right)^{3/2}. \\ &= -N\{\ln X + \ln v_k\}. \end{aligned} \tag{2·10}$$

If $\bar{Z}$ is the first singularity of $G(z, vb)$ on the positive axis, then for volumes smaller than v_g the radius X is given by means of $\bar{Z}$. Here v_g is defined by means of the equation

$$G_1(\bar{Z}, b) = \frac{1}{v_g}. \tag{2·11}$$

In this case the partition function is given by (2·10), with Z replaced by $\bar{Z}$. In both cases we find the same type of equation for the pressure

$$PV = -V\frac{\partial A}{\partial V} = \begin{cases} RTG_0(Z, vb) & v \geqslant v_g, \\ RTG_0(\bar{Z}, vb) & v \leqslant v_g. \end{cases} \tag{2·12}$$

Here V is the total volume Nv. From the second equation we concluded that the pressure remains constant for volumes smaller than v_g, and this region is therefore the region of phase change from the gaseous phase to the condensed phase. The value of $\bar{Z}$ is of course connected with the asymptotic value of the cluster integrals in the same way as X is connected with the asymptotic value of the partition function.

No indication could be obtained from these equations about the condensed phase. This problem will be discussed in the next section.

3. Expansion of the partition function for the condensed phase

The cluster integrals are defined as certain integrals over the configuration space of l particles corresponding to the total volume Nv. The integrand is such that it gives a contribution only if each particle is within the range of forces of the other particles. Since the integration extends over the whole volume, the smaller cluster integrals are obviously independent of the volume. Even if the volume per particle is smaller than the cube of the range of forces, the total volume Nv can still be considered as infinite as long as the number l of particles in the cluster is small compared to N. But if l is of the same order as N, the cluster integrals can depend on the volume.

If the volume v per particle is given, the cluster integrals depend therefore furthermore on the total number of particles; I shall denote them by

$$b_l^{(N)}. \tag{3·1}$$

Now consider the definition (2·3) of the H-functions, it is seen that in each term the coefficients b_l will be different and our theorem about H-functions cannot be applied. This, of course, is the case only if the contribution of the large cluster integrals to the partition function is appreciable. There is therefore no difficulty about the gaseous phase. Even for the densest gases, the cluster integrals can be considered as constants.

The difficulty can be avoided in the following way. I define

$$^N G_\lambda(z) = G_\lambda(z, vb^{(N)}), \quad b_l^{(N)} = 0 \quad \text{if} \quad l > N, \tag{3·2}$$

and correspondingly $$^N H_\lambda^m(x) = H_\lambda^m(x, vb^{(N)}). \tag{3·3}$$

Then the theorem about H-functions holds for every one of these functions. Consequently, it also holds in the limit $N \to \infty$. I therefore define

$$g_\lambda = \lim_{N\to\infty} {}^N G_\lambda, \quad h_\lambda^m = \lim_{N\to\infty} {}^N H_\lambda^m. \tag{3·4}$$

These are the functions which have to be used instead of H_λ^m and G_λ. I obtain the same equation for the partition function in terms of $\bar{Z}$, with the only difference that $\bar{Z}$ is now the first singularity of g_λ on the positive axis; it is therefore given by

$$\frac{1}{\bar{Z}} = \lim_{N\to\infty} (b_N^{(N)})^{1/N}, \tag{3·5}$$

and evidently it can depend on the volume.

Except in the neighbourhood of the critical point, the middle sized clusters do not give any contribution to either the partition function or the series G_λ. They are therefore semi-convergent beyond the singularities and, since the lower cluster integrals do not depend on the volume, they are semi-convergent expansions of g_λ. In this sense the equation (2·10) for the partition function remains correct, if Z is replaced by $\bar{Z}$ as defined by (3·5). Since this quantity depends on the volume, the expression (2·12) for the pressure must be modified; instead

$$PV = RT\left\{G_0(\bar{Z}, vb) - \frac{d\ln\bar{Z}}{d\ln v}(1 - G_1(\bar{Z}, vb))\right\}. \qquad (3\cdot6)$$

Thus, in this region the pressure changes with the volume and it must therefore be identified with the condensed phase.

I therefore define a volume v_c, such that for volumes greater than v_c, $b_N^{(N)}$ and therefore $\bar{Z}$ is constant, and that these quantities depend on the volume for volumes smaller than v_c. Then v_c is the volume of the condensed phase.

Such non-analytical behaviour of the large cluster integrals is easily understood. They are integrals very similar to the integral defining the partition function, though rather more complicated. In the case of the partition function it is easy to understand the discontinuity for $v = v_c$, if we realize that the configurations corresponding to the coexistence of two phases are also included in the integration over the whole configuration space. There is therefore a linear decrease of the free energy corresponding to a linear increase of the number of particles in gaseous configurations. But, since the latter do not contribute to the large cluster integrals, these remain constant for volumes larger than v_c.

4. THE CONDENSATION VOLUME AND VAPOUR PRESSURE

I shall now assume that the free energy of the condensed phase has been obtained. If the condensed phase is the solid phase, this can, for example, be done in the well-known way by integration over all normal modes of vibration. Thus from (2·10)

$$X = \frac{1}{v_k} e^{A/RT}. \qquad (4\cdot1)$$

$\bar{Z}$ can now be obtained from (2·7)

$$\bar{Z} = H_1^1(X, vb) = H_1^1\left(\frac{1}{v_k} e^{A/RT}, vb\right). \qquad (4\cdot2)$$

Applying this equation in particular to the volume v_c, one obtains the value of $\bar{Z}_c$, i.e. the singularity of the G-functions, which governs the process of condensation. The condensation volume of the gaseous phase and the vapour pressure are then given by (2·11), (2·12)

$$\frac{1}{v_g} = G_1(\bar{Z}_c, b), \tag{4·3}$$

$$P_g = P_c = kTG_0(\bar{Z}_c, b). \tag{4·4}$$

Here as in the following equations the indices c and g refer to the evaporation volume v_c of the condensed phase and the condensation volume v_g of the gaseous phase.

The equations (4·4) and (4·5) can be transformed by means of (2·6) and (2·7) with the result

$$\frac{v_c}{v_g} = 1 - \frac{1}{1+H_0^0(X_c, v_c b)}, \quad X_c = \frac{1}{v_k} e^{A_c/RT}. \tag{4·5}$$

$$P_c = \frac{kT}{v_c} H_1^0(X_c, v_c b). \tag{4·6}$$

The volume v_c finally is determined by the condition that the pressure of the solid phase is identical with the vapour pressure

$$-\left(V\frac{\partial A}{\partial V}\right)_{v=v_c} = RTH_1^0(X_c, v_c b). \tag{4·7}$$

The series in these formulae of course converge. They are semi-convergent only for volumes smaller than v_c.

I have therefore expressed the condensation volume v_g and the vapour pressure in terms of the lower cluster integrals and the free energy of the condensed phase. The volume v_c of the condensed phase is expressed as the solution of an equation involving also only the lower cluster integrals and the free energy of the condensed phase.

The cluster integrals furthermore can be expressed in terms of the irreducible integrals β_ν (see I, 3·2), which multiplied by $-\nu/\nu+1$ are identical with the virial coefficients.

In the following the first few terms of the expansions are given. The cluster integrals are

$$b_1 = 1, \quad b_2 = \tfrac{1}{2}\beta_1, \quad b_3 = \tfrac{1}{2}\beta_1^2 + \tfrac{1}{3}\beta_2, \quad b_4 = \tfrac{2}{3}\beta_1^3 + \beta_1\beta_2 + \tfrac{1}{4}\beta_3. \tag{4·8}$$

The equation for v_c is

$$\left(-\frac{1}{kT}\frac{\partial A}{\partial V}\right)_{v=v_c} = \frac{e^{A_c/RT}}{v_k}\left\{1+\frac{v_c+b_2}{v_k}e^{A_c/RT}+\frac{\frac{3}{2}v_c^2+3v_cb_2+b_3}{v_k^2}e^{2A_c/RT} + \frac{\frac{8}{3}v_c^3+8v_c^2b_2+4v_cb_3+2v_cb_2^2+b_4}{v_k^3}e^{3A_c/RT}+\dots\right\}. \tag{4·9}$$

The condensation volume of the gaseous phase is given by

$$\frac{1}{v_g-v_c} = \frac{1}{v_k}e^{A_c/RT}\left\{1+2\frac{v_c+b_2}{v_k}e^{A_c/RT}+3\frac{\frac{3}{2}v_c^2+3v_cb_2+b_3}{v_k^2}e^{2A_c/RT} + 4\frac{\frac{8}{3}v_c^3+8v_c^2b_2+4v_cb_3+2v_cb_2^2+b_4}{v_k^3}e^{3A_c/RT}+\dots\right\}, \tag{4·10}$$

and the vapour pressure by

$$\frac{P_c}{kT} = \frac{1}{v_k}e^{A_c/RT}\left\{1+\frac{v_c+b_2}{v_k}e^{A_c/RT}+\frac{\frac{3}{2}v_c^2+3v_cb_2+b_3}{v_k^2}e^{2A_c/RT} + 4\frac{\frac{8}{3}v_c^3+8v_c^2b_2+4v_cb_3+2v_cb_2^2+b_4}{v_k^3}e^{3A_c/RT}+\dots\right\}. \tag{4·11}$$

If the condensed phase is the solid phase, the free energy may be written in the form

$$\frac{A}{RT} = \frac{\epsilon}{kT} - \frac{3}{2}\ln\frac{kT}{\bar{\nu}^2\,2\pi m} + \ln v_k. \tag{4·12}$$

Taking only the first terms in the expansions (4·10), (4·11) we find

$$v_g - v_c = \left(\frac{kT}{\bar{\nu}^2\,2\pi m}\right)^{3/2} e^{-\epsilon/kT}, \tag{4·13}$$

$$\ln P_c = \frac{\epsilon}{kT} - \frac{1}{2}\ln kT + \frac{3}{2}\ln(\bar{\nu}^2\,2\pi m). \tag{4·14}$$

The last equation is the vapour-pressure formula of Stern (cf. for example, Born 1923). It holds for sufficiently low temperatures. For higher temperatures the next terms in the expansion must be included.

In the same approximation we find for $\bar{Z}$

$$\bar{Z} = \frac{1}{v_k}e^{A_c/RT} = \lim_{N\to\infty}\left(\frac{Q_\tau^{(N)}}{N!}\right)^{-1/N} \tag{4·15}$$

or with (3·5)

$$b_N^{(N)} \fallingdotseq \frac{Q_\tau^{(N)}}{N!}. \tag{4·16}$$

Thus at sufficiently low temperatures at least, the large cluster integrals are identical with that part of the partition function which arises from the integration over the spatial co-ordinates.

REFERENCES

Born, M. 1923 *Atomtheorie des festen Zustandes*, p. 705.
Born, M. and Fuchs, K. 1938 *Proc. Roy. Soc.* A, **166**, 391.
Mayer, J. E. 1937 *J. Chem. Phys.* **5**, 67.
Mayer, J. E. and Ackermann, Ph. G. 1937 *J. Chem. Phys.* **5**, 74.
Mayer, J. E. and Harrison, S. F. 1938 *J. Chem. Phys.* **6**, 87, 101.

The absorption spectra of the cyclic dienes in the vacuum ultra-violet

By W. C. Price and A. D. Walsh
Physical Chemistry Laboratory, Cambridge

(*Communicated by R. G. W. Norrish, F.R.S.—Received* 22 *April* 1941

[Plates 30, 31]

The absorption spectra of cyclohexadiene, cyclopentadiene, pyrrole, thiophene and furan have been investigated in the vacuum ultra-violet. The spectra obtained are due to the excitation of a π electron from the conjugated double-bond electrons $(\chi_1^2\chi_2^2)$. The ionization potentials of the molecules deduced from Rydberg series are respectively 8·4, 8·58, 8·9, 8·91 and 9·01V, these values referring to the outer χ_2 shell of π electrons. A second less certain ionization potential of about 10·8V was obtained for furan.

Some discussion of the electronic structure of the molecules on the basis of their spectra is given, and it is concluded that only in furan is there marked tendency towards homocyclic conjugation. It is also concluded that 'hyperconjugation' does not play so large a part in the interpretation of the spectra of cyclohexadiene and cyclopentadiene as previously supposed.

The absorption spectra of some open-chain dienes in which the double bonds appear to be mainly in the *trans* position have been previously described (Price and Walsh 1940). The present article deals with the spectra of cyclic (*cis*) dienes, the molecules investigated being cyclohexadiene, cyclopentadiene, pyrrole, thiophene and furan. It appears that as in the open-chain dienes the electron which gives rise to the bands is a π electron from the conjugated double bonds. The spectra of the cyclic dienes exhibit considerable similarity amongst themselves. Certain systematic differences which are found indicate the magnitude of the effect of adjacent atoms or groups on these electrons. A comparison of the spectra of the open-chain and cyclic dienes confirms theoretical predictions (Mulliken 1939*b*) on the relative intensities of certain analogous electronic transitions in the *cis* and *trans* positions.

The spectra of the molecules cyclopentadiene, thiophene and furan can be analysed in greater detail than the others for the reason that considerably sharper absorption bands were obtained for these molecules. They will therefore be described first. The main features of cyclic diene absorption having been obtained from them, it will then be seen that cyclohexadiene and pyrrole fit naturally into their places in a sequence, although the data from these molecules is not quite so complete. A vacuum spectrograph with a glass grating was used in these experiments in conjunction with a source of Lyman continuum. The photographic plates were Ilford Q 1, this specially sensitive emulsion being coated on microscope cover-glass (thickness 0·2 mm.) so as to bend easily into the Rowland circle. We have used these plates for several years and have found them extremely satisfactory for work in the vacuum ultra-violet region of the spectrum.

CYCLOPENTADIENE

Monomeric cyclopentadiene was obtained by cracking the dimer under suitable conditions. Its absorption in the Schumann region has been investigated by Scheibe and Grieneisen (1934). Their results and those of most workers in this field are limited by the fact that fluorite spectrographs and the hydrogen continuum were used in their experiments. The use of grating spectrographs and the Lyman continuum enables regions of much shorter wave-lengths to be investigated. A photograph of the absorption spectrum of cyclopentadiene is given in plate 30*b*. It consists of a series of exposures taken at a succession of increasing pressures. The longest wave-length system of bands occurs in the region 2500–2100 A. Similar systems of bands occur in all the dienes. While they are relatively weak in the cyclic (*cis*) dienes they are strong in the open-chain (*trans*) dienes. The spectra in plate 30 have been moved relative to one another so that the second long wave-length absorption systems lie below each other. It can be seen that while in cyclohexadiene and cyclopentadiene these second regions are stronger than the longest wave-length ones, the contrary is true for dimethyl butadiene. The electronic nature of the first transition has been interpreted by Mulliken (1939*b*) as $N \rightarrow V_1$. The bands are diffuse, the main heads being broad maxima superimposed on a background of continuous absorption. Frequency differences of about 1200 cm.$^{-1}$ were found which are probably analogous to the similar differences observed in the corresponding bands of thiophene, pyrrole and furan. They may be interpreted as valence vibrations of the conjugated C=C bonds.

On the short wave-length side of the 2500–2100 A system there is a region of transparency extending to about 1990 A where a system of strong bands starts. Most of these bands are sharp and degraded slightly towards shorter wave-lengths.* While at first sight the vibrational pattern appears fairly complex as might be expected for a molecule having as many possible modes of vibration as cyclopentadiene, a closer inspection shows that two main frequency differences are involved, one of about 1450 cm.$^{-1}$ and the other about 480 cm.$^{-1}$. The first is mainly a valence vibration in the C=C bonds, and as will be shown later occurs also in the analogous systems in furan and thiophene. It probably corresponds to the Raman frequency of 1500 cm.$^{-1}$ (Truchet and Chapron 1934). The 1200 cm.$^{-1}$ separation of the 2500–2100 A system is no doubt the same mode of vibration, though there it suffers greater diminution from its value in the ground state. The second difference (~ 480 cm.$^{-1}$) probably corresponds to a twisting of the CH_2 group, the reasons for supposing this being that (1) a similar difference occurs in the spectrum of ethylene (Price and Tutte 1940) where, by the use of heavy ethylene, the mass factor of the vibration was shown to be hydrogen dependent, and (2) such a difference does not occur in the analogous bands of furan which of course does not have a CH_2 group. Other frequency differences were found to accompany the main pattern, but these give rise to weaker bands. The differences of the stronger bands are shown in table 1.

TABLE 1. FREQUENCIES AND ASSIGNMENTS OF BANDS OF THE 1990–1800 A SYSTEM OF CYCLOPENTADIENE

I	ν obs.	assignment	*I*	ν obs.	assignment
10	50,380	ν_0	3	51,640	$\nu_0+\nu_3+\nu_2$
2	690	—	9	820	$\nu_0+\nu_1$
2	760	—	3	940	$\nu_0+\nu_2+\nu_4$
10	850	$\nu_0+\nu_2$	2	52,140	$\nu_0+\nu_3+2\nu_2$
3	51,180	$\nu_0+\nu_3$	9	310	$\nu_0+\nu_1+\nu_2$
2	330	$\nu_0+2\nu_2$	2	53,270	$\nu_0+2\nu_1$
2	450	$\nu_0+\nu_4$	2	740	$\nu_0+2\nu_1+\nu_2$

---

* This second absorption starts abruptly and is not preceded by the weaker long wave-length step out which is a characteristic feature of the spectra of the cyclic trienes.

ν_1 (1450 cm.$^{-1}$) is probably to be most closely identified with a valence frequency of the conjugated double bonds and ν_2 (480 cm.$^{-1}$) probably a twisting vibration of the CH_2 group. ν_3 and ν_4 are unidentified modes.

After this article had been communicated, a paper by Pickett, Paddock and Sackter (1941) appeared to which the referee kindly called our attention. These authors propose a vibrational analysis for the 1990–1800 A system of cyclopentadiene with which we would agree in the main. We think, however, for reasons already given in this article that the separation of about 480 cm.$^{-1}$ is not an electronic difference as they have suggested but a vibration due to a twisting of the CH_2 group with respect to the plane of the ring. It would not be prevented from appearing by symmetry conditions as is implied in the article by Pickett *et al.*, since they have only considered the symmetrical vibrations of a plane pentagon. It should also be mentioned that our measured frequencies both in cyclopentadiene and furan are less by about 50 cm.$^{-1}$ than those of Miss Pickett.

Towards shorter wave-lengths there is a region of relative transparency followed by somewhat weaker bands in the region below 1650 A. These bands are of a different type and as far as can be ascertained are purely electronic transitions unaccompanied by any appreciable amount of vibrational structure. This is a phenomenon of very frequent occurrence in the absorption spectra of polyatomic molecules in the vacuum ultra-violet. It is clear from the regular decrease in intensity of the bands on going to shorter wave-lengths that we are dealing with a system of electronic bands converging to an ionization potential. Owing to the somewhat diffuse character of the bands and its effect upon the accuracy of the measurements a certain amount of difficulty was experienced in identifying bands belonging to the same Rydberg series. However, a series of bands roughly conforming to the following formula was established with a reasonable degree of certainty:

$$\nu_0^n = 69{,}550 - R/(n+0{\cdot}28)^2. \qquad (1)$$

The reality of this series is supported by the discovery of analogous series in the other *cis* dienes, thiophene and furan, where they were in some cases better developed, and still further by the fact that these series were very similar to those previously discovered in the *trans* dienes (Price and Walsh 1940). The limit corresponds to an ionization potential of 8·58 V. An electron impact value of 8·4 ± 0·1 V, determined in this laboratory by Mr Sugden, also strongly supports this value. A picture of the absorption of dimethyl butadiene is placed beneath that of cyclopentadiene for comparison. It can be seen that analogous bands of the latter molecule fall to the long wave-length side of those of the former. This statement is true of the spectrum as a whole right up to the photo-ionization limit (8·67 V for dimethyl butadiene).

TABLE 2. TABLE SHOWING OBSERVED AND CALCULATED FREQUENCIES OF THE CYCLOPENTADIENE BANDS OF SERIES (1)

n	ν obs.	ν calc.
4	63,540	63,559
5	65,600	65,613
6	66,790	66,766
7	67,440	67,479

THIOPHENE

The absorption spectrum of thiophene is shown in plate 31. Similarities with cyclopentadiene are immediately evident, and it is clear that the whole spectrum is shifted slightly to shorter wave-lengths. In the long wave-length absorption which occurs in thiophene between about 2400 and 2100 A, the bands are much sharper than in cyclopentadiene, and the important frequency difference can be derived here with greater certainty. Menczel (1927) has proposed a tentative vibrational analysis of these bands in which he gives the main frequency difference of the vibrational pattern as ~ 1150 cm.$^{-1}$. Because of the greater contrast of our photographs we were able to measure partially diffuse bands in this neighbourhood at wave-lengths somewhat shorter than he reached. These enable us to show clearly that the main frequency difference of the pattern is ~ 965 cm.$^{-1}$ and not ~ 1150 cm.$^{-1}$ as reported by Menczel. The value corresponds to the valence frequency of the conjugated double bands in the excited state. An additional reason for accepting the lower rather than the higher difference is that this particular vibration is about 100 cm.$^{-1}$ lower for thiophene in the ground state than for the other cyclic pentadienes, i.e. 1404 cm.$^{-1}$ (Bonino and Manzoni-Ansidei 1934) as compared with values ~ 1500 cm.$^{-1}$. Its value in the excited state might be expected to be correspondingly lower than the similar differences in the other dienes (~ 1100 cm.$^{-1}$). Sets of progressions of bands having mean differences of about 965 cm.$^{-1}$ are given in table 3. The separations between the progressions probably correspond to difference frequencies and are not in themselves vibrational frequencies of the upper state.

The 2400–2100 A system is followed by a region of transparency which is terminated fairly abruptly by the start of a strong system of bands about 1880 A. There is strong similarity in appearance, general shape, etc., between this system and the 1980–1800 A system of cyclopentadiene and they are undoubtedly analogous. While the first few bands are sharp, the shorter wave-length members rapidly become diffuse and thus little vibrational analysis could be accomplished for this system. The first two strong bands have a separation of 540 cm. which corresponds to the separation of 470 cm.$^{-1}$ for the first two strong bands of the cyclopentadiene system. It is possible also to pick out the main ethylenic frequency which turns out to be around 1250 cm.$^{-1}$. This is somewhat lower than its value in the corresponding states of cyclopentadiene and furan and is in agreement with the low value of this frequency in the ground state of thiophene (1404 cm.$^{-1}$). There is also some evidence for a ground state frequency of 675 cm.$^{-1}$ appearing just to the long wave-length side of this system.

TABLE 3. PROGRESSIONS WITH MEAN SEPARATION OF 965 CM.$^{-1}$ IN THE 2400–2100 A SYSTEM OF THIOPHENE

I	ν	$\Delta\nu$	I	ν	$\Delta\nu$
0	41,375	—	6	41,715	—
1	42,205	970	9	42,680	965
1	43,300	995	10*d*	43,660	980
	—	—	10	44,645	985
5	41,555	—		—	—
8	42,510	955	2	41,775	—
10	43,480	970	6	42,740	965
10	44,445	965	6*d*	43,720	980
6	45,405	960		—	—
			3	41,990	—
			8	42,920	930
			8	43,900	980
			6	44,860	960

TABLE 4. TABLE SHOWING OBSERVED AND CALCULATED FREQUENCIES OF THE THIOPHENE BANDS OF SERIES (2)

n	ν obs.	ν calc.
4	67,640	67,600
5	69,040	69,018
6	69,820	69,865
7	70,440	70,412

The region between 1600 and 1400 A is occupied by a large number of fairly sharp bands which gradually diminish in intensity towards shorter wave-lengths. These are apparently electronic bands unaccompanied by much if any vibration, converging to an ionization limit ~ 1400 A. Fairly well-developed Rydberg series were found which gave a value of 8·91 ± 0·02V for the ionization potential of the molecule. The following formula represents the most prominent series found:

$$\nu_0^n = 72{,}170 - R/(n+0\cdot90)^2. \qquad (2)$$

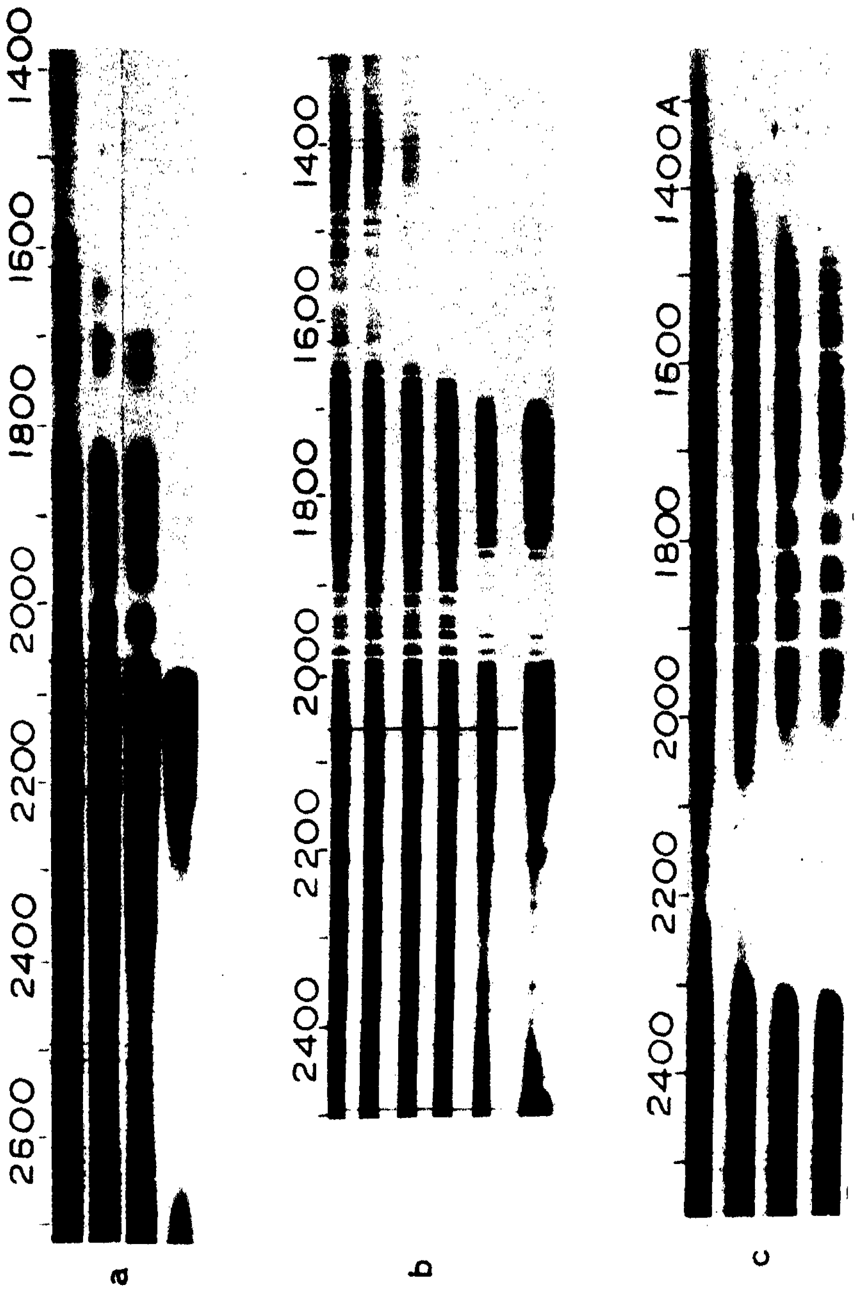

The absorption spectra of (*a*) cyclohexadiene, (*b*) cyclopentadiene, (*c*) $\beta\gamma$ dimethyl butadiene in the vacuum ultra-violet.

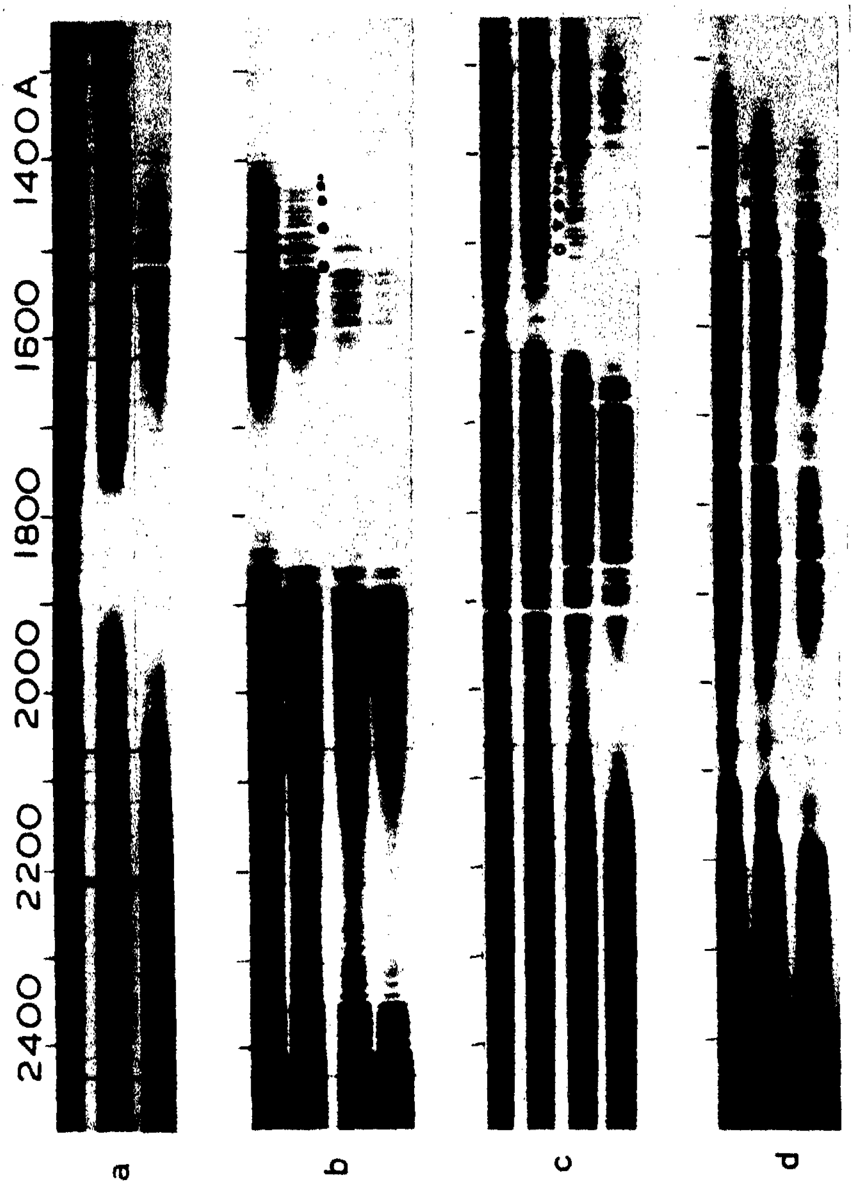

The absorption spectra of (*a*) pyrrole, (*b*) thiophene, (*c*) furan, (*d*) butadiene in the vacuum ultra-violet.

An electron impact value of 9·0 ± 0·05 V to be published shortly supports the value determined from Rydberg series.

FURAN

The absorption of furan is similar in many respects to that of cyclopentadiene and thiophene. It suffers certain wave-length shifts with respect to them, but corresponding systems can be recognized fairly easily. The spectrum in the fluorite region has been photographed by Miss Pickett (1940). Our results confirm hers though of course they extend to considerably shorter wave-lengths. Again the spectrum starts with a relatively weak diffuse system which has broad maxima at about 47,400, 48,800, 50,100, 51,200 cm.$^{-1}$, giving differences of 1200, 1300 and 1100 cm.$^{-1}$ respectively. These differences no doubt correspond to a weakened valence vibration of the conjugated double bonds and are analogous to the differences of ~ 965 cm.$^{-1}$ obtained for thiophene.

On the short wave-length side of this region starts a beautifully sharp system of bands. Its ν_0 band at 1915·6 A is so much stronger than the other bands that it is clear that the vibration frequencies of the molecule have not been much changed by the excitation. This fits in with Miss Pickett's assignments of the vibrational frequencies. Our measurements of this system differ slightly from hers, but what we wish to stress is that here again the most strongly excited vibration (~ 1410 cm.$^{-1}$) must really be interpreted as mainly a valence vibration in the conjugated C=C bonds (1499 cm.$^{-1}$ in the ground state). At first sight it might be thought that this system is not analogous to the 1980–1800 A system of cyclopentadiene and the 1880–1709 A system of thiophene, since if so it would be expected to lie to the short wave-length side of the thiophene bands. This apparent misfit will be discussed later.

A region of transparency extends between 1800 and 1670 A followed on the short wave-length side by a complex system of bands which have the general features of electronic bands converging to an ionization potential. They are similar to the short wave-length bands of cyclopentadiene. Rydberg series established among the higher frequency bands give an ionization potential of 9·01 ± 0·01 V. This is in agreement with our electron impact determination of 9·0 V, and with the order of the short wave-length shift of the spectrum relative to analogous portions of the cyclopentadiene spectrum. Considerable confidence in the series and ionization potential was obtained from the fact that the upper Rydberg series bands are very similar to the corresponding Rydberg bands in butadiene. Analogous members occur at almost the same wave-lengths and the series converges to closely the same ionization potential for both molecules:

$$\nu_0^n = 73{,}080 - R/(n+0\cdot90)^2, \tag{3a}$$

$$\nu_0^n = 73{,}020 - R/(n+0\cdot50)^2. \tag{3b}$$

TABLE 5. SHOWING THE OBSERVED AND CALCULATED FREQUENCIES OF THE FURAN BANDS OF SERIES (3*a*) AND (3*b*)

	series 3*a*		series 3*b*	
n	ν obs.	ν calc.	ν obs.	ν calc.
3	66,030	65,765	—	—
4	68,550	68,510	67,600	67,601
5	69,940	69,228	69,350	65,398
6	70,750	70,775	70,450	70,423

To the short wave-length side of the first ionization limit of furan there occurs a strong band at 1383·7 A which we consider to be a resonance band of the inner pair (χ_1) of the $\chi_1^2\chi_2^2$ group of π electrons. It is accompanied by other bands which are also attributable to the same electron. Their diffuseness and the resultant inaccuracy of their wave-length determinations prevents a definite analysis being given, but our experience indicates that they probably converge to an ionization potential close to 10·8 V. The second ionization potential we obtain from our electron impact measurement is 10·6 V, thus supporting this value.

CYCLOHEXADIENE

The spectrum of cyclohexadiene is similar in its main feature to that of cyclopentadiene, its corresponding bands being shifted somewhat to longer wave-lengths. The NV_1 system has a maximum around 2480 A as compared with 2320 A for cyclopentadiene. Its absorption coefficients have been measured by Henri and Pickett (1939). The next system occurs between 2070 and 1900 A. It is analogous to the 1980–1850 A system of cyclopentadiene and is accordingly much stronger than the NV_1 system. It has been investigated by Carr and Stucklen (1938). The gross structure of this system involves a frequency difference of about 1400 cm.$^{-1}$ which is mainly a valence vibration in the conjugated double bonds (48,790, 50,150, 51,600 cm.$^{-1}$). This is to be compared with the values of about 1450 cm.$^{-1}$ obtained for both cyclopentadiene and furan. The Raman frequency with which it is to be identified is presumably that at 1576 cm.$^{-1}$ (Murray 1935). These main bands of cyclohexadiene are composed of a number of groups of individual bands with separations of about 100 cm.$^{-1}$. It seems probable that these separations correspond to deformation vibrations of the CH_2 groups against each other. The systems falling below 1800 A on our plates were marred by the presence of a small quantity of benzene in our preparation. Unfortunately, a new specimen could not be made as our supply of cyclohexene was cut off as a result of the war. The electron impact value of the ionization potential which we obtained with our purest specimen was 8·4 V, which is in accord with the long wave-length displacement of the spectrum of cyclohexadiene relative to that of cyclopentadiene and the other molecules discussed in this article. The low value is to be attributed to additional charge transfer from the extra CH_2 group.

PYRROLE

The absorption spectrum of this molecule in the Schumann region has been obtained by Scheibe and Grieneisen (1934). Our results confirm theirs and also extend to somewhat shorter wave-lengths. The first relatively weak $N \rightarrow V_1$ absorption occurs between 2220 and 1900 A, being slightly to the long wave-length side of the analogous furan absorption. It overlaps at its short wave-length end, the second region, which is a diffuse region of strong absorption, occurring between about 1870 and 1800 A. This second absorption thus appears to the long wave-length side of the analogous thiophene system and to the short wave-length side of the corresponding furan bands. The relative position of these bands is therefore completely transposed by comparison with the NV_1 bands. This peculiarity will be discussed later. To shorter wave-lengths some individual bands appear which can be correlated with the Rydberg bands of thiophene. Corresponding bands of pyrrole appear slightly to the long wave-length side of analogous thiophene bands. It might thus be expected that the ionization potential of pyrrole is only slightly ($\sim$ 0·005 V) less than that of thiophene (8·9 V). Our electron impact value is about 9·0 V for this molecule.

DISCUSSION

The electronic structures of the cyclic dienes have been treated theoretically by Huckel (1937) and Mulliken (1939*b*). The modifications introduced by further conjugation with an electron pair of 'unsaturation' electrons on the fifth atom have to be considered. In the case of cyclopentadiene (also cyclohexadiene) these are CH_2 molecular orbitals perpendicular to the plane of the molecule, the phenomenon then being termed 'hyperconjugation'.

Mulliken discusses three limiting cases within which it is possible to bracket the electronic structures of known cyclic pentadienes. Case I refers to simple diene conjugation (no cyclic conjugation or hyperconjugation). The molecular orbitals χ_1, χ_2, χ_3, χ_4 are exactly as in butadiene (i.e. energies $-1{\cdot}68\beta$, $-0{\cdot}618\beta$, $0{\cdot}618\beta$, $1{\cdot}618\beta$), and in addition there is an atomic or molecular orbital χ_0 belonging to the fifth atom A. Case II occurs when all the unsaturation electrons are equivalent and is termed homocyclic conjugation. The energies of the associated molecular orbitals have been calculated by Huckel (1937) as $-2{\cdot}000\beta$, $-0{\cdot}618\beta$, $-0{\cdot}618\beta$, $1{\cdot}618\beta$, $1{\cdot}618\beta$. Case III assumes simple conjugation (i.e. case I) modified by localized perturbations between χ_0 and χ_1 (and if A is CH_2 or S, between χ_3 and χ_5). The forms and energies of these orbitals are given in table 1 of Mulliken's article.

The nearest open-chain diene with which we can compare the pentadienes is dimethyl butadiene, since in this molecule the same number of C—C bonds are associated with the conjugated double bonds. The ionization potential of the χ_2 orbital in this case is 8·67 V. Since *cis* and *trans* diene absorption spectra should be nearly alike as regards the frequencies of corresponding systems (though differing considerably in intensity), it should be possible to estimate deviations from case I by observing the shifts of bands of the cyclic pentadiene relative to the corresponding bands of dimethyl butadiene. When the spectrum of cyclopentadiene is compared with that of dimethyl butadiene, it is found that the absorption bands of the former molecule appear to the long wave-length side of corresponding bands of the latter molecule, the frequency shifts diminishing from about 2000 cm.$^{-1}$ for the $N \rightarrow V_1$ bands to about 700 cm.$^{-1}$ for the ionization potentials. Mulliken (1939*b*) explains the appearance of the $N \rightarrow V_1$ bands of cyclopentadiene at relatively long wave-lengths as due to a depression of the excited state ($0{\cdot}618\beta \rightarrow 0{\cdot}618\beta - D'$) by hyperconjugation without much change in the energy of the ground state of the excited orbital. We find that the ground state is elevated, i.e. the ionization potential is reduced, and consider that frequency shift of the $N \rightarrow V_1$ system is not much more than that which is usually associated with such a diminution in the ionization potential. Cyclohexadiene shows a still further shift to the red of the $N \rightarrow V_1$ system ($\lambda_{\text{max.}} \sim 2480$ A). This is interpreted theoretically by Mulliken as being due to an elevation of the ground state and also a depression of the excited state by the same amount D' (which is equal to the theoretical amount by which the upper state is depressed in cyclopentadiene relative to dimethyl butadiene). This fits in with the fact that NV_1 of cyclopentadiene ($\lambda_{\text{max.}}$ 2320 A) lies approximately midway between NV_1 of cyclohexadiene ($\lambda_{\text{max.}}$ 2480 A) and NV_1 of dimethyl butadiene ($\lambda_{\text{max.}}$ 2200 A). On the basis of these values $D = 2580$ cm.$^{-1}$. We do not agree with the larger value of about 4000 cm.$^{-1}$ implicit in the figures that Mulliken gives. The shift of the subsequent bands to shorter wave-length relative to corresponding bands of cyclopentadiene and dimethyl butadiene is consistent with the lowering of the ionization potential to the observed value 8·4 V. On the whole we consider that in both cyclopentadiene and cyclohexadiene the main factor causing the shift of the $N \rightarrow V_1$ absorption to longer wave-lengths is an elevation of the ground state (i.e. a diminution in ionization potential).* However, the $N \rightarrow V_1$ transition in thiophene, on the other hand, does seem to present a clear case of shift to long wave-length resulting from a depression of the excited state (χ_3). This is explained by Mulliken as being mainly due to the interaction of one of the 3*d* sulphur orbitals with χ_3. All the other bands of the thiophene occur at fairly short wave-lengths in accordance with its ionization potential of 9·05 V.

Mulliken in his article classes furan with pyrrole as examples of homocyclic conjugation because of the relatively high intensity of the longest wave-length absorption system which he considers to be a mixture of $N \rightarrow V_1$, V_2, V_3 and V_4, all these transitions occurring at the same wave-length for pure case II. However, it appears to us, judging from the shorter wave-length bands, that pyrrole is much more similar to thiophene than furan. This is in agreement with an alternative explanation of Mulliken's based on Scheibe and Grieneisen's appearance pressure data with which our results agree fairly well. The similarity is particularly apparent for the second longest wave-length region of absorption which appears to have at least some $N \rightarrow V_2$ character. It will be noticed that in both thiophene and pyrrole this absorption is separated considerably from the maximum of the $N \rightarrow V_1$ absorption and appears at the relatively short wave-lengths of 1880–1700 and 1880–1800 A respectively. In furan, however, it follows almost directly on the top of the first absorption region. This tendency of NV_1 and NV_2 absorptions to approach each other is one criterion indicating tendency towards homocyclic conjugation which is complete when the absorptions coincide (see Mulliken 1939*b*). Other criteria, which the spectrum should exhibit, are fairly large shifts towards shorter wave-lengths and a considerable intensification of the NV_1 band as a result of mixing with NV_2. Furan exhibits small shifts towards short wave-lengths and some increase in the relative intensity of the first absorption. Thus we think that even in furan homocyclic conjugation is only partially attained. In both furan and pyrrole Mulliken's conclusions regarding homocyclic conjugation are based on the experimental absorption curves of these substances in hexane solution obtained by Menczel (1927) which yield the very high 'f' values of 0·5 and 0·4 for the bands in the neighbourhood of 2000 A. We think it better to use relative intensities and to consider the appearance of the spectrum over a larger frequency range in drawing these conclusions. When this is done, Mulliken's alternative suggestion which makes pyrrole conform to case III is the only plausible one. That there should be a closer relationship between pyrrole and thiophene than with furan is to be expected from the fact that they both have resonance energies of 31 kcal./mol. as compared with only 23 kcal./mol. for furan. Another point of similarity between them is that the electron pair conjugated with the diene part of the molecule has closely the same ionization potential for these two molecules. This is about 2 V less than the ionization potential of the corresponding electrons in furan, as may be judged from the ionization potentials of H_2S (10·45 V—Price 1936), NH_3 (10·5 ± 0·1 V—Mann, Hustrulid and Tate 1940), H_2O (12·56 V—Price 1936), where the ionization potentials refer to the same electrons as are involved in the cyclic conjugation with the double bonds. A further argument against homocyclic conjugation in pyrrole is the chemical one that pyrrole is a fairly strong base. It could hardly exhibit strong basic properties if the electron pair responsible for these properties were so completely involved with the double-bond electrons.

---

* In a more recent paper (Mulliken, Rieke and Brown 1941) Mulliken has revised his estimates of the contribution of hyperconjugation effects to the energies of excited states and now considers them to be very much less than was originally thought.

If, as Mulliken calculates, the energies of the *cis* and *trans* conjugated dienes are the same, it is difficult to account for the fact that open-chain dienes (and trienes) are practically completely *trans* in their normal state. It seems to us reasonable that the *cis* dienes are relatively unstable because of a mutual repulsion of the electrons in the conjugated double bonds which are closer together in the *cis* than in the *trans* position. This would lead to a lowering of the ionization potentials of the double-bond electrons and might give some explanation of the lower ionization potential of cyclohexadiene and cyclopentadiene relative to corresponding open-chain dienes. Further, resonance to Dewar type structures such as

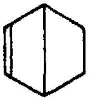

and

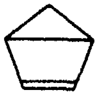

which are quite probable, for the cyclic dienes may also account for the differences of ionization potential between the two classes of compounds. These structures contribute about 20 % of the resonance in benzene and most probably an equal proportion in the cyclic dienes. The lower value of cyclohexadiene relative to cyclopentadiene is probably to be explained as due to additional charge transfer from two CH_2 groups as compared with only one in cyclopentadiene. The higher values for thiophene, pyrrole and furan probably arise from the higher electron affinity of the attached groups in these molecules. This has the effect of withdrawing negative charge from the double bonds and so increasing the ionization potential of the associated electrons.

Mulliken's theory of hyperconjugation was invoked largely to explain the appearance of NV_1 absorption at longer wave-lengths in cyclohexadiene and cyclopentadiene than in the open-chain dienes. This it does by a depression of the excited state without affecting the ground state. It leaves unchanged also the predicted positions of NV_2 bands and bands of a Rydberg type. The observed spectra are not in accord with these predictions, it being found that whenever NV_1 transitions occur at longer wave-lengths all the short wave-length transitions up to and including the ionization potential also suffer comparable depressions. It is therefore concluded that the main cause of the relative displacement of the NV_1 transitions of the closed-chain relative to the open-chain dienes is a change in the energy of the electrons in the ground state corresponding to the observed diminution in ionization potential, a possible explanation of this being that there is greater repulsion between the double bonds in the (near) *cis* than in the far (*trans*) position and greater resonance to Dewar type structures. It should be pointed out that transitions of a pronounced NV character are only obtained for the longest wave-length bands of both open-chain and cyclic dienes. It appears probable that the shorter wave-length systems lose their NV character very quickly because of the greater dimensions of the excited orbit. When the orbit becomes much larger than the molecular structure, it is not then so much modified by this structure.

In conclusion, we should like to thank the Department of Scientific and Industrial Research and Imperial Chemical Industries for financial aid in connexion with this work, and Drs E. H. Farmer and A. Wassermann for advice on the preparation of some of the substances.

References

Bonino and Manzoni-Ansidei 1934 *Z. phys. Chem.* **25B**, 348–362.
Carr and Stucklen 1938 *J. Chem. Phys.* **6**, 55–61.
Henri and Pickett 1939 *J. Chem. Phys.* **7**, 439–440.
Huckel 1937 *Z. Elektrochem.* **43**, 779–845.
Mann, Hustrulid and Tate 1940 *Phys. Rev.* **58**, 340–347.
Menczel 1927 *Z. phys. Chem.* **125**, 161–210.
Mulliken 1939*a* *J. Chem. Phys.* **7**, 121–135.
Mulliken 1939*b* *J. Chem. Phys.* **7**, 339–351.
Mulliken, Rieke and Brown 1941 *J. Amer. Chem. Soc.* **63**, 41–56.
Murray 1935 *J. Chem. Phys.* **3**, 59–60.
Pickett 1940 *J. Chem. Phys.* **8**, 293–297.
Pickett, Paddock and Sackter 1941 *J. Amer. Chem. Soc.* **63**, 1073–1077.
Price and Tutte 1940 *Proc. Roy. Soc.* A, **174**, 207–220.
Price and Walsh 1940 *Proc. Roy. Soc.* A, **174**, 220–234.
Scheibe and Grieneisen 1934 *Z. phys. Chem.* **25B**, 52–56.
Truchet and Chapron 1934 *C.R. Acad. Sci., Paris*, **198**, 1934–1940.

On the heat of sublimation of carbon and on some absorption bands of three mesomeric hydrocarbons

By G. J. Kynch and W. G. Penney

Imperial College of Science and Technology, London

(*Communicated by S. Chapman, F.R.S.—Received* 23 *May* 1941)

Spectroscopic analysis of the CO spectrum, together with thermochemical measurements on the burning of carbon in oxygen, lead to the conclusion that L, the heat of sublimation of carbon, is either 124 or 170 kcal./mol. An estimate of L may be made by calculating the energies of excited states of benzene, butadiene and hexatriene, assuming various values of L, and choosing the one that gives the best agreement with experiment. The theory employed bears a close resemblance to that developed by Eyring for estimating activation energies. Almost exact agreement with experiment is obtained in all three cases by assuming $L = 170$, and no agreement is obtained by assuming $L = 124$. More elaborate calculations are most unlikely to upset this result. The conclusion is therefore that $L = 170$ kcal./mol.

The equilibrium internuclear distances in the excited states are found, and the potential function controlling some of the vibrations about these positions is determined. It is shown that the excited state of benzene has the regular hexagon configuration, the carbon-carbon internuclear distance being 1·45 A, compared with 1·39 in the ground state. The carbon breathing frequency in the excited state is calculated to be 920 cm.$^{-1}$, compared with the experimental value 940 cm.$^{-1}$.

1. INTRODUCTION

The heat of sublimation of carbon is one of the least accurately known quantities in thermochemistry. There are two experimental methods by which it might be measured. One uses the equations

$$\begin{aligned} \mathrm{C(solid)} + \tfrac{1}{2}\mathrm{O_2}(^3\Sigma) &= \mathrm{CO}(X\,^1\Sigma) + 27{\cdot}40\,\mathrm{kcal.}, \\ \mathrm{CO}(X\,^1\Sigma) &= \mathrm{C}(^3P) + \mathrm{O}(^3P) - D_0\,\mathrm{kcal.}, \\ \mathrm{O}(^3P) &= \tfrac{1}{2}\mathrm{O_2}(^3\Sigma) + 58{\cdot}6\,\mathrm{kcal.} \end{aligned}$$

From these it follows that the heat of sublimation of carbon (graphite) is $D_0 - 86$ kcal./mol.

Herzberg reviews the situation in his book (1939) and concludes that the most likely value of D_0 is 9·14 eV, although a much less probable value is 6·92 eV. Another possibility which he does not mention is $D_0 = 11{\cdot}054$ eV, obtained from a predissociation limit. The difficulty is that of fixing the atomic states into which one of the excited levels of the molecule dissociates, and there appears to be no way of doing this spectroscopically. If $D_0 = 9{\cdot}14$ eV, the heat of sublimation $L = 124{\cdot}8$ kcal./mol. and if $D_0 = 11{\cdot}054$ eV, then $L = 168{\cdot}8$ kcal./mol.

The second method of measuring the heat of sublimation is to find the rate of vaporization of carbon as a function of temperature. Then the slope of the log (rate) curve plotted against $1/kT$ gives the heat of sublimation. The experimental difficulties are great, but Marshall and Norton (1933) have succeeded in obtaining a value 176 kcal./mol. Thus the value of L about 170 kcal./mol. does appear to be consistent with both sets of measurements.

Herzberg, Herzfeld and Teller (1937) have, however, created a Gibertian situation by advancing an ingenious argument which states that the rate of evaporization experiment gives an apparent value of L that is $1\frac{1}{2}$ times the true value. Thus, if $L = 125$, the heat of vaporization experiment will appear to give the heat of sublimation about 180 kcal./mol. Therefore, they conclude, the value is actually 125 kcal./mol. Whatever the merits of the argument of Herzberg, Herzfeld and Teller, it has at least eliminated measurements of the rate of vaporization of carbon as an uncontroversial method for determining the heat of vaporization.

In the present paper we explain a new way by which the heat of sublimation of carbon may be estimated, and in three separate applications we find a consistent result 170 ± 10 kcal./mol.

A brief statement of some of our results has already been given (Kynch, Lloyd and Penney 1940), but the details have been deferred because the value of L which we obtained contradicted that found by Herzberg, and his arguments seemed conclusive. Recently, at least two new points have been made by other authors and we have decided, therefore, to give our results in full.

White (1940) states that $D_0 = 11\cdot054$ eV for CO, since this is the only value which can be reconciled with his estimate of the energy of dissociation of CN, taken in conjunction with thermochemical equations similar to those given above and described by Herzberg (1939).

Baughan has pointed out (1941) that the energy of the C-C link in ethane calculated from the reaction $2CH_4 \rightarrow C_2H_6 + H_2$, is 88·2 kcal./mol. This differs by 30 kcal./mol. from the value 58·3 kcal./mol., given by Pauling (1939), assuming $L = 124$ kcal./mol. However, if $L = 170$, then consistent values of the bond energies are obtained. In our opinion this is a strong argument in favour of $L = 170$ kcal./mol.

As a point of interest, it may be stated that a Birge-Sponer extrapolation of the lowest 25 vibration levels in the normal states of CO leads to a dissociation energy into normal atoms of 11·34 eV. Details will be found in the *Report on band spectra*, by Jevons (1932).

Bond energies

Many attempts have been made to construct tables of bond energies. Most of the recent books on molecular structure and thermochemistry give them prominence, and use them frequently. The use of any of these sets of bond energies to estimate the heat of reaction from one set of molecules involving carbon to another set is accurate provided that none of the molecules is mesomeric, because the heat of sublimation of carbon cancels out. If some of the molecules are mesomeric, there is an uncertainty in the estimated heat of the reaction, usually of the order of a few kcal. This is not great enough to permit the experimental value of the heat of the reaction to be used to fix the heat of sublimation of carbon, unless an improved form of the present theories is developed. We have actually tried to do this, and our results will be given later in this paper.

Absorption spectra of mesomeric molecules

Bury (1935) was apparently the first to suggest in any published work that mesomeric molecules should show absorption spectra corresponding with an electronic transition from one mesomeric state to another. Following up this idea, Sklar (1937) made calculations which gave the wave-lengths of these transitions for benzene, fulvene and azulene. His methods are considerably extended in accuracy and application in the present paper.

To illustrate Sklar's arguments, we give briefly the details for benzene. As is well known from the work of Pauling and Wheland (1933), the six *pπ* orbitals of benzene from a resonating system. There are five singlet states; the exchange energy of the most stable state is 2·606J, where J is an exchange integral between neighbours. The next most stable state has an exchange energy OJ. Since all the other terms in the expressions for the energies of the two states are the same, the absorption frequency should be simply 2·606J. There are at least two methods of finding the numerical value of J. Pauling (1933) determines J from a study of the heats of formation of a number of mesomeric molecules and obtains J = 1·55 eV. The corresponding wave-length of the absorption band is approximately 3080 A. The value of J, however, depends considerably upon the value chosen for L, the heat of sublimation of carbon. The value J = 1·55 eV is based on L = 176 kcal./mol. Recently, Pauling has accepted Herzberg's value L = 124 kcal./mol., and the value of J should be modified to 1·0 eV. The absorption band is therefore calculated to appear at 4770 A. Experimentally, the long wave limit of the absorption band is 2700 A, and the maximum absorption is at 2500 A.

Sklar determines J from the observed heats of hydrogenation of various products of benzene, and obtains J = 1·92 eV. The corresponding wavelength of the absorption band is 2450 A. As we show later, the way in which Sklar estimates J may be criticized, although his result happens to be a very good approximation.

These two ways of finding J assume that all bond lengths are the same, whether in the ground state or the excited state, although the excited state may be highly unstable in such a configuration. Further, the energy of the excited state, other than the resonance energy of the *pπ*-electrons, is considerably different from that in the ground state, unless the bond lengths are the same. In some cases the deviations of the individual lengths from the mean is quite small, and the assumption of equality is good. In other cases the approximation is poor. The X-ray measurements of Robertson and Woodward (1938) have shown that all the bonds are not of the same length in the ground state of many mesomeric molecules, e.g. stilbene and tolane, and this fact has been confirmed by the theoretical calculations of Lennard-Jones (1936), Penney (1936), Coulson (1938) and others. There is no experimental evidence on the bond length of the excited molecules, but the improved theoretical method to be described enables these to be calculated and shows that large deviations from the mean length are to be expected.

The experimental data which we use are the energy of the double bond, the normal benzene bond, and the force constants for these bonds. The theory then gives the equilibrium configurations and the energies of the molecules and hence the frequencies of the absorption bands and the heats of hydrogenation. A comparison of these values with experimental results enables the heat of sublimation of carbon to be determined.

2. BOND ENERGIES AND HEATS OF FORMATION

The first part of this discussion closely follows modifications of the pair theory described by Penney and Lloyd (1939).

The $2s$-orbital and two of the $2p$-orbitals of a carbon atom in the valency sp^3 state can hybridize to form three coplanar orbitals directed at angles 120° to each other. Electrons in these orbitals form bonds with unpaired electrons of neighbouring atoms, according to the usual pair theory. We shall refer to these bonds as the trigonal bonds. The carbon atoms in ethylene and benzene are linked to three other atoms in this way. The remaining $2p\pi$-electron either enters into a localized bond with a similar electron on a neighbouring carbon atom, as in ethylene, or else forms part of a resonating system with other similar $2p\pi$-electrons, as in benzene. The exchange energy of the $2p\pi$-electrons can be calculated in terms of an exchange integral $J(r)$ between neighbouring $2p\pi$-electrons. In ethylene, the exchange energy is J; and in benzene it is $2{\cdot}606J$, or $0{\cdot}434J$ per bond. Denote by $S(r)$ the energy per bond, other than that of the exchange energy of the $2p\pi$-electrons. Thus, in $S(r)$, proper account may be taken of non-orthogonality, non-perfect pairing, and interactions between the $2s(2p\sigma)^2$ and the $(2s)^2\,2p\sigma$ configurations of the C atoms.

We do not attempt to determine S and J by quadrature, but follow a well-established practice of fitting them empirically. Thus, with high approximation, the energy of the double bond, as in ethylene, is

$$W_d(r) = S(r) + J(r),$$

and of the mesomeric bond of benzene is

$$W_b(r) = S(r) + 0{\cdot}434J(r).$$

Solving these equations for S and J, it is found that

$$\left.\begin{aligned} J(r) &= 1{\cdot}767(W_d - W_b), \\ S(r) &= W_d - J. \end{aligned}\right\} \qquad (1)$$

Expressions for $W_b(r)$ and $W_d(r)$ may be obtained from experimental data. It is possible to use either the simple form

$$W = W_0 - \tfrac{1}{2}k(r-r_0)^2,$$

or the Morse function

$$W = W_0[2e^{-m(r-r_0)} - e^{-2m(r-r_0)}],$$

where r_0 is the equilibrium length of the bond, W_0 the corresponding energy of formation, k is the force constant and m is a parameter defined by the relation

$$k = 2W_0m^2.$$

The force constant for the double bond is 10×10^5 dynes/cm. and $r_0 = 1{\cdot}33$ A. For the normal benzene bond the force constant is $7{\cdot}5 \times 10^5$ dynes/cm. and $r_0 = 1{\cdot}39$ A.

The values of W_0, and hence of m, for these two bonds depend on the value assumed for the heat of sublimation of carbon. If the bond energies are chosen with respect to one value of the heat of sublimation, and then another value is taken, say Δ kcal./mol. less than before, the double-bond energy must be decreased by Δ, the benzene bond decreased by $3\Delta/4$, the single bond decreased by $\Delta/2$, and the C-H bond energy decreased by $\Delta/4$.

Assuming that the heat of sublimation of carbon is 170 kcal./mol., then $W_d = 151$ for the double bond and $W_b = 124$ for the benzene bond, both in kcal./mol. If, on the other hand, the heat of sublimation is 130 kcal./mol., these figures must be taken as 111 and 94 respectively. Calculations of the energies of butadiene and hexatriene are made for both values, and also for the value $(170+\Delta)$, where Δ is to be determined from the observed absorption spectra.

The energies E of the $p\pi$-electrons in the ground state and in the excited state are the lowest two roots of a determinantal equation. The total energy of the ground state in terms of the n bond lengths r_i of the resonance problem may be expressed

$$W_g(r_1, r_2, \ldots, r_n) = \Sigma(\text{C—C}) + \Sigma(\text{C—H}) + \Sigma S_i + E_g. \tag{2}$$

The summation S_i is over all trigonal carbon-carbon bonds that enters into the resonance problem, and the summation Σ(C—C) is over all the remaining carbon-carbon bonds. We assume that the C—H bonds are unaffected by changes in the (C—C) distances. The length of each (C—H) bond is $1{\cdot}08$ A and its energy is 99 kcal. if the value of L is 170 kcal./mol., and is 89 kcal. if $L = 130$ kcal./mol.

The equilibrium lengths of the bonds are given by the equations

$$\frac{\partial W_g}{\partial r_j} = 0 \quad (j = 1, 2, \ldots, n). \tag{3}$$

A similar expression is obtained for W_e, the energy of the first excited state.

Analytical forms of $W_g(r)$ and $W_e(r)$ are not easy to obtain in practice, and it is necessary to calculate the E for various values of the set j and minimize the W numerically. The minimum values of these total energies we denote by W_g and W_e without the brackets.

Transitions can take place between the two states with absorption of light of suitable energy. The minimum absorption energy is $W_g - W_e$; this transition in general requires a considerable change in the lengths of some of the bonds. This is not, therefore, the most probable transition. According to the Franck-Condon principle, maximum absorption takes place without a change in the lengths. Since the excited molecule is then distorted from the equilibrium position, the frequency of this transition is appreciably higher than the transition from W_g to W_e, in agreement with experiment.

The expression for the total energy (2) also determines the vibration frequencies. The variation of $W(r)$ for changes in the lengths of the bonds without angular variation is obtained by writing $r_j = R_j + x_j$, where R_j is the equilibrium length of the bond j, and expanding $S(r_j)$, E and then $W(r_j)$ as power series in the x_j. Because the molecule is in equilibrium when $x_j = 0$ $(j = 1, 2, \ldots, n)$, the constant term is the energy of formation, terms of the first order in the x_j's are missing, and the second-order terms determine the most important parts of the potential function, neglecting anharmonicity.

We do not at present know the dependence of W upon angular variations, and to this extent the calculated potential function is limited. Empirical terms in the bond angles may be added to explain the observed frequencies.

One interesting feature of the potential functions we obtain is that cross-terms between displacements of bonds far removed from one another are as important as those connecting neighbours.

3. BUTADIENE

The carbon chain in the butadiene molecule C_4H_6 consists of four atoms. The outer links A are equivalent but they are different from the central link B. We must therefore distinguish between the exchange integrals J_a

and J_b for these links. The resonance problem of four electrons and the two values of the energy are well known, and the energy of the molecule is

$$W = 6(\mathrm{C—H}) + 2S_a + S_b \pm [4J_a^2 + J_b^2 - 2J_aJ_b]^{\frac{1}{2}}. \tag{4}$$

The positive sign is to be used for the ground state and the negative sign for the excited state.

Calculations were made first using the two values 170 and 130 kcal./mol. for the heat of sublimation of carbon. The two sets of values of the parameters in the equilibrium position of the molecule are given in table 1, with values for $L = 130$ kcal./mol. in brackets.

TABLE 1. BUTADIENE

	r_a	r_b	J_a	J_b	W
normal	1·331	1·469	51·4	34·4	990·25
	(1·337)	(1·471)	(33·1)	(17·3)	(830·80)
excited	1·553	1·460	26·3	35·4	858·58
	(1·523)	(1·480)	(12·8)	(16·5)	(757·60)

(Lengths are in Angstroms—energies in kcal./mol.)

In the ground state, the outer bonds approximate very closely to double bonds, while the central link is somewhat shorter than a single bond. When the molecule is in the excited state, the central link is slightly shorter, but the outer links are 0·222 A longer than in the ground state. A considerable change of structure takes place in a transition from one level to the other.

If $L = 130$ kcal./mol., the energy $W_g - W_e = 75{\cdot}20$ kcal./mol. or 3·26 eV, corresponding to a wave-length of 3790 A at the edge of the absorption band. If $L = 170$ kcal./mol., the energy of this transition is 131·67 kcal./mol. or 5·71 eV, and the wave-length is 2160 A. The experimental value is 2190 A. Exact agreement between experiment and theory may be obtained by writing $L = 170 + \Delta$, and choosing a suitable value of Δ. We find that

$$W_g = 990{\cdot}25 + 2{\cdot}464\Delta \quad \text{and} \quad W_e = 858{\cdot}58 + 1{\cdot}196\Delta.$$

Thus $W_g - W_e = 131{\cdot}67 + 1{\cdot}27\Delta$, or $(2160 - 20{\cdot}8\Delta)$ A. The best value of Δ is $-1{\cdot}5$ kcal.

Assuming $L = 170$, 50·0 kcal./mol. is required to compress the links A to 1·34 A and extend the link B to 1·47 A in the excited state. Maximum absorption therefore occurs at an energy of 181·7 kcal./mol. or 1580 A.

To obtain the potential functions for symmetrical vibrations about the equilibrium positions we write $r_a = R_a + x_a$, $r_b = R_b + x_b$, and expand the Morse functions of J_a and J_b in ascending powers of x_a and x_b:

$$\left.\begin{aligned} J_a &= 51{\cdot}50 - 136{\cdot}85x_a + 95{\cdot}67x_a^2, \\ J_b &= 34{\cdot}25 - 107{\cdot}37x_b + 117{\cdot}22x_b^2. \end{aligned}\right\} \tag{5}$$

In this way we find that

$$W_g = 990{\cdot}25 - 1401x_a^2 - 104x_a x_b - 330x_b^2. \tag{6}$$

A central force field without cross-terms is nearly correct.

The potential energy of the excited state is

$$W_e = 858{\cdot}58 - 677x_a^2 + 269x_a x_b - 538x_b^2. \tag{7}$$

In these two equations x_a and x_b are measured in Angstroms.

The cross-term in $x_a x_b$ is not small, and hence x_a and x_b are not good approximations to the normal co-ordinates in the excited state.

The force constants for vibrations in the ground state, derived from the above equation, are 4·56 and 19·57 × 10^5 dynes/cm., for the stretching of the B link and the *two* A links respectively. They are close to the single- and double-bond values. The constants for the normal co-ordinates of the excited state are 6·4 and 11·2 × 10^5 dynes/cm. The accuracy of these expressions is not high.

4. HEXATRIENE

The exchange energy of the $p\pi$-electrons of hexatriene is derived from a fourth-order equation. There are five canonical structures, which are shown in figure 1, two of them, III and IV, equivalent owing to the symmetry of the molecule. The two links A and the two links B are equivalent. Three exchange integrals J_a, J_b and J_c remain independent. The equation is

$$f(E) \equiv E^4 + AE^3 + BE^2 + CE + D = 0, \tag{8}$$

where

$$\begin{aligned} A &= 2(J_a + J_b), \\ B &= -2J_c(J_a - J_b + J_c) - 4(J_a^2 - J_a J_b + J_b^2), \\ C &= 2J_c(2J_b^2 - 4J_a^2 - 2J_b J_c - J_a J_c) - 8(J_a^3 + J_b^3), \\ D &= J_c^2(J_c^2 - 2J_b J_c + 2J_a J_c) - 8J_a J_c(J_a^2 - J_b^2) - 4(J_a^2 + J_a J_b - J_b^2)^2. \end{aligned}$$

From this equation we obtain numerically the two lowest roots, for any assigned values of J_a, J_b and J_c. The total energy is

$$W = 8(\mathrm{C{-}H}) + 2S_a + 2S_b + S_c + E. \tag{9}$$

Clearly, W must be minimized by a numerical method.

The equilibrium values of r and J when W is a minimum are given in table 2 for $L = 170$ (and in brackets for $L = 130$).

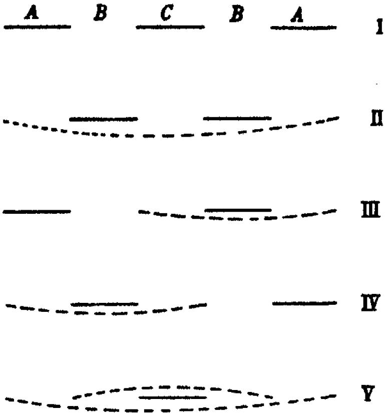

FIGURE 1.

TABLE 2. HEXATRIENE

	r_a	r_b	r_c	J_a	J_b	J_c	W
normal	1·34	1·47	1·34	50·0	34·5	50	1433·3
	(1·34)	(1·47)	(1·34)	(33)	(17)	(33)	(1199)
excited	1·51	1·41	1·43	30·8	41·7	39	1324
	(1·50)	(1·41)	(1·42)	(15·0)	(24·0)	(23·0)	(1133)

If $L = 170 + \Delta$, we find from equation (9) that $W_g = 1433{\cdot}3 + 3{\cdot}89\Delta$, and $W_e = 1324{\cdot}0 + 3{\cdot}043\Delta$.

The energies of the absorption band of hexatriene for these three values of L are 109·3, 65·1, $109{\cdot}3 + 0{\cdot}85\Delta$ kcal./mol. or 2590, 4380 $(2590 - 20\Delta)$ A respectively. Comparing these with the observed value of 2530 we see that the best choice of Δ is 3 kcal., or $L = 173$ kcal./mol.

The longest link of the ground state is almost unchanged in a transition to the excited state, as in butadiene. The outer links increase in length, but the greatest change is in the central link. We should expect, therefore, that it would be easier to extend the central link of normal hexatriene than to extend the outer links, although in the equilibrium position the three links have the same length. It is possible to show this by calculating the potential function. We expand the exchange integrals in powers of x_i, and then the coefficients A, B, C, D according to equations (8). The roots of (8) are assumed to be

$$E = E_g + \Sigma\alpha_i x_i + \Sigma\beta_{ij} x_i x_j + \dots (\beta_{ij} = \beta_{ji}) \quad (i, j = a, b, c), \tag{10}$$

where α_i and β_{ij} are to be evaluated. Then

$$f(E) = f(E_g) + \Sigma\alpha_i x_i \left(\frac{\partial f}{\partial E}\right)_g + \Sigma\beta_{ij} x_i x_j \left(\frac{\partial f}{\partial E}\right)_g + \tfrac{1}{2}\Sigma\alpha_i\alpha_j x_i x_j \left(\frac{\partial^2 f}{\partial E^2}\right)_g + \dots, \tag{11}$$

where $E = E_g$ in the differential coefficients. Since the coefficients of equation (8) are functions of x_i, $f(E)$ can be written

$$f(E) = f_0(E) + \Sigma f_i(E)\, x_i + \Sigma f_{ij}(E)\, x_i x_j + \dots. \tag{12}$$

Hence

$$\left(\frac{\partial f}{\partial E}\right) = f'(E) = f_0'(E) + \Sigma f_i'(E)\, x_i + \Sigma f_{ij}'(E)\, x_i x_j + \dots. \tag{13}$$

Writing $E = E_g$ in equations (12) and (13), substituting in (11), and equating to zero all terms of the first and second order in x_i, we find that $f(E) = 0$ provided

$$f_0(E_g) = 0, \tag{14}$$

$$\alpha_i = -\frac{f_i(E_g)}{f_0'(E_g)}, \tag{15}$$

$$\beta_{ij} = \beta_{ji} = \frac{1}{2\{f_0'\}^2}\{-2f_{ij}f_0' - f_i f_j + f_i f_j' + f_i' f_j\}. \tag{16}$$

Evaluation of the constants α_i and β_{ij} for the ground state shows that

$$W = 1433{\cdot}3 - 664x_a^2 - 611x_b^2 - 308x_c^2 - 308x_a x_b - 194x_b x_c + 349x_c x_a. \tag{17}$$

The most interesting term is the cross-term in $x_a x_c$, representing a coupling of two non-adjacent links of such a type that one link tends to increase with the other. The full potential for all displacements probably contains other cross-terms which are not explicit in our expression for symmetrical displacements. For example, if x_a and x_a' are the changes in the two links A the full potential may contain terms

$$\alpha(x_a^2 + x_a'^2) + 2\beta x_a x_a' = \tfrac{1}{2}(\alpha+\beta)(x_a + x_a')^2 + \tfrac{1}{2}(\alpha-\beta)(x_a - x_a')^2.$$

For a symmetrical displacement $x_a' = x_a$, so that the coefficient of x_a^2 in equation (17) corresponds to $2(\alpha+\beta)$. Since these bonds are the length of double bonds we should expect a force constant of approximately

10^6 dynes/cm. or $\alpha = -700$. Hence $\beta = +380$, a rather large value, although of the same order as the term $x_c x_a$ in (17).

A fifth-order equation, not assuming that the canonical structures III and IV of figure 1 are equivalent, would give the full potential function.

5. BENZENE

The hypothesis of a regular symmetrical shape of benzene in the ground state is supported by a large body of experimental evidence (Ingold and others 1936), and it is confirmed theoretically by calculations such as those of Lennard-Jones using the molecular orbital theory. The heat of formation of the molecule from the constituent atoms is $6(\text{C—H}) + 6W_b = 1338$ kcal./mol. ($L = 170$). It is of considerable interest to know if benzene retains the symmetrical form in its first excited singlet state and, this being so, if it is relatively stable in this form. If the links are equivalent, Pauling (1933) has shown that the exchange energy of this state is OJ and the total energy is $W(r) = 6(\text{C—H}) + 6S(r)$, where r is the length of the equivalent links. This has a minimum when $r = 1{\cdot}445$ A and $W = 1233$ kcal.

To simplify the stability problem we consider only a configuration in which alternate links remain equal in length. Let the length of the links be either r_a or r_b. Certain of the canonical structures are equivalent and the determinantal equation reduces to a cubic

$$E^3 + E^2(J_a + J_b) - 3E(3J_a^2 + 3J_b^2 - 2J_aJ_b) - 9(J_a^2 - J_b^2)(J_a - J_b) = 0. \quad (18)$$

We neglect in this case, as elsewhere, the ionized states.

Using the same technique as for hexatriene, the required root of (18) is obtained in ascending powers of x_a and x_b:

$$\left.\begin{aligned} E &= -693(x_a - x_b)^2, \\ W_e &= 1233 - 1338(x_a - x_b)^2 - 645(x_a + x_b)^2. \end{aligned}\right\} \quad (19)$$

The absence of terms in x_a and x_b shows that the ring is stable in the regular form. In addition, the regular structure is more stable in the excited state for those distortions which retain the hexagonal form, i.e. $x_a = x_b$, than for other types of distortion. The breathing frequency $A_g(2)$, in the notation of Ingold (1936) can be calculated from the above expression for the excited state. It is 918 cm.$^{-1}$. This agrees moderately well with the experimental measurement of 940 cm.$^{-1}$.

The absorption bands of benzene in the ultra-violet region have been observed by a number of experimenters. The superposition of a number of subsidiary maxima upon the main absorption band makes it impossible to fix definitely a wave-length of maximum absorption. Certainly absorption is greatest in the region $\lambda = 2500$ A and diminishes to zero at $\lambda = 2700$ A. The calculated wave-lengths are given in table 3. The results for $L = 170$ give good agreement with the observed wave-lengths, and only a value of L of about this magnitude is compatible with these experimental results.

TABLE 3. BENZENE

Normal state		Excited state	
r	W_g	r	W_e
1·39	1338	1·44	1232·5
(1·39)	(1098)	(1·44)	(1037·4)

$W_g - W_e = 105{\cdot}5\ (60{\cdot}6)$ kcal./mol.

Absorption edge $\lambda = 2690$ (4700) A; max. absorption $\lambda = 2510$ (4220) A.

(Values for $L = 130$ are in brackets.)

6. HYDROGENATION OF BENZENE

We shall now discuss the hydrogenation of benzene to cyclohexadiene, cyclohexene and cyclohexane. Experimentally, it is found that

$$\left.\begin{aligned} C_6H_6 + 3H_2 &= C_6H_{12} + 49{\cdot}8 \text{ kcal.,} \\ C_6H_8 + 2H_2 &= C_6H_{12} + 55{\cdot}4 \text{ kcal.} \end{aligned}\right\} \quad (20)$$

Details will be found in the article by Kistiakowsky (1936).

A third equation may be deduced from those above, namely,

$$C_6H_6 + H_2 = C_6H_8 - 5{\cdot}6 \text{ kcal.} \quad (21)$$

Sklar's argument (1937) for finding J is as follows. Let B kcal./mol. be the hypothetical energy of hydrogenation of a double bond in one Kekule structure of benzene. Then the energy of hydrogenation of benzene to cyclohexane is smaller than $3B$ by the resonance energy of benzene. Using the thermochemical data, we have

$$3B - 1{\cdot}1J = 49{\cdot}8.$$

Similarly, the energy of hydrogenation of benzene to cyclohexadiene is given by

$$B - (1{\cdot}1 - 0{\cdot}232)\,J = -5{\cdot}6.$$

Solving these two equations for B and J leads to

$$B = 32{\cdot}8 \text{ kcal./mol.,} \quad J = 44{\cdot}1 \text{ kcal./mol.}$$

These values are independent of the heat of sublimation of carbon, since they depend only on thermochemical data.

No account is taken in this argument of variations in the carbon-carbon lengths. As it happens, when corrections are made for these variations, large terms practically balance each other out, and Sklar's approximation is a good one.

Consider cyclohexadiene as an example. The structural diagram shows a single bond between the two double bonds. The resonance problem is therefore that of butadiene. The 'double' bonds are of length 1·33 A, and the bond between them is of length 1·47 A. The distance between the two carbon atoms furthest apart in *cis*-butadiene is therefore about 2·80 A. The remaining four sides of the ring in cyclohexadiene are all of the same length, namely about 1·54 A. It will be seen that the six carbon atoms cannot be coplanar. Most probably, not even four of the carbon atoms are coplanar. The molecule is strained, but the loss of energy due to strain is small.

The following are the equations for the heats of formation from normal atoms of the hydrogenation products of benzene, obtained by assuming that the loss of stability due to strain is negligible.

$$\left.\begin{aligned} W(\mathrm{C_6H_8}) &= Bu + 2\mathrm{C{-}H} + 3W_s, \\ W(\mathrm{C_6H_{10}}) &= 5W_s + W_d + 10\mathrm{C{-}H}, \\ W(\mathrm{C_6H_{12}}) &= 6W_s + 12\mathrm{C{-}H}, \end{aligned}\right\} \qquad (22)$$

where Bu stands for the heat of formation of butadiene, and W_s is the energy of a single C-C bond not participating in the resonance.

From these, and the equations

$$\left.\begin{aligned} \mathrm{C_6H_6} + 3\mathrm{H_2} &= \mathrm{C_6H_{12}} + K_1, \\ \mathrm{C_6H_8} + 2\mathrm{H_2} &= \mathrm{C_6H_{12}} + K_2, \end{aligned}\right\} \qquad (23)$$

it is possible to calculate K_1 and K_2.

The values calculated from K_1 and K_2 depend on the heat of sublimation of carbon, but only to a limited extent. If the resonance were negligible, then the result for K_1 and K_2 would be independent of L. One of the molecules, namely benzene, has considerable resonance, and the above equations could be used to fix the value of L, provided all of the quantities on the right-hand sides of (22) were known accurately. Unfortunately, the theory is unable to estimate W_s to within about 3 kcal./mol. All that one can do, therefore, is to determine W_s from the observed value of K_1. Then K_2 may be determined.

If $L = 170$ kcal./mol., then K_2 is calculated to be 48; and if $L = 130$ kcal./

mol., then K_2 is calculated to be 46. The experimental value is 55·4. Clearly, nothing about the magnitude of L can be deduced from these results. The loss of stability due to strain in cyclohexadiene, however, is seen to be about 7 kcal./mol.

7. The heat of vaporization of carbon

As mentioned in the introduction, two sets of measurements of the heat of sublimation are to be found in the literature, giving different values of 124 and 176 kcal./mol. Herzberg, Herzfeld and Teller (1937) made an ingenious proposal to reconcile these two values, supposing that they are both accurate. To explain this, we have drawn a diagram of the corner of a sheet of atoms, as in graphite. There are two possible types of edge. On one type, atoms A and B are each held in position by two bonds. The atom A is removed only by breaking its two bonds, and its removal then leaves B held to the rest of the sheet by only one bond. Therefore twice as much energy is required to remove A as to remove B. On the other type of edge, the same ratio holds for the energies of evaporation of atoms F and G, once the process is started by the removal of the key atom E.

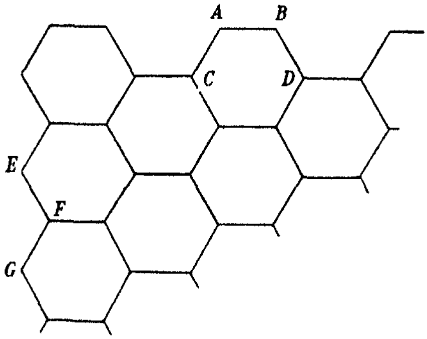

Figure 2.

Now a determination of the rate of any composite process merely measures the rate of the slowest component process. Hence the activation energy of the rate of evaporation of carbon is simply the energy of removing atoms of type A. Marshall and Norton obtain 176 kcal./mol. According to the present argument, only 88 kcal./mol. are required to remove atoms of type B, and the heat of sublimation is the average, 132 kcal./mol.

This argument is attractive, but assumes a very simple theory of chemical bonds. We cannot agree that the figures given are even reasonably correct.

First let us consider the states of the carbon atoms at the edges of a sheet. It simplifies the problem to assume that A and B are in the divalent state (s^2p^2) and C and D are almost entirely in the tetravalent state (sp^3). These states differ in energy by about 160 kcal./mol. As A is removed, C remains bound only to two atoms, and presumably reverts to the divalent state with emission of energy. At the same time the bonds of B are rearranged to strengthen the link BD, also with emission of energy. Both alterations make easier the removal of A, and suggest that the energy of the process is rather less than the sum of the energies of the bonds AC and AB. Moreover, the atom B is now more firmly bound to D by a double bond. More than the original energy of the bond BD is required to remove it, even though the atom D also would take up the divalent state.

This short discussion is sufficient to show that there is no simple relation of the type proposed between the energies of the removal of A and B. Of course, these atoms are not in the divalent state, but in a composite state including both the divalent and tetravalent states of carbon. This only makes the relations between the energies even more complicated. The situation is probably similar to that in methane, where it is found that large energy terms balance one another so that the energies of detachment of successive hydrogen atoms are almost equal.

8. CONCLUSION

Table 4 summarizes our results on the long-wave limits of the absorption bands of benzene, butadiene and hexatriene, calculated earlier in the paper. The first line names the molecule, the next states the calculated wave-length in Angstroms, assuming the heat of sublimation of carbon to be 170 kcal./mol. The next line states the calculated wave-lengths assuming $L = 130$ kcal./mol. The last two lines give the experimental values, and the best possible choice of L to give agreement with these values. The experimental values were kindly supplied to us by Dr W. C. Price.

TABLE 4

	benzene	butadiene	hexatriene
$L = 170$	2690	2160	2590
$L = 130$	4700	3790	4380
experimental	2700	2190	2530
to agree $L =$	170	169	173

Our conclusion is that the heat of vaporization of carbon is about 170 kcal./mol. A more exact value is probably 168·8 kcal. obtained spectroscopically from the predissociation limit $D = 11{\cdot}054$ eV for CO. Supporting this conclusion is the old Birge-Sponer extrapolation limit of the vibrational levels (11·34 eV), the result $L = 176$ kcal./mol. obtained by Marshall and Norton (1933) from a rate of vaporization experiment, the work of White (1940) on the dissociation energy of CN together with thermochemical equations leading to $D_0 = 11{\cdot}054$ eV for CO, and the observation of Baughan (1941) that the 'free radical' reaction $2CH_4 = C_2H_6 + H_2$ requires L to be about 170 kcal./mol. Contrary to these conclusions is only the work of Herzberg (1939) giving $L = 124$ kcal./mol. obtained from an analysis of the CO spectrum, and the argument of Herzberg, Herzfeld and Teller (1937) on the interpretation of the ratè of vaporization experiment. This argument, however, has no strength in itself, and collapses once doubt is thrown on the value $L = 124$ kcal./mol. In our opinion, the weight of evidence in favour of $L = 170$ kcal./mol. is overwhelming.

The theory as presented is easy to handle, but very serious difficulties are encountered in making higher approximations. Goeppert-Mayer and Sklar (1938) have attempted to calculate the absorption frequency of the $\Gamma_1 - \Gamma_{10}$ transition in benzene (the 2690 A band of table 4), beginning with the simple approximation of molecular orbitals, and then constructing molecular wave functions from the molecular orbitals in the form of Slater determinants. They evaluate the energy, including simple exchange interaction between non-neighbours, and non-orthogonality. Those integrals not already tabulated in the literature they evaluate. Unfortunately, as is always the case with this type of calculation, the appropriate values of the effective nuclear charge and the effective internuclear distances are not easy to select, and the results are very sensitive to the choice made. Once again, proper account is not taken of the variation in the bond lengths.

The method of attack that we have described in this paper is essentially similar to the methods developed by Eyring and his collaborators (1935) for estimating activation energies. The splendid results achieved in this field give grounds for confidence in our values.

We wish to express our thanks to Dr A. G. Gaydon for discussions on the spectroscopic work referred to in this article.

REFERENCES

Baughan 1941 *Nature, Lond.*, **147**, 542.
Bury 1935 *J. Amer. Chem. Soc.* **57**, 2115.
Coulson 1938 *Proc. Roy. Soc.* A, **164**, 383.
Eyring, Sherman and Sun 1935 *J. Chem. Phys.* **3**, 107. See this article for earlier references.

Goeppert-Mayer and Sklar 1938 *J. Chem. Phys.* **6**, 645.
Herzberg 1939 *Molecular spectra and molecular structure*, **1**.
Herzberg, Herzfeld and Teller 1937 *J. Phys. Chem.* **41**, 325.
Ingold, Bailey and others 1936 *J. Chem. Soc.* p. 971.
Jevons 1932 *Report on band spectra* (Camb. Univ. Press), p. 195.
Kistiakowsky, Ruhoff, Smith and Vaughan 1936 *J. Amer. Chem. Soc.* **58**, 152.
Kynch, Lloyd and Penney 1940 *Nature, Lond.*, **145**, 777.
Lennard-Jones 1936 *Proc. Roy. Soc.* A, **158**, 280.
Marshall and Norton 1933 *J. Amer. Chem. Soc.* **55**, 431.
Pauling 1939 *The Nature of the Chemical Bond* (Cornell University Press).
Pauling and Wheland 1933 *J. Chem. Phys.* **1**, 365.
Penny 1936 *Proc. Roy. Soc.* A, **158**, 306.
Penney and Kynch 1938 *Proc. Roy. Soc.* A, **164**, 409.
Penney and Lloyd 1939 *Trans. Faraday Soc.* **35**, 835.
Robertson and Woodward 1938 *Proc. Roy. Soc.* A, **164**, 436.
Sklar 1937 *J. Chem. Phys.* **5**, 669.
White 1940 *J. Chem. Phys.* **8**, 459.

Address of the President Sir Henry Dale, C.B.E., at the Anniversary Meeting, 1 December 1941

This is the first occasion on which I have had the great honour of addressing the Royal Society on this anniversary of its foundation. According to custom, I begin with brief mention of those whom death has taken from our Fellowship during the past year, and whose memories we honour.

ALFRED YOUNG (1873–1940), distinguished for his contributions to pure mathematics, was half brother to another of our Fellows, Sydney Young, a chemist of eminence. Alfred Young had an insight into the symbolic structure and manipulation of algebra, which gave him a special place among his mathematical contemporaries. After a successful career at Cambridge he entered the Church, and passed his later years in the country rectory of Birdbrook, Essex. His devotion to mathematics continued, however, throughout his life, and he published a steady stream of work in the branch of algebra which he had invented, and named 'quantitative substitutional analysis'. He lived to see his methods adopted by Weyl in his quantum mechanics and spectroscopy. He was elected to our Fellowship in 1934.

With the death of MILES WALKER (1868–1941) the Society loses a pioneer in large-scale electrical engineering. Walker was a man of wide interests. He was trained first for the law, and even followed its practice for a period. Later he studied electrical engineering under Sylvanus Thompson at the Finsbury Technical College and became his assistant for several years. Thereafter, encouraged by Thompson, he entered St John's College, Cambridge, with a scholarship, and graduated with 1st Class Honours in both the Natural Sciences and the Engineering Tripos.

Having entered the service of the British Westinghouse Company, he was sent by them to the United States of America to study electrical engineering with the parent company in Pittsburgh. On his return to England he became their leading designer of high-speed electrical generators.

In 1911 Walker became, for a year, lecturer in turbo-machinery and rotary-converter design at the Imperial College of Science and Technology, and then, in 1912, was appointed Professor of Electrical Engineering at the Manchester College of Technology. There he instilled into a generation of Manchester electrical engineers the importance of going back to fundamental principles in all discussions of applied problems.

Throughout his life Walker retained an enthusiastic interest in research, and this, together with his enquiring and inventive mind, made him a real source of inspiration to his students. He was elected to our Fellowship in 1931.

HENRY SELBY HELE-SHAW (1854–1941) achieved distinction in scientific research and invention, and also as a pioneer of Technical Education.

After a brilliantly successful career as a student, he became the first Professor of Engineering in Bristol University at the early age of 27. Later he founded two other Schools of Engineering, becoming the first Professor in that faculty at Liverpool University, and first Professor and subsequently Principal of the Transvaal Technical Institution. His last, and perhaps his greatest contribution to technical education is to be found in the part which he played in founding the scheme of 'National Certificates', of which he was joint chairman until 1937. His scientific researches covered several fields, but his most distinctive contribution lay in the development of his stream-line flow methods, which did much to bring hydrodynamics within the range of the experimental sciences. It may be, however, that Hele-Shaw's most lasting fame will be due to his achievements as an inventor. From his intense and active interest in the practical and scientific development of the motor car came his friction clutch and his system of hydraulic transmission. From his researches on stream-line flow came his stream-line filter. From his equally active interest in the development of the aeroplane came his Automatic Variable-Pitch Propeller and his Exactor Control.

Hele-Shaw took a prominent place in the development of the organized professional life of engineers, becoming president of several engineering societies, including the Institution of Mechanical Engineers.

He became a Fellow of our Society in 1899.

CRESSWELL SHEARER (1874–1941) was an interesting personality whose main scientific activities were in experimental embryology. He spent much time at Naples when the Zoological Station there was in, perhaps, its most famous period. He settled in Cambridge in 1910, and shortly afterwards was appointed University Lecturer in Experimental Zoology, being the first to hold that appointment. The ensuing decade was a period of active and productive research for Shearer, and of inspiration to his students. He published important papers on the development of trochosphere larvae and on sex determination in *Dinophilus*; and in 1913 came the well-known monograph in our *Philosophical Transactions*, in collaboration with de Morgan and Munro Fox, on 'The experimental hybridization of echinoids'. Shearer was elected to our Fellowship in 1916, his activities being at that time diverted by the national emergency to war-time bacteriology. Later he carried out important researches on the metabolism of the eggs of sea urchins, being the first to demonstrate the remarkable changes in oxygen consumption which occur for a few seconds, after the fertilizing spermatozoon has entered the egg. Apart from his scientific interests, Shearer was a man of wide culture, and in 1935 published a book on *The renaissance of architecture in southern Italy*.

ARTHUR THOMAS MASTERMAN (1869–1941) studied and graduated at Cambridge, and was early appointed Assistant Professor of Natural History at St Andrews under the late Professor W. C. McIntosh. Under McIntosh's influence he took up the study of the life history of the British food fishes, which for a quarter of a century remained the chief subject of his researches. He became known also for work in other fields of marine zoology, on *Phoronis*, *Cephalodiscus* and *Cribrella*. In 1903 he accepted appointment as a scientific expert attached to the English Ministry of Fisheries, and did important work in reorganizing the statistical records of the Department. On retiring from that post he became interested in a proprietary hypochlorite preparation, and published shortly before his death some investigations made in that connexion.

The death of WILLIAM BULLOCH (1868–1941) has removed a central and familiar figure from the circle of British pathologists and bacteriologists. After a distinguished academic career in medicine at Aberdeen, he went for post-graduate study to Leipzig and other continental centres, forming and retaining an unusually wide circle of friendships and scientific contacts among the pathologists of Europe. Returning to this country, and having worked for a time under Ferrier and Horsley, be became Bacteriologist to the Serum Laboratories of the British Institute (now the Lister Institute) of Preventive Medicine, and later Bacteriologist to the London Hospital, and finally Professor of that subject in its Medical School. Bulloch had a knowledge of his subject unrivalled in its width and detailed accuracy, and he was a consistent and methodical worker; but, though he published observations over a wide range, the more significant dealing with immunology and haemolytic action, he early became more interested in the history of his subject, and in the critical analysis of its records, than in experimental additions to it on his own account. He had inherited a flair for bibliographic enquiries, and he became increasingly concerned with the historical setting of any subject he touched, and with the independent verification of every statement from the original authorities. His critical examination of the recorded pedigrees of familial diseases, for the *Treasury of human inheritance*, ranked him as a pioneer in human genetics; while his *History of bacteriology*, published in 1938, at once attained general recognition as a masterpiece. This Society itself owes an immense debt to Bulloch's scholarly devotion to the history of science and his desire for accurate personal records of those concerned in its advancement. His *Roll of the Fellows of the Royal Society*, embodying the results of many years of unremitting labour, has now been acquired by the Society by friendly arrangement with his widow.

Bulloch was a man of strong and remarkable personality, with an unrivalled store of personal memories of the great figures in the medical science of his time, and had served on a wide range of expert advisory boards and committees.

The name of Sir FREDERICK GRANT BANTING (1891–1941) will always, and rightly, be associated with the discovery of insulin, and the dramatically sudden change which it produced in the accessibility of a distressing disease to treatment. Banting had seen active service and had been seriously wounded in France in 1915, before he was sent back to Toronto to finish his medical course. After the war he went into practice in London, Ontario, holding also a part-time teaching post in physiology at the university. It was there, in 1921, that the vision came to him, and sent him back to Toronto to beg the late Professor Macleod for research facilities in the Department of Physiology. The discovery which resulted from the determined attack by Banting and a still younger collaborator, C. H. Best, on a problem which had baffled so many workers of ripe experience, provided a romantic chapter in the story of modern researches. Banting became a centre of popular interest, and his proud and grateful country provided him with an Institute of Medical Research. It was not to be expected that Banting would produce another discovery to rank with that of insulin in appeal to the world's imagination. Important results, however, were soon coming in steady output from his laboratories; their work on silicosis, a disease of great importance in Canada's mining industry, deserves particular mention. With the outbreak of another war, Banting became a natural leader in the application of Canada's medical researches to military problems, and he threw himself into the work with tremendous energy and enthusiasm. Death came to him in his fiftieth year, through failure of an aircraft which was bringing him on an urgent mission to England. It is idle to speculate as to what he might yet have done for science. His name is for ever linked to a discovery great in itself, and even greater in its influence on subsequent medical researches. He became a Fellow of the Society in 1935.

JOHN SMYTH MACDONALD (1867–1941), after graduating in natural science at Cambridge, completed his medical studies at Liverpool, where his interest in physiology was stimulated by contact with Sir Charles Sherrington. After holding minor appointments in other universities, he became Professor of Physiology at Sheffield, and later, in 1914, succeeded Sir Charles Sherrington at Liverpool. His earlier researches dealt with the relations between electrolytes and colloids in nerve and muscle fibres, and particularly with the localization therein of potassium and chlorides. On these he based conceptions of the electromotive phenomena in these structures, and of muscular contraction. His later work dealt with the production of heat and the output of energy by man during exercise, for the study of which he built a large calorimeter chamber at Sheffield.

HERBERT MAX FREUNDLICH (1880–1941), elected a Foreign Member of the Society in 1939, was born at Charlottenburg in 1880 of a German father and a Scottish mother. A pupil of Wilhelm Ostwald, he worked after graduation for eight years as assistant in Ostwald's Institute. There followed five years as Professor of Physical Chemistry in Braunschweig, and another seventeen as head of a department in Haber's Institute at Dahlem. The revolution in Germany in 1933 brought him to London, as an honorary Research Associate in the Chemistry Department at University College, with support from Imperial Chemical Industries; and in 1938 he went as Distinguished Service Professor of Colloidal Chemistry to the University of Minnesota, Minneapolis, where he died last March. Any approach, even, to detailed mention of Freundlich's contributions to the fundamental physical chemistry of colloidal systems is beyond the scope of this occasion. It must suffice to say that his researches and those of his pupils and collaborators covered an immense field. He created one of the most important schools of research in the chemistry and physics of colloids, and by his books, especially the successive editions of his famous *Kapillarchemie*, as well as by his researches, he became one of the chief founders of the modern science of colloids.

ARTHUR LAPWORTH (1872–1941) was the son of the distinguished first Professor of Geology at Birmingham University.

From 1913 to 1922 he occupied the Chair of Organic Chemistry in the University of Manchester, and from 1922 to 1935 he was Sir Samuel Hall Professor of Chemistry and Director of the Laboratories. He was elected a Fellow of the Society in 1913 and was awarded the Davy Medal in 1931.

Lapworth's scientific work was characterized by remarkable insight and breadth of outlook. His interest was chiefly concentrated on the intimate mechanism of chemical change, and for many years his views were so advanced that his contemporaries paid little attention to them. Now they are the commonplaces of the text-books, and we are able to appreciate what a great part Lapworth played in guiding the course of development of electrochemical theories of organic chemistry. The prophet was also a superb experimentalist, and some of the topics he illuminated were the following: migrations, cyanohydrin formation and decomposition, the constitution of camphor and gingerol, esterification and acid-base catalysis in general, the mechanism of the benzoin reaction, formation and properties of sulphonic acids and their esters, mechanism of bromination of acetone, and many miscellaneous subjects in organic and physical chemistry. Above all he will be remembered for his theoretical papers and his brilliant ideas on the classification of anionoid and cationoid reagents.

By the sudden death of Sir ALBERT SEWARD (1863–1941) we have lost a colleague who had won a position of high distinction and authority in his own departments of science, and who had given generously of his time and his interest to the work of the Society and the promotion of its interests. At the University of Cambridge he was University Lecturer in Botany from 1890 to 1906, Professor of Botany for the ensuing 30 years, and Master of Downing College, in addition, for the last 21 of these. He served his term as Vice-Chancellor, and was an Honorary Fellow of St John's, Emmanuel and Downing Colleges. The progress of scientific studies, and especially of botany, at Cambridge owes much, indeed, to his ability as a teacher and an administrator, and many scientific bodies and institutions were indebted to his wisdom and his energy. His own many and varied contributions to knowledge by research dealt with fossil plants and gave him a leading position among palaeo-botanists. Our Society recognized their distinguished merit by the award of the Royal and the Darwin Medals, and they gave him high standing in geology as in botany. He had been President of the Geological Society, as well as of the Botanical Section of the British Association and of the International Botanical Congress. He worked hard for international co-operation in science and for its re-establishment after the last war. With his friend, the late Professor Went of Utrecht, he was largely responsible for the initiative which led to the formation of the International Union of Biological Sciences, of which he became the President. There was a special fitness therefore in Seward's election in 1934 as the Royal Society's Foreign Secretary. He had already served for two earlier periods on our Council. When he retired from his Cambridge Chair and College Mastership, in 1936, he settled in London, and was able to give even more fully of his time and attention to the affairs of the Society and the maintenance of its foreign connexions. His ripe experience, his wisdom and the charm of his distinguished personality will be sadly missed by a wide circle of men of science in many countries.

GEORGE WILLIAM CLARKSON KAYE (1880–1941) had been since 1922 the Superintendent of the Department of Physics at the National Physical Laboratory. During the earlier part of the war of 1914–18 he had served with distinction in the Royal Engineers and the Royal Air Force, and from 1917 to 1920 he held the post of Chief Inspector of Materials to the Air Ministry. Kaye's public-spirited activities earned for him the gratitude of students and workers in several departments of science. Physicists have had occasion to be grateful for his work as co-author of the book of *Tables of physical and chemical constants.* Those concerned with the use of X-rays and radium for medical and other purposes are deeply indebted to his work on the dangers of repeated exposure and the means of protection against them. He had been President of the Röntgen Society, had acted as honorary editor of journals dealing with radiology and radiography, as Secretary of the International X-ray and Radium Protection Committee, and as Secretary of the National Radium Commission. He devoted much time and thought to the planning of the New Physics Building at the National Physical Laboratory. His greatest pride was in the Acoustics Laboratory, specially designed for the experimental study of the acoustics of buildings; and he was active in the quantitative study of the problem of noise in our modern civilization, with a view to means for its elimination. By his work as a scientific administrator and organizer, indeed, both national and international, Kaye did even greater service to science and to his fellow men than by his own personal work as an investigator. He was elected to our Fellowship in 1939.

Among classical scholars Sir JAMES FRAZER (1854–1941) was a pioneer in the study of the evolution of classical civilization from the rudimentary notions of lowly cultivators, applying the comparative method which his friend and guide, Robertson Smith, had begun to use in his studies of Hebrew Religion. Both Smith and Frazer acknowledged their debt to J. F. M'Lennan. Frazer developed his life-long studies of the evolution of religious ideas and practices into the twelve volumes of *The Golden Bough* and a vast number of accessory works, which have been listed by Besterman in the *Bibliography of Sir James George Frazer* (Macmillan, 1934). In addition to being a Fellow of this Society he was a member of the Order of Merit, a foundation Fellow of the British Academy, an Associate Member of the Institut de France and the recipient of almost innumerable honours from learned societies and universities, honours which seemed not to touch his modest shyness or his care for every detail. He thought that his theories would be overlaid as better data were collected by field workers, and as the divergent adaptations of society to many environments came to be better understood; but he felt that man's thoughts, beliefs and practices were products of natural evolution, and his splendidly phrased expositions impressed that feeling upon a wide public. His was one of the outstanding influences on the thought of our time. He was elected to the Fellowship in 1920.

The name of Lord CADMAN (1877–1941) will always be associated with petroleum, for not only did he found the first school in the Empire of petroleum technology, but he became also head of two of the greatest petroleum companies in the world. For thirteen years he was Professor of Mining in the University of Birmingham and collaborated with the late Professor J. S. Haldane in a fruitful series of investigations into mining hazards.

As a leader of industry he won the admiration of men of science by his unceasing advocacy of the application of science to industry. It has been stated he never looked at to-morrow, but the day after to-morrow, for he looked upon scientific research as shaping the destinies of industry in generations to come.

The scientific development of the oil field in Iran will always be associated with his name, for though his academic life of thirteen years was that of a Professor of Mining, he was extremely well versed in all aspects of geophysical exploration. There was probably no man of his time with the same wide and encyclopaedic knowledge of the oil industry. He was elected a Fellow in 1940.

ROBERT ROBISON (1883–1941) was educated at University College, Nottingham, and at the University of Leipzig. Almost the whole of his scientific career was spent at the Lister Institute, to the staff of which he was appointed in 1913 and where he succeeded the late Sir Arthur Harden as Head of the Department of Biochemistry in 1931.

Robison will be remembered as one of the outstanding British biochemists of the last 20 years, and his name will be particularly associated with two important discoveries. Following up the work of Harden and Young, he isolated from the products of fermentation of sugar by yeast a hexosemonophosphate; this substance, which is now commonly referred to in the scientific literature as the 'Robison ester', has proved to be of great significance in intermediary carbohydrate metabolism. Robison's second important achievement was the demonstration in ossifying cartilage of an enzyme which hydrolyses hexosephosphates; this discovery was followed by a long series of papers on the role of the phosphatase in the process of ossification.

Apart from his personal achievements Robison contributed greatly to the advance of biochemistry by the services which he gave to scientific bodies outside his own Institute and by the example of a life devoted to the highest standards of research. He was elected a Fellow in 1930 and served on the Council from 1934 to 1936.

Sir ARTHUR JOHN EVANS (1851–1941), who died on 11 July, three days after his ninetieth birthday, retained to the last his wide archaeological interests and critical appreciation of ancient craftsmanship. After a precocious childhood guided by his distinguished father, Sir John Evans, a Fellow of this Society and its Treasurer, he spent some years in adventurous travel in Balkan lands, and then became Keeper of the Ashmolean Museum at Oxford in 1882 and transformed it into an active centre of archaeological research. His special interest in engraved gems led him in 1894 to the discovery, on Cretan seal-stones, of a pre-Phoenician system of pictographic and linear writing; and this in turn led to his acquisition and excavation of the site of the prehistoric palace at Knossos, with frescoes and other works of art, and many clay tablets inscribed in the new form of writing. Ably supported throughout by devoted helpers, he retained nevertheless in his own hands the voluminous publication of this vast mass of material, which his wide experience and imaginative insight enabled him to interpret as it deserved. Far beyond his scientific eminence, he will be remembered for the charm and simplicity of his character, his generous use of ample resources, his devotion to his many friends, his unselfish encouragement of colleagues and younger students, and his vigorous defence of national, academic, and intellectual freedom. He was elected a Fellow in 1901 and received the Copley Medal in 1936.

With the death of **Alfred Joseph Clark** (1885–1941), at the early age of 56 years, British pharmacology loses a valued leader, and medical science a stimulating influence and a wise counsellor. After study and graduation at Cambridge and St Bartholomew's Hospital, Clark held Chairs of Pharmacology at Cape Town, University College, London, and finally Edinburgh, being successor to his former chief, A. R. Cushny, in the two last of these. Clark's own researches showed him as concerned primarily with the fundamental physiology of contractile tissues, and with the actions of drugs, mainly for the light which they could throw on these problems. At the same time he had a keen interest in practical medicine, and became an effective and stimulating teacher on the action of drugs as the basis of their rational use in treatment. These two separate streams of interest found expression in his books. He considered the more fundamental problems in books and monographs on *The mode of action of drugs on cells*, *Comparative physiology of the heart*, *Metabolism of the frog's heart*, and *General pharmacology*, and he dealt with practical applications in a stimulating text-book of *Applied pharmacology*. The more practical aspects of his ability came to the front also in the two great wars of our time. In that of 1914–18 he served with distinction as a medical officer in France, being awarded a Military Cross and attaining the rank of Major. In the present war, being on a special mission of medical and scientific liaison with the British Army in France, he took part in the retreat, and did fine emergency service as a regimental medical officer. Clark became a Fellow of the Society in 1931. His death takes all too early from medical science a worker whose imaginative mind, devotion to research and service to human need have exerted a deep and far-reaching influence on its progress.

James Charles Philip (1873–1941), after graduation in chemistry at Aberdeen, went for special experience of physical chemistry to Nernst, in Göttingen. On his return to this country he worked under H. E. Armstrong at South Kensington and with Heycock and Neville in Cambridge. His career from 1900 onwards was closely associated with the Royal College of Science, South Kensington, before and after its incorporation in the Imperial College. He became Assistant Professor in 1909, and the first Professor of Physical Chemistry in 1913, succeeding H. B. Baker as director of the Laboratories of Inorganic and Physical Chemistry in 1932. Philip, until the most recent years, was actively engaged in researches, into which he drew a succession of students in collaboration, covering a wide range of subjects in physical chemistry; and he has left behind him an important and active centre for that subject. But apart from these distinguished personal activities in science, it was characteristic of Philip that for many years he accepted without question, and discharged with quiet efficiency, a load of duties on behalf of his colleagues, of his university and of the nation, such as might well have filled the whole time and interest of a man less unselfish and devoted. Already during the war of 1914–18 he was acting as Secretary of the Royal Society's Committee which organized the services of the nation's chemists, especially for the production of certain needed remedies. In later years he served on the Senate of London University, was dean of the Faculty of Science in 1934 and deputy Vice-Chancellor in 1937–38. Still more recently he was Chairman of the Committee of the Royal Society and the Ministry of Labour dealing with the section of the Central Register concerned with chemists, and accepted, in addition, a long and exacting term of duty, demanding firm friendliness and understanding, as Chairman of the University of London Joint Recruiting Board. He was President of the Society of Chemical Industry from 1939 to 1941, while the Chemical Society, to which he had acted as Secretary for eleven years, and Chairman of its Bureau of Abstracts for nine years, elected him to its Presidential Chair a few months before his sudden death. Though he retired from his Chair at the Imperial College in 1938, he returned to arduous duty as Deputy Rector, when Sir Henry Tizard's services were claimed elsewhere. Seldom has a life been more fully devoted to science, to the public service, and to the interests of colleagues, friends and pupils. Philip was elected to our Fellowship in 1921, and served on our Council from 1928 to 1930.

PAUL SABATIER (1854–1941), who was elected to our Foreign Membership in 1918, began his researches into problems of catalysis in 1897, and in 1900 entered upon his studies of catalytic hydrogenation, which have had such a great influence on the progress of organic chemistry, in research and in industry, and for which he was awarded the Nobel Prize in Chemistry in 1912. Among Sabatier's numerous contributions to this aspect of chemistry may be mentioned his discovery that the same catalyst, by appropriately varying the conditions, can be made effective for either hydrogenation or dehydrogenation, and his studies of selective catalysis, with its suggestive bearing on biological processes. He was led to formulate a theory of catalytic action, involving the formation of temporary combinations, which is similar in essence to that which still prevails. It is sad that the news of his death at Toulouse should come to us under present conditions.

Walter Gardiner (1859–1941). At the time of his election, in 1890, Walter Gardiner was the youngest of our Fellows, being admitted at the early age of 31 years. At the time of his death this year he was one of the veterans, being at the end of his 82nd year. His period of intense scientific activity, however, establishing him as one of the eminent botanists of his time, extended only from 1881 to 1907. The work which brought him fame was concerned with the histological demonstration of the continuity of the cells of vegetable tissues, due to connecting fibrils of protoplasm, the regular presence of which, *ab initio*, he was the first to reveal. He began this work under Sachs at Würzburg in 1882, and continued it mainly in his own private laboratory in Cambridge and the Jodrell Laboratory at Kew. The Royal Society recognized its importance in recommending him for a Royal Medal in 1898. His activities in research, so far as they led to published record, came early to an end, however, in 1907, the later part of his life being clouded by ill-health, so that he was personally unknown to the botanists of the younger generation. This enforced withdrawal from activity, of an investigator of such unusual powers, was a great loss to the science of botany.

Arthur George Green (1864–1941) was one of the veterans of organic chemistry, particularly in its application to the synthetic manufacture of dyestuffs in this country. After training and graduation at University College, London, he went, in succession to Meldola, as research chemist to the firm of Brooke, Simpson and Spiller, which had succeeded to the industrial interests of W. H. Perkin. In nine years with this firm and a further seven with the Clayton Aniline Company, Green made a number of important improvements in artificial dyestuffs and their applications. In 1903 he accepted the Chair of Colour Chemistry and Dyeing at the University of Leeds, and, in the next eleven years, earned a high reputation for that school as a centre of progressive research and teaching in its subject. He returned to work directly for industry in 1916, when he became Director of Research to the British Dyestuffs Corporation, then faced with the task of re-establishing in this country, during war, an industry which had been allowed to pass so predominantly into German hands. In 1923 Green established himself in London as a consultant to a number of firms, both British and American, engaged in chemical manufacture. In this connexion he retained to an unusually advanced age his practical and research activities in the science to which he had given effective service for so many years. He was elected to our Fellowship in 1915.

John Stanley Plaskett (1865–1941) died on 17 October at Victoria, British Columbia, where he had been in charge of the Dominion Astrophysical Observatory from 1917 to 1935. His original work on the application of spectroscopy and the design of spectroscopes for the determination of stellar radial velocities, and on the velocities, distances and properties of the O-type stars, had brought him international recognition, and the honour of having his name attached to the massive bright star, the 'Plaskett Star', which he discovered.

Plaskett's formal, academic education came to him unusually late in life, and he had served an apprenticeship and held a post with the Edison Companies of the United States and Canada before he entered Toronto University and eventually graduated in mathematics and physics. Researches in photography and stereoscopy brought him an astronomical appointment with the Dominion Government, and his successful leadership of an Eclipse Expedition to Labrador was followed by his appointment as astronomer to the Ottawa Observatory. Here he was able to begin his important series of spectroscopic determinations, but the inadequacy of the 15-inch telescope for the purpose led him, with the consent of the Government, to raise funds sufficient for the construction of a 72-inch instrument. This was installed at Victoria, B.C., where Plaskett took charge of it and spent the remainder of his working life.

Many honours and international recognitions came to him, and he was elected to our Fellowship in 1923.

Edgar Vincent, Viscount D'Abernon (1857–1941), elected under Statute 12 in 1934, was a Fellow of the Society of a type much more frequent in its earlier history than in recent years. One can imagine him, indeed, well in the picture among the distinguished group of our founders. A brilliant figure in Society, a connoisseur of the arts and an enthusiastic follower of more than one sport, an able man of affairs and a distinguished public servant, he became a convinced admirer and advocate of science, with a strong sense of the need of its guidance in policy. It was not, however, till relatively late in his career that he made any close scientific contacts. He accepted in 1915 the chairmanship of the Central Control Board (Liquor Traffic) at its war-time foundation, and experience of conflicting propaganda soon determined him to seek a firmer basis for practical action, in independent and strictly scientific evidence concerning the action of alcohol on man. He accordingly appointed a Scientific Advisory Committee to draw up an impartial account of existing knowledge and to plan researches to fill any gaps so revealed. The members of this Committee were Fellows of this Society, and two of them have since occupied this Presidential Chair. Their report, at Lord D'Abernon's request, was cast in a form suitable for general reading, and he himself contributed an able and constructive preface. He found time to pay frequent visits to those who undertook the researches, and even to witness experiments. Some years later, on returning from his historic mission as the first British Ambassador to Berlin after peace was signed, he presented an able statistical report on post-war economic conditions in Germany, and was elected President of the Royal Statistical Society. Later, again, he did service of great importance to different fields and aspects of science, as Chairman of the Royal Commission on Public Museums and Galleries, and finally as Chairman of the Medical Research Council, till the long illness which clouded the remaining years obliged him to withdraw from all activities.

The news of Sir ARTHUR HILL'S (1875–1941) sudden death from a riding accident has come as a shock to a wide circle of friends. Only a few weeks ago the Council had asked him to undertake the obituary notice of Walter Gardiner. It was characteristic of Hill's devotion to the memory of the old teacher who had guided his first steps in research, and of his quiet efficiency in discharging a duty of friendship, that the notice of Gardiner was already written, corrected and lying in page proof in our office, when the tragic mishap took Hill from us.

From Cambridge where his career as a botanist began under Marshall Ward and Gardiner, and where he published important papers on botanical histology, dealing with sieve tubes and continuity of protoplasm between cells, Hill went to Kew in 1907 as assistant director under Sir David Prain. He remained in that position for fifteen years, during which he was able to continue his researches. Though primarily a morphologist, he was interested in plants in all their aspects, and published a number of papers on the taxonomy of different genera. Later he travelled widely with the aid of the Empire Marketing Board, interesting himself in the economic applications of botany as well as in making new contacts for Kew, by which its collections became enriched and its services rendered more widely available. As director at Kew he encouraged travel by his staff to make direct acquaintance with Empire flora, and obtained grants to make these journeys possible. He became, indeed, an effective ambassador for botany in the British Empire. In other circles also Hill was well known and his counsel prized. He kept a warm affection for his old school, Marlborough, and interest in its affairs, and he was an active and valued member of the

University Grants Committee. He served with distinction in the war of 1914–18, and was detailed for special duty as horticultural adviser to the War Graves Commission. He was elected a Fellow in 1920.

Walter Nernst (1864–1941), who was elected to our Foreign Membership in 1932, was a great figure of the period, early in the present century, in which the modern science of physical chemistry was taking shape. He was awarded a Nobel Prize for Physics in 1920. To him was due much of the fundamental work on the reversible galvanic cell and, in relation to the theory of solutions, on diffusion and partition, and on the hydration and dissociation of electrolytes. In 1906 he formulated a thermodynamical theorem by which the free energy could be determined from the known heat of a reaction. This theory, in its full development, found application in the realm of the absolute zero on the one hand, and, on the other, at such high temperatures as exist only in the stars. Nernst was thus led to the discovery that the specific heat of an element vanishes at a sufficiently low temperature—a conclusion which, in its harmony with Einstein's application of Planck's work, provided one of the surest experimental foundations for the quantum theory.

Apart from his own researches, Nernst was one of the great teachers of his time, whose personality and inspiration meant much for science through the pupils and research students who came from all the world to his Institute in Göttingen, and, later, in Berlin.

Nernst's contacts with many of those, who were thus bound to him by ties of friendship and grateful esteem, were twice broken by war. When the present war loomed imminent in July 1939, he wrote thus to one of our Fellows: 'Jedenfalls bin ich sicher dass unsere Freundschaft sich als unzerstörbar sich erweisen wird, was auch kommen mag.' ('In any case I am certain that our friendship will prove to be indestructible, whatever may come.') Nothing that has come will deter us from paying our tribute of respect to the memory of the great man of science, whom death has now taken from our Foreign Membership.

News of the death of Dr Harry Eltringham (1873–1941) comes too recently to allow more than the briefest mention, on this occasion, of his career and his services to science. The son of a shipbuilder, and himself for some time a partner in the family business, he was one of a number of distinguished amateur naturalists who have been elected to our Fellowship, and whose work has made a contribution to the advancement of scientific knowledge which is, perhaps, especially characteristic of British science. Eltringham became a recognized leader in Entomology, serving as Publications Secretary, Vice-President, and President of the Royal Entomological Society of London. He gave to protective mimicry a special preeminence in his studies, and did pioneer work on the minute structure of the sense organs in the Lepidoptera. For some years before he retired to the country he lived in Oxford, carrying out his observations and experiments in connexion with the University Museum. He was elected to our Fellowship in 1930.

Only to-day comes the news of the death, last Friday, of WALCOT GIBSON (1865–1941), who, after geological work in South and East Africa in the early nineties of last century, joined the staff of H.M. Geological Survey and became director of the Survey for Scotland. He was elected to our Fellowship in 1925.

I have made mention of the late Professor Bulloch's very important contribution to our history, in his detailed record of the career and the claims to distinction, so far as these were discoverable, of every one of our Fellows, from the beginning of the Society almost to the present day. Concerning some, whose elections duly appear in our records, no additional information was obtainable, even by Professor Bulloch's researches. It is unlikely that any of these were important contributors to science; the Society in its earlier days, and even up to 1847, having admitted a substantial proportion of Fellows whose interest in its scientific activities was not more than that of onlookers. An interesting article by Sir Henry Lyons, in the recent issue of *Notes and Records*, shows that this was true even of many of the Society's earlier officers. On the other hand, the history of the doings of our Fellows would, over a long period, have comprised practically the whole of the history of science in this country. The failure to discover anything at all about some of them gives new prominence to the lack in our organization, from the beginning of the Society until now, of a system for collecting, during the lives of our Fellows, any but the most meagre items of information concerning them and their doings. This defect is further illustrated by a recent acquisition of papers which concern one of the most important figures in the history of the Society—Sir Robert Moray, who was actually its first President, before the Society received its first Charter, which Moray's influence with King Charles II appears, indeed, to have been largely instrumental in obtaining. Little else was known of the man who played so prominent a part in our foundation, till a life of him was written by the late Alexander Robertson of Edinburgh, though this was not published till after the death of the author in the war of 1914–18. Apart from our earliest Journal Book and certain letters preserved in our library, Robertson obtained his material mainly from the Kincardine papers—a long series of letters from Moray to the second Earl of Kincardine. The originals of these have been lost, and it is not known whether they still exist. Robertson had access to a manuscript copy, but this also disappeared after he had used it. The recent rediscovery of this unique copy is due to the watchful interest of one of our Fellows, Mr Clifford Dobell, who has acquired it and generously offered it to our library, which will henceforward be practically complete in documentary sources for all that is known concerning our first President. In offering the Society's thanks to Mr Dobell for this, not the only example of his generous interest in our library and our history, I venture to appeal to others of our Fellows who are learned in such matters, for help in bringing to the Society's notice opportunities of adding to its treasury of documents bearing on the history of the Society and of science.

So much for the records of the past. A few weeks ago the Fellows received a communication from me, introducing, with the Council's approval, a new scheme which should make good this gap in our equipment, so far as the future is concerned. If we can make this scheme a success, it should provide the Society with a complete set of personal records of all the Fellows from now onwards, containing all the relevant facts concerning the ancestry, parentage and education of each, and a full account of his scientific opportunities, experiences and achievements. For those who now and in the future are newly elected to our Fellowship, it should be a matter of small trouble to provide such accounts of their careers up to the time of election, and then to keep them up to date by annual addenda. It will certainly involve a greater initial trouble for those of us who have become seniors in the Fellowship, in the absence of any system of this kind. On the other hand, it seems to me almost a commonplace to suggest that the memories of some who are still with us cover a period in which the change and the expansion of scientific knowledge have been so rapid and so revolutionary, that the future, looking back upon these times, is likely to regard them as unsurpassed in interest and importance, in the whole history of science. In his Address from this Chair a year ago, Sir William Bragg, speaking of J. J. Thomson and Oliver Lodge, who had passed from us during the year then ending, referred to the memory, still preserved by himself and by others of his own seniority, of 'the brilliant years when these men and their contemporaries were writing the...first pages' of a great new chapter of science. I am appealing to those who keep such memories to put them on record now, and to commit them to the keeping of the Society, for those who will come after them here, and for all who will be interested in tracing and interpreting the history of science over the great epoch of the past half century. No doubt we shall soon have full-scale biographies of men like Thomson and Lodge, in which the attempt will be made to recover, from such correspondence and notes as may be available, their impressions and memories, in turn, of the great men of the generation which went before them. How much, one thinks, might the task of the biographers have been eased, and how much might have been kept for us which no diligence can now recover, if all the leading men of science of that time had been making for the Society records of the kind which we are now trying to inaugurate. To mention another department of science, do we not wish that we had had such a system in use when some of our Fellows could have left us notes of work and discussion with Claude Bernard, Louis Pasteur, Robert Koch, Carl Ludwig and others of that great period of the latter half of the 19th century?

And there are memories of a later generation which we must hope to get now on record, and to hand on to our successors. To quote only one example, there are still a number of us who remember Ernest Rutherford as he first came to Cambridge, as a post-graduate research student from New Zealand, and many more who were later his direct and intimate pupils and collaborators. I am sure, also, that Sir William Bragg was right, when he told us last year that 'our young men of to-day are maintaining in full force the tradition that they have received'. The interval between the two wars showed us how quickly science can return to its normal direction of progress, at some points apparently with even an added vigour, after the forced diversion. I have no doubt at all, that, when we can free ourselves again from such duties as now preoccupy brain and hand for most of us, we shall find that we are still in the great period, and that science will rapidly regain the momentum of its advance. Experience suggests that we may find that it has even, in some directions, made unexpected and almost unnoticed leaps forward. I make a strong appeal, then, to the Fellows also of more recent election to take promptly what, for them, will be the relatively small trouble of rendering and maintaining the accounts of their doings and experiences in science, for the Society's new files of personal records. The present century has witnessed a prodigious growth of the number of those who, in one capacity or another, are directly concerned with the advancement of natural knowledge by research. The election to our Fellowship has, of necessity, become more closely selective and exclusive, and we can hardly expect to avoid a few mistakes of choice in either direction. Nevertheless, I think that we can assume, without undue self-complacency, that a detailed and systematic record, of the scientific activities and contacts of all the Fellows of this Society, will continue to provide a fair picture of the main currents, at least, of scientific progress in this country. Those who in the future endeavour to write the general history of our period may well find in the outburst of scientific achievement its distinguishing and central character, far transcending in importance all changes of political structure. It is not for us, indeed, to anticipate such judgements, but I think that it is part of our duty and concern to see that the material for them is provided. If our Fellows will make the small, systematic effort needed to ensure the success of the new scheme, the future historian of the science of our times, unlike those who now laboriously seek and interpret the scattered relics of its earlier days, should find ready to hand an invaluable body of authentic and contemporary data.

As we come to the end of another year we can see, as yet, no prospect for science of escape from urgent preoccupation with the means of waging war. On the contrary, with the Union of Soviet Russia now locked in a supreme struggle for its own existence and the world's freedom, and with the United States of America rapidly directing its tremendous scientific and technical potential to the support of the same great cause, the diversion of science from its normal uses and objectives has spread right round the world. Yet even this grim necessity has brought with it some measure of compensation, in drawing closer the bonds of friendship, between the men of science in the countries thus united in a common purpose. We in Britain received a tremendous encouragement in the early months of this year, from the visit of President Conant and his associates to establish here, in London, an office for the maintenance of regular and intimate co-operation, between the war researches of our American colleagues and those which are here in hand. More recently, and in spite of all difficulties of communication, the sense of a common peril and a common determination is bringing us into a new and growing intimacy of collaboration with our colleagues of Soviet Russia. The organization of the science of the British Empire for war has brought to London already a number of distinguished colleagues from the Overseas Dominions, and we have heard of others who are on the way. It has been a particular pleasure to gather them here, in the house of the Royal Society, and to invite them to regard it as a centre and a rallying point for discussion of the means by which this new and closer collaboration, arising under the stimulus and the necessity of war, may be perpetuated and strengthened for the purposes of peace.

Generous gifts to the Society, during the year, from sister Societies in America, have given further welcome evidence of the determination of our colleagues there to come to the help of British science in this time of need. The American Philosophical Society, founded in 1743 by Benjamin Franklin, with this Society as his model, sent us ten thousand dollars 'for the aid of science in Britain'. They have confirmed our interpretation of their fraternal gift, as betokening a desire to help us to preserve some measure of normal scientific activity in this country during the war, and to keep alive the tradition of a free pursuit of knowledge for the benefit of all men. We have been able to find good use already for a large part of this benefaction, in the maintenance of a number of important researches, which war conditions had threatened to interrupt or to bring to an end. The American Physiological Society similarly sent us five thousand dollars, as a spontaneous contribution, to the support of scientific publication in Britain, mentioning Physiology as the subject to which they, as physiologists, desired us to give the first consideration. The Rockefeller Foundation, that truly international benefactor and promoter of natural knowledge, had already asked us to be reponsible for the distribution of twelve thousand five hundred dollars in aid of scientific publication in Britain in these difficult times.

As I have taken occasion earlier to state, gifts such as these, welcome for their own intrinsic value and for the practical uses which we are readily finding for them, are even more welcome on account of the evidence that they bring, of the feeling of comradeship between our American colleagues and ourselves. We can do no less, I think, than assure them of our determination that this closer sense of unity in aims and ideals, with them as with our fellow citizens of the British Overseas Dominions, shall not be lost, but rather strengthened, when we face together the new problems which the end of the war will bring.

Though the first and imperative call on the science of all free countries is for the means of winning the war, to save the freedom without which science cannot in any true sense survive, we cannot put aside the duty of preparing for the part which science must play, in rebuilding and maintaining civilization when peace returns. The Conference recently organized by the British Association, on 'Science and World Order', attracted more attention from the Press and the public than is usually given to scientific events and discussions; and it was, indeed, an impressive and significant fact that men of science from a dozen or more different countries, some far distant, should have found it possible now to meet, here in our war-scarred London, and to find the time and the impulse for such debate. We may offer our very sincere congratulations on the success of such an enterprise. Many who took part in these meetings, held at a time when Science finds itself conscript and organized as never before for the destructive purposes of war, were clearly ready to support the view that it should be as fully organized by the governments of a world at peace, for its proper purposes of enriching life and enlarging the opportunities of happiness for all men alike. There were not wanting voices, however, such as that of our Biological Secretary, to sound a warning of dangers which might be entailed, by such fullness of association between science and government as others were advocating with conviction and enthusiasm. Freedom and opportunity, it was pointed out, rather than organization, provide the conditions for the highest types of research, and thus, in the end, for the greatest services which science can give to mankind. I find myself in sympathy with this view, and nobody here, I think, would suggest that it is usually possible to organize the researches which advance boldly into the unknown, and open new vistas to human understanding. Here we shall certainly not overlook the fact that, in the period between the two wars, important funds have been placed at the disposal of the Royal Society by a series of generous benefactors, to be administered for the support of researches over a wide range of subjects, in complete independence of any control by the State.

On the other hand, I think that it will be agreed that the remarkable development in this country, since 1914, of the State support of research administered by the three Research Councils, normally in relation to the needs and the activities of a nation at peace, has taken place without any obvious detriment or danger to the freedom of science. The Royal Society's former function, of advising the Government directly on all scientific matters, and of organizing such systematic researches as were then undertaken in the public interest, has, of necessity, been shared and greatly diminished. We, as a Society, however, can fairly regard this development as, in many respects, a realization of the plans and the dreams of our predecessors here; and I do not think it fanciful to claim that our Society's traditions and standards have been still effective, through the influence of our Fellows on the Research Councils and their Committees, and through the filling of their chief executive offices by men of our Fellowship. As a whole-time research worker myself, since 1914, under the body which became the Medical Research Council, and the senior now in that service, I can bear grateful witness to the freedom of opportunity which can exist under an enlightened organization and control, exercised on behalf of the Government. I have no reason to suppose that the conditions are otherwise under the other Research Councils. Nor should we lose sight of the fact that a further large proportion of the free scientific research of the country is now indebted to support from the State through grants to the Universities, administered without any trace of detailed Government control.

While, therefore, the existing mechanisms for the support of science by the State are doubtless susceptible of improvement at one point or another, I find no reason to fear any threat to the freedom of science from them, or from any natural development on those lines. Nor do I fear it from a wider use of the organized application of science and scientific method to problems of public welfare; nor, again, from a more effective access of scientific knowledge to those responsible for government. A year ago Sir William Bragg told the Society of the formation of the Scientific Advisory Committee to the War Cabinet, under the chairmanship of Lord Hankey, with the President and two Secretaries of this Society as members *ex officio*. The representation of the Society has, indeed, been strengthened since then, and in a manner most welcome, by the fact that, though I have succeeded him *ex officio*, Sir William Bragg still gives his wisdom and experience to the work of that Committee, as an extra member.

There is one direction, however, in which I do find some reason to fear for the freedom of science. If science should become entangled in controversial politics, through the over-eagerness of its advocates and champions to invoke the sanction of science, or to claim its potentialities, in support of any special political doctrine, then indeed I believe that the threat to its freedom might become a real danger. Let there be no misunderstanding of my meaning. I am not abusing the privilege of this Chair by using 'controversial' as an epithet, to be applied to political opinions which I do not happen to share. I see danger if the name of science, or the very cause of its freedom, should become involved as a battle cry in a campaign on behalf of any political system, whether its opponents would describe it as revolutionary or reactionary. If science were allowed thus to be used as a weapon of political pressure, it would be impossible to protect science itself eventually from the pressure of sectional politics. If that should happen the dangers are, I believe, beyond dispute—the danger, for example, that fundamental researches, having no immediately practical appeal, would be allowed to fall into arrears through relative neglect; or the danger that the rigid standards of true science would be relaxed, by allowing the convenience of results for policy or for propaganda to enter into the assessment of their validity as evidence. This Society, with its firm and unbroken tradition of complete aloofness from political controversy, may still find it an important part of its function, to keep watch and, if necessary, to stand without compromise, for the right and the duty of science to seek the truth for its own sake, in complete freedom from any kind of extraneous influence. I hope, indeed, that there will never be need thus to invoke our tradition, in order to protect the freedom and the integrity of science from the enthusiasm and the advocacy of any of its friends.

Awards of Medals, 1941

The COPLEY MEDAL is awarded to Sir THOMAS LEWIS.

Lewis's life's work, still in vigorous progress but for interruption by war duties and war conditions, has been the application of precise and controlled methods of experimental research to problems of Clinical Medicine. This has enabled him to achieve a detailed analysis of abnormalities of function produced by disease, injury, or hereditary defect; and so far his attention has been centred upon the circulation of the blood and its disorders. Being attracted through the work of the late Sir James Mackenzie to the study of abnormal rhythms of the human heart-beat, Lewis recognized, about 1908, the great opportunity for a closer investigation of them offered by the then recent introduction of the string galvanometer by Einthoven. With its aid Lewis had soon made a number of clinical and laboratory studies, such as those in which he finally identified auricular fibrillation as the cause of a particular kind of complete irregularity. He was thus led to undertake, and to extend, with a succession of collaborators from many countries, the remarkable series of investigations, carried through in logical sequence between 1910 and 1923, in which he passed from the laboratory to the clinic and back again as the occasion demanded. It is fitting that special mention should here be made of the series of experimental studies published in our own *Philosophical Transactions* from 1914 to 1916, and presented in brilliant summary by Lewis in his Croonian Lecture to the Society in 1917. In these were traced, with an astonishing precision of measurement and timing, the point of origin and exact course of the rhythmical waves of excitation and contraction in the normally beating heart of the dog, and, finally, for comparison, in the hearts of other classes of vertebrate animals. Considered by itself, this work ranks as one of the outstanding achievements of experimental physiology in our times, and it has given to physiology a large part of its present detailed knowledge of the nature of the heart-beat. For Lewis, however, its greater importance lay in giving to clinical medicine the background for an accurate picture of disturbances of the normal mechanism, therewith a new security of diagnosis and prognosis in dealing with disordered actions of the heart, and ultimately a rational basis for their treatment. A new phase of cardiological thought and practice spread rapidly from Lewis's clinic round the world.

Meanwhile he had begun in 1917, and was to maintain with a series of collaborators for more than another decade, a separate series of investigations, dealing by direct experiment with the blood vessels of the human skin. Thus were elucidated the means by which the resistance of these vessels to the flow of blood is maintained and varied, including their complex reactions to chemical substances akin to histamine, which he proved to be released from the cells of the epidermis by injurious or irritant stimuli. These methods of investigation were later developed and extended to vascular disorders of the limbs, and the experiments of still more recent series have dealt with pain and functional defects in muscles and nerves, due to interruption of the blood supply. Apart from the separate accounts of items and stages of these lines of research, as completed, in papers which have issued from his department in steady sequence, Lewis has assembled and discussed the results, in their appropriate connexions, in a succession of comprehensive monographs. He has been the inspiring leader of a group of younger workers in Clinical Research as an experimental science, has founded a Society for such studies and has devoted to their use a Journal which he had started with a more limited scope.

The work of Thomas Lewis, which we honour to-day with the highest recognition in the gift of the Royal Society, is renewing and carrying forward, with a special directness, the great tradition which William Harvey created, before this Society was founded.

A ROYAL MEDAL has been awarded to Professor EDWARD ARTHUR MILNE.

Milne is distinguished for his work on planetary and stellar atmospheres, on the internal constitution of the stars, and on the theory of relativity. An early paper on various properties of the earth's atmosphere, up to high levels, led later to a valuable improvement of the theory of the escape of planetary atmospheres by the passage of the faster moving molecules out of the range of the gravitational field. Thence he passed on to a long series of investigations on radiative equilibrium and the theory of the atmospheres of the sun and stars.

Next, partly in collaboration with R. H. Fowler, he improved and extended Saha's theory of the absorption lines in stellar spectra, obtaining a relation between the maximum strength of a line and the mean pressure and temperature in the atmosphere. Afterwards Milne generalized this theory, providing a rational foundation for the astronomers' empirical method of determining stellar parallaxes from the spectra.

Later he considered the equilibrium of the calcium chromosphere of the sun, and also discovered a method by which outward moving atoms capable of absorbing radiation in the region of the chief absorption lines can be accelerated and pass beyond the range of the sun's attraction, attaining a limiting speed of about 1000 miles a second. This theory also has an application to 'new' stars.

Milne then considered the deeper layers of the atmosphere (*e.g.* in the case of the sun, the photosphere), which in 1929 he took as the subject of his valuable Bakerian lecture. He has also given a theory of the structure of sunspots and of the circulation associated with them.

In 1929 he began a new series of researches on the radiative equilibrium of gas spheres, designed to improve the theory of the internal constitution of the stars. His work in this field was specially important in focusing attention on the properties of degenerate matter.

In 1932 Milne began an altogether different series of investigations, bearing on the largest topics of astronomy and cosmogony, and providing an alternative to the general theory of relativity developed by Einstein and his followers. He has made a valuable analysis of the concept of time, and his kinematical theory of gravitation has some promise of a possible extension to include also electromagnetism.

Milne's later work has been the subject of much controversy: but the originality and boldness of his attack seem certain to promote our understanding of these great problems, and to open up fresh views and methods of approach to them.

A ROYAL MEDAL is awarded to Professor ERNEST LAURENCE KENNAWAY.

Kennaway is the director of the Chester Beatty Research Institute of the Royal Cancer Hospital, and has been engaged for the past twenty years in investigations on the production of cancers by the continued effects of chemical agents. The long known liability to skin cancer of men whose work involves regular contact with soot, coal tar, or pitch, and the more recently demonstrated production of such cancers in animals by painting the skin with tar, had raised the question whether a specific, chemical agent was concerned, or only a sufficiently persistent irritation. The fractionation of coal tar, in search of a substance revealing its action only after tedious months of experiment, was an undertaking to daunt any but a courageous and devoted investigator. Kennaway embarked on this unpromising quest, and after years of patient and tenacious labour the fluorescence studies of his co-workers Mayneord and Hieger made it possible to isolate a pure substance from tar with intense carcinogenic activity, and ultimately to identify it as benzpyrene. This identification and its confirmation by synthesis were due to J. W. Cook. Meanwhile, the observation that active fractions of the tar had ultraviolet fluorescence spectra resembling those of hydrocarbons of the phenanthrene type led to the testing of various compounds of this nature. The first of these was a dibenzanthracene, which had been synthesized by Clar, and this was found to be carcinogenic. Substances of still greater activity have since been obtained, and some of these have a close structural relationship to naturally occurring sterols. A characteristic nuclear ring-complex thus, surprisingly, provides a link of structural community between these carcinogenic agents and a number of natural substances having intense but widely different biological activities—the D vitamin, a number of hormones concerned with sexual functions, and the highly toxic but remedially important glucosides of the *digitalis* series. One of the most fascinating chapters in organic and biological chemistry has been opened. Identification of these provocative agents does not tell us how they act, and the causes of seemingly spontaneous cancers remain as yet obscure. It cannot be doubted, however, that, when further advances of knowledge enable a correct account to be written of the nature and mode of origin of the malignant tumours, the pioneer work of Kennaway and his able group of co-workers will provide one of the important chapters.

The DAVY MEDAL is awarded to DR HENRY DRYSDALE DAKIN.

Dakin began his researches in the field of biochemistry early in the present century. At that time, in comparison with knowledge of the end products of metabolism, relatively little was known about the chemical activities of the living cells of the animal body. His work has made very important additions to knowledge of the intermediary changes produced by these activities, and also of the chemical structure of natural components of the tissues.

One side of Dakin's work has dealt with enzymes of the animal organs. He was the first to show that such an enzyme will attack at different rates the two optical isomers in a racemic mixture. With Kossel he discovered the enzyme arginase, with its important role in the production of urea from arginine. Later he discovered the enzyme glyoxalase, the wide distribution of which in the tissues must indicate some important though still undefined function in carbohydrate metabolism.

In connexion with the intermediary metabolism of fatty acids, Dakin produced the first convincing evidence for oxidation at the β-carbon-atom as the first stage of their utilization by the body, and showed that this type of oxidation can even be reproduced *in vitro* by the action of hydrogen peroxide.

Dakin's work on the chemistry of the proteins has included a method of partial racemization, bringing subtle differences of molecular pattern into view, which could be related to specific antigenic differences. He also introduced a method of separation which enabled new hydroxyaminoacids to be recognized, and raised much nearer to unity the proportion of a protein-molecule accounted for as known amino-acids. At a wide interval of years, Dakin has made two notable contributions to the chemistry of hormones. In 1905, he was responsible for the first published artificial synthesis of a hormone, adrenaline. In 1936 he described the isolation from liver of a substance which is, at least, a principal factor in the important effect of liver extracts on pernicious anaemia.

Working in France during the war of 1914–18, Dakin introduced the use of a buffered hypochlorite solution for irrigating infected wounds. Later, on a ship bringing the sick and wounded from Gallipoli, he made a similar solution by direct electrolysis of sea-water. Another war is reviving the use of such preparations to meet the same and other needs.

Though Dakin has worked in a private laboratory, with but rare collaboration and no pupils, his work has exercised a wide and powerful influence on the growth of biochemistry and on the strengthening of its links with organic chemistry.

The HUGHES MEDAL is awarded to Professor NEVILL FRANCIS MOTT.

Early in his career Mott's work in the field of atomic collisions attracted widespread attention. He was the first to show that Rutherford's scattering law holds in quantum mechanics, and to give an accurate theory of the effect of symmetry in scattering problems. When he took up his present post as Professor of Theoretical Physics at Bristol, he abandoned this subject for that of the theory of metals and alloys. Within a few years he was recognized as one of the leading international authorities in this field, to which he contributed a number of important papers on electronic bands in metals and on the electrical conductivity of alloys and its temperature coefficient. In establishing a close association between theoretical and experimental workers he has no superior. He has also contributed to the important problem of metals under strain; under his direction Fuchs has calculated the elastic constants of certain metals and obtained good agreement with known values.

Later he turned to semi-conductors and insulators, throwing light on the physical processes involved in the formation of oxide films, and in the electrical conductivity which can be induced by various means in polar crystals. His theory (with Gurney) of the formation of the latent image in a photographic emulsion has found general acceptance, and has stimulated fresh experimental work in research departments of the industry.

This striking record of published work was achieved between 1928 and 1939.

When war broke out Mott found that his activities as a quantum physicist had no direct application to the war. It is a tribute to his versatility and flexibility of mind that he could turn so quickly to a new field in classical physics, and make important contributions to the practical problem in connexion with which he now holds an important post.

Clarke Memorial Medal (1941)—*Royal Society of New South Wales*

The Royal Society of New South Wales has awarded the Clarke Memorial Medal for 1941 to **Frederic Wood-Jones**, F.R.S., now Professor of Anatomy in the University of Manchester. Professor Wood-Jones being unable to attend at Sydney, we have been asked, by our daughter Society of New South Wales, to arrange for the medal to be presented to him here on an appropriate occasion. We have judged that none could be more appropriate than this, on which our own medals are presented, and it gives me just pleasure to be able to make the presentation. The Royal Society of New South Wales have stated the grounds of the award in the following terms: 'The Clarke Memorial Medal, established as a memorial to the late Rev. W. B. Clarke, who for nearly forty years rendered distinguished service to his adopted country, Australia, is awarded "for distinguished work in the Natural Sciences done in or on the Australian Commonwealth and its territories." Professor Wood-Jones is receiving the distinction on account of his very outstanding researches in zoology in Australia, particularly for his work on the mammals of South Australia. Moreover, during his stay in Australia Professor Wood-Jones not only did much research work in South Australia and Victoria, but also took a leading part in scientific endeavour in general.'

On Laplace's differential equations for the tides

By J. PROUDMAN, F.R.S.

(*Received* 22 *May* 1941)

1. INTRODUCTION

This paper is an investigation of the validity of the assumptions made by Laplace in framing his well-known differential equations for the tides of the ocean. Since his time these equations have been used by all the principal workers on the dynamical theory of the tides, but in recent years it has been claimed, mainly in Norway, that they are quite inadequate.

Let ω denote the angular speed of the earth's rotation and let t denote the time; let r denote the distance of a point in the ocean from the earth's centre, and θ the co-latitude of this point; let u, v and w denote the components of the velocity of a particle of water in the directions respectively of increasing θ, east longitude and r. Then the corresponding components of the acceleration of the particle are respectively:

$$\left.\begin{aligned}
&\frac{du}{dt}+\frac{uv}{r}-\frac{v^2}{r}\cot\theta-2\omega\cos\theta v-\omega^2 r\sin\theta\cos\theta,\\
&\frac{dv}{dt}+\frac{vw}{r}+\frac{uv}{r}\cot\theta+2\omega\cos\theta u+2\omega\sin\theta w,\\
&\frac{dw}{dt}-\frac{u^2+v^2}{r}-2\omega\sin\theta v-\omega^2 r\sin^2\theta.
\end{aligned}\right\}\qquad(1\cdot1)$$

In forming his differential equations Laplace neglected all terms of the first two of these expressions involving u, v and w, except those on the left-hand side of the equations (1·2) below; and he dispensed with the use of the third by neglecting the vertical component of the acceleration. By interpreting u and v in the Eulerian sense he neglected product terms and thus restricted his consideration to small motion. He also neglected the vertical component of the tide-generating forces and the vertical variations in the horizontal components of these forces. He assumed the mean surface of the ocean to be the sphere $r = a$. He took the centrifugal terms of (1·1) to be merged in the earth's effective gravity, and assumed the acceleration g

of this effective gravity at the earth's surface to be uniform. His equations of motion thus take the form

$$\left.\begin{aligned}\frac{\partial u}{\partial t}-2\omega\cos\theta v&=-\frac{g}{a}\frac{\partial\zeta'}{\partial\theta},\\ \frac{\partial v}{\partial t}+2\omega\cos\theta u&=-\frac{g}{a\sin\theta}\frac{\partial\zeta'}{\partial\chi},\end{aligned}\right\}\tag{1·2}$$

where χ denotes the east longitude, $\zeta'=\zeta-\bar{\zeta}$, ζ denoting the elevation of the free surface, and $-g\bar{\zeta}$ the variable gravitational potential on $r=a$.

It is a consequence of the equations (1·2) that there is no vertical variation in u and v, and then the equation of continuity takes the form

$$\frac{1}{a\sin\theta}\left\{\frac{\partial}{\partial\theta}(h\sin\theta u)+\frac{\partial}{\partial\chi}(hv)\right\}+\frac{\partial\zeta}{\partial t}=0,\tag{1·3}$$

where h denotes the mean depth of the ocean at any place. It is also a consequence of Laplace's equations that the vertical component of current varies linearly between the ocean bottom and the ocean surface.

In 1933 V. Bjerknes, J. Bjerknes, H. Solberg and T. Bergeron stated that the neglect of the vertical acceleration was a serious error, which might give totally erroneous results for a tidal constituent of period $2\pi/\sigma$ such that $\sigma^2<4\omega^2$. They emphasized the possibility of 'cellular oscillations' associated with negative values of the factor $1-4\omega^2/\sigma^2$, a possibility which was indicated by the presence of this factor in the equations obtained in 1880 by Sir W. Thomson (Lord Kelvin) on the vibrations of a columnar vortex. The main force of their criticism referred to the diurnal constituents, for which σ^2 is near ω^2; they stated that Laplace's equations were not seriously in error for the semi-diurnal constituents, for which σ^2 is near $4\omega^2$. It may be mentioned that the vertical acceleration had been retained by R. O. Street in 1930 in his study of the surface oscillations of water in a rotating cylindrical vessel, but he did not examine the case of $\sigma^2<4\omega^2$.

In 1933 M. Brillouin and J. Coulomb published a detailed study of the oscillations, both free and forced, of the water in a flat circular basin of uniform depth, in which they retained the vertical acceleration. They emphasized the fundamental way in which the distribution of the motions depends on the sign of $1-4\omega^2/\sigma^2$, and they paid particular attention to possible applications to the tides. Their problem of forced tides, when $\sigma^2<4\omega^2$, led to certain difficult questions of convergence. They pointed out that for the semi-diurnal constituent K_2, in which $\sigma^2=4\omega^2$, Laplace's equations did not appear to be valid.

In 1936 H. Solberg published the first part of a monograph on the *free* small oscillations of a homogeneous liquid on a rotating earth, with special reference to the dynamical theory of the tides in the oceans and atmosphere. For the equations of motion he took

$$\left.\begin{aligned} \frac{\partial u}{\partial t} - 2\omega\cos\theta v &= -\frac{1}{r}\frac{\partial P}{\partial \theta}, \\ \frac{\partial v}{\partial t} + 2\omega\cos\theta u + 2\omega\sin\theta w &= -\frac{1}{r\sin\theta}\frac{\partial P}{\partial \chi}, \\ \frac{\partial w}{\partial t} - 2\omega\sin\theta v &= -\frac{\partial P}{\partial r}, \end{aligned}\right\} \tag{1·4}$$

where

$$P = \frac{p}{\rho} + V, \tag{1·5}$$

p denoting the pressure, ρ the density of the water, and V the potential of the gravitational and centrifugal forces. For the equation of continuity he took the general equation

$$\frac{1}{\sin\theta}\frac{\partial}{\partial\theta}(\sin\theta u) + \frac{1}{\sin\theta}\frac{\partial v}{\partial\chi} + \frac{1}{r}\frac{\partial}{\partial r}(r^2 w) = 0. \tag{1·6}$$

He took account of the spheroidal nature of the mean surface of the ocean, and he considered it an 'internal contradiction' to retain the dynamical effect of the earth's rotation on the tides and yet to neglect it on the shape of the mean surface of the ocean.

For the free oscillations of an ocean of uniform depth covering the whole earth, Solberg showed that the analytical character of the solution completely changed as $1-4\omega^2/\sigma^2$ passed through zero. For free oscillations which are the same in all longitudes, and in which $\sigma^2 > 4\omega^2$, he obtained results which are not very different from those obtained by S. S. Hough (1897) on the basis of Laplace's equations. He also gave some attention to the cases in which $\sigma^2 = 4\omega^2$. The detailed development of the cases in which $\sigma^2 < 4\omega^2$, where Solberg expected results differing greatly from those obtained by Hough, he reserved for a second part of his monograph.

2. SUMMARY OF THE PRESENT PAPER

In the present paper consideration is restricted to the tides of the ocean and the water is taken to be homogeneous. *Forced* oscillations are considered, as the actual tides belong to this class. The types of motion can thus be restricted to those corresponding to the actual tides. A direct comparison can also be made between the results of solving Laplace's equations and the results of a more general theory. For this more general theory Solberg's differential equations, viz. (1·4) and (1·6), are used.

First it is shown that it is reasonable to simplify the problem by neglecting the ellipticity of the meridians (§ 3) and the gravitational attraction of the disturbed water (§ 4). With these simplifications the problem is still mathematically self-consistent and the question of cellular oscillations remains.

In §§ 5, 6 the general mathematical formulation is given, and in § 7 it is shown that cellular oscillations are only liable to occur for semi-diurnal constituents near the poles and for long-period constituents near the equator.

Certain cases provided by the vanishing, in turn, of one of the components of current are then considered. It is shown (§ 8) that Laplace's celebrated particular integral for the constituent K_1 in an ocean of uniform depth may be immediately and without approximation extended to Solberg's equations. For a narrow ocean of uniform depth bounded by meridians (§ 9) and for an endless canal of uniform depth along a parallel of latitude (§ 10), it is shown that Laplace's equations always provide a high degree of approximation.

Two basins for which Laplace's equations do not always give valid solutions are next considered. These are a circular sea of uniform depth near the North Pole (§ 11) and a broad channel of uniform depth near the equator (§ 12), and in both cases the curvature of the meridians is neglected. As already indicated, the cases of failure of Laplace's equations are those of semi-diurnal constituents in the first basin and of long-period constituents in the second basin.

Finally, an ocean over which the depth is a function of the latitude only is considered. For the K_2 constituent (§ 13) and for the limiting form of long-period constituents (§ 14) general differential equations in which there is only one independent variable, viz. the latitude, are obtained. When the depth is a very small fraction of the earth's radius, these differential equations reduce to the corresponding ones of Laplace except near the poles for the K_2 constituent and near the equator for the limiting form of long-period constituents. It appears that in §§ 11, 12 the neglect of the curvature of meridians has tended to exaggerate the degree of invalidity of Laplace's equations.

For the diurnal constituents, Laplace's equations appear always to give a good approximation in problems which really resemble those of the actual tides.

In the present paper only such problems as may be solved without the use of expansions in infinite series are considered.

3. NEGLECT OF THE ELLIPTICITY OF MERIDIANS

The ellipticity of a meridian section of the mean surface of the ocean depends on $a\omega^2/g$, while the gyrational effects on the tides depend on ω/σ. From a mathematical point of view, these are independent parameters. If in the solution of the equations (1·4) and (1·6) the latter is retained but the former neglected, and the mean free surface of the ocean is taken as $r = a$, a mathematical problem without any mathematical inconsistency is formulated. And as the solution of this simplified problem will have the same general character as that of the more complete problem, consideration will be given only to the simplified problem.

The contribution to the potential V from the constant part of the earth's gravitation and from the centrifugal force of the earth's rotation is taken to be $g(r-a)$, where g is constant.

4. NEGLECT OF THE GRAVITATIONAL ATTRACTION OF THE DISTURBED WATER

By using spherical harmonics, Hough, in his solution of Laplace's equations for an ocean covering the whole earth, was able to allow for the disturbance of the gravitational field produced by the tides themselves. In a similar way and for the same ocean, Solberg, in the solution of his equations, was able to make the same allowance. But when the ocean does not cover the whole earth, the allowance for the gravitational attraction of the disturbed water is a difficult problem, even in the equilibrium theory of the tides (H. Poincaré 1896, 1910; M. Brillouin 1928). No special cases of the equilibrium theory appear yet to have been worked out, though Brillouin's method makes this possible.

As this matter is not one of those which is the subject of controversy, in the present paper the disturbances in the gravitational field produced by the tides themselves are neglected.

5. CONDITIONS AT FREE SURFACE

From (1·5) and the results of §§ 3, 4,

$$P = \frac{p}{\rho} + g(r-a) - gf(r)\,\zeta, \tag{5·1}$$

where $f(r)$ is a given function of r such that $f(a) = 1$.

At the free surface of the ocean

$$r = a+\zeta, \quad p = 0,$$

so that, from (5·1),
$$P = g\{\zeta - f(r)\,\bar{\zeta}\},$$

but on working to the first order of small quantities only

$$P = g\zeta', \quad w = \frac{\partial\zeta}{\partial t}, \tag{5·2}$$

on $r = a$, since $\zeta - \bar{\zeta} = \zeta'$.

In the differential equations (1·4) and the boundary conditions, P enters as a whole. Hence the function $f(r)$ does not affect the determination of P; it only affects the determination of the pressure p.

For the semi-diurnal, diurnal and long-period constituents of the actual tides

$$\left.\begin{aligned} \frac{\bar{\zeta}}{H} &= \sin^2\theta\cos(\sigma t+2\chi), \\ \frac{\bar{\zeta}}{H} &= \sin\theta\cos\theta\cos(\sigma t+\chi), \\ \frac{\bar{\zeta}}{H} &= \tfrac{1}{2}(3\cos^2\theta-1)\cos\sigma t, \end{aligned}\right\} \tag{5·3}$$

respectively, H denoting a constant length appropriate to each case and σ being positive. By taking

$$\frac{\bar{\zeta}}{H} = F(\theta)\cos(\sigma t+s\chi),$$

σ and s being positive, more than one of these constituents may be considered at the same time, and, when $F(\theta)$ does not include the functions of θ in (5·3), it will be a general member of a sequence of functions specially convenient for the basin in question. The assumption is made that the wavelength of the variations of $\bar{\zeta}$ is large compared with the depth of the ocean. This assumption is important, as it is the basis of our contention that Laplace's equations are valid for constituents other than those of semi-diurnal and long periods. It corresponds to the usual criterion for long waves, and it is only for such motion that Laplace's equations have ever been assumed to hold.

6. HARMONIC MOTION

For harmonic oscillations of period $2\pi/\sigma$ in which t enters only through $e^{i\sigma t}$ Laplace's equations (1·2) yield

$$\left.\begin{aligned} \frac{i\sigma}{g}u &= \frac{-1}{a\left(1-\dfrac{4\omega^2}{\sigma^2}\cos^2\theta\right)}\left(\frac{\partial\zeta'}{\partial\theta}+\frac{2\omega\cos\theta}{i\sigma\sin\theta}\frac{\partial\zeta'}{\partial\chi}\right), \\ \frac{i\sigma}{g}v &= \frac{-1}{a\left(1-\dfrac{4\omega^2}{\sigma^2}\cos^2\theta\right)}\left(\frac{1}{\sin\theta}\frac{\partial\zeta'}{\partial\chi}-\frac{2\omega}{i\sigma}\cos\theta\frac{\partial\zeta'}{\partial\theta}\right), \end{aligned}\right\} \tag{6·1}$$

and then on substituting into the equation of continuity (1·3),

$$\begin{aligned} \frac{1}{\sin\theta}\Bigg\{&\frac{\partial}{\partial\theta}\left(\frac{h\sin\theta}{1-\dfrac{4\omega^2}{\sigma^2}\cos^2\theta}\frac{\partial\zeta'}{\partial\theta}\right)+\frac{1}{\sin\theta}\frac{\partial}{\partial\chi}\left(\frac{h}{1-\dfrac{4\omega^2}{\sigma^2}\cos^2\theta}\frac{\partial\zeta'}{\partial\chi}\right) \\ &+\frac{2\omega}{i\sigma}\left[\frac{\partial}{\partial\theta}\left(\frac{h\cos\theta}{1-\dfrac{4\omega^2}{\sigma^2}\cos^2\theta}\right)\frac{\partial\zeta'}{\partial\chi}-\frac{\partial}{\partial\chi}\left(\frac{h\cos\theta}{1-\dfrac{4\omega^2}{\sigma^2}\cos^2\theta}\right)\frac{\partial\zeta}{\partial\theta}\right]\Bigg\}+\frac{\sigma^2a^2}{g}\zeta = 0. \end{aligned} \tag{6·2}$$

When $\sigma^2 \neq 4\omega^2$, a similar procedure may be followed with the equations (1·4) and (1·6). The equations (1·4) can be solved algebraically so as to give u, v and w in terms of $\partial P/\partial\theta$, $\partial P/\partial\chi$ and $\partial P/\partial r$. The conditions at the ocean bottom, at the surface, and at the coasts can then be expressed in terms of P and of these same derivatives. On substituting into the equation of continuity (1·6), a differential equation of the second order is obtained for P, to be satisfied through the body of the whole ocean. These conditions are sufficient to determine P, u, v, w, ζ and p.

When $\sigma^2 = 4\omega^2$, there is a linear relation between $\partial P/\partial\theta$, $\partial P/\partial\chi$ and $\partial P/\partial r$. To determine u, v and w use must be made of two of the equations (1·4) and the equation (1·6).

The procedure may be illustrated more concisely in cylindrical co-ordinates, and in fact much use will be made of these co-ordinates. Denoting them by ϖ, χ and z with the axis that of the earth, the equations of motion may be written as

$$\left.\begin{aligned} \frac{\partial u}{\partial t}-2\omega v &= -\frac{\partial P}{\partial\varpi}, \\ \frac{\partial v}{\partial t}+2\omega u &= -\frac{1}{\varpi}\frac{\partial P}{\partial\chi}, \\ \frac{\partial w}{\partial t} &= -\frac{\partial P}{\partial z}. \end{aligned}\right\} \tag{6·3}$$

Using the time factor $e^{i\sigma t}$, it is deduced that, when $\sigma^2 \neq 4\omega^2$,

$$\left.\begin{aligned} u &= \frac{i\sigma}{\sigma^2-4\omega^2}\left(\frac{\partial P}{\partial \varpi}+\frac{2\omega}{i\sigma}\frac{1}{\varpi}\frac{\partial P}{\partial \chi}\right), \\ v &= \frac{i\sigma}{\sigma^2-4\omega^2}\left(\frac{1}{\varpi}\frac{\partial P}{\partial \chi}-\frac{2\omega}{i\sigma}\frac{\partial P}{\partial \varpi}\right), \\ w &= -\frac{1}{i\sigma}\frac{\partial P}{\partial z}. \end{aligned}\right\} \tag{6·4}$$

The equation of continuity may be written as

$$\frac{1}{\varpi}\frac{\partial}{\partial \varpi}(\varpi u)+\frac{1}{\varpi}\frac{\partial v}{\partial \chi}+\frac{\partial w}{\partial z} = 0, \tag{6·5}$$

and on substituting from (6·4)

$$\frac{1}{\varpi}\frac{\partial}{\partial \varpi}\left(\varpi\frac{\partial P}{\partial \varpi}\right)+\frac{1}{\varpi^2}\frac{\partial^2 P}{\partial \chi^2}+\left(1-\frac{4\omega^2}{\sigma^2}\right)\frac{\partial P}{\partial z^2} = 0. \tag{6·6}$$

When $\sigma = 2\omega$, it follows from (6·3) or from (6·4), that

$$\varpi\frac{\partial P}{\partial \varpi}-i\frac{\partial P}{\partial \chi} = 0, \tag{6·7}$$

and the equation (6·6) may then be written

$$\left(\varpi\frac{\partial}{\partial \varpi}+i\frac{\partial}{\partial \chi}\right)\left(\varpi\frac{\partial P}{\partial \varpi}-i\frac{\partial P}{\partial \chi}\right) = 0.$$

Also, from (6·3) and (6·5),

$$\frac{\partial}{\partial \varpi}(\varpi u)+i\frac{\partial u}{\partial \chi} = -\frac{i}{\sigma}\left\{\frac{1}{\varpi}\frac{\partial^2 P}{\partial \chi^2}+\varpi\frac{\partial^2 P}{\partial z^2}\right\}. \tag{6·8}$$

7. THE POSSIBILITY OF CELLULAR OSCILLATIONS

Since the depth of the ocean is very small compared with its lateral dimensions, cellular oscillations can only occur when the wave-length of the undulations of P in the vertical direction is very much smaller than the wave-length of these undulations in the horizontal direction. For the possibility of this we examine the equation (6·6), and notice that it depends on very small or very large values of $1-4\omega^2/\sigma^2$.

Near the poles the vertical co-ordinate is z and $\partial^2 P/\partial z^2$ must be large compared with

$$\frac{1}{\varpi}\frac{\partial}{\partial \varpi}\left(\varpi\frac{\partial P}{\partial \varpi}\right). \tag{7·1}$$

This will be the case when $1-4\omega^2/\sigma^2$ is very small, unless

$$\frac{1}{\varpi}\frac{\partial}{\partial\varpi}\left(\varpi\frac{\partial P}{\partial\varpi}\right)+\frac{1}{\varpi^2}\frac{\partial^2 P}{\partial\chi^2} \tag{7·2}$$

is also very small. The matter is examined in detail in §§ 11 and 13.

Near the equator the vertical co-ordinate is ϖ, and for cellular oscillations (7·1) must be very large compared with $\partial^2P/\partial z^2$. This may be the case when $4\omega^2/\sigma^2$ is very large, so that the tides are of long period. The matter is examined in detail in §§ 12 and 14.

For other latitudes and other constituents cellular oscillations do not appear to be possible.

8. LAPLACE'S PARTICULAR INTEGRAL FOR THE CONSTITUENT K_1

When the depth is uniform and $\sigma=\omega$ the equations (1·4), (1·6) and the conditions at the bottom and at the free surface of the ocean are satisfied by

$$\frac{\bar{\zeta}}{H}=\sin\theta\cos\theta\cos(\sigma t+\chi),$$

$$\frac{P}{gH}=-\left(\frac{r}{a}\right)^2\sin\theta\cos\theta\cos(\sigma t+\chi),$$

$$\frac{\sigma a}{gH}u=-\frac{r}{a}\sin(\sigma t+\chi),$$

$$\frac{\sigma a}{gH}v=-\frac{r}{a}\cos\theta\cos(\sigma t+\chi),$$

$$w=0,\quad \zeta=0.$$

As there is zero vertical component of current at all levels, it is clear that the above expressions, with $r=a$, $P=g\zeta'$, also satisfy Laplace's equations; and in fact this is the solution of his equations given by Laplace himself, in which there is no rise and fall of the ocean surface.

Of course the satisfaction of coastal conditions requires the addition of complementary functions which, in general, do involve a rise and fall of the ocean surface.

9. NARROW OCEAN BOUNDED BY MERIDIANS

Consider now a basin of uniform depth h bounded by two meridians which are so near together that there are no transverse currents. Take

$$\frac{\bar{\zeta}}{H} = P_n(\cos\theta)\cos\sigma t, \tag{9·1}$$

where $P_n(\ )$ denotes Legendre's polynomial of integral order n.

On writing $v = 0$ and $\partial v/\partial\chi = 0$ in the equations (1·4) and (1·6), and then on eliminating u and w, it follows that

$$\frac{1}{\sin\theta}\frac{\partial}{\partial\theta}\left(\sin\theta\frac{\partial P}{\partial\theta}\right) + \frac{\partial}{\partial r}\left(r^2\frac{\partial P}{\partial r}\right) = 0, \tag{9·2}$$

an equation which does not contain ω. The solution of all the conditions is given by

$$\left.\begin{aligned}
\frac{P}{gA} &= \left\{\left(\frac{r}{a}\right)^n + \frac{n}{n+1}\left(1-\frac{h}{a}\right)^{2n+1}\left(\frac{a}{r}\right)^{n+1}\right\} P_n(\cos\theta)\cos\sigma t,\\
\frac{u}{\sigma A} &= -\frac{g}{\sigma^2 a}\left\{\left(\frac{r}{a}\right)^{n-1} + \frac{n}{n+1}\left(1-\frac{h}{a}\right)^{2n+1}\left(\frac{a}{r}\right)^{n+2}\right\}\frac{d}{d\theta}P_n(\cos\theta)\sin\sigma t,\\
\frac{w}{\sigma A} &= -\frac{g}{\sigma^2 a}n\left\{\left(\frac{r}{a}\right)^{n-1} - \left(1-\frac{h}{a}\right)^{2n+1}\left(\frac{a}{r}\right)^{n+2}\right\} P_n(\cos\theta)\sin\sigma t,
\end{aligned}\right\} \tag{9·3}$$

where $\qquad \dfrac{H}{A} = n\left\{1-\left(1-\dfrac{h}{a}\right)^{2n+1}\right\}\dfrac{g}{\sigma^2 a} - 1 - \dfrac{n}{n+1}\left(1-\dfrac{h}{a}\right)^{2n+1}.$

When h/a is small, (9·3) gives, to the first order, on $r = a$ and in view of (5·2),

$$\left.\begin{aligned}
\frac{\zeta'}{A'} &= P_n(\cos\theta)\cos\sigma t,\\
\frac{u}{\sigma A'} &= -\frac{g}{\sigma^2 a}\frac{d}{d\theta}P_n(\cos\theta)\sin\sigma t,\\
\frac{w}{\sigma A'} &= -\frac{gh}{\sigma^2 a^2}n(n+1)P_n(\cos\theta)\sin\sigma t,
\end{aligned}\right\} \tag{9·4}$$

where $\qquad \dfrac{H}{A'} = n(n+1)\dfrac{gh}{\sigma^2 a^2} - 1.$

On writing $v = 0$ in Laplace's equations (1·2) and (1·3), and eliminating u, the equation

$$\frac{gh}{\sigma^2 a}\frac{1}{\sin\theta}\frac{\partial}{\partial\theta}\left(\sin\theta\frac{\partial\zeta'}{\partial\theta}\right) + \zeta' = -\bar{\zeta}, \tag{9·5}$$

is obtained. The solution of this equation and the corresponding expressions for u and w are given by (9·4), so that Laplace's equations are valid.

It follows from the first of (9·3) on $r = a$, that

$$\frac{\zeta'}{H} = \frac{P_n(\cos\theta)\cos\sigma t}{q\dfrac{g}{\sigma^2 a} - 1},$$

where q is a known function of h/a. Denoting by q_0 the corresponding part of (9·4), viz. $n(n+1)h/a$, the magnitude of $q/q_0 - 1$ may be used as a measure of the degree of approximation afforded by the solution of Laplace's equations. Now

$$\frac{q}{q_0} - 1 = \frac{\left\{1 - \left(1 - \dfrac{h}{a}\right)^{2n+1}\right\}\dfrac{a}{h}}{n + 1 + n\left(1 - \dfrac{h}{a}\right)^{2n+1}} - 1,$$

and when h/a is small, the principal part of this is

$$-\tfrac{1}{3}n(n+1)\frac{h^2}{a^2}.$$

10. CANAL ALONG PARALLEL OF LATITUDE

Next consider a canal of uniform rectangular section along the parallel of latitude, for which $\theta = \alpha$, and suppose that it is so narrow that there are no transverse currents. Then

$$\frac{\bar{\zeta}}{H} = \cos(\sigma t + s\chi), \tag{10·1}$$

and there is no point in including the case of $s = 0$, as there would then be zero tide-generating forces along the canal. As this rules out cases of long-period constituents no large values of $2\omega/\sigma$ occur.

On writing $u = 0$ and $\partial u/\partial\theta = 0$ in the equations (1·4) and (1·6), and on eliminating v and w, the equation

$$\frac{\partial}{\partial r}\left(r^2\frac{\partial P}{\partial r}\right) + \left(\frac{2s\omega}{\sigma} - \frac{s^2}{\sin^2\alpha}\right)P = 0, \tag{10·2}$$

is obtained, provided that $\sigma^2 \neq 4\omega^2\sin^2\alpha$. On writing

$$\frac{2s\omega}{\sigma} - \frac{s^2}{\sin^2\alpha} = -n(n+1), \tag{10·3}$$

the solution takes the form

$$\left.\begin{aligned}\frac{P}{gA} &= \left\{-\left[1-\frac{(n+1)^2\sin^2\alpha}{s^2}\right]\left(\frac{r}{a}\right)^n+\left[1-\frac{n^2\sin^2\alpha}{s^2}\right]\left(1-\frac{h}{a}\right)^{2n+1}\left(\frac{a}{r}\right)^{n+1}\right\}\\ &\qquad\times\cos(\sigma t+s\chi),\\ \frac{v}{\sigma A} &= -\frac{g}{\sigma^2 a}\frac{\sin\alpha}{s}\left\{(n+1)\left(\frac{r}{a}\right)^{n-1}+n\left(1-\frac{h}{a}\right)^{2n+1}\left(\frac{a}{r}\right)^{n+2}\right\}\cos(\sigma t+s\chi),\\ \frac{w}{\sigma A} &= -\frac{g}{\sigma^2 a}\left\{\left(\frac{r}{a}\right)^{n-1}-\left(1-\frac{h}{a}\right)^{2n+1}\left(\frac{a}{r}\right)^{n+2}\right\}\sin(\sigma t+s\chi),\end{aligned}\right\} \tag{10·4}$$

where

$$\frac{H}{A}=\left\{1-\left(1-\frac{h}{a}\right)^{2n+1}\right\}\frac{g}{\sigma^2 a}+1-\frac{(n+1)^2\sin^2\alpha}{s^2}-\left(1-\frac{n^2\sin^2\alpha}{s^2}\right)\left(1-\frac{h}{a}\right)^{2n+1}.$$

In obtaining the expressions for v and w in (10·4), the factor $\sigma^2-4\omega^2\sin^2\alpha$ has been removed from both numerators and denominators, so that these expressions are determinate when $\sigma=2\omega\sin\alpha$. On starting with $\sigma=2\omega\sin\alpha$, and applying the special method indicated in § 6, the same expressions are obtained directly.

When h/a is small, (10·4) becomes, on $r=a$, and in view of (5·2),

$$\left.\begin{aligned}\frac{\zeta'}{A'} &= \cos(\sigma t+s\chi),\\ \frac{v}{\sigma A'} &= -\frac{s}{\sin\alpha}\frac{g}{\sigma^2 a}\cos(\sigma t+s\chi),\\ \frac{w}{\sigma A'} &= -\frac{s^2}{\sin^2\alpha}\frac{gh}{\sigma^2 a^2}\sin(\sigma t+s\chi),\end{aligned}\right\} \tag{10·5}$$

where
$$\frac{H}{A'}=\frac{s^2}{\sin^2\alpha}\frac{gh}{\sigma^2 a^2}-1,$$

and these expressions are identical with those obtained by solving Laplace's equations (1·2) and (1·3) after writing $u=0$.

It follows from the first of (10·4), on $r=a$, that

$$\frac{\zeta'}{H}=\frac{\cos(\sigma t+s\chi)}{q\dfrac{g}{\sigma^2 a}-1},$$

and on writing the first of (10·5) in the same form with q_0 for q,

$$\frac{q}{q_0}-1=\frac{\left\{1-\left(1-\dfrac{h}{a}\right)^{2n+1}\right\}\dfrac{\sin^2\alpha}{s^2}\dfrac{a}{h}}{-1+(n+1)^2\dfrac{\sin^2\alpha}{s^2}+\left(1-\dfrac{n^2\sin^2\alpha}{s^2}\right)\left(1-\dfrac{h}{a}\right)^{2n+1}}-1.$$

When h/a is small, the principal part of this is

$$\frac{q}{q_0}-1=\left\{\frac{s^2}{\sin^2\alpha}-n(n+1)\right\}\frac{h}{a}=\frac{2s\omega}{\sigma}\frac{h}{a},$$

and this gives a measure of the degree of approximation afforded by the solution of Laplace's equations.

11. FLAT CIRCULAR SEA

Consider next a sea of uniform depth bounded by a parallel of latitude which is so near to the North Pole that the earth's curvature may be neglected. Using the cylindrical co-ordinates ϖ, χ and z the coast is given by $\varpi = c$, the mean sea surface by $z = 0$, and the sea bottom by $z = -h$.

The equation (6·6) has a solution of the form

$$\frac{P}{gA}=J_s(\kappa\varpi)\cos\lambda\kappa(z+h)\cos(\sigma t+s\chi), \tag{11·1}$$

where A is a constant length, κ a constant reciprocal length and

$$\lambda=\left(\frac{4\omega^2}{\sigma^2}-1\right)^{-\frac{1}{2}}.$$

Then from (6·4) it follows that

$$\left.\begin{aligned}\frac{u}{\sigma A}&=\frac{\kappa g\lambda^2}{\sigma^2}\left\{J_s'(\kappa\varpi)+\frac{2s\omega}{\sigma}\frac{J_s(\kappa\varpi)}{\kappa\varpi}\right\}\cos\lambda\kappa(z+h)\sin(\sigma t+s\chi),\\ \frac{v}{\sigma A}&=\frac{\kappa g\lambda^2}{\sigma^2}\left\{\frac{2\omega}{\sigma}J_s'(\kappa\varpi)+\frac{sJ_s(\kappa\varpi)}{\kappa\varpi}\right\}\cos\lambda\kappa(z+h)\cos(\sigma t+s\chi),\\ \frac{w}{\sigma A}&=\frac{\kappa g\lambda}{\sigma^2}J_s(\kappa\varpi)\sin\lambda\kappa(z+h)\sin(\sigma t+s\chi).\end{aligned}\right\} \tag{11·2}$$

From (11·2) it is seen that the condition $w = 0$ at the sea bottom $z = -h$ is satisfied; also that the condition $u = 0$ at the coast $\varpi = c$ will be satisfied if

$$\kappa c J_s'(\kappa c)+\frac{2s\omega}{\sigma}J_s(\kappa c)=0. \tag{11·3}$$

This equation determines κ, and the simplest distribution for a prescribed value of s will be given by the lowest root of (11·3). The conditions (5·2) at the free surface $z = 0$ give

$$\frac{\zeta}{A}=-\left(\frac{\lambda\kappa g}{\sigma^2}\sin\lambda\kappa h+\cos\lambda\kappa h\right)J_s(\kappa\varpi)\cos(\sigma t+s\chi),$$

so that if
$$\frac{\zeta}{H} = J_s(\kappa\varpi)\cos(\sigma t + s\chi), \tag{11·4}$$

then
$$-\frac{H}{A} = \frac{\lambda\kappa g}{\sigma^2}\sin\lambda\kappa h + \cos\lambda\kappa h. \tag{11·5}$$

When $\lambda\kappa h$ is real and sufficiently large, the expressions (11·2) and (11·5) show that cellular oscillations will occur.

When $\lambda\kappa h$ is small, it follows that

$$\left.\begin{aligned} \frac{P}{gA'} &= -J_s(\kappa\varpi)\left\{\frac{4\omega^2-\sigma^2}{\kappa g} - \frac{\sigma^2\kappa}{g}(\tfrac{1}{2}z^2+zh)\right\}\cos(\sigma t+s\chi),\\ \frac{u}{\sigma A'} &= -\left\{J_s'(\kappa\varpi) + \frac{2s\omega}{\sigma}\frac{J_s(\kappa\varpi)}{\kappa\varpi}\right\}\sin(\sigma t+s\chi),\\ \frac{v}{\sigma A'} &= -\left\{\frac{2\omega}{\sigma}J_s'(\kappa\varpi) + s\frac{J_s(\kappa\varpi)}{\kappa\varpi}\right\}\cos(\sigma t+s\chi),\\ \frac{w}{\sigma A'} &= -J_s(\kappa\varpi)\,\kappa(z+h)\sin(\sigma t+s\chi), \end{aligned}\right\} \tag{11·6}$$

where
$$\frac{H}{A'} = \kappa h + \frac{4\omega^2-\sigma^2}{\kappa g},$$

and when $z = 0$ these expressions are identical with those obtained by solving Laplace's equations.

From (11·1) on $z = 0$, and (11·5)

$$\frac{\zeta'}{H} = \frac{J_s(\kappa\varpi)\cos(\sigma t+s\chi)}{q\dfrac{\kappa g}{\sigma^2} - 1},$$

and on writing the first of (11·6) in the same form with q_0 for q, we have

$$\frac{q}{q_0} - 1 = \frac{\tan\lambda\kappa h}{\lambda\kappa h} - 1$$

as a measure of the degree of approximation afforded by the solution of Laplace's equations. When $\lambda\kappa h$ is small, the principal part of $q/q_0 - 1$ is $\frac{1}{3}(\lambda\kappa h)^2$.

For the long-period constituents $\sigma/2\omega$ is small, so that λ is small; also $s = 0$, and then the lowest value of κc is 3·83. Taking $c/h = 100$, then $\kappa h = 0{\cdot}0383$, and Laplace's equations give a very high degree of approximation. For the limiting case in which $\sigma \to 0$ and $\lambda \to 0$, the solution given by (11·1), (11·2) and (11·5) becomes identical with that given by (11·6).

For the constituent K_1, $\sigma = \omega$ so that $\lambda = 0{\cdot}5774$, and $s = 1$, so that the lowest value of κc is 1·84. Again taking $c/h = 100$, then $\lambda\kappa h = 0{\cdot}0106$, and again Laplace's equations give a high degree of approximation.

For the constituent K_2, $s = 2$, and $\lambda \rightarrow \infty$. Then from (11·1), (11·2) and (11·5) it is deduced that P tends to vanish while u and v tend to become infinite; but of course at $z = 0$,

$$\frac{w}{\sigma H} = \frac{1}{\sigma H}\frac{\partial \zeta}{\partial t} = -J_2(\kappa\varpi)\sin(\sigma t + 2\chi).$$

On starting with $\sigma = 2\omega$, (6·7) gives

$$\frac{\partial P}{\partial \varpi} = -2\frac{P}{\varpi},$$

and as the solution of this is

$$P = \left(\frac{c}{\varpi}\right)^2 F(z),$$

it follows that, for finiteness at $\varpi = 0$, $F(z) = 0$. Then $P = 0$ and $w = 0$, so that the conditions (5·2) at the free surface cannot be satisfied. The situation is analogous to that of resonance, in that a boundary condition involving finite elements can only be satisfied by a distribution involving infinite elements. This impossibility of providing, by a finite distribution, the necessary vertical currents at the free surface when λ is infinite, throws a light on the part played by the vertical currents of the cellular oscillations when λ is large.

From the solution (11·6) with $s = 2$, it is seen that, as $\sigma \rightarrow 2\omega$, and κh remains finite

$$\left.\begin{aligned}
\frac{P}{gH} &= J_2(\kappa\varpi)\frac{\sigma^2}{gh}(\tfrac{1}{2}z^2 + zh)\,.\cos(\sigma t + 2\chi),\\
\frac{u}{\sigma H} &= -\frac{1}{\kappa h}\left\{J_2'(\kappa\varpi) + 2\frac{J_2(\kappa\varpi)}{\kappa\varpi}\right\}\sin(\sigma t + 2\chi),\\
\frac{v}{\sigma H} &= -\frac{1}{\kappa h}\left\{J_2'(\kappa\varpi) + 2\frac{J_2(\kappa\varpi)}{\kappa\varpi}\right\}\cos(\sigma t + 2\chi),\\
\frac{w}{\sigma H} &= -J_2(\kappa\varpi)\left(\frac{z}{h} + 1\right)\sin(\sigma t + 2\chi).
\end{aligned}\right| \qquad (11{\cdot}7)$$

In order that these expressions may satisfy the fundamental equations and conditions, it is necessary, according to the different orders of magnitude involved, sometimes to retain P and sometimes to neglect it.

On starting with $\sigma = 2\omega$ in Laplace's equations the same solution with $z = 0$ is obtained. The expressions (11·7) are the result of first taking $\lambda\kappa h$ small with λ finite and then of making $\lambda \to \infty$, and this corresponds to the procedure offered by Laplace's equations. But the conditions of the physical problem require that $\lambda \to \infty$ with κh finite though small, and to this it has been seen that there is no definite solution. Hence for the K_2 constituent, Laplace's equations give a definite solution when the more general equations show that one does not exist. If the curvature of the meridians had been neglected in (5·3) as well as in (1·4) it would have followed that $\bar{\zeta} = 0$ and not (11·4); both Laplace's equations and the more general ones would then have given the same zero solution.

12. BROAD EQUATORIAL CHANNEL

Consider now a channel of uniform rectangular section along the equator, and suppose that it is sufficiently broad to admit of transverse currents. The equations will be simplified by supposing that in the neighbourhood of the channel the earth is cylindrical with gravity perpendicular to its axis. Cylindrical co-ordinates will be used and also

$$\frac{\bar{\zeta}}{H} = \cos kz \cos(\sigma t + s\chi), \tag{12·1}$$

where s is an integer and k is a constant such that at the sides of the channel $\sin kz = 0$. The case of $k = 0$ is not included, as this would exclude transverse currents and merely reproduce the problem of § 10 with $\alpha = \frac{1}{2}\pi$. If the coasts of the channel are given by $z = 0$, $z = b$, it follows that $kb = n\pi$, where n is an integer. But in order to prevent the wave-length of $\bar{\zeta}$ from being of the order of the depth h, n must not be too large. The assumption that kh is small, a consequence of that made in § 5, is important, because it rules out the possibility of cellular oscillations except for long-period constituents.

The appropriate solution of the equation (6·6) is given by

$$\frac{P}{gH} = F(\varpi) \cos kz \cos(\sigma t + s\chi), \tag{12·2}$$

where $F(\varpi)$ satisfies the Bessel's equation:

$$\frac{1}{\varpi}\frac{d}{d\varpi}\left(\varpi\frac{dF}{d\varpi}\right) + \left\{\left(\frac{4\omega^2}{\sigma^2} - 1\right)k^2 - \frac{s^2}{\varpi^2}\right\} F = 0.$$

Then, from (6·4),

$$\left.\begin{aligned}\frac{u}{\sigma H} &= \frac{-g}{\sigma^2-4\omega^2}\left(\frac{dF}{d\varpi}+\frac{2s\omega}{\sigma}\frac{F}{\varpi}\right)\cos kz\sin(\sigma t+s\chi),\\ \frac{v}{\sigma H} &= \frac{-g}{\sigma^2-4\omega^2}\left(\frac{2\omega}{\sigma}\frac{dF}{d\varpi}+s\frac{F}{\varpi}\right)\cos kz\cos(\sigma t+s\chi),\\ \frac{w}{\sigma H} &= \frac{gk}{\sigma^2}F\sin kz\sin(\sigma t+s\chi),\end{aligned}\right\} \tag{12·3}$$

with
$$\frac{dF}{d\varpi}+\frac{2s\omega}{\sigma}\frac{F}{\varpi}=0 \quad (\varpi=a-h),$$

and
$$\frac{g}{\sigma^2-4\omega^2}\left(\frac{dF}{d\varpi}+\frac{2s\omega}{\sigma}\frac{F}{\varpi}\right)=F+1 \quad (\varpi=a),$$

in order to satisfy the conditions at the bottom and the free surface. At the bottom $\varpi=a-h$, it follows that $u=0$, and

$$\frac{v}{\sigma H}=-\frac{sg}{\sigma^2}\frac{F(a-h)}{a-h}\cos kz\cos(\sigma t+s\chi), \tag{12·31}$$

while at the free surface $\varpi=a$,

$$\left.\begin{aligned}\frac{u}{\sigma H} &= -\{F(a)+1\}\cos kz\sin(\sigma t+s\chi),\\ \frac{v}{\sigma H} &= -\left\{\frac{sg}{\sigma^2 a}F(a)+\frac{2\omega}{\sigma}[F(a)+1]\right\}\cos kz\cos(\sigma t+s\chi).\end{aligned}\right\} \tag{12·32}$$

When h/a is so small that it is only necessary to retain the first term of the Taylor expansion of

$$\varpi\frac{dF}{d\varpi}+\frac{2s\omega}{\sigma}F,$$

this function may be taken as

$$h\frac{d}{d\varpi}\left(\varpi\frac{dF}{d\varpi}+\frac{2s\omega}{\sigma}F\right)$$

or
$$h\left(1-\frac{4\omega^2}{\sigma^2}\right)(s^2+k^2a^2)\frac{F(a)}{a}$$

at $\varpi=a$. Then
$$\frac{1}{F(a)}=(s^2+k^2a^2)\frac{gh}{\sigma^2a^2}-1, \tag{12·4}$$

but it is clear that this can only be valid in the absence of cellular oscillations. Under the same condition and to the same order, $F(a-h)/(a-h)$ may be replaced by $F(a)/a$ in (12·31) and the term involving $F(a)+1$ omitted in the expression for v in (12·32), so that the expressions for v in (12·31) and (12·32) become the same. On substituting (12·4) in (12·2), in the third equation of (12·3) and in (12·32), expressions identical with those obtained by solving Laplace's equations are obtained.

The Bessel's equation may be written in the form

$$\frac{d^2}{d\varpi^2}(\varpi^{\frac{1}{2}} F)+\left\{\left(\frac{4\omega^2}{\sigma^2}-1\right)k^2-\frac{s^2-\frac{1}{4}}{\varpi^2}\right\}(\varpi^{\frac{1}{2}} F)=0,$$

and on neglecting the variations of $(s^2-\frac{1}{4})/\varpi^2$, it follows that

$$\frac{d^2}{d\varpi^2}(\varpi^{\frac{1}{2}} F)+\kappa^2(\varpi^{\frac{1}{2}} F)=0, \tag{12·5}$$

where
$$\kappa^2=\left(\frac{4\omega^2}{\sigma^2}-1\right)k^2-\frac{s^2-\frac{1}{4}}{a^2}.$$

Then

$$F(\varpi)=\frac{(a/\varpi)^{\frac{1}{2}}\{\kappa(a-h)\cos\kappa(\varpi-a+h)-\gamma\sin\kappa(\varpi-a+h)\}}{\{\gamma\kappa h\cos\kappa h+[\gamma^2+\kappa^2a(a-h)]\sin\kappa h\}\dfrac{g/a}{4\omega^2-\sigma^2}-\kappa(a-h)\cos\kappa h+\gamma\sin\kappa h}, \tag{12·6}$$

where
$$\gamma=\frac{2s\omega}{\sigma}-\tfrac{1}{2},$$

the form of which indicates the possibility of cellular oscillations. When κh is small, $F(a)$, as given by (12·6), reduces to Laplace's solution (12·4), but again it is clear that this excludes cellular oscillations.

For the constituent K_2, $s=2$, and when in (12·2) and (12·3), $\sigma\rightarrow 2\omega$, it is found, after some reduction, that

$$\left.\begin{aligned}
\frac{P}{gA}&=\left(\frac{a}{\varpi}\right)^2\cos kz\cos(\sigma t+2\chi),\\
\frac{u}{\sigma A}&=\frac{g}{4\omega^2a}\left\{\left(\frac{a}{\varpi}\right)^3+\tfrac{1}{2}k^2a^2\left(\frac{a}{\varpi}\right)-\left[\left(1-\frac{h}{a}\right)^{-4}+\tfrac{1}{2}k^2a^2\left(1-\frac{h}{a}\right)^{-2}\right]\frac{\varpi}{a}\right\}\cos kz\sin(\sigma t+2\chi),\\
\frac{v}{\sigma A}&=\frac{g}{4\omega^2a}\left\{-\left(\frac{a}{\varpi}\right)^3+\tfrac{1}{2}k^2a^2\left(\frac{a}{\varpi}\right)-\left[\left(1-\frac{h}{a}\right)^{-4}+\tfrac{1}{2}k^2a^2\left(1-\frac{h}{a}\right)^{-2}\right]\frac{\varpi}{a}\right\}\cos kz\cos(\sigma t+2\chi),\\
\frac{w}{\sigma A}&=\frac{kg}{\sigma^2}\left(\frac{a}{\varpi}\right)^2\sin kz\sin(\sigma t+2\chi),
\end{aligned}\right\} \tag{12·7}$$

where
$$\frac{H}{A}=\left\{\left(1-\frac{h}{a}\right)^{-4}-1+\tfrac{1}{2}k^2a^2\left[\left(1-\frac{h}{a}\right)^{-2}-1\right]\right\}\frac{g}{4\omega^2a}-1.$$

On starting with $s = 2$ and $\sigma = 2\omega$, and on using the equations (6·7) and (6·8) the result (12·7) is obtained directly. It is clear that (12·7) does not admit of cellular oscillations, and when h/a is small it reduces to Laplace's solution (12·4). From the first of (12·7) on $\varpi = a$

$$\frac{\zeta'}{H} = \frac{\cos kz \cos(\sigma t + 2\chi)}{q\dfrac{g}{4\omega^2 a} - 1}$$

and on writing Laplace's solution in the same form with q_0 for q, we have

$$\frac{q}{q_0} - 1 = \frac{\left(1 - \dfrac{h}{a}\right)^{-4} - 1 + \frac{1}{2}k^2a^2\left[\left(1 - \dfrac{h}{a}\right)^{-2} - 1\right]}{(4 + k^2a^2)\dfrac{h}{a}} - 1$$

as a measure of the degree of approximation afforded by Laplace's solution. When h/a is small, the principal part is given by

$$\frac{q}{q_0} - 1 = \frac{20 + 3k^2a^2}{8 + 2k^2a^2}\frac{h}{a}.$$

For the constituent K_1, $s = 1$ and $\sigma = \omega$, so that

$$\tfrac{1}{3}\kappa^2a^2 = k^2a^2 - \tfrac{1}{4}, \quad \gamma = \tfrac{3}{2}.$$

As kh is small, κh is also small, and cellular oscillations do not occur. Treating (12·4) and (12·6) as before,

$$\frac{q}{q_0} - 1 = \frac{\{\frac{1}{2}\kappa h \cos \kappa h + [\frac{3}{4} + \frac{1}{3}\kappa^2 a(a-h)] \sin \kappa h\}\dfrac{a}{h}}{\{\kappa(a-h)\cos \kappa h - \frac{3}{2}\sin \kappa h\}(1 + k^2a^2)} - 1,$$

the principal part of which is

$$\frac{q}{q_0} - 1 = \frac{11 + 6k^2a^2}{4 + 4k^2a^2}\frac{h}{a}.$$

For long-period constituents, $s = 0$, so that $\gamma = -\frac{1}{2}$; and $2\omega/\sigma$ is large, so that

$$\kappa = \frac{2\omega}{\sigma}k.$$

It is then seen from (12·6), that, to the first order,

$$\left.\begin{aligned}\frac{P}{gA} &= \frac{2\omega\sigma}{kg}\left(\frac{a}{\varpi}\right)^{\frac{1}{2}}\cos\frac{2\omega k}{\sigma}(\varpi-a+h)\cos kz\cos\sigma t,\\ \frac{u}{\sigma A} &= -\left(\frac{a}{\varpi}\right)^{\frac{1}{2}}\sin\frac{2\omega k}{\sigma}(\varpi-a+h)\cos kz\sin\sigma t,\\ \frac{v}{\sigma A} &= -\frac{2\omega}{\sigma}\left(\frac{a}{\varpi}\right)^{\frac{1}{2}}\sin\frac{2\omega k}{\sigma}(\varpi-a+h)\cos kz\cos\sigma t,\\ \frac{w}{\sigma A} &= \frac{2\omega}{\sigma}\left(\frac{a}{\varpi}\right)^{\frac{1}{2}}\cos\frac{2\omega k}{\sigma}(\varpi-a+h)\sin kz\sin\sigma t,\end{aligned}\right\} \qquad (12{\cdot}8)$$

where $$\frac{H}{A} = \sin\frac{2\omega kh}{\sigma}.$$

The motion given by (12·8) involves cellular oscillations, and when h/a is small the expressions do not reduce to those obtained from Laplace's equations.

When in (12·8), $\sigma \to 0$, no definite limiting motion is obtained. On starting with $\sigma = 0$, the equations (14·1) of a later section are found, but the presence of the factor $\cos kz$ requires $P = 0$ and hence $v = 0$ and $\xi = 0$, ξ denoting the radial displacement. It is then impossible to satisfy the condition $\xi = \zeta$ at the free surface. On making $\sigma \to 0$ in Laplace's solution, it follows that $\zeta' \to 0$, $u \to 0$, $v \to 0$, $w \to 0$ which is the equilibrium solution, and the same result is obtained by putting $\sigma = 0$ in Laplace's differential equations. Hence Laplace's equations give a definite limiting form for the constituents of long period when the more general equations show that one does not exist.

13. THE CONSTITUENT K_2

Consider now an ocean over which the depth is a function of the latitude only. On taking $\sigma = 2\omega$ and supposing that t and χ enter P only through the factor $e^{i(\sigma t+2\chi)}$ the equations (6·3) take the form

$$\left.\begin{aligned}\sigma(iu-v) &= -\frac{\partial P}{\partial \varpi},\\ \sigma(iv+u) &= -2i\frac{P}{\varpi},\\ i\sigma w &= -\frac{\partial P}{\partial z}.\end{aligned}\right\} \qquad (13{\cdot}1)$$

From the first two of these equations it is deduced that

$$P = \left(\frac{a}{\varpi}\right)^2 F\left(\frac{z}{a}\right) e^{i(\sigma t+2\chi)},$$

where $F(\;)$ is a function to be determined. For finiteness at the pole it is necessary that

$$F\left(\frac{z}{a}\right) = 0, \quad \text{for} \quad z \geqslant a - h_0,$$

h_0 being the depth of the ocean at the pole. Write, for shortness,

$$F = F\left(\frac{z}{a}\right), \quad F' = a\frac{d}{dz}F\left(\frac{z}{a}\right), \quad F'' = a^2\frac{d^2}{dz^2}F\left(\frac{z}{a}\right).$$

From the third of (13·1) it is seen that

$$i\sigma a w = -\left(\frac{a}{\varpi}\right)^2 F' e^{i(\sigma t+2\chi)}, \tag{13·2}$$

and on substituting for v and w in the equation of continuity (6·5),

$$i\sigma a\left\{\frac{\partial}{\partial\varpi}(\varpi u) - 2u\right\} = \left\{\left(\frac{a}{\varpi}\right)F'' - 4\left(\frac{a}{\varpi}\right)^3 F\right\} e^{i(\sigma t+2\chi)},$$

so that $$i\sigma a u = \left\{-\frac{1}{2}\left(\frac{a}{\varpi}\right)F'' + \left(\frac{a}{\varpi}\right)^3 F + \left(\frac{\varpi}{a}\right) f\left(\frac{z}{a}\right)\right\} e^{i(\sigma t+2\chi)}, \tag{13·3}$$

where $f(z/a)$ is another function to be determined.

Let ψ denote the downward slope of the ocean bottom in the southerly direction, so that $\tan\psi = dh/ad\theta$. The equation of the bottom may be written as

$$\varpi^2 + z^2 = (a-h)^2,$$

and on the bottom both h and ψ may be regarded as functions of z. Take ϖ_1 such that

$$\varpi_1^2 = (a-h)^2 - z^2.$$

Now the component of current normal to the ocean bottom is

$$u\sin(\theta+\psi) + w\cos(\theta+\psi),$$

and on substituting for u and w in terms of z, the vanishing of this normal component gives

$$f\left(\frac{z}{a}\right) = \frac{1}{2}\left(\frac{a}{\varpi_1}\right)^2 F'' - \left(\frac{a}{\varpi_1}\right)^4 F + \cot(\theta+\psi)\left(\frac{a}{\varpi_1}\right)^3 F', \tag{13·4}$$

for $0 \leqslant z < a - h_0$. At the free surface

$$u \sin\theta + w \cos\theta = i\sigma\zeta, \tag{13·5}$$

so that, from (13·2) and (13·3),

$$\left\{\sin\theta\left[-\frac{1}{2}\left(\frac{a}{\varpi}\right)F'' + \left(\frac{a}{\varpi}\right)^3 F + \left(\frac{\varpi}{a}\right)f\right] - \cos\theta\left(\frac{a}{\varpi}\right)^2 F'\right\} e^{i(\sigma t+2\chi)} + \sigma^2 a\zeta = 0. \tag{13·6}$$

Take $\cos a = 1 - h_0/a$. When $h/a = 1/2000$, $\alpha = 1°·8$.

For $\theta \leqslant \alpha$, $F = 0$, so that from (5·2), (13·2) and (13·3), $\zeta' = 0$, $w = 0$,

$$i\sigma a u = \left(\frac{\varpi}{a}\right) f\left(\frac{z}{a}\right) e^{i(\sigma t+2\chi)},$$

and hence, from (13·6),

$$\sin^2\theta f(\cos\theta)\, e^{i(\sigma t+2\chi)} + \sigma^2 a\zeta = 0.$$

This defines $f(z/a)$ from $z = a - h_0$ to $z = a$, and, in fact, on using the first of (5·3),

$$f\left(\frac{z}{a}\right) = -\sigma^2 a H.$$

It is interesting to compare these relationships near the pole with those for the same constituent in the flat sea of § 11. There the vanishing of w made it impossible to satisfy the condition $w = i\sigma\zeta$, while here the curvature of the earth does make it possible to satisfy the corresponding condition (13·5) through the non-vanishing component u.

Now on $r = a$ it is seen that

$$\begin{aligned}
\frac{F}{g} e^{i(\sigma t+2\chi)} &= \sin^2\theta\zeta', \\
\frac{F'}{g} e^{i(\sigma t+2\chi)} &= -\sin\theta\frac{\partial\zeta'}{\partial\theta} - 2\cos\theta\zeta', \\
\frac{F''}{g} e^{i(\sigma t+2\chi)} &= \frac{\partial^2\zeta'}{\partial\theta^2} + 3\cot\theta\frac{\partial\zeta'}{\partial\theta} - 2\zeta',
\end{aligned}$$

so that, from (13·4) and (13·6)

$$\left.\begin{aligned}
&\frac{1}{2}\left\{\left(\frac{a}{\varpi_1}\right)^2 \sin^2\theta - 1\right\}\left\{\frac{\partial^2\zeta'}{\partial\theta^2} + 3\cot\theta\frac{\partial\zeta'}{\partial\theta} - 2\zeta'\right\} \\
&\quad + \left\{\cot\theta - \frac{a\cos\theta\cos\psi - \varpi_1\sin\psi}{\varpi_1\cos\psi + a\cos\theta\sin\psi}\left(\frac{a}{\varpi_1}\right)^3 \sin^3\theta\right\}\left\{\frac{\partial\zeta'}{\partial\theta} + 2\cot\theta\zeta'\right\} \\
&\quad + \left\{1 - \left(\frac{a}{\varpi_1}\right)^4 \sin^4\theta\right\}\zeta' + \frac{\sigma^2 a}{g}\zeta = 0.
\end{aligned}\right\} \tag{13·7}$$

In (13·7) h, which enters through ϖ_1, and ψ, regarded as functions of θ, correspond to that circle of the ocean bottom for which $z = a\cos\theta$. As $\theta \to \alpha$, $\zeta' \to 0$, and the remaining boundary condition is obtained from the coastal condition or that at the other pole. If the ocean does not extend to either pole, then both boundary conditions are obtained from the coastal conditions. As $\theta \to \alpha$, it is seen from (13·7) that it is possible to have

$$\frac{\partial\zeta'}{\partial\theta} \to 0, \quad \frac{\partial^2\zeta}{\partial\theta^2} \to 0,$$

so that, as

$$z \to a - h_0,$$

$$F \to 0, \quad F' \to 0, \quad F'' \to 0,$$

and from (13·3) it is seen that the conditions for the finiteness of u at $\varpi = 0$ are satisfied.

Thus there are two distributions of tides, one on either side of the plane $z = a - h_0$ which is perpendicular to the earth's axis and which touches the ocean bottom immediately under the pole. Across this plane there is continuity of the motion, since on both sides

$$P = 0, \quad \frac{iu}{\sigma H} = \frac{v}{\sigma H} = -\frac{\varpi}{a} e^{i(\sigma t + 2\chi)}, \quad w = 0.$$

When the depth is uniform, h is constant, $\psi = 0$, and on $r = a$,

$$\left(\frac{\varpi_1}{a}\right)^2 = \sin^2\theta - \sin^2\alpha.$$

The equation (13·7) may then be written in the form

$$(\sin^2\theta - \sin^2\alpha)\frac{\partial^2\zeta'}{\partial\theta^2} - (\sin^2\theta + \sin^2\alpha)\cot\theta\frac{\partial\zeta'}{\partial\theta}$$
$$+\left(2\sin^2\theta - 8 + 4\frac{\sin^2\alpha}{\sin^2\theta}\right)\zeta' + (\sin^2\theta - \sin^2\alpha)^2\beta\zeta = 0, \quad (13·8)$$

where

$$\frac{1}{\beta} = \frac{gh}{4\omega^2a^2}\left(1 - \frac{1}{2}\frac{h}{a}\right).$$

When h/a is small compared with $\sin^2\theta$ and ψ also is small, the equation (13·7) takes the form

$$\frac{1}{\sin\theta}\frac{\partial}{\partial\theta}\left(\frac{h}{\sin\theta}\frac{\partial\zeta'}{\partial\theta}\right) + \left\{\frac{2}{\sin\theta}\frac{\partial}{\partial\theta}\left(h\frac{\cos\theta}{\sin^2\theta}\right) - \frac{4h}{\sin^4\theta}\right\}\zeta' + \frac{4\omega^2a^2}{g}\zeta = 0, \quad (13·9)$$

which is identical with Laplace's equation (6·2) when $\sigma = 2\omega$, and χ enters through the factor $e^{2i\chi}$.

In Laplace's solution for an ocean of uniform depth, $\zeta' = 0$ and $\partial\zeta'/\partial\theta = 0$ at $\theta = 0$, whereas in the present solution these conditions obtain at $\theta = \alpha$. As θ increases beyond α the equation (13·8) rapidly approximates to Laplace's equation for uniform depth. From these facts it can be seen that, for an ocean of uniform depth, the solution of the present equations will differ very little from that of Laplace's equations.

When the depth follows the law $h = h_1 \sin^2\theta$, h_1 being constant, so that $h_0 = 0$, and when h_1/a is small, Laplace's equation (13·9) is valid everywhere. In this case the solution takes a very simple form, as noted by Sir G. B. Airy in 1842.

14. LIMITING FORM OF LONG-PERIOD CONSTITUENTS

Again, consider an ocean over which the depth is a function of the latitude only, but now suppose that P is independent of χ and t.

Let ξ and η denote displacement-components in the directions of ϖ and z respectively, so that

$$u = \frac{\partial\xi}{\partial t}, \quad w = \frac{\partial\eta}{\partial t}.$$

Then the equations (6·3) give

$$\left.\begin{aligned} -2\omega v &= -\frac{\partial P}{\partial\varpi}, \\ \frac{\partial v}{\partial t} + 2\omega\frac{\partial\xi}{\partial t} &= 0, \\ 0 &= -\frac{\partial P}{\partial z}, \end{aligned}\right\} \tag{14·1}$$

so that, in the limiting form of periodic motion,

$$P = F(\varpi), \quad v + 2\omega\xi = 0, \quad 4\omega^2\xi = -F', \tag{14·2}$$

where $F(\ )$ is a function to be determined. From the equation of continuity (6·5) it is seen that

$$\frac{1}{\varpi}\frac{d}{d\varpi}(\varpi\xi) + \frac{\partial\eta}{\partial z} = 0,$$

in the limiting form of periodic motion, and hence

$$4\omega^2\frac{\partial\eta}{\partial z} = \frac{1}{\varpi}\frac{d}{d\varpi}(\varpi F'),$$

so that

$$4\omega^2\eta = \frac{z}{\varpi}\frac{d}{d\varpi}(\varpi F') + f(\varpi), \tag{14·3}$$

where $f(\ )$ is another function to be determined.

Take $$z_1^2 = (a-h)^2 - \varpi^2,$$

and ψ as in § 13.

Now the component of displacement normal to the ocean bottom is

$$\xi \sin(\theta+\psi) + \eta\cos(\theta+\psi),$$

and from the vanishing of this at the bottom it is found that

$$f(\varpi) = -\frac{z_1}{\varpi}\frac{d}{d\varpi}(\varpi F') + \tan(\theta+\psi)\,F'. \tag{14·4}$$

The equation (14·4) defines $f(\ )$ in terms of $F(\ )$ for $0 \leqslant \varpi < a - h_1$, where h_1 denotes the depth of the ocean at the equator.

At the surface of the ocean

$$\xi\sin\theta + \eta\cos\theta = \zeta,$$

so that, from (14·2) and (14·3),

$$\sin\theta F' - \cos\theta\left\{\frac{z}{\varpi}\frac{d}{d\varpi}(\varpi F') + f\right\} + 4\omega^2\zeta = 0, \tag{14·5}$$

while
$$F(\varpi) = g\zeta',$$
$$F' = \frac{g}{a\cos\theta}\frac{\partial\zeta'}{\partial\theta},$$
$$\frac{d}{d\varpi}(\varpi F') = \frac{g}{a\cos\theta}\frac{\partial}{\partial\theta}\left(\frac{\sin\theta}{\cos\theta}\frac{\partial\zeta'}{\partial\theta}\right).$$

Take $\sin\alpha = 1 - h_1/a$. When $h_1/a = 1/2000$, $\alpha = 88^\circ{\cdot}2$.

For $\theta < \alpha$, $f(\varpi)$ is given by (14·4), and on substituting into (14·5)

$$\left.\begin{aligned}&\left(\cos\theta - \frac{z_1}{a}\right)\frac{1}{\sin\theta}\frac{\partial}{\partial\theta}\left(\frac{\sin\theta}{\cos\theta}\frac{\partial\zeta'}{\partial\theta}\right)\\ &\quad -\left(\tan\theta - \frac{a\sin\theta\cos\psi + z_1\sin\psi}{z_1\cos\psi - a\sin\theta\sin\psi}\right)\frac{\partial\zeta'}{\partial\theta} - \frac{4\omega^2 a}{g}\zeta = 0,\end{aligned}\right\} \tag{14·6}$$

in which h and ψ, regarded as functions of θ, correspond to the circle of the ocean bottom for which $\varpi = a\sin\theta$. At the equator, where for h and ψ, $\theta = \alpha$, it will be supposed that $\psi = 0$. As $\theta \to \alpha$, it is then deduced from (14·6) that

$$\frac{1}{z_1}\frac{\partial\zeta'}{\partial\theta} \to 0,$$

and it follows, from (14·4) and (14·5), that, as $\varpi \to a - h_1$,

$$f \to 0, \quad F' \to 0, \quad aF'' - \frac{4\omega^2}{\cos^2\theta}\zeta \to 0$$

$\zeta/\cos^2\theta$ being evaluated on $r = a$.

To illustrate the case in which the ocean extends over the equator, it will be taken as symmetrical about the equator. Then, at the equator, $z = 0$, $\partial\zeta'/\partial\theta = 0$, $\eta = 0$, and hence $f(\varpi) = 0$, for $a - h_1 \leqslant \varpi \leqslant a$. The equation (14·5) then becomes

$$\frac{1}{\sin\theta}\frac{\partial}{\partial\theta}\left(\sin\theta\frac{\partial\zeta'}{\partial\theta}\right) - \frac{4\omega^2 a}{g}\zeta = 0 \tag{14·7}$$

for $\theta \geqslant \alpha$; and at $\theta = \alpha$ and $\theta = \frac{1}{2}\pi$, $\partial\zeta'/\partial\theta = 0$. Using the third of (5·3),

$$\frac{\zeta}{H} = \frac{\zeta'}{H} + P_2(\cos\theta) + \text{constant},$$

$P_2(\ )$ denoting Legendre's polynomial of the second order, and hence the solution of (14·7) may be written

$$\frac{\zeta'}{A} = -P_2(\cos\theta) + \frac{P_2'(\cos\alpha)}{R_n'(\cos\alpha)}R_n(\cos\theta) + \text{constant},$$

where

$$\frac{H}{A} = \frac{3g}{2\omega^2 a} + 1, \quad n(n+1) = -\frac{4\omega^2 a}{g},$$

$R_n(\cos\theta)$ denoting the Legendre's function

$$F(-\tfrac{1}{2}n,\ \tfrac{1}{2}+\tfrac{1}{2}n,\ \tfrac{1}{2},\ \cos^2\theta).$$

This distribution gives, at $\varpi = a - h_1$,

$$F' = 0, \quad aF'' - \frac{4\omega^2\zeta}{\cos^2\theta} = 0,$$

$\zeta/\cos^2\theta$ being evaluated on $r = a$, and the value of ζ must be the same as in (14·6). On comparing with § 12, where a definite limiting form did not exist, it is again seen that it is the curvature of the earth which has enabled all the conditions to be satisfied.

Thus there are two distributions of tides, one on either side of the cylinder $\varpi = a - h_1$, which is parallel to the earth's axis and which touches the ocean bottom along the equator. Across this cylinder there is continuity of

$$f,\ F,\ F',\ F'',$$

and hence of P, ξ, η and v.

When the depth is uniform, h is constant, $\psi = 0$, and on $r = a$

$$\left(\frac{z_1}{a}\right)^2 = \cos^2\theta - \cos^2\alpha.$$

The equation (14·6) may then be written in the form

$$\{\cos\theta-[\cos^2\theta-\cos^2\alpha]^{\frac{1}{2}}\}\left\{\frac{1}{\sin\theta}\frac{\partial}{\partial\theta}\left(\frac{\sin\theta}{\cos\theta}\frac{\partial\zeta'}{\partial\theta}\right)\right.$$

$$\left.+\frac{\sin\theta}{\cos\theta[\cos^2\theta-\cos^2\alpha]^{\frac{1}{2}}}\frac{\partial\zeta'}{\partial\theta}\right\}-\frac{4\omega^2a}{g}\zeta=0. \quad (14{\cdot}8)$$

When h/a is small compared with $\cos^2\theta$, and ψ also is small, the equation (14·6) may be written as

$$\frac{1}{\sin\theta}\frac{\partial}{\partial\theta}\left(\frac{h\sin\theta}{\cos^2\theta}\frac{\partial\zeta'}{\partial\theta}\right)-\frac{4\omega^2a^2}{g}\zeta=0, \quad (14{\cdot}9)$$

which is identical with the form taken by Laplace's equation (6·2) when $\sigma\to 0$ and ζ' is independent of χ.

In Laplace's solution for an ocean of uniform depth covering the whole earth, $\partial\zeta'/\partial\theta=0$ at $\theta=90°$, whereas in the present solution this condition obtains at $\theta=\alpha$. As θ decreases from α the equation (14·8) rapidly approximates to Laplace's equation for uniform depth. From these facts it can be seen that the solution of the present equations will differ very little from that of Laplace's equations.

15. COMPARISON WITH PREVIOUS WORK

The chief result of the paper is to modify very considerably the impression created by V. Bjerknes and his co-authors. The emphatic statements of these authors appear to be based on the possibility of the existence of cellular oscillations of diurnal period, and on the possibility of resonance caused by the tide-generating forces of equal period. Now it has been seen that diurnal cellular oscillations are only possible when the horizontal wave-lengths are of the same order of magnitude as the depth. This indeed occurs in the examples given by Bjerknes and his co-authors, but it does not occur in the actual tides of the ocean. The part of the present paper which most nearly corresponds to the examples given by these authors is § 12.

The motion of § 11 may be regarded as one of the elemental motions used by Brillouin and Coulomb in their expansions. There again it is the dynamically possible oscillations of very short horizontal wave-length which cause their difficulties of convergence.

Comparison with Solberg's work is possible in connexion with §§ 13 and 14, as the basins here considered include an ocean of uniform depth covering the whole earth. The two problems here considered occur at the two extreme ends of the range of negative values of $1-4\omega^2/\sigma^2$. It has been shown that though Laplace's equations apply over the greater part of such an ocean, they do not apply near the poles for the constituent K_2 or near the equator for the limiting form of long-period constituents. But for the ocean taken as a whole, the necessary correction to the solution of Laplace's equations is only very slight. Though Solberg does not use cylindrical coordinates explicitly, he does obtain equation equivalent to those of § 13 as far as (13·3). But the distribution of tides which has been taken here to apply only near the poles, Solberg took to apply to the whole ocean, so that he did not obtain the equation (13·7). The problem of § 14 is a limiting case of those to be considered in Solberg's future paper.

REFERENCES

Airy, Sir G. B. 1842 *Tides and waves*. London.

Bjerknes, V., Bjerknes, J., Solberg, H. and Bergeron, T. 1933 *Physikalische Hydrodynamik*, pp. 450–452. Berlin.

Brillouin, M. 1928 *C.R. Acad. Sci., Paris*, **186**, 1665–1669.

Brillouin, M. and Coulomb, J. 1933 *Oscillations d'un liquid pesant dans un bassin cylindrique en rotation*. Inst. Mécan. Fluides Univ. Paris.

Hough, S. S. 1897 *Phil. Trans.* A, **189**, 201–257.

Poincaré, H. 1896 *J. Math. pures appl.* (5), **2**, 57–102.

Poincaré, H. 1910 *Leçons de Mécanique céleste*, **3**. Paris.

Solberg, H. 1936 *Astrophys. Norveg.* **1**, 237–340.

Street, R. O. 1930 *Proc. Camb. Phil. Soc.* **26**, 446–452.

Thomson, Sir W. 1880 *Phil. Mag.* **10**, 155–168. *Math. Phys. Papers*, **4**, 152–165.

Reflexion and scattering of X-rays with change of frequency†

I. Theoretical

By Sir C. V. Raman, F.R.S.

From the Department of Physics, Indian Institute of Science, Bangalore

(*Received* 15 *September* 1941)

The paper sets out in an elementary way the theory of two new phenomena of fundamental importance, namely the quantum reflexion and the quantum scattering of X-rays. (1) The quantum or modified scattering is due to the excitation of the elastic solid or low frequency vibrations of the crystal lattice by the X-ray photon. It has a very low specific intensity proportional to N (the number of lattice cells) and is distributed over a wide range of solid angles. The view expressed by some authors that the elastic solid vibrations of the lattice are responsible for the additional spots visible in Laue diagrams is consequently erroneous. (2) The quantum or modified reflexion is due to the excitation of the infra-red or characteristic high frequency vibrations of the crystal lattice by the X-ray photons. Its intensity, like that of the classical or unmodified reflexions is of the order N^2, though usually smaller in absolute value than the intensity of the classical reflexions. The manner in which the direction and intensity of the quantum reflexions are connected with the specific modes of infra-red vibration is mathematically formulated and discussed. (3) The frequency changes which play a fundamental part in the theory of both phenomena appear as necessary consequences of both the classical and quantum theoretical points of view. The law of temperature dependence of intensity is, however, quite different in the classical and quantum formulations. The experimental study of intensity at low temperatures accordingly furnishes a conclusive criterion both for the reality of the frequency changes and for the quantum mechanical character of the effects. (4) The influence of the modified X-ray reflexions on the intensity of the classical reflexions and their variations with temperature is discussed and shown to be of even greater importance than the effect on the same of the X-ray scattering by the elastic solid vibrations.

1. INTRODUCTION

The scattering of light in crystals with a change of frequency, discovered by me in 1928, has been the subject of intensive investigations at this

---

† These papers were sent as a contribution to the discussion on 'Diffuse reflexions of X-rays by crystals', but arrived too late to be included in the special number of *Proceedings* (A 976) devoted to this discussion.

Institute during the past five years. These are described in numerous memoirs published during the period in the *Proceedings of the Indian Academy of Sciences* and have notably advanced our knowledge of crystal optics and crystal dynamics. That analogous effects should arise also in the X-ray optics of crystals naturally suggested itself, and inspired investigations directed towards placing the behaviour of crystals towards light and X-rays on a common footing. The natural outcome of these researches has been the discovery of two new X-ray phenomena of fundamental importance, namely, the quantum reflexion and the quantum scattering of X-rays in crystals. The observations and theoretical considerations establishing the existence of these effects were published in 1940 (Raman & Nilakantan 1940 *a*, *b*); they may be briefly summarized thus: *The phenomenon of quantum or modified reflexion arises when X-ray photons traverse a crystal and excite the infra-red or high-frequency vibrations of the crystal lattice; the lattice planes of the crystal then reflect the X-rays in geometrically defined directions,* which are, in general, different from those of the well-known classical or Laue reflexions; the reflexions occur with a frequency $(\nu \pm \nu^*)$, ν being the X-ray frequency, and ν^* one or another of the characteristic infra-red frequencies of the crystal. *The quantum scattering by crystals, on the other hand, arises when the X-ray photons excite the elastic or low-frequency vibrations of the crystal lattice; the X-rays are then diffused over a wide range of solid angles* and have a frequency $(\nu \pm \nu^*)$, ν^* the frequency of the excited elastic solid waves being now dependent on the direction of scattering. *The law of temperature dependence of the intensity of the effects is determined, in either case, by the relation between $h\nu^*$ and kT,* k being the Boltzmann constant and T the absolute temperature. If $h\nu^* > kT$, the component of frequency $(\nu - \nu^*)$ *preponderates and the total intensity of quantum reflexion or scattering, as the case may be, is approximately independent of temperature,* while if $h\nu^* < kT$ the two components $(\nu \pm \nu^*)$ are of comparable intensities and *their aggregate increases with rising temperature.* The phenomenon of quantum reflexion comes under the first category at sufficiently low temperatures, while quantum scattering usually comes under the second category.

The further investigations on the subject carried out at Bangalore have completely confirmed the foregoing conclusions. In particular, the general geometric law of quantum reflexion has been derived and has been quantitatively confirmed by measurements made with diamond and a variety of other crystals, both organic and inorganic. The quantum-mechanical nature of the effects and the changes of frequency indicated by the theory have also received experimental confirmation from comparative studies of the intensity of the effects over a range of temperatures including that of liquid air, made with a series of crystals.

2. SOME CLASSICAL CONSIDERATIONS

The quantum theory of radiation phenomena is an application of quantum mechanics to the interactions between matter and the radiation field, the latter being itself considered as essentially Maxwellian. Hence, except in regard to the question of intensities, purely classical ideas suffice in many cases to give a general indication of the nature of the phenomena to be expected in such interactions. It may, in fact, be shown in an elementary fashion that any vibration of the atoms of a crystal through which X-rays pass necessarily involves a change of frequency in the secondary radiations resulting therefrom, and that such changes of frequency play a fundamental part in determining the observed radiation effects.

If the field due to the incident X-rays at the origin be denoted by $E \cos 2\pi\nu t$, the secondary radiations from an individual atom received at a distance R from the origin may be written as

$$\frac{E \sin\beta\, F(\alpha)}{R} \cos\left[2\pi\nu t - 2\pi(R + 2r \sin\alpha/2)/\lambda\right], \tag{1}$$

where α and β are respectively the angles which R makes with the primary rays and with the primary electric vector, $F(\alpha)$ is determined by the structure of the atom, and r is the perpendicular distance of the atom from a plane through the origin bisecting the angle between the incident and the scattered rays. Any oscillation of the atom perpendicular to r would leave the expression unaffected, while an oscillation parallel to r would introduce a periodic variation of the argument of the cosine function in (1). The expression for the scattered radiation may then be written in the form

$$\frac{E \sin\beta\, F(\alpha)}{R} \{\cos(2\pi\nu t - Z)\cos[z\cos(2\pi\nu^* t + \zeta)] \\ + \sin(2\pi\nu t - Z)\sin[z\cos(2\pi\nu^* t + \zeta)]\}, \tag{2}$$

Z being written for the constant part of $2\pi(R + 2r\sin\alpha/2)/\lambda$ and $z\cos(2\pi\nu^* t + \zeta)$ for its periodic part. The expression within the curly brackets in (2) may be expanded in a series of Bessel functions, and written as

$$J_0(z)\cos(2\pi\nu t - Z) \mp J_1(z)\cos[2\pi(\nu \pm \nu^*)t - Z \pm \zeta] \\ - J_2(z)\cos[2\pi(\nu \pm 2\nu^*)t - Z \pm 2\zeta] \\ \mp \text{etc., etc.} \tag{3}$$

The principles of the wave theory indicate that all secondary radiations having the same frequency are necessarily coherent, while those which differ in frequency by howsoever little, are necessarily incoherent with each other. Hence, in considering the interferences of the secondary radiations from the oscillating atoms with each other, it is necessary first to separate them according to the distinct frequencies as indicated by (3) and consider the secondary radiations of frequency ν, $(\nu+\nu^*)$, $(\nu-\nu^*)$, $(\nu+2\nu^*)$, $(\nu-2\nu^*)$, etc., separately. The relative importance of these frequency components depends upon the absolute value of the quantity z which appears as the argument of the Bessel functions. If z be sufficiently small, $J_0(z)$ is nearly equal to unity, $J_1(z)$ may be written as $\frac{1}{2}z$, while $J_2(z)$, etc., may be neglected. From equation (3) it will be seen that the interferences of unmodified frequency are determined by the values of Z giving the phases of the secondary radiations, in other words, by the equilibrium positions of the atoms. The interferences of the radiations of modified frequency $(\nu+\nu^*)$ and $(\nu-\nu^*)$ are, on the other hand, determined by the values of $Z-\zeta$ and $Z+\zeta$ respectively, in other words, jointly by the equilibrium positions of the atoms and by the relative phases of their vibrations. The significance of these results is readily appreciated by reference to figure 1 in which the lines marked ddd represent a set of lattice planes in the crystal, the lines $\Delta\Delta\Delta$ represent a set of equidistant parallel planes along which the phases of the atomic vibrations are identical, while $d^*d^*d^*$ are the diagonal planes passing through the intersections of ddd and $\Delta\Delta\Delta$. It is evident from (3) that the lines $d^*d^*d^*$ represent the planes of atoms from which the secondary radiations of frequency $(\nu\pm\nu^*)$ have the same resultant phase. The differing signs of ζ in (3) indicate that the direction of advancing phase, in other words,

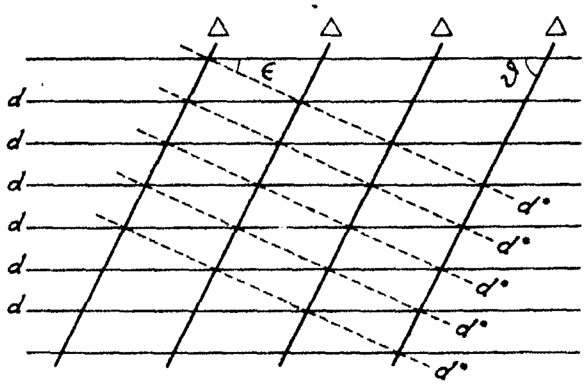

FIGURE 1. Geometric relation between static and dynamic stratifications.

the direction of movement of the waves $\Delta\Delta\Delta$, must be opposite for the frequencies $(\nu + \nu^*)$ and $(\nu - \nu^*)$, if the same diagonal planes are to represent the resultant in both cases.

3. SCATTERING OF X-RAYS BY ELASTIC-SOLID WAVES

The planes marked *ddd* in figure 1 evidently represent a static periodicity of electron density in the crystal, while $d^*d^*d^*$ represent the dynamic stratifications due to the oscillation of the atoms in these layers, the resultant effect of which has the frequency $(\nu \pm \nu^*)$ as indicated by (3). If the waves marked $\Delta\Delta\Delta$ are of such a nature as directly to involve variations of electron density in the solid, viz. if they are longitudinal elastic waves producing compressions and dilatations, they should themselves be regarded as dynamic stratifications of electron density irrespective of the atomic layers in the crystal. Such longitudinal or compressional waves should therefore be capable of giving a scattering of X-rays by the sound waves entirely analogous to that actually observed with ordinary light in liquids and in crystals. The angle through which the rays are scattered is given by the familiar optical formula

$$2\Delta \sin \alpha/2 = \lambda, \qquad (4)$$

and therefore ranges from the value $\alpha = 0$ for $\Delta = \infty$ upwards to the value of α found from (4) by putting Δ equal to the smallest permissible wave-length for sound waves in the crystal. The scattered rays thus form a diffuse cone surrounding the primary beam, their frequency change ν^* being dependent on the angle of scattering. Such a frequency shift in the acoustic scattering of radiation (originally predicted by L. Brillouin) has found experimental verification in the case of light. It is important to remark that though compressional and distortional elastic waves are both operative with light in the effect now under discussion, only the former need be considered in the case of X-rays.

Elastic waves of both types and especially waves of distortional type give rise to a diffuse scattering of X-rays in another way, namely, by disturbing the regularity of arrangement of the lattice cells in the crystal. The effect of such disturbance has been considered by Laue (*Ann. Phys., Lpz.*, December 1926) in a very complete manner, taking into account the changes of frequency indicated by classical considerations. Laue's results are readily intelligible from the geometric considerations indicated in figure 1. Here, the planes $\Delta\Delta\Delta$ represent the elastic solid waves traversing the crystal. Acting on the static atomic layers *ddd*, the waves create dynamic stratifications $d^*d^*d^*$ whose structure amplitude is proportional to $J_1(z)$ as indicated by equation (3). These stratifications have a sensible optical effect only when the relation

$$2d^* \sin\psi = n\lambda \qquad (5)$$

is satisfied. Here, ψ is the angle of incidence of the primary X-rays on the dynamic stratifications, d^* being the spacing of the latter. From figure 1 we write

$$d^* \sin\vartheta = d \sin(\vartheta+\epsilon) = \Delta \sin\epsilon, \qquad (6)$$

where ϑ and ϵ are the angles which the crystal spacings make respectively with the elastic waves and the dynamic stratifications. Combining (5) and (6), we obtain the formula

$$2d \sin\psi \sin(\vartheta+\epsilon) = n\lambda \sin\vartheta. \qquad (7)$$

Now, the plane of the elastic waves is entirely arbitrary; in other words, the angle ϑ appearing in equation (7) may have all possible values, and hence the angle of scattering which is 2ψ and the plane in which the scattered rays appear are both completely indeterminate. In other words, *the elastic solid waves can give only a diffuse scattering of the X-rays spread over a wide range of solid angles.*

Since elastic waves displace the atoms in a lattice cell to the same extent, in other words involve no appreciable distortion of their basic grouping, the static and dynamic structure amplitudes are proportional to each other. The intensity of the scattering by waves of specified frequency ν^* acting on a particular set of crystal planes may therefore be readily expressed as a fraction of the intensity of the unmodified reflexion by the same planes in the absence of any disturbance. From equation (3), it is seen that, apart from the variations of the factor $\sin^2\beta\, F^2(\alpha)$, the ratio under consideration would be $2J_1^2(z)$. When z is small, this may be taken as $\frac{1}{2}z^2$. Its magnitude is therefore directly proportional to the energy of vibration with frequency ν^*, the amplitude A of which is connected with z by the relation $z \approx 4\pi A \sin\psi/\lambda$. With the aid of equations (5) and (6), the energy of the oscillation may be written in the form $\frac{1}{2}z^2 M s^2 \sin^2\epsilon/\sin^2\vartheta$, where M is the mass of the whole crystal, and s is the velocity of the elastic waves in it. Putting this expression equal to kT (classical mechanics) or $h\nu^*$ (quantum mechanics), it is easily seen that the intensity ratio $\frac{1}{2}z^2$ of the modified scattering in any specified direction to the intensity of the unmodified reflexion is an exceedingly small quantity, being, in fact, of the order of magnitude $1/N$, where N is the total number of lattice cells. For a crystal large enough to be the subject of experiment but not so large as to invalidate the simple theory, *this ratio becomes a vanishingly* *small quantity. In practice, it is easily possible to record the classical X-ray reflexions by using thin crystal plates and fine X-ray beams, and it is evident that when such a technique is employed the effect due to the scattering by the elastic solid waves would be inappreciable.* The multiplying factor $\sin^2\vartheta/\sin^2\epsilon$ appearing as a numerical factor in the ratio cannot alter the position stated above. For it is a number which may range from say 100 → 10,000, according to the setting of the crystal and the direction of the scattered ray, while, on the other hand, the value of N is of an altogether larger order of magnitude, say 10^{12}, for a crystal traversed by X-rays in the circumstances in which these considerations are valid.

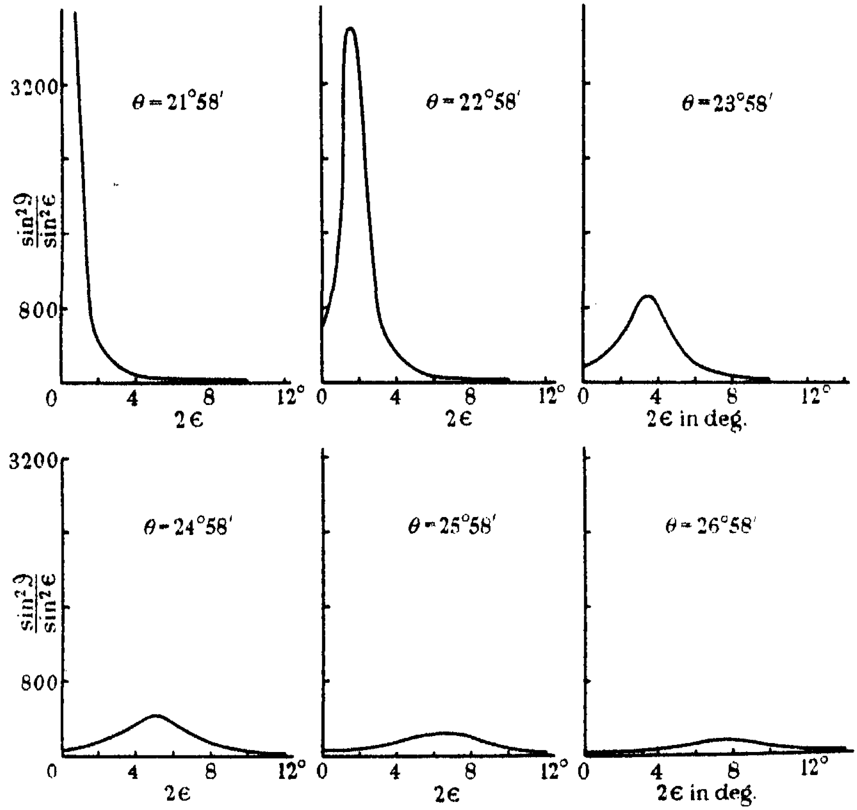

FIGURE 2. Graph of $\sin^2\vartheta/\sin^2\epsilon$ against 2ϵ (in degrees of angle); crystal spacing is that of (111) planes in diamond, using Cu K_α radiation.

Omitting the variation of the structure factor $F^2(\alpha)$, the function $\sin^2\vartheta/\sin^2\epsilon$ represents the manner in which the intensity of the scattered radiation varies with the direction of the scattered ray. Its value can readily be calculated using the formulae (5), (6) and (7), and its variation with 2ϵ (the angle between the Laue spot and a scattered ray assumed to lie in the plane of incidence) is shown graphically in figure 2 for a series of settings of the crystal. It will be seen from the graphs that the scattering intensity shows a maximum or 'peak' when the setting of the crystal planes is nearly that required for reflecting the incident monochromatic X-rays. The position of this peak for each setting corresponds to the direction in which the elastic waves having the longest wave-length or the lowest frequency (and therefore possessing the largest amplitude) are effective in scattering the X-rays. It will be seen, however, that the peak falls away very rapidly both in height and in sharpness and becomes an extremely diffuse 'hump' when the crystal is moved away from the setting at which the peak coincides with the Laue spot. It is evident from figure 2 and from the considerations regarding the absolute intensity of the scattering already set out, that *such scattering cannot give rise to any phenomenon even remotely resembling a geometric reflexion which persists over a wide range of settings of the crystal and is of sufficient intensity to be observed under the same experimental conditions as the ordinary Laue spots.*

It may be remarked here that Zachariasen, Lonsdale, Jahn and others who have considered the possible effects arising from the scattering of X-rays by the elastic solid waves have perhaps overlooked the fundamental considerations dealt with above. The conclusions which they have arrived at are, in consequence, in my opinion wholly illusory. As will be shown in Part II of this paper, all the observed characters of the 'modified' reflexions, namely, their intensity, their sharpness, geometric positions, and their behaviour at low temperatures, seem to contradict completely the idea that the scattering by elastic solid waves is responsible for their origin.

4. CLASSICAL THEORY OF MODIFIED X-RAY REFLEXION

We now proceed to consider the effect on the X-rays of vibrations in the crystal having one or another of the characteristic infra-red frequencies. The character of such vibrations differs fundamentally from those of the elastic-solid type, and the resulting optical effects are therefore also completely different. While the elastic-solid vibrations displace the lattice cells without disturbing the atomic grouping within them, the situation is reversed in the infra-red vibrations; the lattice cells now remain undisturbed in their equilibrium positions, while the atoms within the cells oscillate relatively to each other. As the result of such vibration the structure amplitudes of the lattice planes become periodic in time and give rise to geometric reflexions having a dynamic character and an altered frequency. Viewed from a purely classical standpoint, the preliminary discussion in § 2 continues valid; a change of frequency of the secondary radiations appears as a necessary consequence of the classical wave principles. The considerations contained in § 3, however, require radical modification in view of the altered nature of the vibrations with which we are now concerned.

It is obvious that in the present case the manner in which the secondary radiations from the different atoms in the unit cell sum up is different for the modified and the unmodified radiations. The resultant of the latter is expressed by

$$\sum_p F_p(\alpha)\, J_0(z_p) \cos Z_p, \tag{8}$$

and of the former by

$$\sum_p F_p(\alpha)\, J_1(z_p) \cos Z_p, \tag{9}$$

it being remarked that the displacements z_p for the p atoms are different though their phases ζ_p may be taken as identical. Formula (9) indicates that the vibration amplitudes of the atoms in any particular infra-red mode as well as their positions enter into the calculation of the final resultant. It may well happen that in a particular case, expression (9) vanishes while (8) is finite, or vice versa.

A general idea of the results to be expected in the present case may be obtained by regarding the N cells of the lattice as N oscillators having an identical vibration frequency, namely, ν^*. Each lattice cell may then be assigned a vibration energy kT (classical mechanics) or $h\nu^*$ (quantum mechanics). If we further assume that the phases of the secondary radiations from the N cells are in complete agreement as received in the direction of observation, their final effect would be the maximum possible and would be proportional to N^2 multiplied by the square of the expression (9). The amplitude of the oscillation of the atoms in the individual cells would be of the order $\sqrt{(kT/2\pi^2\mu\nu^{*2})}$ (classical mechanics) or $\sqrt{(h/4\pi^2\mu\nu^*)}$ (quantum mechanics), μ being the reduced mass of the lattice cell. Choosing appropriate values for μ and ν^*, the expressions may be evaluated, *and it is readily verified that the intensity of the modified X-ray reflexions would be from a hundredth to a thousandth part of that of the unmodified ones.* The general procedure indicated above would be approximately valid even when the coupling between the N cells is taken into account. For, the effect of such coupling is to endow the crystal with N separate frequencies of which a large proportion cluster round some particular value. Accordingly, though the resultant intensity would be smaller than that indicated above, it would still remain proportional to N^2.

The phase relations subsisting between the vibrations of the different lattice cells determine the directions in which the resultant of the modified secondary radiations is observable. The geometric representation in figure 1, and the formulae (5), (6) and (7), continue to be applicable. The same diagram and formulae were employed in § 3 to represent the diffuse scattering by the elastic-solid waves. In the present case they describe a geometric reflexion because the nature of the vibrations is quite different. The orientation and azimuth of the phase waves are properties of the particular mode of vibration under discussion and would be determined by the symmetry of the mode in relation to the symmetry properties of the crystal. They may be expected, therefore, to have specific values in relation to the lattice planes of which the structure amplitude is varied by the vibration. The situation may be pictured geometrically by setting out the possible values of $\overrightarrow{1/\Delta}$ as vectors from the origin in a three-dimensional diagram. The vectors thus drawn would then all be in the same straight line (or along one or another of a few straight lines determined by symmetry considerations) having a specific inclination to the reciprocal vector $\overrightarrow{1/d}$ of the crystal spacing. It follows immediately that the direction of the resulting dynamic reflexion would be represented by a single point (or a few specific points) on the sphere of reflexion.

The manner in which the N degrees of freedom corresponding to a particular infra-red mode of vibration are distributed amongst the various possible values of $\overrightarrow{1/\Delta}$ is evidently a matter of great importance, since it determines the intensity of the observed reflexions. It is evident that when Δ is large, the vibrations in neighbouring cells do not appreciably differ in phase. Prima facie, therefore, the frequency of a vibration of the atomic grouping within a cell would be influenced to a negligible extent by the value of Δ, so long as this is many times greater than the lattice spacing; the frequencies would diverge from the limiting value only when Δ becomes a small multiple of the lattice spacing. In other words, the discrete frequencies of the system cluster together very densely round the limiting frequency and are more sparsely distributed when they diverge from it. Accordingly, in the enumeration of the modes of vibration and their geometric representation on the vector diagram of $\overrightarrow{1/\Delta}$, the great majority of the representative points would be located at or near the origin of the diagram, while the remainder are distributed along the line or lines mentioned in the preceding paragraph, the density falling off quickly with increasing distance from the origin. Accordingly, also, the intensity of the modified reflexion would be a maximum when it falls upon the classical reflexion, and would diminish rapidly when it separates and moves away from the same in altered settings of the crystal.

5. QUANTUM THEORETICAL CONSIDERATIONS

The theory so far developed indicates that the components of the modified radiations with frequencies $(\nu \pm \nu^*)$ have equal intensities. This is a characteristic consequence of a classical treatment of the interaction between matter and radiation; in the analogous case of the light scattering in crystals, the result is definitely contradicted by experiment, the spectral component of diminished frequency having an enormously greater intensity than the component of increased frequency when $h\nu^* > kT$. This feature finds a ready explanation on the quantum mechanical view of the interactions. The incidence of the photon on the crystal induces a transition from a lower to a higher level of energy of vibration or vice versa, the photon supplying or taking up the requisite quantum of energy and appearing after the encounter with diminished or increased energy, as the case may be. When $h\nu^* \gg kT$, the crystal finds itself at the lowest energy level, and transitions are therefore only possible in one direction. As the temperature is raised, some of the higher energy states are thermally excited, and hence the photon can induce transitions either to the next higher states or in the reverse direction to the next lower states of energy. The quantitative formulation of these ideas shows that the intensity of the component of frequency $(\nu - \nu^*)$ should be proportional to $1/(1-e^{-h\nu^*/kT})$ and that of the component of frequency $(\nu + \nu^*)$ to $1/(e^{h\nu^*/kT}-1)$. At low temperatures, therefore, the former component reaches the limiting value unity, while the latter vanishes. At high temperatures, on the other hand, the intensities of both components approach equality and ultimately become proportional to the absolute temperature.

The foregoing considerations are of such general validity and so closely related to our present problem that they must necessarily be regarded as applicable to it. Indeed, the change of frequency indicated classically by equation (3), and the classical condition for reflexion indicated in equation (5), appear independently from the quantum theory as consequences of the conservation of energy and momentum respectively in the encounter between the photon and the crystal. The modified reflexion and modified scattering must therefore necessarily be regarded as quantum effects and their intensities as determined by the principles of the quantum mechanics. From an experimental point of view, we are concerned now with the summation of the intensities of the two components of frequency $(\nu \pm \nu^*)$, since they both overlap. In the parallel case of light scattering, this sum is proportional to

$$(e^{h\nu^*/kT}+1)/(e^{h\nu^*/kT}-1), \tag{10}$$

and this expression should therefore also represent the intensity of modified X-ray reflexion as a function of temperature, unless the latter be so high that the basic assumptions of theory cease to be valid.

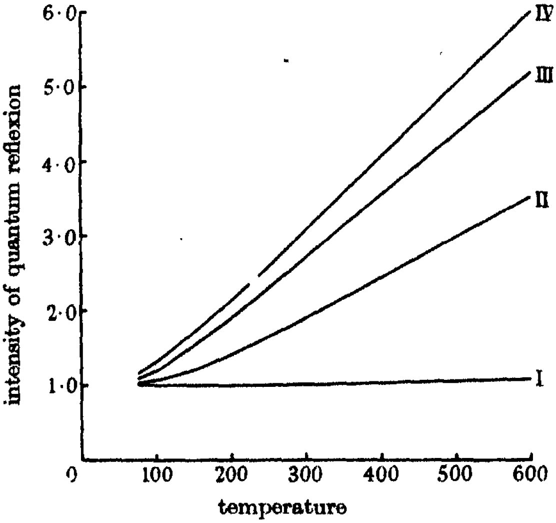

FIGURE 3. Intensity of quantum reflexion as a function of temperature. I, Diamond; II, NaF; III, NaCl; IV, KCl.

In figure 3 the function appearing in (10) has been represented graphically for four different values of ν^*, being respectively the characteristic frequencies for diamond, sodium fluoride, sodium chloride and potassium chloride. It will be seen that the increase of intensity with temperature is quite negligible in the case of diamond and becomes the more conspicuous the lower the characteristic frequency of the crystal. The graph, however, indicates that in all cases, the function remains finite and reaches the limiting value unity at low temperatures. In other words, the *modified reflexions should persist at the lowest temperatures and their intensity should then be independent of temperature variations.*

6. RELATION TO THE INTENSITY OF CLASSICAL REFLEXION

We have already seen that the theory of the quantum or modified reflexion essentially rests on the fact that each of the characteristic infra-red modes represents the superposition of N co-existent vibrations of the crystal having practically identical frequency. It is easily seen that the result of such superposition would be to endow the atoms of the crystal with relatively large amplitudes of vibration. Indeed, if all the N modes were assumed to possess identical frequencies and phases, their amplitudes would be superposed and the secondary radiations from a lattice cell would be expressed by

$$\sum_p F_p(\alpha)\, J_0(Nz_p) \cos Z_p \tag{11}$$

and

$$\sum_p F_p(\alpha)\, J_1(Nz_p) \cos Z_p \tag{12}$$

respectively. Though the values of z_p would be very small compared with unity, the arguments Nz_p of the Bessel functions $J_0(Nz_p)$ and $J_1(Nz_p)$ may easily assume large values; the greatly increased values of the expression (12) for the modified reflexion would then involve a corresponding diminution in the expression for the classical or unmodified reflexions given by (11).

The effect of the co-existence of N modes of vibrations having slightly different frequencies may, of course, be worked out completely ab initio from the expression (1) of § 2. It is obvious, however, that the general nature of the result, so far as it concerns the intensity of the unmodified reflexion, cannot differ much from the situation indicated in (11) and (12) above, namely, that the existence of strong modified reflexions by any particular set of crystal planes would usually involve a large diminution of the intensity of the unmodified reflexion by the same planes. Combining this with the indications of the graphs in figure 3, it also follows that the *increased intensity of the modified reflexions at high temperatures involves a diminished intensity of the unmodified ones. Further, the expressions* (11) *and* (12) *indicate that these reciprocal relationships would usually be selective, in other words, just those planes which show increased intensity of modified reflexions would also show a large diminution of intensity of the unmodified reflexion.*

From the foregoing discussion, it is evident that the characteristic infra-red vibrations of the crystal lattice play a fundamental part in the theory of the temperature effect in X-ray reflexion, even more than the elastic vibrations considered by Laue and his predecessors in the field. As in the majority of actual crystals the number of degrees of freedom associated with the infra-red modes is much larger than the number associated with the elastic vibrations of the lattice, the importance of this remark should be evident.

REFERENCES

Raman, C. V. & Nilakantan, P. 1940*a* *Curr. Sci.* **9**, 165.
Raman, C. V. & Nilakantan, P. 1940*b* *Proc. Indian Acad. Sci.* A, **11**, 379, 389, 398.
Laue, M. von 1926 *Ann. Phys., Lpz.*, **81**, 877.

Reflexion and scattering of X-rays with change of frequency

II. Experimental

By Sir C. V. Raman, F.R.S.

From the Department of Physics, Indian Institute of Science, Bangalore

(*Received* 15 *September* 1941)

[Plates 32, 33]

It is shown that the quantum theory of X-ray reflexion and scattering in crystals developed in Part I is in full accord with the experimental facts. The theory succeeds in giving a quantitative explanation of the experimental facts concerning these phenomena as observed with diamond, viz. (1) the specular character of the quantum reflexion from the (111) planes, (2) the geometric law of such reflexion and especially the fact that, in general, the reflexion falls outside the plane of incidence, (3) the subsidiary features accompanying the reflexion, viz. faint elliptic spots and elongated streamers noticed in certain special cases, (4) the absolute intensity of the reflexion which is an appreciable fraction of the intensity of the classical reflexion, (5) the failure of the (110) planes to exhibit similar reflexions, (6) the persistence of the reflexions by the (111) planes with undiminished intensity at liquid air temperature and the relatively small increase of intensity at high temperatures, and (7) the appearance of a diffuse scattering having an undiminished intensity at low temperatures. The differences between diamond and other crystals in respect of these X-ray phenomena are explained by taking into consideration the differences in the frequency and character of their lattice vibrations in the infra-red region as revealed by the spectroscope.

1. INTRODUCTION

The two fundamental results emerging from the theory outlined in Part I are, first, that we are here concerned with phenomena of a quantum-mechanical nature, and secondly, that the infra-red or high frequency vibrations of the lattice produce effects radically different in their character from the X-ray scattering by the elastic vibrations, being in fact of an altogether higher order of intensity and in the nature of a geometric reflexion by the lattice planes of the crystal. The latter of these two results escaped recognition in the classical investigations of Debye, Waller and Laue on the temperature problem in X-rays. The reason for this is to be found in their acceptance of Born's postulate that *all the vibrations* of the lattice have wave-lengths forming a three-dimensional harmonic sequence determined by the dimensions of the crystal; accepting the postulate, it follows at once that the infra-red and the elastic vibrations alike result merely in a diffusion of the X-rays, the effect of the former being even less conspicuous than that of the latter owing to the higher frequency and correspondingly smaller amplitude. The recognition that Born's postulate does not correctly represent the infra-red vibrations of a crystal lattice is thus as important for the present subject as an appreciation of the fact that the classical mechanics does not correctly determine the results of an interaction between the X-rays and the crystal lattice.

Conclusive evidence bearing on these fundamental points of theory was furnished by the experimental work of Dr P. Nilakantan and myself (1940*a*, *b*). The decisive character of the experimental results set out in those papers was due to the fact that the crystal employed, namely, diamond, shows the effects contemplated in the theory with ideal perfection, and indeed in such manner as totally to exclude all alternative explanations. The experiments disclosed the following features, amongst others of scarcely less interest, namely, the strictly geometric or specular character of the dynamic X-ray reflexions exhibited by the (111) lattice planes of diamond, their great intensity comparable with that of the ordinary Laue spots in specially favourable settings of the crystal, their visibility with undiminished sharpness over a wide range of settings of the crystal though with greatly diminished intensity, and above all, the practically constant intensity of the reflexion over a wide range of temperature. These features, taken together, left no room for doubt that the observed effects were due to the excitation of the characteristic high-frequency vibrations of the lattice by the incidence of the X-rays. Subsequent investigations with this and other crystals have furnished useful information and enabled some details to be more fully elucidated. But the case for the theory as stated in the papers quoted was essentially a complete one.

A good deal of literature has recently appeared on this subject which seeks to show, on the one hand, that the theory of X-ray scattering due to Faxén and Waller explains the facts of the case, and on the other hand seeks to convey the impression that the fundamental observations and conclusions reported by myself and Dr Nilakantan had been anticipated in earlier publications from other laboratories. The first of these claims has already been dealt with in the theoretical part of this paper, and its erroneous character will become even more evident when we proceed to consider the experimental facts. As regards the second claim, while the literature does contain numerous observations on diffuse streaks and spots in Laue patterns for which very varied explanations had been put forward, *I wish to point out that the existence of a distinct new type of specular X-ray reflexion of a dynamic kind by the lattice planes of a crystal was for the first time recognized and its physical characters elucidated in the publications from this Institute quoted above.*

I shall now set out briefly the relevant experimental evidence under each of the heads mentioned above, commenting at each stage upon its relation to the theoretical aspects dealt with in Part I of the paper.

2. THE SPECULAR CHARACTER OF QUANTUM REFLEXION

In the earliest published photographs, the dynamic reflexions by the (111) planes of diamond appear as round spots whose diameter in strongly exposed pictures is about the same as or a little less than the major axis of the elliptic Laue spots, thereby indicating that their size is determined by the thickness of the crystal and the divergence of the incident X-ray beam and *not* by any inherent diffuseness of the reflexion. This inference has since been thoroughly tested by using thin plates of diamond with a fine slit as the source of X-rays and giving long exposures to bring out the reflexions with full intensity. Two such pictures are shown as figure 1 *a* and *b* in plate 32 for two different settings of the diamond. The quantum reflexions (indicated by arrows) appear in the record as fine lines, their measured widths being exactly that resulting from the finite thickness of the plate and the width of the slit used. Further, it is most significant that there is no change in the width of the reflexion as between the two settings. The experimental situation indicated in figure 1 *b* in plate 32 may be compared directly with the curve for the same glancing angle, namely 25° 58′, drawn in figure 2 of Part I. The 'diffuse maximum' of scattering in the latter curve extends over fully 12° of arc, while the reflexion appearing in figure 1 *b* as stated above has no measurable width. *The observed facts thus completely discredit the idea that the scattering of X-rays by elastic waves is in any way responsible for the phenomenon with which we are now concerned.* They also show that the term 'diffuse reflexion' is inappropriate as a description of it, since such diffuseness is clearly not an essential feature of the phenomenon. The observed sharpness of the quantum reflexions in diamond is equally decisive against the postulate of Born as applied to the infra-red vibrations of the lattice. For it demonstrates that the orientation and azimuth of the phase-waves are uniquely defined and independent of their wave-length, instead of having an infinite number of possible values as assumed in Born's postulate.

The sharpness of the quantum reflexion is closely related to the geometric law of such reflexion, being in fact a measure of the precision with which such law can be stated. It is evident that the reflexion can be perfectly specular only when the crystal is *dynamically homogeneous*, which would be the case if the lattice vibrations are represented by sharp lines in the spectrum of the light scattered by the crystal, as is actually found with diamond. Any cause, e.g. thermal agitation, which disturbs the dynamic homogeneity and results in increasing the width of these spectral lines must therefore also impair the specular character of the quantum reflexions. The lattice vibrations appear in the spectra of the great majority of crystals as rather diffuse lines which, however, become sharper at low temperatures. Accordingly, it is not surprising that the phenomenon of quantum reflexion is not shown with the same perfection as in diamond by other crystals. Nevertheless, in many cases, e.g. calcite or rock-salt, the quantum reflexions appear fairly sharp, their angular spread being only a small fraction of the angular separation between the Laue and the quantum reflexions. Indeed, the experimental facts as observed with the majority of crystals bear no resemblance to the situation represented in the series of curves in figure 2 of Part I. It is thus patent that the Faxén-Waller theory of X-ray scattering is completely irrelevant to the phenomenon now under consideration.

The manner in which a dynamic inhomogeneity of the lattice would influence the quantum reflexions may be readily appreciated by reference to the three-dimensional representation of the lattice vibrations against the reciprocal wave-length $\overrightarrow{1/\Lambda}$. As already remarked in §4 of Part I, the N representative points lie densely clustered at the origin, the stragglers being distributed along a specific line (or lines) defining the permitted orientation and azimuth of the phase waves. The intersection of this line (or lines) with the sphere of reflexion determines the direction in which the reflexion is observed. A dynamic inhomogeneity of the lattice would result in this line, instead of being rigid and fixed in direction, becoming ill-defined. Since, however, the origin from which the line is drawn is firmly fixed, *it follows that the resulting spread of the quantum reflexion would be negligible when it lies very near the Laue reflexion and would progressively increase as its angular separation from the latter increases.* This is exactly what was observed and pointed out in the case of sodium nitrate and rock-salt (Raman & Nilakantan 1940*b*, *c*) and is indeed a general feature. As the lattice lines in the spectra of most crystals sharpen at low temperatures, a corresponding sharpening of the quantum reflexions may be expected in the same circumstances.

3. GEOMETRIC LAW OF QUANTUM REFLEXION

The earliest measurements with diamond showed that the dynamic spacing d^* of the (111) planes altered continuously with the setting of the crystal, coinciding with the static spacing d only when the classical and quantum reflexions appeared superposed. This made it evident that the phase waves were not transverse to the crystal spacing in diamond, though in other cases, e.g. sodium nitrate, rock-salt and calcite, the measurements appeared to support the assumption of transversality. The explanation of these and other facts was furnished by the general theory of quantum reflexion (Raman & Nagendra Nath 1940) which yielded the formula

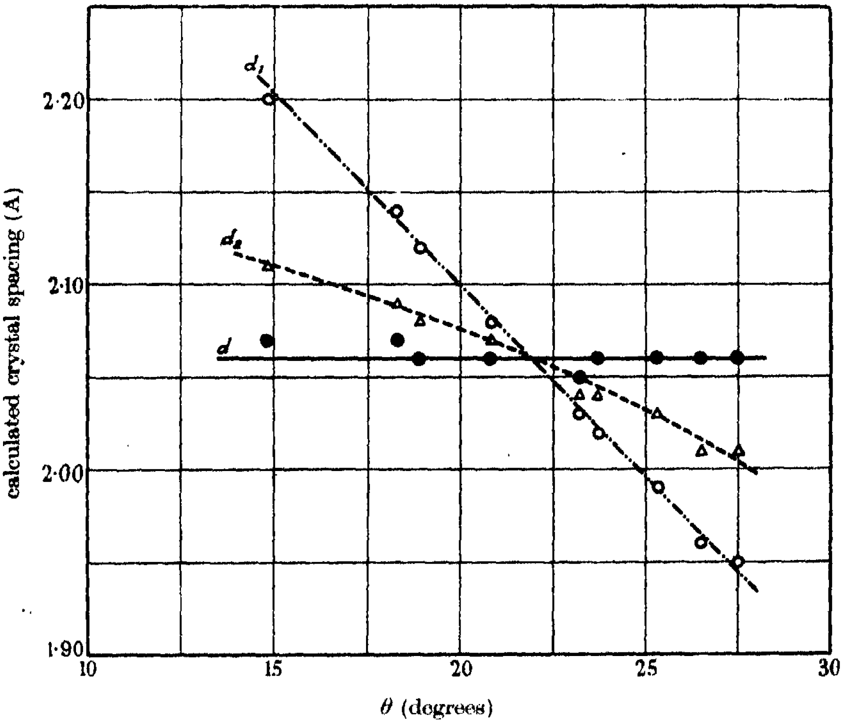

FIGURE 2. Showing the failure of the Faxén formula.

$$2d \sin\psi \sin(\vartheta+\epsilon) = n\lambda \sin\vartheta, \tag{1}$$

ϑ and ϵ having the significance already indicated in Part I. *Since the plane of the reflexion is that of incidence of the X-rays on the dynamic stratifications, it will not in general coincide with the plane of incidence on the static crystal* *planes.* In the particular case, however, when $\epsilon = 0$ and the classical and quantum reflexions therefore coincide, and also generally when the plane of the phase waves is transverse to the plane of incidence on the static spacings, the reflexion indicated by (1) would appear in the same plane. We may then write (1) in the form

$$2d\sin\tfrac{1}{2}(\theta+\phi)\sin\left(\vartheta+\frac{\theta-\phi}{2}\right) = n\lambda\sin\vartheta, \qquad (2)$$

θ and ϕ being respectively the glancing angles of incidence and quantum reflexion measured with reference to the crystal planes. The earliest measurements as well as more elaborate ones made a few months later over a wider range of settings for the quantum reflexions by the (111) planes of diamond fitted the formula (1) rigorously, ϑ coming out as 54° 44′, that is half the tetrahedral valence angle. The measurements made for the particular case in which the plane of incidence is transverse to the (100) planes are shown graphically in figure 2.

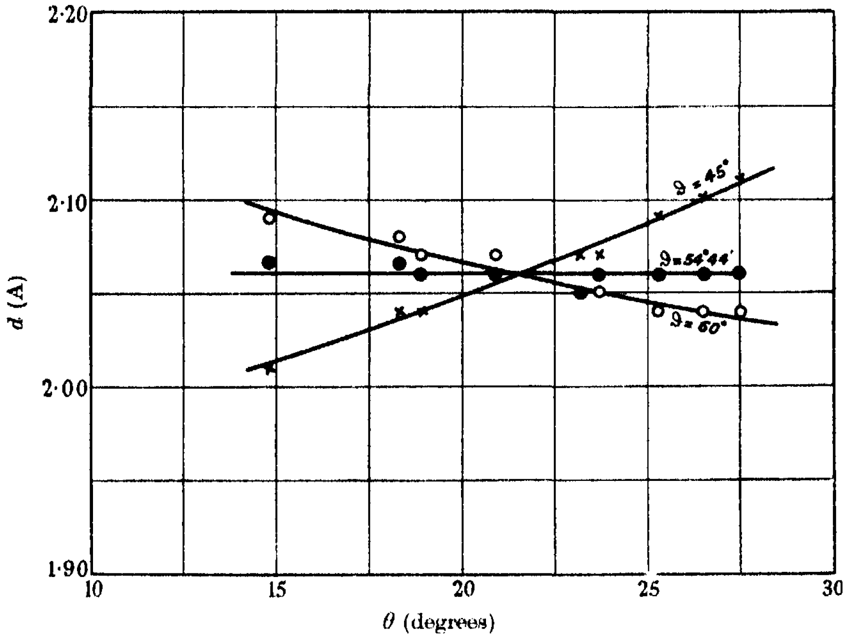

FIGURE 3. Fixing the orientation of the phase waves in diamond.

In figure 2 the line marked d represents the crystal spacing calculated from the experimental data and equation (2), while the lines d_1 and d_2 were respectively drawn assuming the formulae

$$2d_1 \sin \tfrac{1}{2}(\theta+\phi) = \lambda, \tag{3}$$

$$d_2 \sin(\theta+\phi) = \lambda \cos\phi. \tag{4}$$

In figure 3 the same data are plotted from the formula (2) assuming different values of ϑ to illustrate the accuracy with which this angle can be evaluated and also the agreement between the evaluated and the known crystal spacing (2·055 A). Formula (4) was derived by Faxén to give the position of the diffuse maximum in the intensity of scattered X-radiations. *The total lack of agreement between the calculated and known crystal spacings, and the curvature of the line indicate that the considerations on which the Faxén formula is based are altogether irrelevant to our present subject.*

The experimental result stated above (Raman & Nilakantan 1941) is of extraordinary interest, for it indicates that the *phase waves of the infra-red vibration which give the* (111) *reflexions have a completely fixed orientation parallel to the* (100) *planes of the crystal.* Its significance from the point of view of crystal dynamics becomes clear when it is remarked that the (111) planes are normal to the valence bonds between the carbon atoms, while the (100) planes bisect the angles between them, and that the atomic layers in both these planes belong alternately to the two interpenetrating lattices of carbon atoms of which the oscillation as rigid wholes relative to each other gives the characteristic infra-red frequency (1332 cm.$^{-1}$) of diamond.

As remarked above, the reflexion given by the formula (1) ceases to appear in the plane of incidence (except in the special case where $\epsilon = 0$) if the phase waves are not transverse to that plane. *If, therefore, the diamond is so set that the* (100) *planes are inclined to the plane of incidence, the Laue and quantum reflexions by the* (111) *spacings should appear in different planes.* This remarkable result indicated by the theory was verified experimentally by Dr P. Nilakantan and myself and is illustrated in figure 4 in plate 32; the observed and calculated inclinations between the plane of incidence and the plane in which the quantum reflexion appears are found to be in full agreement.

Other remarkable results also follow from the theory. From considerations of symmetry, it is evident that if there is a set of phase waves parallel to the (100) planes, there must also be two other sets parallel respectively to the (010) and (001) planes. *Diamond must therefore show three quantum reflexions from the* (111) *planes and not one,* their relative positions being determined by the angle of incidence of the X-rays and the azimuth in which the crystal is set, while their relative intensities would depend on the numerical values of the three reciprocal phase vectors $\overrightarrow{1/\Delta_1}$, $\overrightarrow{1/\Delta_2}$ and $\overrightarrow{1/\Delta_3}$. These conclusions, extraordinary as they may seem, have been completely confirmed by the experimental investigations made at this Institute. Mr P. R. Pisharoty has worked out the geometrical implications of the theory in a most detailed manner and shown that in spite of the perfectly specular character of the quantum reflexion, by taking into account the angular divergence of the incident X-ray beam, all the observed phenomena, including especially the oblique streamers diverging from the Laue spots in some settings and the elongated elliptic spots on the opposite side in other settings are quantitatively explained (see figures 5*a*, *b*, *c*, *d* in plate 32). The oblique streamers are, in fact, the result of two of the phase vectors being nearly tangential to the sphere of reflexion instead of meeting it sharply. The intensity and extension of the streamers are determined by precisely the same considerations as the brightness and positions of the discrete spots. *Thus, the theory of phase waves put forward in April* 1940 *has found a most detailed and satisfactory experimental confirmation in the case of diamond.*

Formula (3) follows from the general formula (1) as an approximation if ϑ is assumed equal to $\frac{1}{2}\pi$, and ϵ is small. It suffices roughly to describe the observed geometric behaviour of the quantum reflexion in many cases. An appropriate choice of the angle ϑ in the general formula should lead to better concord with observation in all cases.

4. INTENSITY OF QUANTUM REFLEXIONS

Optical theory indicates that when the secondary radiations from N dipoles are of identical frequency and in coherent phase relationship, their resultant appears as a directed geometric pencil of intensity proportional to N^2, while if there is no such identity of frequency, the resultant is a diffuse radiation of which the intensity is proportional to N. The translatory movements of the lattice units in a crystal due to its elastic vibrations have a continuous spectrum of frequencies, and the case therefore comes under the second category. On the other hand, the characteristic infra-red vibrations are shown by the spectroscope to have precisely definable frequencies and their effect therefore comes naturally under the first category. The geometric character of the quantum reflexions, their physical origin and observed intensity are thus seen to be related to each other in a very intimate fashion, while the diffuse character of the quantum scattering, its physical origin and its intensity are similarly connected.

The intensities of the quantum reflexions like those of the classical ones are thus necessarily proportional to the square of the volume of the irradiated crystal (if this be not too large), while that of the scattering is proportional to the volume. This situation may be readily verified experimentally by reducing the effective volume to the minimum possible, e.g. by using the thinnest possible crystal and the finest possible X-ray beams. The classical and quantum reflexions are then seen physically to stand in the same category, continuing to be visible in the photographic record, while the diffuse or background scattering becomes too feeble to produce any sensible effect.

As explained in Part I, the intensity of the quantum reflexion may be evaluated theoretically by setting the energy of the individual oscillators equal to $h\nu^*$ and assuming them to be in an identical phase of vibration. This procedure yields the limiting intensity at the lowest temperatures and for the most favourable setting of the crystal, and comes out as a small but easily observable fraction of the intensity of the classical reflexion, of the order of about 1/100 to 1/1000, depending on the particular circumstances. *Though no precise experimental determinations are available, this indication of theory is at least of the right order of magnitude.* In making an exact test of the theory, it would be preferable not to rely on comparisons between the classical and quantum reflexions, but to make a calculation of the absolute intensity as well as a direct experimental determination of the same. Investigations of this kind have been undertaken at this Institute by Mr Pisharoty and are now in progress.

As already mentioned in Part I, theory indicates that the intensity of the quantum reflexions by different lattice planes in a crystal need not necessarily stand in the same ratio as the intensities of the classical reflexions by the same planes. We may, as an example, consider the case of diamond. The atoms belonging to the two interpenetrating lattices in the crystal appear interleaved in the (111) and the (100) planes, dividing these spacings in the ratios 1 : 2 and 1 : 1 respectively. On the other hand, they appear interspersed in equal numbers in the (110) planes. From these facts and formula (9) of Part I, it follows that neither the (110) nor the (100) planes can give any modified reflexion as the result of an oscillation of the interpenetrating lattices, though the (111) planes can. Though the classical reflexions by the (110) planes have an intensity one-third of that of the (111) planes, *prolonged exposures fail to yield any modified reflexions by the* (110) *planes, in agreement with the indications of the theory.*

5. QUANTUM REFLEXION AT LOW TEMPERATURES

In the scattering of light with altered frequency by crystals, the quantum mechanical nature of the effect is strikingly revealed in the spectroscope by the enormous disparity in intensity of the radiations with frequencies $(\nu-\nu^*)$ and $(\nu+\nu^*)$ respectively, the disparity increasing rapidly with the magnitude of ν^*. In the X-ray problem, the components $(\nu\pm\nu^*)$ overlap, but this does not obscure the situation altogether, since the sum of their intensities continues to behave quite differently in the classical and quantum theories. As illustrated in figure 3 of Part I, the course of the intensity curve depends on ν^*. The greater its value, the more nearly horizontal is the curve at ordinary temperatures and the greater the deviation from the simple proportionality to the absolute temperature indicated by the classical mechanics. Per contra, the smaller the value of ν^*, the lower the temperature we must reach before the curve flattens out and becomes horizontal. Hence, the quantitative study of the intensity at low temperatures is of decisive importance for the subject. Not only does it furnish a test of the quantum mechanical nature of the phenomenon, but the course of the curve also enables us to measure the frequency of the lattice vibrations responsible for the reflexion and thus to establish the physical reality of the frequency shift. It also enables us to demonstrate the error of seeking an explanation of modified X-ray reflexion in the Faxén-Waller theory of X-ray scattering. For, in the latter theory, the elastic-solid waves giving the 'diffuse maxima' of the scattered radiation are those of which the frequency is the lowest possible, diminishing without limit as the position of the 'maximum' approaches the Laue spot. Hence, the intensity of the 'maximum' should diminish proportionally with temperature down to the absolute zero and indeed for all crystals, including even diamond.

The theoretical relation between the intensity of quantum reflexion and temperature was clearly set out (Raman & Nilakantan 1940*a*, *b*) dealing with the case of diamond, and observations at high temperatures were also described which supported its indications. It was confidently predicted that the intensity of the quantum reflexion by diamond should remain undiminished at liquid air temperature. When the necessary experimental technique had been developed, this prediction was found to be in complete accord with the facts (Raman & Nilakantan 1940*d*).

A proper experimental procedure is obviously imperative for all quantitative investigations of intensity. The simple method of dipping the crystal into liquid air which has been adopted in this connexion by the workers at the Davy-Faraday Laboratory (Preston 1941) is obviously incapable of giving trustworthy results, as the absorption and diffusion of X-rays by the liquid air would mask the effects due to the crystal. *The conclusions which have been drawn from photographs in which the halo due to the liquid air appears superposed on the crystal pattern are therefore quite illusory.* To obtain results having a real significance, a high-vacuum low-temperature X-ray camera was constructed and employed by Dr P. Nilakantan at this Institute with very satisfactory results for the investigations with diamond. The design of the apparatus is illustrated in figure 6. Both the crystal and the photographic film are placed inside a high vacuum, the crystal being held firmly in contact with a metal block attached to the vessel containing liquid air or other refrigerant. It should be remarked also that for such quantitative work, *intensifying screens should*

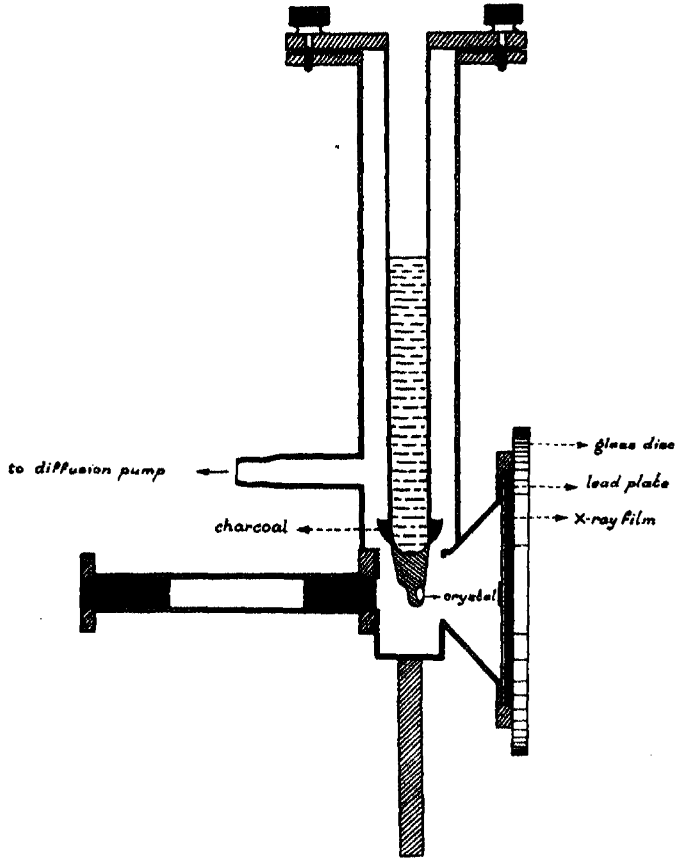

FIGURE 6. Design of low-temperature high-vacuum X-ray camera.

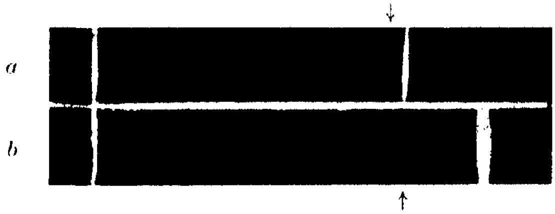

FIGURE 1. Showing sharpness of quantum reflexions in diamond.

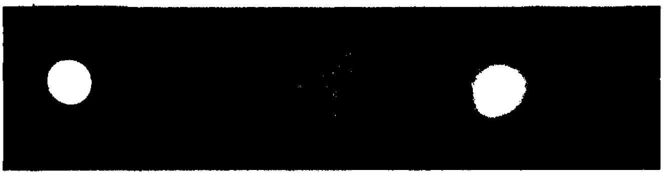

FIGURE 4. Showing reflexions from diamond not in the plane of incidence.

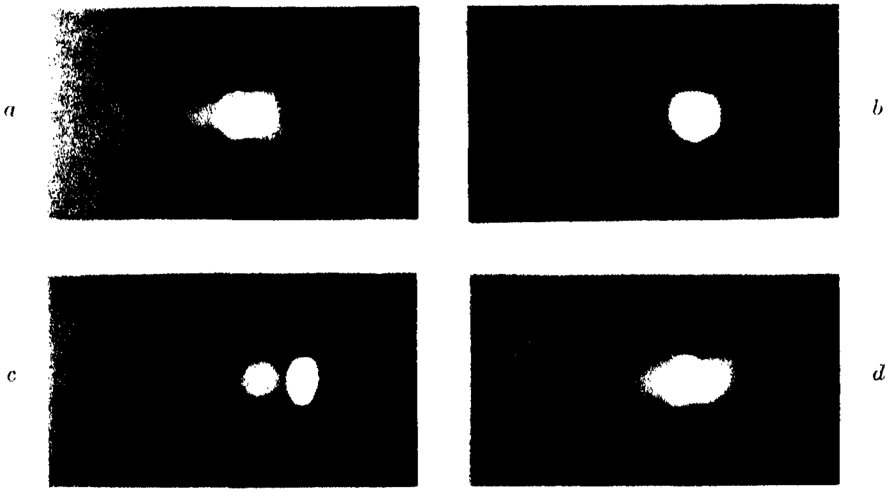

FIGURE 5. Showing streamers and other subsidiary phenomena.

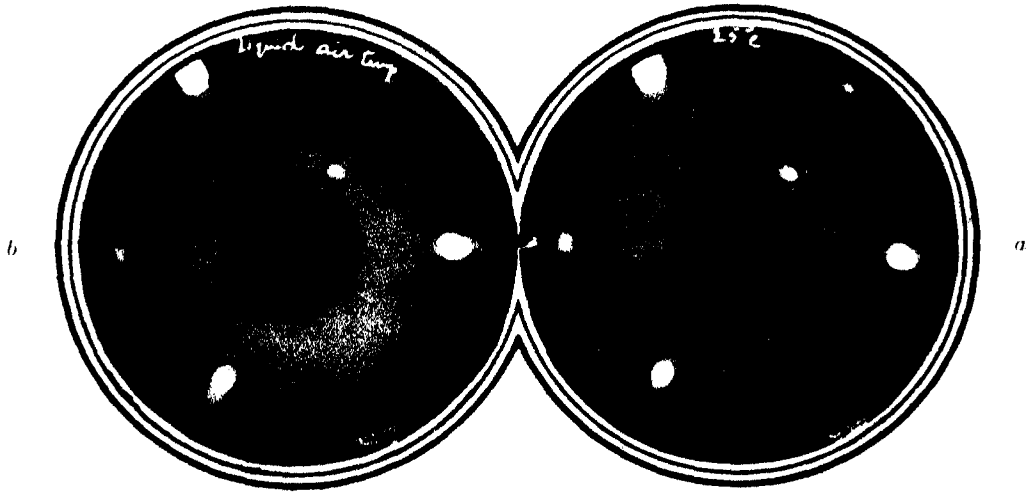

FIGURE 7. Comparison of intensities at room and liquid air temperatures.

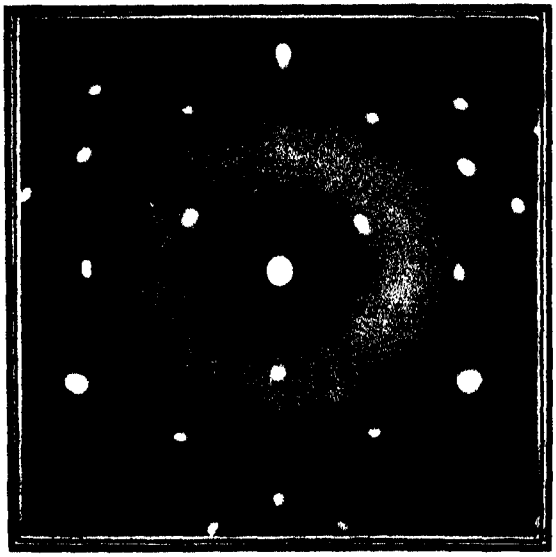

FIGURE 8. Quantum scattering in diamond.

not be used, as they cannot be relied upon to maintain a constant behaviour. Two photographs for diamond taken with this camera at room and liquid air temperatures respectively are shown in figure 7 *a* and *b* in plate 33. A camera of improved design which enables rectangular X-ray films of larger size to be used has more recently been constructed and employed by Dr C. S. Venkateswaran in highly successful investigations with crystals of carborundum, rock-salt and pentaerythritol. These crystals were chosen as having high, medium, and low frequencies respectively in the infra-red spectrum. The results obtained with them at various temperatures completely confirm the theoretical conclusions already set out in the foregoing pages.

6. QUANTUM REFLEXION AT HIGH TEMPERATURES

The majority of crystals have numerous characteristic infra-red frequencies. The different modes of vibration are, however, far from being of equal importance in relation to our present subject. At the lowest temperatures, the intensity of the quantum reflexions is proportional to $h/4\pi^2\mu\nu^*$, while at sufficiently high temperatures it becomes proportional to $kT/2\pi^2\mu\nu^{*2}$. Thus in nearly all cases and particularly at high temperatures, the infra-red modes which have the lowest frequencies would make the largest contribution to the observed intensities of the modified reflexions. It may also be remarked, as shown by the formula (11) and (12) of Part I, that the static and dynamic structure amplitudes of the different lattice planes would be influenced even by the same mode of vibration to different extents. Hence by a comparative study of the modified reflexions from several lattice planes at various temperatures, it should be possible to correlate the X-ray facts with the known spectroscopic behaviour of the crystal, particularly in regard to the infra-red vibrations of the lowest frequencies.

The intimate relationship between modified X-ray reflexion and the infra-red spectrum is strikingly illustrated by the behaviour of the (210) planes of sodium nitrate investigated by Dr Nilakantan and the present writer. It is found that pari passu with the rapid decrease in the intensity of the classical reflexions by these planes which occurs in the temperature range from 180 to 275° C, there is an enormous increase in the intensity of the modified reflexions by the same planes. *This behaviour is not shared by other planes in the crystal*, the intensity of reflexion by which is altered by rise of temperature to a relatively small extent; it is thus evident that *we are concerned with a particular mode of vibration of the sodium nitrate lattice which is strongly excited in this temperature range*, and not with the general increase of the thermal agitation. The same inference is indicated also by the specific heat data, and by spectroscopic observations on the light scattered in sodium nitrate crystals.

7. QUANTUM SCATTERING OF X-RAYS

Since the scattering of X-rays by the elastic vibrations of the crystal lattice involves a change of frequency, it is a quantum effect which should persist at the lowest temperatures. The observed intensity would, however, be then sensible only if $h\nu^* > kT$, in other words when the scattering is due to elastic waves of high frequency for which this condition is satisfied. Such an effect is actually exhibited by diamond, the scattering appearing as a diffuse halo at a considerable angular distance from the primary beam (figure 8 in plate 33). The dark ring at the centre of the halo and the distinct maximum of intensity towards its outer margin are noteworthy features of the phenomenon. It will be seen on a comparison of figure 7 *a* and *b* in plate 33 that the halo does not disappear at liquid air temperature, but that, on the other hand, it is actually more conspicuous and better defined. The effect presumably arises from the scattering of X-rays by longitudinal elastic waves of high frequency. The peculiar distribution of intensity in the halo is probably due to the increasing value of $h\nu^*$ to which the intensity is proportional for larger angles of scattering. The variation in the number of elastic modes of vibration with the reciprocal wave-length $\overrightarrow{1/\Delta}$ will, of course, also have to be taken into consideration.

8. CONCLUDING REMARKS

Though the present report is written by me, it is largely based on the work of past and present members of the department, including especially Dr P. Nilakantan with whom these investigations were first undertaken, Dr N. S. Nagendra Nath, Dr C. S. Venkateswaran and Mr P. R. Pisharoty, all of whom have contributed notably to the development of the subject. I desire to place on record my warmest appreciation of their collaboration.

REFERENCES

Preston, G. D. 1941 *Nature, Lond.*, **147**, 467.
Raman, C. V. & Nagendra Nath, N. S. 1940 *Proc. Indian Acad. Sci.* A, **12**, 427.
Raman, C. V. & Nilakantan, P. 1940*a* *Curr. Sci.* **9**, 165.
Raman, C. V. & Nilakantan, P. 1940*b* *Proc. Indian Acad. Sci.* A, **11**, 379, 389, 398.
Raman, C. V. & Nilakantan, P. 1940*c* *Proc. Indian Acad. Sci.* A. **12**, 141.
Raman, C. V. & Nilakantan, P. 1941 *Nature, Lond.*, **147**, 118.

Extra reflexions from the two types of diamond*

By Kathleen Lonsdale
Royal Institution

(*Communicated by Sir William Bragg, F.R.S.—Received* 21 *October* 1941)

[Plates 34–39]

New experimental facts about diamond, supported by X-ray photographs, are as follows: There are two kinds of extra reflexions to be seen on well-exposed Laue photographs. All diamonds show *primary* diffuse reflexions, which are temperature-sensitive but not structure-sensitive. These correspond to the diffuse reflexions observed under suitable conditions for all other substances. Type I diamonds, only, show the *secondary* reflexions (sharp spots, streaks and groups of spots) which have been previously described and which are not at all typical of diffuse spots in general. They are not really diffuse, they are not (or only slightly) temperature-sensitive and they are strongly structure-sensitive. *Primary and secondary* reflexions have been observed for many diamonds and in various orientations, associated with the {111} {220} {113} {331} Laue reflexions, using filtered and unfiltered radiation from copper and iron targets. There is as yet no explanation of the *secondary* reflexions which can account satisfactorily for the structure-sensitiveness, the presence of {220} spots, and the apparent incompleteness of the groups of spots actually observed.

When Sir C. V. Raman sent the preceding contribution to the discussion on diffuse reflexions of X-rays by crystals (*Proc. Roy. Soc.*, A, **179**, 1–101, 1941), he was necessarily unaware of various experimental developments, since briefly reported (Lonsdale & Smith, 1941), which must have a considerable bearing on his, and other, theoretical arguments. These further experimental facts are as follows:

(1) *Two kinds of extra reflexions.* The extra reflexions given by different diamonds are not all alike. They may be divided into two classes, which we have called *primary* and *secondary* reflexions.

(2) *Primary reflexions* (*all diamonds*). All diamonds so far examined show the *primary* reflexion. This consists of a single, nearly spherical spot, which really is diffuse and which accompanies the Laue spot when the diamond orientation is not more than about ± 3–5° from the Bragg position for any given plane. With the [$1\bar{1}0$] axis vertical (as it was throughout almost all

---

* This paper is an addition to the series of papers published as a Discussion on 'Diffuse reflexions of X-rays by crystals' in consequence of the receipt of the preceding paper by Sir C. Venkata Raman.

our experiments), *primary* reflexions have been observed for the {111} {220} {113} {004} {331} planes, using Cu $K\alpha$ and $K\beta$ radiations, and for the first three of these using Fe $K\alpha$ and $K\beta$ radiations. Examples of *primary* spots may be seen on plates 34 *a–d*, 35 *e*, *f*, 36 *a–d*, 37 *a*, *b*, *d*, 38 *a–e*, 39 *a–d*.

(3) *Secondary reflexions* (*type I diamonds only*). Only some diamonds show the *secondary* reflexions. In particular, those rare diamonds classed by Robertson, Fox & Martin (1934, 1936) as being of type II do not show them at all. [The diamonds actually tested were D 2, D 16, D 19, D 22, in their classification.*] When the [1$\bar{1}$0] axis is vertical, the *secondary* reflexion consists of single sharp spots or of well-defined streaks (or both), or of groups of sharp spots, according to the angle and direction of incidence. These *secondary* spots are very persistent, being still visible even at an angle of + 12° or − 8° from the Bragg angle for the (111) plane. Such *secondary* reflexions have been observed, using Cu $K\alpha$ and $K\beta$ radiations, for the {111} {220} {113} {331} planes, but not for the {004} planes; and using Fe $K\alpha$ and $K\beta$ radiations, for the first three of these. Examples are given in plates 34 *b*, *d*, 35 *b*, *d*, *e*, *f*, 36 *a*, *b*, *c*, 37 *a–e*, 38 *a–e* and (very weakly) 39 *a*, *b*, *c*. Photographs previously reproduced in the course of this Discussion (Lonsdale & Smith, Sir W. H. Bragg, Sir C. V. Raman) have shown only {111} *secondary* effects.

(4) *Intensity of the extra reflexions*. The intensity of the *primary* reflexions does not vary appreciably from one diamond to another. The *secondary* reflexions are, however, markedly structure-sensitive. They appear strongly for some diamonds, weakly for others and not at all for type II diamonds. Of the diamonds examined and classed as type I by Robertson *et al.*, the following have been examined:

D 1, a spinel twin, showed weak *secondary* spots and streaks from both individuals;

D 20 showed a moderate effect;

D 21 and D 23 showed relatively strong effects.

The most intense *secondary* reflexions were obtained from D (2), a small octahedral diamond of weight 1 mg. which was found to give uniformly intense, sharp spots, streaks or groups of spots in all crystallographically equivalent orientations, that is, associated with each of the eight {111} planes, twelve {220} planes, etc. D (4), another small (slightly deformed) octahedral diamond of about the same weight, showed only extremely weak *secondary* effects (plate 39 *a*, *b*, *c*), while D (3), a beautiful octahedral plate from Sierra Leone, 0·6 mm. thick, weight 0·047 g., and of great purity, also gave exceedingly good *secondary* reflexions in the various orientations. D (2), D (3) and D (4) were not among the diamonds examined and described by Robertson *et al.*

---

* Mr Smith and I are indebted to Professor W. T. Gordon for the loan of these and all other diamonds examined.

(5) *Intensity of normal reflexion.* It was noticeable that the intensity of ordinary selective reflexion also varied greatly from one diamond to another; the more intense the *secondary* reflexions, the greater was the extinction of the normal reflexion. Type II diamonds, and those of type I which gave poor *secondary* effects, showed very little extinction and were therefore particularly fine monochromators; the normal reflexions from the {111} {220} and {113} planes could be seen in broad daylight on a fluorescent screen.

(6) *Position of extra reflexions.* The position of the *primary* spots is given reasonably closely by Faxén's simple formula, and corresponds therefore to the intersections of the sphere of reflexion with an approximately spherical (and very limited) extension of reflecting power about the reciprocal lattice points. These *primary* reflexions became weaker and more diffuse (and therefore more difficult to measure) as the angle of missetting increases (plate 36 *a*, *c*) and soon disappear.

The position of the *secondary* spots and streaks corresponds geometrically, as Sir C. V. Raman has pointed out, with their being the intersections of the sphere of reflexion with cubic directions in reciprocal space (see also Lonsdale & Smith, this Discussion, p. 44). It follows that the *primary* reflexion lies at the centre of the triangle of *secondary* (111) reflexions (plates 34 *b*, *d*, 36 *a*, 37 *a*, *b*, etc.) or, in the alternate orientation, it forms an approximate background to the sharp *secondary* (111) spot from which may proceed the streaks described by Sir C. V. Raman (plates 35 *f*, 38 *d*, *e*). In this latter orientation the *primary* reflexion may well be overlooked altogether, but it is most clearly seen when a small slit (0·5 mm. or less diameter) and thin crystal are used; it is, of course, quite obvious for type II diamonds, for which the sharp *secondary* spot and streaks are absent (plates 34 *a*, *c*, 39 *d*).

(7) *Temperature-sensitiveness of extra reflexions.* The *primary* reflexion is quite markedly temperature-sensitive. This has been proved beyond doubt for both types of diamond, the temperature range covered being $750 \leftrightarrows 30 \leftrightarrows -180^\circ$ C for type I diamonds, and $30 \leftrightarrows -180^\circ$ C for type II diamonds. At high temperatures, the general background is rather more intense, but the *primary* reflexion intensity is increased by a factor of at least three or four, relative to that at room temperatures. Even when the exposure times are varied, the *primary* reflexions (unlike the Laue and *secondary* spots) are still considerably stronger than those observed on a

room-temperature photograph given double the exposure (plates 38*a*, *b*, *c*, *d*, *e*, 39*a*, *b*, *c*). At liquid air temperatures the *primary* reflexions are weakened in intensity (plates 37*b*, *c*, 39*d*, *e*).

The *secondary* reflexions are only slightly temperature-sensitive. This agrees with Sir C. V. Raman's observation, although it should be noticed that there *is* a slight apparent increase in intensity at high temperatures and a slight diminution at low ones (plates 37*b*, *c*, 38*a*, *b*, *c*, *d*, *e*).

In the low-temperature experiments that part of the diamond under irradiation remained covered with a very thin film of liquid air, but the general excellence of the Laue photographs obtained under these conditions showed that no appreciable absorption or scattering by the liquid air itself could have affected the validity of the results. It was also found that while no ice formed on the part of the diamond in actual contact with liquid air, ice did form on the surface only 1 mm. away. This evidence of the extremely low thermal conductivity of diamond makes it doubtful whether any method which does not surround the irradiated part of the specimen with the desired temperature (that is, which depends upon conductivity for its success) can possibly be satisfactory.

(8) *Extra reflexions from* {110} *planes.* Sir C. V. Raman has referred specifically to the absence of any extra spots corresponding to the (110) reflexion. Diamond, crystallizing as it does in a face-centred cubic lattice, cannot of course give any *first-order* selective or extra reflexions from the {110} planes. The intensity of the (220) selective reflexion is about 46 % of that of the (111). When diamonds of type I are so orientated ($[1\bar{1}0]$ vertical, angle of incidence near to 37·65° for Cu $K\alpha$, 50·1° for Fe $K\alpha$ radiation) as to give an (*hh*0) Laue reflexion near to the (220) Bragg position, strong *primary and secondary* reflexions may be observed with quite a short exposure (20 min. for the 5 kW tube). Diamonds of type II give only the *primary* reflexion. In all orientations some 5° or less from the Bragg angle, the *secondary* (220) reflexion consists of a pair of sharp, inclined spots, vertically above and below the Laue spot; the *primary* spot is to one side and is, of course, much more diffuse in character (plate 36*b*, *c*). Some photographs show *primary* and *secondary* reflexions from the (111) (202) (022) and (113) planes simultaneously (plate 37*a*). The (202) and (022) extra reflexions seen on such photographs consist of a sharp *secondary* spot superposed on a more diffuse *primary* spot and sometimes accompanied by a sharp streak (plate 36*a*).

(9) *Extra reflexions from* {113} {331} {004} *planes.* The (113) *secondary* reflexions (in alternative orientations) are shown in plates 35*d*, 37*a*, *d*, *e*. The (331) *secondary* reflexion has also been found in both alternative orienta-

tions, and (131) (311) (313) (133) reflexions observed, with the $[1\bar{1}0]$ axis vertical.

The (004) Laue reflexion (plates 35 *e*, 36 *d*) is apparently accompanied by a *primary* reflexion only. It may be pointed out, however, that any *secondary* reflexions corresponding to reflecting points on the [001] axis would coincide with the Laue spot in every orientation and could not therefore be observed, except by the use of strictly monochromatized radiation. This has not been attempted. Detailed contours of the reflecting regions in reciprocal space corresponding to the observed *primary* and *secondary* reflexions will be published later, but it is significant that the (220) and (113) *secondary* reflexions correspond to reflecting points along the [100] and [010] directions only. There are no *secondary* spots associated with either the (220) or the (113) reflexions which would correspond to points on the [001] axis. The (331) *seondary* reflexion corresponds mainly to reciprocal lattice reflecting points along the [001] direction, though there may be weak [100] [010] branches.

CONCLUSIONS

It would appear from Sir C. V. Raman's paper that the existence of the {220} extra reflexions is incompatible with his theory. We have already pointed out (Lonsdale & Smith, 1941) that the structure-sensitiveness of the *secondary* reflexions shows that these cannot be explained on the Faxén-Waller heat theory. Nor can the simple diffraction theory, as it stands, explain the absence of *secondary* spots corresponding to the [001] direction for the (220) (113) reflexions. At present these experimental facts, therefore, have received no satisfactory theoretical explanation.

On the other hand, it must be emphasized that type I diamonds are not typical, or even ideal, crystals. The *primary* diffuse reflexions, found for all diamonds, correspond closely to the diffuse reflexions observed under suitable conditions of orientation, wave-length and temperature for all other crystalline substances. The *secondary* reflexions are quite different in character, and indeed, as Sir C. V. Raman has insisted, are not diffuse reflexions at all. They are analogous in some respects to the sharp spots or scratches which are occasionally observed, superposed on the ordinary diffuse spots, in the case of cleaved or cold-worked crystals (Lonsdale & Smith; this Discussion, p. 26). Examples of these 'strain' spots have even been found on some photographs of type II diamonds with worked faces, but they disappear when the diamond is shifted slightly. They are not temperature-sensitive (plate 39 *d*, *e*).

If the *secondary* diamond reflexions are to be explained on the basis of strain, however, it must be a strain which is cubic in symmetry and inherent in the majority of diamonds, although in differing degree. The interdependence of *secondary* effects and extinction, and their variation with the diamond examined, make it obvious that intensity measurements, whether relative or absolute, will apply only to the particular diamonds used, and cannot be used for purposes of generalization.

Mr H. Smith has been associated with me throughout the entire course of this research. We are indebted to Sir W. H. Bragg and to colleagues both in the Davy Faraday Laboratory and elsewhere for much help and interested encouragement.

REFERENCES

Lonsdale & Smith 1941*a* *Nature, Lond.*, **148**, 112, 257.
Lonsdale & Smith 1941*b* *Proc. Phys. Soc.* **53**, 529.
Robertson, Fox & Martin 1934 *Phil. Trans.* A, **232**, 463.
Robertson, Fox & Martin 1936 *Proc. Roy. Soc.* A, **157**, 579.

Diffuse scattering of X-rays by crystals

The Faxén-Waller theory and the surfaces of isodiffusion for cubic crystals

By H. A. Jahn

Davy Faraday Laboratory, Royal Institution

(*Communicated by Sir William Bragg, F.R.S.—Received* 5 *July* 1941)

An elementary derivation is given of the Faxén-Waller formula for the diffuse scattering of X-rays by thermally excited lattice vibrations and the shapes of the surfaces of isodiffusion in reciprocal space for cubic crystals investigated. It is shown that for substances with high elastic anisotropy large deviations from spherical character are to be expected for the surfaces of isodiffusion belonging to each of the individual lattice planes and, moreover, marked differences in shape between surfaces belonging to different lattice planes. The theory is illustrated by calculations made for a single crystal of sodium.

Recent experimental work (Laval 1939; Preston 1939; Raman and Nilakantan 1940; Lonsdale, Knaggs and Smith 1940; Siegel and Zachariasen 1940; Jauncey and Baltzer 1941) has brought added interest to the fundamental theoretical work of Faxén (1923) and Waller (1925) on the effect of

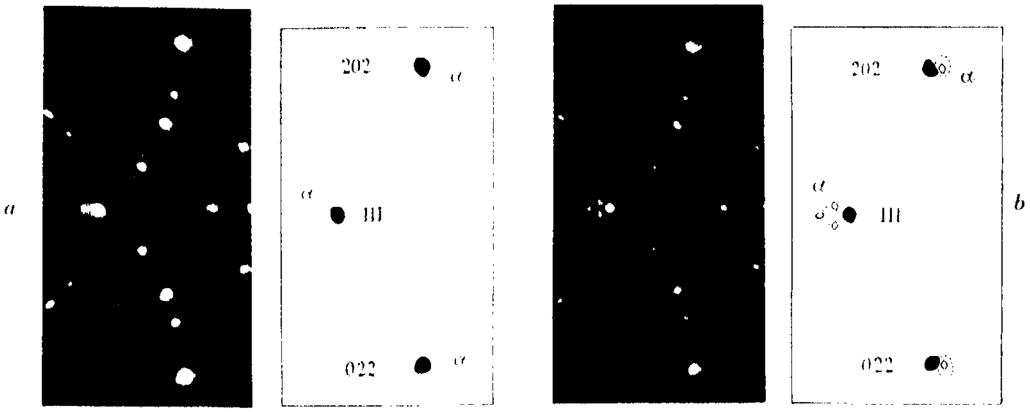

Cu unfiltered radiation, $\theta_{111} = -23\cdot8^\circ$. Film normal at 68° to undeviated incident beam; ● Laue spot, ○ primary, ○ secondary spot. *a*, D 16, type II diamond showing no secondary reflexions; *b*, D (2), type I diamond showing strong secondary reflexions.

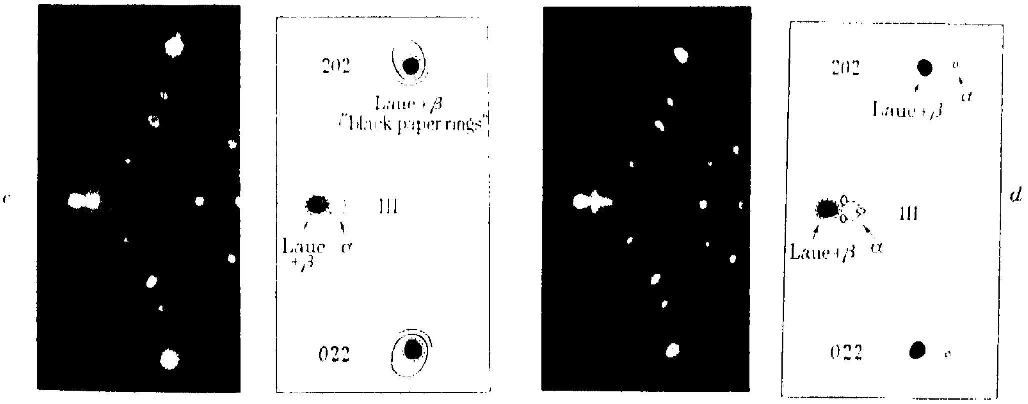

Cu unfiltered radiation, $\theta_{111} = -20^\circ$. Film normal at 68° to undeviated incident beam; ellipses around 202, 022 Laue spots (in *c*) are due to reflexion of intense Cu $K\beta$ beam by black paper covering film-holder; *c*, D 22, type II diamond; *d*, D(3), type I diamond.

[110] vertical in all photographs. Film distance, 2·85 → 4·15 cm. No intensifying screens were used, as these would have spoilt the definition of the photographs.

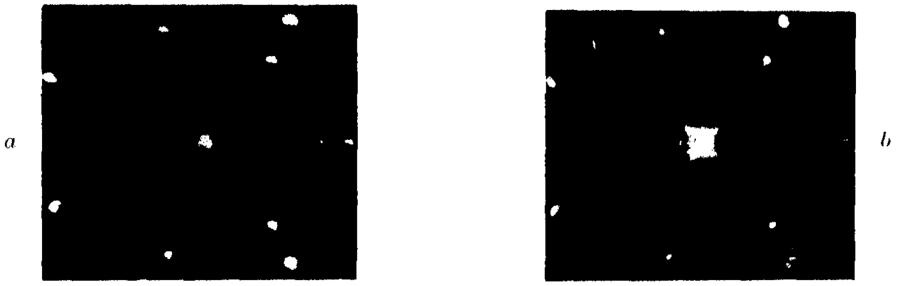

Fe unfiltered radiation, $\theta_{111} = +28\cdot35°$. Film normal at 56·1° to undeviated incident beam. *a*, D22, type II; *b*, D(2), type I.

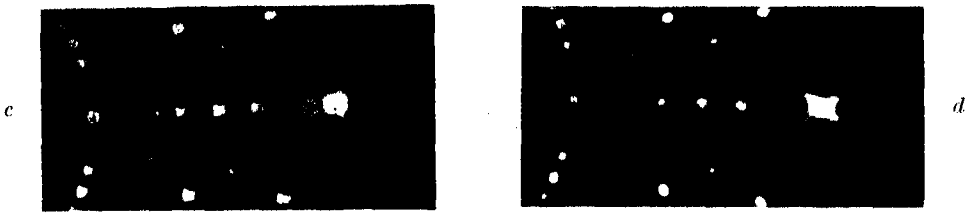

Fe unfiltered radiation, $\theta_{113} = +64\cdot2°$. Film normal at 80° to undeviated incident beam. *c*, D22; *d*, D(2), showing secondary streaks. The ellipses on *c* and *d* and the circles on *a* and *b* are due to Fe $K\alpha$ reflexion by the black paper of the film-holder (*see* Lonsdale and Smith 1941*b*).

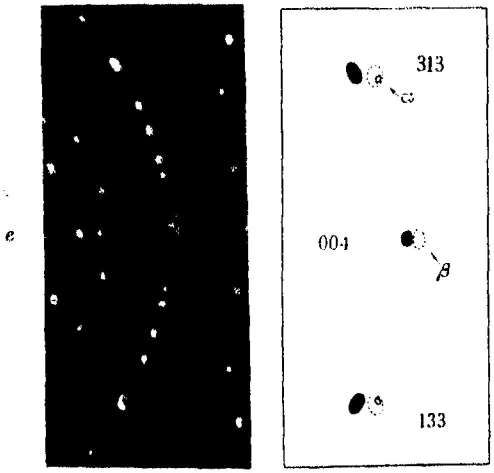

e, D(2), Cu, $\theta_{001} = 50\cdot4°$. Film parallel to undeviated incident beam.

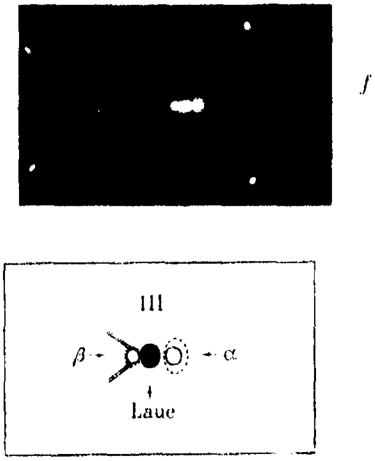

f, D(2), Fe, $\theta_{111} = +26\cdot85°$. Film normal at 56·1° to undeviated incident beam.

a

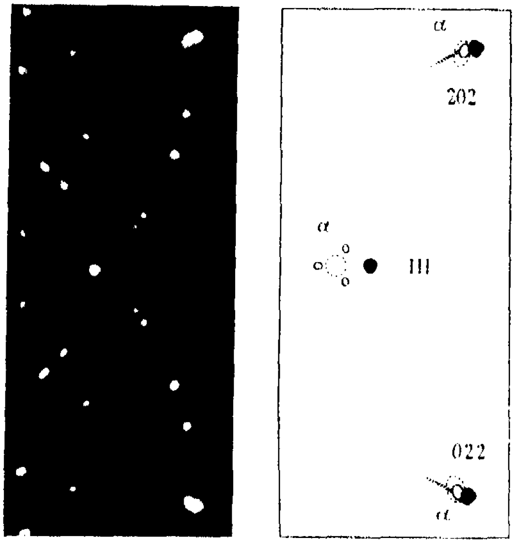

D(2), Cu radiation, $\theta_{111} = -27°$. Film normal at 44° to undeviated incident beam. Differential printing adopted to bring out detail of film.

b

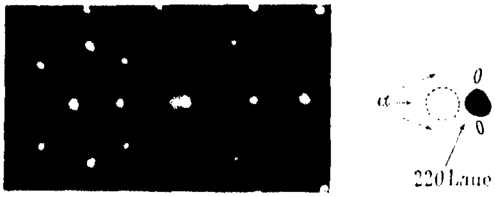

D(2), Cu radiation, $\theta_{110} = 39·75°$. Film normal at 75·3° to undeviated incident beam.

c

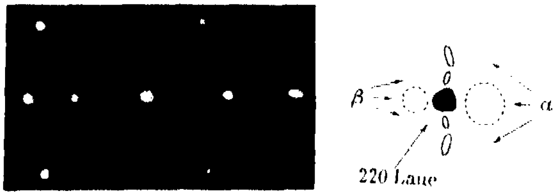

D(2), Fe radiation, $\theta_{110} = 46·1°$. Film normal at 80° to undeviated incident beam.

d

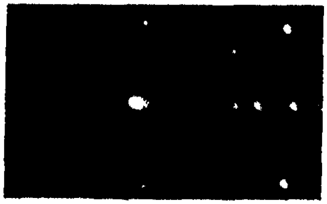

D(2), Cu radiation, $\theta_{001} = 61·7°$. Film normal at 80° to undeviated incident beam. No secondary, only primary (Cu $K\alpha$) diffuse spot just by 004 Laue.

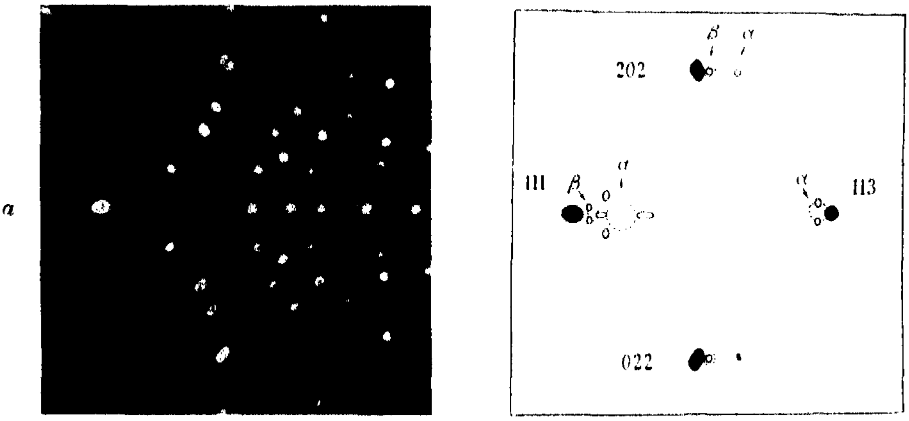

a, D(2), Cu radiation (partly filtered); $\theta_{111} = -18{\cdot}1°$. Film normal at 80 to undeviated incident beam. Room temperature.

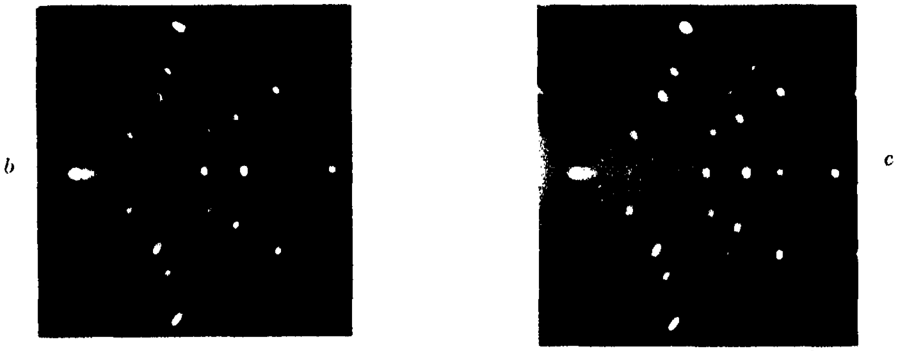

D(3), Cu unfiltered radiation, $\theta_{111} = -18{\cdot}6°$. Film normal at 68·5° to undeviated incident beam. *b*, 30° C, 9 min.; *c*, −180° C, 15 min.

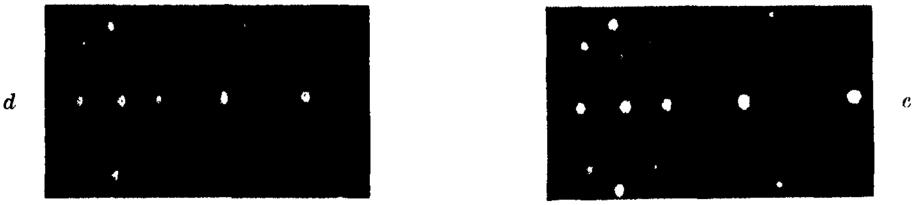

D(2), Fe unfiltered radiation. Film parallel to undeviated incident beam. *d*, $\theta_{113} = -62{\cdot}75°$; *e*, $\theta_{113} = -66{\cdot}75°$ (Bragg angle 64·2°).

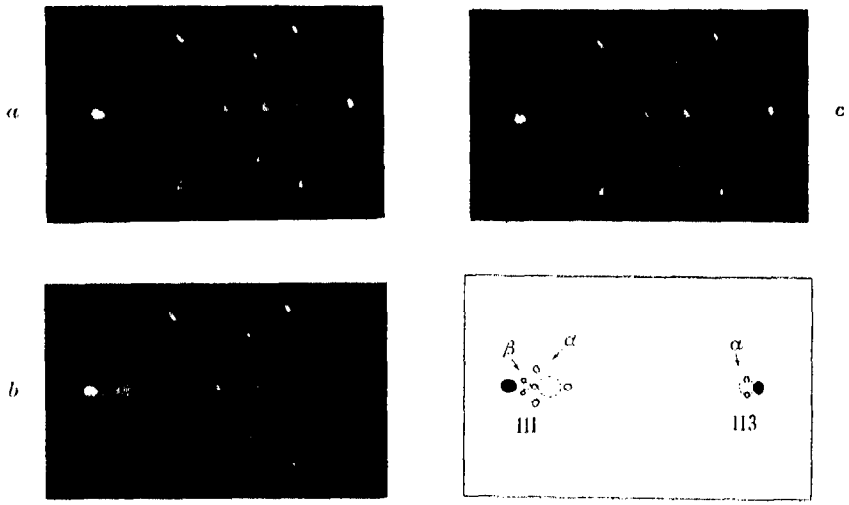

D(2), Cu unfiltered radiation, $\theta_{111} = -18°$. Film normal at 69° to undeviated incident beam. *a*, 30° C, 10 min.; *b*, 650° C, 10 min.; *c*, 650° C, 5 min.

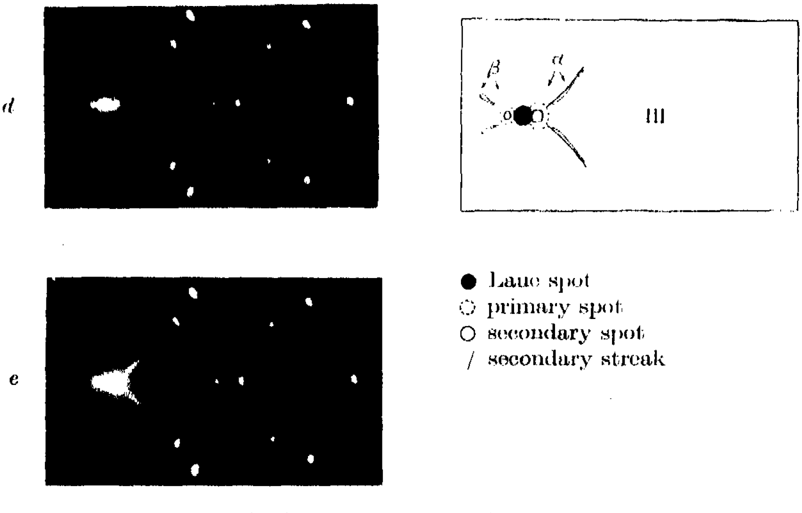

D(2), Cu unfiltered radiation, $\theta_{111} = +21\cdot2°$. Film normal at 60° to undeviated incident beam. *d*, 25° C, 30 min.; *e*, 650° C, 30 min. D(2) is a type I diamond, giving strong secondary effects.

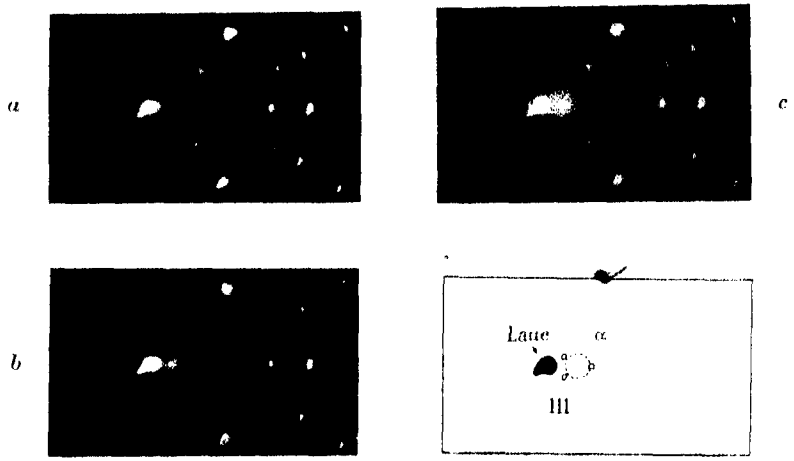

D(4), type I diamond, giving very weak secondary effects. Cu unfiltered radiation, $\theta_{111} = -19°$. Film normal at 68° to undeviated incident beam. *a*, 25° C, 10 min.; *b*, 650° C, 5 min.; *c*, 650° C, 10 min.

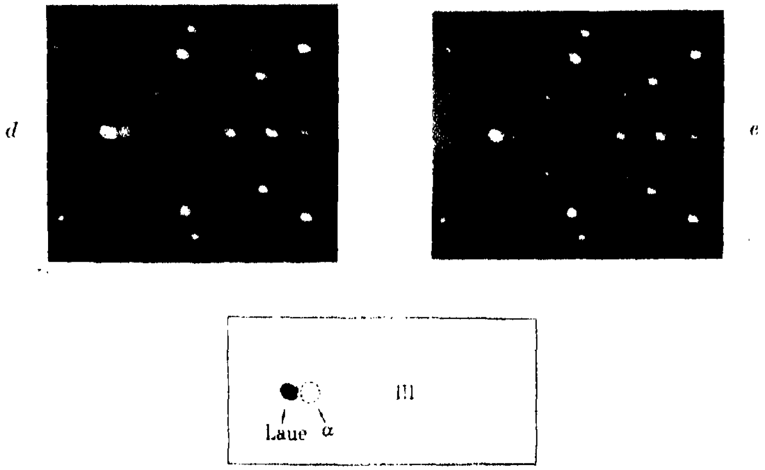

D2, type II diamond giving no secondary effects. Cu unfiltered radiation, $\theta_{111} = -20°$. Film normal at 68° to undeviated incident beam. *d*, 25° C, 5 min.; *e*, −180° C, 10 min.

thermally excited lattice vibrations on the scattering of X-rays by crystals. This theory of Faxén and Waller has been recapitulated recently by Zachariasen (1940), who has shown that it is capable of giving general agreement with the experimental results. Zachariasen used, however, a less general expression than the complete Faxén-Waller formula, his final formula not taking into account the full elastic anisotropy of the crystal. It is the purpose of this paper to deduce from the general expression given by both Faxén and Waller the manner in which the shape of the surfaces of isodiffusion discussed by Laval (1939) depend upon the three fundamental elastic constants of a cubic crystal. It is found that for substances with high elastic anisotropy such as sodium, large deviations from spherical character are to be expected for the surfaces of isodiffusion belonging to each of the individual lattice planes and, moreover, marked differences in shape between surfaces belonging to different lattice planes. Theoretically, therefore, the diffuse scattering phenomenon is capable of being developed into a method of determining the elastic constants of crystals, although the experimental difficulties may be very great (one of them being, for example, the certainty that the crystal under investigation is free from internal strains or other imperfections).* These theoretically predicted variations will also be of importance in connexion with the rival theories (Preston-Bragg-Jauncey block hypothesis, Raman's modified radiation hypothesis†) which claim to explain the experimental results as well as the Faxén-Waller-Zachariasen theory. Measurements on a strain-free single crystal of sodium might well settle this controversy once and for all.

The theory of Faxén and Waller was in the nature of a correction to the original work of Debye (1914) on the subject. Debye's calculation was equivalent to a process of first averaging over the thermal motion of the atoms, leading thereby to a temperature-dependent Gaussian distribution about each lattice point, and then calculating the scattering of X-rays from such a distribution (cf. Ewald 1940). Faxén and Waller, on the other hand, pointed out that since the scattering takes place from the instantaneous configuration of the crystal (neglecting retardation effects), calculation should first be made of the scattering from the instantaneous configuration and then an average taken over the thermal motion, instead of vice versa as Debye had done. The calculation of Faxén and Waller and of Zachariasen has, however, been carried out in a manner which tends to obscure the simple physical basis of the theory. A much more direct approach to the theory has been outlined by Mauguin and Laval (1939) in a note on the Fourier transforms of lattice vibrations, and it would not be difficult to develop their method into a completely rigorous and physically satisfying derivation of the whole Faxén-Waller theory. Preference is given, however, to the following very elementary but far from rigorous derivation of the fundamental Faxén-Waller formula, which should help to clarify the subject, being based as it is on ideas familiar to all crystal physicists.

---

* For instance, I at one time held the opinion that the triangular spots and the streaks found for diamond (Jahn and Lonsdale 1941) were indicative of a considerable elastic anisotropy for the diamond crystal, but recent experiments of Lonsdale and Smith which prove that these effects are found only with the one type of diamond and not the other and that, moreover, the variation for different Bragg spots is not in accordance with the variation to be expected from the Faxén-Waller theory, show conclusively that the effect in the one type of diamond is not due to thermally excited lattice vibrations of the unstrained perfect crystal.

† See, for example, Jauncey (1941) and Raman (1941).

1. Elementary derivation of the Faxén-Waller formula

The fundamental idea behind this derivation is that if the instantaneous configuration of a crystal traversed by a single plane wave is considered, the successive wave fronts of which make integral intercepts on the crystal axes, then the original fundamental basis of the translational lattice is replaced by a larger basis determined by these intercepts. This larger basis leads to a finer subdivision of the reciprocal space and to a structure factor which depends upon the wave form. Thus it can be said that a plane wave has the effect of dividing the crystal up into a lattice of congruent, similarly oriented and similarly deformed, crystal blocks, the size of the individual block being proportional to the wave-length of the wave. The existence of the whole lattice of blocks entails sharp scattering only, and the wave nature of the deformation of each block entails sharp restrictions on the directions for which scattering occurs. In fact, it is found that the single plane wave leads finally, so long as its amplitude is sufficiently small, only to two extra sharp scattering directions about each Bragg reflexion of the undisturbed crystal. Further, making use of the well-known resolution of the thermal motion into independent plane waves (normal modes of vibration), each with its own temperature excitation function depending upon the fundamental frequency of vibration of the mode, it is found that to the first approximation each plane wave scatters independently. Thus it is seen how each Bragg reflexion is surrounded by a cloud of sharp scattering directions, each of which is due to a different lattice vibration, i.e. to a different very large set of crystal blocks, in each particular set the blocks possessing the same size and deformation but different sets differing in the size and deformation of the individual blocks, each atom in the crystal belonging simultaneously to every set. The fundamental difference between the Faxén-Waller-Zachariasen theory and the Preston-Bragg-Jauncey block hypothesis is here clearly seen, for the essence of the latter was to derive this whole cloud of scattering directions from the well-known diffuseness of scattering from one small single crystal block.

Next consider a crystal with one atom in the unit cell. Let $\mathbf{a}_1$, $\mathbf{a}_2$, $\mathbf{a}_3$ be the fundamental translational vectors of the lattice, $\mathbf{b}_1$, $\mathbf{b}_2$, $\mathbf{b}_3$ the fundamental vectors of the reciprocal lattice. Consider the instantaneous configuration of the crystal due to a single plane wave described by

$$\mathbf{u}_l = q\mathbf{e}\sin 2\pi\left(\frac{l_1}{L_1}+\frac{l_2}{L_2}+\frac{l_3}{L_3}\right), \tag{1}$$

where $\mathbf{u}_l$ is the displacement vector of the atom having the equilibrium position $\mathbf{X}_l = l_1\mathbf{a}_1 + l_2\mathbf{a}_2 + l_3\mathbf{a}_3$ (l_1, l_2, l_3 integral), q the small amplitude of the wave, and $\mathbf{e}$ a unit vector describing the direction of polarization of the elastic wave (for a general direction of propagation in a crystal the motion is in general neither purely longitudinal nor purely transversal). The expression (1) can be written in the form

$$\mathbf{u}_l = q\mathbf{e}\sin 2\pi(\mathbf{W}, \mathbf{X}_l),$$

with

$$\mathbf{W} = \frac{1}{L_1}\mathbf{b}_1 + \frac{1}{L_2}\mathbf{b}_2 + \frac{1}{L_3}\mathbf{b}_3.$$

Thus $\mathbf{W}$ is the wave vector of the wave (1). It is known from lattice theory that if from the origin of the reciprocal lattice are drawn the wave vectors $\mathbf{W}$ of all possible lattice waves, then for a large crystal the end-points of these vectors cover with uniform density the first Brillouin zone of the reciprocal lattice. Hence for a large crystal and fairly long waves a sufficiently fine selection of waves is obtained by restricting L_1, L_2, L_3 to integral values. It is then seen that the instantaneous configuration described by (1) forms a complex lattice with $L_1L_2L_3$ atoms in the unit cell, the new fundamental translational vectors being

$$\mathbf{A}_1 = L_1\mathbf{a}_1, \quad \mathbf{A}_2 = L_2\mathbf{a}_2, \quad \mathbf{A}_3 = L_3\mathbf{a}_3,$$

with corresponding reciprocal lattice vectors

$$\mathbf{B}_1 = \mathbf{b}_1/L_1, \quad \mathbf{B}_2 = \mathbf{b}_2/L_2, \quad \mathbf{B}_3 = \mathbf{b}_3/L_3.$$

Consider now the scattering of X-rays from this complex lattice. Elementary theory shows that if

$$\mathbf{B} = \frac{\boldsymbol{\epsilon}-\boldsymbol{\epsilon}_0}{\lambda},$$

where $\boldsymbol{\epsilon}_0$, $\boldsymbol{\epsilon}$ are unit vectors in the direction of incident and reflected rays, λ the wave-length of the radiation, then Bragg reflexions take place only when

$$\mathbf{B} = \mathbf{B}_N = N_1\mathbf{B}_1 + N_2\mathbf{B}_2 + N_3\mathbf{B}_3 \quad (N_1, N_2, N_3 \text{ integral}).$$

Further, the intensity of scattering in the direction determined by $\mathbf{B}_N$ is proportional to the square of the structure factor or weight function $S(\mathbf{B}_N)$ in the reciprocal space of the complex lattice at the point $\mathbf{B}_N$. This is given by

$$S(\mathbf{B}_N) = \frac{1}{V}\sum_{l_1=1}^{L_1}\sum_{l_2=1}^{L_2}\sum_{l_3=1}^{L_3} e^{2\pi i(\mathbf{X}_l+\mathbf{u}_l,\mathbf{B}_N)},$$

where V = volume of unit cell of complex lattice $= L_1L_2L_3v$, v being the volume of the unit cell of the undisturbed crystal. Now if the amplitude q of the wave is sufficiently small, this can be written in the form

$$S(\mathbf{B}_N) = \frac{1}{V}\sum_{l_1=1}^{L_1}\sum_{l_2=1}^{L_2}\sum_{l_3=1}^{L_3} e^{2\pi i(\mathbf{X}_l,\mathbf{B}_N)}\{1 + 2\pi iq(\mathbf{e},\mathbf{B}_N)\sin 2\pi(\mathbf{W},\mathbf{X}_l)\},$$

neglecting the higher powers of q. Putting

$$\sin 2\pi(\mathbf{W},\mathbf{X}_l) = \frac{1}{2i}\{e^{2\pi i(\mathbf{W},\mathbf{X}_l)} - e^{-2\pi i(\mathbf{W},\mathbf{X}_l)}\}$$

and $$(\mathbf{W},\mathbf{X}_l) = \frac{l_1}{L_1} + \frac{l_2}{L_2} + \frac{l_3}{L_3}, \quad (\mathbf{X}_l,\mathbf{B}_N) = N_1\frac{l_1}{L_1} + N_2\frac{l_2}{L_2} + N_3\frac{l_3}{L_3},$$

then

$$\begin{aligned}S(\mathbf{B}_N) = {} & \frac{1}{V}\sum_{l_1=1}^{L_1}\sum_{l_2=1}^{L_2}\sum_{l_3=1}^{L_3}\exp\left[2\pi i\left(\frac{l_1}{L_1}N_1 + \frac{l_2}{L_2}N_2 + \frac{l_3}{L_3}N_3\right)\right] \\ & + \pi q(\mathbf{e},\mathbf{B}_N)\frac{1}{V}\sum_{l_1=1}^{L_1}\sum_{l_2=1}^{L_2}\sum_{l_3=1}^{L_3}\left[\exp\left[2\pi i\left\{\frac{l_1}{L_1}(N_1+1) + \frac{l_2}{L_2}(N_2+1) + \frac{l_3}{L_3}(N_3+1)\right\}\right]\right. \\ & \left. - \exp\left[2\pi i\left\{\frac{l_1}{L_1}(N_1-1) + \frac{l_2}{L_2}(N_2-1) + \frac{l_3}{L_3}(N_3-1)\right\}\right]\right].\end{aligned}$$

Now $$\sum_{l_1=1}^{L_1}\sum_{l_2=1}^{L_2}\sum_{l_3=1}^{L_3}\exp\left[2\pi i\left(\frac{l_1}{L_1}N_1 + \frac{l_2}{L_2}N_2 + \frac{l_3}{L_3}N_3\right)\right]$$

is zero unless $N_1 = n_1L_1$, $N_2 = n_2L_2$, $N_3 = n_3L_3$ (n_1, n_2, n_3 integral) when it has the value $L_1L_2L_3$. Similarly

$$\sum_{l_1=1}^{L_1}\sum_{l_2=1}^{L_2}\sum_{l_3=1}^{L_3}\exp\left[2\pi i\left\{\frac{l_1}{L_1}(N_1+1) + \frac{l_2}{L_2}(N_2+1) + \frac{l_3}{L_3}(N_3+1)\right\}\right]$$

and $$\sum_{l_1=1}^{L_1}\sum_{l_2=1}^{L_2}\sum_{l_3=1}^{L_3}\exp\left[2\pi i\left\{\frac{l_1}{L_1}(N_1-1) + \frac{l_2}{L_2}(N_2-1) + \frac{l_3}{L_3}(N_3-1)\right\}\right]$$

are zero unless

$$N_1+1 = n_1L_1, \quad N_2+1 = n_2L_2, \quad N_3+1 = n_3L_3$$

and $$N_1-1 = n_1L_1, \quad N_2-1 = n_2L_2, \quad N_3-1 = n_3L_3,$$

respectively. Thus remembering

$$\mathbf{B}_N = N_1\mathbf{B}_1+N_2\mathbf{B}_2+N_3\mathbf{B}_3$$

and putting $$\mathbf{b}_n = n_1\mathbf{b}_1+n_2\mathbf{b}_2+n_3\mathbf{b}_3$$
$$= n_1L_1\mathbf{B}_1+n_2L_2\mathbf{B}_2+n_3L_3\mathbf{B}_3$$

and $$\mathbf{W} = \frac{1}{L_1}\mathbf{b}_1+\frac{1}{L_2}\mathbf{b}_2+\frac{1}{L_3}\mathbf{b}_3$$
$$= \mathbf{B}_1+\mathbf{B}_2+\mathbf{B}_3,$$

it is seen that $S(\mathbf{B}_N)$ vanishes except for

$$\mathbf{B}_N = \mathbf{b}_n, \quad \text{when} \quad S(\mathbf{B}_N) = \frac{1}{v},$$

$$\mathbf{B}_N = \mathbf{b}_n-\mathbf{W}, \quad \text{when} \quad S(\mathbf{B}_N) = \frac{1}{v}\pi q(\mathbf{e},\mathbf{B}_N),$$

or $$\mathbf{B}_N = \mathbf{b}_n+\mathbf{W}, \quad \text{when} \quad S(\mathbf{B}_N) = -\frac{1}{v}\pi q(\mathbf{e},\mathbf{B}_N).$$

Thus the Faxén-Waller vector condition is reached. Further, the intensity of scattering in the direction determined by $\mathbf{B} = \mathbf{b}_n+\mathbf{W}$ is proportional to $q^2(\mathbf{B},\mathbf{e})^2$. It is known that the mean square amplitude $\overline{q^2}$ of a harmonic oscillator is proportional to the mean energy $\bar{E}$ divided by the square of the frequency:

$$\overline{q^2} \sim \frac{\bar{E}}{\nu^2} = \frac{1}{\nu^2}\left\{\frac{h\nu}{e^{h\nu/kT}-1}+\tfrac{1}{2}h\nu\right\} = \frac{kT}{\nu^2} \quad \text{for } h\nu \ll kT,$$

i.e. for long elastic waves.

Considering now the superposition of a number of plane waves, it is easy to see that in the present approximation (assumption of small amplitudes) each plane wave scatters independently in the above manner. Thus taking into account the existence of three independent modes of vibration with frequencies ν_1, ν_2, ν_3 and directions of oscillation $\mathbf{e}_1$, $\mathbf{e}_2$, $\mathbf{e}_3$ for any given wave vector $\mathbf{W}$ in the Brillouin zone, the Faxén-Waller formula

$$I(\mathbf{B}) \sim \frac{(\mathbf{B},\mathbf{e}_1)^2}{\nu_1^2}+\frac{(\mathbf{B},\mathbf{e}_2)^2}{\nu_2^2}+\frac{(\mathbf{B},\mathbf{e}_3)^2}{\nu_3^2}$$

for the intensity of scattering in the direction determined by the vector **B** drawn from the origin of the reciprocal lattice is reached, where, as stated above,

$$\mathbf{B} = (\boldsymbol{\epsilon} - \boldsymbol{\epsilon}_0)/\lambda$$

($\boldsymbol{\epsilon}_0$, $\boldsymbol{\epsilon}$ unit vectors in the direction of incident and reflected ray, λ the wave-length of the monochromatic X-rays) and **B** and **W** are related by the Faxén-Waller vector condition

$$\mathbf{B} = \mathbf{b}_n + \mathbf{W},$$

where $\mathbf{b}_n$ is that reciprocal lattice vector of the undisturbed crystal whose end-point lies nearest to that of **B**, i.e. which lies in the same Brillouin zone as **B**.

2. SURFACES OF ISODIFFUSION FOR CUBIC CRYSTALS

Now write the Faxén-Waller formula

$$I(\mathbf{B}) = \frac{(\mathbf{b}_n + \mathbf{W}, \mathbf{e}_1)^2}{\nu_1^2} + \frac{(\mathbf{b}_n + \mathbf{W}, \mathbf{e}_2)^2}{\nu_2^2} + \frac{(\mathbf{b}_n + \mathbf{W}, \mathbf{e}_3)^2}{\nu_3^2}$$

in the form

$$\begin{aligned} I(\mathbf{B}) = {} & \frac{(\mathbf{b}_n, \mathbf{e}_1)^2}{\nu_1^2} + \frac{(\mathbf{b}_n, \mathbf{e}_2)^2}{\nu_2^2} + \frac{(\mathbf{b}_n, \mathbf{e}_3)^2}{\nu_3^2} \\ & + 2\left\{\frac{(\mathbf{b}_n, \mathbf{e}_1)(\mathbf{W}, \mathbf{e}_1)}{\nu_1^2} + \frac{(\mathbf{b}_n, \mathbf{e}_2)(\mathbf{W}, \mathbf{e}_2)}{\nu_2^2} + \frac{(\mathbf{b}_n, \mathbf{e}_3)(\mathbf{W}, \mathbf{e}_3)}{\nu_3^2}\right\} \\ & + \frac{(\mathbf{W}, \mathbf{e}_1)^2}{\nu_1^2} + \frac{(\mathbf{W}, \mathbf{e}_2)^2}{\nu_2^2} + \frac{(\mathbf{W}, \mathbf{e}_3)^2}{\nu_3^2}. \end{aligned}$$

Let l, m, n denote the direction cosines of **W** relative to the cubic axes, L, M, N those of $\mathbf{b}_n$. Then if

$$\mathbf{b}_n = R(L, M, N),$$
$$\mathbf{W} = r(l, m, n),$$

R is the distance of the reciprocal lattice point under consideration from the origin and r is the distance of the end-point of **B** from the end-point of $\mathbf{b}_n$. r is also the reciprocal wave-length of the lattice wave, i.e.

$$\nu_i = rc_i \quad (i = 1, 2, 3),$$

where c_i is the velocity of the wave of frequency ν_i. Further, let A_i, B_i, C_i denote the direction cosines of the unit polarization vectors $\mathbf{e}_i$:

$$\mathbf{e}_i = (A_i, B_i, C_i) \quad (i = 1, 2, 3).$$

Then

$$I(\mathbf{B}) = \frac{R^2}{r^2}\sum_{i=1}^{3}\frac{(LA_i+MB_i+NC_i)^2}{c_i^2} + \frac{2R}{r}\sum_{i=1}^{3}\frac{(LA_i+MB_i+NC_i)(lA_i+mB_i+nC_i)}{c_i^2} + \sum_{i=1}^{3}\frac{(lA_i+mB_i+nC_i)^2}{c_i^2}.$$

If $r \ll R$ (proximity to Bragg setting), only the first term need be considered, and it is found that for the radial co-ordinate r of the surface of equidiffusion (i.e. values of r for which $I(\mathbf{B})$ is constant)

$$r^2 \sim \sum_{i=1}^{3}\frac{(LA_i+MB_i+NC_i)^2}{c_i^2}.$$

In this approximation the surfaces of isodiffusion possess a centre of symmetry; the second term which we have neglected would introduce asymmetry for larger values of r for which however the whole acoustical approximation to which we are restricting ourselves (neglect of dispersion of the lattice waves) no longer applies.

Now the velocities c_1, c_2, c_3 and polarization vectors $\mathbf{e}_1$, $\mathbf{e}_2$, $\mathbf{e}_3$ of the three elastic waves of wave vector $\mathbf{W}$ having direction cosines l, m, n relative to the cubic axes are given by the three solutions of the simultaneous equations:

$$\left.\begin{aligned} \{c_{11}l^2+c_{44}(m^2+n^2)-\rho c_i^2\}A_i+(c_{12}+c_{44})(lmB_i+lnC_i) &= 0,\\ \{c_{11}m^2+c_{44}(l^2+n^2)-\rho c_i^2\}B_i+(c_{12}+c_{44})(lmA_i+mnC_i) &= 0,\\ \{c_{11}n^2+c_{44}(l^2+m^2)-\rho c_i^2\}C_i+(c_{12}+c_{44})(lnA_i+mnB_i) &= 0,\end{aligned}\right\} \qquad (2)$$

where c_{11}, c_{12}, c_{44} are the three elastic constants and ρ the density of the cubic crystal. These equations can be factorized into three independent equations for waves propagated along special directions in the crystal, viz. for waves propagated along the 100, 110, 111 and crystallographic equivalent directions, for along these directions the lattice waves take the form of one pure longitudinal and two pure transverse waves. This gives rise to simple expressions for the relative intercepts of the surfaces of isodiffusion on these major crystallographic directions about any one of the reciprocal lattice points. These three special cases are treated below (§ 3). The expressions derived there together with the condition of centre of symmetry give us the intercepts in 26 directions about the reciprocal lattice point with direction cosines L, M, N and hence give a fairly complete picture of the shape of the isodiffusion surfaces corresponding to any crystal plane. For a general direction of propagation (l, m, n) there are neither pure transverse nor pure longitudinal waves, and the intensity expression then becomes much more complicated (in the general case the velocities are roots of cubic equations). Nevertheless, a general expression can be found for the intercepts of the isodiffusion surface in an arbitrary direction for a general crystal plane in a manner indicated by Waller in his dissertation by which the explicit solution of the cubic equations is avoided. This general expression is derived in § 4 and used to obtain complete expressions for the contours of special plane sections of particular isodiffusion surfaces. In § 5 the diffuse scattering surrounding the central beam is investigated separately and finally in § 6 some consequences of the theory for the special case of sodium are indicated.

3. INTERCEPTS OF THE ISODIFFUSION SURFACES IN SPECIAL DIRECTIONS

(1) *Elastic waves propagated along a four-fold cubic axis*

For example $l = 1, \quad m = n = 0.$

The determining equations (2) become

$$(c_{11}-\rho c_i^2)A_i = 0,$$
$$(c_{44}-\rho c_i^2)B_i = 0,$$
$$(c_{44}-\rho c_i^2)C_i = 0,$$

giving the solutions

$$\rho c_1^2 = c_{11}, \quad A_1 = 1, \quad B_1 = C_1 = 0,$$
$$\rho c_2^2 = c_{44}, \quad B_1 = 1, \quad A_1 = C_1 = 0,$$
$$\rho c_3^2 = c_{44}, \quad C_1 = 1, \quad A_1 = B_1 = 0,$$

corresponding to a longitudinal wave of velocity $\sqrt{(c_{11}/\rho)}$ and two transverse waves of the same velocity $\sqrt{(c_{44}/\rho)}$. Substitution in the expression

$$r^2 = \sum_{i=1}^{3} \frac{(LA_i+MB_i+NC_i)^2}{\rho c_i^2} \tag{3}$$

gives

$$r^2(100) = \frac{L^2}{c_{11}} + \frac{M^2+N^2}{c_{44}}$$

for the square of the relative intercept on the x axis. By symmetry it is found for the intercepts on the y and z axes

$$r^2(010) = \frac{M^2}{c_{11}} + \frac{L^2+N^2}{c_{44}},$$

$$r^2(001) = \frac{N^2}{c_{11}} + \frac{L^2+M^2}{c_{44}}.$$

(2) *Elastic waves propagated along a digonal axis*

For example $l = m = 1/\sqrt{2}, \quad n = 0.$

The equations become

$$\{\tfrac{1}{2}(c_{11}+c_{44})-\rho c_i^2\}\,A_i+\tfrac{1}{2}(c_{12}+c_{44})\,B_i = 0,$$

$$\{\tfrac{1}{2}(c_{11}+c_{44})-\rho c_i^2\}\,B_i+\tfrac{1}{2}(c_{12}+c_{44})\,A_i = 0,$$

$$(c_{44}-\rho c_i^2)\,C_i = 0.$$

By combining the first two equations

$$\{\tfrac{1}{2}(c_{11}+c_{12}+2c_{44})-\rho c_i^2\}\,(A_i+B_i) = 0,$$

$$\{\tfrac{1}{2}(c_{11}-c_{12})-\rho c_i^2\}\,(A_i-B_i) = 0,$$

giving the three solutions

$$\begin{aligned}
\rho c_1^2 &= \tfrac{1}{2}(c_{11}+c_{12}+2c_{44}), & A_1 &= B_1 = 1/\sqrt{2},\ C_1 = 0,\\
\rho c_2^2 &= \tfrac{1}{2}(c_{11}-c_{12}), & A_2 &= -B_2 = 1/\sqrt{2},\ C_2 = 0,\\
\rho c_3^2 &= c_{44}, & A_3 &= B_3 = 0,\ C_3 = 1,
\end{aligned}$$

the first being a pure longitudinal wave and the other two transverse waves, this time with different frequencies. Substitution in (3) gives

$$r^2(110) = \frac{(L+M)^2}{c_{11}+c_{12}+2c_{44}}+\frac{(L-M)^2}{c_{11}-c_{12}}+\frac{N^2}{c_{44}},$$

and by symmetry

$$r^2(101) = \frac{(L+N)^2}{c_{11}+c_{12}+2c_{44}}+\frac{(L-N)^2}{c_{11}-c_{12}}+\frac{M^2}{c_{44}},$$

$$r^2(011) = \frac{(M+N)^2}{c_{11}+c_{12}+2c_{44}}+\frac{(M-N)^2}{c_{11}-c_{12}}+\frac{L^2}{c_{44}}.$$

Similarly for the $1\bar{1}0$ direction, i.e. $l = -m = 1/\sqrt{2}$, $n = 0$,

$$\{\tfrac{1}{2}(c_{11}-c_{12})-\rho c_i^2\}\,(A_i+B_i) = 0,$$

$$\{\tfrac{1}{2}(c_{11}+c_{12}+2c_{44})-\rho c_i^2\}\,(A_i-B_i) = 0,$$

$$(c_{44}-\rho c_i^2)\,C_i = 0,$$

giving the intercepts

$$r^2(1\bar{1}0) = \frac{(L-M)^2}{c_{11}+c_{12}+2c_{44}}+\frac{(L+M)^2}{c_{11}-c_{12}}+\frac{N^2}{c_{44}},$$

and by symmetry

$$r^2(10\bar{1}) = \frac{(L-N)^2}{c_{11}+c_{12}+2c_{44}} + \frac{(L+N)^2}{c_{11}-c_{12}} + \frac{M^2}{c_{44}},$$

$$r^2(01\bar{1}) = \frac{(M-N)^2}{c_{11}+c_{12}+2c_{44}} + \frac{(M+N)^2}{c_{11}-c_{12}} + \frac{L^2}{c_{44}}.$$

(3) *Elastic waves propagated along a trigonal axis*

For example 111 direction, i.e. $l = m = n = 1/\sqrt{3}$.
The equations become

$$\{\tfrac{1}{3}(c_{11}+2c_{44}) - \rho c_i^2\} A_i + \tfrac{1}{3}(c_{12}+c_{44})(B_i+C_i) = 0,$$

$$\{\tfrac{1}{3}(c_{11}+2c_{44}) - \rho c_i^2\} B_i + \tfrac{1}{3}(c_{12}+c_{44})(A_i+C_i) = 0,$$

$$\{\tfrac{1}{3}(c_{11}+2c_{44}) - \rho c_i^2\} C_i + \tfrac{1}{3}(c_{12}+c_{44})(A_i+B_i) = 0,$$

from which

$$\{\tfrac{1}{3}(c_{11}+2c_{12}+4c_{44}) - \rho c_i^2\}(A_i+B_i+C_i) = 0,$$

$$\{\tfrac{1}{3}(c_{11}-c_{12}+c_{44}) - \rho c_i^2\}(A_i-B_i) = 0,$$

$$\{\tfrac{1}{3}(c_{11}-c_{12}+c_{44}) - \rho c_i^2\}(A_i+B_i-2C_i) = 0,$$

giving the solutions

$$\rho c_1^2 = \tfrac{1}{3}(c_{11}+2c_{12}+4c_{44}), \quad A_1 = B_1 = C_1 = 1/\sqrt{3},$$

$$\rho c_2^2 = \tfrac{1}{3}(c_{11}-c_{12}+c_{44}), \quad A_2 = -B_2 = 1/\sqrt{2},\ C_2 = 0,$$

$$\rho c_3^2 = \tfrac{1}{3}(c_{11}-c_{12}+c_{44}), \quad A_3 = B_3 = -\tfrac{1}{2}C_3 = 1/\sqrt{6}.$$

Here the two transverse waves are degenerate (i.e. have the same frequency), and hence the corresponding modes are arbitrary apart from mutual orthogonality and orthogonality to the longitudinal mode. Then

$$r^2(111) = \frac{(L+M+N)^2}{c_{11}+2c_{12}+4c_{44}} + \frac{3}{c_{11}-c_{12}+c_{44}}\left\{\frac{(L-M)^2}{2} + \frac{(L+M-2N)^2}{6}\right\}$$

$$= \frac{(L+M+N)^2}{c_{11}+2c_{12}+4c_{44}} + \frac{2\{1-(LM+LN+MN)\}}{c_{11}-c_{12}+c_{44}},$$

TABLE 1. RELATIVE INTERCEPTS OF SURFACES OF ISODIFFUSION ALONG SPECIAL CRYSTALLOGRAPHIC DIRECTIONS

W \ B		(L, M, N)	001	110	111
a	100	$\sqrt{\left(\frac{L^2}{c_{11}}+\frac{M^2+N^2}{c_{44}}\right)}$	$\sqrt{\frac{1}{c_{44}}}$	$\sqrt{\left(\frac{1}{2c_{11}}+\frac{1}{2c_{44}}\right)}$	$\sqrt{\left(\frac{1}{3c_{11}}+\frac{2}{3c_{44}}\right)}$
b	010	$\sqrt{\left(\frac{M^2}{c_{11}}+\frac{L^2+N^2}{c_{44}}\right)}$	$\sqrt{\frac{1}{c_{44}}}$	$\sqrt{\left(\frac{1}{2c_{11}}+\frac{1}{2c_{44}}\right)}$	$\sqrt{\left(\frac{1}{3c_{11}}+\frac{2}{3c_{44}}\right)}$
c	001	$\sqrt{\left(\frac{N^2}{c_{11}}+\frac{L^2+M^2}{c_{44}}\right)}$	$\sqrt{\frac{1}{c_{11}}}$	$\sqrt{\frac{1}{c_{44}}}$	$\sqrt{\left(\frac{1}{3c_{11}}+\frac{2}{3c_{44}}\right)}$
d	110	$\sqrt{\left(\frac{(L+M)^2}{c_{11}+c_{12}+2c_{44}}+\frac{(L-M)^2}{c_{11}-c_{12}}+\frac{N^2}{c_{44}}\right)}$	$\sqrt{\frac{1}{c_{44}}}$	$\sqrt{\frac{2}{c_{11}+c_{12}+2c_{44}}}$	$\sqrt{\left(\frac{1}{3c_{44}}+\frac{4}{3(c_{11}+c_{12}+2c_{44})}\right)}$
e	101	$\sqrt{\left(\frac{(L+N)^2}{c_{11}+c_{12}+2c_{44}}+\frac{(L-N)^2}{c_{11}-c_{12}}+\frac{M^2}{c_{44}}\right)}$	$\sqrt{\left(\frac{1}{c_{11}+c_{12}+2c_{44}}+\frac{1}{c_{11}-c_{12}}\right)}$	$\sqrt{\left(\frac{1}{2c_{44}}+\frac{1}{2(c_{11}+c_{12}+2c_{44})}+\frac{1}{2(c_{11}-c_{12})}\right)}$	$\sqrt{\left(\frac{1}{3c_{44}}+\frac{4}{3(c_{11}+c_{12}+2c_{44})}\right)}$
f	011	$\sqrt{\left(\frac{(M+N)^2}{c_{11}+c_{12}+2c_{44}}+\frac{(M-N)^2}{c_{11}-c_{12}}+\frac{L^2}{c_{44}}\right)}$	$\sqrt{\left(\frac{1}{c_{11}+c_{12}+2c_{44}}+\frac{1}{c_{11}-c_{12}}\right)}$	$\sqrt{\left(\frac{1}{2c_{44}}+\frac{1}{2(c_{11}+c_{12}+2c_{44})}+\frac{1}{2(c_{11}-c_{12})}\right)}$	$\sqrt{\left(\frac{1}{3c_{44}}+\frac{4}{3(c_{11}+c_{12}+2c_{44})}\right)}$
g	$1\bar{1}0$	$\sqrt{\left(\frac{(L-M)^2}{c_{11}+c_{12}+2c_{44}}+\frac{(L+M)^2}{c_{11}-c_{12}}+\frac{N^2}{c_{44}}\right)}$	$\sqrt{\frac{1}{c_{44}}}$	$\sqrt{\frac{2}{c_{11}-c_{12}}}$	$\sqrt{\left(\frac{1}{3c_{44}}+\frac{4}{3(c_{11}-c_{12})}\right)}$
h	$10\bar{1}$	$\sqrt{\left(\frac{(L-N)^2}{c_{11}+c_{12}+2c_{44}}+\frac{(L+N)^2}{c_{11}-c_{12}}+\frac{M^2}{c_{44}}\right)}$	$\sqrt{\left(\frac{1}{c_{11}+c_{12}+2c_{44}}+\frac{1}{c_{11}-c_{12}}\right)}$	$\sqrt{\left(\frac{1}{2c_{44}}+\frac{1}{2(c_{11}+c_{12}+2c_{44})}+\frac{1}{2(c_{11}-c_{12})}\right)}$	$\sqrt{\left(\frac{1}{3c_{44}}+\frac{4}{3(c_{11}-c_{12})}\right)}$
i	$01\bar{1}$	$\sqrt{\left(\frac{(M-N)^2}{c_{11}+c_{12}+2c_{44}}+\frac{(M+N)^2}{c_{11}-c_{12}}+\frac{L^2}{c_{44}}\right)}$	$\sqrt{\left(\frac{1}{c_{11}+c_{12}+2c_{44}}+\frac{1}{c_{11}-c_{12}}\right)}$	$\sqrt{\left(\frac{1}{2c_{44}}+\frac{1}{2(c_{11}+c_{12}+2c_{44})}+\frac{1}{2(c_{11}-c_{12})}\right)}$	$\sqrt{\left(\frac{1}{3c_{44}}+\frac{4}{3(c_{11}-c_{12})}\right)}$
j	111	$\sqrt{\left(\frac{(L+M+N)^2}{c_{11}+2c_{12}+4c_{44}}+\frac{2(1-LM-LN-MN)}{c_{11}-c_{12}+c_{44}}\right)}$	$\sqrt{\left(\frac{1}{c_{11}+2c_{12}+4c_{44}}+\frac{2}{c_{11}-c_{12}+c_{44}}\right)}$	$\sqrt{\left(\frac{2}{c_{11}+2c_{12}+4c_{44}}+\frac{1}{c_{11}-c_{12}+c_{44}}\right)}$	$\sqrt{\frac{3}{c_{11}+2c_{12}+4c_{44}}}$
k	$11\bar{1}$	$\sqrt{\left(\frac{(L+M-N)^2}{c_{11}+2c_{12}+4c_{44}}+\frac{2(1-LM+LN+MN)}{c_{11}-c_{12}+c_{44}}\right)}$	$\sqrt{\left(\frac{1}{c_{11}+2c_{12}+4c_{44}}+\frac{2}{c_{11}-c_{12}+c_{44}}\right)}$	$\sqrt{\left(\frac{2}{c_{11}+2c_{12}+4c_{44}}+\frac{1}{c_{11}-c_{12}+c_{44}}\right)}$	$\sqrt{\left(\frac{1}{3(c_{11}+2c_{12}+4c_{44})}+\frac{8}{3(c_{11}-c_{12}+c_{44})}\right)}$
l	$1\bar{1}1$	$\sqrt{\left(\frac{(L-M+N)^2}{c_{11}+2c_{12}+4c_{44}}+\frac{2(1+LM-LN+MN)}{c_{11}-c_{12}+c_{44}}\right)}$	$\sqrt{\left(\frac{1}{c_{11}+2c_{12}+4c_{44}}+\frac{2}{c_{11}-c_{12}+c_{44}}\right)}$	$\sqrt{\frac{3}{c_{11}-c_{12}+c_{44}}}$	$\sqrt{\left(\frac{1}{3(c_{11}+2c_{12}+4c_{44})}+\frac{8}{3(c_{11}-c_{12}+c_{44})}\right)}$
m	$\bar{1}11$	$\sqrt{\left(\frac{(-L+M+N)^2}{c_{11}+2c_{12}+4c_{44}}+\frac{2(1+LM+LN-MN)}{c_{11}-c_{12}+c_{44}}\right)}$	$\sqrt{\left(\frac{1}{c_{11}+2c_{12}+4c_{44}}+\frac{2}{c_{11}-c_{12}+c_{44}}\right)}$	$\sqrt{\frac{3}{c_{11}-c_{12}+c_{44}}}$	$\sqrt{\left(\frac{1}{3(c_{11}+2c_{12}+4c_{44})}+\frac{8}{3(c_{11}-c_{12}+c_{44})}\right)}$

making use of $L^2+M^2+N^2=1$. By symmetry it is found for the crystallographic equivalent directions that

$$r^2(11\bar{1})=\frac{(L+M-N)^2}{c_{11}+2c_{12}+4c_{44}}+\frac{2\{1-(LM-LN-MN)\}}{c_{11}-c_{12}+c_{44}},$$

$$r^2(1\bar{1}1)=\frac{(L-M+N)^2}{c_{11}+2c_{12}+4c_{44}}+\frac{2\{1-(-LM+LN-MN)\}}{c_{11}-c_{12}+c_{44}},$$

$$r^2(\bar{1}11)=\frac{(-L+M+N)^2}{c_{11}+2c_{12}+4c_{44}}+\frac{2\{1-(-LM-LN+MN)\}}{c_{11}-c_{12}+c_{44}}.$$

These general expressions, together with their special values for particular values of L, M, N, i.e. for particular lattice planes, are listed in table 1. The special directions are lettered from a to m and shown in the accompanying diagram (figure 1).

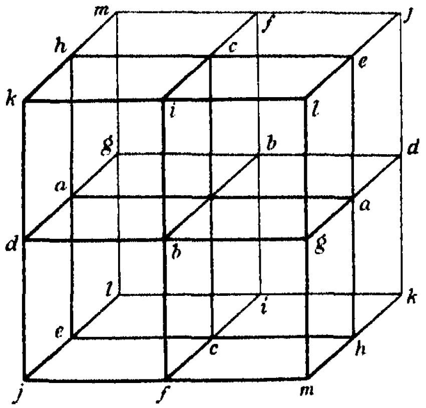

FIGURE 1

4. INTERCEPTS OF THE ISODIFFUSION SURFACES IN ARBITRARY DIRECTIONS

Now proceed to calculate the relative intercepts of the isodiffusion surfaces in arbitrary directions. Restriction is again made to scattering by the acoustical vibrations in close proximity to the Bragg setting. Strictly speaking this expression is valid only for a crystal with one atom in the unit cell, but it can be used also for a general crystal so long as the intermixture of the optical and acoustical modes can be neglected, i.e. if there are no exceptionally small optical frequencies.

Thus, for $r \ll R$,

$$\begin{aligned} r^2 &= \sum_{i=1}^{3} \frac{(LA_i + MB_i + NC_i)^2}{\rho c_i^2} \\ &= L^2 \sum_i \frac{A_i^2}{\rho c_i^2} + M^2 \sum_i \frac{B_i^2}{\rho c_i^2} + N^2 \sum_i \frac{C_i^2}{\rho c_i^2} \\ &\qquad + 2LM \sum_i \frac{A_i B_i}{\rho c_i^2} + 2LN \sum_i \frac{A_i C_i}{\rho c_i^2} + 2MN \sum_i \frac{B_i C_i}{\rho c_i^2}. \end{aligned}$$

Here A_i, B_i, C_i and the velocities c_i are determined by the equations

$$\left.\begin{aligned} A_i &= A_{11}\frac{A_i}{\rho c_i^2} + A_{12}\frac{B_i}{\rho c_i^2} + A_{13}\frac{C_i}{\rho c_i^2}, \\ B_i &= A_{12}\frac{A_i}{\rho c_i^2} + A_{22}\frac{B_i}{\rho c_i^2} + A_{23}\frac{C_i}{\rho c_i^2}, \\ C_i &= A_{13}\frac{A_i}{\rho c_i^2} + A_{23}\frac{B_i}{\rho c_i^2} + A_{33}\frac{C_i}{\rho c_i^2}, \end{aligned}\right\} \quad (i = 1, 2, 3) \qquad (4)$$

where for a general crystal with 21 elastic constants c_{rs} ($r \leqq s = 1, \ldots, 6$)

$$\begin{aligned} A_{11} &= c_{11} l^2 + c_{66} m^2 + c_{55} n^2 + 2c_{56} mn + 2c_{15} ln + 2c_{16} lm, \\ A_{22} &= c_{66} l^2 + c_{22} m^2 + c_{44} n^2 + 2c_{24} mn + 2c_{46} ln + 2c_{26} lm, \\ A_{33} &= c_{55} l^2 + c_{44} m^2 + c_{33} n^2 + 2c_{34} mn + 2c_{35} ln + 2c_{45} lm, \\ A_{12} &= c_{16} l^2 + c_{26} m^2 + c_{45} n^2 + (c_{25} + c_{46}) mn + (c_{14} + c_{56}) ln + (c_{12} + c_{66}) lm, \\ A_{13} &= c_{15} l^2 + c_{46} m^2 + c_{35} n^2 + (c_{36} + c_{45}) mn + (c_{13} + c_{55}) ln + (c_{14} + c_{56}) lm, \\ A_{23} &= c_{56} l^2 + c_{24} m^2 + c_{34} n^2 + (c_{23} + c_{44}) mn + (c_{36} + c_{45}) ln + (c_{25} + c_{46}) lm \end{aligned}$$

(cf. Love, *Theory of elasticity*, p. 287).

From (4) it is found that

$$\begin{aligned} \sum_{i=1}^{3} A_i^2 &= A_{11} \sum_i \frac{A_i^2}{\rho c_i^2} + A_{12} \sum_i \frac{A_i B_i}{\rho c_i^2} + A_{13} \sum_i \frac{A_i C_i}{\rho c_i^2} = 1, \\ \sum_{i=1}^{3} A_i B_i &= A_{12} \sum_i \frac{A_i^2}{\rho c_i^2} + A_{22} \sum_i \frac{A_i B_i}{\rho c_i^2} + A_{23} \sum_i \frac{A_i C_i}{\rho c_i^2} = 0, \\ \sum_{i=1}^{3} A_i C_i &= A_{13} \sum_i \frac{A_i^2}{\rho c_i^2} + A_{23} \sum_i \frac{A_i B_i}{\rho c_i^2} + A_{33} \sum_i \frac{A_i C_i}{\rho c_i^2} = 0, \end{aligned}$$

since the polarization vectors are unit and orthogonal vectors. Thus

$$\sum_i \frac{A_i^2}{\rho c_i^2} = \frac{\begin{vmatrix} A_{22} & A_{23} \\ A_{23} & A_{33} \end{vmatrix}}{\Delta} = (A^{-1})_{11},$$

$$\sum_i \frac{A_i B_i}{\rho c_i^2} = -\frac{\begin{vmatrix} A_{12} & A_{23} \\ A_{13} & A_{33} \end{vmatrix}}{\Delta} = (A^{-1})_{12},$$

$$\sum_i \frac{A_i C_i}{\rho c_i^2} = \frac{\begin{vmatrix} A_{12} & A_{22} \\ A_{13} & A_{23} \end{vmatrix}}{\Delta} = (A^{-1})_{13},$$

where

$$\Delta = \begin{vmatrix} A_{11} & A_{12} & A_{13} \\ A_{12} & A_{22} & A_{23} \\ A_{13} & A_{23} & A_{33} \end{vmatrix}$$

and $(A^{-1})_{ij}$ denotes an element of the matrix A^{-1} inverse to A.

In a similar manner

$$\sum_i \frac{B_i^2}{\rho c_i^2} = (A^{-1})_{22}, \quad \sum_i \frac{C_i^2}{\rho c_i^2} = (A^{-1})_{33}, \quad \sum_i \frac{B_i C_i}{\rho c_i^2} = (A^{-1})_{23}.$$

Thus the general expression for the shape of the surfaces of iso-diffusion in close proximity to the reciprocal lattice point with direction cosines L, M, N is

$$r^2(l,m,n) = L^2(A^{-1})_{11} + M^2(A^{-1})_{22} + N^2(A^{-1})_{33} + 2LM(A^{-1})_{12} + 2LN(A^{-1})_{13} + 2MN(A^{-1})_{23}.$$

For a cubic crystal

$$A_{11} = c_{11}l^2 + c_{44}(m^2+n^2),$$

$$A_{22} = c_{11}m^2 + c_{44}(l^2+n^2),$$

$$A_{33} = c_{11}n^2 + c_{44}(l^2+m^2),$$

$$A_{12} = (c_{12}+c_{44})lm,$$

$$A_{13} = (c_{12}+c_{44})ln,$$

$$A_{23} = (c_{12}+c_{44})mn.$$

It then follows easily for a cubic crystal (cf. Waller)

$$r^2(l,m,n) = \frac{1}{\begin{bmatrix} c_{11}c_{44}^2 + c_{44}(c_{11}+c_{12})(c_{11}-c_{12}-2c_{44})(l^2m^2+l^2n^2+m^2n^2) \\ \qquad + (c_{11}+2c_{12}+c_{44})(c_{11}-c_{12}-2c_{44})^2 l^2m^2n^2 \end{bmatrix}}$$

$$\begin{aligned} &\times [L^2\{c_{44}^2 + c_{44}(c_{11}-c_{44})(m^2+n^2) + (c_{11}+c_{12})(c_{11}-c_{12}-2c_{44})m^2n^2\} \\ &+ M^2\{c_{44}^2 + c_{44}(c_{11}-c_{44})(l^2+n^2) + (c_{11}+c_{12})(c_{11}-c_{12}-2c_{44})l^2n^2\} \\ &+ N^2\{c_{44}^2 + c_{44}(c_{11}-c_{44})(l^2+m^2) + (c_{11}+c_{12})(c_{11}-c_{12}-2c_{44})l^2m^2\} \\ &- 2LM(c_{12}+c_{44})\{c_{44} + (c_{11}-c_{12}-2c_{44})n^2\}\, lm \\ &- 2LN(c_{12}+c_{44})\{c_{44} + (c_{11}-c_{12}-2c_{44})m^2\}\, ln \\ &- 2MN(c_{12}+c_{44})\{c_{44} + (c_{11}-c_{12}-2c_{44})l^2\}\, mn]. \end{aligned}$$

The complicated nature of this expression should cause no surprise in view of the fact that it contains implicitly a complete account of the full acoustical spectrum (frequencies and directions of polarization) of the cubic crystal. It must, for instance, include as special values all the special formulae listed in table 1 above. That this is the case is easily verified. For example, for $l = 1/\sqrt{2}$, $m = -1/\sqrt{2}$, $n = 0$,

$$r^2(1\bar{1}0) = \frac{\begin{bmatrix} c_{44}^2(L^2+M^2+N^2) + c_{44}(c_{11}-c_{44})\left\{\dfrac{L^2+M^2}{2} + N^2\right\} \\ + \dfrac{(c_{11}+c_{12})(c_{11}-c_{12}-2c_{44})}{4}N^2 + c_{44}(c_{12}+c_{44})LM \end{bmatrix}}{c_{11}c_{44}^2 + \dfrac{c_{44}(c_{11}+c_{12})(c_{11}-c_{12}-2c_{44})}{4}}$$

$$= \frac{\begin{bmatrix} 2c_{44}(c_{11}+c_{44})(L^2+M^2) + (c_{11}-c_{12}) \\ \times (c_{11}+c_{12}+2c_{44})N^2 + 4c_{44}(c_{12}+c_{44})LM \end{bmatrix}}{4c_{11}c_{44}^2 + c_{44}(c_{11}+c_{12})(c_{11}-c_{12}-2c_{44})}.$$

One verifies

$$c_{44}(c_{11}-c_{12})(c_{11}+c_{12}+2c_{44}) = c_{44}\{4c_{11}c_{44} + (c_{11}+c_{12})(c_{11}-c_{12}-2c_{44})\},$$

and putting
$$2(L^2+M^2) = (L-M)^2 + (L+M)^2,$$
$$4LM = (L+M)^2 - (L-M)^2,$$

it is found that

$$r^2(1\bar{1}0) = \frac{\begin{bmatrix} c_{44}(c_{11}-c_{12})(L-M)^2 + c_{44}(c_{11}+c_{12}+2c_{44}) \\ \times (L+M)^2 + (c_{11}-c_{12})(c_{11}+c_{12}+2c_{44})N^2 \end{bmatrix}}{c_{44}(c_{11}-c_{12})(c_{11}+c_{12}+2c_{44})}$$

$$= \frac{(L-M)^2}{c_{11}+c_{12}+2c_{44}} + \frac{(L+M)^2}{c_{11}-c_{12}} + \frac{N^2}{c_{44}},$$

as given above (table 1).

The above general formula can be used to derive expressions for the contours of isodiffusion in special planes of the reciprocal lattice. For example, for the contours in the 100, 010 plane of the reciprocal lattice put

$$N = 0, \quad L = \cos\Phi, \quad M = \sin\Phi,$$
$$n = 0, \quad l = \cos\phi, \quad m = \sin\phi,$$

and it is easily found that

$$r^2(\Phi,\phi) = \frac{c_{44}\cos^2(\Phi-\phi) + c_{11}\sin^2(\Phi-\phi) + \frac{c_{11}-c_{12}-2c_{44}}{2}\sin 2\Phi \sin 2\phi}{c_{11}c_{44} + \frac{1}{4}(c_{11}+c_{12})(c_{11}-c_{12}-2c_{44})\sin^2 2\phi}$$
$$= \frac{c_{11}+c_{44}+(c_{44}-c_{11})\cos 2\Phi \cos 2\phi - (c_{12}+c_{44})\sin 2\Phi \sin 2\phi}{2c_{11}c_{44} + \frac{1}{2}(c_{11}+c_{12})(c_{11}-c_{12}-2c_{44})\sin^2 2\phi}.$$

For $\Phi = 0$ (100 reflexion) this becomes

$$r^2(0,\phi) = \frac{c_{44}\cos^2\phi + c_{11}\sin^2\phi}{c_{11}c_{44} + \frac{1}{4}(c_{11}+c_{12})(c_{11}-c_{12}-2c_{44})\sin^2 2\phi}$$

and for $\Phi = 45^\circ$ (110 reflexion)

$$r^2(45^\circ,\phi) = \frac{c_{11}+c_{44}-(c_{12}+c_{44})\sin 2\phi}{2c_{11}c_{44} + \frac{1}{2}(c_{11}+c_{12})(c_{11}-c_{12}-2c_{44})\sin^2 2\phi}.$$

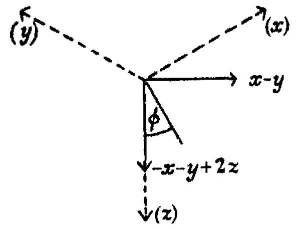

FIGURE 2

Further, expressions for the contours of special plane sections of special reciprocal lattice regions can be derived. Thus a section through the 001 reciprocal lattice point perpendicular to the 001 axis is given by

$$n = 0, \quad l^2+m^2 = 1, \quad L = M = 0, \quad N = 1,$$

from which

$$r^2 = \frac{c_{11}c_{44} + (c_{11}+c_{12})(c_{11}-c_{12}-2c_{44})l^2m^2}{c_{44}\{c_{11}c_{44} + (c_{11}+c_{12})(c_{11}-c_{12}-2c_{44})l^2m^2\}} = \frac{1}{c_{44}},$$

and these particular sections are circular for all cubic crystals. On the other hand, for a plane section through the 111 reciprocal lattice point perpendicular to the trigonal axis, the contours have only trigonal symmetry. For, letting ϕ denote the angle between the radius vector in the plane and the projection of the z-axis on the plane (figure 2), it is found that

$$l = -\frac{\cos\phi}{\sqrt{6}} + \frac{\sin\phi}{\sqrt{2}},$$

$$m = -\frac{\cos\phi}{\sqrt{6}} - \frac{\sin\phi}{\sqrt{2}},$$

$$n = \frac{2}{\sqrt{6}}\cos\phi,$$

giving

$$l+m+n = 0,$$

$$lm+ln+mn = -\tfrac{1}{2},$$

$$l^2m^2+l^2n^2+m^2n^2 = \tfrac{1}{4},$$

$$l^2m^2n^2 = \tfrac{1}{54}\cos^2 3\phi,$$

so that with $L = M = N = 1/\sqrt{3}$

$$r^2(\phi) = \frac{c_{44}^2 + \frac{2}{3}c_{44}(c_{11}-c_{44}) + \frac{1}{12}(c_{11}+c_{12})(c_{11}-c_{12}-2c_{44}) + \frac{1}{3}c_{44}(c_{12}+c_{44})}{\left[\begin{array}{l} c_{11}c_{44}^2 + \frac{1}{4}c_{44}(c_{11}+c_{12})(c_{11}-c_{12}-2c_{44}) + \frac{1}{54}(c_{11}+2c_{12}+c_{44}) \\ \qquad\qquad\qquad\qquad\qquad \times (c_{11}-c_{12}-2c_{44})^2\cos^2 3\phi \end{array}\right]}.$$

This theoretical result would appear to be more reasonable than the generalization Laval makes from his experimental results, namely, that the contours in all cases in a plane perpendicular to the axis joining the reciprocal lattice point to the origin would be circular.

5. Diffuse scattering about the central beam

Consider finally the scattering at small angles near the central beam, i.e. the diffuse scattering belonging to the 000 reflexion. The particular term considered above vanishes here because $R = 0$. Returning to the general Faxén-Waller formula, it is found that for the 000 scattering

$$\begin{aligned} I(l,m,n) &= \sum_{i=1}^{3}\frac{(lA_i+mB_i+nC_i)^2}{\rho c_i^2} \\ &= l^2\sum_i\frac{A_i^2}{\rho c_i^2} + m^2\sum_i\frac{B_i^2}{\rho c_i^2} + n^2\sum_i\frac{C_i^2}{\rho c_i^2} \\ &\quad + 2lm\sum_i\frac{A_iB_i}{\rho c_i^2} + 2ln\sum_i\frac{A_iC_i}{\rho c_i^2} + 2mn\sum_i\frac{B_iC_i}{\rho c_i^2}. \end{aligned}$$

For a cubic crystal this becomes

$$I(l,m,n) = \frac{\begin{bmatrix} c_{44}^2 + 2c_{44}(c_{11}-c_{12}-2c_{44})\,(l^2m^2+l^2n^2+m^2n^2) \\ \hfill +\,3(c_{11}-c_{12}-2c_{44})^2\,l^2m^2n^2 \end{bmatrix}}{\begin{bmatrix} c_{11}c_{44}^2 + c_{44}(c_{11}+c_{12})\,(c_{11}-c_{12}-2c_{44})\,(l^2m^2+l^2n^2+m^2n^2) \\ \hfill +\,(c_{11}+2c_{12}+c_{44})\,(c_{11}-c_{12}-2c_{44})^2\,l^2m^2n^2 \end{bmatrix}}.$$

Thus in the present approximation (neglect of the dispersion of the lattice waves), the scattering intensity depends only on the direction cosines of the lattice wave determining the direction of scattering (see figure 3). Thus the contours of isodiffusion in the Brillouin zone surrounding the 000 point of the reciprocal lattice are straight lines through the origin in this approximation.

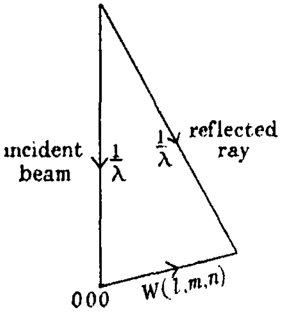

FIGURE 3

6. SCATTERING FOR SODIUM SINGLE CRYSTALS

Illustration of this theory may be made by evaluating certain of the above formulae for the special case of sodium. Taking the values of the elastic constants given by Quimby and Siegel (1938), viz.

$$c_{12} = 0{\cdot}760c_{11}, \quad c_{44} = 0{\cdot}914c_{11} \quad \text{(at } 200^\circ\,\text{K)}$$

(relative values only), the relative intercepts of the isodiffusion surfaces belonging to the 002, 110, 222 Bragg reflexions are found to have the values given in table 2 for the 26 directions shown in figure 1 (putting $c_{11} = 1$).

As is seen a large anisotropy of the isodiffusion surfaces for sodium is predicted by the Faxén-Waller theory. This is due essentially to the smallness of the fundamental elastic constant $c_{11}-c_{12}$ which has as a consequence the existence of transverse waves of particularly small frequency along the digonal axes of the crystal. Finally, calculation has been made of some of the curves of isodiffusion in the 200, 020 plane of the reciprocal lattice (cf. Jahn 1941). Sodium crystallizes in a simple body-centred lattice, so that, as is well known, the reciprocal lattice of the undisturbed crystal is face centred. A part of the 200, 020 plane of this reciprocal lattice is shown in figure 4 together with the shape of curves of isodiffusion surrounding the reciprocal lattice points. It is to be hoped that experiments will be forthcoming to test these predictions of the Faxén-Waller theory.

TABLE 2

B *W*		002	110	222
a	100	1·05	1·02	1·03
b	010	1·05	1·02	1·03
c	001	1	1·05	1·03
d	110	1·05	0·748	0·857
e	101	2·11	1·66	0·857
f	011	2·11	1·66	0·857
g	$1\bar{1}0$	1·05	2·89	2·43
h	$10\bar{1}$	2·11	1·66	2·43
i	$01\bar{1}$	2·11	1·66	2·43
j	111	1·38	1·09	0·698
k	$11\bar{1}$	1·38	1·09	1·54
l	$1\bar{1}1$	1·38	1·62	1·54
m	$\bar{1}11$	1·38	1·62	1·54

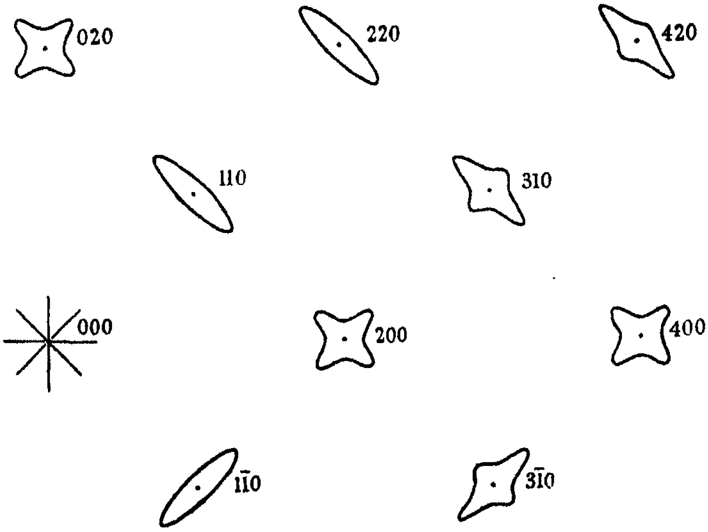

FIGURE 4. Part of 200,020 plane of reciprocal lattice, showing shapes of sections of isodiffusion surfaces predicted by the Faxén-Waller theory.

REFERENCES

Debye, P. 1914 *Ann. Phys., Lpz.*, **43**, 49.
Ewald, P. P. 1940 *Proc. Phys. Soc.* **52**, 167.
Faxén, H. 1923 *Z. Phys.* **17**, 266.
Jahn, H. A. 1941 *Nature, Lond.*, **147**, 511.
Jahn, H. A. and Lonsdale, K. 1941 *Nature, Lond.*, **147**, 88.
Jauncey, G. E. M. 1941 *Phys. Rev.* **59**, 456.
Jauncey, G. E. M. and Baltzer, O. J. 1941 *Phys. Rev.* **59**, 699.
Laval, J. 1939 *Bull. Soc. franç. Minér.* **62**, 137.
Lonsdale, K., Knaggs, I. E. and Smith, H. 1940 *Nature, Lond.*, **146**, 332
Mauguin, C. and Laval, J. 1939 *C.R. Acad. Sci., Paris*, **208**, 1446.
Preston, G. D. 1939 *Proc. Roy. Soc.* A, **172**, 116.
Quimby, S. L. and Siegel, S. 1938 *Phys. Rev.* **54**, 293.
Raman, C. V. 1941 *Proc. Indian Acad. Sci.* B, **13**, 1.
Raman, C. V. and Nilakantan, P. 1940 *Proc. Indian Acad. Sci.* A, **11**, 379.
Siegel, S. and Zachariasen, W. H. 1940 *Phys. Rev.* **57**, 795.
Waller, I. 1925 *Uppsala Univ. Årssk.*
Zachariasen, W. H. 1940 *Phys. Rev.* **57**, 597.

Statistical mechanics of binary systems

BY KLAUS FUCHS
University of Edinburgh

(*Communicated by M. Born, F.R.S.—Received* 31 *March* 1941—
Revised 17 *June* 1941)

Mayer's method for the expansion of the partition function of a gas is adapted to the calculation of the partition function of a binary solid solution. The partition function is expanded in powers of the atomic fraction. Singularities in this expansion correspond to a phase transition. The singularity can be calculated in the simplest case of a binary solution with a two-phase region. This case is treated in full; the limits of solubility and the specific heat are obtained. The latter is discontinuous at the phase boundaries.

1. INTRODUCTION

The simplest approximation in calculating the partition function of binary systems is obtained by assuming that the atoms of the two substances are distributed at random over the lattice points. In actual fact the random distribution is not the most probable configuration, owing to the fact that the interaction energies between like and unlike atoms in general differ. Therefore, even in solution, like atoms will tend to coagulate or to keep apart from each other as the case may be. This effect is well known from Bethe's theory of superstructure (1935); according to this theory there remains a certain degree of 'short distance order', even above the critical temperature, when no superstructure remains. Early attempts to take this fact into account usually had to introduce some more or less arbitrary assumption (cf. Guggenheim 1935). The development of the theory of superstructure supplied methods by means of which an approximate treatment of the present problem could be given. This was done by Rushbrooke (1938), who used Bethe's methods, and by Kirkwood (1939), who applied his own order-disorder theory to this problem.

In this paper I wish to treat this problem by another method. The situation is very similar to that found in the evaluation of the partition function of a gas. In the ideal gas the most probable configuration is a random distribution of the molecules. In actual fact the probability that two molecules are near each other is greater than the probability given by a random distribution, owing to the attraction between the molecules. This problem has been solved by Mayer and his collaborators (Mayer 1937; Mayer and Ackermann 1937; Mayer and Harrison 1938; Mayer and Goepert-Mayer 1940). He obtained an expansion of the partition function of the gas in terms of the reciprocal volume and was able to show that certain singularities in this expansion are connected with the transition to the condensed phase.

In this paper I shall employ the same method in order to obtain the partition function of a binary system, assuming central forces between the particles. The partition function is obtained as an expansion in powers of the atomic fraction. *The singularities in this expansion are connected* either with the appearance of superstructure or with a two-phase region. The former case will not be treated in this paper.

In attempting to determine the singularities of the expansion we meet the same difficulty as in the theory of gases. In principle the singularities are determined by the asymptotic value of the coefficients in the expansion; however, it is extremely difficult to assess this value without introducing assumptions which are not easily justified. As in the theory of condensation, indirect methods must be used and this can be done very easily for a binary solution with a two-phase region. Once this is done, the free energy and therefore also the thermal energy and specific heat can be obtained for any atomic fraction.

The notation used by Born and Fuchs (1938, in the following quoted as I) will be employed throughout, and I shall quote freely from that paper since many equations need only slight modifications in order to be applied to the present problem.

Numerical calculations in this paper refer to the body-centred cubic lattice.

2. THE CONFIGURATIONAL ENERGY AND THE PARTITION FUNCTION

Consider a system of N atoms, composed of c_aN A-atoms and c_bN B-atoms. Here c_a and c_b are the atomic fractions; their sum is unity

$$c_a + c_b = 1. \tag{2·1}$$

The N atoms are distributed over N lattice points. Any distribution constitutes a thermodynamical configuration.

I introduce the following simplifications:

(1) The thermal oscillations are independent of the configuration. I may then disregard them altogether, since they give only an additive constant. Only if changes of volume are taken into account should the volume dependence of the thermal frequencies be included.

(2) The interactions between like and unlike particles differ only if the two particles are nearest neighbours, but not if they are farther apart. This simplification is not essential for the application of the following method, but it should be a good approximation if the difference in the interaction arises mainly from the repulsive forces.

With these simplifications the total energy of a configuration can be expressed in terms of the numbers a, b, c of nearest neighbour bonds between two A-atoms, two B-atoms or an A-atom and a B-atom:

$$E = aV_{aa} + bV_{bb} + cV_{ab} + NV'. \tag{2·2}$$

Here V_{aa}, V_{bb} and V_{ab} are the interaction energies between the corresponding pairs of particles when they are nearest neighbours, and V' represents the remainder of the energy.

The bond number a obviously depends only on the configuration of the A-atoms. But, if the latter is given, the B-atoms must necessarily occupy the remaining vacant lattice points, so that the total configuration is also determined apart from trivial interchanges of the B-atoms. I should therefore expect that the three bond numbers a, b, c are not independent of each other.

Indeed, a short calculation gives (cf. Guggenheim 1935)

$$E = aV + NV'', \tag{2·3}$$

where
$$V = V_{aa} + V_{bb} - 2V_{ab}, \tag{2·4}$$
$$V'' = V' + \tfrac{1}{2}nV_{bb} + nc_a(V_{ab} - V_{bb}). \tag{2·5}$$

The partition function of the system is now given by the sum over all configurations
$$Q_N = \frac{1}{(c_a N)!}\frac{1}{(c_b N)!}\sum_{\text{conf.}} e^{-E/kT}. \tag{2·6}$$

I mentioned above that it is in fact sufficient to consider only the configurations of A-atoms; thus the partition function can also be written in the following form:
$$Q_N = \frac{1}{(c_A N)!}\sum_{A\text{-conf.}} e^{-E/kT} = \frac{e^{-NV''/kT}}{(c_A N)!}\sum_{A\text{-conf.}} e^{-aV/kT}. \tag{2·7}$$

Apart from the factor $\exp(-nV''/kT)$, this partition function is the partition function of a system of $c_a N$ particles distributed over N lattice points, with an interaction energy v between two particles given by
$$v = \begin{cases} \infty & \text{if the two atoms are at the same lattice point,} \\ V & \text{if the two atoms are nearest neighbours,} \\ 0 & \text{otherwise.} \end{cases} \tag{2·8}$$

Let v_{ij} denote the potential (2·8) between the ith and jth particle at the lattice points l_i, l_j. Then the partition function may be written in the form
$$Q_N e^{NV''/kT} = \frac{1}{(c_a N)!}\sum_{l_1=1}^{N}\sum_{l_2=1}^{N}\cdots\sum_{l_M=1}^{N}\prod_{M\geqslant i>j\geqslant 1} e^{-v_{ij}/kT} \quad (M = c_a N). \tag{2·9}$$

3. EXPANSION OF THE PARTITION FUNCTION

The expression on the right-hand side of equation (2·9) is exactly analogous to the expression of the configurational partition function $Q_\tau/N!$ of a gas, except that the integration over the co-ordinates r_{ij} is replaced by the summation over all lattice points and that N is replaced by $c_a N$ (cf. I, 1·3).

I introduce as in I
$$f_{ij} = e^{-v_{ij}/kT} - 1 = \begin{cases} -1 & \text{if the two atoms are at the same lattice point,} \\ e^{-V/kT} - 1 & \text{if the two atoms are nearest neighbours,} \\ 0 & \text{otherwise.} \end{cases} \tag{3·1}$$

I now proceed with the expansion of the partition function analogous to Mayer's expansion. The calculation is exactly the same and need not be repeated. Instead of the cluster integrals and irreducible cluster integrals (cf. I, 1·6 and § 2), I obtain here cluster sums and irreducible cluster sums, which will be denoted by the same symbols b_l and β_ν respectively. Instead of the total volume, arising from the integration over the co-ordinates of a particle, with the integrand equal to 1, I obtain a summation over the lattice points, giving the total number N of lattice points. The volume v per particle must then be replaced by $N/c_a N = f_a$, where f_a is defined by

$$f_a = \frac{1}{c_a}. \tag{3·2}$$

Analogous to (I, 3·2) the partition function (2·9) is

$$Q_N e^{NV''/kT} = F(c_a N, c_a N, f_a b_l), \tag{3·3}$$

where the F-functions are defined by (I, 3·1). The relation between the cluster sums and the irreducible cluster sums is the same as for the corresponding integrals (cf. I, 3·2)

$$l^2 b_l = F(l-1, l, \beta_\nu). \tag{3·4}$$

As in I we introduce the G-functions

$$G_\lambda(z, f_a b_l) = \sum_{l=1}^{\infty} l^\lambda f_a b_l z^l = f_a G_\lambda(z, b_l), \tag{3·5}$$

$$G_\lambda(y, \beta_\nu) = \sum_{\nu=1}^{\infty} \nu^\lambda \beta_\nu y^\nu. \tag{3·6}$$

The expression of the F-functions in terms of the G-functions was proved in I in general, and can be applied immediately.

Let then $\bar{Z}$ be the smallest singularity of $G_\lambda(z, f_a b_l)$ on the positive z-axis and define

$$G_1(\bar{Z}, b_l) = \bar{c}_a. \tag{3·7}$$

Then c_a takes the place of the reciprocal condensation volume. For c_a smaller than $\bar{c}_a$ we find, corresponding to (I, 6·10),

$$\lim_{N \to \infty} \frac{1}{c_a N} \ln (Q_N e^{NV''/kT}) = G_0(Z, f_a b_l) - \ln Z, \tag{3·8}$$

where Z is the root of the equation $G_1(Z, f_a b_l) = 1$, or with (3·2)

$$G_1(Z, b_l) = c_a. \tag{3·9}$$

The free energy is defined by

$$A = -kT \ln Q = -RT \lim_{N \to \infty} \frac{1}{N} \ln Q_N. \tag{3·10}$$

Substituting (3·8) and the expression (2·5) for V'' this gives

$$A = N\left\{kT(c_a \ln Z - G_0(Z, b_l)) + nc_a(V_{ab} - V_{bb}) + \frac{n}{2}V_{bb} + V'\right\}. \tag{3·11}$$

For c_a greater than $\bar{c}_a$, the free energy is given by the same expression with Z replaced by $\bar{Z}$.

$\ln Z$ and $G_0(Z, b_l)$ can be expressed in power series of the atomic fraction corresponding to the power series in the reciprocal volume for the gas. From (I, 6·8) we have

$$\ln Z = \ln c_a - G_0(c_a, \beta_\nu), \tag{3·12}$$

and from (I, 6·5)

$$G_0(Z, b_l) = c_a(1 - G_{0,1}(c_a, \beta_\nu)). \tag{3·13}$$

Thus the free energy (3·11) can also be written in the form

$$\frac{A}{N} = kT\{\ln c_a - 1 - G_0(c_a, \beta_\nu) + G_{0,1}(c_a, \beta_\nu)\}\, c_a + nc_a(V_{ab} - V_{bb}) + \frac{n}{2}V_{bb} + V' \qquad (c_a \leqslant \bar{c}_a), \tag{3·14}$$

$$\frac{A}{N} = kT\{c_a(\ln \bar{c}_a - G_0(\bar{c}_a, \beta_\nu)) - \bar{c}_a(1 - G_{0,1}(\bar{c}_a, \beta_\nu))\} + nc_a(V_{ab} - V_{bb}) + \frac{n}{2}V_{bb} + V' \qquad (c_a \geqslant \bar{c}_a). \tag{3·15}$$

By exchanging the indices a and b we obtain similar equations for the free energy for small concentrations of the B-atoms

$$\frac{A}{N} = kT\{\ln c_b - 1 - G_0(c_b, \beta_\nu) + G_{0,1}(c_b, \beta_\nu)\}\, c_b + nc_b(V_{ab} - V_{aa}) + \frac{n}{2}V_{aa} + V' \qquad (c_b \leqslant \bar{c}_b), \tag{3·16}$$

$$\frac{A}{N} = kT\{c_b[\ln \bar{c}_b - G_0(\bar{c}_b, \beta_\nu)] - c_b[1 - G_{0,1}(\bar{c}_b, \beta_\nu)]\} + nc_b(V_{ab} - V_{aa}) + \frac{n}{2}V_{aa} + V' \qquad (c_b \geqslant \bar{c}_b), \tag{3·17}$$

where

$$G_1(\bar{Z}, b_l) = \bar{c}_b. \tag{3·18}$$

If $\bar{c}_a$ or $\bar{c}_b$ are greater than 1 the expressions (3·14) and (3·16) hold over the whole range of concentrations and the two substances form a solid solution for any concentration. The same is clearly the case if $\bar{c}_a + \bar{c}_b$ is greater than unity. In the latter case the expressions (3·14), (3·16) have a common region of validity, in which they must be identical; it follows that neither of them can have a singularity throughout the whole region of atomic fractions and $\bar{c}_a$ as well as $\bar{c}_b$ must be greater than unity.

If we neglect the change of volume with the atomic fraction it follows of course that $\bar{c}_a$ and $\bar{c}_b$ are identical, since in this case the definitions (3·7) and (3·18) coincide.

4. BINARY SOLUTIONS WITH A TWO-PHASE REGION

The expression (3·15) for the free energy holds up to an atomic fraction for which the large cluster sums b_l begin to depend on the size of the lattice. In this region the free energy is linear in the atomic fraction. For c_a greater than $1-\bar{c}_b$ the free energy, according to (3·16), is not linear. It follows that this atomic fraction, for which the linear expression (3·15) breaks down, is smaller than or equal to $1-\bar{c}_b$.

Consider the case that (3·15) holds right up to $1-\bar{c}_b$. Then there are three distinct regions: small atomic fractions of A-atoms ($c_a \leqslant \bar{c}_a$), small atomic fractions of B-atoms ($c_b \leqslant \bar{c}_b$), and a region in between in which the free energy is linear. In the first two regions the two substances form a solid solution; in the middle region we have clearly a two-phase region.

The atomic fractions $\bar{c}_a$, $\bar{c}_b$ then are the limits of solubility. In principle they are given by the asymptotic value of the irreducible cluster sums. But in practice it is impossible to evaluate them. One can, however, determine the limits of solubility by an indirect method. In the two-phase region we have two different expressions (3·15) and (3·17) for the free energy. They must be identical. Since the free energy in this region is linear, I obtain two conditions which are sufficient to determine the two limits of solubility. If I wish to take into account the change of volume between the two atomic fractions, the irreducible cluster integrals and the interaction energies in the two expressions (3·15) and (3·17) are not identical, and I shall add a suffix a or b, indicating that the values of these quantities for the volumes corresponding to the atomic fractions $\bar{c}_a$ and $\bar{c}_b$ are understood. Furthermore, I have to add in this case the free energy $A_{\text{osc.}}$ due to the thermal oscillations. The two conditions then are

$$kT\{\ln \bar{c}_a + \ln \bar{c}_b - G_0(\bar{c}_a, \beta_\nu^{(a)}) - G_0(\bar{c}_b, \beta_\nu^{(b)})\} = n\{V_{aa}^{(b)} + V_{bb}^{(a)} - V_{ab}^{(b)} - V_{ab}^{(a)}\}, \quad (4·1)$$

$$kT\{2[G_{0,1}(\bar{c}_a, \beta_\nu^{(a)}) - G_{0,1}(\bar{c}_b, \beta_\nu^{(b)}) - \bar{c}_a + \bar{c}_b] + \ln \bar{c}_a - \ln \bar{c}_b - G_0(\bar{c}_a, \beta_\nu^{(a)}) + G_0(\bar{c}_b, \beta_\nu^{(b)})\} = n\{V_{ab}^{(b)} - V_{ab}^{(a)} + 2V'^{(b)} - 2V'^{(a)}\} + \frac{2}{N}\{A_{\text{osc.}}^{(b)} - A_{\text{osc.}}^{(a)}\}. \quad (4·2)$$

If the change of volume can be neglected, the last equation is identically satisfied. The first reduces to

$$kT\{\ln \bar{c}_a - G_0(\bar{c}_a, \beta_\nu)\} = \tfrac{1}{2}nV. \quad (4·3)$$

With (3·12) this can also be written in the form

$$\bar{Z} = e^{nV/2kT}, \tag{4·4}$$

which shows the physical significance of $\bar{Z}$.

With (3·7) the solution of (4·3) is now

$$\bar{c}_a = \bar{c}_b = G_1(e^{nV/2kT}, b_l). \tag{4·5}$$

A few words are necessary to explain how it is possible that the series (3·7) defining $\bar{c}_a$ can 'know' which volume will be the correct volume at the other side of the two-phase region. Strictly speaking this is not the case according to our definitions, and the singularity $\bar{Z}$ is always given by (4·4). But a slight change in the definition of the partition function (2·9) will supply the large cluster sums in (3·7) with the necessary 'knowledge'. If I include in this definition an integration over all possible lattice constants, the cluster sums must also be integrated over the lattice constant and then the large cluster sums will automatically take their maximum value as a function of the lattice constant. Now, the important large cluster sums in the definition of $\bar{c}_a$ must be those corresponding to the most probable configuration on the other side of the two-phase region, and they will therefore take their values for the corresponding lattice constant. The strict calculation would introduce further complications. But instead of starting a priori from the total partition function (including various lattice constants), we may start from a partial partition function and then apply the two-phase rule. This is what I have done in fact in deriving the equations (4·1) and (4·2) for the limits of solubility.

5. THE CLUSTER SUMS FOR $V = 0$

Consider the special case that the interaction V vanishes

$$V = V_{aa} + V_{bb} - 2V_{ab} = 0. \tag{5·1}$$

Then the energy is the same for any configuration. Taking, for example, complete separation of the two substances, the energy is

$$E = \frac{Nn}{2}\{c_a V_{aa} + c_b V_{bb}\} + NV' = N\left\{c_a n(V_{ab} - V_{bb}) + \frac{n}{2}V_{bb} + V'\right\}. \tag{5·2}$$

The Boltzman factor in the partition function (2·6) is now constant and the sum gives the total number of configurations $N!$:

$$Q_N = \frac{N!}{(c_a N)!\,(c_b N)!}e^{-E/kT}. \tag{5·3}$$

By means of Stirling's formula the free energy is

$$A = N\left\{kT(c_a \ln c_a + c_b \ln c_b) + c_a n(V_{ab} - V_{bb}) + \frac{n}{2}V_{bb} + V'\right\}. \tag{5·4}$$

Comparison of this expression with (3·14) gives

$$c_a\{1 + G_0(c_a, \beta_\nu) - G_{0,1}(c_a, \beta_\nu)\} = -(1-c_a)\ln(1-c_a). \tag{5·5}$$

Expanding the logarithm and comparing coefficients I find

$$\beta_\nu = -\frac{1}{\nu}. \tag{5·6}$$

With this value of the irreducible cluster integrals the G-functions can easily be summed. The result is

$$G_0(c_a, \beta_\nu) = \ln(1-c_a), \quad G_{0,1}(c_a, \beta_\nu) = \frac{\ln(1-c_a)}{c_a} + 1, \tag{5·7}$$

$$G_1(c_a, \beta_\nu) = -\frac{c_a}{1-c_a}, \tag{5·8}$$

$$G_2(c_a, \beta_\nu) = -\frac{c_a}{(1-c_a)^2}. \tag{5·9}$$

Now, we have the following expansion of the exponential function (cf. I, 3·4)

$$e^{lG_0(c_a, \beta_\nu)} = \sum_{l'=0}^{\infty} F(l', l, \beta_\nu)\, c_a^{\nu}.$$

Introducing the value (5·7) for G_0,

$$(1-c_a)^l = \sum_{l'=0}^{\infty} F(l', l, \beta_\nu)\, c_a^{l'}.$$

Comparison of the coefficients yields

$$F(l', l, \beta_\nu) = \begin{cases} (-1)^{l'}\dfrac{l!}{l'!(l-l')!} & (0 \leqslant l' \leqslant l), \\ 0 & (l' > l). \end{cases} \tag{5·10}$$

For $l' = l-1$ the F-function gives, according to (3·4), the cluster sum b_l

$$b_l = \frac{1}{l^2}F(l-1, l, \beta_\nu) = -\frac{(-1)^l}{l}. \tag{5·11}$$

6. BINARY SOLUTIONS AT HIGH TEMPERATURES

At sufficiently high temperatures we can expand f_{ij}, given by (3·1), and therefore also the cluster sums in powers of the reciprocal temperature

$$f_{ij} = \begin{cases} -1 & l_i = l_j, \\ -\dfrac{V}{kT}+\dfrac{1}{2}\left(\dfrac{V}{kT}\right)^2-\dots & l_i,\, l_j \text{ neighbouring lattice points,} \\ 0 & \text{otherwise,} \end{cases} \tag{6·1}$$

$$\beta_\nu = \beta_\nu^{(0)}+\beta_\nu^{(1)}\frac{V}{kT}+\beta_\nu^{(2)}\left(\frac{V}{kT}\right)^2+\dots. \tag{6·2}$$

Now, the limiting cases $T \to \infty$ and $V \to 0$ are clearly identical. The temperature-independent parts of the cluster sums are therefore identical with those found in the last section

$$\beta_\nu^{(0)} = -\frac{1}{\nu}. \tag{6·3}$$

Furthermore, since in each irreducible cluster sum each particle is connected with at least two others, we shall obtain in the temperature-dependent part at least two factors $1/kT$; the only exception is β_1, which contains only one bond between the two particles. The value of β_1 is easily obtained. Thus (n is the co-ordination number)

$$\beta_\nu^{(1)} = \begin{cases} -n & (\nu = 1), \\ 0 & (\nu > 1). \end{cases} \tag{6·4}$$

I now split β into three parts

$$\beta = \beta_\nu^{(0)}+\beta_\nu^{(1)}\frac{V}{kT}+\beta_\nu'. \tag{6·5}$$

The G-functions are linear in the β_ν and therefore additive,

$$G_\lambda(c_a,\beta_\nu) = G_\lambda(c_a,\beta_\nu^{(0)})+\frac{V}{kT}G_\lambda(c_a,\beta_\nu^{(1)})+G_\lambda(c_a,\beta_\nu'). \tag{6·6}$$

The G-functions with $\beta^{(1)}$ contain according to (6·4) only one term,

$$G_\lambda(c_a,\beta_\nu^{(1)}) = -nc_a, \quad G_{0,1}(c_a,\beta_\nu^{(1)}) = -\tfrac{1}{2}nc_a. \tag{6·7}$$

With the help of this expression and (5·7) the partition function (3·14) can be written in the form

$$\frac{A}{N} = kT\{c_a \ln c_a + (1-c_a)\ln(1-c_a) - c_a G_0(c_a, \beta'_\nu) + c_a G_{0,1}(c_a, \beta'_\nu)\}$$
$$+\frac{n}{2} V c_a^2 + n c_a (V_{ab} - V_{bb}) + \frac{n}{2} V_{bb} + V' \quad (c_a \leqslant \bar{c}_a), \qquad (6·8)$$

and a similar expression for small values of c_b.

At very high temperatures one need consider in first approximation only the temperature-independent part. In that case, however, the expansion (6·8) has no singularity and holds for all atomic fractions. The same holds for the corresponding expression in c_b. The two expressions must therefore be identical. This gives the following equation:

$$c_a\{G_0(c_a, \beta'_\nu) - G_{0,1}(c_a, \beta'_\nu)\} = (1-c_a)\{G_0(1-c_a, \beta'_\nu) - G_{0,1}(1-c_a, \beta'_\nu)\}. \qquad (6·9)$$

Successive differentiation with regard to c_a gives

$$G_0(c_a, \beta'_\nu) = -G_0(1-c_a, \beta'_\nu), \qquad (6·10)$$

$$\frac{1}{c_a} G_1(c_a, \beta'_\nu) = \frac{1}{1-c_a} G_1(1-c_a, \beta'_\nu), \qquad (6·11)$$

$$\frac{1}{c_a^2}\{G_2(c_a, \beta'_\nu) - G_1(c_a, \beta'_\nu)\} = -\frac{1}{(1-c_a)^2}\{G_2(1-c_a, \beta'_\nu) - G_1(1-c_a, \beta'_\nu)\}. \qquad (6·12)$$

In particular for $c_a = 1 - c_a = \frac{1}{2}$

$$G_0(\tfrac{1}{2}, \beta'_\nu) = 0, \quad G_2(\tfrac{1}{2}, \beta'_\nu) = G_1(\tfrac{1}{2}, \beta'_\nu). \qquad (6·13)$$

7. THE CRITICAL TEMPERATURE

It has been seen in the last section that for high temperatures the two substances form a solid solution for any atomic fraction. If for low temperatures this is not the case, there must be a critical temperature T_c, such that above this temperature the two substances form a solid solution for all atomic fractions but not below this temperature.

For the critical temperature and the corresponding critical atomic fraction C we obtain formulae analogous to those in I (cf. I, 7·3)

$$G_1(C, \beta_\nu) = 1, \quad G_2(C, \beta_\nu) = 0 \quad (T = T_c). \qquad (7·1)$$

These two equations are sufficient to determine the critical temperature and atomic fraction. However, the critical atomic fraction can be obtained easily in a different way. For the critical temperature the two limits $\bar{c}_a$ and

$\bar{c}_b$ correspond to the same atomic fraction, i.e. $\bar{c}_b = 1-\bar{c}_a$. In that case, however, the volume is the same for both atomic fractions and therefore $\bar{c}_a = \bar{c}_b$. The solution of these two equations gives the critical atomic fraction

$$C = \tfrac{1}{2}. \tag{7·2}$$

Introducing this value in (7·1) we obtain two equations for T_c

$$G_1(\tfrac{1}{2}, \beta_\nu) = 1, \quad G_2(\tfrac{1}{2}, \beta_\nu) = 0 \quad (T = T_c). \tag{7·3}$$

It can easily be shown that there exists an identity between these two equations. With (5·8), (5·9) and (6·7) they can be written in the form

$$G_1(\tfrac{1}{2}, \beta'_\nu) = 2+\frac{n}{2}\frac{V}{kT}, \quad G_2(\tfrac{1}{2}, \beta'_\nu) = 2+\frac{n}{2}\frac{V}{kT} \quad (T = T_c). \tag{7·4}$$

According to (6·13) these two equations are identical.

The numerical solution of this equation is given in the Appendix. The result for the body-centred lattice is

$$-\frac{V}{kT_c} = 0{\cdot}60. \tag{7·5}$$

It is interesting to note that there is no solution for positive values of V. The critical temperature corresponding to the appearance of superstructure is therefore not given by these equations.

8. THE LIMITS OF SOLUBILITY

Below the critical temperature there exists a two-phase region between the limits of solubility $\bar{c}_a$ and $\bar{c}_b$. These are given either by a singularity in the series $G_\lambda(c_a, \beta_\nu)$ or by the equation $G_1(\bar{c}_a, \beta_\nu) = 1$, whichever gives the smaller value (cf. I, § 6). In both cases the equation (4·3) must hold, which has been derived in general,

$$\ln \bar{c}_a - G_0(\bar{c}_a, \beta_\nu) = \frac{n}{2}\frac{V}{kT}. \tag{8·1}$$

Now, it can easily be proved that the solution of this equation does not coincide with the solution of $G_1 = 1$, the latter being in fact larger than the former (strictly speaking there is no solution of $G_1 = 1$, since beyond the singularity this series is only semi-convergent).

It follows that below the critical point $\bar{c}_a$ is a singular point* and that

$$G_1(\bar{c}_a, \beta_\nu) < 1 \quad (T < T_c). \tag{8·2}$$

---

* Mayer and Harrison (1938) has found for gases a small region below the critical temperature where the condensation volume (corresponding to our $\bar{c}_a$) is given by $G_1 = 1$. No such region occurs for binary solutions with a two-phase region.

With (5·7) and (6·7) the equation (8·1) can be written in the form

$$\ln \bar{c}_a - \ln(1-\bar{c}_a) - G_0(\bar{c}_a, \beta'_\nu) = \frac{n}{2}\frac{V}{kT}(1-2c_a). \tag{8·3}$$

The series in this equation converges well even near the critical temperature. For low temperatures, however, it is more convenient to use the series (4·5) since it gives directly the solution $\bar{c}_a$. The calculation is carried out in the Appendix. The result is given in figure 1.

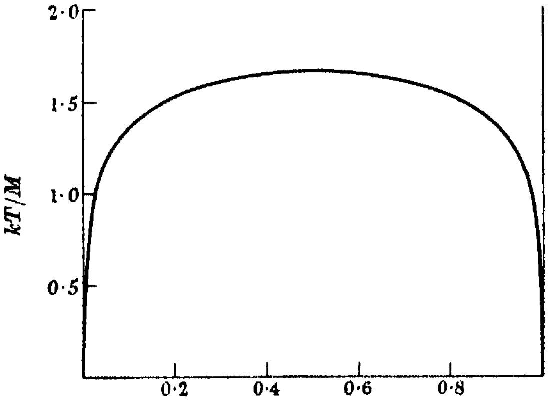

FIGURE 1. The phase diagram of binary solid solutions with a two-phase region in the body-centred lattice.

At very low temperatures it is sufficient to consider only the first term in the series (4·5). Then we have

$$\bar{c}_a = e^{nV/2kT} \quad (kT \ll |V|). \tag{8·4}$$

V being negative, the limits of solubility tend to zero for T against zero.

9. THE SPECIFIC HEAT

Now consider a binary solution with a definite atomic fraction c_a. As the temperature changes, the most probable configuration will change with the temperature. At low temperatures like atoms tend to keep apart from each other, as it is energetically more favourable; but at higher temperatures the probability of like atoms being in neighbouring positions increases, until for infinite temperature it coincides with the probability obtained from a random distribution. This change is accompanied by an increase in energy and leads therefore to an additional specific heat. The total thermal energy absorbed in this way can be obtained immediately. At zero temperature there is complete separation of the two substances. The energy is then

$$N\frac{n}{2}\{c_a V_{aa} + c_b V_{bb}\}. \tag{9·1}$$

At infinite temperature there is random distribution with an energy

$$Nn\left\{\frac{c_a^2}{2}V_{aa} + c_a c_b V_{ab} + \frac{c_b^2}{2}V_{bb}\right\}. \tag{9·2}$$

The difference is

$$-\frac{Nn}{2}c_a c_b V. \tag{9·3}$$

In order to obtain the thermal energy for any temperature, we use the thermodynamical connexion between the free energy and the thermal energy. It will be most convenient for this purpose to introduce instead of the temperature the variable ξ defined by

$$\xi = \frac{V}{kT}. \tag{9·4}$$

The mean value of the energy is then from (2·7)

$$\bar{E} = -\frac{V}{Q}\frac{\partial Q}{\partial \xi} + NV'', \tag{9·5}$$

or, introducing the free energy (3·10),

$$\bar{E} = V\frac{\partial}{\partial \xi}\left(\frac{A}{kT}\right) + NV''. \tag{9·6}$$

Using the expression (3·14) for the free energy, we obtain

$$\bar{E} = VN\left\{G_{0,1}\left(c_a, \frac{\partial \beta_\nu}{\partial \xi}\right) - G_0\left(c_a, \frac{\partial \beta_\nu}{\partial \xi}\right)\right\}c_a + NV'' \quad (c_a < \bar{c}_a). \tag{9·7}$$

In the two-phase region we have to take into account that $\bar{c}_a$ is also a function of the temperature. From (4·3) and (4·5) one obtains the alternative equations

$$\frac{\partial \bar{c}_a}{\partial \xi} = \bar{c}_a \frac{\frac{1}{2}n + G_0\left(\bar{c}_a, \dfrac{\partial \beta_\nu}{\partial \xi}\right)}{1 - G_1(\bar{c}_a, \beta_\nu)} = \tfrac{1}{2}nG_2(e^{\frac{1}{2}n\xi}, b_l) + G_1\left(e^{\frac{1}{2}n\xi}, \frac{\partial b_l}{\partial \xi}\right). \tag{9·8}$$

Using the expression (3·15) for the free energy in the two-phase region, the mean energy is

$$\bar{E} = NV\left\{\bar{c}_a G_{0,1}\left(\bar{c}_a, \frac{\partial \beta_\nu}{\partial \xi}\right) - \bar{c}_a G_0\left(\bar{c}_a, \frac{\partial \beta_\nu}{\partial \xi}\right) + (c_a - \bar{c}_a)\,\tfrac{1}{2}n\right\} + NV'' \quad (c_a > \bar{c}_a). \tag{9·9}$$

Comparing this expression with (9·7), it will be seen that the two expressions coincide for $c_a = \bar{c}_a$. There is therefore no heat of transformation for the transition from the two-phase region to the region of solubility.

At low temperatures it is more convenient to use in the two-phase region the expansion of the free energy in terms of the cluster sums b_l; it is given

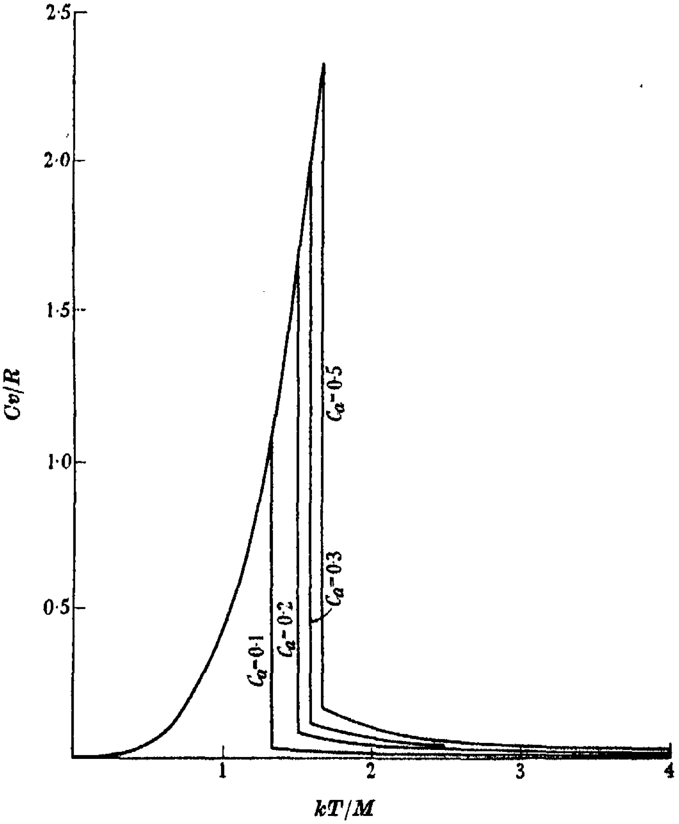

FIGURE 2. The specific heat for various atomic fractions of binary solid solutions with a two-phase region in the body-centred lattice.

by (3·11), if in that equation Z is replaced by $\bar{Z}$, the latter being given by (4·4). The result is

$$\bar{E} = NV\left\{\tfrac{1}{2}n(c_a - G_1(e^{\frac{1}{2}n\xi}, b_l)) - G_0\left(e^{\frac{1}{2}n\xi}, \frac{\partial b_l}{\partial \xi}\right)\right\} + NV'' \quad (c_a > \bar{c}_a). \quad (9{\cdot}10)$$

The specific heat is given by

$$c_v = \frac{d\bar{E}}{dT} = -\frac{V}{kT^2}\frac{\partial \bar{E}}{\partial \xi}. \quad (9{\cdot}11)$$

From (9·7), (9·9) and (9·10) we obtain

$$c_v = Nk\xi^2 c_a\left\{G_0\left(c_a, \frac{\partial^2\beta_\nu}{\partial\xi^2}\right) - G_{0,1}\left(c_a, \frac{\partial^2\beta_\nu}{\partial\xi^2}\right)\right\} \quad (c_a < \bar{c}_a), \tag{9·12}$$

$$c_v = Nk\xi^2 \bar{c}_a\left\{G_0\left(\bar{c}_a, \frac{\partial^2\beta_\nu}{\partial\xi^2}\right) - G_{0,1}\left(\bar{c}_a, \frac{\partial^2\beta_\nu}{\partial\xi^2}\right) + \frac{\left[\frac{1}{2}n + G_0\left(\bar{c}_a, \frac{\partial\beta_\nu}{\partial\xi}\right)\right]^2}{1 - G_1(\bar{c}_a, \beta_\nu)}\right\} \quad (c_a > \bar{c}_a), \tag{9·13}$$

$$c_v = Nk\xi^2\left\{G_0\left(e^{\frac{1}{2}n\xi}, \frac{\partial^2 b_l}{\partial\xi^2}\right) + nG_1\left(e^{\frac{1}{2}n\xi}, \frac{\partial b_l}{\partial\xi}\right) + \tfrac{1}{4}n^2 G_2(e^{\frac{1}{2}n\xi}, b_l)\right\} \quad (c_a > \bar{c}_a). \tag{9·14}$$

It is interesting to note that in the two-phase region the specific heat does not depend on the atomic fraction.

Comparison of (9·12) and (9·13) shows that the specific heat is discontinuous at a temperature $T(c_a)$, for which the given atomic fraction c_a is identical with the limit of solubility $\bar{c}_a$. Since G_0 and G_1 converge for the singularity $\bar{c}_a$ and G_1 is smaller than unity, the specific heat below the temperature $T(c_a)$ is larger than above by the finite amount

$$\Delta c_v = \lim_{\epsilon \to 0}\,[c_v(T(c_a)+\epsilon) - c_v(T(c_a)-\epsilon)] = Nk\xi^2 c_a \frac{\left\{\frac{1}{2}n + G_0\left(c_a, \frac{\partial\beta_\nu}{\partial\xi}\right)\right\}^2}{1 - G_1(c_a, \beta_\nu)}. \tag{9·15}$$

The numerical calculation for the body centred lattice is given in the Appendix. The result is shown in figure 2.

10. COMPARISON WITH THE THEORIES OF RUSHBROOKE AND KIRKWOOD

Let us, in conclusion, compare the results of the present paper with those obtained by Rushbrooke (1938) and Kirkwood (1939). It will be sufficient to compare the formulae for the free energy and the critical temperature.

Rushbrooke's result for the deviation of the free energy from the free energy of a perfect solution (i.e. $V = 0$) is given in the formula at the bottom of p. 298 of his paper up to terms in the square of the atomic fraction. Higher terms can easily be obtained from the equation for $\bar{X}$ on the same page. The result is in the present notation

$$\begin{aligned}\Delta A = RT\{&-c_a c_b \tfrac{1}{2}n\xi + c_a^2 c_b^2 \tfrac{1}{2}n(1 - \xi - e^{-\xi}) + c_a^3 c_b^3 n(\tfrac{3}{2} - \xi - 2e^{-\xi} + \tfrac{1}{2}e^{-2\xi}) \\ &+ \tfrac{5}{2}c_a^4 c_b^4 n(\tfrac{11}{6} - \xi - 3e^{-\xi} + \tfrac{3}{2}e^{-2\xi} - \tfrac{1}{3}e^{-3\xi})\} \quad \text{(Rushbrooke).}\end{aligned} \tag{10·1}$$

Substituting for the G-series in (6·8) according to the equations (A. 5) and (A. 7) of the appendix,

$$\begin{aligned}\Delta A &= A - \tfrac{1}{2}nV_{aa}c_a - \tfrac{1}{2}nV_{bb}c_b - RT\{c_a \ln c_a + c_b \ln c_b\} \\ &= RT\left\{-\tfrac{1}{2}n\xi c_a c_b - \sum_{\nu=1}^{\infty} \frac{\gamma_\nu}{\nu+1} c_a^{\nu+1} c_b^{\nu+1}\right\}. \qquad (10\cdot 2)\end{aligned}$$

With the γ_ν given by (A. 9) and $n = 8$, it follows that Rushbrooke's equation agrees with (10·2) up to the third power in $c_a c_b$.

For the critical temperature Rushbrooke finds the equation (cf. p. 309 of his paper)

$$e^{\xi/2} = 1 - \frac{2}{n} \quad \text{(Rushbrooke)}, \qquad (10\cdot 3)$$

which agrees with the equation (A. 14) of the appendix up to the third power in ξ.

Kirkwood obtains a priori an expansion in powers of the reciprocal temperature. He finds (equation (23) of his paper gives the 'free energy of mixing' from which $(c_a \ln c_a + c_b \ln c_b)\, NkT$ must be subtracted in order to obtain ΔA)

$$\Delta A = RT\{-\tfrac{1}{2}n\xi c_a c_b - \tfrac{1}{4}n\xi^2 c_a^2 c_b^2 + \tfrac{1}{12}n\xi^3 c_a^2 c_b^2 (c_a - c_b)^2\} \quad \text{(Kirkwood)}. \qquad (10\cdot 4)$$

On substitution of the value (A. 10) for γ_ν in the equation (10·2), it is found that this equation reduces to (10·4), if only terms to the third power in ξ are retained.

Similarly Kirkwood's equation (32) for the critical temperature

$$2 + \tfrac{1}{2}n\xi + \tfrac{1}{8}n\xi^2 = 0 \quad \text{(Kirkwood)}, \qquad (10\cdot 5)$$

is obtained from the equation (A. 14) of the appendix by retaining only terms to the second power in ξ.

APPENDIX

1. *The irreducible cluster sums*

The first few irreducible cluster sums are

$$\left.\begin{aligned}&\beta_1 = \sum_{l_2} f_{12}, \quad \beta_2 = \tfrac{1}{2}\sum_{l_2}\sum_{l_3} f_{12}f_{23}f_{31}, \\ &\beta_3 = \tfrac{1}{6}(3\beta_{30} + 6\beta_{31} + \beta_{32}), \\ &\beta_4 = \tfrac{1}{24}(12\beta_{40} + 60\beta_{41} + 10\beta_{42} + 60\beta_{43} + 10\beta_{44} \\ &\qquad + 30\beta_{45} + 30\beta_{46} + 15\beta_{47} + 10\beta_{48} + \beta_{49}).\end{aligned}\right\} \qquad (A.\ 1)$$

Here the sum extends over all lattice points and the function f_{ij} is given by (3·1).

The component sums of β_3 and β_4 are best illustrated by means of the corresponding 'bond figures', each bond representing a factor f_{ij} under the summation sign. They are shown in figure 3.

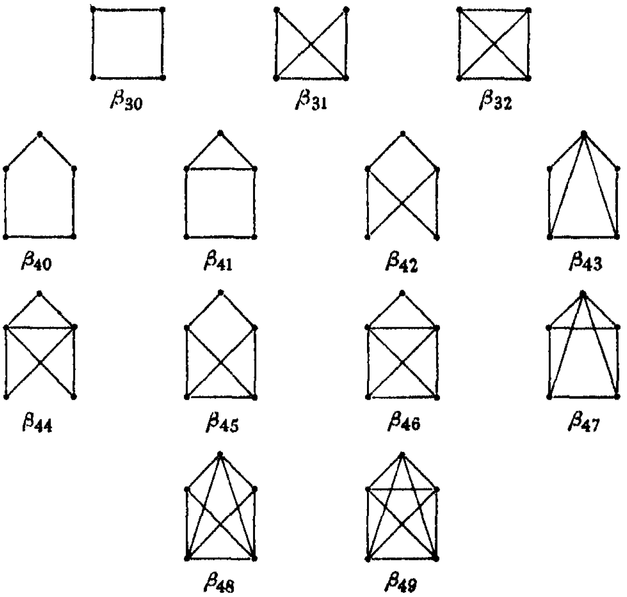

FIGURE 3. Bond figures of the component irreducible sums of β_3 and β_4.

The summation over the lattice points is tedious but elementary. The result for the body-centred lattice is

$$\left.\begin{aligned} \beta_1 &= -1+8f, \quad \beta_2 = -\tfrac{1}{2}+12f^2, \\ \beta_3 &= -\tfrac{1}{3}+8f^2+\tfrac{80}{3}f^3+48f^4, \\ \beta_4 &= -\tfrac{1}{4}-40f^3-310f^4-480f^5+60f^6, \end{aligned}\right\} \tag{A.2}$$

where

$$f = e^{-V/kT}-1 = e^{-\xi}-1. \tag{A.3}$$

The cluster sums b_l can now be obtained from (3·4). The first few are

$$\left.\begin{aligned} b_1 &= 1, \quad b_2 = \tfrac{1}{2}\beta_1, \\ b_3 &= \tfrac{1}{2}\beta_1^2+\tfrac{1}{3}\beta_2, \quad b_4 = \tfrac{2}{3}\beta_1^3+\beta_1\beta_2+\tfrac{1}{4}\beta_3, \\ b_5 &= \tfrac{25}{24}\beta_1^4+\tfrac{1}{2}\beta_2^2+\tfrac{5}{2}\beta_1^2\beta_2+\beta_1\beta_3+\tfrac{1}{5}\beta_4. \end{aligned}\right\} \tag{A.4}$$

2. *The G-functions*

First consider the function

$$c_a\{G_0(c_a,\beta'_\nu)-G_{0,1}(c_a,\beta'_\nu)\} = \sum_{\nu=1}^{\infty}\frac{\beta'_\nu}{\nu+1}c_a^{\nu+1}. \tag{A. 5}$$

Here the β'_ν are in accordance with (6·3), (6·4) and (6·5),

$$\begin{aligned}\beta'_1 &= \beta_1+1+8\xi,\\ \beta'_\nu &= \beta_\nu+\frac{1}{\nu}\quad(\nu>1).\end{aligned} \tag{A. 6}$$

From the equation (6·9) it follows that the function (A. 5) is symmetric in c_a and $c_b = 1-c_a$. It can therefore be written in the form

$$\sum_{\nu=1}^{\infty}\frac{\beta'_\nu}{\nu+1}c_a^{\nu+1} = \sum_{\nu=1}^{\infty}\frac{\gamma_\nu}{\nu+1}c_a^{\nu+1}(1-c_a)^{\nu+1}. \tag{A. 7}$$

In this form it converges more easily than in the form (A. 5). By expanding the right-hand side and comparing coefficients we find

$$\left.\begin{aligned}&\beta'_1 = \gamma_1,\quad \beta'_2 = \gamma_2-3\gamma_1,\\ &\beta'_\nu = (\nu+1)\sum_{0\leqslant\lambda\leqslant\frac{1}{2}(\nu+1)}\frac{(-1)^\lambda\gamma_{\nu-\lambda}(\nu-\lambda)!}{\lambda!(\nu+1-2\lambda)!}\quad(\nu>2).\end{aligned}\right\} \tag{A. 8}$$

From these equations the γ_ν can be obtained successively. With (A. 2), (A. 6) one finds

$$\left.\begin{aligned}\gamma_1 &= 8(f+\xi),\\ \gamma_2 &= 24(f+\xi)-12f^2,\\ \gamma_3 &= 80(f+\xi)-40f^2+\tfrac{80}{3}f^3+48f^4,\\ \gamma_4 &= 280(f+\xi)-140f^2+\tfrac{280}{3}f^3-70f^4-480f^5+60f^6.\end{aligned}\right\} \tag{A. 9}$$

Expand these expressions for high temperatures ($kT\gg V$); then

$$\left.\begin{aligned}\gamma_1 &= 4\xi^2-\tfrac{4}{3}\xi^3+\tfrac{1}{3}\xi^4-\tfrac{1}{15}\xi^5+\dots,\\ \gamma_2 &= 8\xi^3-6\xi^4+\tfrac{14}{5}\xi^6+\dots,\\ \gamma_3 &= 68\xi^4-120\xi^5,\\ \gamma_4 &= 536\xi^5+\dots.\end{aligned}\right\} \tag{A. 10}$$

It seems that each γ_ν starts only with the $(\nu+1)$th power of $\xi = V/kT$, though I have not been able to prove this in general. It is therefore probable that at high temperatures the expansion up to the term with γ_4 is correct up to the fifth power in the reciprocal temperature.

Differentiation of (A. 7) gives the equations

$$\left.\begin{aligned} G_0(c_a, \beta'_\nu) &= \Sigma \beta'_\nu c_a^\nu = (1-2c_a)\,\Sigma \gamma_\nu c_a^\nu (1-c_a)^\nu, \\ \frac{1}{c_a} G_1(c_a, \beta'_\nu) &= \Sigma \nu \beta'_\nu c_a^{\nu-1} = (1-2c_a)^2\,\Sigma \nu \gamma_\nu c_a^{\nu-1}(1-c_a)^{\nu-1} - 2\Sigma \gamma_\nu c_a^\nu (1-c_a)^\nu. \end{aligned}\right\} \tag{A. 11}$$

3. *The limits of solubility*

At low temperatures it is possible to use the expansion (4·5), with the cluster sums b_l given by (A. 4). But this expansion converges rather badly at higher temperatures, where it is more convenient to use the equation (8·3). Substituting for G_0 the value (A. 11) it takes the form

$$\ln \bar{c}_a - \ln(1-\bar{c}_a) = (1-2\bar{c}_a)\{\tfrac{1}{2}n\xi + \Sigma \gamma_\nu \bar{c}_a^\nu (1-\bar{c}_a)^\nu\}, \tag{A. 12}$$

which is best suited for numerical calculation. The values of the limits of solubility obtained from this equation with the γ_ν values (A. 10) join smoothly with those obtained for lower temperatures from (4·5), a fact which gives a good check on the accuracy of the calculation.

4. *The critical temperature*

The critical value $\xi_{\text{crit.}}$ corresponding to the critical temperature satisfies the equation (7·4). With (A. 11) it takes the form

$$2 + 4\xi + \Sigma \gamma_\nu (\tfrac{1}{4})^\nu = 0. \tag{A. 13}$$

With (A. 10) this equation reduces to

$$2 + 4\xi + \xi^2 + \tfrac{1}{6}\xi^3 + \tfrac{37}{48}\xi^4 + \tfrac{181}{480}\xi^5 + \ldots = 0, \tag{A. 14}$$

with the solution

$$\xi_{\text{crit.}} = -0{\cdot}60. \tag{A. 15}$$

5. *The specific heat*

The specific heat above the temperature $T(c_a)$ is given by (9·12), or, after introducing the expressions (A. 5), (A. 7), by the equation

$$c_v = Nk\xi^2 \Sigma \frac{c_a^{\nu+1}(1-c_a)^{\nu+1}}{\nu+1} \frac{\partial^2 \gamma_\nu}{\partial \xi^2} \quad (c_a < \bar{c}_a). \tag{A. 16}$$

For values of c_a near $\frac{1}{2}$ and temperatures near $T(c_a)$ this series does not converge as well as those we have met before, but it is still possible to obtain a fair estimate of the specific heat, which is found to be very small ndeed.

Below $T(c_a)$ the specific heat is given by the alternative expressions (9·13) or (9·14). The latter converges badly except at low temperatures. The G-functions occurring in (9·13) are (cf. (5·7), (5·8), (6·7) and (A. 11))

$$G_0\left(\bar{c}_a, \frac{\partial\beta_\nu}{\partial\xi}\right) + \tfrac{1}{2}n = (1-2\bar{c}_a)\left\{\tfrac{1}{2}n + \Sigma\frac{\partial\gamma_\nu}{\partial\xi}\bar{c}_a^\nu(1-\bar{c}_a)^\nu\right\}, \tag{A. 17}$$

$$1 - G_1(\bar{c}_a, \beta_\nu) = \frac{1}{1-\bar{c}_a} + n\xi\bar{c}_a - \bar{c}_a\{(1-2\bar{c}_a)^2\,\Sigma\nu\gamma_\nu\bar{c}_a^{\nu-1}(1-\bar{c}_a)^{\nu-1} \\ - 2\Sigma\gamma_\nu\bar{c}_a^\nu(1-\bar{c}_a)^\nu\}. \tag{A. 18}$$

With the help of (A. 12) the latter equation can be reduced to

$$1 - G_1(\bar{c}_a, \beta_\nu) = \frac{1}{1-\bar{c}_a} + \bar{c}_a\frac{\ln\bar{c}_a - \ln(1-\bar{c}_a)}{1-2\bar{c}_a} - \bar{c}_a(1-2c_a)^2\,\Sigma\nu\gamma_\nu\bar{c}_a^{\nu-1}(1-\bar{c}_a)^{\nu-1}. \tag{A. 19}$$

Substituting these expressions the specific heat (9·13) is

$$c_v = Nk\xi^2\left[\Sigma\frac{\bar{c}_a^{\nu+1}(1-\bar{c}_a)^{\nu+1}}{\nu+1}\frac{\partial^2\gamma_\nu}{\partial\xi^2} \right. \\ \left. + \frac{\bar{c}_a(1-\bar{c}_a)(1-2\bar{c}_a)^3\left\{\frac{n}{2} + \Sigma\frac{\partial\gamma_\nu}{\partial\xi}\bar{c}_a^\nu(1-\bar{c}_a)^\nu\right\}^2}{1-2\bar{c}_a+\bar{c}_a(1-\bar{c}_a)\{\ln\bar{c}_a - \ln(1-\bar{c}_a) - (1-2\bar{c}_a)^2\,\Sigma\nu\gamma_\nu\bar{c}_a^{\nu-1}(1-\bar{c}_a)^{\nu-1}\}}\right]. \tag{A. 20}$$

The sums in the second term converge very badly (except at low temperatures) and it is only possible to obtain the order of magnitude. Fortunately they turn out to be small compared with the other terms (not more than 10 %). Neglecting them altogether (A. 20) becomes

$$c_v \doteqdot Nk\xi^2\left[\Sigma\frac{\bar{c}_a^{\nu+1}(1-\bar{c}_a)^{\nu+1}}{\nu+1}\frac{\partial^2\gamma_\nu}{\partial\xi^2} + \frac{n^2}{4}\frac{\bar{c}_a(1-\bar{c}_a)(1-2\bar{c}_a)^3}{1-2\bar{c}_a+\bar{c}_a(1-\bar{c}_a)\{\ln\bar{c}_a-\ln(1-\bar{c}_a)\}}\right], \tag{A. 21}$$

which has been used for numerical calculation. If $\bar{c}_a$ tends to $\frac{1}{2}$ both numerator and denominator in the second term of (A. 21) tend to zero, but the quotient remains finite. It can easily be verified in general that this also holds for the exact expression.

REFERENCES

Bethe, H. A. 1935 *Proc. Roy. Soc.* A, **150**, 552.
Born, M. and Fuchs, K. 1938 *Proc. Roy. Soc.* A, **166**, 391.
Guggenheim, E. A. 1935 *Proc. Roy. Soc.* A, **148**, 304.

Kirkwood, J. G. 1939 *J. Phys. Chem.* **43**, 97.
Mayer, J. E. 1937 *J. Chem. Phys.* **5**, 67.
Mayer, J. E. and Ackermann, Ph. G. 1937 *J. Chem. Phys.* **5**, 74.
Mayer, J. E. and Harrison, S. F. 1938 *J. Chem. Phys.* **6**, 87, 101.
Mayer, J. E. and Goepert-Mayer, M. 1940 *Statistical mechanics*. New York.
Rushbrooke, G. S. 1938 *Proc. Roy. Soc.* A, **166**, 296. (See also the account of Rushbrooke's theory in Fowler, R. H. and Guggenheim, E. A., *Statistical thermodynamics*, Cambridge, 1939.)

Penetrating cosmic-ray showers

By L. Jánossy
Physical Laboratories, University, Manchester

(*Communicated by P. M. S. Blackett, F.R.S.—Received* 13 *June* 1941)

[Plate 40]

Observations giving evidence for the existence of showers penetrating at least 50 cm. of lead are reported. These penetrating showers are shown to be parts of extensive air showers. A detailed discussion shows that the penetrating showers are neither energetic cascades nor knock-on showers; they are, however, probably connected with the production of mesons. The connexion of the penetrating showers observed at sea-level with the production of mesons in the atmosphere is discussed with the following alternative assumptions: (1) that the mesons are produced by photons, (2) that the mesons are mainly produced by protons and possibly neutrons.

1. Introduction

It is now recognized that most of the cosmic-ray showers consist of primary cascades and knock-on showers, e.g. W.M. Nielsen (1938), Jánossy (1938), though another view is held by Schmeiser and Bothe (1938). It has been pointed out, however, by Auger and co-workers (1939) that the high penetrating power of the extensive air showers suggests that they contain a small number of mesons. Furthermore, the analysis carried out by Euler and Wergeland (1940) on Auger's data shows that the observed spread of extensive air showers covering up to 10^5 sq. m. can only be accounted for by assuming the presence of a small number of penetrating particles in the showers. This view is, however, not supported by the recent calculations of Bethe (1941).

Cloud-chamber photographs have not yet given any clear evidence for the presence of mesons or protons in extensive air showers (P. Auger and

Daudin 1939; Jánossy and Lovell 1938). However, by means of counter experiments penetrating showers containing more than one penetrating particle have been observed independently by Wataghin and co-workers (1940) and Jánossy and Ingleby (1940) and Jánossy (1941).

2. THE EXPERIMENTAL ARRANGEMENT

(i) The observations were carried out with the counter arrangement reproduced in figure 1. The counters shown joined with lines were connected in parallel. Fivefold coincidences 1–2–3–*A*–*B* were recorded. By means of eight neon indicator tubes it was recorded photographically which of the counters *H* were discharged simultaneously with each individual coincidence. A sample of such a photographic record is reproduced in figure 2 (plate 40). The dimensions of the counters are given in table 1.

TABLE 1. *Dimensions of counters*

description	diameter, cm.	length, cm.
1, *A*, *B*	3·5	40
H	3·5	60
2, 3	2·5	40

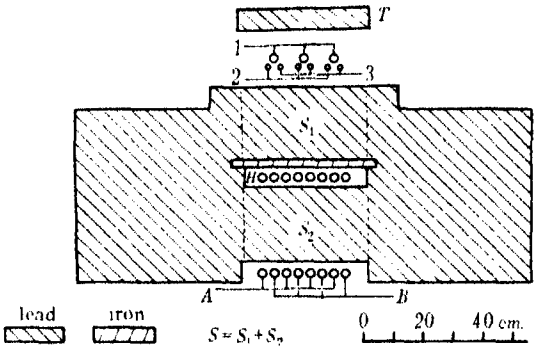

FIGURE 1. The experimental arrangement.

The circuit controlling the neon lamps will be described elsewhere. It is important to note that the resolving power of the circuit was found by control experiments to be such that less than one accidental neon flash on any of the eight lamps was to be expected for 100 fivefold coincidences. The efficiency of the neon lamps for recording counter discharges was greater than 99 %. The resolving power of the coincidence circuit was so high that casual coincidences could be neglected.

(ii) The object of the experiments was to observe showers penetrating up to 50 cm. Pb. For this purpose the absorbing material ($S = S_1 + S_2$) which could be varied from 0 to 50 cm. lead was placed between the top counters 1–2–3 and the bottom counters A–B as shown in figure 1. The whole counter arrangement was surrounded by 50 cm. Pb in order to absorb all side showers whose penetration was less than this thickness of lead. The total weight of the absorber was 15 tons, and the general lay-out of the apparatus is shown in figure 3 (plate 40).

A shower was only recorded when it discharged more than one counter near the top of S and more than one near the bottom of S. This arrangement was chosen to prevent ordinary knock-on showers being recorded. The arrangement responded, however, to certain multiple knock-on showers, the contribution of which will be discussed later (§ 3 (ii)). The photographic records showing the discharges of the counters H give evidence of the size of the showers.

A variable absorber T was placed close above the top counters to investigate transition phenomena.

(iii) In table 2 observations are given which show the occurrence of showers with a range of at least 50 cm. Pb at sea-level.

TABLE 2

S = 50 cm. Pb, T = 1·8 cm. Pb*

n =	0	1	2	3	4	5	6	7	8
number of cases with n counters discharged in H	77	64	14	9	13	9	7	7	5
rate per 100 hour	—	—	—	—	—	—	—	—	—

n =	0–1	2–8	total count	time
number of cases with n counters discharged in H	141	64	205	278 hr. 15 min.
rate per 100 hour	51 ± 4	23 ± 3	74 ± 5	—

These showers are clearly far more penetrating than those observed formerly (Jánossy 1938; Schmeiser and Bothe 1938). These very penetrating showers are so very rare that they could not be detected by the experiments referred to, and thus the present experiments are not at all in contradiction with previous results. For the same reason these results do not contradict those derived from cloud-chamber photographs by Lovell (1939).

---

* Owing to a slight change in the counter arrangement the figures given in table 2 are slightly higher than those reported earlier by Jánossy and Ingleby (1940).

3. DISCUSSION OF THE NATURE OF THE SHOWERS

The following arguments appear to prove that the observations referred to in table 2 cannot be accounted for in terms either of energetic cascade showers or of knock-on showers, unless the theory of either or both of these processes breaks down completely for high energies. Since there is no evidence for such a breakdown, we conclude that the observations establish the existence of a new type of penetrating shower.

(i) *Cascades.* (*a*) The absorber $S = 50$ cm. of lead corresponds to $l = 125$ in cascade units. According to a rough extrapolation of Bhabha and Heitler's data, an initial energy of about 10^{19} eV is required for an electron to produce a cascade shower penetrating through this absorber. Assuming the electron spectrum to be of the type

$$S_e(E) \sim dE/E^{\gamma+1} \quad (1 < \gamma < 2), \tag{1}$$

the frequency of occurrence of electrons of 10^{19} eV is estimated to be less than 2×10^{-5} per m.^{2} per hr. Thus the rate of occurrence of electrons sufficiently energetic to produce cascades penetrating S is negligible compared with the rate of showers observed which is 0·23 per hr.

The extrapolation of the energy spectrum up to energies of the order 10^{19} eV appears justified by recent considerations of Blackett and Lovell (1941) and of Blackett (1941). Nevertheless, it appears worth while to give two other independent arguments, which do not involve any assumption about the energy spectrum of electrons, to show that the penetrating showers are not cascades. First, a cascade shower of 10^{19} eV must contain an enormous number of particles and would always give rise to records $n = 8$ which is contrary to observation. Secondly, the ionization produced by the total cosmic radiation in the lead surrounding the apparatus ($\approx 1{\cdot}5 \times 10^6$ c.c.) can be estimated to be about 10^{14} ions per hour. The average energy to produce an ion is 32 V, therefore the energy dissipated in the absorber is of the order of 3×10^{15} eV per hour. On the other hand, an electron cascade of 10^{19} eV initial energy must be almost completely stopped in the absorber S and so will convert almost all its energy into ionization. Thus the ionization produced in S by one cascade shower penetrating 50 cm. of lead can be assumed to exceed 10^{19} eV. Since the contribution of showers and bursts to the total ionization is known to be small, the frequency of cascades penetrating S must be smaller than

$$\frac{\text{rate of ionization}}{\text{ionization per cascade}} = 3 \times 10^{15}/10^{19} = 3 \times 10^{-4} \text{ per hour.}$$

This rate is negligible compared with the rate of showers observed, and therefore the penetrating showers cannot be accounted for in terms of energetic cascades.

These considerations would be invalidated if the cross-section for radiation loss and pair production for high energies should prove to be much smaller than predicted by the theory of Bethe and Heitler. Since there is no evidence for a breakdown of this theory we think that the observed showers are not cascades.

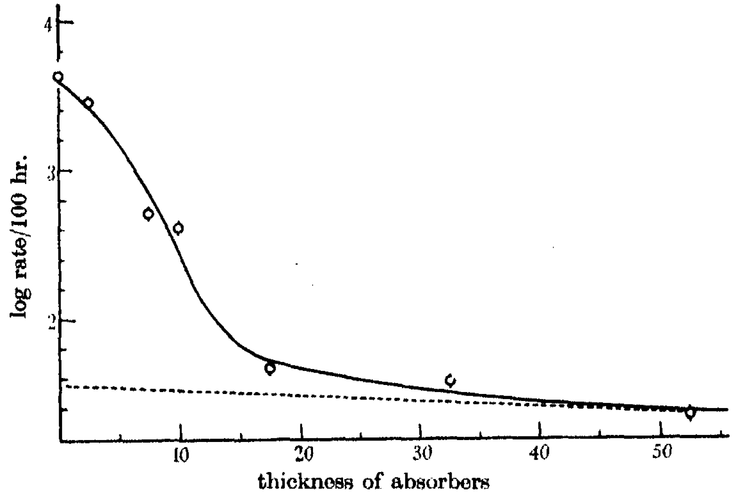

FIGURE 4. The shower absorption curve.

(*b*) Apart from these quantitative considerations the following observations suggest that the more penetrating showers are distinct from cascades. In figure 4 the logarithm of the shower rate $R(T = 1{\cdot}8$ cm. Pb, $n \geqq 2)$ is plotted against the thickness of the absorber S. This curve shows a marked change of slope near $S = 15$ cm. Pb, indicating that the showers which predominate in the region $S < 15$ cm. Pb and those predominant in the region $S > 15$ cm. Pb are of two distinct types. The slope in the region up to 15 cm. Pb agrees well with that predicted by the cascade theory for cascade showers, while the slope of the second part of the absorption curve is of the order of that corresponding to the absorption in lead of the penetrating component near sea-level, which is shown by the broken line.

In figure 5 the frequency of occurrence of records with $n = 0, 1, \ldots, 8$ are given for three different thicknesses of S, namely, 0, 7·5 and 30 cm. Pb. The scales have been chosen as to make the area of each diagram (*a*), (*b*) and (*c*) the same. The distributions in the cascade region ($S = 0, 7\cdot5$) are somewhat different from that observed under the thicker absorber ($S = 30$), thus suggesting again a different mechanism.

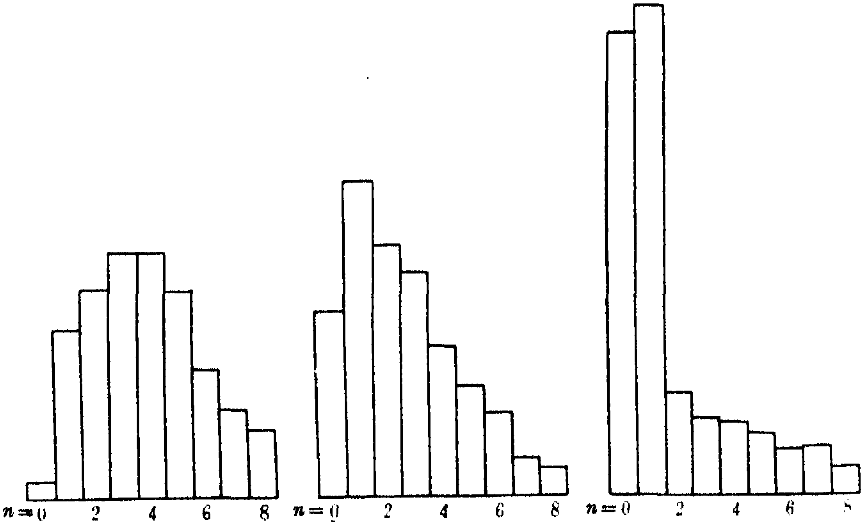

(*a*) $S = 0$ (*b*) $S = 7\cdot5$ (*c*) $S = 30$

FIGURE 5. Size distribution of showers with various absorbers. $T = 1\cdot8$ cm. Pb.

(ii) *Knock-on showers.* It has already been pointed out that our experimental arrangement does not record ordinary knock-on showers. But a double knock-on shower, i.e. a meson producing a secondary near the top set of counters and producing an independent secondary near the bottom counters could give rise to a fivefold coincidence 1–2–3–*A*–*B*, and such a process would be recorded. A double knock-on gives rise to a photographic record $n = 0$ or 1 according to whether the meson passes through a gap between the counters or discharges one of the counters *H*. Similarly, records with $n \geqq 2$ cannot be due to double knock-on showers but they might be due to triple knock-on showers, that is, to processes in which one meson produces three independent secondaries at suitable points. We discuss the contributions of these processes to our records by reference to the data collected in table 3.

In table 3 (1, 2, 3) means counters 1, 2 and 3 connected in parallel; (*A*)–(*B*) means counters *A* and *B* in coincidence. R_2 represents the rate of mesons crossing the apparatus. The coincidences R_3 are mainly due to knock-on showers, a secondary being produced near the bottom counters. Thus the average probability per meson of producing such a knock-on is

$R_3/R_2 = 2\ \%$. Similarly, R_4 represents the rate of knock-on showers where secondaries are produced near the top counters. The probability for this process is $R_4/R_2 = 1{\cdot}1\ \%$. Assuming that the production of secondaries near the top takes place independently of the production of secondaries near

TABLE 3

$T = 10$ cm. Pb, $S = 30$ cm. Pb

description	*symbol*	*rate per hour*
double coincidences (1, 2, 3)–(A, B)	R_2	3400
triple coincidences (1, 2, 3)–(A)–(B)	R_3	68
fourfold coincidences (1)–(2)–(3)–(A, B)	R_4	38
fivefold coincidences $n = 0,\ 1$; (1)–(2)–(3)–(A)–(B)	R_5	0·68

the bottom, the probability for a double knock-on giving rise to a fivefold coincidence 1–2–3–A–B is the product of the two probabilities given above. The calculated rate of double knock-on showers is therefore equal to

$$R_3 R_4/R_2 = 76 \text{ per 100 hour.}$$

This rate is very nearly equal to the observed rate R_5 of records $n = 0, 1$ given in table 3. From the close agreement between these two rates we conclude that most of the records R ($n = 0, 1$) are due to double knock-on showers.

Since the lead above the counters H is placed in much the same way as the lead above the counters A, B, the probability of a knock-on secondary actuating the counters H can be assumed to be nearly equal to R_3/R_2, i.e. the probability of a knock-on actuating the counters A, B. Thus the rate of triple knock-on showers is expected to be

$$R_3^2 R_4/R_2^2 = 1{\cdot}5 \text{ per 100 hour.}$$

This rate is very much smaller than the rate of the records for $n \geqslant 2$ and $S = 30$, which is found to be

$$R(n \geqq 2) = 36 \pm 5.$$

Thus the records for $R(n \geqq 2)$ cannot be attributed to triple knock-on processes.

In order to meet a possible objection to this argument we have to discuss the validity of the assumption that the productions of subsequent secondaries by the same meson can be regarded as independent processes. In fact, this assumption is not strictly valid since the cross-section for the production of secondaries increases with the energy of the primary. Therefore, on the average, a meson which has already given rise to a secondary is likely to be of more than average energy and so will have more than an average chance to produce subsequent secondaries. Using, however, the cross sections given either by Bhabha (1938) or, by Massey and Corben (1939) this effect appears to be negligible. Cloud chamber observations of Wilson (1938*b*) have verified these cross sections up to about 3×10^9 eV.

One can, however, account for the records with $n \geqq 2$ in terms of knock-on showers by making the assumption that for very high energies the theoretical cross-section is much too small. The observations of Wilson (1938*b*) do not necessarily contradict such an assumption since high-energy mesons are very rare.

Assume for instance that the probability of a meson greater than 10^{11} eV energy being accompanied by secondaries is of the order of 100 %. All the records with $n \geqq 2$ in terms of triple knock-on showers can then be accounted for. The average number of secondaries per meson greater than 10^9 eV is, however, hardly affected by the contributions of the secondaries due to mesons of about 10^{11} eV energy, owing to the small number of the latter.

Since the records with $n = 0, 1$ are already well accounted for in terms of double knock-on showers due to mesons with average energies, the functional dependence of the knock-on cross-section on energy must be such that the rate of double knock-on showers due to high-energy mesons becomes small compared with the observed rate of records $n = 0, 1$.

It is therefore possible to account for the records $n \geqq 2$ in terms of triple knock-on showers, but the assumptions required for this purpose are rather artificial. It appears therefore reasonable to assume that our records are not due to knock-on showers.

4. PROPERTIES OF THE PENETRATING SHOWERS

In discussing the properties of penetrating showers it is essential to distinguish clearly the two most probable types of processes, namely:

(1) The simultaneous production of several penetrating particles.

(2) The production by a single penetrating agent of several soft secondaries on its way through matter.

The experimental data available at present do not yield sufficient evidence to distinguish between these two possibilities. It is likely, however, that the mesons in the atmosphere are produced by a process of the type (1), while no evidence exists for the occurrence of a process of the type (2). It is assumed therefore in the following sections as a working hypothesis that the penetrating showers are due rather to process (1) than to process (2).

(i) *The absorption effect.* The absorption curve of the penetrating showers is reproduced in figure 4, and the corresponding data are collected in table 4.

TABLE 4

$T = 1{\cdot}8$ cm. Pb

S (cm. Pb)	rate $n \geqq 2$
15	47 ± 5
30	$38 \pm 3{\cdot}5$
50	23 ± 3

The order of magnitude of the absorption effect is that of the penetrating component of cosmic radiation. It is therefore reasonable to assume that the showers consist of mesons. The assumption that associated mesons do occur is supported by some cloud-chamber photographs taken by Braddick and Hensby (1939), Herzog and Bostick (1940), Powell (1940).

(ii) *The size of the showers.* Penetrating showers giving rise to records with $n \geqq 2$ must consist of at least two mesons both penetrating S. Thus for $S = 50$ cm. Pb the minimum energy of showers with $n \geqq 2$ is $1{\cdot}2 \times 10^9$ eV and the average value of n (including only the values $n \geqq 2$) is approximately 4. The frequency of records with $n = 8$ corresponding to showers of energies greater than 6×10^9 eV is still appreciable. It is difficult to estimate the total energy of the showers, since the actual number of particles is unknown. The following effect, however, gives some indication.

The flashes on individual records are not entirely distributed at random but show a tendency to form groups as is illustrated in table 5. This tendency of the showers to discharge groups of neighbouring counters suggests that the average density of the particles in a shower is greater than one particle per counter. A rough estimate based on this effect gives the lower limit for the average particle density as two particles per counter, i.e. one particle per 100 cm.^{2}.

TABLE 5

number of records with $n = 4$ or 5		50
number of cases in which the counters discharged are lying side by side	observed	17
	calculated for random distribution	3·6

(iii) *Connexion with the extensive air showers.* A single counter C was placed at a distance of 3 m. from the centre of S and sixfold coincidences 1–2–3–A–B–C were recorded. Results obtained with this arrangement are given in table 6. The frequency of these showers is 11 ± 2 per 100 hr. and is of the same order as the frequency of records with $n \geqq 2$ obtained with $T = 0$

and S = 30 cm. Pb (see table 7). This indicates that all the penetrating showers observed with $T = 0$ are parts of extensive air showers.

TABLE 6

S = 30 cm. Pb

T	numbers observed $n = 0$	1	2	3	4	5	6	7	8	rate per 100 hour
light roof only	1	3	0	1	4	0	0	1	1	11 ± 3
1·8 cm. Pb	0	3	0	1	2	3	3	1	2	11 ± 3

The records with $n = 0$, 1 form a comparatively small fraction of the records given in table 7. This is in accordance with the view that most of the records with $n = 0$, 1 while recording fivefold coincidences are due to double knock-on showers.

(iv) *Transition effect.* The absorber T was varied while S was kept constant and equal to 30 cm. Pb. The results of these observations are collected in table 7. The transition curves are plotted on an equivalent mass scale in figure 5 and the following conclusions are based upon these observations:

TABLE 7

T			rates per 100 hour	
cm.	g./cm.	material	$n = 0$ to 8	$n = 2$
0	—	light roof only	56 ± 4	16 ± 2
0·8	8·5	lead	89 ± 6	30 ± 3·5
1·8	20·0		127 ± 6	38 ± 3·5
5·0	56·5		99 ± 8	44 ± 5·5
10·0	113·0		104 ± 9	36 ± 5
2·0	5·4	aluminium	73 ± 5·5	17 ± 2·5
6·5	17·5		91 ± 5	23 ± 2
22·0	60		115 ± 6	37 ± 3·5
38·0	103		136 ± 5·5	41 ± 3

(*a*) The penetrating showers observed with $T = 0$ come from the air, and a few from the light roof. The frequency of showers increases however considerably above this zero as the thickness of the absorber T increases. An increase of T from 0 to 1·8 cm. Pb produces for instance an increase in the rate of showers with $n \geqq 2$ of 22 ± 4 per 100 hour. Therefore about half of the penetrating showers are produced in T. If the penetrating showers consist of mesons, then the result shows that mesons must be created in the absorber T.

The creation of mesons by a non-ionizing agent at high altitudes has been recently observed by Schein and co-workers (1940).

(*b*) The initial slopes of the transition curves in lead and aluminium define the relative cross-sections for the production of the showers in these materials. The observed slopes can be well accounted for by assuming that the cross-sections in various materials are proportional to Z^2 (Z atomic number); to show this, curves with slopes corresponding to Z^2 cross-sections have been drawn through the observed points in figure 6.

The Z^2 dependence suggests that the process responsible for the production of penetrating showers involves an interaction with the Coulomb field of the nuclei.

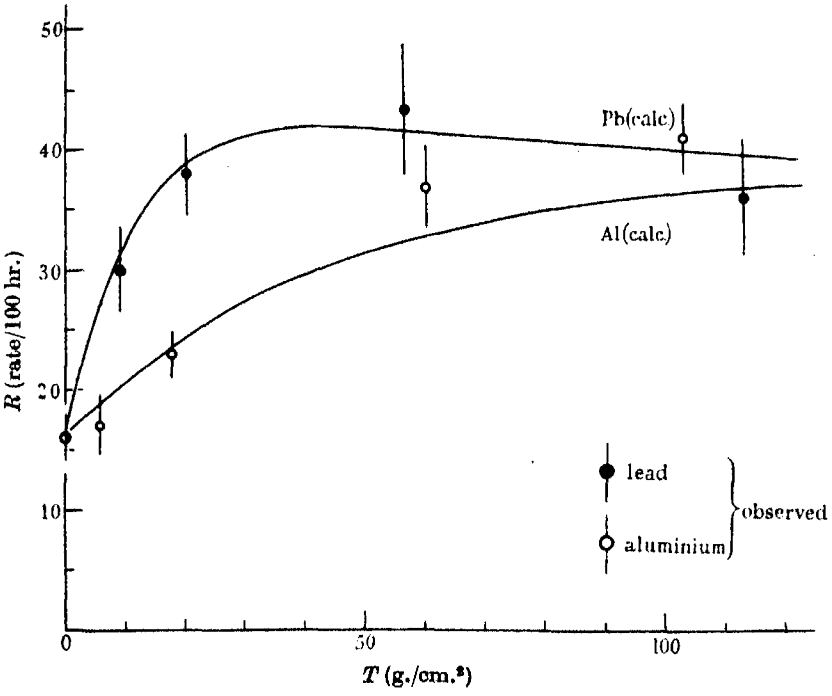

FIGURE 6. The transition effect of penetrating showers in lead and aluminium.

(*c*) The lead transition effect shows saturation for thicknesses exceeding about 5 cm. Pb. Therefore the radiation producing the penetrating showers has a range of this order. One is inclined to identify this radiation with the soft component of cosmic rays. That the showers are initiated by the soft component is also supported by the fact that saturation is reached for aluminium absorbers at a greater mass equivalent than for lead absorbers.

Both effects, the range of the shower producing radiation and the Z^2 dependence of the cross-section for shower production, can be accounted for by assuming that the showers are due to meson pair production by energetic photons or electrons. The curves fitted to the experimental points in figure 6 are calculated on this assumption. The simultaneous agreement of the calculated lead and aluminium curves with the observed points is noteworthy.

Nevertheless, the possibility cannot be ruled out that the close agreement of the range of the radiation producing the penetrating showers with that of electron cascades in lead is accidental and that the radiation producing the showers consists of, say, protons or neutrons, provided one assumes that protons or neutrons of high energy are suitably absorbed in lead and aluminium.

Observations of Rochester and Bound (1940) seem to favour the assumption that protons suffer an absorption in lead exceeding that due to ionization alone. Further, the abnormal energy loss for cosmic-ray particles traversing a lead plate observed by Wilson (1938*a*) might be due to protons.

The proton hypothesis accounts for the penetrating showers in a less simple way than the photon hypothesis. But a general argument by Johnson (1939) gives strong evidence for the view that most mesons are produced by primary protons and not by the soft component. It seems therefore important to explore both the proton and the photon hypothesis.

5. PENETRATING SHOWERS AND MESON PRODUCTION

In the following section it will be assumed that the penetrating showers consist of simultaneously produced mesons. An attempt will be made to show that simple assumptions about the processes involved can be found which account for both the production of mesons in the atmosphere and the penetrating showers at sea level.

(i) *The photon hypothesis.* The value of the cross-section for the production of mesons or groups of mesons by photons can be derived from the penetrating shower data as follows.

rate of cosmic-ray particles crossing the arrangement figure 1	4000 per hour
rate of photons, energy greater $E_c = 1\cdot5 \times 10^8$ eV	400 per hour
rate of photons having an energy sufficient to produce two mesons each with a range exceeding 30 cm. Pb, i.e. photons $E > 10^9$ eV ($E^{-1\cdot5}$ spectrum)	27 per hour
rate of showers giving records $n \geqq 2$ produced in the first cm. of T	0·12 per hour

Since the mean free path of photons in lead is about 1 cm., the probability for a photon $E > 10^9$ eV to produce mesons instead of giving rise to an electron pair is roughly $0{\cdot}12/27 \sim 5 \times 10^{-3}$.

The cross-section for the production of a meson pair by a photon is according to Booth and Wilson (1940)

$$\Phi_{\text{meson}} = \frac{5}{9}\frac{Z^2}{137}\left(\frac{c^2}{\mu c^2}\right)\frac{h\nu}{\mu c^2} \quad (\mu \text{ mass of the meson}).$$

This compared with the cross-section for the production of electron pairs in lead gives

$$\Phi_{\text{meson}}/\Phi_{\text{electron}} = 100(m/\mu)^3 \frac{h\nu}{10^9\,\text{eV}} \quad \text{(theory)}$$

and for $\mu = 170$ m. and $h\nu = 10^9$ eV we get

$$\Phi_{\text{meson}}/\Phi_{\text{electron}} = \begin{cases} 2 \times 10^{-5} & \text{(theory)} \\ 5 \times 10^{-3} & \text{(observation of penetrating showers).} \end{cases}$$

Thus the theoretical cross-section is about 250 times too small to account for penetrating showers. The disagreement is even more pronounced if one remembers that the average penetrating shower contains at least ten penetrating particles (§ 4 (ii)).

The cross-section for meson pair production in lead as derived here from the penetrating shower observations is of the right order of magnitude to account for the meson flux produced in the atmosphere assuming the cross-section varies as Z^2. This is shown in an unpublished calculation (Jánossy and Lockett). Compare also Heitler (1938) and Nordheim and Hebb (1939).

It may be noted that in order to account for the atmospheric mesons it is essential to assume that the cross-section for meson production is proportional to Z^2. If one were to assume, for instance, that the cross-section varies with Z instead of Z^2, then the rate of mesons produced in the atmosphere would be expected to be greater by the factor $Z_{\text{Pb}}/Z_{\text{air}} = 11$. Thus the frequency of mesons produced in the atmosphere estimated using Z cross-section would be larger than the observed meson flux.

(ii) *Proton hypothesis*. The consequences of the assumption that both the penetrating showers and the atmospheric mesons are due to primary protons will be discussed.

(*a*) To account for the properties of the penetrating showers obtained in § 4 in terms of incident protons a process of the following type is suggested.

A proton suffering a close collision with a nucleus is either slowed down considerably emitting a number of mesons or else it disintegrates into a number of mesons (and possibly other particles).

According to §4 (4*b*) the probability for such a collision is proportional to Z^2 and therefore the mean free path of a proton expressed in cascade units should be independent of the material; it amounts to 2–3 cascade units (figure 5).

The rate of incident protons will be roughly equal to the rate of penetrating showers observed. Thus near sea-level one expects in 3 hr. about one energetic proton of suitable direction incident on T. This corresponds to one proton among 12,000 cosmic-ray particles, an estimate which includes only fast protons and is therefore not in disagreement with the much higher rates observed for slower protons.

(*b*) It will now be shown that the particular process for the production of mesons by protons described above can be used to give a reasonable account of the production of the meson component in the atmosphere by primary protons.

Suppose for the moment that the primary cosmic radiation consists of protons only. The primary energy flux is according to Regener (1933) and to Bowen and Neher (1938) about 2×10^{11} eV per cm.^{2} per min. The primaries must have energies exceeding 3×10^9 eV according to a general argument based on the latitude effect. Thus the average energy of the primaries can be assumed to be about 6×10^9 eV and therefore the number of primaries per cm.^{2} per min. at the top of the atmosphere is estimated to be $2 \times 10^{11}/6 \times 10^9 = 33$ per cm.^{2} per min. According to (*a*) the frequency of fast protons at sea-level is about 1/12,000 per cm.^{2} per min.

The protons, if absorbed 'catastrophically' by the act of meson production, decline in number exponentially through the atmosphere. The mean free path of a fast proton is thus obtained by comparing the intensities at the top of the atmosphere and at sea-level as follows

$$\lambda_{\text{proton}} = \frac{H}{\log_e (I_{\text{top}}/I_{\text{sea level}})} = \frac{29}{12{\cdot}7} = 2{\cdot}2 \text{ cascade units.}$$

This value for the mean free path of protons is in good agreement with that derived for the radiation producing the penetrating showers from the transition effect. The curves fitted to the observed points in figure 6 are based on a mean free path of 2·5 cascade units.

We conclude, therefore, that the proton hypothesis gives as good an account of the production of mesons in the atmosphere and the penetrating showers observed at sea level as the photon hypothesis. The obvious advantage of the proton hypothesis is that it does not lead to difficulties with the east-west effect.

(*c*) The assumption made above that the primary radiation consists of protons only is not essential to maintain the order of magnitude of the value obtained for λ_{proton}. Assuming for instance that only 10 % of the primaries are protons, the calculated free path is 2·7 instead of 2·2 cascade units again in sufficient agreement with the experiment.

The fact, however, that the penetrating showers are parts of the extensive air showers makes it very likely that the whole of the soft component is of secondary origin and that the primaries are protons and possibly neutrons.

Regarding the actual process of production of the soft component, it is not very likely that the extensive air showers which have frequently energies up to 10^{13}–10^{16} eV are due to energetic decay electrons and knock-on secondaries only. It appears more likely that electrons or photons are produced simultaneously with the mesons.

Finally, the proton hypothesis is not necessarily in disagreement with the observations of Schein and co-workers (1939, 1940) giving evidence for the production of mesons by non-ionising agents, since it can be assumed that fast neutrons have properties similar to fast protons and that the mesons observed by Schein were produced by neutrons.

[*Note added in proof.* A process for the production of the meson component similar to that given in § 5 (ii*a*) has been suggested by Hilberry (1941) based on theoretical considerations by Carlson and Schein (1941). I received these papers after the conclusion of the present paper.]

This work was started early in 1939 in collaboration with P. Ingleby who lost his life in an air accident, while engaged in experimental work for the Air Ministry.

I wish to thank Professor P.M.S. Blackett for much encouragement and valuable discussions. My thanks are also due to Dr W. Heitler for many inspiring discussions throughout the work, and to Dr G. D. Rochester for his friendly assistance.

REFERENCES

Auger, P. and Daudin, J. 1939 *C.R. Acad. Sci., Paris*, **209**, 481.
Auger, P., Maze, R., Ehrenfest, P. jr and Fréon, A. 1939 *J. Phys. Radium*, **10**, 39.
Bethe, A. H. 1941 *Phys. Rev.* **59**, 684.
Bhabha, H. J. 1938 *Proc. Roy. Soc.* A, **164**, 151.
Blackett, P. M. S. 1941 *Proc. Phys. Soc.* **53**, 203.
Blackett, P. M. S. and Lovell, A. C. B. 1941 *Proc. Roy. Soc.* A, **177**, 183.
Booth, F. and Wilson, A. H. 1940 *Proc. Roy. Soc.* A, **175**, 483.
Bowen, I S. and Neher, H. V. 1938 *Phys. Rev.* **52**, 217.

Braddick, H. J. J. and Hensby, G. S. 1939 *Nature, Lond.*, **144**, 1012.
Carlson, J. F. and Schein, M. 1941 *Phys. Rev.* **59**, 840.
Euler, H. and Wergeland 1940 *Astrophys. Norv.* **3**, 165.
Heitler, W. 1938 *Proc. Roy. Soc.* A, **166**, 529.
Herzog, G. and Bostick, W. H. 1940 *Phys. Rev.* **58**, 278.
Hilberry, N. 1941 *Phys. Rev.* **60**, 1.
Jánossy, L. 1938 *Proc. Camb. Phil. Soc.* **34**, 614.
Jánossy, L. 1941 *Nature, Lond.*, **147**, 56.
Jánossy, L. and Ingleby, P. 1940 *Nature, Lond.*, **145**, 511.
Jánossy, L. and Lovell, A. C. B. 1938 *Nature, Lond.*, **142**, 716.
Johnson, T. H. 1939 *Rev. Mod. Phys.* **11**, 208.
Lovell, A. C. B. 1939 *Proc. Roy. Soc.* A, **172**, 568.
Massey, H. S. W. and Corben, H. C. 1939 *Proc. Camb. Phil. Soc.* **35**, 463.
Nielsen, W. M. 1938 *J. Franklin Inst.* **226**, 601.
Nordheim, L. W. and Hebb, M. H. 1939 *Phys. Rev.* **56**, 484.
Powell, W. M. 1940 *Phys. Rev.* **58**, 474.
Regener, E. 1933 *Nature, Lond.*, **131**, 130 and *Z. Phys.* **80**, 666.
Rochester, G. D. and Bound, M. 1940 *Nature, Lond.*, **146**, 745.
Schein, M. and Wilson, V. C. 1939 *Rev. Mod. Phys.* **11**, 292.
Schein, M., Wollan, E. O. and Groetzingen 1940 *Phys. Rev.* **58**, 1027.
Schmeiser, K. and Bothe, W. 1938 *Ann. Phys., Lpz.*, **32**, 161.
Wataghin, G., de Souze, M. and Pompia, P. A. 1940 *Phys. Rev.* **57**, 61, 339.
Wilson, J. G. 1938*a* *Proc. Roy. Soc.* A, **166**, 482.
Wilson, J. G. 1938*b* *Nature, Lond.*, **142**, 73.

EXPLANATION OF PLATE 40

FIGURE 2. Each vertical column represents the discharges of one of the counters H. Each horizontal line represents the discharges of the counters H occurring simultaneously with a fivefold coincidence 1–2–3–A–B. The first and last lines of the photograph are time marks. The second horizontal line is the record of a coincidence 1–2–3–A–B accompanied by the discharge of the counter H no. 2, this is an example of a record $n = 1$. Similarly, the next line is an example of a record $n = 4$.

FIGURE 3. The experimental arrangement.

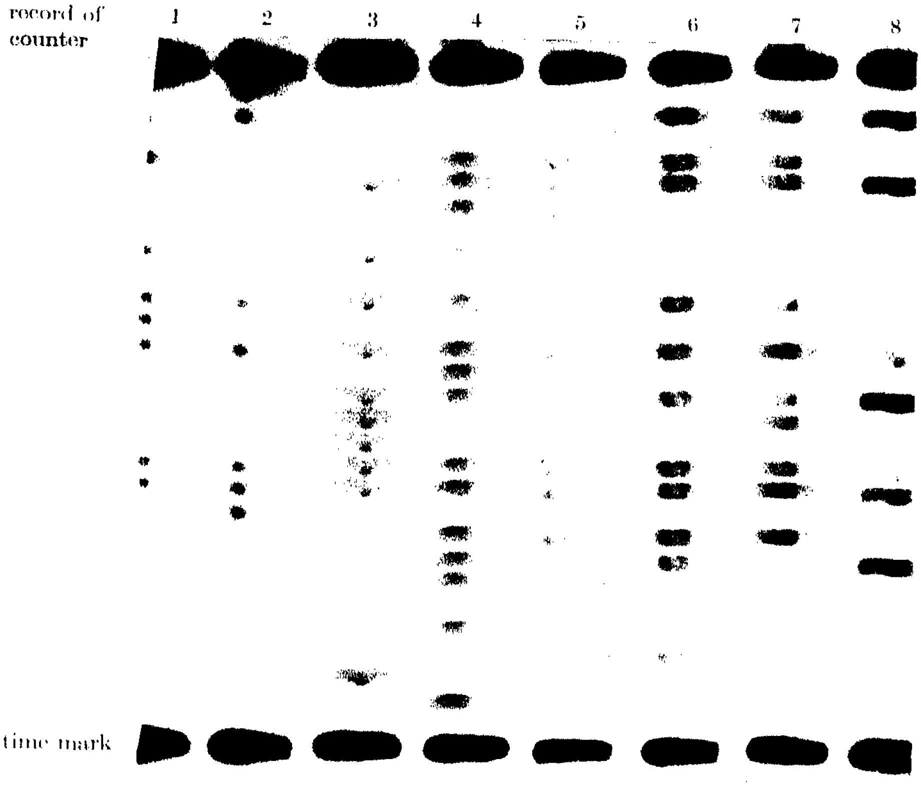

FIGURE 2

FIGURE 3

The summation of infinite harmonic series

By F. Soddy, F.R.S.

(*Received* 11 *June* 1941.—*Revised* 8 *September* 1941)

Infinite harmonic series with alternating signs, capable of being extended to infinity in both directions, of which the Leibnitz series for $\frac{1}{4}\pi$, $2a = d = 2$, is typical ($S_D = \frac{1}{4}\pi$), can be very simply transformed into very rapidly converging doubly infinite series, termed S_D^T, in which the successive terms are the reciprocals of any number, $n+1$, of factors in arithmetical progression, the first *two* (in one case the first three) factors of the successive terms constituting the same arithmetical progression:

$$S_D = \sum_{M=-\infty}^{M=+\infty} \frac{(-1)^M}{a+Md}$$
$$= 2(\tfrac{1}{2}d)^n n! \sum_{M=-\infty}^{M=+\infty} \frac{1}{(a+2Md)\,(a+\overline{2M+1}.d)\ldots(a+\overline{2M+n}.d)} = S_D^T,$$

as for example

$$\frac{\pi}{4.n!} = \sum_{M=-\infty}^{M=+\infty} \frac{1}{(4M+1)\,(4M+3)\ldots(4M+2n+1)} \quad (n = 0, 1, 2, 3, \ldots, \infty).$$

With $n = 9$, five pairs of equal terms give the result correct to 1 part in 17 millions. With $n = 39$, the computation of eleven terms gave 14 places and of twenty-five terms 31 places of decimals.

The method may be extended to harmonic series, as that for which $a = d = 1$, summing to $\log_e 2$, for which, in the doubly infinite form, the denominator of one of the terms vanishes, by use of a special set of numerators termed Summate Numerators. When n is large this is the quickest way of computing the first large terms of S_D^T and also of the Euler transformation series, termed S^T,

$$S_s^T = \sum_{M=1}^{M=\infty} \frac{(M-1)!\,d^{M-1}}{2^M} \left[\frac{1}{a(a+d)\ldots(a+\overline{M-1})\,d}\right],$$

the relation of which to S^T is discussed.

The transformation of an infinite harmonic series into one very rapidly converging can be effected very simply for the doubly infinite form

$$S_D = \sum_{M=-\infty}^{M=+\infty} \frac{(-1)^M}{a+Md} = \ldots + \frac{1}{a-2d} - \frac{1}{a-d} + \frac{1}{a} - \frac{1}{a+d} + \frac{1}{a+2d} - \ldots, \quad (1)$$

where d is the common difference and a is the 'first term', now become the mid-term, of an arithmetical progression. It is denoted by S_D, and its relation to the ordinary singly infinite series S_S is given by

$$S_D = \left[\frac{1}{a} - \frac{1}{a+d} + \frac{1}{a+2d} - \dots\right] - \left[\frac{1}{a-d} - \frac{1}{a-2d} + \frac{1}{a-3d} - \dots\right] = S_S - S_{-S}, \quad (1a)$$

in which S_D is expressed as the difference between two singly infinite harmonic series termed S_S and S_{-S}.

The commonest examples of S_S are the series summing to $\log_e 2$, for which $a = d = 1$, and the Leibnitz series for $\frac{1}{4}\pi$ for which $2a = d = 2$, and which are here characterized and distinguished by single and double dashes, as S'_S and S''_S respectively. When a is an integral multiple of d, as in S'_S, the method is not directly applicable as the denominator of one of the terms of the series vanishes and the further consideration of the $\log_e 2$ series may be deferred. For S''_S, S''_{-S} is $-\frac{1}{4}\pi$, S''_D is $\frac{1}{2}\pi$, and the method may be illustrated for this series and those derivable from it.

The algebra is similar to that on which the generalized theory of finite differences is largely based, as, for example, in the Euler transformation, which, however, deals with algebraic identities and is therefore generally applicable though not generally useful. In the case described the result follows from a particular property of the harmonic series which is transformed into a very rapidly convergent set of series. This will be denoted by S^τ to distinguish it from the Euler transformed series which will be termed S^T:

$$S^T_S = \sum_{M=1}^{M=\infty} \frac{(M-1)!\,d^{M-1}}{2^M} \left[\frac{1}{a(a+d)\dots(a+\overline{M-1})\,d}\right].$$

With this method the latter is obtainable from the former by a further transformation. It would appear that S^T for the harmonic series is a concisely formulizable general expression only because of the peculiarity of the harmonic series mentioned. To facilitate computation and also to include the $\log_e 2$ series and derivatives, in which a is an integral multiple of d, a summation of the initial terms of both S^τ and S^T by means of what are termed Summate Numerators is described.

The harmonic series have the particular property that any number, $n+1$, of terms, if the unit numerators are replaced by the binomial coefficients of the expansion $(1-x)^n$, sum to a single term, in which the denominator is the product of the $(n+1)$ denominators of the single terms, and the numerator is the same whatever part of the series is summed, being independent of a and a function only of n and d. Thus using $-c_1$, $+c_2$, $-c_3$, ..., $(-1)^n c_n$ to denote these coefficients, where c_0 and c_n are unity; c_1 and $c_{n-1} = n$; c_2 and $c_{n-2} = \{n(n-1)\}/2!$; c_3 and $c_{n-3} = \{n(n-1)(n-2)\}/3!$; and so on:

$$\frac{c_0}{a+bd} - \frac{c_1}{a+\overline{b+1}\,.\,d} + \frac{c_2}{a+\overline{b+2}\,.\,d} - \dots (-1)^n \frac{c_n}{a+\overline{b+n}\,.\,d}$$

$$= \frac{d^n n!}{(a+bd)(a+\overline{b+1}\,.\,d)(a+\overline{b+2}\,.\,d)\dots(a+\overline{b+n}\,.\,d)}. \tag{2}$$

n is any + integer, including 0 if 0! is conventionally reckoned unity, and the method derives from the fact that b may be any integer, + or −, without the expression (2) being invalidated. The partial fraction of $(n+1)$ terms on the left will be termed P_n, and the rational fraction with $(n+1)$ factors in the denominator on the right by R_n. The summation of these is a way of summing the original series, if an appropriate spacing factor, s, or number of terms of P_n separating the successive terms summed, is used. Then b is sM, as M assumes successive integral values over the range of summation. The spacing factor is denoted by a left-hand subscript as ${}_sP_n$ or ${}_sR_n$. It is convenient to start sometimes with a negative term of P_n, which may give a different series, and in this case the suffix s is preceded by a minus sign as ${}_{-s}P_n$. Thus

$$\Sigma_{-s}P_n \quad \text{or} \quad \Sigma_{-s}R_n = -\Sigma_s P_n \quad \text{or} \quad -\Sigma_s R_n. \tag{2a}$$

A particular term of the series may be indicated by a right-hand superscript as P_n^M or R_n^M.

When $s = 1$, because of the equality of the sum of the + and − coefficients,

$$\sum_{M=-\infty}^{M=+\infty} {}_1P_n = \sum_{M=-\infty}^{M=+\infty} {}_1R_n = 0 \quad \text{and} \quad \sum_{M=p}^{M=q} {}_1P_n = \sum_{M=p}^{M=q} {}_1R_n = R_{n-1}^p - R_{n-1}^{q+1}. \tag{3}^*$$

The second relation of (3) is a form of the well-known solution for the sum of a finite number of terms of a series, the terms of which are + and the reciprocals of any number of factors in arithmetical progression, the *first* factors of the successive terms constituting the same arithmetical progression.

---

* The expressions throughout with asterisked numbers are arrived at when successive terms of ${}_sP_n$ with the assigned spacing are arrayed in successive horizontal lines and summed vertically.

When $s = 2$, because the $+$ and $-$ coefficients both sum to 2^{n-1},

$$\left.\begin{aligned} \sum_{M=-\infty}^{M=+\infty} {}_2P_n &= 2^{n-1}\sum_{M=-\infty}^{M=+\infty}\frac{(-1)^M}{a+Md} = 2^{n-1}S_D, \\ S_D &= 2^{1-n}\sum_{M=-\infty}^{M=+\infty} {}_2R_n = S_D^{\tau} \\ &= 2(\tfrac{1}{2}d)^n n!\sum_{M=-\infty}^{M=+\infty}\frac{1}{(a+2Md)(a+\overline{2M+1}\,.\,d)(a+\overline{2M+2}\,.\,d)\dots(a+\overline{2M+n}\,.\,d)}. \end{aligned}\right\} \quad (4)^*$$

$$\left.\begin{aligned} \text{Also}\quad S_D &= 2^{1-n}\sum_{M=-\infty}^{M=+\infty} {}_{-2}R_n = S_D^{\tau} \\ &= 2(\tfrac{1}{2}d)^n n!\sum_{M=-\infty}^{M=+\infty}\frac{-1}{(a+\overline{2M+1}\,.\,d)(a+\overline{2M+2}\,.\,d)\dots(a+\overline{2M+n+1}\,.\,d)}. \end{aligned}\right\} \quad (4a)$$

In this way the doubly infinite harmonic series with alternating signs, S_D, is transformed into the doubly infinite series S^{τ}, the terms of which are the reciprocals of any number $(n+1)$ of factors in arithmetical progression, the *first two* factors of the successive terms constituting the same arithmetical progression, multiplied by the constant $2(\frac{1}{2}d)^n n!$.

Applying the general expressions (4) and (4a) to the Leibnitz series, for which S_D is $\frac{1}{4}\pi$, the result is

$$\frac{\pi}{4\,.\,n!} = \sum_{M=-\infty}^{M=+\infty}\frac{1}{(4M+1)(4M+3)\dots(4M+2n+1)} \qquad (5)$$

$$(n = 0, 1, 2, 3, \dots, \infty),$$

$$= \sum_{M=-\infty}^{M=+\infty}\frac{-1}{(4M+3)(4M+5)\dots(4M+2n+3)} \qquad (5a)$$

$$(n = 0, 1, 2, 3, \dots, \infty).$$

Both forms with $n = 0$ reproduce the Leibnitz series, which thus appears as the first of an infinite number of the series denoted S_D^{τ}. With $n = 1$, the two forms (5) and (5a) give the Leibnitz series with pairs of successive $+$ and $-$, or $-$ and $+$ terms, respectively, combined. For (5), which may be regarded as the normal form, when n is odd, owing to the negative factors in the denominator occurring in pairs, all the terms are $+$, and two cases arise according as $\frac{1}{2}(n+1)$ is even or odd. For the first, there is a single central term for $M = -\frac{1}{4}(n+1)$, of the form $\dfrac{1}{(1\,.\,3\,.\,5\dots n)^2}$, the terms equidistant on either side being equal. For the second, the series divides into two identical series extending respectively from $M = -\frac{1}{4}(n-1)$ to $+\infty$, and from $M = -\frac{1}{4}(n+3)$ to $-\infty$. They are reformulized as (5*b*) and (5*c*):

$$\frac{\pi}{8\,.\,n!} = \frac{1}{2(1\,.\,3\,.\,5\,\ldots\,n)^2} + \sum_{M=-\frac{1}{4}(n-3)}^{M=+\infty} \frac{1}{(4M+1)(4M+3)\ldots(4M+2n+1)} \tag{5b}$$

$$(n = 3, 7, 11, \ldots, \infty),$$

$$\frac{\pi}{8\,.\,n!} = \sum_{M=-\frac{1}{4}(n-1)}^{M=+\infty} \frac{1}{(4M+1)(4M+3)\ldots(4M+2n+1)} \tag{5c}$$

$$(n = 1, 5, 9, \ldots, \infty).$$

For even values of n in (5) the terms are + from $-\frac{1}{2}n$ to $+\infty$, the others being negative, so that, when arranged in order of magnitude, after $\frac{1}{2}n+1$ + terms the signs alternate, the *first* factors of the successive terms then being in arithmetical progression. This is useful in computation in that the limit is approached from either side alternately, but otherwise they need no separate consideration because combination of successive + and − pairs gives the forms with the next higher (odd) values of n just reformulized. Before considering these new π series further a few other variants may be noted.

For odd values of n using form (5) when $\frac{1}{2}(n+1)$ is even and form (5*a*) when it is odd, and adjusting the value of M to make the denominators symmetrical, as is allowable since the summation is to ∞ in both directions, S_D^T becomes

$$\frac{\pi}{4\,.\,n!} = \sum_{M=-\infty}^{M=+\infty} \frac{(-1)^{\frac{1}{2}(n+1)}}{[16M^2-n^2][16M^2-(n-2)^2]\ldots[16M^2-1]} \tag{5d}$$

$$(n = 1, 3, 5, \ldots, \infty),$$

which may be combined with the easily derivable series

$$\frac{\pi}{3} = \sum_{M=-\infty}^{M=+\infty} \frac{1}{(16M^2-1)(4M^2-1)}$$

to give

$$\frac{\pi}{(n+2)\,n!} = \sum_{M=-\infty}^{M=+\infty} \frac{(-1)^{\frac{1}{2}(n+3)}}{[16M^2-n^2][16M^2-(n-2)^2]\ldots[16M^2-1][4M^2-1]} \tag{5e}$$

$$(n = 1, 3, 5, \ldots, \infty).$$

By removing the second, fifth and every subsequent third term from the Leibnitz series, which sum to $-\frac{1}{12}\pi$, there remains

$$\left.\begin{aligned} \frac{\pi}{3} = \sum_{M=-\infty}^{M=+\infty} \frac{(-1)^M}{6M+1} \quad &\text{or} \quad \sum_{M=-\infty}^{M=+\infty} \frac{(-1)^M}{6M+5} \\ &\text{or} \quad \sum_{M=0}^{M=+\infty} (-1)^M \left[\frac{1}{6M+1} + \frac{1}{6M+5}\right], \end{aligned}\right\} \tag{5f}$$

for which d is 6, and applying (4) gives

$$\frac{\pi}{2\,.\,3^{n+1}\,.\,n!}=\sum_{M=-\infty}^{M=+\infty}\frac{1}{(12M+1)(12M+7)\ldots(12M+6n+1)} \qquad (5g)$$

$$(n=1,2,3,\ldots,\infty).$$

A curiosity, got from the Leibnitz series by using the same device with $s=6$ for even values of n, is

$$\frac{\pi}{6}=\frac{2^n\,.\,n!}{2^{n-1}-1}\sum_{M=-\infty}^{M=+\infty}\frac{(-1)^{\frac{1}{2}n}}{(12M-n-3)(12M-n-1)\ldots(12M+n-3)} \qquad (5h)^*$$

$$(n=0,2,4,6,\ldots,\infty),$$

in which it is now the first *three* factors of the successive terms of alternating sign that are in the same arithmetical progression as the factors of each term, thus

$$\left.\begin{aligned}\frac{\pi}{48}&=\frac{1}{1\,.\,3\,.\,5}-\frac{1}{7\,.\,9\,.\,11}+\frac{1}{13\,.\,15\,.\,17}-\ldots;\\ \frac{7\pi}{2304}&=-\frac{1}{-1\,.\,1\,.\,3\,.\,5\,.\,7}+\frac{1}{5\,.\,7\,.\,9\,.\,11\,.\,13}-\frac{1}{11\,.\,13\,.\,15\,.\,17\,.\,19}+\ldots;\end{aligned}\right\} \qquad (5i)$$

and so on, the signs being alternating.

Lastly may be noted the form from (5) by summation also of n from 0 to ∞,

$$\frac{\pi e}{4}=\sum_{n=0}^{n=\infty}\sum_{M=-\infty}^{M=+\infty}\frac{1}{(4M+1)(4M+3)\ldots(4M+2n+1)}. \qquad (5j)$$

In the same way π/e is derived from $(5e)$, $\frac{1}{6}\{\pi(e^{\frac{1}{2}}-1)\}$ from $(5g)$, and from $(5h)$,

$$\tfrac{1}{24}[\pi(e-2e^{\frac{1}{2}}-2e^{-\frac{1}{2}}+e^{-1})].$$

The curious law of convergence for these π series may be illustrated for expression $(5c)$ with $n=9$:

$$\begin{aligned}&M=\quad -2\text{ and }-3 \qquad\qquad\qquad -1\text{ and }-4\\ &\frac{\pi}{8\,.\,9!}=\frac{1}{(1\,.\,3\,.\,5\,.\,7)^2\,.\,9\,.\,11}+\frac{1}{(1\,.\,3)^2\,.\,5\,.\,7\,.\,9\,.\,11\,.\,13\,.\,15}\\ &\qquad\qquad\qquad 0\text{ and }-5 \qquad\qquad 1\text{ and }-6 \qquad\qquad 2\text{ and }-7\\ &\qquad+\frac{1}{1\,.\,3\,.\,5\ldots17\,.\,19}+\frac{1}{5\,.\,7\ldots21\,.\,23}+\frac{1}{9\,.\,11\ldots25\,.\,27}+\ldots,\end{aligned} \qquad (6)$$

$$\text{Ratio }\frac{5\,.\,7}{13\,.\,15}=0{\cdot}18,\quad \frac{1\,.\,3}{17\,.\,19}=0{\cdot}0093,\quad \frac{1\,.\,3}{21\,.\,23}=0{\cdot}0062,\quad \frac{5\,.\,7}{25\,.\,27}=0{\cdot}052,$$

Values for π:

$$2{\cdot}65974026+0{\cdot}47738928+0{\cdot}00443396+0{\cdot}000027540+0{\cdot}00000143+\dots$$

$$3{\cdot}13712954 \quad 3{\cdot}14156350 \quad 3{\cdot}14159104 \quad 3{\cdot}14159247$$

Deficit at 5th term, one in $17{\cdot}5\times 10^6$. Remainder $0{\cdot}00000018\dots$.

Thus, even with quite moderate values of n, the first $\frac{1}{4}(n-1)$ doubled terms comprise nearly the whole sum. These are referred to as 'large terms' in contradistinction to the 'small terms' for the values of M from 0 to $+\infty$. The rate of convergence is at its maximum with this form for $M=1$, being $(1\,.\,3)/\{(2n+3)(2n+5)\}$, or $\frac{1}{160}$ with $n=9$, and it only reached $\frac{1}{2}$, the asymptotic limit of the Euler transformed series, when M, reckoned from $-\frac{1}{4}(n-1)$ as zero, is greater than $\sqrt{2}(n)$. For form (5*b*) the maximum convergence at $M=1$, $1/\{(2n+3)(2n+5)\}$ is three times greater. With large values of n the sum of the small terms is infinitesimal.

In a computation of π by (5*b*), $n=39$, the ten large terms (one central and nine double) of themselves gave the result correct to 11 places of decimals. The first small term added gave three more places, with five the result was correct to 22 places, with ten to 27 and with fifteen to 31 places. The method could not perhaps yet compete with those developed over centuries with the entirely special methods for this one constant from the geometry of the circle by which Shanks ultimately obtained a value for π correct to over 700 places of decimals, though that is perhaps a question of the number of digits that could be incorporated in a calculating machine. For large values of M, it compares unfavourably with the Euler transformed series, in that the asymptotic limit of its rate of convergence is zero, and, after M is greater than about $2n$, quicker computation would be got by increasing n rather than M. But the method is universally applicable to any harmonic series with alternating signs, including the S_S series for $\log_e 2$ and its derivatives, about to be considered, and is extremely powerful over any conceivably useful range.

When n is large, the computation is assisted by another method of summing the large terms, which is equally applicable to the S_S series, including that for $\log_e 2$. For these, owing to the summation starting at $M=0$, there is a deficiency, termed D_{n-2}, which is easy to evaluate, due to the numerators of the first $(n-1)$ terms (two less than the number of terms in P_n) not reaching the constant value 2^{n-1}:

$$\sum_{M=0}^{M=+\infty} {}_2P_n = 2^{n-1}\sum_{M=0}^{M=+\infty}\frac{(-1)^M}{a+Md} - D_{n-2} \quad \text{or} \quad 2^{n-1}[S_S - {}^0\Delta_{n-2}], \tag{7}$$

where for $2^{1-n}D_{n-2}$ is written ${}^0\Delta_{n-2}$, which will be called the deficiency term, the left-hand superscript being the value of M from which the summation starts, and the right-hand subscript denoting that the number of terms involved is two less than for P_n. The deficiency term may be evaluated as follows:

$$\begin{aligned} D_{n-2} &= 2^{n-1}.{}^0\Delta_{n-2} \\ &= \frac{C_0}{a} - \frac{C_1}{a+d} + \frac{C_2}{a+2d} - \ldots + \frac{(-1)^{n-3}C_{n-3}}{a+\overline{n-3}\,.d} + \frac{(-1)^{n-2}C_{n-2}}{a+\overline{n-2}\,.d}, \end{aligned} \qquad (8)^*$$

where $C_0, C_1, C_2, \ldots, C_{n-3}, C_{n-2}$ are a special set of numerators, called summate numerators, derived from the binomial coefficients as follows:

$$\begin{aligned} &C_0 = c_2+c_4+c_6+\ldots; \quad C_1 = c_3+c_5+c_7+\ldots; \\ &C_2 = c_4+c_6+c_8+\ldots; \quad C_3 = c_5+c_7+c_9+\ldots \quad \text{and so on,} \end{aligned} \qquad (9)$$

C_0 being $2^{n-1}-1$; C_1, $2^{n-1}-n$; …; C_{n-3}, n; and C_{n-2}, 1. The summate numerators are the same for all S_S series, and even when n is large are quickly computed. Hence

$$\begin{aligned} S_S^r &= {}^0\Delta_{n-2} \\ &\quad + 2(\tfrac{1}{2}d)^n.n!\sum_{M=0}^{M=+\infty}\frac{1}{(a+2Md)(a+\overline{2M+1}\,.d)\ldots(a+\overline{2M+n}\,.d)}, \end{aligned} \qquad (10)$$

$$\log_e 2 = {}^0\Delta'_{n-2} + 2^{1-n}.n!\sum_{M=0}^{M=+\infty}\frac{1}{(2M+1)(2M+2)\ldots(\overline{2M+n+1})}, \qquad (11)$$

$$\frac{\pi}{4} = {}^0\Delta''_{n-2} + 2n!\sum_{M=0}^{M=+\infty}\frac{1}{(4M+1)(4M+3)\ldots(4M+2n+1)}. \qquad (12)$$

Comparing (12) and (5)

$$\begin{aligned} {}^0\Delta''_{n-2} &= n!\left[\sum_{-\infty}^{+\infty}\frac{1}{(4M+1)(4M+3)\ldots(4M+2n+1)}\right. \\ &\qquad \left. -2\sum_{0}^{+\infty}\frac{1}{(4M+1)(4M+3)\ldots(4M+2n+1)}\right] \\ &= n!\sum_{M=-\frac{1}{2}(n-1)}^{M=-1}\frac{1}{(4M+1)(4M+3)\ldots(4M+2n+1)}, \end{aligned} \qquad (13)$$

because, with n odd, the set of terms from $M = 0$ to $+\infty$ is identical with the set from $-\frac{1}{2}(n+1)$ to $-\infty$. Hence the deficiency term is the sum of the large terms multiplied by $n!$.

Generally for any S_S^T series, D_{n-2} may also be written

$$\left.\begin{aligned} D_{n-2} = 2^{n-1}.{}^0\Delta_{n-2} &= {}^0P_{n-2}+2.{}^0P_{n-3}+2^2.{}^0P_{n-4}+2^3.{}^0P_{n-5}+\ldots+2^{n-2}.{}^0P_0 \\ \text{and}\qquad {}^0\Delta_{n-2} &= \frac{1}{2a}+\frac{d}{2^2a(a+d)}+\frac{2!\,d^2}{2^3a(a+d)(a+2d)}+\ldots \\ &\quad +\frac{(n-2)!\,d^{n-2}}{2^{n-1}a(a+d)(a+2d)\ldots(a+\overline{n-2}\,.\,d)} = \sum_{M=1}^{M=n-1} S_S^T. \end{aligned}\right\} \quad (14)^*$$

Thus the sum of the $\frac{1}{2}(n-1)$ large terms of S_D^T equals the sum of the first $(n-1)$ terms of the Euler transformed series S_S^T.

Applying (14) to expressions (11) and (12)

$$\log_e 2 = \sum_{M=1}^{M=(n-1)} \frac{1}{2^M M} + 2^{1-n}.n!\sum_{M=0}^{M=+\infty}\frac{1}{(2M+1)(2M+2)\ldots(2M+n+1)}, \quad (15)$$

$$\frac{\pi}{4} = \sum_{M=1}^{M=(n-1)}\frac{(M-1)!}{2(1.3\ldots\overline{2M-1})}$$

$$+2.n!\sum_{M=0}^{M=+\infty}\frac{1}{(4M+1)(4M+3)\ldots(4M+2n+1)}. \quad (16)$$

For (15) and (16) $n = 2, 3, \ldots, \infty$. These three different ways of computing the large terms are illustrated for $\frac{1}{4}\pi$, $n = 9$, the first being by summate numerators, the second by the Euler transformation, and the last by the direct method first described. When n is large the first is preferable to the third and both are shorter than the Euler method. It is perhaps noteworthy that the 'degree of evenness' of the numerator of the first expression within brackets reduced to a rational fraction is necessarily of the order of *twice* n:

$$2^{-8}\left[255-\frac{247}{3}+\frac{219}{5}-\frac{163}{7}+\frac{93}{9}-\frac{37}{11}+\frac{9}{13}-\frac{1}{15}\right] \quad \text{or} \quad 2^9\left[\frac{23}{7.11.13.15}\right]$$

$$=\frac{1}{2}+\frac{1}{6}+\frac{1}{15}+\frac{1}{35}+\frac{4}{315}+\frac{4}{693}+\frac{8}{3003}+\frac{8}{6435}$$

$$=\frac{2.9!}{(1.3.5.7)^2.9.11}+\frac{2.9!}{(1.3)^2.5.7.9.11.13.15}. \quad (17)$$

Finally, the general expression for the relation between the $\frac{1}{2}(n-1)$ large terms and the Euler series, independently of the a/d ratio so long as it is not a whole number, may be recorded, $n = 3, 5, 7, \ldots, \infty$.

$$2(\tfrac{1}{2}d)^n . n! \sum_{M=-\frac{1}{2}(n-1)}^{M=-1} \frac{1}{(a+2Md)(a+\overline{2M+1}.d)\ldots(a+\overline{2M+n}.d)}$$
$$= \sum_{M=1}^{M=(n-1)} \left[\frac{(M-1)!\,d^{M-1}}{2^M}\left\{\frac{1}{a(a+d)\ldots(a+\overline{M-1}.d)} - \frac{(-1)^{M-1}}{(a-d)(a-2d)\ldots(a-Md)}\right\}\right]$$
$$= \sum_{M=1}^{M=(n-1)} (S^T_S - S^T_{-S}) \quad \text{or} \quad \sum_{M=1}^{M=(n-1)} S^T_D. \tag{18}$$

All the terms of S^T_D are $+$, if $d > a$.

The stone-iron meteorites called pallasites: a synthetic study of their structure and probable mode of formation

By Lord Rayleigh, F.R.S.

(*Received* 16 *June* 1941—*Revised* 18 *July* 1941)

[Plates 41, 42]

Pallasites possess a remarkable structure of olivine, enclosed in a sponge or three-dimensional net of nickel iron. Structures which are more or less of this character are obtained in metallurgy, but pallasites cannot have originated in the same way, because the included olivine is less fusible than the metal, while iron slag is more fusible. The structure of the specimens figured can, however, be closely imitated by pouring molten alloy into a compact layer of stone fragments. The fragments used are angular or rounded, according to the character of the pallasite to be imitated.

Meteorites, as is well known, fall for the most part into two classes: those consisting mainly of iron, and those consisting mainly of stone. There is, however, an intermediate and much rarer class, of which less has been written. This consists of olivine in a three-dimensional net or sponge of iron. Such meteorites are known as pallasites, from the original example reported of iron from Asiatic Russia, by P. S. Pallas, in 1776.

Pallasites have been classed by Wadsworth (1884, pp. 75–83) with certain terrestrial rocks consisting of magnetite and olivine. The magnetite is considered as a secondary alteration of metallic iron, but, beyond the general resemblance of structure to the meteoric pallasites, no evidence of this is offered. The suggestion has not, so far as I am aware, been taken up by subsequent writers.

As regards the origin of pallasites, very little seems to have been written. Daubrée (1879) says that they resemble certain metallurgical products. Merrill (1902) considers that in the Admire pallasite described by him the iron is of later introduction than the olivine. He seems, if I understand him rightly, to think it probable that the iron has been reduced chemically in situ from lawrencite and troilite (1902, p. 11). The views of Goldschmidt (1922) will be referred to later. Paneth (1940, p. 18) considers that 'a complete mixture of the two phases iron and stone must have been a preliminary stage. There are many other proofs for the original molten state of iron meteorites, for instance the regularities in the distribution of rarer chemical elements between the iron, iron sulphide and stone phases can hardly be explained under any other assumption.'

One of the typical pallasites is that from Imilac in the desert of Atacama, Chile (Fletcher 1889, p. 243), of which there is a very large specimen in the British Museum. I purchased many years ago a specimen of this meteorite (see plate 41, no. I) which came from the collection of Mr James R. Gregory, of 88 Charlotte Street, Fitzroy Square, and have often looked at it and speculated how this curious structure could have come into existence. The simple difficulty which I felt was this—the material was evidently to be classed as an igneous rock; and if it had ever been in a state of fusion, why did it not separate into two layers, iron at the bottom and stone at the top? I considered, as Sorby (1864) and Goldschmidt (1922) had done earlier, whether it could have been formed under conditions where gravity was scarcely operative. But in such a case the interfaces would be controlled by surface tension, and the structure of my specimen at any rate did not suggest anything of the kind.

With regard to Daubrée's remark about similar structures obtained in metallurgical operations, I consulted Dr C. H. Desch, F.R.S., who suggested examining 'puddled ball', which is iron containing slag, and is produced at one stage in the manufacture of wrought iron.

He kindly procured a specimen for me. The amount of slag contained is usually small compared with what there is in the pallasites. However, on tentatively grinding flats with a carborundum wheel on a number of pieces, one was picked out which more nearly corresponded to these, and the flat surface, after smoothing with fine carborundum, was photographed, using a low-power microscopic objective. The photograph is reproduced, plate 41, no. II, with 13·5-fold magnification. It will be seen that this magnification brings the structure about up to the coarseness of the meteorite (no. I). Apart from the difference of scale, these structures have some points of resemblance, though the slag particles in the iron are less angular in outline than in the meteorite. It is to be remarked that the iron is worked into this form in a pasty condition, which explains why it does not separate into a distinct layer.

I have succeeded in producing a similar but much coarser structure using sodium as the metallic component, and paraffin wax as the non-metallic one. The sodium was melted, with a layer of molten paraffin above it, and when partially solidified it was vigorously stirred with an iron rod. On cooling, the mass could be exposed in sections by paring with a knife, and a structure very similar to no. II (plate 41) was obtained, but much coarser, nearly as coarse as the meteorite itself. This is reproduced in no. III, but it is not now thought to have any real bearing on the problem in hand. Paraffin wax is more fusible than sodium, while olivine is much less fusible than iron: thus the above process cannot well represent what happens in the formation of the meteorite. Similarly the slag contained in puddled iron is more fusible than iron, and this apparently comparable case is not really helpful.

The high melting-point of olivine was only realized (with disappointment) after I had spent a good deal of time on the problem. Bowen and Schairer (1935, p. 163) give the melting and solidifying points of various mixtures of Mg_2SiO_4 and Fe_2SiO_4 in the form of curves. These show the temperatures at which solidification begins and is complete as a function of the percentage of Fe_2SiO_4 in the initial mixture.

The olivine from the Pallas meteorite contains SiO_2 40·24 %, MgO 47·41 %, FeO 11·80 %. This is equivalent to 83 % Mg_2SiO_4 and 16·8 % Fe_2SiO_4. Such a composition should melt completely at 1840° C and solidify completely at 1690° C, according to Bowen and Schairer's curves. The melting-point of iron is 1530° C, and of the nickel iron of the meteorite no doubt somewhat less, so that there is an ample margin of certainty in saying that the nickel iron will melt at a temperature at which the olivine remains solid.

This being so, it is evidently possible to pour molten iron into a mass of olivine fragments without melting them, and the possibility is opened that the structure may have arisen thus.

It is a question for experiment how good an imitation of the pallasite can be made in this way. My laboratory is not equipped for casting iron and steel or for slicing hard materials, but it seemed that a satisfactory experiment could be made without this. Steatite was selected to represent the olivine, and plumber's solder to represent the iron. An iron mould was constructed (see figure 1) consisting of a slightly conical tube of 5 cm. diameter, with flat end-plates clamped on, and a small tube at the top for pouring. This was filled with angular fragments of steatite of various sizes, none of them much larger than a pea, and free from dust. The mould was heated so that the metal should not be prematurely chilled, and was filled up with the molten solder.

To exhibit the structure, the cylindrical mass was cut up into disks with a hack saw, and these were filed flat. It was found to be a very satisfactory copy of the structure of the meteorite, as may be seen by comparing the two halves of the composite photograph no. IV (plate 41), which shows how very similar are the shapes and mutual relations of the fragments as seen in section.

I conclude rather definitely therefore that the structure of the Imilac meteorite and others like it has arisen in the same way. In the experiment, the particles are prevented from floating up by being packed tight in the mould. In nature we may suppose that they are held by the pressure of superincumbent material.

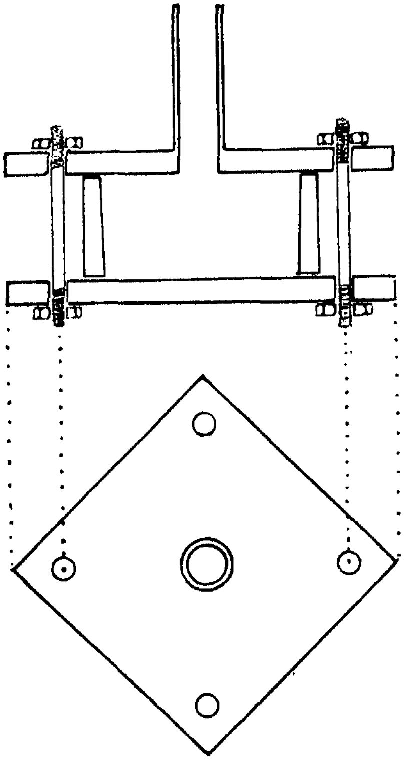

FIGURE 1

Fletcher (1896, p. 38) remarks that stony meteorites (he is not here speaking of pallasites) appear to be made up chiefly of irregular angular fragments, and that many of them resemble volcanic tuffs. According to the view here taken the pallasite structure has arisen in a similar way, angular fragments of olivine have become immersed in melted nickel iron, and in this way what may be called a breccia with a metallic cement has been formed.

There is no reason to doubt that the same result would be obtained with nickel-iron and olivine, and in this way artificial products almost or quite indistinguishable from the pallasite itself might be produced by an experimenter who had the necessary facilities. But it is doubtful whether much more would be learnt from this than from the present experiment.

The experiments of this paper were originally inspired by examining a single specimen of a pallasite—the only one conveniently accessible to me. I have since examined another like it—the Eagle Station pallasite—in the Mineralogical Department at Cambridge. My artificial imitation reproduces this as well or better than it reproduces Imilac. Most of the illustrations of pallasites which I have seen show very much the same structure; for example, the Brahin figured by Daubrée (1879) and one figured by Wadsworth (1884). Others are figured by Merrill (1916) from Ahumada, Chihuahua, Mexico, and from Admire, Lyon Co., Kansas, though no precise information as to scale is given. There appears to be no special reason for doubting that the conclusions drawn from the Imilac meteorite apply to these also.

Certain other pallasites, in particular the Brenham pallasite (Kunz 1890), no. V (plate 42) and the Springwater pallasite (Nininger 1932), no. VI (plate 42), left-hand half, contain rounded grains of olivine in nickel iron, some of them drop-like. A photograph of the Brenham pallasite is also given by V. M. Goldschmidt (1929), and he expresses the view that the rounded grains of olivine result from drops melted in situ, their shape being determined by surface tension in the absence of any strong gravitational field. I have been allowed to examine and photograph specimens of these meteorites in the British Museum (Natural History) and wish to thank Mr F. O. Bannister and Dr M. Hey for their kindness in giving me facilities under the present difficult conditions.

It must, I think, be admitted that most of these rounded olivine grains are very far from possessing the perfectly spherical form shown, e.g. by the oil drops suspended in a mixture of alcohol and water in Plateau's experiments. If all the sections were perfectly circular, that would no doubt prove that the grains were spherical. An occasional circular section does not prove that the grain in question is spherical, or even that it has a figure of revolution. Consider, for example, an ellipsoidal pebble, and many pebbles approximate to this. Two of the sections of an ellipsoid through the centre are circular, and any sections parallel to them are also circular.

It seemed worth while to try whether the structure of these meteorites could not be successfully imitated by the method used in the case of the

Imilac meteorite, substituting pebbles rounded by attrition for the angular fragments that were used in that case. Angular fragments of steatite of suitable size were mixed with steel hexagon nuts, and put in a box of elongated shape. This box was kept in slow rotation about one of its shorter axes, and the contents which only filled a fraction of it, fell to the opposite end every half-second. About an hour of this reduced the angular fragments of steatite to a rounded outline. These rounded pieces were packed into the mould as before. Molten solder was poured in, and the casting cut up into slices. One of these is shown in no. VI (plate 42), with the Springwater pallasite for comparison. It would seem that the essential features are fairly well reproduced in the experiment.

The extent to which the process of rounding the pebbles by attrition is carried is of course arbitrary, and it may be that it was not carried quite far enough to get the best imitation. My stock of steatite was used up, and several attempts to get more were unsuccessful. However, it was found that chalk was a fairly satisfactory substitute, and fragments of this were rounded by attrition until something like the ultimate approximately ellipsoidal form had been attained. Photograph no. VI (plate 42) shows a casting containing these. They were intentionally packed somewhat loosely in the mould, and the photograph shows how they may sometimes appear isolated in the section without apparent contact with their neighbours. The contacts are of course really in other planes than that of the section. Their resemblance to Plateau's suspended oil drops is illusory, and the same probably applies to apparently isolated drops in the meteorites. As might be expected, some of the sections are approximately circular.

A point worthy of attention is the distribution of the metal near the point of contact of two rounded grains or pebbles. Melted metals in general, as in the familiar case of mercury, do not wet stone surfaces. Thus the melted metal would not fill up the narrow spaces near the point of contact, and a neck characterized by the *absence* of metal would apparently join the two rounded pebbles, forming more or less of a dumbell shape. This neck would be originally a cavity, but in cutting the section it gets filled up with debris from the cutting operation. The expected appearance is found in the artificial castings (plate 42, nos. V and VI) and also in the meteorites (nos. V and VI).

It seems then that the two kinds of pallasites can both be imitated by these methods, using angular fragments for the one and rounded pebbles for the other. The conception of a general fusion of both metal and stone in the absence of a gravitational field* will certainly not help us in the case of the Imilac meteorite and others like it, because angular outlines would not be consistent with this mode of origin. It seems, therefore, better not to appeal to this hypothesis in the other case either, but to regard the one as a breccia and the other as a conglomerate, each with metallic cement.

My assistant, Mr R. Thompson, has given efficient help in these experiments.

REFERENCES

Bowen, N. L. and Schairer, J. F. 1935 *Amer. J. Sci.* **29**, 151–227.
Daubrée, A. 1879 *Études Synthétiques de Geologie Experimentale.* Paris.
Fletcher, L. 1889 *Mineral. Mag.* **8**, 223–264.
Fletcher, L. 1896 *Introduction to the Study of Meteorites.* London.
Goldschmidt, V. M. 1922 *Naturwissenschaften*, Heft 42, p. 2.
Goldschmidt, V. M. 1929 *Not. Proc. Roy. Instn*, **26**, 73–86.
Goldschmidt, V. M. 1929 *Stahl u. Eisen*, **49**, *Düsseldorf*, 601–612.
Kunz, G. F. 1890 *Amer. J. Sci.* **40**, 312–323.
Merrill, G. P. 1902 *Proc. U.S. Nat. Mus.* **24**.
Merrill, G. P. 1916 *Handbook and Descriptive Catalogue of the Meteorite Collections in the U.S. National Museum.* Washington.
Merrill, G. P. 1920 *Proc. U.S. Nat. Mus. Wash.* **57**, 97.
Nininger, H. H. 1932 *Amer. Min.* **17**, 396.
Paneth, F. A. 1940 *The Origin of Meteorites.* Halley Lecture. Oxford.
Sorby, H. C. 1864 *Rep. Brit. Ass.* p. 70.
Wadsworth, M. 1884 *Lithological Studies.* Cambridge, Mass.

DESCRIPTION OF PLATES 41, 42

I. Imilac meteorite (pallasite). The bright part is nickel iron, the dark part olivine. Actual size.

II. Puddled ball obtained in the manufacture of wrought iron. The bright part is iron, the dark part slag. × 13·5 diameters.

III. Aggregate obtained by stirring up sodium in course of solidification with paraffin wax. Sodium bright. Paraffin dark. Actual size.

---

* As a matter of scientific taste, most would probably prefer not to resort to the hypothesis that gravity was absent unless they were compelled. There appears to be positive evidence that, in some cases at least, meteorites have not acquired their present structure under the action of gravity. Merrill (1920), describing the Cumberland Falls Meteorite, considers that it is composed of detrital material which must have been deeply buried and compressed. 'This', he says, 'carries with it the supposition that the meteorite is but a sprawl from a very much larger mass....How large such a mass must be it is impossible to say, but that it must have been of planetary dimensions would seemingly be a safe assumption.'

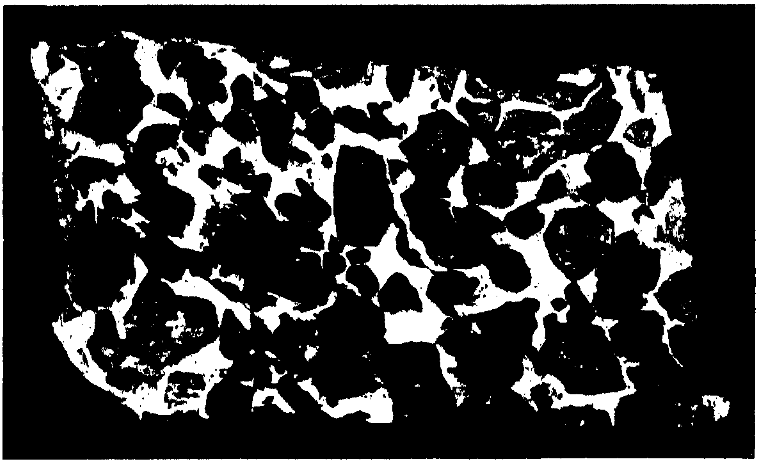

I

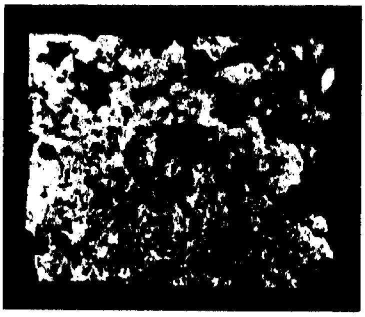

II

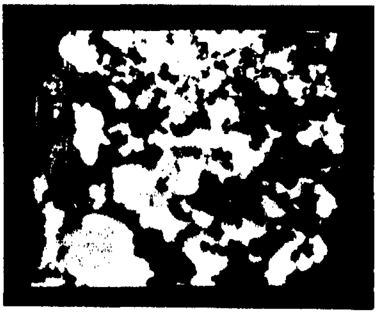

III

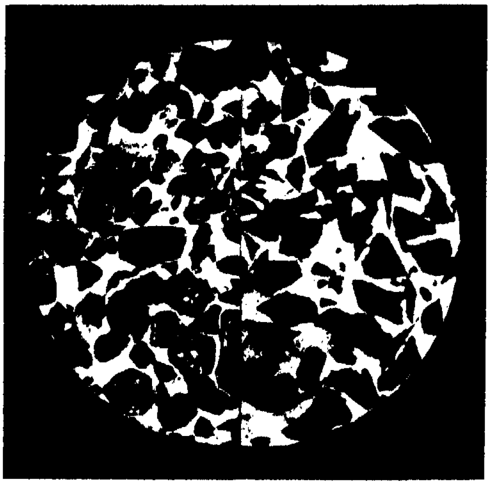

IV

(Facing p. 392)

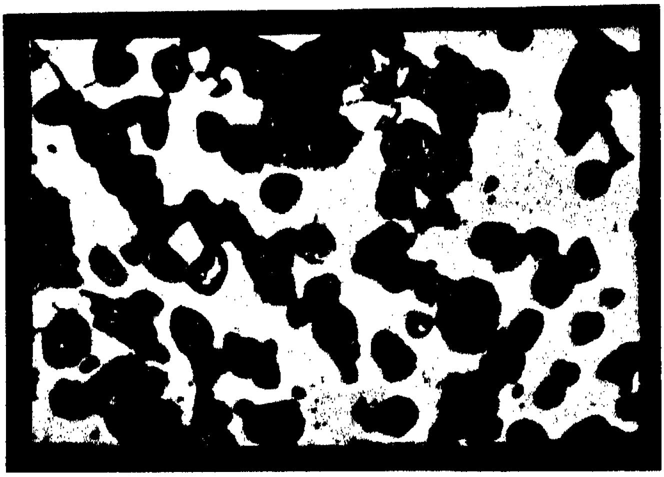

V

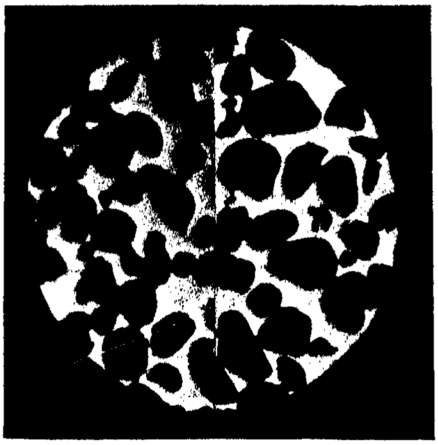

VI

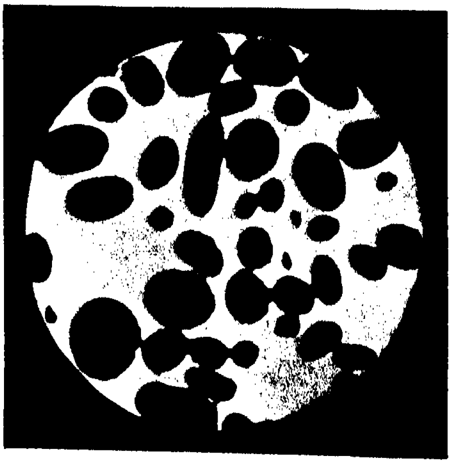

VII

IV. *Left-hand half.* Imilac meteorite $\frac{2}{3}$ actual size. *Right-hand half.* Artificial 'pallasite' structure, made by charging a mould with angular fragments of steatite and filling up with plumber's solder. Actual size.

V. Brenham pallasite. Actual size. From a specimen in the British Museum.

VI. *Left-hand half.* Springwater pallasite. Actual size. From a specimen in the British Museum. *Right-hand half.* Artificial 'pallasite' structure made by charging a mould with fragments of steatite rounded by attrition and filling up with plumber's solder. Actual size.

VII. Fragments of chalk rounded by prolonged attrition. In plumber's solder.

Interaction between adsorbed substances of simple constitution and insoluble monolayers. II

BY KENNETH G. A. PANKHURST

(*Communicated by N. K. Adam, F.R.S.—
Received* 14 *March* 1941—*Revised* 20 *June* 1941)

Penetration of monolayers of aliphatic substances and sterols, by aliphatic alcohols and acids of chain length from five to eight carbons, is similar to that by the four-carbon alcohol and acid except that it is much more powerful. *p*-Ethyl phenol penetrates much more than phenol. Each CH_2 group added to the hydrocarbon chain decreases the concentration required for equal penetration by a factor of about 4·5. The penetration is, with these substances, non-specific, resulting only in a disruption of the cohesion of the monolayer.

A single-wire surface balance, sensitive to 0·01 dyne/cm., is described.

The principal interaction between insoluble monolayers and solutions of phenol, butyric acid and butyl alcohol was shown by Adam, Askew and Pankhurst (1939) to consist in a non-specific penetration of the monolayer by the dissolved substance, with the disruption of its cohesion. There was also some displacement of the adsorbed molecules of the soluble substance from the surface, by the insoluble monolayer; but there was no evidence of any specific interaction between the polar groups of the soluble and insoluble substances. In this paper the work is extended to higher homologues of these soluble substances, fatty acids and alcohols up to eight carbon atoms and *p*-ethyl phenol.

RESULTS AND DISCUSSION

The interaction was similar to that previously found, but as would be expected the longer chain soluble molecules penetrate at much lower bulk concentrations and up to much higher surface pressures than do the lower homologues previously investigated. A much greater degree of cohesion in the monolayers can be disrupted with the eight-carbon than with the four-carbon penetrants.

Figures 1–4 show some typical results which should be compared with figures 1–7 of the previous paper. The 0·001 % solution of octyl alcohol has *greater penetrating power than even the* 0·3 % *solution* of butyl alcohol; 0·05 % *p*-ethyl phenol is more effective than 0·5 % phenol. Similar relations hold good for penetration into cholesterol and its ketone, coprostenone; and as before, coprostenone is more easily penetrated than cholesterol, probably because its molecules are considerably tilted in the monolayer, and there is less cohesion than in cholesterol. Table 1 indicates the extent to which the cohesion of the various monolayers is destroyed; a perfect gaseous film would have a pressure of 1 dyne/cm. at 400 sq. A and 4 dynes/cm. at 100 sq. A; in some cases the observed pressure approaches quite closely to these figures, showing that practically no cohesion remains in the film.

TABLE 1. SURFACE PRESSURES AT LARGE AREAS (20–22° C)

monolayer	area	N/50 HCl	*n*-amyl alcohol		*n*-hexyl alcohol	*sec.*-octyl alcohol		*n*-caprylic acid		*p*-ethyl phenol	
			0·05 %	0·10 %	0·03 %	0·001 %	0·003 %	0·001 %	0·003 %	0·05 %	0·10 %
lauric acid	100	(0·46)	(1·36)	(2·00)	(3·02)	1·83	4·53	2·42	3·48	—	—
	400	(0·29)	(0·47)	(0·90)	(0·52)	0·50	0·82	0·88	1·20	—	—
myristic acid	100	0·21	0·78	(1·42)	2·07	2·50	3·50	2·96	3·95	3·50	(1·60)
	400	0·18	0·73	(0·98)	1·01	0·32	0·99	0·95	0·95	1·15	(0·55)
palmitic acid	100	0·07	0·27	0·52	0·82	0·42	1·32	2·01	3·81	3·70	3·88
	400	0·04	0·13	0·31	0·30	0·38	0·47	0·35	1·16	0·86	0·94
behenic acid	100	0·05	0·14	0·30	0·33	0·37	0·98	1·57	2·20	0·60	1·01
	400	0·01	0·09	0·17	0·27	0·32	0·50	0·25	0·48	0·27	0·48
palmitonitrile	100	0·16	1·03	1·51	2·00	1·10	2·70	2·29	3·80	3·83	(1·95)
	400	0·16	0·31	0·57	0·54	0·57	0·95	0·57	1·60	0·58	(0·41)

Figures in parentheses indicate that some collapse or solution was taking place. These pressures are therefore less accurate and low.

Table 2 compares the penetration into monolayers of cholesterol and coprostenone. In all cases penetration is greater into that monolayer which has the smaller cohesion initially.

From the above results an estimate can be made of the concentrations in bulk solution, at which a substance of one chain length has a similar

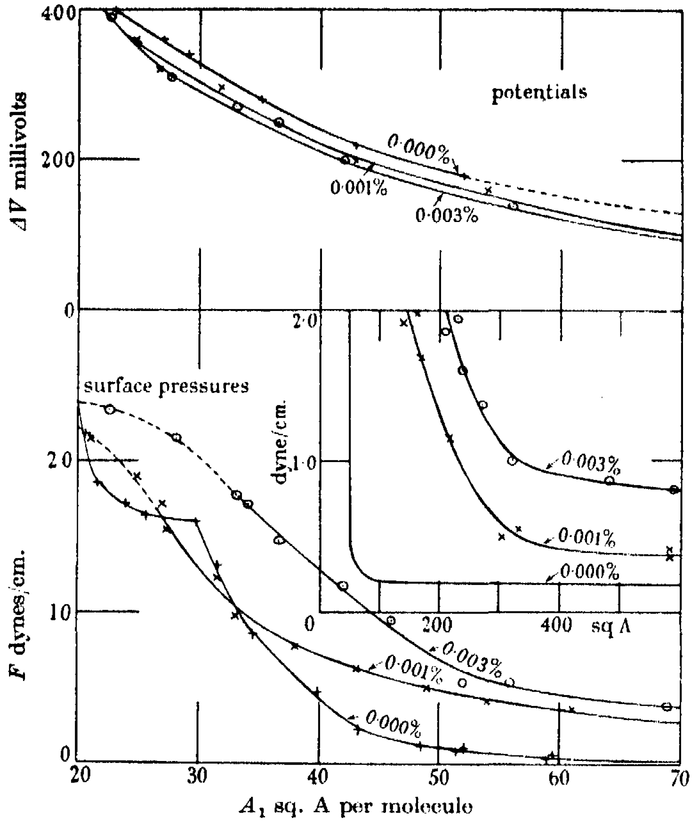

FIGURE 1. Myristic acid on *sec.*-octyl alcohol, 20–22° C.

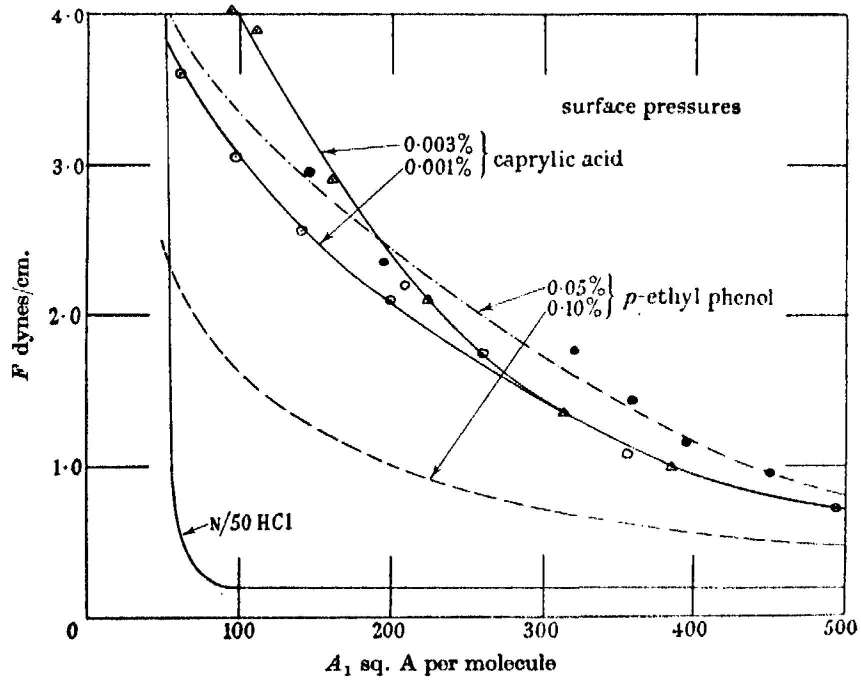

FIGURE 2. Myristic acid on *n*-caprylic acid (full lines) and *p*-ethyl phenol (broken lines), 20° C. —·— Stable film; ——— film collapsing.

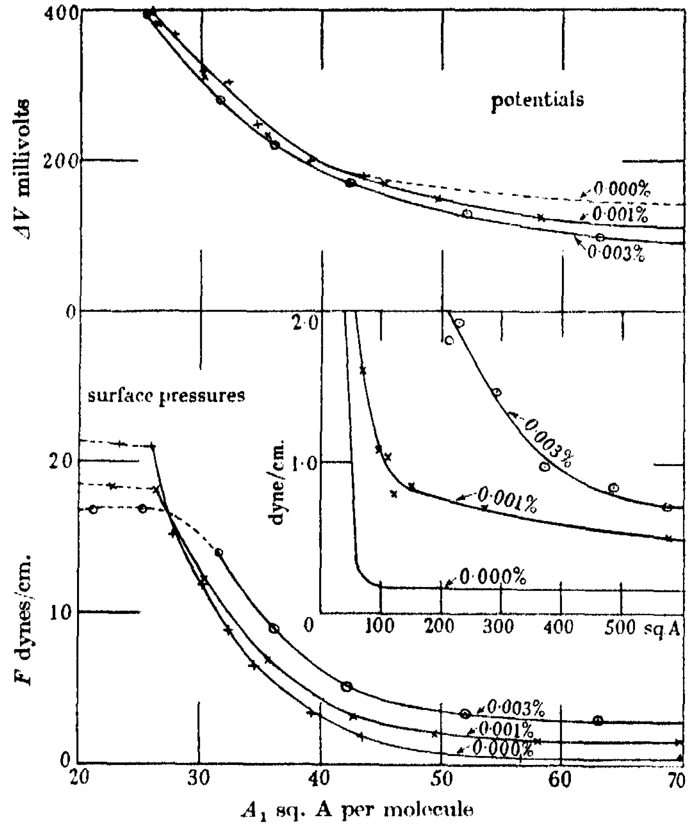

FIGURE 3. Palmitonitrile on *sec.*-octyl alcohol, 20–22° C.

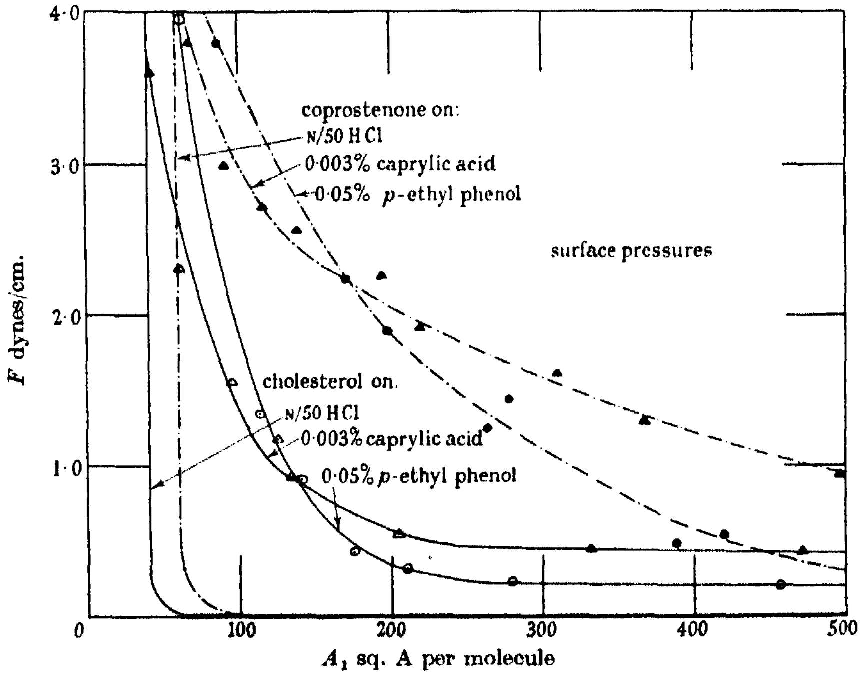

FIGURE 4. Cholesterol (full lines) and coprostenone (broken lines) on *n*-caprylic acid (triangles) and *p*-ethyl phenol (circles), 20° C.

penetrating effect to a higher or lower homologue differing in length of chain by several carbon atoms. Comparing myristic acid on butyl and octyl alcohols, 0·001 % octyl alcohol (M/13,000) penetrates more than 0·3 % butyl alcohol (M/24·7); the ratio of concentrations for equal penetration being of the order of 600 or possibly more. This gives, for the ratio of concentrations for the addition of only one carbon atom to the chain, a factor of about five. Traube's well-known rule states that for simple adsorption at a water-air surface, the factor is of the order of three. Langmuir (1917) showed that this factor indicates a decrease in free energy on adsorption of 640 cal./mole for each CH_2 group in the chain. The factor of five is unusually high and indicates a free-energy decrease in penetration of the order of 1000 cal./mole for each CH_2 group in the penetrant.

TABLE 2. SURFACE PRESSURES OF CHOLESTEROL AND COPROSTENONE ON SOLUTIONS OF *p*-ETHYL PHENOL AND CAPRYLIC ACID (20° C)

		N/50	*p*-ethyl phenol		caprylic acid	
monolayer	area	HCl	0·05 %	0·10 %	0·001 %	0·003 %
cholesterol	100	0·04	1·65	(1·10)	0·58	1·38
	400	0·02	0·21	(0·30)	0·14	0·45
coprostenone	100	0·02	3·55	—	1·65	2·90
	400	0·01	0·53	—	0·13	1·20

A survey of the remaining results in this paper and in Part I gives a mean value for the ratio of concentrations required to produce equal increases in surface pressure, by disruption of cohesion, of *ca.* 4·5, extremes varying from 3·7 to 6·2. A rough estimate of the concentrations of solution required to abolish fluctuations of surface potential found at areas greater than the limiting area of coherent films shows a ratio of 4·5–5·0 for each CH_2 added to the chain. The decrease of free energy when these simple molecules penetrate an insoluble monolayer thus appears to be definitely larger than when such molecules are adsorbed at an air-water surface, although the present experiments do not permit a close estimate of the difference to be made.

EXPERIMENTAL

The technique of surface pressure and surface potential measurement was the same in principle as in the previous paper, except that a single-wire torsion balance was used instead of a two-wire instrument for measuring surface pressures, the mirror indicating the position of the float being mounted on the torsion wire used for applying the force to the float.

Sensitivity to 0·01 dyne/cm., which is believed to be much greater than has hitherto been achieved with a balance of this type, was attained by attention to the following details. The horizontal torsion wire, 19·4 cm. long and 4·9 cm. above the surface of the water, carried the mirror and a light rigid framework with two prongs fitting slightly loosely through holes in the mica float. The float was connected to the sides of the trough by silk threads *lightly* paraffined or vaselined (Guastalla 1929). Using a phosphorbronze wire of 0·20 mm. diameter, the sensitivity was 0·20 dyne/cm./degree of twist of the torsion head; a wire of 0·11 mm. diameter gave 0·019 dyne/cm./degree. The wires could easily be changed, with a soldering iron, in a few minutes.

TABLE 3

solute	concentration %	ΔV mV	$-\Delta\gamma$ dynes/cm.
n-amyl alcohol	0·05	85	6·1
	0·10	113	8·2
n-hexyl alcohol	0·03	63	7·3
sec.-octyl alcohol	0·001	23	1·0
	0·003	67	6·5
n-caprylic acid	0·001	—	1·7
	0·003	—	6·9
p-ethyl phenol	0·05	—	10·6
	0·10	—	20·7

The alcohols and acids were purified until the boiling range was usually 2° C or less (caprylic acid and octyl alcohol, 3° C). *p*-Ethyl phenol, m.p. 45° C, was prepared by acetylation of anisole and reduction by the Clemmensen reaction, and purified by crystallisation from carefully distilled light petroleum (b.p. 40–60° C). The surface tensions of the solutions used as substrata were determined by the drop-volume method using a micrometer syringe (cf. Adam 1938, pp. 376–82) and their surface potentials by Sawai's method (1935) using a polonium air-electrode. Table 3 shows the results.

My thanks are due to Professor N. K. Adam, F.R.S. for his interest and valuable criticism and for supplying most of the pure long-chain compounds, to Dr C. Dorée and Dr V. A. Petrow who kindly provided the sterols, to Mr J. S. F. Gill for preparing the *p*-ethyl phenol, and to Mr G. W. Alliss who constructed the new surface pressure balance. Part of the cost of the apparatus was met by a grant from the Dixon Fund of the University of London.

REFERENCES

Adam, N. K. 1938 *The physics and chemistry of surfaces.* 2nd ed. Oxford.
Adam, N. K., Askew, F. A. and Pankhurst, K. G. A. 1939 *Proc. Roy. Soc.* **A, 170,** 485.
Guastalla, J. 1929 *C.R. Acad. Sci., Paris,* **189,** 241.
Langmuir, I. 1917 *J. Amer. Chem. Soc.* **39,** 1893.
Sawai, I. 1935 *Trans. Faraday Soc.* **31,** 765.

Structure and thermal properties associated with some hydrogen bonds in crystals

IV. Isotope effects in some acid phosphates

BY A. R. UBBELOHDE AND I. WOODWARD

(*Communicated by Sir William Bragg, F.R.S.—Received 4 April* 1941)

[Plate 43]

The isotope effect has been measured for $(NH_4)H_2PO_4$. Expansion of the crystal lattice takes place on substituting deuterium for hydrogen. The expansion is in the direction of the hydrogen bonds, and is of the same magnitude as in the isomorphous KH_2PO_4. A contraction of the lattice at right angles to the plane containing the hydrogen bonds is considerably larger for $(NH_4)H_2PO_4$ than for KH_2PO_4. From an application of the calculus of errors, the accuracy of the results is estimated to be

$$\alpha_{11} = +0{\cdot}00269 \pm 0{\cdot}00006, \quad \alpha_{33} = -0{\cdot}00123 \pm 0{\cdot}00009.$$

Further investigations on the monoclinic form of KD_2PO_4 has shown the presence of curious diffuse reflexions in moving-film photographs. Attempts to obtain $(NH_4)D_2PO_4$ or KH_2PO_4 in the monoclinic structure were unsuccessful.

In acid phosphates of the general formulae MH_2PO_4 and M_2HPO_4, it is possible to make comparatively small perturbations in the structure of crystals, both by varying the positive ion, and by substituting deuterium for hydrogen. As was described in previous publications, one effect of substituting deuterium for hydrogen in KH_2PO_4 is that the acid phosphate crystallizes spontaneously from solution in a new form (Ubbelohde and Woodward 1939; Ubbelohde 1939*b*). The tetragonal form of KD_2PO_4 could only be obtained by special nucleation, and when compared with the tetragonal form of KH_2PO_4 it showed an expansion of the crystal lattice in the direction of the deuterium bonds.

Experiments described in the present paper were carried out to obtain fresh information on the role of hydrogen bonds in determining the structure of acid phosphates. Preliminary information on the structure of the monoclinic form of KD_2PO_4 includes studies of intensities of X-ray reflexions, of pyro-electric properties, and of the curious streaks in moving-film X-ray photographs of single crystals. Further light on the occurrence of the monoclinic form of KD_2PO_4 was also obtained from experiments on the structure and isotope effects of $(NH_4)H_2PO_4$. Attempts to obtain the monoclinic forms of $(ND_4)D_2PO_4$ and of KH_2PO_4 were unsuccessful. The main conclusion from all these experiments is that in the acid phosphates the hydrogen bonds must make a contribution to the lattice structure such that quite different arrangements of atoms can have much the same stability and lattice free-energy. This may have an important bearing on the thermodynamical properties of the crystals.

THE ISOTOPE EFFECT FOR $(NH_4)H_2PO_4$

The monoclinic form of $(ND_4)D_2PO_4$. It was shown by Hassel (1925; cf. Wyckoff 1931) that $(NH_4)H_2PO_4$ is isomorphous with KH_2PO_4, and crystallizes in the tetragonal sphenoidal system, space group $D_{2d}^{12} - I\bar{4}2d$, $a = b = 7{\cdot}53$ A, $c = 7{\cdot}54$ A, with four molecules to the unit cell. If $(ND_4)D_2PO_4$ showed a behaviour similar to KD_2PO_4, and could be crystallized in both tetragonal and monoclinic forms, much information about the structure could be obtained by comparing intensities of X-ray reflexions in isomorphous potassium and ammonium salts. To test this possibility, $(ND_4)D_2PO_4$ was prepared by repeated crystallization of $(NH_4)H_2PO_4$ of analytical purity from D_2O. The final crystallizations were made from 99·6 % D_2O, so as to leave approximately this proportion of deuterium atoms in the product.

In contrast with the behaviour of KD_2PO_4, it was found that in all spontaneous crystallizations of $(ND_4)D_2PO_4$ from supersaturated solutions of varying concentration, only tetragonal crystals were obtained. A further attempt to obtain a monoclinic form of the ammonium salt was made by dropping freshly prepared nuclei of monoclinic KD_2PO_4 into supersaturated solutions of $(ND_4)D_2PO_4$ in 99·6 % D_2O. The crystals obtained could frequently be identified by their external habit, but in doubtful cases the crystal form was identified by taking X-ray rotation photographs. Only the tetragonal form was found. Even the small crystallites adhering firmly to the needle of monoclinic KD_2PO_4 were found to be tetragonal crystals of $(ND_4)D_2PO_4$, on examination with a low-power microscope. Preferred directions of growth of these crystallites, relative to the nucleating crystal, were evident on visual inspection, but could not be established with great precision. The c axis of the growths made an angle of about 20° with the (001) plane of the nucleating crystal.

The conclusion from these nucleation experiments is that $(ND_4)D_2PO_4$ shows far less tendency to crystallize in a monoclinic form than KD_2PO_4. The failure to obtain the ammonium crystals in a monoclinic form makes investigations of the structure of the potassium salt much more difficult.

The tetragonal form of $(ND_4)D_2PO_4$. Lattice spacings of the deuterium and hydrogen compounds were compared using a multiple exposure X-ray spectrometer (Ubbelohde 1939*a*). To minimize errors due to absorption, all the crystals used were of similar size and shape. Oscillation and some rotation photographs were taken with crystals mounted for both a and c axes, and unfiltered Cu K radiation from a gas tube was used so as to give β as well as α reflexions.

In a tetragonal crystal, the axes of the expansion ellipsoid coincide with the crystal axes, and are equal in the direction of the a and b axes. The expansion α' along a plane normally inclined at an angle ξ to the c axis is given by the simple expression

$$\alpha' = A + B\cos 2\xi,$$

where $$\alpha_{11} = \alpha_{22} = A - B, \quad \alpha_{33} = A + B.$$

Twelve such equations, each obtained from the mean of several independent measurements of α', were used to calculate the best values of A and B by the method of least squares. The best values were found to be

$$A = +0{\cdot}00073 \pm 0{\cdot}00005, \quad B = -0{\cdot}00196 \pm 0{\cdot}0006,$$

from which α_{11} and α_{33} can at once be calculated.

In view of present refinements in the theory of bond lengths in crystals, it is highly desirable to have a reliable estimate of the range of uncertainty attached to any experimental results. For actual bond lengths, such as that of hydrogen bonds as determined by Fourier methods, estimates of ranges of uncertainty present a problem not yet completely solved, owing to the fact that no systematic calculus of errors has been devised (Robertson and Woodward 1936; Brill, Hermann and Peters 1939; Robertson 1940). The magnitude of isotope effects can be determined with much greater precision than that of actual bond lengths, both on account of the fact that relative measurements are involved, and because a standard calculus of errors is directly applicable to the results (Whittaker and Robinson 1937). To apply this calculus to obtain the probable errors in the values of α_{11} and α_{33}, the original equations are preferably rewritten in the form

$$\alpha' = \alpha_{11}[1-\cos 2\xi]/2+\alpha_{33}[1+\cos 2\xi]/2.$$

Standard methods when applied to the twelve independent values of α' give

$$\alpha_{11} = +0{\cdot}00269 \pm 0{\cdot}00006, \quad \alpha_{33} = -0{\cdot}00123 \pm 0{\cdot}00009.$$

A plot of the smoothed curve showing expansion in different directions is given for comparison with the observed values of α' in figure 1, and a polar diagram showing the relation of the expansions to the approximate positions of the hydrogen bonds in the crystal is given in figure 2 (plate 43).

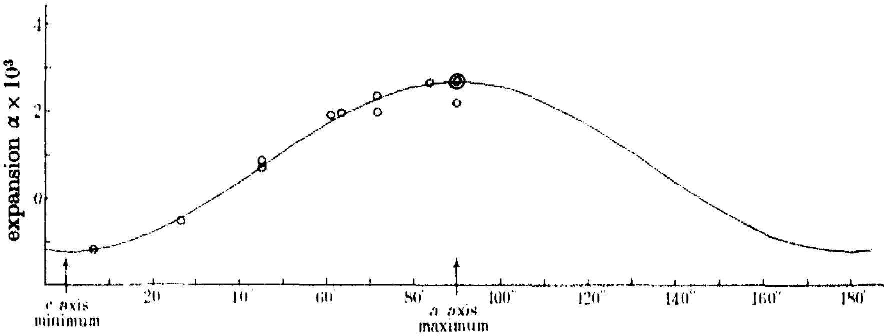

FIGURE 1. Lattice deformation (isotope effect, D for H) for $(NH_4)H_2PO_4$.

It will be noted that the isotope effect (D for H) in $(NH_4)H_2PO_4$ is closely similar in direction and magnitude to the effect in tetragonal KH_2PO_4. (An obvious misprint occurs in III, p. 422, but the correct figures are given in the adjoining diagram.) This makes it all the more puzzling that the monoclinic form of the ammonium salt has not yet been obtained. Further points are discussed below.

THE MONOCLINIC FORM OF KD_2PO_4

In addition to using the tests previously described (Ubbelohde 1939*b*), the chemical identity of the crystals was verified from direct phosphate analyses on a semi-micro scale, using single crystals whose monoclinic structure was previously established by X-ray rotation photographs. An average content of P_2O_5 found for the monoclinic crystals of KD_2PO_4 was 51·47 % (theory 51·64 %). Together with the molecular weight determination from the X-ray data, this evidence excludes any simple acid salt other than KD_2PO_4, and is probably as definite as can be obtained with comparatively small amounts of material. The fact that repeated crystallization from pure 99·6 % D_2O gave the same salt as crystallization from the original mother liquors is a further argument against any acid salt of composition other than KD_2PO_4. One or two tetragonal crystals were occasionally found amongst the mass of monoclinic crystals of KD_2PO_4 which separate from supersaturated solutions.

In order to minimize the effects of slow reversion to the tetragonal form (see below) X-ray studies were usually carried out with crystals separated from solution shortly before exposure.

The crystal axes as determined by rotation photographs were found to be (cf. Ubbelohde and Woodward 1939)

$$a = 7{\cdot}37 \pm 0{\cdot}01\,\text{A}, \quad b = 14{\cdot}73 \pm 0{\cdot}01\,\text{A}, \quad c = 7{\cdot}17 \pm 0{\cdot}01\,\text{A}; \quad \beta = 92^\circ.$$

It is estimated that any systematic errors in the above results are unlikely to exceed the order of magnitude of the random errors, which have been calculated according to standard methods, and are as indicated.

Moving-film rotation photographs of the zero layer lines for the three axes of monoclinic KD_2PO_4 show that the $(0k0)$ reflexion is halved when k is odd. (On a well-exposed film this was observed up to $k = 15$.) No other halvings are present, so that the space group is $C_2^2 - P2_1$. A notable feature of the $(hk0)$ zone is that the reflexions are very much stronger when h is even. The reflexions are particularly strong and uniform when $h = 2$, and are practically absent when $h = 1$.

On immersion into liquid air, the crystals develop a strong polarity in the direction of the b axis. A marked cleavage is exhibited parallel to the (001) face, and a less pronounced cleavage parallel to the (100). After immersion in liquid air the (001) cleavage is still more marked. The development of faces in the $(hk0)$ and $(0kl)$ zones is asymmetric, confirming the polarity of the crystal.

Reversion of monoclinic to tetragonal crystals

When finely powdered, the monoclinic form appears to revert to the tetragonal form of KD_2PO_4 within a few days. For larger crystals, reversion is slower. One specimen, with a, b, c approximately 0·6, 1·0, 2·4 mm., has been investigated with fixed and moving-film rotation photographs during a period of 14 months. Whilst there has been a growth of powder rings, and of splitting into small crystallites, the reflexions characteristic of the original crystal still persist. Certain reflexions, such as the (102), remain undivided and well defined during the change, whereas reflexions such as that corresponding to (200) show that splitting into crystallites takes place in preferred directions, in this instance with rotation about the *b* axis. The persistence of some small spacing planes is noteworthy, such as (70$\bar{2}$) and (60$\bar{4}$). Furthermore, inspection of another monoclinic crystal after 10 months exposure to the atmosphere, on a Hutchinson goniometer, showed that after this interval there was much diffuseness in the reflexion from the (100), but not from the (010) face. These and similar observations show that although a partial rearrangement of the atoms slowly takes place in the monoclinic crystals, the increased stability does not appear to be sufficient to lead to a very radical break up of the original structure.

DIFFUSE REFLEXIONS FROM FRESHLY PREPARED MONOCLINIC CRYSTALS

A remarkable feature of moving-film photographs of crystals of KD_2PO_4, even when freshly separated from solution, is the occurrence of diffuse reflexion streaks, whose intensity is comparable with that of the sharp reflexions (cf. figure 3, plate 43). To verify that these were not due to white radiation from the gas tube used (filtered Cu $K\alpha$ radiation), a standard crystal of oxalic acid dihydrate was mounted on the second spindle of a two-crystal moving-film spectrometer (Robertson 1934). Although the sharp reflexions from the oxalic acid were much more intense than those from the KD_2PO_4 exposed at the same time, there were practically no streaks connected with them. This showed that the phenomenon was not primarily connected with white radiation from the tube.

The streaks in KD_2PO_4 also showed characteristic differences for rotations about the three axes. For *c* axis rotations, streaks occurred in the sequence of moderately strong sharp reflexions. For example, the approximate centres of large spacing streaks corresponded with the weak or absent (*hk*0) reflexions with *h* odd. There was no obvious correlation between streaks and Bragg reflexions in rotations about the other axes. Special features illustrated in figure 3 (plate 43) are

(1) That streaks are frequently independent of any Bragg reflexions, as at (*a*).

(2) That the extension of streaks with decreasing Bragg angle is very variable; in (*b*) and (*c*) the streaks end at approximately $\theta = 6°$, whereas at (*d*) the streaks persist to the very edge of the film.

(3) In certain parts of the film streaks are grouped together in threes, with angular interval of about 7°.

Further comment on the diffuse reflexions is made below.

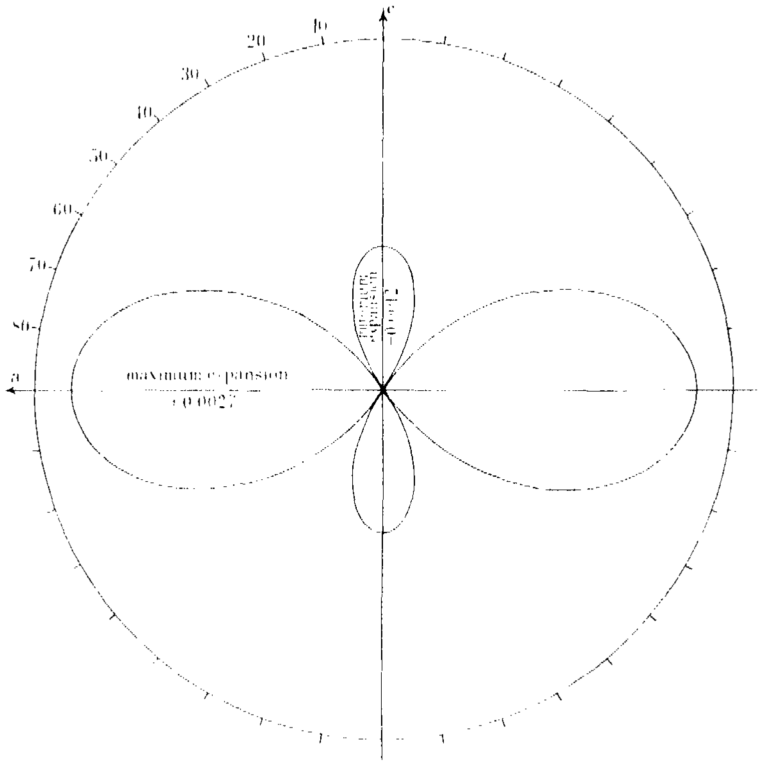

FIGURE 2. Isotope effect (D for H) in relation to hydrogen bond directions, which are within 2° or 3° of *a* axis.

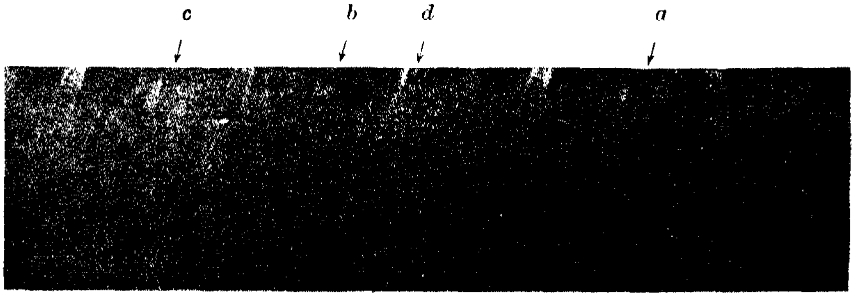

FIGURE 3. Diffuse reflexion streaks in moving film exposure of KD_2PO_4.

DISCUSSION

The main conclusions from the experiments are as follows:

(1) In $(NH_4)H_2PO_4$ the replacement of H by D leads to an expansion of the crystal, at right angles to the c axis.

Assuming that the hydrogen bonds lie nearly parallel to the (001) plane, as in the isomorphous KH_2PO_4, this implies that the hydrogen bonds expand on substituting deuterium. Within the experimental error, the expansion is the same as in KH_2PO_4, though the contraction at right angles is some three times as large in the ammonium salts.

By applying the calculus of errors, a comparatively high accuracy can be attained in the measurement of isotope effects.

(2) No definitive attempt can yet be made at calculating the detailed structure of monoclinic KD_2PO_4. This is partly due to lack of isomorphous salts, and partly to the streaks or diffuse reflexions which are a prominent feature in moving-film X-ray photographs of this salt. The high absorption coefficient ($\mu = 147$ per cm. for $\lambda = 1{\cdot}54$) imposed a further limitation on estimates of the absolute intensities of reflexion from single crystals. It may be noted that after assuming a model of the phosphate group, there are still 32 parameters to be adjusted in proposing a trial structure.

Tentative conclusions can, however, be drawn about the positions of the potassium atoms, since these are the dominating factors governing the intensity of the large spacing planes. The strength and uniformity of the $(0k0)$ series, when k is even, suggests that the potassium atoms lie near to planes parallel to (010), and a distance $\frac{1}{2}b$ apart. Inspection of the axial series, and the $(hk0)$ projection, suggests that the projections of the potassium atoms are displaced from the corners of rectangles, with edges $\frac{1}{2}a$, $\frac{1}{2}c$. The distance between adjacent potassium atoms is of the order 3·7 A.

(3) A comparison of $(NH_4)H_2PO_4$ with KH_2PO_4 suggests that the ammonium ion may have only a tetrahedral symmetry at the temperature investigated. This suggestion is of some interest in view of possible rotational transitions in the phosphates (cf. *Annual Reports* 1940). Thermal investigations are being carried out on these crystals, but in the meantime a brief summary may be given of the structural evidence.

From a detailed study of the structure of KH_2PO_4 (West 1930), it was concluded that the phosphate ion probably exhibited a slight distortion from tetrahedral symmetry. Each potassium atom was found to be surrounded by eight oxygen atoms, four at a distance of 2·79 A and four at a distance of 2·81 A. The shortest distance between oxygen atoms on neighbouring phosphate groups (i.e. the length of the hydrogen bond) was found to be 2·54 A. An alternative structure, with phosphate groups showing complete tetrahedral symmetry, was not in such good agreement with the experimental results. In this structure, the K—O distances were 2·82 A, and the length of the hydrogen bond 2·48 A.

When either of these phosphate groups is inserted into the lattice of $(NH_4)H_2PO_4$, placing the phosphorus and nitrogen atoms at positions corresponding with phosphorus and potassium atoms in KH_2PO_4, the following results are calculated:

H bond	distance (NH_4)—O
distorted phosphate ion 2·57 A	4 O atoms at 3·06 A 4 O atoms at 2·91 A
tetrahedral phosphate ion 2·53 A	4 O atoms at 3·13 A 4 O atoms at 2·89 A

Unlike the potassium ion, which is surrounded by eight oxygen atoms at practically equal distances, it will be seen that the ammonium ion appears to behave like a sphere deformed by tetrahedral bulges. Some uncertainty attaches to calculations of the greatest and least radii of this deformed sphere, but the difference of radii is estimated to lie between 0·15 and 0·24 A. The only way to avoid the conclusion that the ammonium ion behaves in this way is to equalize the (NH_4)—O distances, and this would involve a phosphate ion even more distorted than in West's model, and also an elongation of the hydrogen bond. From the close agreement in the magnitude of the isotope effect in the potassium and ammonium salts any great difference in the length of the hydrogen bond is unlikely.

The fact that the ammonium salt shows a markedly bigger contraction (cf. figure 2) at right angles to the directions of the hydrogen bonds, on replacing H by D, than was observed for tetragonal KH_2PO_4, is probably associated with the longer c axis and more open packing in this direction in the ammonium salt. This might lead to a larger Poisson contraction accompanying the expansion of the hydrogen bonds. In view of the precision with which isotope effects can be measured, a knowledge of the coefficients of elasticity of the phosphate crystals in various directions would be of value, and might lead to a direct estimate of the strength of the hydrogen bond.

Finally, attention may be drawn to the unsolved problem of the origin of the diffuse streaks in moving-film photographs of monoclinic KD_2PO_4. The possibility has not yet been completely eliminated that these are similar in origin to the diffuse spots observed for a variety of crystals when these are set up to give Laue reflexions (Preston 1939; W. H. Bragg 1940; Lonsdale, Knaggs and Smith 1940). With Cu K radiation, the fogging of the film was too extensive, on account of the high absorption of the crystals, to establish diffuse spots in Laue photographs of monoclinic KD_2PO_4, but they were readily obtained using molybdenum radiation from the 5 kW tube.

No complete correlation has yet been established between these diffuse spots and the streaks obtained in moving-film photographs, though the results emphasize the value of moving-film technique, in characterizing diffuse reflexions more completely than is possible from stationary photographs. An alternative possibility which is receiving attention is that the KD_2PO_4 crystals contain lattice imperfections which are essential for the stability of the monoclinic structure. If the single crystals were merely strained owing to their rapid separation from solution, and exhibited various types of slip, it would be difficult to explain why KH_2PO_4 does not show streaks in moving-film photographs in corresponding intensity, or alternatively, why KD_2PO_4 does not at once separate in the tetragonal unstrained form. Further discussion of the curious behaviour of KD_2PO_4 must await fresh experimental information.

Thanks are due to the Managers of the Royal Institution for the facilities provided, and to Mr H. Smith for his collaboration in some of the experiments.

References

Ann. Rep. Chem. Soc. 1940, p. 160.
Bragg, W. H. 1940 *Nature, Lond.*, **146**, 509.
Brill, Hermann and Peters 1939 *Naturwissenschaften*, p. 677.
Hassel 1925 *Z. Elektrochem.* **31**, 523.
Lonsdale, Knaggs and Smith 1940 *Nature, Lond.*, **146**, 332.
Preston 1939 *Proc. Roy. Soc.* A, **172**, 116.
Robertson 1934 *Phil. Mag.* **18**, 729.
Robertson 1940 *Trans. Faraday Soc.* **36**, 913.
Robertson and Woodward 1936 *J. Chem. Soc.* p. 1817.
Ubbelohde 1939*a* *J. Sci. Instrum.* **16**, 155.
Ubbelohde 1939*b* *Proc. Roy. Soc.* A, **173**, 417.
Ubbelohde and Woodward 1939 *Nature, Lond.*, **144**, 632.
West 1930 *Z. Kristallogr.* **174**, 306.
Whittaker and Robinson 1937 *Calculus of observations*. Blackie.
Wyckoff 1931 *Structure of crystals*. Chemical Catalog Company.

The statistical mechanics of many component gases

By K. Fuchs

The University of Edinburgh

(*Communicated by M. Born, F.R.S.—Received* 22 *May* 1941.—
Revised 5 *August* 1941)

The theory of condensing systems of J. E. Mayer is generalized for a mixture of an arbitrary number of gases.

Strict equations for chemical equilibrium in a mixture of gases are derived. For sufficiently small pressures they reduce to the law of mass action.

1. Introduction

The methods for the strict evaluation of the partition function of a gas as developed by Mayer and his collaborators (1937–40), by Born and Fuchs (1938) and by Uhlenbeck and Kahn (1938), have been applied by Mayer (1939) to the calculation of the partition of a mixture of two gases.

From the consideration of certain phenomena connected with the order-disorder transition in alloys, I was led to consider this problem for a system composed of an arbitrary number of gases. Since this problem is of interest by itself, I shall develop in this paper the theory without further reference to the problem which originally led to this investigation.

The theory is of particular interest in connexion with the problem of chemical equilibrium in a gas mixture; this problem could not be treated by means of the previous theories, since such a system contains at least three components; the two original substances and the compound formed by them. The strict law of chemical equilibrium is derived in the last section. For sufficiently small pressures it reduces to the well-known law of mass action.

The present investigation follows closely the calculations of Mayer (1939) for the two-component system and of Born and Fuchs (1938, in the following quoted as I) for the one-component system. In spite of the existence of these investigations the generalization for the many-component system requires a great deal of mathematical analysis, since for the most intricate parts of the calculation even the theory of the two-component system does not give any indication as to the results for the many-component system (e.g. the reduction of the cluster integrals to the irreducible cluster integrals).

2. The partition function

Consider a system composed of ρ different types of particles. Let N_i be the number of particles of type i ($i = 1, 2, \ldots, \rho$) and m_i their mass. Let $r_{ij}^{\alpha\beta}$ be the distance between the αth particle of type i and the βth particle of type j and $v_{ij}(r_{ij}^{\alpha\beta})$ the potential energy between them. Then the total potential energy is

$$E = \sum_{i=1}^{\rho} \sum_{j>i}^{\rho} \sum_{\alpha=1}^{N_i} \sum_{\beta=1}^{N_j} v_{ij}(r_{ij}^{\alpha\beta}) + \sum_{i=1}^{\rho} \sum_{\alpha=1}^{N_i} \sum_{\beta>\alpha}^{N_i} v_{ii}(r_{ii}^{\alpha\beta}). \tag{2·1}$$

The partition function is

$$Q = \prod_i \left(\frac{2\pi m_i kT}{h^2}\right)^{\frac{3}{2}N_i} Q_\tau, \tag{2·2}$$

where N is the total number of particles,

$$N = \sum_{i=1}^{\rho} N_i, \tag{2·3}$$

and Q_τ is defined by

$$Q_\tau = \frac{1}{\prod_{i=1}^{\rho} N_i!} \iint \ldots \int e^{-E/kT} \prod_{i=1}^{\rho} \prod_{\alpha=1}^{N_i} d\tau_{i\alpha}. \tag{2·4}$$

Here $d\tau_{i\alpha}$ is the volume element of the αth particle of type i.

Introduce $$f_{ij}^{\alpha\beta} = \exp\{-v_{ij}(r_{ij}^{\alpha\beta})/kT\} - 1 \tag{2·5}$$

and expand (2·4)

$$Q_\tau = \frac{1}{\prod_i N_i!} \iint \ldots \int [1 + \Sigma f_{ij}^{\alpha\beta} + \Sigma\Sigma f_{ij}^{\alpha\beta} f_{i'j'}^{\alpha'\beta'} + \ldots] \prod_i \prod_\alpha d\tau_{i\alpha}. \tag{2·6}$$

Here the summation is over all values i, j, α, β as shown explicitly in (2·1).

Each factor $f_{ij}^{\alpha\beta}$ will be referred to as a 'bond' between the two particles concerned. A 'cluster' of particles of size $(\mathbf{l}) = (l_1, l_2, \ldots, l_\rho)$ is a system of l_1 particles of type 1, l_2 particles of type 2, etc., each particle being directly or indirectly connected with every other particle of the cluster by means of bonds, but not connected with any particle outside the cluster. The cluster integral $b(\mathbf{l})$ connected with such a cluster is defined by*

$$Vb(\mathbf{l}) = \frac{1}{\prod_i l_i!} \Sigma \iint \ldots \int \Pi f_{ij}^{\alpha\beta} \prod_{i=1}^{\rho} \prod_{\alpha=1}^{l_i} d\tau_{i\alpha}, \tag{2·7}$$

---

* Throughout this paper letters in heavy type represent a set of numbers or variables.

where the sum extends over all products of different bonds $f_{ij}^{\alpha\beta}$ ($\alpha = 1, 2, \ldots, l_i$; $\beta = 1, 2, \ldots, l_j$) consistent with the definition of the cluster. V is the total volume; the factor V in (2·7) is introduced, since the integration over the co-ordinates of the 'last' particle gives a factor V.

The partition function can then be expressed as follows (cf. I, 1·7):

$$Q_r = \sum_{m(\mathbf{l})} \prod_{(\mathbf{l})} \frac{\{Nvb(\mathbf{l})\}^{m(\mathbf{l})}}{m(\mathbf{l})!}, \tag{2·8}$$

where the summation extends over all sets of values $m(\mathbf{l})$, which satisfy the condition

$$\sum_{(\mathbf{l})} l_i m(\mathbf{l}) = N_i, \tag{2·9}$$

and

$$v = V/N \tag{2·10}$$

is the volume per particle.

3. Reduction of the cluster integrals

By the definition of the cluster one may pass from one particle of a cluster to any other particle of the cluster by means of a sequence of bonds. In general there will be several different sequences. Now, it may be possible to divide the particles of the cluster into different groups, in such a way that one particular particle (the 'connecting' particle) must always be passed in order to pass from a particle of one group to a particle of a different group. The only exceptions are the connecting particles, which may be counted as belonging to two or more groups. This is illustrated in figure 1. The dots and crosses inside each ellipse represent one of these groups. They may be directly connected by means of a bond with any particle inside the same ellipse, but not with a particle outside. The ellipses overlap owing to the connecting particles denoted by crosses. Such bond configurations will be called 'reducible'. A configuration is irreducible only if we can pass from any particle to any other by means of at least two different sequences of bonds passing through two mutually exclusive sets of particles.

If there are ν_i particles of type i in such a cluster, it is called an irreducible cluster of size $(\boldsymbol{\nu}) = (\nu_1, \nu_2, \ldots, \nu_\rho)$. The corresponding irreducible cluster integral is defined by

$$VB(\boldsymbol{\nu}) = \frac{1}{\prod\limits_i \nu_i!} \sum \iint \cdots \int \prod f_{ij}^{\alpha\beta} \prod_{i=1}^{\rho} \prod_{\alpha=1}^{\nu_i} d\tau_{i\alpha}, \tag{3·1}$$

where the sum extends over all products of different bonds $f_{ij}^{\alpha\beta}$ ($\alpha = 1, 2, \ldots, \nu_i$; $\beta = 1, 2, \ldots, \nu_j$), which are consistent with the definition of the irreducible cluster. The definition (3·1) differs from that used in (I); it agrees with the definition used by Mayer (1939) for the two-component system.

Consider now a definite bond configuration of a cluster of size (l). It may be assumed without loss of generality that the first σ of the numbers l_i are greater than zero, and that the remaining l_i vanish. Then for the purposes of this section the indices i, j, k run from 1 to σ.

I now single out arbitrarily one particular particle—say the first particle of type 1. I next collect all the particles which belong to the same irreducible cluster as the first one. These particles (excluding the first) will be called an incomplete cluster. If it is of size ($\boldsymbol{\nu}$), it contains $\nu_1 - 1, \nu_2, \ldots, \nu_\sigma$ numbered particles of type 1, 2, etc. If this cluster is detached from the first particle, it has a free place for a particle of type 1, which I shall consider as an unnumbered particle of type 1. By identifying it with the first particle the incomplete cluster is 'attached' to the first particle. If the first particle is a connecting particle between several irreducible clusters, one obtains correspondingly at this first stage several incomplete clusters. This is illustrated in figure 1. The cross in the centre represents the first particle. Each fully drawn ellipse represents an irreducible cluster containing the first particle. The particles inside each of these ellipses, denoted by dots and crosses, with the exception of the first constitute the incomplete clusters.

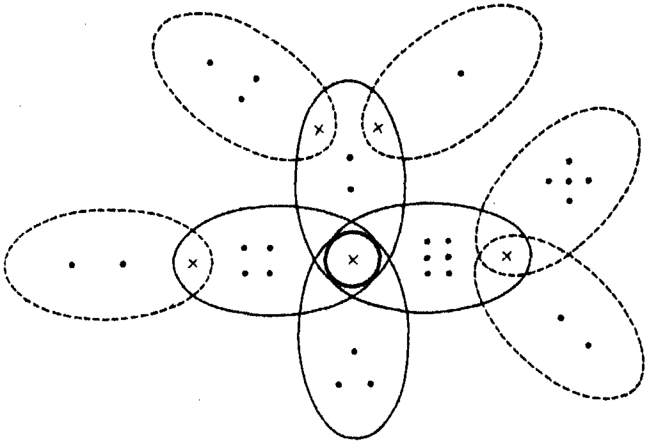

FIGURE 1. Reduction of the reducible clusters to irreducible clusters. Dots and crosses inside the same ellipse represent particles belonging to the same irreducible cluster. Crosses represent connecting particles between several irreducible clusters.

Among the particles collected at this first stage there will again be a number of connecting particles, denoted by crosses in the figure. I now treat these particles in the same way as the first particle, obtaining in this way another set of incomplete clusters, indicated by the ellipses with broken outlines. This procedure is continued, until all particles are assigned to the incomplete clusters. It will be noted that in this way not only the assignment of the particles to the incomplete clusters is uniquely determined, but also the unnumbered particle in each incomplete cluster, so that different sets of unnumbered particles lead to different bond configurations, provided of course we start always from the same first particle.

If I now integrate over the co-ordinates of the numbered particles of one of the last incomplete clusters, the result is independent of the co-ordinates of all the other particles. Proceeding step by step a number of factors are obtained, all independent of the position of the remaining particles. Summing over all bond configurations which are consistent with the splitting of the cluster into the given incomplete clusters, the product of the corresponding irreducible cluster integrals is found. Integration over the co-ordinates of the first particle finally gives the factor V which cancels against the corresponding factor in the definition (2·7) of the cluster integral $b(\mathbf{l})$.

If the unnumbered particle of an incomplete cluster is of type i, I shall call it a cluster of type i. Such a cluster contains

$$\nu_j - \delta_{ij} \quad \left(\delta_{ij} = \begin{cases} 1 & \text{if } i = j \\ 0 & \text{if } i \neq j \end{cases}\right)$$

numbered particles of type j. The first particle will also be referred to as a cluster of type 0 and of size $(\boldsymbol{\nu}^0)$, where

$$\nu_i^0 = \begin{cases} 1 & \text{if } i = 1, \\ 0 & \text{if } i \neq 1. \end{cases} \tag{3·2}$$

Let there be $\mu_i(\boldsymbol{\nu})$ incomplete clusters of type i and size $(\boldsymbol{\nu})$. Then the total number of particles of type i is

$$\nu_i^0 + \sum_j \sum_{(\boldsymbol{\nu})} (\nu_i - \delta_{ij})\,\mu_j(\boldsymbol{\nu}) = l_i. \tag{3·3}$$

If no distinction is made between clusters of the same type and same size, the $l_1 - \nu_1^0$ particles of type 1, the $l_2 - \nu_2^0$ particles of type 2, etc., can be distributed over the incomplete clusters in

$$\prod_i \left\{(l_i - \nu_i^0)!\prod_{(\boldsymbol{\nu})} \frac{\nu_i^{\mu_i(\boldsymbol{\nu})}}{\mu_i(\boldsymbol{\nu})!\,(\prod_j \nu_j!)^{\mu_i(\boldsymbol{\nu})}}\right\} = \frac{1}{l_1}\prod_i \left\{l_i!\prod_{(\boldsymbol{\nu})} \frac{\nu_i^{\mu_i(\boldsymbol{\nu})}}{\mu_i(\boldsymbol{\nu})!\,(\prod_j \nu_j!)^{\mu_i(\boldsymbol{\nu})}}\right\} \tag{3·4}$$

different ways.

Further let $p\{\mu_i(\boldsymbol{\nu})\}$ be the number of ways in which the incomplete clusters can be attached to each other so as to form a reducible cluster. Cancelling the factorials in the definition of the cluster integrals and the irreducible cluster integrals, it follows with (3·4) that $b(1)$ is given by

$$l_1 b(1) = \sum_{\mu_i(\boldsymbol{\nu})} p\{\mu_i(\boldsymbol{\nu})\} \prod_i \prod_{(\boldsymbol{\nu})} \frac{\{\nu_i B(\boldsymbol{\nu})\}^{\mu_i(\boldsymbol{\nu})}}{\mu_i(\boldsymbol{\nu})!}, \tag{3·5}$$

where the sum extends over all sets of numbers $\mu_i(\boldsymbol{\nu}) \geqslant 0$ compatible with the condition (3·3).

Let now m_i be the total number of clusters of type i. It follows that

$$m_i = \sum_{(\boldsymbol{\nu})} \mu_i(\boldsymbol{\nu}). \tag{3·6}$$

Arrange the clusters in any order and number them by two indices: An index i, j denoting the type of the cluster and an index $\alpha, \beta = 1, 2, \ldots, m_i$ denoting the particular cluster of the given type. Thus $\nu_i^{j\alpha}$ is the number of particles of type i of the αth cluster of type j. Then

$$\sum_{\alpha=1}^{m_j} (\nu_i^{j\alpha} - \delta_{ij}) = \sum_{(\boldsymbol{\nu})} (\nu_i - \delta_{ij})\, \mu_j(\boldsymbol{\nu}). \tag{3·7}$$

Consequently (3·3) may be written in the form

$$\nu_i^0 + \sum_{j=1}^{\sigma} \sum_{\alpha=1}^{m_j} (\nu_i^{j\alpha} - \delta_{ij}) = l_i. \tag{3·8}$$

If now a cluster $(\boldsymbol{\nu}^{i\alpha})$ is attached to a cluster $(\boldsymbol{\nu}^{j\beta})$, this can be done by identifying the unnumbered particle of the former with any one of the numbered particles of type i of the latter, i.e. in $\nu_i^{j\beta} - \delta_{ij}$ different ways. If the cluster is attached to the cluster $(\boldsymbol{\nu}^0)$, this can be done in ν_i^0 different ways.

Any definite way of attaching the incomplete clusters to each other, irrespective of the particular numbered particle used for the purpose, is here called a 'pattern' of the irreducible clusters. Such a pattern can be characterized by the numbers $n_i^{j\alpha}$ of clusters of type i attached to the cluster $(\boldsymbol{\nu}^{j\alpha})$ and the number n_i^0 attached to $(\boldsymbol{\nu}^0)$. Then the number of ways of attaching the clusters so as to give the given pattern is

$$\prod_i \left\{ {\nu_i^0}^{n_i^0} \prod_j \prod_\alpha (\nu_i^{j\alpha} - \delta_{ij})^{n_i^{j\alpha}} \right\}. \tag{3·9}$$

Let further $q(n_i^0, n_i^{j\alpha})$ be the number of different patterns which are characterized by the same numbers n_i^0, $n_i^{j\alpha}$. Then $p\{\mu_i(\boldsymbol{\nu})\}$ is given by

$$p\{\mu_i(\boldsymbol{\nu})\} = \sum_{n_i^0,\, n_i^{j\alpha}} q(n_i^0, n_i^{j\alpha}) \prod_i \left\{ {\nu_i^0}^{n_i^0} \prod_j \prod_\alpha (\nu_i^{j\alpha} - \delta_{ij})^{n_i^{j\alpha}} \right\}. \tag{3·10}$$

Here the summation goes over all sets of integers n_i^0, $n_i^{j\alpha} \geqslant 0$ subject to the following conditions:

$$n_i^0 + \sum_j \sum_\alpha n_i^{j\alpha} = m_i, \tag{3·11}$$

$$\sum_i n_i^0 \geqslant 1, \tag{3·12}$$

$$\sum_\alpha n_i^{i\alpha} < m_i. \tag{3·13}$$

The first of these arises because there are m_i clusters of type i to be attached, the second because at least one cluster must be attached to the cluster $(\mathbf{v}^0)$, and the third because the m_i clusters of type i cannot be attached exclusively among each other, but at least one of them must be attached to a cluster of a different type.

In calculating q one must distinguish those indices i for which m_i vanishes. Assume that m_i is positive for i smaller or equal to τ and that it vanishes for i greater than τ. I shall prove that

$$q(n_i^0, n_i^{j\alpha}) = \left| m_i \delta_{ij} - \sum_\alpha n_i^{j\alpha} \right|_\tau \prod_{i=1}^{\tau} \frac{(m_i - 1)!}{n_i^0! \prod_j \prod_\alpha n_i^{j\alpha}!}, \tag{3·14}$$

where the first factor represents the determinant with the term $m_i \delta_{ij} - \sum_\alpha n_i^{j\alpha}$ in the ith row and jth column, and the index τ signifies that the indices i, j run from 1 to τ.

I first prove (3·14) for the special case $m_1 = 1$, $m_2 = m_3 = \ldots = m_\rho = 0$. In this case there is only one cluster, which must be attached to the cluster $(\mathbf{v}^0)$, so that $q = 1$. Furthermore, $n_1^0 = 1$ and all other n_i^0, $n_i^{j\alpha}$ vanish. Since τ is equal to 1, it follows easily that in this case (3·14) gives indeed the value $q = 1$.

I now proceed by induction. Owing to (3·11) and (3·12) there exists at least one cluster (the cluster attached last) which has no cluster attached to it. Let the γth cluster of type k be such a cluster so that

$$n_1^{k\gamma} = n_2^{k\gamma} = \ldots = n_\tau^{k\gamma} = 0. \tag{3·15}$$

I now assume (3·14) has been proved for a set of values m_i' given by

$$m_i' = \begin{cases} m_i - 1 & \text{if } i = k, \\ m_i & \text{if } i \neq k. \end{cases} \tag{3·16}$$

Consider all patterns of the m_i clusters in which the cluster $(\mathbf{v}^{k\gamma})$ is attached to the cluster $(\mathbf{v}^{k'\beta})$, and which belong to the given set of numbers n_i^0, $n_i^{j\alpha}$.

If the cluster $(\mathbf{v}^{k\gamma})$ is detached, one obtains all patterns of the m'_i clusters belonging to a set of numbers

$$n'^0_i = n^0_i, \quad n'^{j\alpha}_i = \begin{cases} n^{j\alpha}_i - 1 & \text{if } j = k', \alpha = \beta, i = k, \\ n^{j\alpha}_i & \text{otherwise.} \end{cases}$$

According to (3·14) the number of such patterns is given by

$$\left| m'_i \delta_{ij} - \sum_\alpha n'^{j\alpha}_i \right|_\tau \prod_i \frac{(m'_i - 1)!}{n'^0_i! \prod\limits_{j,\alpha} n'^{j\alpha}_i!} = \left| m'_i \delta_{ij} - \sum_\alpha n'^{j\alpha}_i \right|_\tau \prod_i \frac{(m_i - 1)!}{n^0_i! \prod\limits_{j,\alpha} n^{j\alpha}_i!} \frac{n^{k'\beta}_k}{m_k - 1}. \tag{3·17}$$

Here the sum and product over j, α does not include the term $\alpha = \gamma$, $j = k$. But, in view of (3·15), there is no error in including this term. It should be noted that the second form of equation (3·17) also holds if $n^{k'\beta}_k = 0$.

Similar expressions are obtained if the cluster $(\mathbf{v}^{k\gamma})$ is attached to any other cluster or to the cluster $(\mathbf{v}^0)$. Summing over all expressions, the total number of patterns is found to be

$$q(n^0_i, n^{j\alpha}_i) = \frac{1}{m_k - 1} \left\{ \sum_{k',\beta} \left| m'_i \delta_{ij} - \sum_\alpha n'^{j\alpha}_i \right|_\tau n^{k'\beta}_k \right.$$
$$\left. + \left| m'_i \delta_{ij} - \sum_\alpha n^{j\alpha}_i \right|_\tau n^0_k \right\} \prod_i \frac{(m_i - 1)!}{n^0_i! \prod\limits_{j,\alpha} n^{j\alpha}_i!}.$$

Expanding the determinant with respect to the kth row and denoting the sub-determinants by upper indices, it is found that

$$q(n^0_i, n^{j\alpha}_i) = \frac{1}{m_k - 1} \sum_j \| |^{kj}_\tau \left[n^0_k \left\{ (m_k - 1)\delta_{kj} - \sum_\alpha n^{j\alpha}_k \right\} \right.$$
$$\left. + \sum_{k',\beta} n^{k'\beta}_k \left\{ (m_k - 1)\delta_{kj} - \sum_\alpha (n^{j\alpha}_k - \delta_{jk'}\delta_{\alpha\beta}) \right\} \right] \prod_i \frac{(m_i - 1)!}{n^0_i! \prod\limits_{j,\alpha} n^{j\alpha}_i!}$$
$$= \sum_j \| |^{kj}_\tau \left[\left\{ n^0_k + \sum_{k',\beta} n^{k'\beta}_k \right\} \left\{ \delta_{kj} - \frac{1}{m_k - 1} \sum_\alpha n^{j\alpha}_k \right\} + \frac{1}{m_k - 1} \sum_\alpha n^{j\alpha}_k \right] \prod_i \frac{(m_i - 1)!}{n^0_i! \prod\limits_{j,\alpha} n^{j\alpha}_i!};$$

with (3·11) this gives

$$q(n^0_i, n^{j\alpha}_i) = \sum_j \| |^{kj}_\tau \left\{ m_k \delta_{kj} - \sum_\alpha n^{j\alpha}_k \right\} \prod_i \frac{(m_i - 1)!}{n^0_i! \prod\limits_{j,\alpha} n^{j\alpha}_i!}$$

which is the expansion of (3·14) with respect to the kth row.

Particular attention must be paid to the case that $m_k = 1$. As (3·14) does not depend on the order of the indices, it may be assumed that $k = \tau$. There is then only one cluster of type $k = \tau$ and (3·15) implies the equations

$$\sum_{\alpha=1}^{m_\tau} n_1^{\tau\alpha} = \sum_\alpha n_2^{\tau\alpha} = \ldots = \sum_\alpha n_\tau^{\tau\alpha} = 0. \qquad (3{\cdot}18)$$

Furthermore, it follows from (3·11) that all numbers n_τ^0, $n_\tau^{j\alpha}$ vanish, except one which is equal to unity, say $n_\tau^{k'\beta} = 1$. The cluster $(\nu^{\tau\gamma})$ must therefore be attached to the cluster $(\nu^{k'\beta})$, and consequently the number of patterns of the m_i clusters is the same as the number of patterns of the m_i' clusters. It is therefore necessary to prove that in this particular case

$$\left| m_i\delta_{ij} - \sum_\alpha n_i^{j\alpha} \right|_\tau \prod_{i=1}^{\tau} \frac{(m_i-1)!}{n_i^0!\prod\limits_{j,\alpha} n_i^{j\alpha}!} = \left| m_i\delta_{ij} - \sum_\alpha n_i^{j\alpha} \right|_{\tau-1} \prod_{i=1}^{\tau-1} \frac{(m_i-1)!}{n_i^0!\prod\limits_{j,\alpha} n_i^{j\alpha}!}.$$

All elements of the τth column of the determinant on the left-hand side vanish, except the diagonal element, in view of (3·18). The diagonal element is equal to $m_\tau = 1$. Therefore the determinants on the right- and left-hand sides are identical. Similarly, the products on both sides are identical, since they differ only by factors $0!$ and $1!$.

Since any set of numbers n_i^0, $n_i^{j\alpha}$ can be reached by a succession of such steps, it follows that the equation (3·14) is proved.

Let us consider finally the forbidden cases (3·12) and (3·13). If (3·13) is violated for an index $i = k$, it follows from (3·11) that

$$n_i^0 = n_i^{j\alpha} = 0 \quad \text{for } i = k,\ j \neq i,$$

and consequently $$m_i\delta_{ij} - \sum_\alpha n_i^{j\alpha} = 0 \quad \text{for } i = k.$$

Therefore the determinant in (3·14) has only zero elements in the kth row and it vanishes.

If (3·12) is violated, (3·11) may be written in the form

$$\sum_j \left\{ m_i\delta_{ij} - \sum_\alpha n_i^{j\alpha} \right\} = 0,$$

which constitutes a linear relation between the rows of the determinant (3·14). Consequently, it vanishes again.

Thus the two cases excluded by (3·12) and (3·13) give no contributions and these conditions may therefore be disregarded.

We now insert (3·14) into (3·10):

$$p(\mu_i(\boldsymbol{\nu})) = \sum_{n_i^0,\, n_i^{j\alpha}} \left| m_i\delta_{ij} - \sum_{\alpha} n_i^{j\alpha} \right|_{\tau} \prod_{i=1}^{\tau} (m_i-1)!\,\frac{\nu_i^{0\,n_i^0}}{n_i^0!} \prod_{j,\alpha} \frac{(\nu_i^{j\alpha}-\delta_{ij})^{n_i^{j\alpha}}}{n_i^{j\alpha}!}.$$

This may also be written in the form

$$p(\mu_i(\boldsymbol{\nu})) = \left| \delta_{ij} - \frac{1}{m_i}\sum_{\alpha} (\nu_i^{j\alpha}-\delta_{ij})\frac{\partial}{\partial \nu_i^{j\alpha}} \right|_{\tau} \sum_{n_i^0,\, n_i^{j\alpha}} \prod_{i} m_i!\,\frac{\nu_i^{0\,n_i^0}}{n_i^0!} \prod_{j,\alpha} \frac{(\nu_i^{j\alpha}-\delta_{ij})^{n_i^{j\alpha}}}{n_i^{j\alpha}!}.$$

The summation, subject to the condition (3·11), can be carried out and gives

$$p(\mu_i(\boldsymbol{\nu})) = \left| \delta_{ij} - \frac{1}{m_i}\sum_{\alpha} (\nu_i^{j\alpha}-\delta_{ij})\frac{\partial}{\partial \nu_i^{j\alpha}} \right|_{\tau} \prod_{i} \left\{ \nu_i^0 + \sum_{j,\alpha} (\nu_i^{j\alpha}-\delta_{ij}) \right\}^{m_i}.$$

After completing the differentiation we may substitute according to (3·6), (3·7), (3·8) and find

$$p(\mu_i(\boldsymbol{\nu})) = \left| \delta_{ij} - \frac{1}{l_j}\sum_{(\boldsymbol{\nu})} (\nu_i-\delta_{ij})\,\mu_j(\boldsymbol{\nu}) \right|_{\tau} \prod_{i=1}^{\tau} l_i^{\sum\limits_{(\boldsymbol{\nu})}\mu_i(\boldsymbol{\nu})}. \tag{3·19}$$

We shall now prove that this expression is identical with

$$p(\mu_i(\boldsymbol{\nu})) = \left| \delta_{ij} - \frac{1}{l_j}\sum_{(\boldsymbol{\nu})} (\nu_i-\delta_{ij})\,\mu_j(\boldsymbol{\nu}) \right|_{\sigma} \prod_{i=1}^{\sigma} l_i^{\sum\limits_{(\boldsymbol{\nu})}\mu_i(\boldsymbol{\nu})}. \tag{3·20}$$

Remembering that $\sum\limits_{(\boldsymbol{\nu})}\mu_i(\boldsymbol{\nu}) = 0$ for $\tau < i \leqslant \sigma$, it follows that the columns $\tau < i \leqslant \sigma$ of the determinant (3·20) contain only zero elements, with the exception of the diagonal elements, which are equal to unity. Thus the two determinants in (3·20) and (3·19) are identical and (3·20) is proved.

Finally, by substituting (3·20) into (3·5) the following expression for the cluster integrals is found:

$$l_1 b(1) = \sum_{\mu_i(\boldsymbol{\nu})} \left| \delta_{ij} - \frac{1}{l_j}\sum_{(\boldsymbol{\nu})} (\nu_i-\delta_{ij})\,\mu_j(\boldsymbol{\nu}) \right|_{\sigma} \prod_{i=1}^{\sigma} \prod_{(\boldsymbol{\nu})} \frac{\{l_i \nu_i B(\boldsymbol{\nu})\}^{\mu_i(\boldsymbol{\nu})}}{\mu_i(\boldsymbol{\nu})!}, \tag{3·21}$$

where the summation extends over all sets of integers $\mu_i(\boldsymbol{\nu}) \geqslant 0$ subject to the condition (3·3). With (3·2) this condition reads

$$\sum_{j=1}^{\sigma} \sum_{(\boldsymbol{\nu})} (\nu_i-\delta_{ij})\,\mu_j(\boldsymbol{\nu}) = \begin{cases} l_i & \text{if } i \neq 1, \\ l_i - 1 & \text{if } i = 1. \end{cases} \tag{3·22}$$

If the index 1 is exchanged with any other index, corresponding expressions for $l_2 b(1)$, $l_3 b(1)$, etc. can be found.

4. INTEGRAL REPRESENTATION OF THE CLUSTER INTEGRALS AND THE PARTITION FUNCTION

I introduce the functions

$$G^\sigma\{\xi_1, \xi_2, \ldots, \xi_\sigma, B(\nu_1, \nu_2, \ldots, \nu_\sigma, 0, \ldots, 0)\}$$
$$= \sum_{\nu_1, \nu_2, \ldots, \nu_\sigma} B(\nu_1, \nu_2, \ldots, \nu_\sigma, 0, \ldots, 0)\, \xi_1^{\nu_1} \xi_2^{\nu_2} \ldots \xi_\sigma^{\nu_\sigma},$$

or written in short $\quad G^\sigma\{\boldsymbol{\xi}, B(\boldsymbol{\nu})\} = \sum_{\nu_1, \ldots, \nu_\sigma} B(\boldsymbol{\nu}) \prod_{k=1}^{\sigma} \xi_k^{\nu_k}. \qquad (4·1)$

Let a lower index denote differentiation, i.e.

$$G_i^\sigma = \frac{\partial G^\sigma}{\partial \xi_i} = \sum_{(\boldsymbol{\nu})} \nu_i B(\boldsymbol{\nu}) \prod_{k=1}^{\sigma} \xi_k^{\nu_k - \delta_{ik}}, \tag{4·2}$$

$$G_{ij}^\sigma = \frac{\partial^2 G^\sigma}{\partial \xi_i \partial \xi_j}. \tag{4·3}$$

I now expand the exponential

$$e^{l_j G_j^\sigma} = \sum_{\mu(\boldsymbol{\nu})} \prod_{(\boldsymbol{\nu})} \frac{\left\{ l_j \nu_j B(\boldsymbol{\nu}) \prod_{k=1}^{\sigma} \xi_k^{\nu_k - \delta_{jk}} \right\}^{\mu(\boldsymbol{\nu})}}{\mu(\boldsymbol{\nu})!},$$

and form the expressions

$$\left(\delta_{ij} - \frac{\xi_i}{l_j} \frac{\partial}{\partial \xi_i}\right) e^{l_j G_j^\sigma} = \sum_{\mu(\boldsymbol{\nu})} \left(\delta_{ij} - \frac{1}{l_j} \sum_{(\boldsymbol{\nu})} (\nu_i - \delta_{ij})\, \mu(\boldsymbol{\nu})\right) \prod_{(\boldsymbol{\nu})} \frac{\left\{ l_j \nu_j B(\boldsymbol{\nu}) \prod_{k=1}^{\sigma} \xi_k^{\nu_k - \delta_{jk}} \right\}^{\mu(\boldsymbol{\nu})}}{\mu(\boldsymbol{\nu})!}.$$

If a determinant is formed with such sums as elements, it can be transformed into a multiple sum of determinants. Taking the common factor in each column out of these determinants, I find

$$\left| \left(\delta_{ij} - \frac{\xi_i}{l_j} \frac{\partial}{\partial \xi_i}\right) e^{l_j G_j^\tau} \right|_\sigma = \sum_{\mu_j(\boldsymbol{\nu})} \left| \delta_{ij} - \frac{1}{l_j} \sum_{(\boldsymbol{\nu})} (\nu_i - \delta_{ij})\, \mu_j(\boldsymbol{\nu}) \right|_\sigma$$
$$\times \prod_{j=1}^{\sigma} \prod_{(\boldsymbol{\nu})} \frac{\left\{ l_j \nu_j B(\boldsymbol{\nu}) \prod_{k} \xi_k^{\nu_k - \delta_{jk}} \right\}^{\mu_j(\boldsymbol{\nu})}}{\mu_j(\boldsymbol{\nu})!}. \tag{4·4}$$

The dummy index j in the product can of course be changed into an index i. Comparison with (3·21) shows that $l_1 b(\mathbf{l})$ is the coefficient of $\prod_i \xi_i^{l_i}/\xi_1$ in the expansion (4·4). Therefore $l_1 b(\mathbf{l})$ can be written in the form of a multiple Cauchy integral

$$l_1 b(\mathbf{l}) = \left(\frac{1}{2\pi i}\right)^\sigma \oint \oint \ldots \oint \xi_1 \left| \left(\delta_{ij} - \frac{\xi_i}{l_j} \frac{\partial}{\partial \xi_i}\right) e^{l_j G_j^\sigma} \right|_\sigma \prod_{i=1}^{\sigma} \frac{d\xi_i}{\xi_i^{l_i+1}}. \tag{4·5}$$

The differentiation yields

$$l_1 b(\mathbf{l}) = \left(\frac{1}{2\pi\iota}\right)^{\sigma} \oint\oint \dots \oint \xi_1 \,|\, \delta_{ij} - \xi_i G^{\sigma}_{ji} \,|_{\sigma} \prod_{i=1}^{\sigma} \frac{e^{l_i G^{\sigma}_i}}{\xi_i^{l_i+1}} d\xi_i. \tag{4·6}$$

I shall now prove that this expression is identical with

$$l_1 b(\mathbf{l}) = \left(\frac{1}{2\pi\iota}\right)^{\rho} \oint\oint \dots \oint \xi_1 \,|\, \delta_{ij} - \xi_i G_{ji} \,|_{\rho} \prod_{i=1}^{\rho} \frac{e^{l_i G_i}}{\xi_i^{l_i+1}} d\xi_i, \tag{4·7}$$

where the index ρ of the G-functions is omitted,

$$G \equiv G^{\rho}, \quad G_i \equiv G^{\rho}_i, \quad G_{ij} \equiv G^{\rho}_{ij}. \tag{4·8}$$

It follows easily that

$$G^{\sigma}(\xi_1, \xi_2, \dots, \xi_{\sigma}) = G(\xi_1, \dots, \xi_{\sigma}, \xi_{\sigma+1} = \dots = \xi_{\rho} = 0). \tag{4·9}$$

In considering (4·7) it should be remembered that $l_i = 0$ for $\sigma < i \leqslant \rho$. Therefore the integrand in (4·7) has a pole of the first order in the variables $\xi_{\sigma+1}, \dots, \xi_{\rho}$. The residue is obtained by putting $\xi_{\sigma+1} = \dots = \xi_{\rho} = 0$ in the numerator. Thus (4·7) reduces to

$$l_1 b(\mathbf{l}) = \left(\frac{1}{2\pi\iota}\right)^{\sigma} \oint \dots \oint [\xi_1 \,|\, \delta_{ij} - \xi_i G_{ji} \,|_{\rho}]_{\xi_{\sigma+1} = \dots = \xi_{\rho} = 0} \prod_{i=1}^{\sigma} \frac{e^{l_i G_i(\xi_{\sigma+1} = \dots = \xi_{\rho} = 0)}}{\xi_i^{l_i+1}} d\xi_i,$$

which, with the help of (4·9), is easily shown to be identical with (4·6). Thus (4·7) is proved.

The proof has been given only for a set of numbers such that $l_1, l_2, \dots, l_{\sigma}$ differ from zero and that $l_{\sigma+1}, \dots, l_{\rho}$ vanish. Since the order of the indices i, j in (4·7) is irrelevant, it follows that this equation holds for any arbitrary set of numbers l_i.

This is also true if l_1 vanishes. In this case the left-hand side is zero. In the integrand on the right-hand side, the factor ξ_1 in the denominator cancels against the same factor in the numerator and the integrand, as a function of ξ_1, is regular. The integral therefore vanishes.

The corresponding integral representation of the partition function (2·8) is easily obtained. I define

$$g\{\eta, b(\mathbf{l})\} = \sum_{(\mathbf{l})} b(\mathbf{l}) \prod_{k=1}^{\rho} \eta_k^{l_k}, \tag{4·10}$$

and form the exponential function $\exp(Nvg)$. On expansion it is found that the partition function is the coefficient of $\prod_i \eta_i^{N_i}$. The integral representation of the partition function is therefore given by

$$Q_{\tau}(\mathbf{N}) = \left(\frac{1}{2\pi\iota}\right)^{\rho} \oint\oint \dots \oint e^{Nvg} \prod_{i=1}^{\rho} \frac{d\eta_i}{\eta_i^{N_i+1}}. \tag{4·11}$$

5. THE GENERATING FUNCTION OF THE PARTITION FUNCTION

The generating function of the partition function is

$$H(\mathbf{x}) = \sum_{N_1=0}^{\infty} \cdots \sum_{N_\rho=0}^{\infty} Q_\tau(\mathrm{N}) \prod_{i=1}^{\rho} x_i^{N_i} = \sum_{(N)} Q_\tau(\mathrm{N}) \prod_i x_i^{N_i}. \tag{5·1}$$

In order to calculate it I substitute the integral representation (4·11) of Q_τ and obtain a manifold geometric series, which can be summed provided

$$\frac{x_i e^{vg(\eta)}}{\eta_i} < 1 \tag{5·2}$$

for all values of i. The result is

$$H(\mathbf{x}) = \left(\frac{1}{2\pi\iota}\right)^\rho \oint\oint \cdots \oint \prod_i \frac{1}{\eta_i - x_i e^{vg}} d\eta_i. \tag{5·3}$$

I shall prove by induction that for $i \leqslant \rho$

$$\left(\frac{1}{2\pi\iota}\right)^i \oint \cdots \oint \prod_{j=1}^{i} \frac{d\eta_j}{\eta_j - x_j e^{vg(\eta)}} = \frac{1}{1 - \sum\limits_{j=1}^{i} v z_j g_j(z_1, z_2, \ldots, z_i, \eta_{i+1}, \ldots, \eta_\rho)}, \tag{5·4}$$

where the z_j are the solutions of the equations

$$z_j = x_j e^{vg(z_1 \cdots z_i, \eta_{i+1} \cdots \eta_\rho)} \quad (j = 1, 2, \ldots, i) \tag{5·5}$$

and $g_j = \partial g / \partial z_j$.

Furthermore, it will be shown that for sufficiently small values of x_i the path of integration can always be chosen in such a way that

$$\sum_{j=1}^{i} v z_j g_j(z_1 \ldots z_i, \eta_{i+1} \ldots \eta_\rho) < 1 \tag{5·6}$$

inside the path of integration.

Let us assume the equations (5·4), (5·5) and (5·6) have been proved for $i-1$. It then follows that (in view of (5·2) the factor $1/\{\eta_i - x_i \exp(vg)\}$ is regular for the integration over $\eta_1 \ldots \eta_{i-1}$)

$$\left(\frac{1}{2\pi\iota}\right)^i \oint \cdots \oint \prod_{j=1}^{i} \frac{d\eta_i}{\eta_j - x_j e^{vg}} = \frac{1}{2\pi\iota} \oint \frac{1}{\eta_i - x_i e^{vg(z_1 \ldots z_{i-1}, \eta_i \ldots \eta_\rho)}} \frac{1}{1 - \sum\limits_{j=1}^{i-1} v z_j g_j}, \tag{5·7}$$

where $$z_j = x_j e^{vg(z_1 \dots z_{i-1}, \eta_i \dots \eta_\rho)} \quad (j = 1, 2, \dots, i-1) \tag{5·8}$$

must now be considered as functions of η_i.

Differentiation of the logarithm of (5·8) gives

$$\sum_{k=1}^{i-1} (\delta_{jk} - vz_k g_k) \frac{dz_k}{z_k} = vg_i d\eta_i. \tag{5·9}$$

The difference of any two of these equations gives the result

$$\frac{dz_1}{z_1} = \frac{dz_2}{z_2} = \dots = \frac{dz_{i-1}}{z_{i-1}}.$$

Substitution in (5·9) yields

$$\frac{\partial z_j}{\partial \eta_i}\left(1 - \sum_{k=1}^{i-1} vz_k g_k\right) = z_j v g_i. \tag{5·10}$$

Now, in view of (5·6) (which has been assumed to be proved for $i-1$), the second factor in the integral (5·7) is regular. I shall show below that the first factor has only one pole for $\eta_i = z_i$, where z_i is given by

$$z_i = x_i e^{vg(z_1, z_2, \dots, z_i, \eta_{i+1} \dots \eta_\rho)}. \tag{5·11}$$

The residuum at this pole is obtained by replacing the denominator by its derivative at the pole

$$\left(\frac{1}{2\pi i}\right)^i \oint \dots \oint \prod_{j=1}^{i} \frac{d\eta_j}{\eta_j - x_j e^{vg}} = \frac{1}{1 - vz_i g_i - \sum_{j=1}^{i-1} vz_i g_j \frac{\partial z_j}{\partial \eta_i}} \frac{1}{1 - \sum_{j=1}^{i-1} vz_j g_j}.$$

Substitution of (5·10) gives the equation (5·4).

The derivation just given holds also for the first step (i.e. for $i = 1$), so that (5·4) is proved, provided it can be shown that the statements about the path of integration are correct.

Now the path of integration in (5·7) must be chosen in such a way that it includes $\eta_i = 0$ and that (5·2) is satisfied along the path of integration. The function on the left-hand side of (5·2) has a pole of the first order for $\eta_i = 0$. The curves of constant absolute value are therefore closed curves going around the pole, provided they do not enclose a saddle point. If as path of integration such a closed curve with constant value smaller than unity is chosen, then (5·2) is satisfied on the path of integration and there is one and only one point inside the path of integration, for which (5·11) is satisfied.

It is only left to prove that the path of integration can be chosen in this way without including a saddle point. The condition for a saddle point is

$$\frac{d}{d\eta_i}\left(\frac{x_i e^{vg}}{\eta_i}\right) = -\frac{x_i e^{vg}}{\eta_i^2}\left(1 - v\eta_i g_i - \eta_i \sum_{j=1}^{i-1} v g_j \frac{\partial z_j}{\partial \eta_i}\right) = 0,$$

or with (5·10)

$$\frac{x_i e^{vg}}{\eta_i^2} \frac{1 - \sum\limits_{j=1}^{i-1} v z_j g_j - v\eta_i g_i}{1 - \sum\limits_{j=1}^{i-1} v z_j g_j} = 0.$$

Therefore

$$1 - \sum_{j=1}^{i-1} v z_j g_j - v\eta_i g_i \neq 0 \tag{5·12}$$

inside the path of integration. Now η_i can be made as small as we please provided the x_i are sufficiently small. Since the series in (5·12) have no constant terms, they can therefore be made smaller than 1 for sufficiently small values of x_i. Thus the statements about the path of integration and the equation (5·6) are proved.

For $i = \rho$, (5·4) gives the series (5·3), which is therefore given by

$$H(\mathbf{x}) = \frac{1}{1 - \sum\limits_{i=1}^{\rho} v z_i g_i(\mathbf{z})}, \tag{5·13}$$

$$x_i = z_i e^{-vg(\mathbf{z})}. \tag{5·14}$$

6. THEOREM ON ASSOCIATED RADII OF CONVERGENCE OF A MULTIPLE POWER SERIES WITH POSITIVE COEFFICIENTS

In order to investigate the convergence properties of the power series (5·1), I use the method of associated radii, applied by Mayer (1939) to the two component system.

I use the following theorem (cf. Borel 1901):

Let $K_1, K_2, \ldots, K_{\rho-1}$ be certain constants. Let $\lambda(\mathbf{K})$ be the greatest limit of

$$\left\{Q_r(\mathrm{N}) \prod_{i=1}^{\rho-1} K_i^{N_i}\right\}^{1/N}, \quad N = \sum_{i=1}^{\rho} N_i \tag{6·1}$$

in the limit $N \to \infty$. Then the equations

$$\frac{X_1}{K_1} = \frac{X_2}{K_2} = \ldots = \frac{X_{\rho-1}}{K_{\rho-1}} = X_\rho = \frac{1}{\lambda(\mathbf{K})} \tag{6·2}$$

give a set of associated radii of convergence $X_1, X_2, \ldots, X_\rho$.

I define
$$c_i = \frac{N_i}{N}, \tag{6·3}$$

$$\lim_{N\to\infty} \frac{1}{N} \ln Q_\tau(\mathbf{N}) = \ln q(\mathbf{c}), \tag{6·4}$$

$$\ln \lambda(\mathbf{c}, \mathbf{K}) = \ln q(\mathbf{c}) + \sum_{i=1}^{\rho-1} c_i \ln K_i. \tag{6·5}$$

The c_i must satisfy the condition
$$\sum_{i=1}^{\rho} c_i = 1. \tag{6·6}$$

Then $\lambda(\mathbf{K})$ is given by
$$\lambda(\mathbf{K}) = \lambda(\mathbf{c}^0, \mathbf{K}), \tag{6·7}$$

where the c_i^0 are determined in such a way that the variation of λ with c_i (subject to the condition (6·6)) vanishes
$$[\delta_c \ln \lambda(\mathbf{c}, \mathbf{K})]_{c_i = c_i^0} = \sum_i \left[\frac{\partial \ln \lambda}{\partial c_i}\right]_{c_i = c_i^0} \delta c_i = 0. \tag{6·8}$$

Introduce the function
$$f(\mathbf{c}, \mathbf{X}) = \ln q(\mathbf{c}) + \sum_{i=1}^{\rho} c_i \ln X_i = \ln \lambda\left(\mathbf{c}, \frac{\mathbf{X}}{X_\rho}\right) + \ln X_\rho, \tag{6·9}$$

where c_i, X_i are to be considered as independent variables. Therefore the variation of $\ln \lambda(\mathbf{c}, \mathbf{K})$ with c_i is identical with the variation of f with c_i and it follows from (6·8) that
$$[\delta_c f(\mathbf{c}, \mathbf{X})]_{c_i = c_i^0} = 0. \tag{6·10}$$

Further, it follows from (6·7) and (6·2) that for c_i^0 the function (6·9) vanishes
$$f(\mathbf{c}^0, \mathbf{X}) = 0. \tag{6·11}$$

This equation constitutes a relation between the values c_i^0 (determined by (6·10)) and the radii of convergence X_i. Now consider a simultaneous variation of these quantities, so that (6·11) remains unchanged
$$\delta f(\mathbf{c}^0, \mathbf{X}) = [\delta_c f(\mathbf{c}, \mathbf{X}) + \delta_X f(\mathbf{c}, \mathbf{X})]_{c_i = c_i^0} = 0. \tag{6·12}$$

With (6·10) it follows that
$$\delta_X f(\mathbf{c}^0, \mathbf{X}) = 0, \tag{6·13}$$

or with (6·9)
$$\delta_X \sum_{i=1}^{\rho} c_i^0 \ln X_i = 0. \tag{6·14}$$

Here the variations δX_i are subject to the condition that the X_i as well as the $X_i + \delta X_i$ are associated radii of convergence.

7. EXPANSION OF THE FREE ENERGY BY MEANS OF THE CLUSTER INTEGRALS

The theorem proved in the last section is now applied to the series (5·1). According to (5·13) a set of associated radii is given by

$$X_i = Z_i e^{-vg(\mathbf{Z})}, \tag{7·1}$$

where the Z_i satisfy the equation

$$\sum_{i=1}^{\rho} vZ_i g_i(\mathbf{Z}) = 1. \tag{7·2}$$

Introducing the Z_i as independent variables, (6·14) can be written in the form

$$\delta_{\mathbf{Z}}\left(\sum_i c_i^0 \ln Z_i - vg(\mathbf{Z})\right) = 0, \tag{7·3}$$

where the variation is subject to the condition (7·2). This leads to the variational equations

$$\frac{1}{Z_i}(c_i^0 - vZ_i g_i) + \lambda\left(vg_i + \sum_{j=1}^{\rho} vZ_j g_{ij}\right) = 0. \tag{7·4}$$

Now λ must be determined in such a way that (7·2) is satisfied. Multiplying (7·4) by Z_i, and summing over all i, we find with (6·6) and (7·2)

$$\lambda\left(1 + \sum_{i,j} vZ_i Z_j g_{ij}\right) = 0. \tag{7·5}$$

Therefore $\lambda = 0$ and (7·4) gives

$$vZ_i g_i = c_i^0. \tag{7·6}$$

Introducing the values satisfying this equation into (6·11), it follows with (6·9) and (7·1) that

$$\ln q(\mathbf{c}^0) = -\sum_{i=1}^{\rho} c_i^0 \ln Z_i + vg(\mathbf{Z}). \tag{7·7}$$

The configurational free energy is defined by

$$A_r = -RT \lim_{N\to\infty} \frac{1}{N} \ln Q_r(\mathrm{N}). \tag{7·8}$$

Hence it follows from (6·4) and (7·7) that

$$A_r = RT\left\{-vg(\mathbf{Z}) + \sum_{i=1}^{\rho} c_i^0 \ln Z_i\right\}. \tag{7·9}$$

Here the c_i^0, according to (6·3), represent the atomic fractions of the various substances constituting the gas.

8. EXPANSION OF THE FREE ENERGY IN TERMS OF THE IRREDUCIBLE CLUSTER INTEGRALS

I shall now make use of the integral representation (4·7) of the cluster integrals. Then

$$z_1 g_1(\mathbf{z}) = \sum_{(\mathbf{l})} l_1 b(\mathbf{l}) \prod_{i=1}^{\rho} z_i^{l_i}$$

$$= \sum_{(\mathbf{l})} \left(\frac{1}{2\pi\iota}\right)^{\rho} \oint \cdots \oint \xi_1 \,|\, \delta_{ij} - \xi_i G_{ji} \,|_{\rho} \prod_{i=1}^{\rho} \left(\frac{z_i e^{G_i}}{\xi_i}\right)^{l_i} \frac{d\xi_i}{\xi_i}. \tag{8·1}$$

The summation can be carried out provided

$$\frac{z_i e^{G_i}}{\xi_i} < 1 \tag{8·2}$$

along the path of integration. The result is

$$z_1 g_1(\mathbf{z}) = \left(\frac{1}{2\pi\iota}\right)^{\rho} \oint \cdots \oint \xi_1 \,|\, \delta_{ij} - \xi_i G_{ji} \,|_{\rho} \prod_{i=1}^{\rho} \frac{d\xi_i}{\xi_i - z_i e^{G_i}}. \tag{8·3}$$

I shall prove by induction that

$$\left(\frac{1}{2\pi\iota}\right)^{k} \oint \cdots \oint \prod_{i=1}^{k} \frac{d\xi_i}{\xi_i - z_i e^{G_i(\xi)}} = \frac{1}{|\, \delta_{ij} - y_i G_{ij}(y_1 \ldots y_k, \xi_{k+1} \ldots \xi_{\rho}) \,|_k}, \tag{8·4}$$

where the y_i are given by

$$y_i = z_i e^{G_i(y_1 \ldots y_k, \xi_{k+1} \ldots \xi_{\rho})} \quad (i = 1, 2, \ldots, k). \tag{8·5}$$

Furthermore, it can be shown that the path of integration can be chosen in such a way that

$$|\, \delta_{ij} - y_i G_{ij} \,|_k \neq 0 \tag{8·6}$$

inside the path of integration.

The statement is immediately evident for $k = 1$. Let us assume then that it has been proved for $k-1$. Then (owing to (8·2))

$$\left(\frac{1}{2\pi\iota}\right)^{k} \oint \cdots \oint \prod_{i=1}^{k} \frac{d\xi_i}{\xi_i - z_i e^{G_i}} = \frac{1}{2\pi\iota} \oint \frac{1}{\xi_k - z_k e^{G_k}} \frac{1}{|\, \delta_{ij} - y_i G_{ij} \,|_{k-1}} d\xi_k, \tag{8·7}$$

with

$$y_i = z_i e^{G_i(z_1 \ldots z_{k-1}, \xi_k \ldots \xi_{\rho})}, \tag{8·8}$$

which are now to be considered as functions of ξ_k.

Differentiation of the logarithm of (8·8) gives

$$\sum_{j=1}^{k-1} \frac{dy_j}{y_j} (\delta_{ij} - y_j G_{ij}) - \frac{d\xi_k}{\xi_k} \xi_k G_{ki} = 0. \tag{8·9}$$

The solutions of these equations are

$$\frac{\xi_k \partial y_j}{y_j \partial \xi_k} = \frac{\left|\delta_{ij} - y_j G_{ij}\right|^{kj}_{k}}{\left|\delta_{ij} - y_j G_{ij}\right|_{k-1}}, \tag{8·10}$$

where the upper indices denote the jth subdeterminant in the development of the determinant with respect to the kth row, and y_k in the determinant is to be replaced by ξ_k.

The discussion of the path of integration is exactly the same as in § 5. It may therefore be omitted. Suffice it to say that there is exactly one point $\xi_k = y_k$ inside the path of integration for which the integrand has a pole, where y_k is given by

$$y_k = z_k e^{G_k(y_1 \dots y_k, \xi_{k+1} \dots \xi_\rho)}. \tag{8·11}$$

The residuum is obtained by differentiation of the denominator

$$\left[\left(1 - y_k G_{kk} - y_k \sum_{i=1}^{k-1} G_{ki} \frac{\partial y_i}{\partial \xi_k}\right) \left|\delta_{ij} - y_i G_{ij}\right|_{k-1}\right]^{-1}_{\xi_k = y_k}$$

or with (8·10)

$$\left[(1 - y_k G_{kk}) \left|\delta_{ij} - y_i G_{ij}\right|_{k-1} - \sum_{i=1}^{k-1} y_i G_{ki} \left|\delta_{ij} \quad y_i G_{ij}\right|^{ki}_{k}\right]^{-1}.$$

Now the first determinant in this expression is identical with the subdeterminant with indices kk. Therefore the denominator is identical with the expansion of the determinant

$$\left|\delta_{ij} - y_i G_{ij}(y_1 \dots y_k, \xi_{k+1} \dots \xi_\rho)\right|_k,$$

with respect to the kth row, and (8·4) is proved.

Now return to the integral (8·3). The additional factors in the integrand do not make any difference, since they contain no singularities. Therefore (8·4) can be applied immediately. Putting $k = \rho$, it follows that

$$z_1 g_1(\mathbf{z}) = y_1, \tag{8·12}$$

where the y_i are the solutions of the equations

$$z_i = y_i e^{-G_i(y_1 \dots y_\rho)}. \tag{8·13}$$

Similarly

$$z_i g_i(z_1 \dots z_\rho) = y_i. \tag{8·14}$$

Furthermore, the expansion of $g(\mathbf{z})$ in terms of the irreducible integrals will be needed. I shall prove that

$$g(\mathbf{z}) = G(\mathbf{y}) + \sum_{i=1}^{\rho} y_i(\ln z_i - \ln y_i + 1). \tag{8·15}$$

Differentiation with respect to z_k gives

$$z_k g_k = y_k + z_k \sum_{i=1}^{\rho} \{G_i + \ln z_i - \ln y_i\} \frac{\partial y_i}{\partial z_k}. \tag{8·16}$$

Here the sum vanishes in view of (8·13), and (8·16) therefore reduces to the correct expressions (8·14). Thus (8·15) is correct apart from a constant of integration. The latter however vanishes, since for $z_i = 0$ also $y_i = 0$ and both sides of (8·15) vanish.

Let now Y_i be those values of y_i which correspond to Z_i, so that from (8·13)

$$Z_i = Y_i e^{-G_i(\mathbf{Y})}. \tag{8·17}$$

Introduce these values into (7·9); then with (8·15)

$$A_\tau = RT\left[-vG(\mathbf{Y}) + \sum_{i=1}^{\rho} \{c_i^0(\ln Y_i - G_i) + vY_i(G_i - 1)\}\right]. \tag{8·18}$$

The Z_i are determined by the equations (7·6). Comparison with (8·14) shows that the Y_i are given by

$$Y_i = \frac{c_i^0}{v}. \tag{8·19}$$

Therefore (8·18) gives an expansion of the free energy in powers of the reciprocal volume and the atomic fractions c_i^0.

With (2·2) the total free energy is then given by

$$A = RT\left[\ln\left(\frac{h^2}{2\pi kT}\right)^{\frac{3}{2}} - \tfrac{3}{2}\sum_i c_i^0 \ln m_i - \ln v - 1 - vG\left(\frac{c_1^0}{v}, \ldots, \frac{c_\rho^0}{v}\right) + \sum_{i=1}^{\rho} c_i^0 \ln c_i^0\right]. \tag{8·20}$$

The free energy (8·20) yields by differentiation the pressure

$$PV = -v\frac{\partial A}{\partial v} = RT\left[1 + vG\left(\frac{c_1^0}{v}, \ldots, \frac{c_\rho^0}{v}\right) - \sum_{i=1}^{\rho} c_i^0 G_i\left(\frac{c_1^0}{v}, \ldots, \frac{c_\rho^0}{v}\right)\right]. \tag{8·21}$$

Here the subscript i denotes differentiation in accordance with the definition (4·2).

The Gibbs's free energy is given by

$$F = A + PV = RT\left[\ln\left(\frac{h^2}{2\pi kT}\right)^{\frac{3}{2}} - \tfrac{3}{2}\sum_i c_i^0 \ln m_i - \ln v + \sum_{i=1}^{\rho} c_i^0 \left\{\ln c_i^0 - G_i\left(\frac{c_1^0}{v}, \ldots, \frac{c_\rho^0}{v}\right)\right\}\right], \tag{8·22}$$

where V must be considered as a function of P and T given by (8·21).

The equations (8·20)–(8·22) are identical with the equations for a mixture of perfect gases, if the G-series are omitted. The latter give the deviations from the perfect gas.

9. CHEMICAL EQUILIBRIUM IN A GAS MIXTURE

The equations derived in the preceding section can be applied to the problem of chemical equilibrium in a gas mixture.

It will be sufficient to consider two substances A_1 and A_2, which may form a chemical compound A_3. The more general case does not lead to any difficulties.

Let us assume that ν_1 molecules of the substance A_1 and ν_2 molecules of the substance A_2 form together $-\nu_3$ molecules of the compound A_3 (ν_3 is therefore negative). Let further N_1, N_2 be the total number of molecules of the substances A_1 and A_2, if all molecules of the compound A_3 are dissociated. Now assume that some of these molecules have combined to form n_3 molecules of the compound, leaving n_1 molecules of the substance A_1 and n_2 molecules of A_2. Hence the equations

$$\nu_3 N_1 = \nu_3 n_1 - \nu_1 n_3, \quad \nu_3 N_2 = \nu_3 n_2 - \nu_2 n_3. \tag{9·1}$$

The molar fractions (dropping the index 0, used in the previous sections) are given by

$$c_i = \frac{n_i}{n_1+n_2+n_3}. \tag{9·2}$$

Then (9·1) can be written in the form

$$\nu_3 \frac{N_1}{n_1+n_2+n_3} = \nu_3 c_1 - \nu_1 c_3, \quad \nu_3 \frac{N_2}{n_1+n_2+n_3} = \nu_3 c_2 - \nu_2 c_3. \tag{9·3}$$

I further introduce the mole fractions C_1, C_2 of the two substances A_1 and A_2, if all molecules of the compound are dissociated

$$C_1 = \frac{N_1}{N_1+N_2}, \quad C_2 = \frac{N_2}{N_1+N_2}. \tag{9·4}$$

Then, from (9·3)

$$C_1 = \frac{\nu_3 c_1 - \nu_1 c_3}{\nu_3 - c_3(\nu_1+\nu_2+\nu_3)}, \quad C_2 = \frac{\nu_3 c_2 - \nu_2 c_3}{\nu_3 - c_3(\nu_1+\nu_2+\nu_3)}. \tag{9·5}$$

These equations represent two relations between the mole fractions c_1, c_2 and c_3, since for any definite system the mole fractions C_1, C_2 are given constants. A third relation must be obtained from the condition of thermodynamical equilibrium with regard to the chemical reaction.

When forming the partition function in the previous sections, it was tacitly assumed that the zero level of the energy is given by the total energy of the system, when all particles are at infinite distance from each other.

Furthermore, I have neglected all internal processes (molecular rotations, vibrations, etc.). This is of course justified, since these processes give additive terms, which do not influence the equation of state, though they must of course be added, if the heat content or specific heat is calculated.

But if one considers chemical equilibrium, one must compare systems with different total numbers n_i of composing particles. Since each type of particle gives a different additive term, the total of these additive terms does not remain constant during a chemical reaction and therefore they influence the equilibrium. It will be convenient to introduce the chemical potentials μ_i of the three substances considered as perfect gases. They are of the form (cf. Fowler and Guggenheim, 1939)

$$\mu_i(P,T) = \epsilon_i + kT\ln P - TC_p^i \ln T - kT\Sigma \ln q_v^i(T) - kTj_i - kT\Sigma\ln\rho_i. \quad (9\cdot 6)$$

Here ϵ_i are the internal energies of the molecules at the absolute zero of temperature; C_p^i are the heat capacities per molecule at constant pressure arising from the translational and rotational movements of the molecules; q_v^i are the free energies of the molecular vibrations, which have to be summed over all vibrations; j_i are the chemical constants and ρ_i the nuclear spin weights, which have to be summed over all nuclei. The latter of course do not influence the chemical equilibrium and may be disregarded.

For perfect gases (9·6) may be written in the form

$$\mu_i(V,T) = \epsilon_i + kT\ln\frac{kT}{v} - TC_p^i \ln T - kT\Sigma \ln q_v^i(T) - kTj_i - kT\Sigma\ln\rho_i. \quad (9\cdot 7)$$

For imperfect gases, I shall use (9·6) and (9·7) as definitions. For monatomic gases one has (cf. Fowler and Guggenheim 1939)

$$C_p^i = \tfrac{5}{2}k, \quad j_i = \ln\frac{(2\pi m_i)^{\frac{3}{2}}k^{\frac{5}{2}}}{h^3}v_0, \quad q_v^i = 1,$$

where v_0 is the electronic weight of the normal state. With these expressions (9·7) gives

$$\mu_i(V,T) = \epsilon_i \underline{-kT\left[\ln v + \ln\left(\frac{2\pi m_i kT}{h^2}\right)^{\frac{3}{2}}\right]} - kT\ln v_0 - kT\Sigma\ln\rho_i. \quad (9\cdot 8)$$

If, furthermore, one puts $\epsilon_i = 0$ and $v_0 = \rho_i = 1$, one obtains the assumptions under which the equations of the previous sections were derived. In this case only the term which has been underlined in (9·8) remains. Therefore one must replace this term in the expression (8·20) for the free energy by the more general expression (9·7). The free energy is therefore

$$A = kT\left[\sum_i n_i\left\{\frac{\mu_i(V,T)}{kT}+\ln\frac{n_i}{n_1+n_2+n_3}-1\right\}-VG\left(\frac{n_1}{V},\frac{n_2}{V},\frac{n_3}{V}\right)\right]. \qquad (9\cdot9)$$

Here R has been replaced by $(n_1+n_2+n_3)\,k$ and the c_i have been eliminated by means of the definitions (9·2).

Before proceeding any further, it is necessary to see how the μ_i depend on the numbers n_i. Now all terms in (9·7) are independent of n_i except the term containing the volume per particle $v = V/(n_1+n_2+n_3)$. Introducing the quantity

$$\mu_i' = \mu_i - kT\ln(n_1+n_2+n_3), \qquad (9\cdot10)$$

it follows that μ_i' does not depend on the numbers n_i. (9·9) may now be written in the form

$$A = kT\left[\sum_i n_i\left\{\frac{\mu_i'(V,T)}{kT}+\ln n_i-1\right\}-VG\left(\frac{n_1}{V},\frac{n_2}{V},\frac{n_3}{V}\right)\right], \qquad (9\cdot11)$$

which shows explicitly the dependence of this expression on the n_i. Chemical equilibrium is established, if A is a minimum for the chemical reaction, i.e. for a variation of the numbers n_i subject to the conditions (9·1); the latter lead to the relations

$$\nu_3\delta n_1 = \nu_1\delta n_3, \quad \nu_3\delta n_2 = \nu_2\delta n_3. \qquad (9\cdot12)$$

The variation of A then leads to the equation

$$\sum_i \nu_i\left\{\ln n_i+\frac{\mu_i'(V,T)}{kT}-G_i\right\} = 0. \qquad (9\cdot13)$$

If here one introduces again the mole fractions c_i, one finds

$$\sum_i \nu_i\left\{\ln c_i+\frac{\mu_i(V,T)}{kT}-G_i\left(\frac{c_1}{v},\frac{c_2}{v},\frac{c_3}{v}\right)\right\} = 0. \qquad (9\cdot14)$$

For small pressures, i.e. large volumes, the G_i-series can be neglected with the result

$$\sum_i \nu_i\left(\ln c_i+\frac{\mu_i}{kT}\right) = 0 \quad (P\rightarrow 0). \qquad (9\cdot15)$$

Here the argument of μ_i has been omitted, since in the limit $P \to 0$ $\mu_i(V,T)$ and $\mu_i(P,T)$ are identical. If in the expression (9·6) for μ_i the vibrational partition functions can be omitted, then

$$\sum_i \nu_i \frac{\mu_i}{kT} = \frac{B}{T} + \nu \ln P - \frac{C_p}{k} \ln T - J, \tag{9·16}$$

where $$kB = \sum_i \nu_i \epsilon_i, \quad C_p = \sum_i \nu_i C_p^i, \quad J = \sum_i \nu_i j_i, \quad \nu = \sum_i \nu_i. \tag{9·17}$$

Substituting (9·16) into (9·15), the well-known law of mass action is found (cf. Planck 1927):

$$K = \prod_i c_i^{\nu_i} = e^J e^{-B/T} P^{-\nu} T^{C_p/k}. \tag{9·18}$$

In general (9·15) is the integral of the van 't Hoff equation. This follows from the thermodynamic relations

$$\mu = \frac{F}{N}, \tag{9·19}$$

where F is Gibbs's free energy and

$$\left(\frac{\partial}{\partial T}\frac{F}{kT}\right)_p = \left(\frac{\partial}{\partial T}\frac{A}{kT}\right)_v = \frac{1}{kT^2} E, \tag{9·20}$$

where E is the heat content. Differentiation of (9·15) then gives

$$\left(\frac{\partial \ln K}{\partial T}\right)_p = \left(\frac{\partial}{\partial T} \sum_i \nu_i \ln c_i\right)_p = -\frac{1}{RT^2} \sum_i \nu_i E_i \quad (P \to 0). \tag{9·21}$$

Here $-\Sigma \nu_i E_i$ is the heat content produced by the reaction. Thus (9·21) is identical with the van 't Hoff equation (cf. Mayer and Goeppert-Mayer 1940).

I shall now consider the deviations from this law for increasing pressure. For this purpose, one must take into account the difference between $\mu_i(V,T)$ and $\mu_i(P,T)$. Hence, with (9·6), (9·7) and (8·21),

$$\frac{\mu_i(P,T) - \mu_i(V,T)}{kT} = \ln \frac{VP}{RT} = \ln\left[1 + vG - \sum_i c_i G_i\right]. \tag{9·22}$$

I form the expression $$\ln K_p = \sum_i \nu_i \{\ln c_i + \ln P\}. \tag{9·23}$$

With (9·14) and (9·22) it is given by

$$\ln K_p = \sum_i \nu_i \frac{\mu_i(P,T) - kT \ln P}{kT} + \nu \ln\left(1 + vG - \sum_i c_i G_i\right) + \sum_i \nu_i G_i. \tag{9·24}$$

Now, the first term on the right-hand side is independent of the pressure, according to the definition (9·6). The second and third terms vanish for $P \to 0$. Therefore (9·24) can be written in the form

$$\left.\begin{aligned} \ln K_p &= \ln K_p^0 + \nu \ln\left[1 + vG - \sum_i c_i G_i\right] + \sum_i \nu_i G_i, \\ \ln K_p^0 &= \lim_{P\to 0} \ln K_p = \sum_i \nu_i \frac{\mu_i(P,T) - kT\ln P}{kT}. \end{aligned}\right\} \qquad (9{\cdot}25)$$

Here the last two terms give the pressure dependence of the equilibrium constant K_p and the deviation from van 't Hoff's law, if the volume is eliminated by means of the equation (8·21).

I wish to thank Professor M. Born, F.R.S. for his interest in the present investigation.

REFERENCES

Borel, É. 1901 *Leçons sur les séries divergentes*, 1st ed. (see p. 88). Paris.
Born, M. and Fuchs, K. 1938 *Proc. Roy. Soc.* A, **166**, 391.
Fowler, R. H. and Guggenheim, E. A. 1939 *Statistical thermodynamics* (see p. 171, equ. (510·9), (510·10)). Cambridge.
Mayer, J. E. 1937 *J. Chem. Phys.* **5**, 67.
Mayer, J. E. 1939 *J. Phys. Chem.* **43**, 71.
Mayer, J. E. and Ackermann, Ph. G. 1937 *J. Chem. Phys.* **5**, 74.
Mayer, J. E. and Goeppert-Mayer, M. 1940 *Statistical mechanics* (see p. 298, equ. (9)). New York.
Mayer, J. E. and Harrison, S. F. 1938 *J. Chem. Phys.* **6**, 87, 107.
Planck, M. 1927 *Thermodynamik*, 8th ed. (see p. 219, equ. (203*a*)). Berlin and Leipzig.
Uhlenbeck, G. E. and Kahn, B. 1938 *Physica*, **5**, 399.

Pressure dependence of the equilibrium constant of ammonia

By Klaus Fuchs
The University of Edinburgh

(*Communicated by M. Born, F.R.S.—Received* 11 *August* 1941)

The pressure dependence of the equilibrium constant of a slightly imperfect gas is calculated. At sufficiently high temperatures, the constants occurring in the formula for the equilibrium constant can be expressed in terms of the van der Waals constants. The latter can be obtained from the second virial coefficients.

Numerical results for ammonia give good agreement between the theory and experiments.

1. Introduction

Experimental results of the equilibrium constants of gaseous mixtures are usually represented as integrals of the van't Hoff equation. The constants in this integral are then adjusted so as to represent the equilibrium constant over a fair range of temperatures and pressures.

However, the van't Hoff equation is correct only in the limiting case of zero pressure, owing to the fact that for non-vanishing pressure the heat content produced by the reaction depends explicitly on the concentration. It seems therefore worth while to consider the theory of the pressure dependence of the equilibrium constant for a particular example, although at present a calculation of more than the first order term—corresponding to the second virial coefficient—seems to be impracticable.

In a recent paper (Fuchs 1941) the general theory of a mixture of imperfect gases has been developed and the general equations determining chemical equilibrium have been derived. For the purposes of the present paper, however, the far simpler theory of slightly imperfect gases is sufficient. Those readers who are more interested in the connexion with the general theory, will easily establish the relation with the paper just quoted.

2. Chemical equilibrium of slightly imperfect gases

I use in the following the notation of Fowler and Guggenheim (1939). The free energy of a mixture of slightly imperfect gases is given by (cf. Fowler and Guggenheim, p. 265, equ. (704·3))

$$A = kT\left[\sum_A N_A\left(\ln\frac{N_A}{\phi_A V} - 1\right) + \sum_{AB}\frac{N_A N_B}{V}B_{AB}(T)\right]. \qquad (2\cdot 1)$$

Here N_A is the number of molecules of type A; B_{AB} are essentially the generalized second virial coefficients

$$B_{AB}(T) = \tfrac{1}{2}\int_0^\infty (1 - e^{-\epsilon_{AB}(r)/kT})\, 4\pi r^2 dr, \tag{2·2}$$

and ϕ_A is given by (cf. Fowler and Guggenheim, p. 257, equ. (701·8))

$$\phi_A = \frac{(2\pi m_A kT)^{\frac{3}{2}}}{h^3} j_A(T). \tag{2·3}$$

Here the first factor arises from that part of the partition function due to the integration over the momentum coordinates and the second factor $j_A(T)$ is the internal partition function of the molecule.

Consider now a chemical reaction given by the equation

$$\sum_A \nu_A(A) = 0. \tag{2·4}$$

Here (A) represents a molecule of type A and ν_A are the number of molecules taking part in the reaction.

Consider next a variation of the number N_A of molecules of type A due to the reaction. From (2·4) follows that the variations δN_A satisfy the relations

$$\frac{\delta N_A}{\nu_A} = \frac{\delta N_B}{\nu_B}. \tag{2·5}$$

Chemical equilibrium is established, if the variation of the free energy vanishes, i.e.

$$\sum_A \frac{\partial A}{\partial N_A} \delta N_A = 0 \tag{2·6}$$

with (2·5) follows

$$\sum_A \nu_A \frac{\partial A}{\partial N_A} = \sum_A \nu_A \mu_A = 0. \tag{2·7}$$

Here $\mu_A = \partial A/\partial N_A$ is the chemical potential of the molecules of type A in the mixture. It can be obtained from the free energy (2·1) (cf. also Fowler and Guggenheim, equ. (704·5)) with the result

$$\sum_A \nu_A \ln \frac{N_A}{\phi_A V} + 2\sum_{A,B} \nu_A \frac{N_B}{V} B_{AB} = 0. \tag{2·8}$$

I now form the expression

$$\ln K_p = \sum_A \nu_A \left(\ln \frac{N_A}{N} + \ln P\right), \quad N = \sum_A N_A, \tag{2·9}$$

which is connected with the equilibrium constant K by the equation

$$K = K_p P^{-\nu}, \quad \nu = \sum_A \nu_A. \tag{2·10}$$

Now, the pressure P is given by (cf. Fowler and Guggenheim, equ. (704·4))

$$P = \frac{kTN}{V}\left(1 + \sum_{A,B} \frac{N_A N_B}{NV} B_{AB}\right). \tag{2·11}$$

With the help of (2·11) and (2·8) we find for K_p

$$\ln K_p = \sum_A \nu_A \ln(\phi_A kT) - 2\sum_{A,B} \nu_A \frac{N_B}{V} B_{AB} + \nu \ln\left(1 + \sum_{A,B} \frac{N_A N_B}{NV} B_{AB}\right). \tag{2·12}$$

If the volume V is now eliminated by means of (2·11), one must neglect the second order terms, since they give only terms of the third order in (2·12). Similarly in the expansion of the logarithm only the first term need be taken into account. Thus

$$\ln K_p = \sum_A \nu_A \ln(\phi_A kT) + \frac{P}{kT} \sum_{A,B} B_{AB}\left\{\nu \frac{N_A N_B}{N^2} - 2\frac{\nu_A N_B}{N}\right\}. \tag{2·13}$$

The first term

$$\ln K_p^0 = \sum_A \nu_A \ln(\phi_A kT) \tag{2·14}$$

is independent of the pressure. I further introduce the mole fractions $c_A = N_A/N$. Then (2·13) takes the form

$$\ln K_p = \ln K_p^0 + \frac{P}{kT} \sum_{A,B} (\nu c_A c_B - 2\nu_A c_B) B_{AB}. \tag{2·15}$$

At sufficiently high temperatures the B_{AB} can be expressed in terms of the van der Waals constants. Considering the molecules as rigid spheres of radii ρ_A and an interaction $\epsilon_{AB}(r)$, if they do not overlap, it follows that

$$B_{AB} = \frac{1}{2}\left\{\frac{4\pi}{3}(\rho_A + \rho_B)^3 - \frac{\alpha_{AB}}{kT}\right\}, \quad \alpha_{AB} = -\int_{\rho_A+\rho_B}^{\infty} \epsilon_{AB}(r)\, 4\pi r^2 dr. \tag{2·16}$$

The constants in this equation are related to the van der Waals constants a_A, b_A of the pure gases as follows

$$2a_A = N\alpha_{AA}, \quad 2b_A = \frac{4\pi}{3} N(2\rho_A)^3, \tag{2·17}$$

(2·15) may then be written in the form

$$\ln K_p = \ln K_p^0 + \frac{P}{kT} \sum_{A,B} \{\tfrac{1}{2}\nu c_A c_B - \nu_A c_B\}\left\{\frac{4\pi}{3}(\rho_A + \rho_B)^3 - \frac{\alpha_{AB}}{kT}\right\}. \tag{2·18}$$

3. PRESSURE DEPENDENCE OF THE EQUILIBRIUM CONSTANT OF AMMONIA

In conclusion let us consider the chemical equilibrium for a specified substance. I choose ammonia for this purpose, since the chemical equilibrium of this gas has been investigated over a wide range of pressures. This was done by Larson and Dodge (1923) and Larson (1924).

The chemical equation for ammonia is

$$\tfrac{3}{2}H_2 + \tfrac{1}{2}N_2 = NH_3. \tag{3·1}$$

Thus we have $$\nu_1 = \tfrac{3}{2}, \quad \nu_2 = \tfrac{1}{2}, \quad \nu_3 = -1, \quad \nu = 1. \tag{3·2}$$

Furthermore, starting with pure ammonia, the mole fractions for complete dissociation are $\tfrac{3}{4}$ and $\tfrac{1}{4}$.

If x is the mole fraction of ammonia in the mixture, it follows that

$$c_1 = \tfrac{3}{4}(1-x), \quad c_2 = \tfrac{1}{4}(1-x), \quad c_3 = x. \tag{3·3}$$

K_p defined by (2·9) is now

$$\ln K_p = \tfrac{3}{2}\ln 3 - 2\ln 4 + \ln\frac{(1-x)^2 P}{x}. \tag{3·4}$$

On the other hand, from (2·15)

$$\ln K_p = \ln K_p^o - \frac{P}{kT}[D_0 + D_1 x + D_2 x^2], \tag{3·5}$$

$$\left.\begin{aligned} D_0 &= \tfrac{1}{16}\{27B_{11} + 18B_{12} + 3B_{22} - 24B_{13} - 8B_{23}\}, \\ D_1 &= \tfrac{1}{8}\{24B_{13} + 8B_{23} - 9B_{11} - 6B_{12} - B_{22} - 16B_{33}\}, \\ D_2 &= \tfrac{1}{16}\{16B_{33} + 24B_{13} + 8B_{23} - 9B_{11} - 6B_{12} - B_{22}\}. \end{aligned}\right\} \tag{3·6}$$

I am here interested chiefly in the pressure dependence of K_p. I shall therefore assume for K_p^o the experimental values of Larson and Dodge (1923). The comparison with the theory in this limit has in fact already been made by Larson and Dodge, who analysed their experimental values with the help of van't Hoff's equation. But, as pointed out in the introduction, there is no justification for using van't Hoff's equation except in the limit $P \rightarrow 0$. It is therefore not astonishing that Larson and Dodge had to adjust the constants in the experimental expressions for the heat content produced by the reaction so as to obtain agreement with experiment, and that these adjusted constants turned out to depend on the pressure.

The van der Waals constants can be estimated from the second virial coefficients in the equation of state (cf. Landolt-Boernstein, 1935). In the temperature intervals used for this purpose the virial coefficients are linear in the reciprocal temperature so that the approximation (2·16) is justified.

The temperature interval in which we shall apply these values is at even higher temperatures. The values obtained are collected in the first three columns of table 1.

The 'mixed' van der Waals constants α_{ij} cannot be obtained in this way, except by a thorough analysis of the influence of the chemical reaction on the virial coefficients. However, we can obtain a good approximation in the following way.

London (1930) has shown the close connexion between the polarizability and the van der Waals forces, the latter being proportional to the square of the polarizability. It is plausible to assume that α_{ij} is proportional to the product of the polarizabilities of the two substances. In fact, corresponding to London's estimate of the van der Waals forces for two molecules of the same type (see equation (13) of his paper), we find easily

$$\frac{3}{4}\frac{\alpha\alpha'}{r^6}\sqrt{(V_a V_a')} \leqslant -\epsilon(r) \leqslant \frac{3}{4}\frac{\alpha\alpha'}{r^6}\sqrt{(V_j V_j')}$$

where α, α' are the polarizabilities, V_a, V_a' the excitation energies and V_j, V_j' the ionization energies. London found furthermore that the actual values of the van der Waals forces are always very near the same place in the interval given by the above estimate. I therefore assume

$$\epsilon_{AB}(r) = \sqrt{\{\epsilon_{AA}(r)\,\epsilon_{BB}(r)\}}.$$

As the dependence on r is the same for all ϵ_{AB}, it follows that

$$\alpha_{ij} = \sqrt{(\alpha_{ii}\alpha_{jj})}. \tag{3·7}$$

In the case of NH_3 there is a complication, as this molecule has a dipole moment. Apart from the dispersion effect, also the induction and direction effect will give contributions to the van der Waals forces. The latter however is important only at low temperatures; the induction effect has been calculated by London (1930) and he has shown that it is only 10 % of the dispersion effect (see table 4 of his paper). Therefore it will not influence equation (3·7) appreciably.

The 'mixed' b values on the other hand can be obtained easily by assuming additivity of the radii as in (2·16).

The results are collected in the table 1.

TABLE 1. VAN DER WAALS'S CONSTANTS

	H_2	N_2	NH_3	H_2–N_2	H_2–NH_3	N_2–NH_3	units
a/R^2	12·15	227	354	52·4	65·6	284	degree²/atm.
b/R	0·223	0·685	0·408	0·410	0·306	0·535	degree/atm.

With the help of this table the B_{ij} can be calculated as given by (2·16), (2·17). Substitution in (3·5) yields

$$\ln K_p = \ln K_p^0 - \frac{P}{T}\left[\frac{119}{T} + 0{\cdot}431 + x\left\{\frac{309}{T} - 0{\cdot}390\right\} + x^2\left\{\frac{554}{T} - 0{\cdot}621\right\}\right]. \quad (3{\cdot}8)$$

Here P is to be measured in atmospheres.

Equating (3·4) and (3·8) we obtain an equation for x. The results are best illustrated by plotting the logarithm of the equilibrium constant K_p as a function of the pressure. This is done in figure 1. The curves represent the theoretical values for various temperatures, the crosses represent the experimental values of Larson and Dodge (1923) and Larson (1924). It will be seen that the slope of the curves for small pressures gives very good agreement between the theoretical and experimental values. For higher pressures, however, deviations occur, which must be due to the higher virial coefficients.

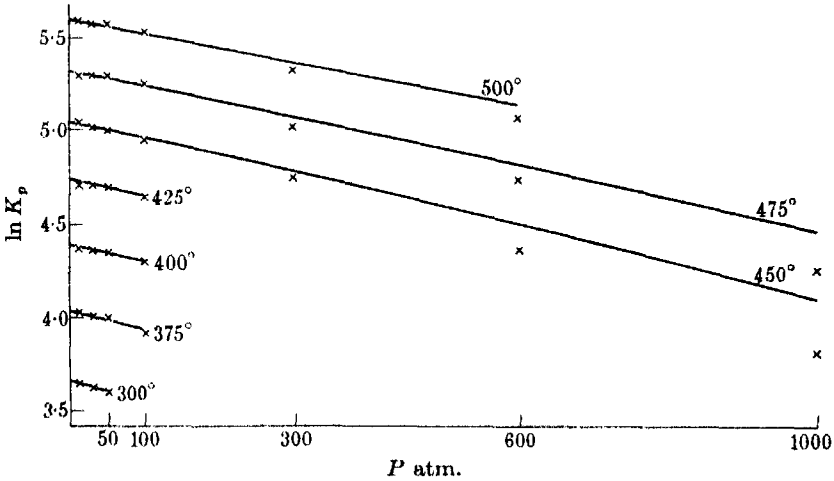

FIGURE 1. The equilibrium constant K_p as a function of the pressure for various temperatures. The curves represent the calculated values. The crosses indicate the experimental values of Larson and Dodge.

REFERENCES

Fowler, R. H. and Guggenheim, E. A. 1939 *Statistical Thermodynamics*, Cambridge University Press.

Fuchs, K. 1941 *Proc. Roy. Soc.* A, **179**, 408.

Landolt-Boernstein 1935 *Physikalisch Chemische Tabellen*, Eg. III*a*, pp. **94**, **96**, **100**.

Larson, A. T. 1924 *J. Amer. Chem. Soc.* **46**, 367.

Larson, A. T. and Dodge, R. L. 1923 *J. Amer. Chem. Soc.* **45**, 2918.

London, F. 1930 *Z. Phys.* **63**, 245.

The spectra of chilled hydrocarbon flames

By A. G. Gaydon, Ph.D. *Leverhulme Research Fellow, Chemical Technology Department, Imperial College, London, S.W. 7*

(*Communicated by A. C. Egerton, Sec.R.S.—Received* 26 *May* 1941)

[Plates 44, 45]

It has been found that the spectrum of the outer cone of hydrocarbon flames struck back in a water-cooled steel burner shows the hydrocarbon flame bands in the ultra-violet which are usually known as the ethylene flame bands. Under suitable conditions these bands are relatively very strong, being almost the sole feature of the spectrum. Chemical tests show that the occurrence of these hydrocarbon flame bands is closely associated with the formation of a peroxide, probably an alkyl peroxide. The bands are not necessarily associated with the presence of aldehydes in the inter-conal gases. Various catalysts have little effect on the spectrum.

A brief discussion on the nature of the emitter of the hydrocarbon flame bands is given. The present observations favour the radical HCO as the emitter, this being formed perhaps by the breaking up of peroxides in much the same way as CH is known spectroscopically to be formed in the breaking up of hydrocarbons.

INTRODUCTION

The spectra associated with normal flames of burning hydrocarbons are well known, being indeed among the first spectra to be studied. The inner cone of the ordinary Bunsen-type flame shows chiefly the Swan bands of C_2, the CH bands at 4315 and 3900 A, and the OH bands at 3064 and 2811 A. There is also present in the *inner* cone a weaker system of bands in the near ultra-violet which were first described in detail by Vaidya (1934) and which have been referred to as the ethylene flame bands but are more appropriately called the hydrocarbon flame bands (Vaidya 1941); these bands have been studied by Bell (1937) and Smith (1940) as well as by Vaidya (1934, 1941), and have been variously attributed to CH_2, CHOH and HCO. The outer cone of a Bunsen-type flame shows mostly OH, with weak CH bands and a background of the continuous and banded carbon monoxide flame spectrum.

Following previous work on the spectrum and afterburning of CO (Gaydon 1940, 1941) some observations were made on the spectra of gases burning in a very fast stream of air; it was found that under suitable conditions the tip of a town's gas flame, corresponding to the *outer* cone, showed the hydrocarbon flame bands relatively very strongly. These observations were followed up by a study of the spectra of hydrocarbon flames under various conditions of combustion accompanied by chemical tests on the combustion products, examination of the absorption spectrum of the partly burnt gases, and by studying the effects of catalysts on the flames. The results of these investigations are presented here, and are followed by a brief discussion of the effect of chilling hydrocarbon flames, and on the origin of the hydrocarbon flame bands.

BURNER DESIGN AND APPEARANCE OF FLAMES

The original burner consisted of two long concentric mild steel tubes, internal diameters $\frac{1}{8}$ in. and $\frac{1}{2}$ in. arranged so that the inner tube was supplied with the inflammable gas admixed with a little primary air. The outer tube was closed by a steel ring at one end through which the inner tube slid. A fast stream of secondary air was injected into the outer tube near the closed end. A diagram is shown in figure 1.

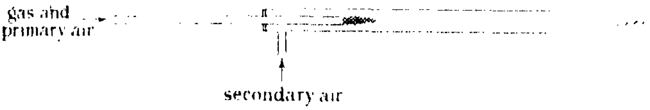

FIGURE 1.

When the gas and air supplies were suitably adjusted the flame was located at the tip of the inner tube, as indicated by the shading in the diagram. With reduced air supply the gas could also be lit at the end of the outer tube, the burner thus resembling somewhat a Smithell's flame separator. The flame, however, showed some unusual characteristics which are best described by giving an account of the appearance of the flame with varying air supply. Using town's gas, with the inner tube drawn about 15 to 18 in. inside the larger tube, and with a ratio of primary to secondary air of about 1 : 3, the following were the principal features of the flame, the various conditions being lettered for convenience of later reference:

air supply	inner cone	outer cone	condition (for later reference)
very little	short blue	long flame with luminous tip	A
little	short bluish green	long non-luminous flame, easily blown out	B
moderate	moderate bluish green	no flame or glow	C_1
fairly fast	fairly long bluish green	blue glow about 8 in. long	D_1
fast	fairly long blue	blue glow only about 2 in. long	E_1
very fast	moderate blue-violet	no glow or flame	F_1

With the primary air supply cut nearly off the appearance of the flame was rather different, being described below:

air supply	inner cone	outer cone	condition
very little	as condition A above		
little	as condition B above		
moderate	fairly long blue, luminous tip	faint luminosity	C_2
fairly fast	very long, extending to end of tube, luminous	luminous jet from end of tube, with blue tip	D_2
fast	as D_2	long smoky luminous jet from end of tube, with blue tip	E_2
very fast	long smoky luminous flame	short smoky jet of flame projecting from end of tube	F_2

The conditions described as D_1 and D_2 were of most interest spectroscopically. The blue glow consisted of a long thin streak of blue luminosity which, unlike the flame in conditions A and B, could not be blown out. This blue streak appeared within a definite, rather narrow, range of air supply; with the inner steel tube only pulled in about 12 in. from the open end of the outer tube, the limits of air supply were widened and condition C_1 was eliminated altogether; if the inner steel tube was drawn further in, the limits of air supply over which the blue streak appeared were narrowed, until, when the tube was about 22 in. in, no such streak could be obtained. This blue glow was not very bright, but could just comfortably be seen in a normally lighted room; it increased in brightness as the inner steel tube was moved out so that the distance between the inner and outer cones was reduced. With a smaller ratio of primary to secondary air the adjustment of the total air supply for the appearance of the blue tip to the luminous jet of flame (condition D_2) was less critical, the luminous jet gradually appearing out of the end of the tube, lengthening, and then shrinking back as the air supply was increased.

It was found that the centring of the inner tube within the outer affected both the appearance of the flame and its spectrum. If the tube was poorly centred, the flame became rather noisy, owing to turbulence, and the blue glow of condition D_1 took on the appearance of jagged tongues of pale blue flame surrounding a non-luminous core; this core gradually became luminous (yellow from incandescent particles) as the ratio of primary to secondary air supply was reduced (condition D_2).

Preliminary spectroscopic investigations showed that the spectrum was influenced by the temperature of the tube, and hence the outer steel tube was fitted with a water-cooling jacket. In order to ensure accurate centring the inner tube was fitted with steel supporting pins. For some experiments similar tubes made of fused silica were used, and in other experiments slight modifications of the steel burner were made; these are described in the next section. For all these burners it was usually necessary, to make the flame strike back on to the inner tube, to thrust the inner tube forward until within an inch or two of the outer end and then to draw it back gently into the required position.

SPECTROSCOPIC OBSERVATIONS

Experimental. Most of the spectra were explored using a small quartz (Hilger E 3) instrument with a wide slit. Ilford Fast Blue Sensitive, Zenith and H.P. 2 plates were used for most of the work and exposure times varied from a few minutes to five hours. A few plates were also taken on a medium size quartz spectrograph (E 2) with normal slit width. All the investigations described in this section were made with town's gas (approximate composition 50 % H_2, 24 % CH_4, 12·5 % CO, 8 % N_2, 2·4 % CO_2 and 2·3 % C_nH_{2n}) as the fast flow of gas and long exposures used such large quantities of gas.

Effect of burner design. The first burner used consisted of steel tubes about 18 in. long which were poorly centred, so that the inner cone impinged slightly on to the inner wall of the outer tube. It was found that in condition D_1 the spectrum of the blue glow consisted chiefly of the hydrocarbon flame bands with relatively weak bands of OH and CH and some CO flame spectrum as background. When, however, a second burner consisting of tubes 3 ft. long, which were accurately centred by supporting pins, was used the spectrum did not show the hydrocarbon flame bands so clearly. This effect was at first associated with the reduced turbulence in the new tube. To test this hypothesis the end of the inner tube was closed and holes were drilled about an inch from the end; with this modification the inner cone did not settle right on to the inner tube, but remained a fraction of an inch from the end of the tube where a very noisy turbulent flame was produced; the spectrum did not, however, show the hydrocarbon flame bands any more clearly, the OH band and CO flame spectrum being the strongest features. Some observations were then made using a burner consisting of two silica tubes (internal diameters ½ and ¾ in.), but with this burner the appearance of the flame was rather different, usually showing slightly luminous because of carbon deposition, and the spectrum only showed the hydrocarbon flame bands weakly on a much heavier background of CO flame spectrum and OH.

Thus it seemed that the occurrence of the hydrocarbon bands depended on either temperature or surface action. A water-cooling jacket was therefore fitted to the outer tube of the 3 ft. steel burner, the inner tube of which was altered back to the original open-end design but with the supporting pins to ensure centring being retained. This resulted in the hydrocarbon flame bands showing up very clearly, thus presumably indicating that their presence was favoured by chilling the inner cone of the flame. This conclusion was checked by direct comparison of the spectra under otherwise similar conditions using the water-cooled tube and the same tube without the cooling on, and also with a silica outer tube which, being a poor thermal conductor, ran very hot. These spectra are shown in plate 44 *a*, *b* and *c*, and clearly show the increase in relative intensity of the hydrocarbon flame bands produced by cooling.

Effect of variation of air supply. Using the water-cooled tube the spectrum of the outer cone of the flame has been studied for the various conditions already listed, and the following is a brief description of the principal features of the spectrum under these conditions of air supply.

Condition *A*. The long blue flame showed a spectrum very similar to that of a just non-luminous Bunsen. The OH bands were very strong with CH bands at 4315 and 3900 A of moderate intensity and weak hydrocarbon flame bands on a weak continuous background, due probably to the CO flame spectrum.

Condition *B*. This was rather similar to the above, but with the hydrocarbon flame bands showing up more clearly, these being especially marked when the inner tube was drawn far in so that the separation between the inner and outer cones was considerable. See plate 44 *d*, *e*.

Condition C_1. No light.

Condition C_2. Probably continuum.

Condition D_1. The blue streak showed the hydrocarbon flame bands clearly, with the OH and CH bands also present. As with condition *B* the hydrocarbon bands were favoured by drawing the inner tube far in, although this decreased the intensity of the spectrum as a whole, necessitating long exposures. See plate 44 *f*, *g*.

Condition D_2. The blue tip to the flame also showed the hydrocarbon flame bands very clearly with a little OH and CH. The spectrum was rather stronger than in condition D_1, enabling a corresponding reduction in exposure times. See plates 44 *h* and 45 *h*. The base of the flame of course showed continuous spectrum from incandescent carbon.

Condition E_1. This showed chiefly the CO flame spectrum with some OH, CH and hydrocarbon flame bands.

Condition E_2. Similar to D_2 but with the blue tip less bright.

Condition F_1. Very little light at all.

Condition F_2. Only continuum in red and orange from hot carbon particles.

Other observations. For comparison with the above spectra plates were also taken of the spectrum of the flame when not struck back. With the air supply just sufficient to render the flame non-luminous the OH bands were strong, with moderate CH and C_2 bands and a fairly strong continuous background (probably CO flame), while the hydrocarbon flame bands were barely detectable. See plate 45*f*. With a full air supply, producing a roaring Bunsen-type flame, the OH, CH and C_2 bands were all strong with the hydrocarbon flame bands rather weak but definitely present. See plate 45*g*.

Using a transparent silica outer tube to the burner the spectrum of the inner cone was studied, but showed no unusual features, being generally the same as that of a Bunsen burner with corresponding conditions of air supply.

The hydrocarbon flame bands, as observed in the spectra of these chilled flames, include both the *A* and *B* groups of bands listed by Vaidya (1934). The separation of the bands into two groups is not supported by any of the author's observations, and is indeed not very obvious in Vaidya's published spectrograms.

CHEMICAL TESTS

In conjunction with the spectroscopic observations described above, some chemical tests were made. The gases were drawn, by suction from a water pump, from a point within the flame of the outer cone about 2 in. from the end of the tube, through a short length of quartz tube into either a few c.c. of testing solution or into distilled water. The gases were bubbled through the testing solution for varying times, but most of the tests were made after a period of 10 min. The quartz sampling tube was cooled by winding a thin coil of copper tubing, through which a flow of water was maintained, round the outside of the quartz tube right up to the tip which was in the flame; this was done to prevent decomposition of peroxides or other unstable substances by the hot walls of the sampling tube.

Aldehydes. Tests with Schiff's reagent showed that there was strong aldehyde formation in the chilled flame, this being strongest in conditions *A* and *B*, but only slight in conditions D_1 and D_2 which were especially favourable for the ethylene flame bands. These tests for aldehydes are summarized with other observations in table 1. The speed of the reaction with Schiff's reagent indicated that the aldehyde was largely present as formaldehyde, but tests with iodine and potassium iodide in caustic potash gave a slight liberation of iodoform, indicating the presence of acetaldehyde and this was confirmed by the formation of a crystalline precipitate with 2, 4-dinitrophenylhydrazine in dilute hydrochloric acid.

Peroxides. Strong peroxide formation occurred in the chilled flame, this being particularly marked in conditions D_1 and D_2. The results are again summarized in table 1, from which it will be seen that the occurrence of peroxides and of the ethylene flame bands behaves in a closely similar manner. The tests for peroxides were at first rather inconsistent until it was found that the test was very sensitive to the initial pH of the distilled water. If this was slightly acid no peroxide was collected, but with neutral or slightly alkaline water the peroxide was rapidly collected under suitable conditions of the flame. The neutral solution liberated a little iodine immediately from potassium iodide, but strong liberation of iodine was only obtained with potassium iodide acidified with acetic acid, and then came up rather slowly. This appears to indicate that there was a little peracid present, but that most of the peroxide was present as an alkyl peroxide. Burning pure ethylene instead of town's gas (see later) only alkyl peroxide appeared to be formed.

Acidity. The solution obtained by bubbling the gases through water for 10 min. was found to be slightly acid, having a pH of about 3 or 4.

Nitrogen peroxide. The acidity of the solution suggested that this might be due to nitrogen peroxide formation. The brown ring test with ferrous sulphate and sulphuric acid, however, gave negative or negligibly weak indications for nitric acid. This test is not a very sensitive one, but it appears safe to conclude that nitrogen peroxide was not present in sufficient quantity to account for the observed acidity or peroxide formation.

Methyl alcohol. This is rather difficult to test for in small quantities. Tests with benzoyl chloride gave no positive indication.

Acetylene. Tests with ammoniacal cuprous chloride solution did not show the formation of copper acetylide.

The results for the tests for aldehydes and peroxides are presented with the spectroscopic observations in table 1. The approximate intensity estimates on a scale of 0 to 5 may be taken as indicating that the result of the test was negative, very weak, weak, moderate, fairly strong, strong, or very strong respectively. The intensity of the hydrocarbon flame bands is estimated relative to the other features of the spectrum and does not take account of the total brightness of the flame.

It was noticed that when burning either town's gas or pure hydrocarbons in the water-cooled burner, an unpleasant smell was produced, this being reminiscent of that given by the exhaust of a petrol motor when starting up.

TABLE 1. CHEMICAL TESTS AND SPECTROSCOPIC OBSERVATIONS ON THE OUTER CONE OF THE FLAMES

fuel	condition	aldehyde	peroxide	hydrocarbon flame bands	other strong features of spectrum
town's gas	*A*	5	3	2	OH, CH
,,	*B* 6 in. in	5	2	2	OH, CH
,,	*B* 20 in. in	5	4	4	OH, CH
,,	*C*	4	3	—	—
,,	D_1	2	5	5	little OH, CH
,,	D_2	4	5	5	little OH, CH
,,	E_1	0	4	3	OH, CO flame
,,	*F*	0	0	—	—
,,	not struck back	3	0	0	CH, OH, C_2
C_2H_4	*A* to *B*	5	2	1	OH, CH
,,	*D*	1	5	5	trace OH, CH
,,	*E* to *F*	0	4	2?	CO flame, OH

ABSORPTION SPECTRA

A T-shaped attachment was fitted to the end of the burner so that the flame was split into two, thus enabling the absorption spectrum of the gases between the end of the inner cone and the outer cones to be examined. A hydrogen discharge tube was used as source of continuum and the spectra were studied with an E 2 quartz instrument using a fine slit and careful adjustment of the spectrograph. The absorption spectrum of the chilled flame in both conditions *D* and *B* showed only a gentle cut-off at the ultra-violet end (from around 2300 A) and only the merest trace of the formaldehyde absorption bands, these latter being doubtfully present. The weak absorption in the far ultra-violet is consistent with the presence of peroxides, but gives little help in identifying the emitter of the hydrocarbon flame bands.

EXPERIMENTS WITH PURE HYDROCARBONS

In addition to the investigations made with town's gas, some similar experiments were also made using pure hydrocarbons as fuel.

Ethylene. This gas behaved in much the same manner as town's gas, except that more primary air was required to prevent the flame being too smoky and luminous. The spectrum of the outer cone of the chilled flame in condition D (intermediate between D_1 and D_2) showed the hydrocarbon flame bands very clearly, both the OH and CH bands being very weak. See plate 45*a*. With this gas the CO flame spectrum came up rather more readily, and was the dominating feature in condition E. Chemical tests showed that aldehydes (mostly formaldehyde) and peroxides were present. With ethylene the collection of the peroxide was not appreciably affected by the pH of the collecting solution; liberation of iodine from KI only occurred from an acidified solution, and then only slowly but very strongly; this seems to indicate that only alkyl peroxide was formed, and that this was not the same peroxide as formed from town's gas (methane). The results are included in table 1.

Butane. This gas also behaved similarly to town's gas. Owing to the slightly lower flame speed it was necessary to reduce the rate of flow of both gas and air slightly. Condition C, in which no outer cone was obtainable, covered a rather greater range of relative air supply than with town's gas. A spectrogram taken in condition B showed the hydrocarbon flame bands rather more clearly than did town's gas under similar conditions. See plate 45*b*.

Methane. Owing to the low flame speed of methane-air mixtures this gas would not strike back in the steel water-cooled burner. Using the wider bore silica burner, spectrograms were obtained of conditions approximating to conditions B and D_1 which showed the hydrocarbon flame bands together with strong OH and CH bands and a little CO flame spectrum. The hydrocarbon flame bands were rather stronger, using the silica burner, for pure methane than for town's gas (consisting of 24 % methane diluted chiefly with hydrogen and carbon monoxide) under similar conditions. Chemical tests again showed fairly strong formation of both peroxide and formaldehyde.

It may thus be concluded that the production of the hydrocarbon flame bands in the spectra of these chilled flames, together with the formation of aldehydes and peroxides, is a general property of hydrocarbons.

EFFECT OF CATALYSTS

Propyl bromide. Propyl bromide is known to act as a negative catalyst (inhibitor) in the combustion of town's gas, and investigations carried out in these laboratories by Dr H. Zentler Gordon show that a few per cent of the vapour reduces the flame speed considerably. The introduction of some propyl bromide vapour was not observed to produce any marked effects on the appearance of the outer cone of the chilled flame, apart from those necessitated by variation of the gas and air supplies because of the reduced flame speed. The spectrum was apparently unaltered in both conditions *B* and *D*, apart from the appearance of a weak band of unknown origin at around 2905 A. The spectrum in condition *B* is shown in plate 45*e*; this spectrogram was rather heavily exposed, and the appearance of the strong C_2 bands is due to this overexposure, and not to any change in the spectrum, as can be seen from the negative.

Ethyl nitrate. Ethyl nitrate is known to act as a positive catalyst (promoter) for the combustion of CO and some other gases. No change in the condition of the chilled flame was observed when the vapour was introduced with the gas supply. In condition *B*, bands of NH and CN made their appearance, and the hydrocarbon flame bands may have been suppressed slightly, although still weakly present. In condition *D* the spectrum was very similar to that of the flame without the introduction of the catalyst, but close examination showed that the λ 3883 band of CN was superposed on the 3900 A band of CH. See plate 45*c*, *d*.

Thus it seems that catalysts had no marked effect on the phenomena peculiar to the chilled flame.

DISCUSSION

These experiments on the spectra of chilled hydrocarbon flames seem to indicate that the production of the hydrocarbon flame bands is associated with the formation of peroxides, probably alkyl peroxides. The occurrence of the bands does not seem to follow the presence of aldehydes in the interconal gases, and, as it has been shown (Bell 1937) that formaldehyde flames do not show the hydrocarbon flame bands, it seems safe to assume that they are produced at some stage of the combustion prior to the formation of formaldehyde.

Numerous possible radicals which might occur in the combustion and breaking up of hydrocarbons can be postulated on either the hydroxylation or peroxide theories of combustion, but the production of the bands from such simple substances as methane, ethylene and acetylene limits the choice considerably.

Bell suggested CH_2 as the emitter of the flame bands, but this suggestion has not received general acceptance. Geib and Vaidya's recent experiments (1941) with atomic oxygen indicate that oxygen is necessary, although it might be argued that atomic oxygen and methane would, on a modified hydroxylation theory (Norrish 1935), give water and CH_2 radicals, which might not be produced by atomic hydrogen; the definite occurrence of the bands in the inner cone of the flame of acetylene (confirmed by own observations) seems, however, to rule out any emitter with more than one hydrogen atom directly linked to the carbon.

Smith (1940) expressed the opinion that the emitter might be an isomeric formaldehyde molecule $CH.OH$. The formation of this by collision of OH and CH radicals would probably require the presence of a third body which would also then probably stabilize the new molecule to formaldehyde itself; it is shown in the present work that formaldehyde is not necessarily associated with the production of the bands. Moreover there is no record of the occurrence of the hydrocarbon flame bands in discharge tubes although such sources may produce both CH and OH strongly.

Vaidya (1934, 1941) has provisionally assigned the bands to the radical HCO. This seems quite reasonable if the bands are produced by the decomposition of peroxides. It is known spectroscopically that radicals of CH are produced in the breaking up of hydrocarbons, either by combustion or in electric discharges, and thus peroxides may well be expected to break up into radicals such as HCO or HCO_2. Professor Egerton has suggested that, for example, methane might first form an unstable complex $CH_4.O_2$ which might then either stabilize into the alkyl peroxide CH_3OOH, which is rapidly decomposed at high temperatures, or might break down into $HCO+H_2+OH$. The chilling of the flame, which would slow down the decomposition of the peroxide, would enable this to be carried through to the outer cone of the flame where its subsequent combustion would account for the appearance of the hydrocarbon flame bands in the spectrum of the outer cone. Thus it may be concluded that an explanation of the present experiments can be given which is consistent with the emitter of the hydrocarbon flame bands being HCO, which may be produced in the decomposition of peroxidic substances, but it must be admitted that alternative explanations cannot be entirely ruled out. The experiments are being continued.

In conclusion I should like to express my sincere thanks to Professor A. C. Egerton and to Dr D. M. Newitt for their interest in the work and for their many helpful suggestions, and to Dr H. E. Edulgee for advice and assistance with some of the chemical tests.

References

Bell, J. 1937 *Proc. Roy. Soc.* A, **158**, 429.
Gaydon, A. G. 1940 *Proc. Roy. Soc.* A, **176**, 505.
Gaydon, A. G. 1941 *Proc. Roy. Soc.* A, **178**, 61.
Geib, K. H. and Vaidya, W. M. 1941 *Proc. Roy. Soc.* A, **178**, 351.
Norrish, R. G. W. 1935 *Proc. Roy. Soc.* A, **150**, 36.
Smith, E. C. W. 1940 *Proc. Roy. Soc.* A, **174**, 110.
Vaidya, W. M. 1934 *Proc. Roy. Soc.* A, **147**, 513.
Vaidya, W. M. 1941 *Proc. Roy. Soc.* A, **178**, 356.

Description of plates 44, 45

All the plates were taken on a small quartz spectrograph with (except for plate 45*h*) a rather wide slit. Plates 44*e*, 44*h*, and 45*b*–*h* were taken on Fast Blue Sensitive plates, and the remainder on Zenith plates. All the plates are of burning town's gas except 45*a* and 45*b* which are of ethylene and butane respectively. The distance in inches refers to the separation between the two cones of the flame.

The following are the exposure times in minutes: 44*a*, 60; *b*, 60; *c*, 20; *d*, 15; *e*, 15; *f*, 5; *g*, 60; *h*, 225; 45*a*, 35; *b*, 20; *c*, 15; *d*, 20; *e*, 15; *f*, 8; *g*, 4; *h*, 150.

A stress-strain curve for the atomic lattice of mild steel, and the physical significance of the yield point of a metal

By S. L. Smith, D.Sc., F.C.G.I., *Engineering Department*
and W. A. Wood, D.Sc., *Physics Department*
National Physical Laboratory, Teddington, Middlesex

(*Communicated by Sir Edward Appleton, F.R.S.—Received* 29 *May* 1941)

[Plate 46]

A stress-strain curve is obtained for the atomic lattice of mild steel subjected to tensile stress. A set of atomic planes is selected of which the spacing is practically perpendicular to the direction of the stress applied to the tensile test specimen, and which should contract with the cross-section as the specimen extends along its length. It is shown that up to the external yield point the lattice spacing contracts in proportion to the applied stress in conformity with Hooke's Law; but at the external yield point, instead of a continued contraction, the spacing undergoes an abrupt expansion. As the stress is still further increased, the lattice dimension remains approximately constant in the expanded condition. It is further shown that the sudden

a

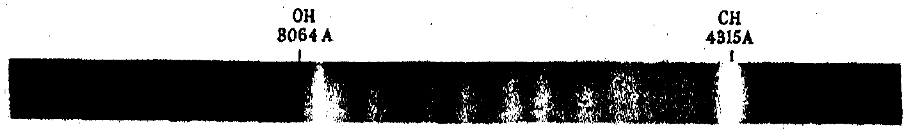

condition D 16 in. in, water-cooled

b

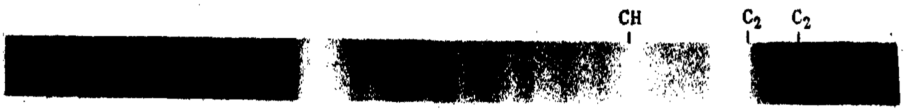

condition D 16 in. in, not cooled

c

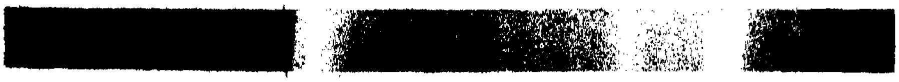

condition D 16 in. in, silica tube running hot

d

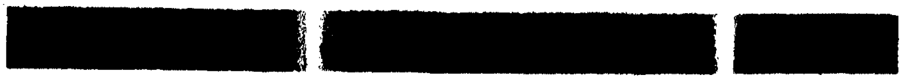

condition B 12 in. in

e

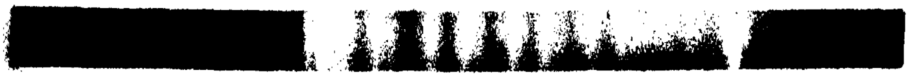

condition B 33 in. in

f

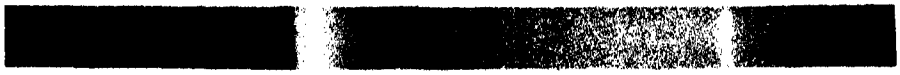

condition D_1 12 in. in

g

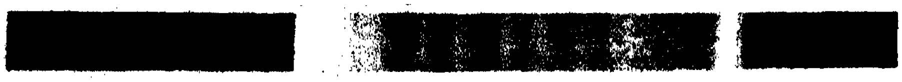

condition D_1 16 in. in

h

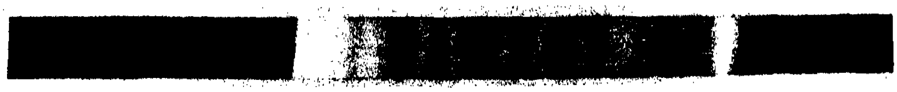

condition D_2 21 in. in

a

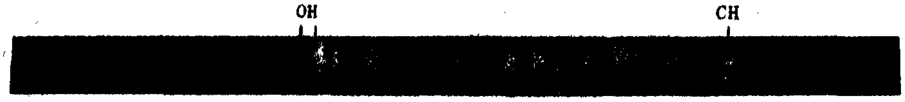

ethylene, condition *D* 16 in. in

b

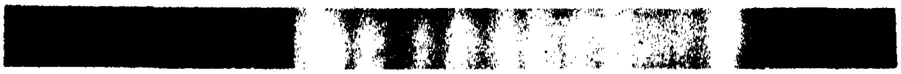

butane, condition *B* 14 in. in

c

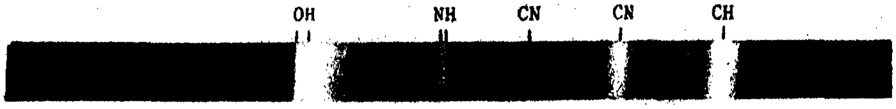

with ethyl nitrate, condition *B* 14 in. in

d

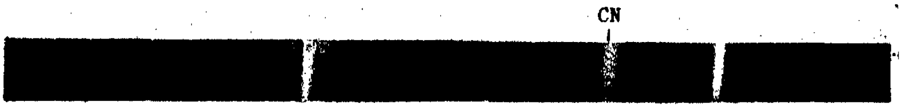

with ethyl nitrate, condition D_2 18 in. in

e

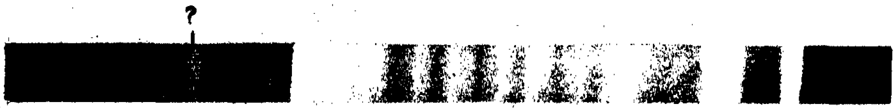

with propyl bromide, condition *B* 14 in. in

f

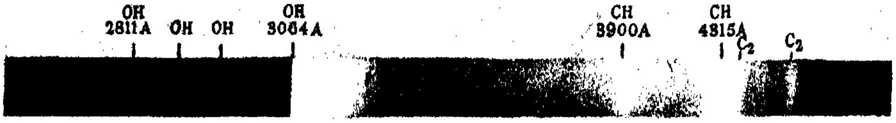

burner not struck back, just non-luminous

g

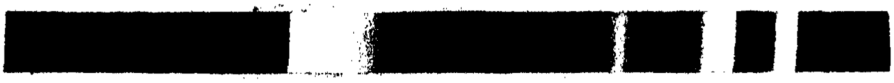

burner not struck back, roaring

h

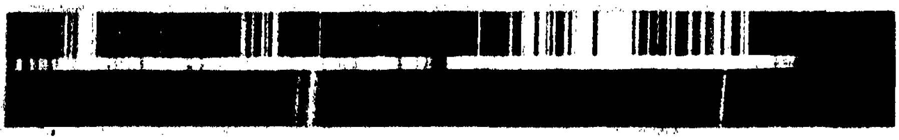

condition D_2 20 in. in, fine slit and iron arc comparison

expansion which sets in at the yield point while the specimen is under load is fully retained as the load is removed. Also that with the application of increasing stress, the permanent expansion imposed on the lattice spacing systematically increases up to the ultimate stress preceding fracture. It is found in addition that the sharp changes in the lattice spacing at the yield are accompanied by a striking drop in the intensity of the X-ray diffraction ring on which the spacing measurements are based. The experiments have established that the atomic lattice of a metal itself possesses a yield point which marks the onset of permanent lattice strains of an unexpected character and of direct technical interest in connexion with the mechanical properties of metals.

INTRODUCTION

In recent work a stress-strain curve for the atomic lattice of pure iron subjected to tensile stress was determined (Smith and Wood 1940*a*, 1941). This curve gave the displacement of the atoms from their normal positions in the lattice under stress, and the extent of their recovery when at any point the stress was removed. The results revealed some of the principles governing the response of a metallic lattice to applied stresses.

In these experiments, specimens were stretched under tensile loading. For convenience of technique, the lattice measurements were concerned with the related contraction which takes place at right angles to the stress direction; they referred in particular to the spacing of atomic planes which lay approximately parallel to the stress direction, and which would be brought closer together as the specimen extended and the cross-section diminished. The main features of the results may be summarized here for reference:

(1) Up to the external yield point, the spacing of the atomic planes contracted in proportion to the applied stress. When the stress was removed the lattice reverted to its original dimensions. In this range the lattice obeyed Hooke's Law.

(2) Beyond the external yield point, the contraction of the spacing slowed down as the stress was increased and quickly reached a limit.

(3) When in this latter range the stress was removed, the lattice spacing did not return to its original value, but passed through that figure and attained a value greater than the original. The lattice was left with a permanent expansion. The magnitude of this expansion grew systematically as the stress applied to the specimen increased and the cross-section diminished.

The first point might have been anticipated. The second and third indicated mechanical properties of the lattice not previously observed. A striking inference was that the increase in apparent elastic range, here contraction, which may be exhibited by a metal as the stress exceeds the yield point, does not arise because the atoms can be forced closer and closer together, but because they begin their movement from positions which are further and further apart.

In the present work, these experiments are extended to mild steel. They demonstrate a further result, that the lattice of a metal possesses a 'yield point'.

EXPERIMENTAL

The apparatus employed was a combined tensile testing machine and back-reflexion X-ray spectrometer, recently designed for these researches. The principles of the apparatus have been described in a previous paper (Smith and Wood 1940*b*). The changes in external dimensions of a specimen are given by an extensometer attachment. The changes in a selected atomic spacing are measured by changes in diameter of a sensitive X-ray diffraction ring obtained whilst the specimen is loaded to known stresses.

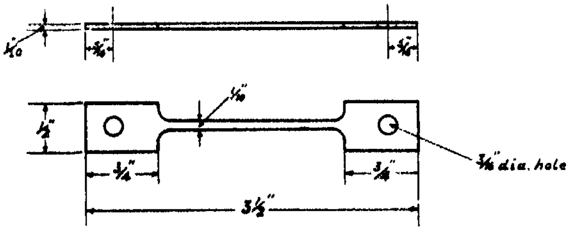

FIGURE 1. Shape and dimensions of X-ray and tensile test piece.

The material used was a mild steel (0·1 % C), received in the normalized condition and given a further heat treatment at 950° C for 15 min. and air cooled. The specimens were machined to the shape and dimensions shown in figure 1, after which they were subjected to a second heat treatment in vacuo similar to the first, and then etched. The sharpness of the X-ray reflexions from the grains of the test pieces indicated that the structure was reasonably free from distortion before the experiments were commenced.

The results are best described by considering (*a*) the external tensile stress-strain curve of the material, (*b*) the lattice stress-strain curve, and (*c*) the changes under slow cycles of stress.

External stress-strain curve

The tensile stress-strain curve for a typical specimen is given in figure 2. In addition to measurements on the special test pieces, other measurements were made in a standard tensile testing machine on specimens of circular cross-section. From these, Poisson's ratio was also determined. The characteristics of the curve differ from those of the pure iron previously examined (Smith and Wood 1941); the steel exhibits a longer range of primitive elasticity and a much more marked yield, features which are specially relevant to the aims of the present work. The principal mechanical data were:

Young's modulus	$1 \cdot 3 \times 10^4$ tons/sq. in.
Poisson's ratio	0·28
Yield stress	16·8 tons/sq. in.
Ultimate stress	27·7 tons/sq. in.

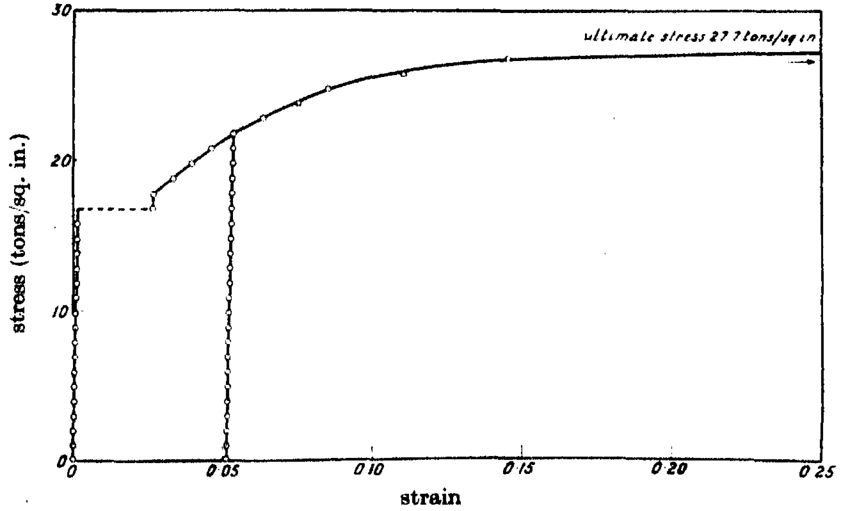

FIGURE 2. External tensile stress-strain curve.

Lattice stress-strain curve

In studying the changes in lattice dimensions, it is most convenient to direct the X-ray beam at right angles to the length of the specimen, in order to avoid the grips attached to the ends of the test piece. The measurements are then related to the contraction in cross-section which occurs as the specimen is stretched.

A further point is that whereas the external measurements represent an integrated effect over a large number of anisotropic grains, each of which will behave differently according to its crystallographic orientation relative to the stress direction, the X-ray measurements automatically divide the grains into groups, and refer to one group at a time. A group is characterized by the feature that each member behaves in a similar manner since it possesses the same orientation with respect to the incident X-ray beam, in order to satisfy the Bragg condition for reflexion on to a particular

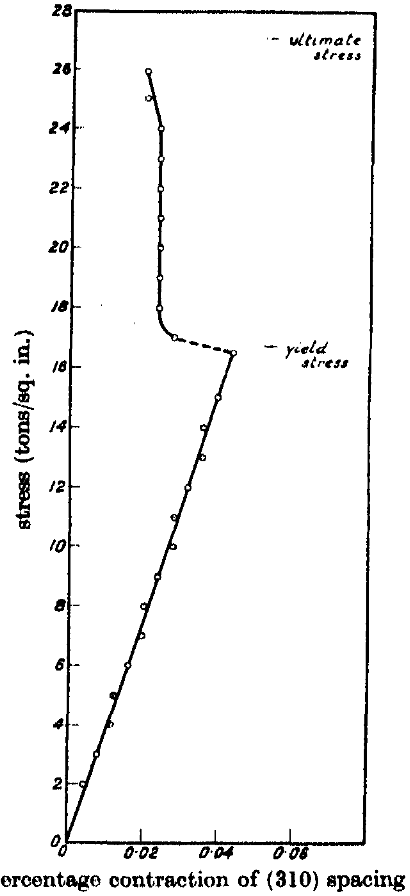

FIGURE 3. Lattice stress-strain curve. Relation of percentage contraction of (310) planes, practically perpendicular to stress direction, to applied stress.

diffraction ring. In the present experiments, using cobalt K radiation, the group of grains involved was that in each of which the (310) atomic planes were inclined at $\frac{1}{2}\pi - 9^\circ$ to the incident beam, or 9° to the length of the specimen. These may therefore be regarded as approximately parallel to the stress direction, and the perpendicular spacing between them should contract as a load is applied to the specimen. This spacing change plotted against the applied tensile stress then gives the lattice stress-strain curve shown in figure 3. This curve suffices to illustrate the points in the behaviour of the atomic lattice to which it is desired to draw attention.

It will be seen that at a definite stress, the curve shows a strongly marked discontinuity. Below this stress, the lattice spacing contracts linearly with increasing load. At the critical stress, instead of a continued contraction, the spacing undergoes an abrupt expansion. As the stress is further increased, the lattice dimensions remain approximately constant in their expanded condition.

This discontinuous change occurs simultaneously with the external yield. As indicated previously, the mild steel exhibits a particularly well-defined external yield. By taking advantage of this feature, and showing that the lattice spacing exhibits a correspondingly abrupt change at the same stress, the relation between the external yield and the newly observed lattice changes may be regarded as established.

The external yield is defined not only by the increase in the rate of external deformation with stress but also by the onset of a different process of deformation, the plastic strain, caused by the relative translation of large groups of atoms within each grain by irreversible processes of slip and fragmentation. The above experiments show that the lattice change at a yield stress is also marked both by a discontinuity in the rate of deformation and by the appearance of entirely new factors in the mechanism of internal deformation. Therefore the lattice also possesses a true 'yield point'. We propose to term this the 'lattice yield point'.

Irreversible lattice strains

The results described in the present section show that the expansion of spacing observed at the lattice yield point becomes permanently superimposed on the lattice dimensions.

Specimens were taken through slow cycles of stress and photographed at the peak stress and at the zero stress between each cycle. After an initial photograph under zero stress, the specimen was photographed under the load of 1 ton/sq. in. and then again at zero stress when this load had been removed. The specimen was next photographed at the stress 2 tons/sq. in. and then again at zero stress. The process was continued until fracture, photographs thus being obtained at the following sequence of stresses: 0; 1, 0; 2, 0; 3, 0; ... tons/sq. in. It was possible that the treatment imposed in this way on the structure of the specimens before the yield point was reached might have modified the characteristics of the yield. With other specimens therefore the preliminary cycles were omitted, and the first cycle was made between zero stress and a load just below the yield. Also, with further specimens, particular cycles were examined in greater detail; photographs were taken at intermediate points on both the increasing and decreasing halves of the stress cycle. The time taken for a photograph was of the order of 10 min., and a specimen was held at each point of examination for about 20 min. before the next point was taken. The results are conveniently set out in the lattice stress-strain diagram shown in figure 4.

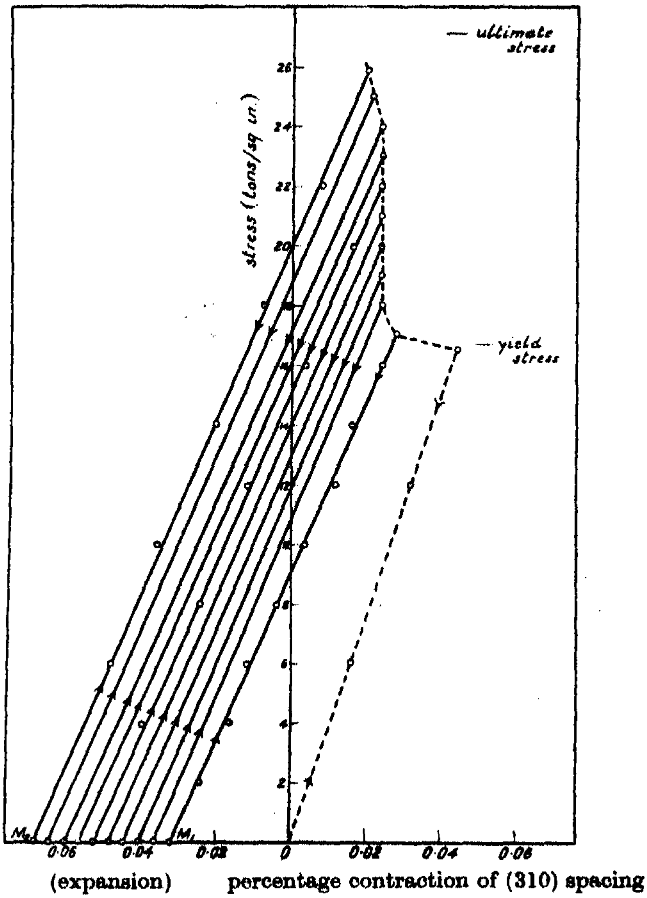

FIGURE 4. Changes in (310) spacing on loading and unloading of tensile specimens.

The main feature of interest occurs at the lattice yield point. Below this stage the atomic displacements are reversible. At the critical point,

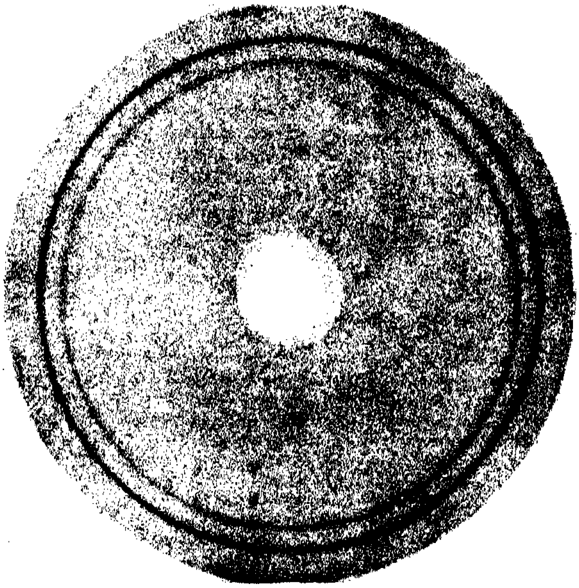

FIGURE 5. Before yield.

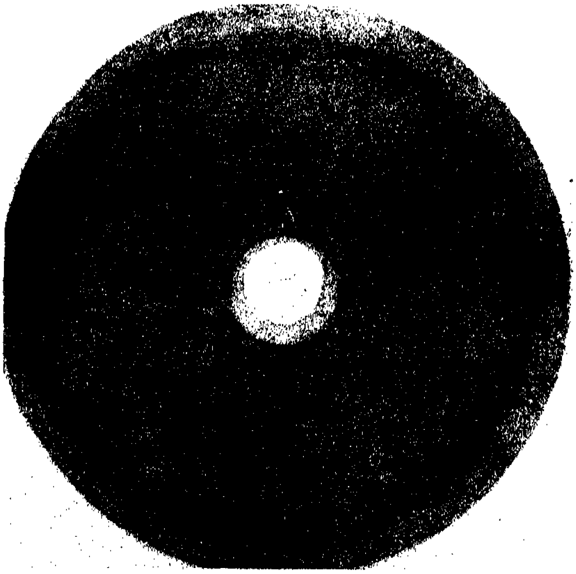

FIGURE 6. After yield.

FIGURES 5 and 6, obtained under identical conditions, illustrate the drop in intensity of X-ray reflexion which occurs when the tensile specimen passes through the yield point.

(Facing p. 457)

the expansion of spacing which sets in sharply while the specimen is under load is fully retained as the load is removed. The change is shown by OM_1 in figure 4. As the stress is further increased, the permanent expansion imposed on the lattice spacing grows from OM_1 to OM_2, the value obtained after the ultimate stress had been applied to the specimen. In this latter respect, the behaviour of the mild steel resembles that of the pure iron previously investigated. In the iron, however, the internal lattice strain set in less abruptly; there was no large jump corresponding to OM_1. The difference appears to be due to the fact that the external yield was much less marked than in the mild steel.

The curve again illustrates the interesting point that, after the yield point, as the stress to which the specimen has been subjected is increased, so the permanent expansion imposed on the lattice after that stress is removed becomes greater. The actual change in dimensions exhibited by the lattice under a particular stress is then the resultant of the permanent expansion and the ordinary reversible elastic contraction. The permanent expansion effect, however, increases with the higher stress values at such a rate that the resultant contraction observed never exceeds a limiting value. There is thus a limit to the contraction of the lattice under stress. Also, the apparent increase in elastic range at the higher stresses arises because the atoms move between the position of limited contraction and a continually expanded zero position. The lattice expansion effect thus plays a primary part in determining the mechanical properties of a metal.

Effect of yield on X-ray diffraction intensities

In addition to the sharp changes in the lattice spacings at the yield, it was found that the intensity of the (310) diffraction ring under observation exhibited a marked drop.

The effect is amply illustrated on comparison of figures 5 and 6 (plate 46); figure 5 shows the diffraction ring when stressed to a value just before yield, and figure 6 immediately after yield, the exposure conditions being the same. To ensure constancy in reproduction, the original negatives have been printed and subsequently processed simultaneously. For studying the intensity changes of this type, a check was kept on the output of the X-ray tube so that the exposure given to the specimen should be standardized. The X-ray tube possessed two windows on opposite sides and symmetrically placed with respect to the focal line on the target. On one side of the tube was the X-ray and tensile testing apparatus, and on the other a second X-ray back-reflexion spectrometer. A standard specimen in this spectrometer could thus be exposed simultaneously with the test specimen. The intensity of the diffraction ring from the standard thus bore, for all practical purposes, a constant ratio to that from the test specimen. If the intensity from the standard was the same in the two exposures given, for instance, to the test specimen before and after yield, then it could be safely assumed that changes in intensity of reflexion from the latter were due only to changes in the specimen itself. This was the case in figures 5 and 6. Actually the change is large, and well beyond possible experimental error. In fact, it was necessary to increase the intensity of reflexion from a specimen after yield had occurred by doubling the power put through the X-ray tube in order to bring up the intensity to the same order as that of the diffraction rings obtained before yield, so that the diameters might be effectively measured. The drop in intensity at the yield point is of the order of 50 %. In practice, the intensity changes may ultimately prove a more sensitive indicator of the permanent lattice strains than the changes in lattice spacing. Also they may be more easily applied in technical testing, since the intensity measurements do not call for the exacting experimental conditions required to measure small spacing changes.

The effect of the lattice yield on the X-ray spectrum is thus analogous to the effect of raising the temperature of the specimen. Each would produce an expansion of spacing, and each would cause a reduction in the peak intensity of the X-ray diffraction ring.

Quantitative measurements

The relation between the diameters of the diffraction rings from the (310) planes and the spacing of the planes was linear within the range of variation. A change of 1 mm. in diameter corresponded to a percentage change of spacing of 0·037 %.

The following measurements are of special interest:

(i) In the initial elastic range of the lattice stress-strain curve the contraction of the (310) spacing per unit increase of stress (ton/sq. in.) is $0{\cdot}0027_5$ %.

This value obtains when the planes are inclined at 9° to the length of the specimen. The corresponding contraction if the planes were actually parallel to the length of the specimen, and their spacing thus perpendicular to the stress direction, should be given approximately by dividing by cos 9°. The contraction is then 0·0028 %.

(ii) The corresponding external elastic contraction of the specimen, also in the direction perpendicular to the stress direction, is given by the measured extension and Poisson's ratio. This value of the contraction is

0·0022 %. It will be noted that the value is not identical with (i), a difference ascribed to the fact that the grains are not isotropic.

(iii) The permanent expansion of spacing which sets in at the lattice yield point, OM_1 in figure 4, is 0·03 %.

The magnitude finally reached by the permanent expansion effect prior to fracture, OM_2 in figure 4, is 0·07 %. This expansion is actually greater than the maximum elastic contraction which is reached under the stress of 16 tons/sq. in. near the extreme of the initial elastic range. The figure for the contraction at that point is 0·04 %. As a matter of interest, taking the linear coefficient of expansion as 11×10^{-6}, the rise in temperature required to produce the expansion OM_2 would be 64° C.

DISCUSSION

The observations described in this paper clearly establish the presence of a yield point in the atomic lattice of a metal under stress, and the existence of significant properties of the lattice itself which are revealed at the yield point. These results mark a definite step in the recent studies on the structure of a metal in relation to its mechanical properties. It may be of interest at this stage to summarize some of the points which have emerged and which appear to play a leading part in the behaviour of the metallic state.

First is the existence of a lower limiting crystallite size. It has been established that the grains break down rapidly on plastic deformation into component parts of widely varying orientations, but this fragmentation does not proceed beyond a definite lower limit of size, depending on the metal. This indicates potential units of structure in the metallic grain; these have been termed crystallites (Wood 1939).

Secondly, there is a characteristic sequence in the structural changes on deformation. Up to the yield point, the degree of fragmentation is negligible. The break-down commences at the yield and approaches the limit as the fracture stage is reached. After very severe deformation, such as that obtainable by such processes as cold rolling, the crystallites finally assume a well-defined preferred orientation (Wood 1932, 1940).

Thirdly, there is a speed effect. It has been shown that the fragmentation may be inhibited under alternating stresses when the frequency of alternation is high, even though the peak of the cycle employed is considerably in excess of the static yield point of the material (Wood and Thorpe 1940).

Fourthly, the grains in a polycrystalline metal under stress may change in dimensions at different rates. The percentage change of dimensions measured in a given direction will then vary from grain to grain according to its crystallographic orientation relative to the direction of the applied stress (Smith and Wood 1940*b*). Consequently a critical condition will develop at the boundaries of neighbouring grains which have different orientations. We have suggested that this condition may be the cause of the abrupt fragmentation which is a feature of the yield point, where the grains attempt to preserve continuity of structure by forming a set of intermediate orientations. In this connexion it is of interest to note that the extent of the fragmentation for a given degree of plastic deformation is more marked in a polycrystalline metal than in a single large metal crystal; in the latter the rate of deformation from point to point is not complicated by abrupt changes in crystallographic orientation. It is further of interest that by assuming a preferred orientation after particularly severe deformation, as indicated above, the crystallites tend to revert a polycrystalline specimen to the form of a single crystal, and thereby again diminish the disruptive effect of the differential rate of strain from point to point.

Finally, we have the new aspects, as described in the present paper, which arise from direct examination of the behaviour of the atomic lattice itself whilst under load; of these, perhaps the most important is the observation of a lattice yield point and the systematic growth in the lattice of an internal strain which is stable at room temperature and which is of immediate interest in the technical testing of metals.

The work described above has been carried out as part of the research programme of the National Physical Laboratory, and this paper is published by permission of the Director of the Laboratory.

REFERENCES

Smith, S. L. and Wood, W. A. 1940*a* *Nature, Lond.*, **146**, 400.
Smith, S. L. and Wood, W. A. 1940*b* *Proc. Roy. Soc.* A, **176**, 398.
Smith, S. L. and Wood, W. A. 1941 *Proc. Roy. Soc.* A, **178**, 93.
Wood, W. A. 1932 *Phil. Mag.* **14**, 656.
Wood, W. A. 1939 *Proc. Roy. Soc.* A, **172**, 231.
Wood, W. A. 1940 *Proc. Phys. Soc.* **52**, 110.
Wood, W. A. and Thorpe, P. L. 1940 *Proc. Roy. Soc.* A, **174**, 310.

An elementary theory of thermal diffusion

By R. Fürth
The University, Edinburgh

(*Communicated by M. Born, F.R.S.—Received* 6 *June* 1941.—
Revised 31 *July* 1941)

Although a rigorous theory of thermal diffusion has been developed by Chapman and Enskog, it is desirable to have an approximate but elementary theory which reveals the physical mechanism of the phenomenon. This is given in the present paper by the application of a method similar to that used by Meyer for the treatment of ordinary diffusion in gases. It leads to an approximate formula for the thermal diffusion ratio, a discussion of which shows that it accounts for many of the characteristic properties of thermal diffusion.

1. The phenomenon of thermal diffusion in gases, although theoretically predicted by Enskog in 1912, and independently by Chapman in 1916, and for the first time observed by Chapman and Dootson in 1917, did not particularly attract the attention of physicists. It was only regarded as a curious effect, perhaps usable for the determination of the field of force surrounding molecules. Clusius and Dickel (1938, 1939) have recently applied it as a method of separation of gaseous mixtures, and it is now considered as the most effective device for this purpose, and is in operation in many laboratories.

It is always desirable that the experimenter investigating or using a certain phenomenon should be in a position to understand the fundamental principles of the underlying theory. It seems that this need is not often met in the case of thermal diffusion owing to the great difficulties of the general kinetic theory of non-uniform gases on which the theory of thermal diffusion is based. Although the strict theory of ordinary diffusion is not simpler, an elementary theory of this phenomenon had been given long ago (Meyer 1877), which is easily understandable by every physicist and the results of which are in fairly good agreement with the results of the rigorous theory. It is hard to comprehend why the theory of thermal diffusion, a phenomenon not less conspicuous than ordinary diffusion, should be unexplainable from an elementary point of view (see e.g. Chapman 1928). It can indeed be shown that a satisfactory elementary theory of thermal diffusion can be given on almost the same lines as the elementary theory of ordinary diffusion, and that the results of this treatment agree well with the results of the rigorous theory in all significant aspects.* It should be kept in mind, however, that this theory, like any other elementary theory of a rather complicated phenomenon, can by no means be regarded as a complete equivalent of the strict theory as given, for instance, in the book by Chapman and Cowling on the theory of non-uniform gases (1939), which should be consulted by everyone who wishes to refer to the more rigorous treatment.

2. Thermal diffusion, like all the other transport phenomena, is essentially due to the deviations in non-uniform gases from the Maxwellian law of distribution of molecular velocities in uniform gases. Accordingly the rigorous theory starts by deriving this distribution law which is then applied to the treatment of the phenomenon in question. The elementary theories of 'transport phenomena' use the method of mean free paths which assumes that all the particles colliding with each other in a certain volume element obey Maxwell's distribution law relating to the local density and temperature, and that they are able to carry the attribute of this distribution over a certain distance, the mean free path. Hence the actual velocity distribution at a certain point results from the superposition of the frequencies of the velocities of all the molecules coming from volume elements within the range of the free path where they have undergone their last collisions. It will therefore generally be different from Maxwell's distribution. Although this procedure is not rigorous and is open to some criticism (Chapman 1928) it has the advantage of revealing clearly the physical mechanism of the phenomenon, and it will therefore be adopted in the present paper.

3. Let us consider a mixture of two ideal gases at rest, each consisting of identical molecules of mass m_1 and m_2 respectively. Let n_1 be the average number of molecules of the first kind and n_2 the corresponding number of molecules of the second kind, both varying in space. I further assume that the pressure p is uniform throughout the system, but that the temperature T is not uniform, being a given function of the co-ordinates. I finally assume that within a sufficiently small region the equipartition law is satisfied relating to the local temperature for all the molecules colliding with each other in this region. Thus

$$m_1 v_1^2 = m_2 v_2^2 = 3kT, \tag{1}$$

$$(n_1 + n_2)\,kT = p = \text{constant}. \tag{2}$$

---

* After this paper had been completed I noticed a publication of L. J. Gillespie (1939) in which he also tries an elementary treatment of the thermal diffusion process. The methods used, however, are too primitive, and the results therefore do not account for the dependence of the effect on the size of the particles and their mutual forces.

Here v_1^2, v_2^2 are the mean squares of the thermal velocities $\mathbf{u}_1$, $\mathbf{u}_2$ of the two kinds of molecules. As usual in elementary kinetic theories, we shall identify v_1 and v_2 with the average of the speeds u_1, u_2 of the thermal motion of the two kinds of particles; by this simplification the final result is affected only by a slight change in the numerical factor. On the thermal velocities of the molecules there will be generally superposed a common stream velocity $\mathbf{v}$, relative to which the distribution of the thermal velocities is assumed to be of spherical symmetry.

I now suppose that n_1, n_2 and T, and consequently also v_1, v_2, as functions of the co-ordinates x, y, z, can be developed in power series in the vicinity of any point P inside the gas; this point can always be chosen as origin of co-ordinates. If the variation of these quantities in space is sufficiently small, all terms of u higher than the first order within a distance from the origin of the order of magnitude of a mean free path can be neglected. Hence

$$\left.\begin{aligned} n_i &= n_i^0+\left(\frac{\partial n_i}{\partial x}\right)_0 x+\left(\frac{\partial n_i}{\partial y}\right)_0 y+\left(\frac{\partial n_i}{\partial z}\right)_0 z \\ v_i &= v_i^0+\left(\frac{\partial v_i}{\partial x}\right)_0 x+\left(\frac{\partial v_i}{\partial y}\right)_0 y+\left(\frac{\partial v_i}{\partial z}\right)_0 z \end{aligned} \quad (i = 1, 2).\right\} \tag{3}$$

The average surplus number $\nu_1^0 d\omega$ of particles of the first kind, passing in unit time through an element of area $d\omega$ of the y-z-plane around P in the direction of increasing x, over the number of particles crossing in the opposite direction, is given by

$$\nu_1^0 = \overline{[n_1(\mathbf{v}+\mathbf{u}_1)_x]} = v_x \, . \, \overline{n_1}+\overline{(n_1 u_{1x})} \tag{4}$$

where the bar denotes averaging over all the particles crossing $d\omega$.

On account of the supposed symmetrical distribution of the local thermal velocities, this is equivalent to the average over all the volume elements in position $\mathbf{r}(x, y, z)$ from which the molecules transfer the physical quantities connected with them through $d\omega$. Let l_1 be the mean distance over which the molecules travelling in the direction $\mathbf{r}$ carry the attribute n_1 of their distribution, and l_1' the analogous mean distance for carrying the quantity v_1. Using the developments (3) and introducing the direction cosines a, b, c of $\mathbf{r}$, we have the expressions

$$\left.\begin{aligned} n_1 &= n_1^0-\left(\frac{\partial n_1}{\partial x}\right)_0 l_1 a-\left(\frac{\partial n_1}{\partial y}\right)_0 l_1 b-\left(\frac{\partial n_1}{\partial z}\right)_0 l_1 c, \\ u_{1x} &= v_1 . a = v_1^0 a-\left(\frac{\partial v_1}{\partial x}\right)_0 l_1' a^2-\left(\frac{\partial v_1}{\partial y}\right)_0 l_1' ab-\left(\frac{\partial v_1}{\partial z}\right)_0 l_1' ac, \end{aligned}\right\} \tag{5}$$

which are to be substituted in (4). We thus have averaged over all possible distances r and over all possible values of the thermal velocities in the direction a, b, c.

In this way I obtain

$$\begin{aligned}\nu_1^0 = v_x\Big[n_1^0 - \left(\frac{\partial n_1}{\partial x}\right)_0 (\overline{l_1 a}) - \left(\frac{\partial n_1}{\partial y}\right)_0 (\overline{l_1 b}) - \left(\frac{\partial n_1}{\partial z}\right) (\overline{l_1 c})\Big] + n_1^0 v_1^0 . \bar{a} \\ - l_1 v_1^0\Big[\left(\frac{\partial n_1}{\partial x}\right)_0 \overline{a^2} + \left(\frac{\partial n_1}{\partial y}\right)_0 (\overline{ab}) + \left(\frac{\partial n_1}{\partial z}\right)_0 (\overline{ac})\Big] \\ - l_1' n_1^0\Big[\left(\frac{\partial v_1}{\partial x}\right)_0 \overline{a^2} + \left(\frac{\partial v_1}{\partial y}\right)_0 (\overline{ab}) + \left(\frac{\partial v_1}{\partial z}\right)_0 (\overline{ac})\Big],\end{aligned} \tag{6}$$

where the bars now denote averaging over all possible directions.

l_1 and l_1' will generally depend on a, b, c, for they depend on n_1, n_2, v_1, v_2. Since according to our assumption the variation of these quantities in dimensions of the order of magnitude l_1 and l_1' is only very slight this dependence can be neglected within the limits of the approximation adopted. However l_1 and l_1' will generally differ according to the different definitions for them given above.

Because all the averages in (6) vanish by reasons of symmetry with the exception of $\overline{a^2} = 1/3$, it follows that

$$\nu_1 = v_x n_1 - \tfrac{1}{3} l_1 v_1 \frac{\partial n_1}{\partial x} - \tfrac{1}{3} l_1' n_1 \frac{\partial v_1}{\partial x}, \tag{7}$$

where the superficies have been omitted since P can be an arbitrary point of the system. Similarly we get for the particles of the second kind

$$\nu_2 = v_x n_2 - \tfrac{1}{3} l_2 v_2 \frac{\partial n_2}{\partial x} - \tfrac{1}{3} l_2' n_2 \frac{\partial v_2}{\partial x}. \tag{8}$$

ν_1 represents the current density of a flow of particles of the first kind in the positive x-direction, the speed of which is equal to ν_1/n_1; similarly the speed of the flow of particles of the second kind is ν_2/n_2. The rate of mutual diffusion is usually measured by the difference q_{12} of these speeds

$$q_{12} = \nu_1/n_1 - \nu_2/n_2. \tag{9}$$

Hence, substituting from (7) and (8) into (9),

$$q_{12} = -\frac{1}{3}\left(\frac{l_1 v_1}{n_1}\frac{\partial n_1}{\partial x} - \frac{l_2 v_2}{n_2}\frac{\partial n_2}{\partial x}\right) - \frac{1}{3}\left(l_1' \frac{\partial v_1}{\partial x} - l_2' \frac{\partial v_2}{\partial x}\right). \tag{10}$$

We now introduce the molar fractions of the two components defined by

$$\gamma_1 = \frac{n_1}{n_1+n_2}, \quad \gamma_2 = \frac{n_2}{n_1+n_2}, \tag{11}$$

which satisfy the identity $\qquad \gamma_1+\gamma_2 = 1. \qquad (12)$

According to (2) we have therefore

$$n_1 = \frac{\gamma_1 p}{kT}, \quad n_2 = \frac{\gamma_2 p}{kT}. \tag{13}$$

By means of (1) and (13) the derivatives of the n's and the v's appearing in equation (10) can be expressed in terms of the derivatives of the γ's and T which are observable quantities, namely

$$\left.\begin{aligned} \frac{\partial v_1}{\partial x} &= \frac{1}{2}\sqrt{\left(\frac{3k}{m_1}\right)}\frac{1}{\sqrt{T}}\frac{\partial T}{\partial x}, \\ \frac{\partial v_2}{\partial x} &= \frac{1}{2}\sqrt{\left(\frac{3k}{m_2}\right)}\frac{1}{\sqrt{T}}\frac{\partial T}{\partial x}, \end{aligned}\right\} \tag{14}$$

$$\left.\begin{aligned} \frac{v_1}{n_1}\frac{\partial n_1}{\partial x} &= \sqrt{\left(\frac{3k}{m_1}\right)}\left(\frac{\sqrt{T}}{\gamma_1}\frac{\partial \gamma_1}{\partial x} - \frac{1}{\sqrt{T}}\frac{\partial T}{\partial x}\right), \\ \frac{v_2}{n_2}\frac{\partial n_2}{\partial x} &= \sqrt{\left(\frac{3k}{m_2}\right)}\left(\frac{\sqrt{T}}{\gamma_2}\frac{\partial \gamma_2}{\partial x} - \frac{1}{\sqrt{T}}\frac{\partial T}{\partial x}\right). \end{aligned}\right\} \tag{15}$$

Substituting from here into (10), by means of (12), we obtain

$$q_{12} = -\sqrt{\left(\frac{kT}{3}\right)}\left\{\frac{1}{\gamma_1\gamma_2}\left(\frac{l_1}{\sqrt{m_1}}\gamma_2 + \frac{l_2}{\sqrt{m_2}}\gamma_1\right)\frac{\partial \gamma_1}{\partial x} + \left(\frac{l_2 - l_2'/2}{\sqrt{m_2}} - \frac{l_1 - l_1'/2}{\sqrt{m_1}}\right)\frac{1}{T}\frac{\partial T}{\partial x}\right\}, \tag{16}$$

which can be rewritten as

$$q_{12} = -\frac{D_{12}}{\gamma_1\gamma_2}\left\{\frac{\partial \gamma_1}{\partial x} + k_T\frac{\partial \log T}{\partial x}\right\}. \tag{17}$$

Here $\qquad D_{12} = \sqrt{\left(\frac{kT}{3m_1m_2}\right)}\left(l_2\sqrt{m_1}\,.\,\gamma_1 + l_1\sqrt{m_2}\,.\,\gamma_2\right) \qquad (18)$

is the well-known expression for the coefficient of ordinary diffusion according to Meyer's theory if l_1 and l_2 are identified with the 'mean free paths' of the two kinds of particles responsible for this phenomenon. k_T is the expression

$$k_T = \frac{(l_2 - l_2'/2)\sqrt{m_1} - (l_1 - l_1'/2)\sqrt{m_2}}{l_2\sqrt{m_1}\,.\,\gamma_1 + l_1\sqrt{m_2}\,.\,\gamma_2}\gamma_1\gamma_2. \tag{19}$$

Since, in the preceding, the direction of the x-axis has been arbitrarily chosen, equation (17) can be replaced by the general vector formula

$$q_{12} = -\frac{D_{12}}{\gamma_1\gamma_2}\{\operatorname{grad}\gamma_1 + k_T \operatorname{grad}\log T\}, \tag{20}$$

which is identical with the corresponding formula derived by the rigorous theory. The second term in the brackets represents the thermal diffusion, and the coefficient k_T is the 'thermal diffusion ratio'.

Formula (19) shows how the quantity k_T, which determines the rate of thermal diffusion, depends on the concentration, the masses of the two sorts of molecules, and on the quantities l and l' which again depend on the behaviour of the molecules in collision, i.e. on their sizes and their mutual forces.

It has already been seen that our theory provides the same expression (18) for the coefficient D_{12} of ordinary diffusion as Meyer's theory. Consequently I follow the procedure of Meyer in assuming that l_1, l_2 are the mean free paths of Maxwell's elementary theory which for a mixture of two components take the form

$$\left.\begin{aligned} 1/l_1 &= \pi(\sqrt{2}\,n_1\sigma_1^2 + n_2\sqrt{(1+m_1/m_2)}\,.\,\sigma_{12}^2),\\ 1/l_2 &= \pi(\sqrt{2}\,n_2\sigma_2^2 + n_1\sqrt{(1+m_2/m_1)}\,.\,\sigma_{12}^2).\end{aligned}\right\} \tag{21}$$

Here σ_1, σ_2 are the radii of the two kinds of molecules and

$$\sigma_{12} = \tfrac{1}{2}(\sigma_1+\sigma_2). \tag{22}$$

The corresponding formulae of Tait, who uses a definition of the mean free path different from that of Maxwell, differ from (21) only in that the numerical constant has a slightly different value.

It is known, of course, that formula (18) does not, as the rigorous theory does, give the correct dependence of D_{12} on the concentration and the mass ratio of the molecules if the expressions (21) for l_1 and l_2 are used, because certain important effects, e.g. the 'persistence of velocities' are not taken into account (see e.g. Jeans 1925). But as these refinements far exceed the limits of an elementary theory like the present one, the formulae given above will suffice, in spite of the fact that they are to a certain extent incorrect.

I have already mentioned that l_1 and l_1' (and also l_2 and l_2') will generally be different from each other since they refer to different processes. This difference will certainly depend on the forces acting between the particles in collision. In order to simplify the problem I shall assume that the field of forces surrounding a molecule is identical for both kinds of particles. In this case it is reasonable to assume that l_1' differs from l_1 only by a numerical factor α the value of which depends mainly on the force law. I assume that l_2' and l_2 differ in this case by the same factor α. Hence

$$l_1' = \alpha l_1, \quad l_2' = \alpha l_2. \tag{23}$$

No attempt will be made to determine the actual value of α for any particular kind of force law, since this would again require considerations similar to those used in the theory of persistence of velocities, and is therefore beyond the scope of this theory. But it can be stated without calculation that α will have its smallest value for hard molecules and will increase with increasing 'softness' of the molecules. For l' is by definition the mean distance over which a particular molecule has to travel before its original velocity becomes assimilated to the local thermal velocity, and this is achieved only partially in the first collision with another molecule, that is after travelling through a distance l, if the field of interaction forces extends over a finite region instead of being concentrated in the point of contact. I shall return to this point in § 4.

Substituting from (23) into (19),

$$k_T = \left(1-\frac{\alpha}{2}\right)\frac{\sqrt{m_1/l_1}-\sqrt{m_2/l_2}}{\gamma_1\sqrt{m_1/l_1}+\gamma_2\sqrt{m_2/l_2}}\gamma_1\gamma_2, \tag{24}$$

and finally by means of (21) and (11)

$$k_T = \left(1-\frac{\alpha}{2}\right)\gamma_1\gamma_2\frac{a_1\gamma_1-a_2\gamma_2}{b_1\gamma_1^2+b_2\gamma_2^2+b_{12}\gamma_1\gamma_2} \tag{25}$$

with

$$\left.\begin{aligned}
a_1 &= \sqrt{(2m_1)}\,.\,\sigma_1^2-\sqrt{\left(\frac{m_2}{m_1}(m_1+m_2)\right)}\,.\,\sigma_{12}^2,\\
a_2 &= \sqrt{(2m_2)}\,.\,\sigma_2^2-\sqrt{\left(\frac{m_1}{m_2}(m_1+m_2)\right)}\,.\,\sigma_{12}^2,\\
b_1 &= \sqrt{(2m_1)}\,.\,\sigma_1^2,\\
b_2 &= \sqrt{(2m_2)}\,.\,\sigma_2^2,\\
b_{12} &= \sqrt{\left(\frac{(m_1+m_2)^3}{m_1m_2}\right)}\,.\,\sigma_{12}^2.
\end{aligned}\right\} \tag{26}$$

4. The following brief discussion of the formulae (25) and (26) will show that the results of the present elementary theory of thermal diffusion account for many of its characteristic properties.

(*a*) Dependence of k_T on the concentration. According to (25) k_T vanishes for $\gamma_1 = 0$ and $\gamma_2 = 0$ (or $\gamma_1 = 1$), and it has therefore at least one extremum for a certain finite concentration which will be the most suitable for separating a mixture of gases by means of thermal diffusion. The denominator of (25) is always positive; hence if a_1 and a_2 are opposite in sign, the sign of k_T is the same for all concentrations. If, however, a_1 and a_2 have both the same sign, k_T must vanish for a particular finite concentration and its sign depends on the concentration.

(*b*) Dependence of k_T on the force law. The influence of the force law controlling the behaviour of the molecules in collision is expressed by the first factor on the right-hand side of (25) which is positive for $\alpha < 2$ and negative for $\alpha > 2$. According to the statements in § 3 this means, that in a gas consisting of a certain standard type of molecules for which α is exactly equal to 2, no thermal diffusion can occur, and that in a gas consisting of 'harder' molecules than these the effect has the opposite sign than in a gas consisting of 'softer' molecules.

This is in agreement with the results of the rigorous theory of Chapman and Enskog, quoted above, which provides, besides, the formalism for calculating the factor corresponding to our $(1-\frac{1}{2}\alpha)$ for any supposed law of mutual forces. This calculation has been performed for the case where the forces between two particles of different kind are repulsive and proportional to an inverse power s of their mutual distance. It is shown that this factor is positive for $s > 5$, negative for $s < 5$ and zero for $s = 5$, the famous Maxwell 'fifth power law' (1868), which therefore corresponds to our $\alpha = 2$.*

This certainly proves a defect of the elementary theory compared with the rigorous theory. But this defect is not so bad, since the result of the general theory could be checked by experiment only if the force law were known beforehand. As this is not the case, the normal procedure is to determine a value for the exponent s of the hypothetical force law by comparing the theoretical formula with the measurements. This s can be considered as a measure for the hardness of the molecule. By using our formula (25) in the same way a value for α can be determined which is also a measure for the hardness of the molecule, no particular force law having been presupposed.

(*c*) Molecules of equal size and different mass. In this case from (26) and (22), by putting $\sigma_1 = \sigma_2 = \sigma$,

$$\left.\begin{aligned} a_1 &= \sigma^2\left[\sqrt{(2m_1)} - \sqrt{\left(\frac{m_2}{m_1}(m_1+m_2)\right)}\right], \\ a_2 &= \sigma^2\left[\sqrt{(2m_2)} - \sqrt{\left(\frac{m_1}{m_2}(m_1+m_2)\right)}\right]. \end{aligned}\right\} \qquad (27)$$

---

* An interesting attempt to account for this surprising fact by an elementary consideration on dimensions is contained in a short paper of Frankel (1940).

Hence for $m_1 > m_2$: $a_1 > 0, \quad a_2 < 0,$

and for $m_1 < m_2$: $a_1 < 0, \quad a_2 > 0.$

This means that (provided $\alpha < 2$) the heavier molecules always tend to diffuse into the cooler region.

(*d*) Molecules of equal mass and different size. Putting $m_1 = m_2 = m$ in this case, from (26)

$$\left.\begin{aligned} a_1 &= \sqrt{(2m)}\,(\sigma_1^2 - \sigma_{12}^2), \\ a_2 &= \sqrt{(2m)}\,(\sigma_2^2 - \sigma_{12}^2). \end{aligned}\right\} \tag{28}$$

Hence for $\sigma_1 > \sigma_2$: $a_1 > 0, \quad a_2 < 0,$

and for $\sigma_1 < \sigma_2$: $a_1 < 0, \quad a_2 > 0.$

Thus (again provided $\alpha < 2$) the larger molecules always tend to diffuse into the cooler region.

I am very obliged to Professor Born and Professor Chapman for their interest in this investigation and for valuable discussion and criticism.

REFERENCES

Chapman, S. 1916 *Proc. Roy. Soc.* A, **93**, 1.

Chapman, S. 1928 *Phil. Mag.* **5** (7), 630.

Chapman, S. and Dootson, F. W. 1917 *Phil. Mag.* **33**, 268.

Chapman, S. and Cowling, T. G. 1939 *The mathematical theory of non-uniform gases.* Cambridge.

Clusius, K. and Dickel, G. 1938 *Naturwissenschaften*, **26**, 546.

Clusius, K. and Dickel, G. 1939 *Naturwissenschaften*, **27**, 148.

Enskog, D. 1911 *Phys. Z.* **2**, 538.

Enskog, D. 1912 *Phys. Z.* **3**, 742.

Frankel, S. P. 1940 *Phys. Rev.* **57**, 661.

Gillespie, L. J. 1939 *J. Chem. Phys.* **7**, 530.

Jeans, J. H. 1925 *The dynamical theory of gases.* Cambridge.

Maxwell, J. C. 1868 *Collected works*, **2**.

Meyer, O. E. 1877 *Kinetic theory of gases.*

Tait, P. G. 1886 *Trans. Roy. Soc. Edinb.* **33**, 74.

The role of hydrogen bonds in condensed monolayers

By A. E. Alexander

Colloid Science Department, The University, Cambridge

(*Communicated by Eric K. Rideal, F.R.S.—Received* 11 *June* 1941)

From the behaviour of monolayers of compounds containing the —CO.NH— linkage it is concluded that intermolecular hydrogen bonding can play a major role in determining the properties of condensed monolayers. Such effects, which are well marked in the ureas, amides, acetanilides, unsubstituted and α-amino acids, tend to bring about condensation and solidification, and a marked increase in the half-expansion temperature.

A detailed examination of the acetamides has been made in both the expanded and condensed regions by combined force area and surface potential methods. Comparison of the condensed films with those of the analogous acetates, where no such intermolecular hydrogen bonding is possible, shows several striking differences. With the acetamides and ureas the hydrogen bonding has been shown to be quite sensitive to the pH of the substrate, very acid substrates leading to complete liquefaction.

The hydrogen bond distances can be calculated and the values so obtained are found to agree quite well with those in the crystal for the same or similar head groups.

The free energy difference between the —CO.NH— group when forming hydrogen bonds to water (as in the expanded films), and when cross-linked (as in the low temperature form), is calculated for the acetamides to be about 840 cal./g.mol. Values of the same order can be calculated for the other systems discussed.

The importance of such measurements in determining the part played by the hydrogen bond in the protein molecule is pointed out.

Although during recent years considerable progress has been made towards an understanding of the hydrogen bond, the extent to which this contributes towards the stability and structure of the protein molecule is still very speculative. Astbury (1940) has recently reviewed the question. Owing to the very fundamental part played by the —CO.NH— group, it is of great interest to study the behaviour of this and similar groups in simple compounds, particularly in an aqueous medium. The monolayer technique is very suitable for this (Rideal 1937), and, as already shown, indicates that the polar group structure in an aqueous medium *may* differ very markedly from that in non-polar media (Alexander 1939). Since the study of the hydrogen bond by X-ray or infra-red methods is mainly limited to the solid state or to non-polar solvents, the importance of such an examination is readily apparent. From the experimental data discussed below it would seem that the hydrogen bond plays a large part in determining the monolayer characteristics of compounds containing the —CO.NH— linkage (Alexander and Rideal 1941). Accordingly it becomes possible to study the effect of such compounds as denaturing and swelling agents on the hydrogen bond between simple molecules containing this linkage, a question of great importance in elucidating their behaviour towards the protein molecule. The question of the nature of the cross-linkages in protein monolayers, which is far from settled, may also be clarified.

From general reasoning it might be anticipated that two factors would be operative in determining the extent of cross-hydrogen bonding in the monolayer. The first and most important is the steric one. Since in monolayers the minimum cross-sectional area occupied by an unsubstituted hydrocarbon chain is 19–20 A^2, the polar groups cannot approach more closely than about 4·5 A. Consequently such simple groups as —OH are prohibited from forming direct intermolecular bonds, and can only form hydrogen bonds with water. (They may, of course, form cross-linkages through the intermediary of a water molecule, as discussed later.) Larger groups, however, such as —COOH, —CO.NH—, and —NH.CO.NH$_2$, can bridge distances of this size, and, as shown below, often tend to do so. The second factor to be considered is the strength of the cross-hydrogen bond as compared with that to water. If the former greatly exceeds the latter, and provided that the molecular area is suitable, a strong tendency towards formation of solid or gel-like films should result. This is well shown by the ureas and α-amino acids which are described below.

The only previously suggested example showing cross-hydrogen bonding in a single long-chain component monolayer (as contrasted to the two component systems present in mixed monolayers) was the *trans* dihydroxy behenic acid (Marsden and Rideal 1938). Davies (1940*b*), however, has shown that in the solid state both *cis* and *trans* compounds show precisely similar intramolecular hydrogen bonding, and, as he points out, the difference in monolayer behaviour may be due solely to the greater ease of packing of the long chains in the *trans* compound. Further doubt follows from a calculation of the intermolecular hydrogen bond distance in the monolayer, which has a minimum value of *ca.* 3·1 A for the *trans* compound, a rather high value as compared with *ca.* 2·7 A in the alcohols. (The calculation follows that given below for the acetamides.)

In mixed monolayers of two long-chain components the tendency towards solidification and condensation is well shown in those examples where cross hydrogen bonding would be expected, e.g. octadecylamine hydrochloride (pH 2) and octadecyl methyl ether (Marsden and Schulman

1938), cetyl alcohol and sodium cetyl sulphate (Schulman and Stenhagen 1938). Sodium cetyl sulphate shows a very powerful interaction with cholesterol, but a very weak one with cholesterol acetate (Schulman and Rideal 1937), readily explicable on this basis since no hydrogen bonding can occur with the latter. It may be suggested also that part of the differences observed on varying the hydrophobic portion of the molecule, e.g. oleyl, elaidyl and octadecyl alcohols with sodium cetyl sulphate (Schulman and Stenhagen 1938), can be ascribed to steric effects modifying the strength of the cross-hydrogen bonding, as indicated in this paper.

The rather sharp transition temperatures shown by condensed monolayers of ureas, acetamides and acetanilides (Adam 1922, 1923; Adam and Dyer 1924), the large areas of unionized acid films and the shrinkage on partial ionization, can also be readily explained. Again, a comparison between substituted amides and analogous esters with very similar head groups, but where the latter cannot form cross-linkages, shows many striking differences.

TABLE 1. CHAIN LENGTH $C_{16}H_{33}$ IN ALL CASES

head group	$T_{\frac{1}{2}}$°	nature of condensed film
$—OCOCH_3$	20	Liquid
$—COCH_3$	33	Liquid
$—COOCH_3$	34	Liquid
—COOH	37·5	'Plastic solid'
—CHNOH	42	Solid
$—CONH_2$	44	Solid
$—NHCONH_2$	48	Solid

An increase in the expansion temperature should also be brought about by such cross-hydrogen bonding. This is well shown by table 1, giving the half-expansion temperatures ($T_{\frac{1}{2}}$) under a standard pressure of 1·44 dynes/cm. (Adam 1938). Other factors enter as well, but the general trend is quite clear, as is also the change in physical state.

A detailed discussion of films of acetamides, ureas, amides, acetanilides, aldoximes, unsubstituted and α-amino acids is given below.

EXPERIMENTAL METHODS

The apparatus, which allowed of simultaneous force, area and potential observations, needs no description. The temperature could be raised by means of a heating coil below the trough, and could easily be kept constant to within 0·2° over the time of an experiment (generally about 20 min.). The time taken for each observation was approximately 1 min. These are rather important variables, particularly with some of these films, owing to hysteresis effects. Solutions of the substances spread were made up in redistilled benzene, owing to insufficient solubility in petrol ether. The aqueous substrate was N/1000 HCl unless otherwise stated.

(a) *Acetamides*, $R.NHCOCH_3$

Condensed films of acetamides were found by Adam and Dyer (1924) to exist in two forms with a definite transition temperature, the high-temperature form being liquid with a limiting area of *ca.* 24·2 A^2, the low-temperature one solid with a limiting area of *ca.* 20·5 A^2. A very simple explanation would appear possible from the suggested configurations II and III shown in figure 1. Here the high-temperature condensed form is seen to resemble the acetate and methyl ketone head-group configuration very closely, in agreement with the observed area and liquid state (see Alexander 1941). The low-temperature condensed form is assumed to be stabilized by cross-hydrogen bonds, in accord with its solid state and great stability as compared with the liquid, rather unstable films given by the acetates and methyl ketones. Spontaneous formation of configuration III would be opposed by thermal agitation and by the work necessary to immerse the methyl group (Alexander and Schulman 1937). Compression

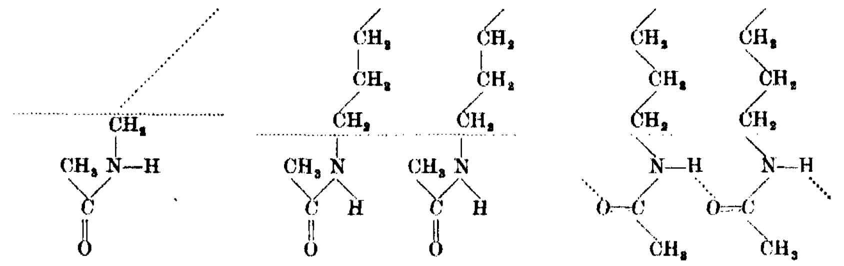

Configuration I
Expanded form. $A > 47$ A^2. $\mu = 302$ m.-Debyes. No cross-hydrogen bonds. Liquid film.

Configuration II
High-temperature condensed form. A *ca.* 24 A^2. μ *ca.* 350 m.-Debyes. Hydrogen bond distance *ca.* 4 A, i.e. no direct bonds. Liquid film. Chains inclined at *ca.* 30° to vertical. Resembles acetates and methyl ketones.

Configuration III
Low-temperature condensed form. $A < 21$ A^2. μ *ca.* 390 m.-Debyes. Strong hydrogen bonds (bond distance *ca.* 2·8 A). Rigid solid film. Normal area of close-packed, vertical chains. No analogous form known in acetates and methyl ketones.

FIGURE 1. (In this and subsequent figures the water surface is to be taken as parallel to the horizontal dotted line. All values of μ are given in milli-Debyes.)

should thus tend to facilitate the change from II to III, that is, increasing F should raise the transition temperature. Adam and Dyer (1924) found experimentally that increasing F by 8·5 dynes/cm. raised the transition temperature about 2°.

The above explanation was tested by examining the force area and surface potential characteristics of monolayers of the C_{16}, C_{17} and C_{18} acetamides, since it might reasonably be anticipated that the changes postulated would be shown up by changes in the surface moment μ. The results are shown in figure 2. The F-A curves agree closely with those of Adam and Dyer (1924), and the marked hysteresis they described was fully confirmed; the F-A curves being very sensitive to temperature, rate of compression, and even the area at which the film was initially spread. This was especially marked for the C_{17} compound, which showed an intermediate behaviour between the C_{16} and C_{18} homologues, and so no F-A curve is given for this. The surface potential curve, however, includes

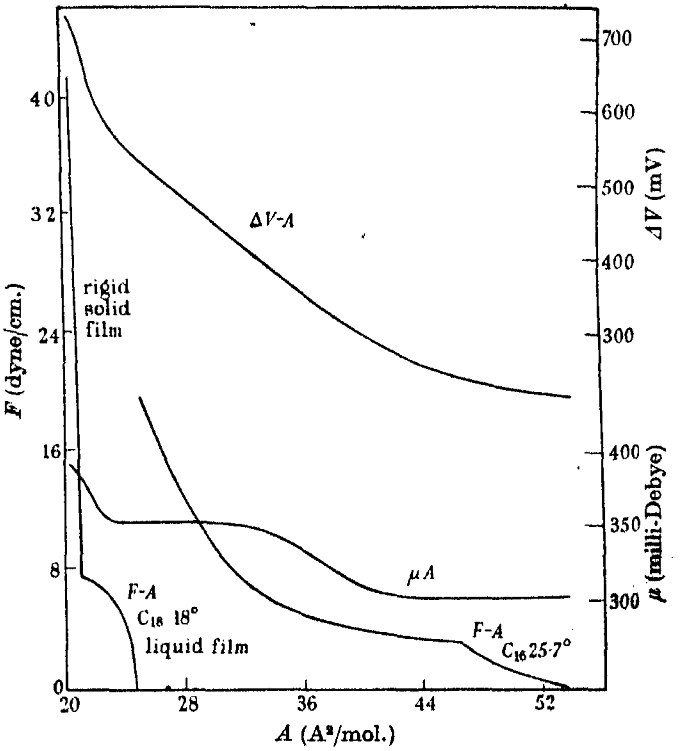

FIGURE 2

values from all three compounds and at temperatures between 18 and 26°, since no differences greater than about 10–15 mV were observed. Owing to the above hysteresis effects this curve is less definite over the range 46–26 A^2 than in the expanded region (46·5–54 A^2) or in the condensed at less than 25 A^2, where the potentials agreed to within 5 mV. Slight collapse was observed in the highly condensed films ($A < 21$ A^2), but even at 50 dynes pressure this was extremely slow.

The μ-A curve shows that μ is constant at 302 m.-Debyes in the expanded region, commences to rise when condensation sets in, shows a fairly flat region from about 30–24 A^2, and then rises very rapidly when transition from the liquid large-area to the solid low-area form sets in, reaching a final value of about 390 m.-Debyes. The total increase in moment is thus about 30 %. An *increase* of this magnitude is most unusual, the only other example being the cyanides (see Alexander 1941), but the following explanation can be suggested.

The configuration in the expanded state is almost certainly that of I in figure 1, with the resultant dipole vertically orientated, and no possibility of cross-hydrogen bonding on account of the large areas occupied. On transition to the condensed forms II and III the C=O group reorientation will tend to decrease μ, particularly in configuration III, and in order to account for the observed *increase* in this configuration it would seem that a very large moment, approximating to that of an ionic link, has to be ascribed to the hydrogen bond. This is readily explicable on Pauling's view of the essentially ionic nature of this bond (Pauling 1939), although objections have been raised against this view in certain cases (Davies 1940*a*).

The validity of configurations II and III can also be tested by calculating the hydrogen bond distances (i.e. the N...O separations), which in the latter should approach the value for the crystal. This was done assuming that the minimum cross-sectional area of the chain was 21·0 A^2 (from figure 2), that the thickness of the hydrocarbon chain perpendicular to the planar zigzags (i.e. to the plane of the paper in figure 1) was 4·6 A in all cases, and that in configuration II the chains were tilted over so as to fill the available space. The value of 4·6 A, although to some extent arbitrary since the exact mode of packing of the long chains is uncertain, is a reasonable one, being that found by Müller (1932) from X-ray measurements upon hydrocarbons at the melting-point. These points are discussed in more detail in the following paper. The bond distances and angles are taken from Pauling (1939), unless otherwise stated.

Calculation upon the above assumptions gives at 24 A^2 a minimum separation of close to 4 A between the N and O atoms, corresponding to a chain inclination of about 30° to the vertical. Since this distance is considerably greater than the normal distance of 2·8–3·0 A found in the crystal, only negligible direct hydrogen bonding can take place, and so the film remains fluid. The increase in μ from the expanded state does, however, indicate some change in the head-group structure, and a rather speculative suggestion is that cross-linking occurs through the OH bond of a single water molecule. Further reduction in the N to O distance is impossible in this configuration, since the necessary increased tilt of the hydrocarbon chain would require an area greater than 24 A^2. (Taking the minimum cross-section as 21 A^2, a tilt of 30° corresponds to an area of 24·3 A^2.) This reduction can, however, take place by transition to configuration III, where at 21 A^2 a similar calculation to that above gives the hydrogen bond distance as 2·8 A, very close to the X-ray value of 2·85 A in diketopiperazine (see Astbury 1940). The observed great rigidity fits in well with this. Thus these calculations upon the hydrogen bond distances are in accord with the postulated structures.

Further confirmation is obtained by a comparison with octadecyl acetate and heptadecyl methyl ketone which cannot form such intermolecular hydrogen bonds. These are very much less stable in the condensed state, giving *liquid* films at all compressions, and as shown by the μ-A curves, no reorientation of the methyl group occurs, since this would reduce the moment very much more than observed experimentally (see Alexander (1941), and the following paper).

The stabilizing action of the cross-hydrogen bonds can be so weakened by the action of strongly acid substrates (e.g. 5N . H_2SO_4), that liquefaction is brought about. Certain other reagents, such as urea, may exert a similar effect.

(*b*) *Ureas*, R.$NHCONH_2$

The ureas were found by Adam (1922, 1923) and by Adam and Dyer (1924) to resemble the acetamides in showing a fairly definite transition in the condensed region, but in this case the high-area form (limiting area *ca.* 25 A^2) was the stable one at low temperatures, and the low-area form (limiting area *ca.* 21 A^2) at high temperatures. This high-area form resembles the α-amino acids in existing as a solid film at areas considerably greater than that of close-packed, vertically orientated chains (see following paper). These facts and others presented below are again very simply explained by intermolecular hydrogen bonds, the suggested head-group configurations being shown in figure 3.

As discussed in the following paper it would seem that μ is at its maximum value at the limiting area, so assuming cross-hydrogen bonding to be the cause of the observed solidity and large area in configuration I, then transition to II should tend to decrease μ. This is confirmed experimentally as shown by figure 4. Also transition from I to II should be favoured by increase of pressure and of temperature (the latter by tending to weaken the hydrogen bonding). This agrees with Adam's observation (Adam 1922, 1923) that the transition temperature is lowered a few degrees by lateral compression. The reason for configuration I being preferred to II is probably due to the stronger hydrogen bonds formed with the unsubstituted $-NH_2$ group, owing to the smaller negative character of the substituted nitrogen atom.

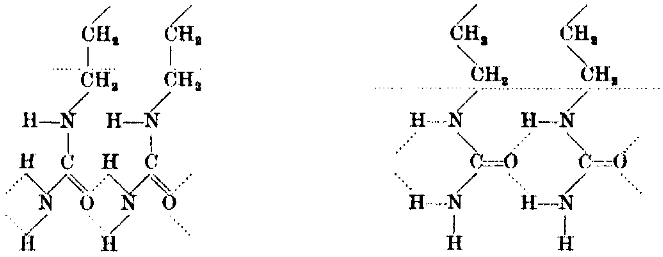

Configuration I
Low-temperature form. A *ca.* 25 A^2. μ *ca.* 364 m.-Debyes. Solid film. Chains inclined at *ca.* 30° to vertical.

Configuration II
High-temperature form. $A < 21$ A^2. μ *ca.* 328 m.-Debyes. Solid film. Vertical close-packed chains.

FIGURE 3

As with the acetamides, the assumption of cross-hydrogen bonding can be tested by calculation of the hydrogen bond distance. (Urea gives values of 2·98 and 3·03 A—see Astbury 1940.) A calculation using the same assumptions as for the acetamides gives at the limiting area of 25·5 A^2 a value of 3·1 A, at 25 A^2 one of 3·0 A. The chain tilt in both cases is approximately 30° to the vertical. (The mean value of 25·5 A^2 for the limiting area is taken from the above results of Adam, those of Cockbain (1939), and those of the author.) The vertical configuration II is seen to be identical with configuration III in the acetamides, so a similar hydrogen bond distance of 2·8 A is found.

The experimental results with hexadecyl urea in the low and high temperature forms upon N/1000 HCl substrate are shown in figure 4. (The spreading solution was benzene containing 5 % ethyl alcohol.) The F-A curve given is that obtained on initial compression. After compression and expansion the hysteresis effects are much reduced and a value close to 25 A^2 is obtained for the limiting area. There is seen to be no abrupt change in μ during the transition from one form to the other, in agreement with the suggested structures.

The *F*-*A* curves given by Adam (1922, 1923), by Adam and Dyer (1924), and by Cockbain (1939) are in quite close agreement with each other, but differ somewhat from those given here, particularly in that their high-area form had a much lower compressibility and gave a much more solid film. It was suspected that this difference was due to the difference in substrate pH modifying the strength of the hydrogen bonding. (The substrate used by Adam was distilled water; by Cockbain phosphate buffer pH 8·0.) Accordingly the *F*-*A* curve for hexadecyl urea was determined using N.HCl as substrate ($T = 19°$), since this should bring about a much more pronounced effect. A very marked effect was indeed found, the *F*-*A* curve now being of the 'normal' type as given by most condensed films (see figure 1 of the following paper), with an extrapolated area for the *X Y*

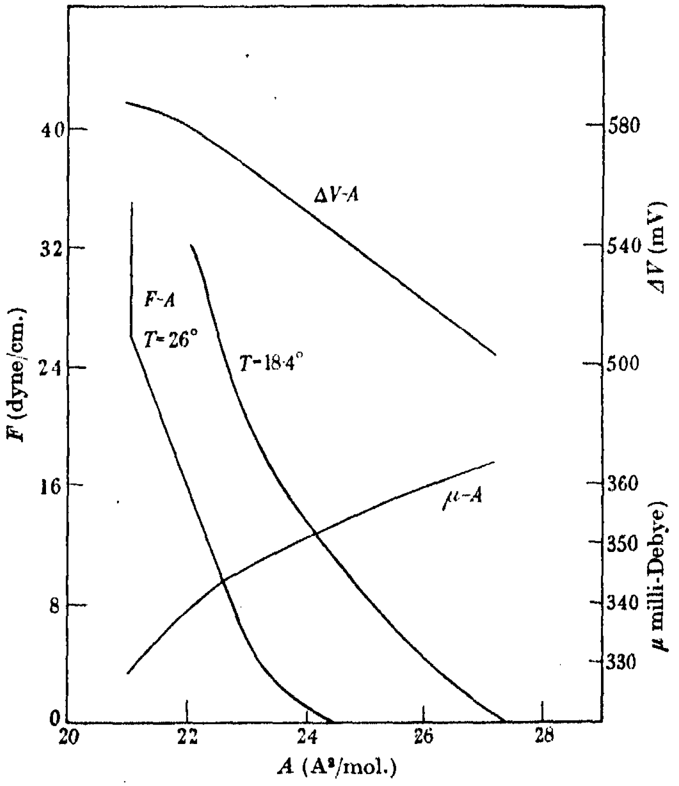

FIGURE 4

region of *ca.* 25 A², and the kink-point Y at close to 21 A² (F *ca.* 28 dynes/cm.). The film was a viscous liquid or very weak solid at the largest areas and never became a strong solid even below 21 A². Thus it is evident that the hydrogen ion can modify the strength of the intermolecular hydrogen bonding very considerably, as also shown above with the acetamides. This observation probably accounts for the variation with pH, and the much greater stability upon very acid substrates, of stearic anilide monolayers (Rideal and Mitchell 1937).

(*c*) *Amides*, $R.\mathrm{CONH_2}$

Similar considerations to those already put forward should apply to the simple and mono-substituted amides, since they both contain the —CO.NH— group. Little has been done on the unsubstituted amides, although Adam (1922, 1923) records that they form very rigid films. Of the mono-substituted derivatives only methyl stearamide appears to have been examined.

(*d*) *Methyl stearamide*, $C_{17}H_{35}CONHCH_3$

Mitchell (1939) records that this gives a rigid solid film even at 23 A² ($T = 25°$), and the surface moment μ varies quite markedly with pH (cf. the dependence of F-A curve of ureas upon pH). Thus it differs greatly from the very similar compound methyl stearate $C_{17}H_{35}COOCH_3$ which gives a *liquid* film at all areas, and where μ appears to be independent of the pH (Alexander and Schulman 1937; Alexander and Rideal 1937).

It is possible to put forward a structure at the limiting area (given by Cockbain (1939) as *ca.* 24·5 A²), based as in previous examples upon the assumption that intermolecular hydrogen bonding is the determining factor. A similar calculation as in the acetamides shows that the minimum hydrogen bond distance is *ca.* 2·9 A at 24·5 A², with a chain tilt of *ca.* 30° to the vertical (configuration I, figure 5). The similarity to the picture suggested below for the acids (configuration I, figure 7) is quite striking.

On compression from the limiting area the necessary alteration in tilt of the hydrocarbon chain brings about an *increase* in the hydrogen bond distance, suggesting once again that the limiting area in these cases is determined by such cross hydrogen bonding. At 21 A² the suggested configuration (II in figure 5) has a hydrogen bond distance of *ca.* 3·15 A. It differs somewhat from that suggested for the acids at this area (figure 7, configuration II), since a precisely similar one is excluded on account of the presence of the methyl group, but, as might be expected in view of their similar head groups, closely resembles that for the condensed form of ethyl stearate (Alexander and Schulman 1937).

As in the ureas and acids, transition from configuration I to II decreases μ quite considerably (Cockbain 1939), indicating that the free energy of the head-group/water system is a minimum at the limiting area. This aspect is further discussed in the following paper.

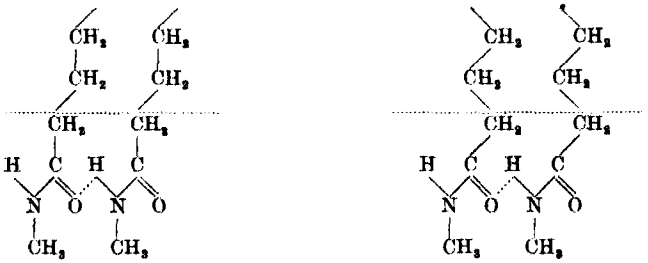

Configuration I
$A = 24{\cdot}5$ A². Hydrogen bond distance *ca.* 2·9 A. *Chains tilted at ca.* 30° *to vertical.*

Configuration II
$A = 21$ A². Hydrogen bond distance *ca.* 3·1 A. Vertical chains.

FIGURE 5

Cockbain (1939) made the interesting observation that in a 1 : 1 mixed film of methyl stearamide and hexadecyl urea at 20°, the latter is present as the low-area form, normally the one stable at high temperature (> 24°). No explanation was attempted, but from the considerations advanced in this paper it would seem that a modification of the cross-hydrogen bonding between the urea molecules, as might be expected from the nature of the second component, would provide a plausible explanation. As shown above a similar change can be brought about by using very acid substrates.

(*e*) *Acetanilides*, $R.C_6H_4.NHCOCH_3$

Hexadecyl acetanilide was found by Adam (1923) to give two types of condensed film, one of limiting area 28·2 A² ($T < 24°$), the other of 25·8 A² ($T > 29°$). Again, a simple explanation would be that the large area form is stabilized by directed hydrogen bonds as in configuration I of figure 6. Increase of temperature breaks down this structure, thus permitting the methyl group and C=O dipole to reorientate themselves into a configuration similar to that of the acetates and methyl ketones (configuration II, figure 6).

This is supported by calculation of the hydrogen bond distances in the two configurations, using the data for stearic anilide as given by Rideal and Mitchell (1937). It is rather striking that using the same configuration as for the acetamides (configuration III, figure 1), an identical hydrogen bond distance of 2·8 A is obtained. Taking the area occupied by closely packed benzene rings in the monolayer as 23·8 A^2 (Adam 1923), and the angle between the nitrogen valencies for simplicity as 110°, then the area occupied by these rings in configuration I is about 29 A^2, very close to the experimental one of 28·2 A^2. Evidently this structure is partially stabilized by such close-packed rings, just as the acetamides were by close-packed hydrocarbon chains.

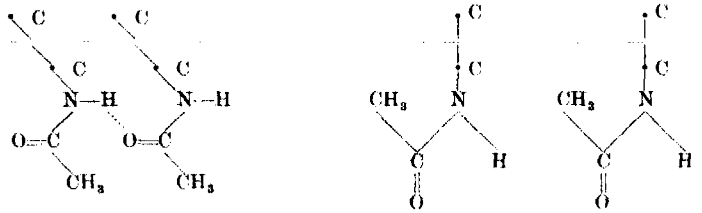

Configuration I
Low-temperature condensed form. $A = 28{\cdot}2$ A^2. Strong hydrogen bonding (bond distance *ca.* 2·8 A).

Configuration II
High-temperature condensed form. $A = 25{\cdot}8$ A^2. Negligible direct hydrogen bonding (bond distance *ca.* 4 A).

FIGURE 6. (Hydrocarbon chains not represented.)

The high-temperature form (configuration II) is seen to be precisely similar to the corresponding form of the acetamides (configuration II, figure 1), with an identical value of *ca.* 4 A for the hydrogen bond distance. It is evident that no direct bonding can occur, but by analogy with the acetamides it can be suggested that cross-linkage occurs through the OH bond of a single water molecule. The surface potentials in the expanded and condensed states would help towards a more detailed understanding. The rather larger area occupied by configuration II as compared with the unsubstituted anilines is readily ascribed to the 'acetate' configuration of the head group (see Alexander and Schulman 1937).

(*f*) *Aldoximes*, *R*.CH=NOH

These appear to be somewhat anomalous, as discussed in the following paper, in showing no fall in μ in the condensed state, but this may well be due to intermolecular hydrogen bonding offsetting the change in dipole orientation as shown in some of the previous examples. Solid films would then be expected in the most compressed region. This is not recorded in any published work (Adam 1923; Adam, Danielli and Harding 1934), but has been confirmed by Professor Adam (private communication) and by experiments by the author. The films are liquid along *XY* (see figure 1 of following paper) and solidify close to the kink-point *Y*.

To explain the increase in μ at the limiting area (*ca.* 25 A^2) over that in the expanded state a similar explanation as for the acetamides can be put forward, namely that cross-linkage occurs through the OH bond of a single water molecule.

(*g*) *Acids*, *R*.COOH

As is well known, condensed films of acids on dilute acid substrates show a limiting area of about 24 A^2 (Nutting and Harkins 1939), a rather high value in view of the simple head group. It can be suggested that this is due to directed hydrogen bonds stabilizing a comparatively open structure as in ice. Increase of pressure, either externally by increasing *F*, or internally by increasing the chain length, should tend to decrease the limiting area, in accord with experiment (Nutting and Harkins 1939; Adam and Dyer 1924). Also the surface moment should decrease on compression and differ from that in the expanded state. The absolute values in the expanded region differ somewhat (possibly owing to solubility effects), but it does seem that μ is a maximum at 24–25 A^2 and decreases at both smaller and larger areas (Schulman and Rideal 1931; Adam and Harding 1932; Addink 1934; Dervichian 1936). The suggested structures in the condensed films are given in figure 7.

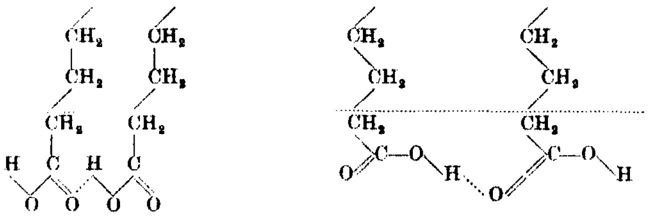

Configuration I
A = 24 A^2. Hydrogen bond distance *ca.* 2·8 A. Tilted chains.

Configuration II
A = 21 A^2. Hydrogen bond distance *ca.* 3·2 A. Vertical chains.

FIGURE 7

At 24 A^2, a similar calculation to the previous ones gives a minimum hydrogen bond distance of 2·8 A, with the chains tilted at approximately 30° to the vertical. This distance is again quite close to the value found in the crystal (e.g. 2·67 A in formic acid dimer, 2·6 A in oxalic acid—see Robertson 1940). Also the tilt corresponds to an effective area occupied by the hydrocarbon chain of about 24·3 A^2, which fits in very well with the observed area. In the condensed state at 21 A^2, where vertical chains are assumed, the hydrogen bond distance is seen from figure 7 to have increased to about 3·2 A, and so the limiting area of 24 A^2 seems to be mainly due to the spatial arrangement required by the intermolecular hydrogen bonding.

As the pH is increased the limiting area decreases until a completely condensed, solid film, is obtained. As suggested in the introduction, this may be due to strong hydrogen bonding between the ionized and unionized molecules, owing to the very negative character of the carboxyl ion. The calculated value of the minimum hydrogen bond distance is 3·1 A at 21 A^2.

(*h*) *α-amino acids*, R.CH.NH$_2$COOH *or* R.CH.NH$_3^+$COO′

The behaviour of these simple zwitterions should help towards elucidating the part played by similar groupings in the protein molecule, where one of the cross-linkages is assumed to be that between acidic and basic side chains. These are generally termed 'salt' or 'salt-like' linkages, but may also be considered as hydrogen bridges (for a review see Astbury 1940).

Monolayers of α-amino stearic acid have been investigated by Porter (1937), but no mention is made of their physical state. Askew and Danielli (1940) have pointed out that α-amino palmitic acid gives a solid monolayer at the oil/water interface at areas less than about 50 A^2 (pH 4). This latter compound has now been examined at the air/water interface at pH 7·2 (M/40 phosphate buffer). The spreading solution was made up according to the directions given by Porter (1937).

Very considerable hysteresis was observed, the limiting area on initial compression being about 48 A^2, reduced by compression and re-expansion to about 38 A^2. The film was fluid at areas down to about 36 A^2, when gelation set in, becoming a very strong gel at about 30 A^2, and a rigid stable solid at smaller areas. Pressures of over 50 dynes/cm. were easily withstood.

The resemblance between these monolayers and those given by the ureas is very obvious. Assuming intermolecular hydrogen bonding to be the cause, this should be very strong on account of the zwitterionic nature of the head group. Calculation of the hydrogen bond distance, using the angles and distances for glycine as given by Albrecht and Corey (1939), and the assumptions used in earlier examples, gives a value of 4·2 A at 36 A^2 (commencement of gelation), 3·0 A at 30 A^2 (strong gel), and 2·7 A at 29 A^2 (rigid solid). The latter two agree well with values found in the glycine crystal (2·76, 2·88, 2·93 and 3·05 A), the former, which is the value at the commencement of gelation, may possibly be due to cross-linking through a water molecule, as suggested above in several instances.

CALCULATION OF THE HYDROGEN BOND ENERGIES

From the above results on the acetamides it is possible to make an approximate calculation of the difference in energy of the —CO.NH— group when forming hydrogen bonds with water molecules, as in the expanded films (configuration I, figure 1), and when cross-linked as in the low temperature condensed form (configuration III, figure 1). The magnitude of this difference will, of course, decide the part played by the latter type towards stabilizing the protein molecule.

Since μ increases by about 90 m.-Debyes during this transition, then the energy of the head-group/water system has been decreased by an amount $H\Delta\mu$, where $\Delta\mu = 90$ m.-Debyes, and H is the field strength at the interface. Taking this to be constant at $1{\cdot}5 \times 10^8$ V/cm. (Mitchell 1936), this corresponds to about 640 cal./g.mol. The transition, however, also involves a rotation of the methyl group which is known to require about 200 cal./g.mol. (Alexander and Schulman 1937). Hence the difference in free energy is very approximately 840 cal./g.mol., showing that in this case intermolecular hydrogen bonding brings about an appreciable *increase* in stability.

Similar ideas should hold for the other systems discussed in this paper, and so far as the data permit, this would seem to be so. Thus as pointed out, in the case of the acids μ is a maximum at 24–25 A^2, being some 30 m.-Debyes greater than in the expanded region. Again, with the aldoximes μ increases by about 70 m.-Debyes from the expanded to the condensed state (Adam, Danielli and Harding 1934). It is also extremely significant that in the examples of mixed films discussed by Marsden and Schulman (1938) and by Harkins and Florence (1938), those in which hydrogen bonding would seem to be most probable (e.g. amine and ether at pH 2) give very marked *increases* in surface potential over the mean value expected.

CONCLUSION

It would seem from the above examples that cross-hydrogen bonding is a factor which in certain cases can play a predominant part in determining the characteristics of monolayers. Using such simple compounds as the acetamides, the action of such reagents as urea, thiocyanates, etc., upon the keto-imino hydrogen bond can now be examined, and some correlation with their effect upon the protein molecule may be possible. Also, using the α-amino acids, this may be extended to observing their effect upon the 'salt' linkages in proteins.

I have much pleasure in thanking Professor N. K. Adam, F.R.S. for a gift of the compounds used in this investigation, and Professor E. K. Rideal, F.R.S. and Dr M. M. Davies for helpful discussions.

REFERENCES

Adam, N. K. 1922 *Proc. Roy. Soc.* A, **101**, 452–471.
Adam, N. K. 1923 *Proc. Roy. Soc.* A, **103**, 676–695.
Adam, N. K. 1938 *The physics and chemistry of surfaces*, 2nd ed. Oxford.
Adam, N. K., Danielli, J. F. and Harding, J. B. 1934 *Proc. Roy. Soc.* A, **147**, 491–499.
Adam, N. K. and Dyer, J. W. 1924 *Proc. Roy. Soc.* A, **106**, 694–709.
Adam, N. K. and Harding, J. B. 1932 *Proc. Roy. Soc.* A, **138**, 411–430.
Adam, N. K. and Miller, J. G. 1933 *Proc. Roy. Soc.* A, **142**, 401–422.
Addink, N. W. 1934 *J. Chem. Phys.* **2**, 574–577.
Albrecht, G. and Corey, R. B. 1939 *J. Amer. Chem. Soc.* **61**, 1087–1103.
Alexander, A. E. 1939 *J. Chem. Soc.* pp. 177–181.
Alexander, A. E. 1941 *Trans. Faraday Soc.* **37**, 426–437.
Alexander, A. E. and Rideal, E. K. 1937 *Proc. Roy. Soc.* A, **163**, 70–89.
Alexander, A. E. and Rideal, E. K. 1941 *Nature, Lond.*, **147**, 541.
Alexander, A. E. and Schulman, J. H. 1937 *Proc. Roy. Soc.* A, **161**, 115–127.
Askew, F. A. and Danielli, J. F. 1940 *Trans. Faraday Soc.* **36**, 785–794.
Astbury, W. T. 1940 *Trans. Faraday Soc.* **36**, 871–880.
Cockbain, G. 1939 Dissertation, Cambridge.
Davies, M. M. 1940*a* *Trans. Faraday Soc.* **36**, 333–344.
Davies, M. M. 1940*b* *J. Chem. Phys.* **8**, 577–587.
Dervichian, D. 1936 Thesis, Masson, Paris.
Harkins, W. D. and Florence, R. T. 1938 *J. Chem. Phys.* **6**, 847–855.
Marsden, J. and Rideal, E. K. 1938 *J. Chem. Soc.* pp. 1163–1171.
Marsden, J. and Schulman, J. H. 1938 *Trans. Faraday Soc.* **34**, 748–758.
Mitchell, J. S. 1936 *Proc. Roy. Soc.* A, **155**, 696–701.
Mitchell, J. S. 1939 *Tabulae Biologicae*, **19**, 292.
Müller, A. 1932 *Proc. Roy. Soc.* A, **138**, 514–530.
Nutting, G. C. and Harkins, W. D. 1939 *J. Amer. Chem. Soc.* **61**, 1180–1187.
Pauling, L. 1939 *The nature of the chemical bond.* Cornell.
Porter, E. F. 1937 *J. Amer. Chem. Soc.* **59**, 1883–1888.
Rideal, E. K. 1937 Institute of Chemistry Lectures.
Rideal, E. K. and Mitchell, J. S. 1937 *Proc. Roy. Soc.* A, **159**, 206–228.
Robertson, J. M. 1940 *Trans. Faraday Soc.* **36**, 913–921.
Schulman, J. H. and Rideal, E. K. 1931 *Proc. Roy. Soc.* A, **130**, 268–294.
Schulman, J. H. and Rideal, E. K. 1937 *Proc. Roy. Soc.* B, **122**, 29–57.
Schulman, J. H. and Stenhagen, E. 1938 *Proc. Roy. Soc.* B, **126**, 356–369.

A proposed general structure for condensed monomolecular films

By A. E. Alexander

Colloid Science Department, The University, Cambridge

(*Communicated by Eric K. Rideal, F.R.S.—Received* 11 *June* 1941)

A very brief review is given of the theories put forward by earlier workers to explain the observed characteristics of condensed monolayers.

From the detailed structures of numerous condensed films as discussed in a previous publication, certain generalizations are now suggested.

For the least compressible region (YZ) evidence based upon surface potential measurements, upon the X-ray structure of hydrocarbons near the melting-point, and upon the compressibility, strongly support the statement that in this region the long chains are vertically orientated and close-packed, but not as tightly as is possible in the three-dimensional crystal.

In the more compressible region (XY) the behaviour appears to be intermediate between that in the YZ region (determined only by the hydrocarbon chain packing), and in the expanded state (determined only by the head-group dipole orientation). The most general statement possible is that the configuration at the limiting area X is determined *both* by the orientation of the head-group dipole with respect to the surface, and by the long-chain packing. All known classes of condensed monolayers are grouped according to the factors thought to be primarily responsible for determining the limiting area X, namely, the 'size' of the head group, hydrogen bond formation between the head groups, and the hydrocarbon chain packing.

The physical states of monolayers, and the factors by which they are influenced, are briefly discussed. Forces both between the polar head groups and between the hydrophobic tails have to be considered.

In a recent publication (Alexander 1941*b*) previous theories advanced to explain the characteristics of condensed monolayers have been reviewed and critically examined. The monolayer characteristics are derived from a study of the changes in surface tension (F), surface potential (ΔV), and surface viscosity and rigidity, measured as a function of the area per molecule (A). The 'surface moment' μ is obtained from the change in surface potential by means of the equation $\Delta V = 4\pi n\mu$, where $n = 1/A$.

The usual force-area (F-A) curve for a completely condensed monolayer, as shown in figure 1, consists of two approximately linear sections, one of which (XY) shows a much higher compressibility than the second (YZ). Adam (1921) early suggested that the two parts XY and YZ could be ascribed to the close-packed heads and close-packed chains respectively, a view which, with slight modifications, he still retains (Adam 1938).

Lyons and Rideal (1929) made the alternative suggestion that the behaviour was determined by the packing of the hydrocarbon chains at those definite angles of tilt (26·5 or 45° to the vertical), which allowed the zigzags to interlock. More recently Dervichian (1939) has attempted to draw a very close analogy between condensed films and the three-dimensional state as shown by his statement (Dervichian 1939, p. 939), 'The lattice structure and tilt of the molecules in the different forms are the same in two and three dimensions.' An examination of this postulate in the light of the variety of data now available showed that, as a general explanation, it was most improbable (Alexander 1941*b*).

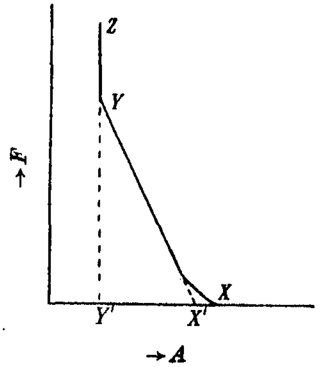

FIGURE 1

In order to go into the question still further the individual behaviour of all classes of compounds, excluding only the more complex ones such as the sterols, was examined, and in many cases possible configurations for the head group and long chain were put forward (Alexander 1941*b*). These results show certain generalizations which it is the object of this paper to examine in detail, and for convenience the XY and YZ regions are considered separately.

THE LEAST COMPRESSIBLE REGION YZ

In contrast to Dervichian's idea of inclined chains in this region (Dervichian 1939), it is now postulated that the long chains are close-packed and vertically orientated *in all cases*. Three independent lines of evidence give support to this.

First, the surface moment of condensed films of ethyl stearate definitely demands vertically orientated chains (Alexander and Schulman 1937).

The calculated values for the four possible configurations with the chains tilted at 26·5° to the vertical are 277, 80, 7, and – 139 m.-Debyes, whereas the vertical configuration gives 198, in good agreement with the experimental value of 193.

The second point in favour of vertical chains is the magnitude of the areas at the kink-point Y which, as shown in table 1, are seen to lie between 19 and 21 A^2 for the straight-chain compounds. Vertical orientation would apparently require an area of about 18·5 A^2; an inclination of 26½° to the vertical one of about 20·7 A^2. The areas at zero compression which are slightly greater than the values at Y certainly appear at first sight to support an inclined structure, but the matter is more complicated as the following remarks show. The value of 18·5 A^2 quoted above was the value obtained by Müller (1927, 1928), from X-ray analysis of the hydrocarbon $C_{29}H_{60}$ and of stearic acid at room temperature (the actual values being 18·5 and 18·3 A^2 respectively). Later work, however (Müller 1932), showed that this cross-sectional area increases very considerably as the temperature approaches the melting-point, the values for the hydrocarbons then lying between 19·0 and 20·1 A^2 with an average value of 19·5 A^2. The values obtained by Buckingham (1934) for the α-forms (the forms stable near the melting-point) of ethyl behenate and hexacosane agree well with Müller's, being 19·64 and 19·43 A^2 for the α_1 and α_2 forms of the former and 19·89 A^2 for the α_1 form of the latter.

The cross-sectional area of the hydrocarbon molecule in the liquid state can also be obtained from density measurements. Assuming hexagonally packed chains the average value so obtained for the C_{20} to C_{30} members is 22·0 A^2 (Müller 1932).

Now, as has already been mentioned (Alexander 1941*b*), the melting-point of monolayers on water seems to be invariably very much less than in the crystal, and in very many cases fluid monolayers are obtained from substances solid at the same temperature. Hence it would seem much more logical to compare the monolayer cross-sections in the YZ region with the values in crystals near the melting-point rather than with those at room temperature. Although, owing to lack of data, comparison can only be made with the hydrocarbons, there is seen to be a close correspondence between the two, the values being intermediate between those calculated from the X-ray and those from the density measurements. The tendency for the monolayer values to be slightly greater than the X-ray values may be due to the conditions not being strictly comparable, such as might arise from some hydration of the chains in the monolayer (Alexander 1941*a*). Also, as pointed out (Alexander 1941*b*), collapse seems to occur

TABLE 1

compound		temp. °C	substrate pH	area at Y (A^2)	extrapolated area X' (A^2)	area at X (A^2)	reference
n-acids	C_{22}	17·8	2	20·3	24·0	*ca.* 25·0	Adam and Harding (1932)
	C_{20}	25·0	2	19·2	23·6	*ca.* 23·8	Nutting and Harkins (1939)
	C_{19}	25·0	2	20·1	24·0	*ca.* 24·0	Nutting and Harkins (1939)
	C_{18}	25·0	2	—	24·5	*ca.* 24·6	Nutting and Harkins (1939)
	C_{18}	25·0	2	20·8	26·0	*ca.* 26·4	Hoffman, Ralston and Ziegler (1939)
	C_{18}	25·0	3	20·1	24·3	24·3	Harkins and Florence (1938)
	C_{18}	24·5	8·2	19·3	20·5	20·5	Harkins and Anderson (1937)
	C_{18}	22–25	3·2	20·1	25·4	*ca.* 27·0	Porter (1937)
	C_{17}	25·0	2	20·2	24·6	*ca.* 24·7	Nutting and Harkins (1939)
	C_{16}	18·3	2	20·4	24·7	*ca.* 26·0	Adam and Harding (1932)
n-alcohols	C_{20}	25·0	2	20·2	22·2	*ca.* 22·7	Schulman and Hughes (1932)
	C_{20}	16·0	2	19·6	21·1	*ca.* 21·4	Schulman and Hughes (1932)
	C_{18}	25·0	3	20·3	21·9	*ca.* 21·9	Harkins and Florence (1938)
	C_{18}	20·0	2	20·4	21·8	*ca.* 21·8	Nutting and Harkins (1939)
	C_{18}	Room T	—	20·0	22·5	*ca.* 24·0	Adam, Danielli and Harding (1934)
	C_{17}	25·0	2	20·4	21·8	*ca.* 21·8	Nutting and Harkins (1939)
	C_{16}	25·0	2	20·6	21·8	*ca.* 21·8	Nutting and Harkins (1939)
	C_{16}	20·0	2 and 7·8	*ca.* 20·3	*ca.* 22·0	*ca.* 23·0	Marsden and Schulman (1938)
	C_{16}	Room T	—	20·0	22·5	*ca.* 24·0	Adam, Danielli and Harding (1934)
	C_{16}	20·0	—	20·7	21·85	21·85	Harkins, Young and Boyd (1940)
	C_{16}	7·5	—	20·3	21·5	21·5	Harkins, Young and Boyd (1940)
n-amines	C_{18}	20·0	7·8	*ca.* 20·4	—	*ca.* 21·8	Marsden and Schulman (1938)
	C_{17}	22–25	9·1	*ca.* 21·5	—	*ca.* 24·0	Porter (1937)
methyl ketones	C_{17}	25·0	2	20·5	21·6	21·8	Hoffman, Ralston and Ziegler (1939)
	C_{17}	Room T	—	*ca.* 20·5	—	*ca.* 22·0	Adam, Danielli and Harding (1934)
aldoximes	C_{16}	Room T	—	20·5	23·5	—	Adam, Danielli and Harding (1934)
	C_{15}	Room T	—	20·1	25·0	*ca.* 28·0	Adam, Danielli and Harding (1934)
esters:							
ethyl stearate		20–21	2	19·0	20·9	*ca.* 21·5	Alexander and Schulman (1937)
methyl stearate		21·0	2	19·7	21·8	*ca.* 22·8	Alexander and Schulman (1937)
ethyl margarate		15·0	—	20·7	*ca.* 22·4	—	Harkins and Boyd (1941)
octadecyl acetate		20–21	2	—	22·7	*ca.* 23·5	Alexander and Schulman (1937)
methyl ethers	C_{18}	20·0	2	*ca.* 19·0	*ca.* 20·5	*ca.* 21·0	Marsden and Schulman (1938)
acetamides	C_{18}	18·0	3	21·0	24·8	*ca.* 24·8	preceding paper
ureas	C_{16}	26·0	3	21·1	23·5	*ca.* 24·5	preceding paper

invariably at much greater areas than that of 18·3 A^2 found in crystals of stearic acid and heptadecyl methyl ketone, two of the most accurately investigated compounds. Hence the areas at the kink-point *Y* favour vertical, rather than inclined, chains in the *YZ* region.

The third point is based upon the very low compressibility in the *YZ* region which, as Adam (1938) has pointed out, is only about 25 % greater than for a long-chain paraffin in bulk, where the complications of extension and hydration of the long chains are not possible. Harkins and Boyd (1940) have recently pointed this out in connexion with the acids and alcohols. This cannot be reconciled with an inclined chain structure (as for example on Dervichian's theory) without postulating a very high energy barrier between the inclined and vertical positions, and in view of the ease with which the inclined changes into the vertical form in long-chain hydrocarbons (Müller 1927, 1928, 1932) and esters and glycerides (Malkin and others 1934, 1936, 1937), this would appear to be highly improbable. Also, if transition from an inclined to a vertical form did take place, then the compressibility curve should show a further discontinuity corresponding to the compression of vertically orientated molecules at an area of about 18·3 A^2. This, however, has never been observed and all films at smaller areas than about 19 A^2 seem to be partially collapsed (Alexander 1941*b*).

One of the results from the X-ray structure of built-up films (Stenhagen 1938; Alexander 1939; Bernstein 1940) is that the long X-ray spacing is in general appreciably greater than the optical spacing and therefore than the height of the monolayer on water (since the deposition ratio is always very close to unity), even for substances such as calcium stearate which show only the typical *YZ* film. This must mean that even at oleic acid pressure (*ca.* 33 dynes/cm.) such condensed films are still considerably removed from the structure in the crystal, and indicates very large forces to be operative during crystallization; the change being perhaps associated with dehydration during the transition from the monolayer to the crystal.

Hence it is concluded that along *YZ* the long chains are vertically orientated and close-packed, but not so tightly as is possible in the crystalline state.

With regard to the packing of the polar head groups in this region, the surface potential measurements should assist, since it would be expected that if these became close-packed at any point then a distinct change in the surface moment μ would occur there. From the data so far available, only in the case of ethyl and methyl stearates has a sharp break been noticed, in this case at the kink-point *Y* (Alexander and Schulman 1937).

This appears to be in agreement with the suggested configuration, since the short chain, and therefore the head group, must start to be compressed at the same area as the long one, that is, at the kink-point Y. The question of the head-group packing is considered in more detail below.

THE MORE COMPRESSIBLE REGION XY

The rather opposed views of Lyons and Rideal (1929) and of Adam (1921, 1938), with the former focusing attention solely upon the packing of the hydrocarbon chain and the latter solely upon that of the head groups, have been given in the introduction. As pointed out below, however, both these appear to be correct to a certain degree, and to be the two main factors of a generally composite phenomenon.

As discussed in detail above it appears that in the YZ region, with A less than *ca.* 20 A^2, only the hydrocarbon chain packing need be considered, so the polar group can evidently play only a very subordinate role except in determining the ease with which this structure is attained. In the expanded films, however, this state of affairs is completely reversed. Thus in the equation of state $(F-F_0)(A-A_0)=C$, which is valid for this region (Langmuir 1933) and for the oil/water interface (Alexander and Teorell 1939), the A_0 term is determined *only* by the nature of the head group, there being no evidence for any preferred chain orientation. (This equation holds for areas down to about 30 A^2 with simple compounds such as alcohols and acids.) Also, as pointed out theoretically by Mitchell (1936) and supported by experiments upon expanded ester films (Alexander and Schulman 1937), it appears that at the limiting area the resultant dipole is vertically orientated owing to the very powerful interfacial field (*ca.* 10^8 V/cm.). The A_0 term is thus related to the area taken up by the head group as so orientated in the interface. In the XY region, with areas in general between 20 and 30 A^2, a behaviour intermediate between that in the expanded and most condensed regions might then be reasonably anticipated.

At the cohering point X there exists an equilibrium, under the surface vapour pressure, between the various forces, some tending to expand, others to compress, the film; the monolayer/water system as a whole being in its minimum energy position. It is convenient to discuss the forces between the long chains and those between the head groups separately.

The chains would normally tend to give close-packed, vertical chains at an area of *ca.* 20 A^2 (see table 1), although this may be complicated by the possibility of energy minima at definite angles of tilt. (For reasons pointed out earlier (see Alexander 1941*b*) only the first possibility, viz. 26·5° tilt from the vertical, is considered here.) Close packing of the chains would be assisted by increase of chain length, opposed by steric effects in certain cases (e.g. unsaturated and α-methyl acids), by the head-group packing if this occupies an area greater than *ca.* 20 A^2, and in general by the kinetic energy associated with the two-dimensional translatory movements, with the rotation of the chains about the long axis, and with the torsional oscillations of the chain. (In a few cases the kinetic agitation of the molecule may actually assist close packing of the chains by breaking down a more open structure maintained by directed hydrogen bonds (e.g. the low-temperature form of the ureas), as discussed in the preceding paper.) Any rotation of the long chains would seem to be most improbable in the monolayer, involving as it would a tilt of the stabilizing dipole away from its position of minimum energy, whereas from the recent experiments of Müller (1940) considerable torsional oscillation might be expected, even at room temperature, on account of the lowering of the melting-point produced by the aqueous substrate (see Alexander 1941*b*, Part I).

The calculations of Bresler and Frenkel (1939) to determine the extent of such torsional oscillations show that, with a potential barrier restricting free rotation about each C—C bond of 3·6 kcal., long-chain molecules remain practically rigid in solution. Thus for a sixteen-carbon chain the statistical length would be approximately that for a fully extended one of fourteen carbon atoms, and gives some justification for the assumption of a planar zigzag hydrocarbon chain, as used in previous papers (see Alexander 1941*b*). Assuming the volume to remain constant, then these torsional oscillations would be sufficient, taking the close-packed form as 20 A^2, to give an area in the film of up to about 23 A^2, still with the average orientation perpendicular to the surface. This is the structure suggested for the long chains in such monolayers as ethyl stearate, where the head-group structure indicates approximately vertical chain orientation and yet the area per molecule can exceed that of close-packed chains by some 2 A^2.

Considering now the head groups, these would, if non-polar, pack together into the configuration of minimum energy as determined by the usual van der Waals's attractive and the short-range repulsive forces, but since they are invariably polar and are immersed in a polar medium, additional complications arise. The electrostatic forces between an array of similarly orientated dipoles should produce a net repulsive force and hence an increase in spreading pressure, but calculation by Langmuir (1933) and experimental study by Marsden and Schulman (1938) show this effect to be quite small. Also in those numerous cases where hydrogen bonding can take place (see the preceding paper), it would seem that the electrostatic forces between the head-group dipoles are attractive rather than repulsive. Fully ionized head groups however, such as in the soaps, produce sufficiently powerful electrostatic repulsive forces to break down the hydrocarbon chain attractions very largely, giving vapour expanded or gaseous films (Adam and Miller 1933; Adam 1938, p. 129). This strong repulsion can be changed into strong attraction by addition of a suitable second component, for example, by adding calcium ions to sodium stearate, or a long-chain ether to a long-chain amine hydrochloride (Marsden and Schulman 1938). In such cases the XY region is completely eliminated, leaving only the close-packed YZ structure.

In addition to these electrostatic head-group interactions and the usual disordering thermal forces, there remains that between the head-group dipole and the interfacial field which, as pointed out above, tends to orientate the resultant dipole vertically in the surface. In general, owing to the asymmetry of the resultant dipole with respect to the long-chain axis, this preferred dipole orientation opposes vertical orientation of the long chains. If the tilt of the hydrocarbon chain away from the vertical caused no increase in energy, then the dipole orientation would be normal to the surface, and the limiting area X would correspond either to the cross-sectional area of the head group, or to that of the long chain, depending upon which occupied the larger area in the configuration imposed by this dipole orientation.

It is clearly evident from the examples of the methyl ketones, acetates and ethers (Alexander 1941*b*), that if a close-packed configuration with vertical chains entails a zero or very small moment (see for example, Alexander 1941*b*, figure 2, configuration IV), then such a configuration is *never* obtained, even in the YZ region. At the point X the configuration actually taken up is one with chains tilted at close to 26·5° to the vertical and with a comparatively high moment, often approaching that in the expanded state. This would appear to indicate that the energy difference between the vertical and inclined forms is small at this tilt, but increases beyond that point, in agreement with the results of Harkins, Young and Boyd (1940). With pentadecylic acid these authors have shown that only small energy changes occur in the condensed region (i.e. up to 24 A^2), although this example may be complicated by variation in the hydrogen bond energy (see preceding paper).

One very general point arises from the detailed examples previously discussed (Alexander 1941*b*), namely that μ *falls* on compression from the point X. (The exceptions are the cyanides and those compounds such as the acetamides, where decrease of area permits cross hydrogen bonding.) This indicates that compression *increases* the energy of the head-group/water system, and since such compression tends to *decrease* that of the hydrocarbon chain system (until close-packed, vertical chains are obtained at the point Y), there is evidently a compromise between these two opposing tendencies at the point X. Further evidence of such a balance at X comes from the effect of increasing the chain length which, from the above, should tend to decrease the area X. This was indicated by the early work of Adam and Dyer (1924) with very long-chain compounds, and recently confirmed by the accurate measurements of Nutting and Harkins (1939) with the acids. Also, as pointed out above, very strong head-group attractive forces, as in calcium stearate, completely eliminate the XY region.

Below is given the proposed classification for condensed monolayers in the XY region, according to the factor thought to be primarily responsible for determining the area X. It must be pointed out, however, that a much more definite division would be possible if the surface moments of all the compounds considered had been examined in both the condensed and expanded regions. A systematic study of surface potentials, on the lines of the force-area measurements of Adam and his collaborators, would be of real value in this connexion.

CLASSIFICATION OF CONDENSED MONOLAYERS IN THE XY REGION, ACCORDING TO THE FACTOR PRIMARILY DETERMINING THE LIMITING AREA X

The detailed results for the various compounds have been given in a previous publication (Alexander 1941*b*), to which reference should be made for any statements quoted below.

(1) '*Size*' *of the head group*

This seems to be the determining factor for the *p*-alkyl phenols, anisoles and anilines, and similarly for the *p*-alkyl cyclohexanols, if the ring is taken as part of the head group. If, however, the latter term is restricted so as to include only the —OH, —OCH_3 or —NH_2 groups, then these compounds show only the YZ region with close-packed phenyl groups and so should not be included in this part of the discussion at all. In the case of cholesterol, for example, it would seem better to regard the sterol skeleton as forming part of the hydrophobic portion rather than of the head group, and to classify such sterols with compounds showing *only* the YZ region.

Other benzene derivatives (anilides, resorcinols, etc.), and other ring structures such as the lactones, also ethyl and methyl stearates, glycerides (mono-, di- and tri-), glycols, pentaerythritol tetrapalmitate, cyanides and α-bromo acids, may be explained similarly on the basis of closely packed head groups. At the same time, however, it should be noted that the packing taken up appears to be that consistent with the maximum surface moment, as is well shown by such examples as the lactones and α-bromo acids.

(2) *Cross-hydrogen bonding*

In the preceding paper it has been suggested that this factor determines the limiting area in the case of the unsubstituted fatty acids, ureas, the low-temperature form of the acetamides and acetanilides, methyl stearamide and probably the amides generally.

In certain other cases where hydrogen bonding might be expected but for steric restrictions, it was postulated that cross-linkage occurred through the OH bond of a single water molecule. Such an explanation was given for the alcohols, amines, aldoximes and high temperature form of the acetamides. The α-amino acids should probably be included here as well.

(3) *Packing of the chains*

Examples where the long chain packing appeared to be the deciding factor were given particularly by the *cis* and *trans* unsaturated compounds, and the differences between the *cis* and *trans* dihydroxy behenic acids seemed to be best explicable on a similar basis. Iso-oleic acid and its ethyl ester may be included here or in section (1), since the double bond may be regarded as part of the long chain or of the head group.

In a number of cases, namely, the methyl ketones, acetates, cetyl palmitate and propionate, it appeared that the head-group orientation corresponded to a chain tilt of close to 26·5° to the vertical, giving evidence for a minimum in the chain energy at one orientation other than the vertical. A similar explanation seemed the most probable one for the ethers. It is perhaps significant that for all these compounds any attractive forces between the head groups, arising, for example, from hydrogen bonding, are most unlikely.

Even in these cases, however, as pointed out above, it is clear that since the interaction between the head-group dipole and the substrate can prohibit the simplest packing with vertical chains, the tilted chain configuration is determined by the orientation of the head group *as well as* by that of the long chain.

From the above discussion and classification the most general statement possible would appear to be that, for the usual chain lengths of 14–20 carbon atoms, the configuration of minimum energy at the limiting area X is determined *both* by the orientation of the dipole with respect to the surface and by the long-chain packing. The area at X may correspond either to that of the head group or to that of the hydrocarbon chain, depending upon which occupies the larger area in their respective orientations at this point.

FACTORS INFLUENCING THE PHYSICAL STATE OF CONDENSED MONOLAYERS

In two-dimensional condensed films true fluid, anisotropic fluid (sometimes termed 'plastic solid'), and true solid states have been observed, exactly as in three-dimensional matter. A correct distinction between these requires quantitative viscosity and rigidity measurements, and so far such data are limited to the alcohols, acids and esters (Fourt and Harkins 1938; Boyd and Harkins 1939; Trapeznikov 1938, 1939). Hence in all other cases referred to below, fluid and solid films are distinguished solely by qualitative blowing experiments, and a clear-cut differentiation is not always possible. To classify all films in the YZ region as 'solid', as Dervichian (1939) and Harkins and Boyd (1941) have done, seems rather misleading in view of the obvious fluidity of such films as methyl ketones, acetates, many other simple esters, and the alcohols; and since in the case of pentadecylic acid (Harkins, Young and Boyd 1940) no heat is required to melt the 'solid'. The esters and alcohols do, however, show anomalous viscosity along YZ, and this is quite possibly a general phenomenon for all liquid films in this region, but it would seem better to restrict the term 'solid' to those films with a definite elastic modulus (Trapeznikov 1938, 1939).

Excluding compounds containing ring structures which are discussed below, it would seem that solid films are rarely obtained unless the long chains are close-packed and vertically orientated (i.e. unless the YZ region exists), since compounds with large substituents in the chain, giving films stable in the XY region only, give only liquid films. The importance of this packing effect is clearly shown by the α-methyl, α-triazo and α-bromo acids, which give liquid films even as the calcium salts (Alexander 1939), and by the *cis* and *trans* unsaturated compounds (Marsden and Rideal 1938; Alexander 1939). These latter can pack together much more readily if the chains are in the *trans* position; accordingly *trans* compounds tend to give solid and the *cis* liquid films.

The exceptions to the above generalization appear to be the ureas (Adam 1922, 1923), a long-chain sulphate (Stenhagen 1940), and α-amino acids (preceding paper). The unusual solidity of the ureas and α-amino acids in the XY region can be ascribed to cross-hydrogen bonding (see preceding paper), that of sodium docosyl sulphate to traces of divalent cations, as indicated by the work of Langmuir and Waugh (1940), and by the fact that on an acid substrate, where such cations are known to exert a diminished effect and are less likely to be present, solidification only occurs at the kink-point Y.

Increasing the van der Waals cohesive forces by increasing the chain length has been shown to bring about solidification in the case of the esters and alcohols (Adam and Dyer 1924; Schulman and Hughes 1932; Trapeznikov 1938, 1939). The non-polar association can also be increased by replacing the flexible long chain by more complex planar ring systems, e.g. benzene, porphin, etc., which are known to have a high mutual cohesion. Thus *p*-hexadecyl phenol (Adam 1923) and mesoporphyrin dimethyl ester (Alexander 1937) give very rigid films showing no liquid region at all.

Solidification of the film can also be brought about by increasing the attractive forces between the head groups. These forces may be of a physical nature (e.g. due to ion-ion, ion-dipole, or dipole-dipole interactions), or chemical, as for example, when several acid radicals are linked together by means of a glycerol or other polyhydric alcohol in the esters. That such chemical links tend to bring about solidification is shown, for example, by a comparison of methyl stearate and tristearin. Work on mixed films by Marsden and Schulman (1938) shows that, unless hydrogen bonding is possible, forces between dipoles are insufficient to bring about solidification, but those between an ion and a dipole, or between two oppositely charged ions, are much greater and can bring about such changes. A more detailed discussion of the part played by hydrogen bonding has been given in the preceding paper.

GENERAL CONCLUSION

It is hoped that this discussion and the previous paper on this topic (Alexander 1941*b*) have served to point out some of the main factors which appear to be operative in determining the structure of condensed monolayers. Regarding any future investigations certain ones seem to be called for, particularly a systematic surface potential examination of all known compounds in both expanded and condensed states, and whether very long chain compounds can bring about a closer packing in the YZ as well as in the XY region. From the above analysis this should be so, but very accurate work with pure compounds would be necessary since the changes must necessarily be small. In all future experiments upon condensed films quantitative surface viscosity and rigidity measurements should be included, so that the physical states can be more accurately defined.

I have much pleasure in thanking Professor N. K. Adam, F.R.S. and Professor E. K. Rideal, F.R.S. for very helpful criticisms and discussions.

REFERENCES

Adam, N. K. 1921 *Proc. Roy. Soc.* A, **99**, 336–351.
Adam, N. K. 1922 *Proc. Roy. Soc.* A, **101**, 452–471.
Adam, N. K. 1923 *Proc. Roy. Soc.* A, **103**, 676–695.
Adam, N. K. 1938 *Physics and chemistry of surfaces*, 2nd ed. Oxford.
Adam, N. K., Danielli, J. F. and Harding, J. B. 1934 *Proc. Roy. Soc.* A, **147**, 491–499.
Adam, N. K. and Dyer, J. W. 1924 *Proc. Roy. Soc.* A, **106**, 694–709.
Adam, N. K. and Harding, J. B. 1932 *Proc. Roy. Soc.* A, **138**, 411–430.
Adam, N. K. and Miller, J. G. 1933 *Proc. Roy. Soc.* A, **142**, 401–422.
Alexander, A. E. 1937 *J. Chem. Soc.* pp. 1813–1816.
Alexander, A. E. 1939 *J. Chem. Soc.* pp. 777–781.
Alexander, A. E. 1941*a* *Trans. Faraday Soc.* **37**, 15, 192.
Alexander, A. E. 1941*b* *Trans. Faraday Soc.* **37**, 426–437.
Alexander, A. E. and Schulman, J. H. 1937 *Proc. Roy. Soc.* A, **161**, 115–127.
Alexander, A. E. and Teorell, T. 1939 *Trans. Faraday Soc.* **35**, 727–737.
Bernstein, S. 1940 *J. Amer. Chem. Soc.* **62**, 374–378.
Boyd, E. and Harkins, W. D. 1939 *J. Amer. Chem. Soc.* **61**, 1188–1195.
Bresler, S. and Frenkel, J. 1939 *Acta Physicochim. U.R.S.S.* **11**, 485–504.
Buckingham, R. 1934 *Trans. Faraday Soc.* **30**, 377–386.
Dervichian, D. G. 1939 *J. Chem. Phys.* **7**, 931–948.
Fourt, L. and Harkins, W. D. 1938 *J. Phys. Chem.* **42**, 897–910.
Harkins, W. D. and Anderson, T. F. 1937 *J. Amer. Chem. Soc.* **59**, 2189–2197.
Harkins, W. D. and Boyd, E. 1940 *J. Chem. Phys.* **8**, 129.
Harkins, W. D. and Boyd, E. 1941 *J. Phys. Chem.* **45**, 20–43.
Harkins, W. D. and Florence, R. T. 1938 *J. Chem. Phys.* **6**, 847–855.
Harkins, W. D., Young, T. F. and Boyd, E. 1940 *J. Chem. Phys.* **8**, 954–965.
Hoffman, E. J., Ralston, A. W. and Ziegler, G. E. 1939 *J. Phys. Chem.* **43**, 301–307.
Langmuir, I. 1933 *J. Chem. Phys.* **1**, 756–776.
Langmuir, I. and Waugh, D. 1940 *J. Amer. Chem. Soc.* **62**, 2771–2793.
Lyons, C. C. and Rideal, E. K. 1929 *Proc. Roy. Soc.* A, **124**, 322–355.
Malkin, T. and others 1934 *J. Chem. Soc.* pp. 666–671.
Malkin, T. and others 1936 *J. Chem. Soc.* pp. 1628–1634.
Malkin, T. and others 1937 *J. Chem. Soc.* pp. 1409–1413.
Marsden, J. and Rideal, E. K. 1938 *J. Chem. Soc.* pp. 1163–1171.
Marsden, J. and Schulman, J. H. 1938 *Trans. Faraday Soc.* **34**, 748–758.
Mitchell, J. S. 1936 *Proc. Roy. Soc.* A, **155**, 696–701.

Müller, A. 1927 *Proc. Roy. Soc.* A, **114**, 542–561.
Müller, A. 1928 *Proc. Roy. Soc.* A, **120**, 437–459.
Müller, A. 1932 *Proc. Roy. Soc.* A, **138**, 514–530.
Müller, A. 1940 *Proc. Roy. Soc.* A, **174**, 137–144.
Nutting, G. C. and Harkins, W. D. 1939 *J. Amer. Chem. Soc.* **61**, 1180–1187.
Porter, E. F. 1937 *J. Amer. Chem. Soc.* **59**, 1883–1888.
Schulman, J. H. and Hughes, A. H. 1932 *Proc. Roy. Soc.* A, **138**, 430–450.
Stenhagen, E. 1938 *Trans. Faraday Soc.* **34**, 1328–1337.
Stenhagen, E. 1940 *Trans. Faraday Soc.* **36**, 496–499.
Trapeznikov, A. A. 1938 *Acta Physicochim. U.R.S.S.* **9**, 273–312.
Trapeznikov, A. A. 1939 *Acta Physicochim. U.R.S.S.* **10**, 65–82.

Supersonic dispersion in gases. The vibrational activation of the acetaldehyde molecule

By E. A. Alexander and J. D. Lambert

(*Communicated by C. N. Hinshelwood, F.R.S.—Received* 7 *July* 1941)

An investigation of the supersonic dispersion in acetaldehyde vapour was carried out in piezoelectric, magnetostriction and Kundt's tube interferometers over as wide a range of frequency and pressure as possible. Acetaldehyde is found to exhibit a multiple dispersion region which is independently confirmed by absorption measurements. This implies that certain intramolecular vibrations are activated independently.

INTRODUCTION

The transfer of energy from the translational to the vibrational degrees of freedom in a gas molecule is generally an inefficient process, several thousand intramolecular collisions being necessary for each quantum of vibrational energy acquired (Kneser 1931). When a gas absorbs heat, a finite 'period of relaxation' is therefore necessary before the vibrational energy of the molecules rises to its equilibrium value. When a gas transmits sound waves whose period is comparable with the period of relaxation, the equilibrium value between the translational and vibrational degrees of freedom is not attained. This results in a variation with frequency of the apparent ratio of the specific heats (γ_ν) and hence the velocity of sound in the gas. This often occurs at supersonic frequencies and gives rise to supersonic dispersion accompanied by absorption of energy over a limited frequency range.

In molecules where more than one intramolecular vibration is possible, it might be expected that the ease of excitation should vary considerably for the different vibrations. There would then be a separate dispersion region corresponding to the period of relaxation for each different vibration. A complex dispersion of this type has not previously been found with pure gases. The dispersion in carbon dioxide and nitrous oxide has been investigated at temperatures where *both* the deformational vibration *and* the valency vibration are excited, and there is only a single dispersion region giving *one* period of relaxation for the excitation of both vibrations (Eucken and Nümann 1937). This may be explained on the grounds that energy flows into the deformational vibration first and then subsequently activates the valency vibration. This transfer occurs more easily when there is a possibility of resonance between the higher states of the deformational vibration and the valency vibration. Hence only the single period of relaxation of the deformational vibration is observed.

In view of this it seemed interesting to investigate the supersonic dispersion of a more complex molecule in which there are several different deformational vibrations. Acetaldehyde was chosen as there is already evidence from chemical kinetics suggesting the existence of different modes of vibrational activation of the molecule with different probabilities of decomposition (Hinshelwood and Fletcher 1933).

EXPERIMENTAL

Preparation of materials

Air was purified by passing it through a series of tubes containing sofnolite, calcium chloride and redistilled phosphorus pentoxide.

Acetaldehyde was carefully fractionated and the middle fraction was distilled under reduced pressure into the storage bulb of the apparatus, and the first and last fractions were again discarded. It was protected from light.

Apparatus

In essentials an acoustic interferometer consists of an oscillator of constant frequency and a movable reflector which is associated with some recording device. Whenever the distance between the oscillator and reflector corresponds to an integral number of half wave-lengths, stationary waves are set up and are detected by various means. This enables the wave-length of the sound to be estimated.

The investigation of supersonic waves in acetaldehyde vapour was carried out principally in a piezoelectric interferometer over as wide a range of frequency and pressure as possible. As the pressure range at room temperature is smaller than at higher temperatures, a magnetostriction interferometer was used to extend the scope of the measurements at room temperature by operating at lower frequencies. Finally a Kundt's tube interferometer was used for measurements at a very low frequency where no dispersion occurs.

The piezoelectric interferometer was originally devised by Pierce (1925); the design used here is similar to that of Eucken and Nümann (1937) and is shown diagrammatically in figure 1.

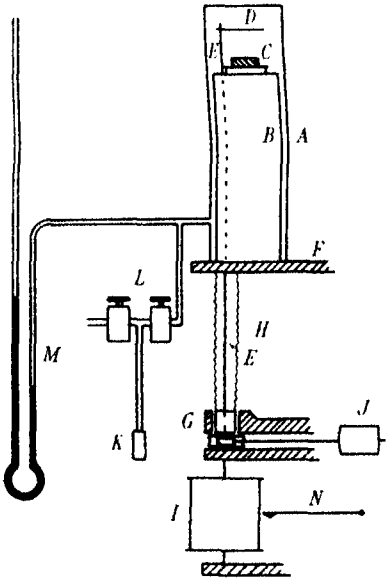

FIGURE 1

The outer cylindrical case (A) covers an inner cylinder (B) which supports the piezoelectric quartz oscillator (C) and carries a guide tube for the reflector (D) and reflector shaft (E). Both these cylinders are bolted down to a common base (F) and thin lead washers are used to make vacuum-tight joints. The outer cylinder is 10 cm. wide thus avoiding tube corrections for the velocity of sound. The apparatus has to withstand pressure, vacuum and temperatures up to 400° C. For the latter reason both the inner and outer cylinders are long so that the part containing the quartz and reflector can be heated to 400° C, while the lower end containing the lead washers is not heated above 100° C. Hence the reflector shaft consists of an invar rod which is not affected by the temperature gradient.

The reflector and shaft are moved by a set screw and collar (G). Vacuum-tight conditions between the movable collar and the fixed base (F) are effected by a metal tombac tube (H). A recording drum (I) is attached to the same shaft as the set screw and hence rotates as the reflector is moved. A smooth steady motion is achieved by using an electric motor (J) which is geared down (22,500 revolutions to 1), and the coupling shaft is fitted with special devices to prevent vibrations being transmitted from the motor to the apparatus.

The apparatus was connected to an evacuating system consisting of a large efficient oil pump, an electrically heated mercury-vapour pump, a liquid air trap interposed between the apparatus and the pumps, and finally a discharge tube for testing the degree of evacuation. High pressures of condensable gases were developed by the freezing chamber (K). Special metal tombac valves were used to prevent the rest of the glass apparatus being subjected to the pressure. The gas was frozen in the bulb (K) and then allowed to evaporate into the interferometer to give the required pressure which was registered directly on an 18 ft. mercury manometer (M). When working with acetaldehyde the manometer and all the connecting tubing was heated to 100° C. High pressures of non-condensable gas mixtures were developed by a special mercury compressor.

When the interferometer was in operation the reflector was moved steadily away from (or towards) the oscillator which was connected to the grid and filament of a thermionic valve in an oscillating electric circuit. Whenever the distance between the reflector and oscillator corresponds to an integral number of half wave-lengths, stationary waves are set up and the intervening gas acts as a resonator, absorbing energy from the oscillator. Hence the resonances can be detected by a sensitive galvanometer as they produce fluctuations in the anode current of the oscillating electric circuit. These are recorded by a tapping key operating an electromagnetic pen (N) which marks a strip of paper wrapped around the recording drum. This enables the wave-length of the sound to be estimated. This interferometer can also be used to measure the absorption of the sound in the gas by observing the varying intensity of the successive fluctuations in the anode current. But before the ratio of the specific heats can be calculated for acetaldehyde, the second virial coefficient, which gives the deviation from the perfect gas laws, must be determined.

The magnetostriction interferometer was also originally devised by Pierce (1928), and is in principle the same as the previous one. Here the oscillator consists of a metal rod set in vibration by magnetostriction in an alternating electromagnetic field which is produced by the coils of an oscillating electric circuit. The oscillator is mounted in a glass tube with the coils on the outside. The reflector consists of a glass plunger attached to a soft iron disk so that it can be operated from outside by a strong magnet. Stationary waves are detected in the same way as before.

It was not possible owing to experimental difficulties to use a tube of diameter larger than 1 cm. This involves a considerable tube correction which was estimated from the actual measurements by comparison with results from the piezoelectric interferometer. In view of this the results are not so reliable as those obtained by the former method.

The Kundt's tube interferometer was operated in the usual way using a long glass rod as the oscillator. It could, however, be evacuated and used at pressures below atmospheric. The reflector consisted of a soft iron spool which was operated from the outside by an electromagnet. The diameter of the tube was 6 cm. giving a negligible tube correction. This apparatus is not capable of a high degree of accuracy.

RESULTS

Pure air was chosen as a standard and all the results were obtained by comparison with it. A measurement was first taken with air and then immediately afterwards with the required gas under the same experimental conditions. The accuracy of the interferometers were tested with dry and moist carbon dioxide.

The ratio of the specific heats (γ_ν) is calculated from the equation

$$\frac{\gamma_{\nu_1}}{\gamma_{\nu_2}} = \frac{M_1\lambda_1^2(T_2+2B_2P_2/R)}{M_2\lambda_2^2(T_1+2B_1P_1/R)},$$

where M is the molecular weight, λ the wave-length, T the absolute temperature, B the second virial coefficient, P the pressure and R the gas constant.

The value of the second virial coefficient of acetaldehyde was calculated from critical data by the Berthelot equation:

$$B_a = 42{\cdot}1 - 53{\cdot}6 \times 10^6/T^2 \text{ c.c./mol.}$$

Acetaldehyde vapour is dimerized to a small extent (Alexander and Lambert 1941), hence the complete expression for the second virial coefficient is

$$B = \{2\alpha/(1+\alpha)\}\,B_a + \{(1-\alpha)/(1+\alpha)\}\,B_d,$$

where $(1-\alpha)$ is the degree of dimerization, B_a and B_d the second virial coefficient of monomeric and dimerized acetaldehyde respectively. But as the degree of dimerization is very small, even at room temperature, it may be assumed that B is approximately equal to B_a.

The ratio of the specific heats (γ_ν) is pressure dependent and is corrected in the usual way by extrapolation to zero pressure (γ_0), where

$$\gamma_0 = 1 + 1 \Big/ \left[\frac{1}{(\gamma_\nu - 1)} + \left\{\frac{2dB}{dT}\left(\frac{\gamma_\nu}{\gamma_\nu - 1}\right) + \frac{Td^2B}{dT^2}\right\}\frac{P}{R}\right].$$

The results at room temperature and 110° C are given in tables 1 and 2 respectively, and the plots of γ_0 against $\log \nu/P$ (Eucken and Becker 1934) are shown in figures 2 and 3 respectively. All the tabulated results and the air standards (from which the frequency of the oscillators was calculated) are averages of two separate recordings, one with the reflector moving towards the oscillator and the other with it moving away from the oscillator.

During the experiments the acetaldehyde was changed after each result and was not allowed to remain in the apparatus longer than was absolutely necessary. With old samples of acetaldehyde the dispersion regions are displaced slightly towards the region of higher frequencies. This is probably due to a minute trace of paraldehyde in the acetaldehyde vapour. Reproducible results were always obtained with fresh samples of acetaldehyde.

It is difficult to assess the accuracy of γ_0 as it varies with temperature, pressure and frequency, but the probable error in γ_0 determined by the piezoelectric, magnetostriction and Kundt's tube interferometers is ± 0·1, ± 0·35 and ± 0·5 % respectively.

Calculation of the absorption coefficient per wave-length (μ)

If I_0 is the intensity of the galvanometer deflexion for the first resonance maximum, then I the intensity of any other is given by

$$I = I_0 e^{-\mu x/\lambda},$$

where x is the distance of the reflector above the oscillator and λ the wave-length.

Hence $$\mu = 2{\cdot}303\,(\lambda/x)\log I_0/I.$$

In practice λ/x is plotted against $\log I$ and μ is determined from the slope of the plot. The values of μ, where possible, are included in tables 1 and 2 and the plots of μ against $\log \nu/P$ are shown in figures 2 and 3.

TABLE 1

number	temp. (°C)	press. (atm.)	ν (kcyc./sec.)	γ_ν	γ_0	μ
1	20·1	0·242	2·452*	1·135	1·132	—
2	20·1	0·401	„	1·143	1·135	—
3	20·1	0·556	„	1·146	1·134	—
4	17·1	0·302	30·15†	1·160	1·153	—
5	17·1	0·416	„	1·153	1·145	—
6	17·3	0·631	„	1·158	1·147	—
7	17·1	0·661	„	1·153	1·141	—
8	17·0	0·211	34·13†	1·158	1·152	—
9	17·0	0·291	„	1·158	1·151	—
10	17·0	0·387	„	1·157	1·149	—
11	17·0	0·624	„	1·156	1·145	—
12	16·5	0·214	40·92†	1·155	1·149	—
13	16·7	0·307	„	1·161	1·154	—
14	16·8	0·524	„	1·160	1·151	—
15	20·7	0·145	229·5‡	1·188	1·181	0·053
16	22·2	0·303	„	1·182	1·177	0·056
17	22·0	0·501	„	1·174	1·167	0·067
18	21·2	0·628	„	1·170	1·161	0·071
19	20·9	0·778	„	1·170	1·158	0·065
20	22·5	1·012	„	1·169	1·155	0·025
21	24·2	1·113	„	1·168	1·152	0·024
22	20·0	0·097	574·0‡	1·188	1·185	0·01
23	18·2	0·224	„	1·191	1·184	0·01
24	18·8	0·437	„	1·190	1·182	0·01
25	19·3	0·921	„	1·189	1·173	0·015
26	16·1	0·096	1247 ‡	1·199	1·197	—
27	15·0	0·120	„	1·196	1·193	—
28	15·4	0·161	„	1·192	1·188	—
29	15·7	0·218	„	1·190	1·185	—
30	16·8	0·302	„	1·190	1·185	—
31	16·0	0·400	„	1·192	1·186	—
32	16·3	0·603	„	1·194	1·185	—
33	16·5	0·851	„	1·195	1·184	—
34	16·9	0·101	„	—	—	0·20
35	16·9	0·153	„	—	—	0·183
36	16·9	0·205	„	—	—	0·147
37	16·8	0·421	„	—	—	0·131
38	16·8	0·604	„	—	—	0·129
39	16·7	0·854	„	—	—	0·127

* Kundt's tube interferometer.
† Magnetostriction interferometer.
‡ Piezoelectric interferometer.

TABLE 2

number	temp. (°C)	press. (atm.)	ν (kcyc./sec.)	γ_ν	γ_0	μ
1	99·9	0·167	2·472*	1·112	1·111	—
2	99·9	0·344	,,	1·111	1·107	—
3	99·9	0·621	,,	1·109	1·104	—
4	110·0	0·128	226·8†	1·138	1·137	—
5	110·1	0·287	,,	1·134	1·132	0·030
6	110·0	0·475	,,	1·135	1·132	0·030
7	108·8	1·015	,,	1·132	1·128	0·023
8	109·4	1·683	,,	1·128	1·121	0·016
9	109·0	2·175	,,	1·114	1·107	0·021
10	109·9	2·803	,,	1·117	1·104	0·046
11	110·0	3·784	,,	1·119	1·102	0·064
12	110·0	4·418	,,	1·123	1·105	0·039
13	109·0	0·382	231·0†	1·137	1·133	0·026
14	109·5	0·694	,,	1·135	1·131	0·025
15	109·2	1·480	,,	1·125	1·118	0·020
16	110·0	1·923	,,	1·123	1·116	0·025
17	109·1	2·198	,,	1·121	1·112	0·031
18	110·1	2·534	,,	1·119	1·109	0·034
19	110·2	2·971	,,	1·120	1·103	0·053
20	110·1	3·910	,,	1·121	1·107	0·048
21	108·9	0·119	572·2†	1·170	1·169	0·045
22	109·0	0·159	,,	1·165	1·163	0·048
23	108·9	0·201	,,	1·158	1·155	0·054
24	109·0	0·302	,,	1·150	1·148	0·028
25	108·2	0·394	,,	1·145	1·142	0·010
26	110·6	0·465	,,	1·137	1·134	0·005
27	110·0	0·734	,,	1·140	1·135	0·007
28	109·0	1·536	,,	1·143	1·134	—
29	110·2	1·538	,,	1·140	1·131	0·009
30	110·4	1·993	,,	1·142	1·132	0·018
31	109·0	2·420	,,	1·146	1·131	—
32	110·1	2·469	,,	1·144	1·129	0·016
33	110·0	2·800	,,	1·147	1·131	0·018
34	110·0	3·379	,,	1·132	1·123	0·016
35	110·0	3·764	,,	1·136	1·125	0·016
36	110·1	0·147	1269†	1·170	1·169	—
37	110·0	0·182	,,	1·170	1·169	—
38	110·2	0·201	,,	1·170	1·168	—
39	110·4	0·288	,,	1·169	1·167	—
40	110·8	0·390	,,	1·162	1·159	—
41	110·7	0·552	,,	1·155	1·151	—
42	110·6	0·741	,,	1·149	1·144	—
43	110·9	0·902	,,	1·145	1·139	—

* Kundt's tube interferometer.

† Piezoelectric interferometer.

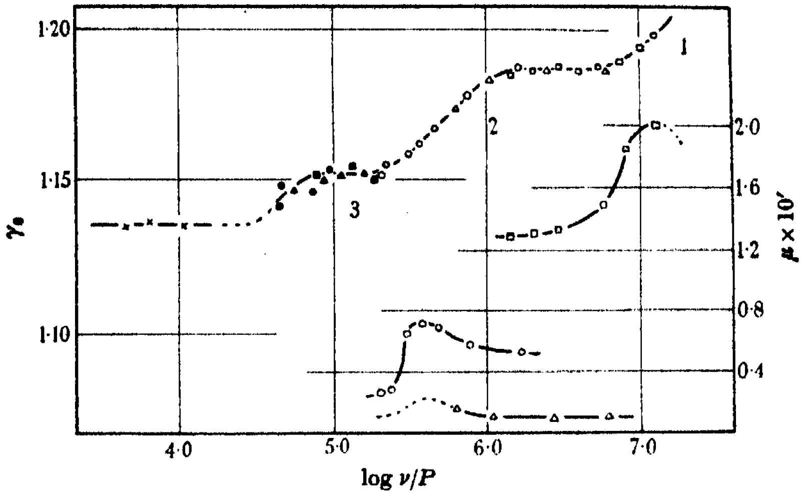

FIGURE 2

□ 1247 kcyc./sec. △ 574·0 kcyc./sec. ○ 229·5 kcyc./sec. ■ 40·9 kcyc./sec.
▲ 34·1 kcyc./sec. ● 30·2 kcyc./sec. × 2·45 kcyc./sec.

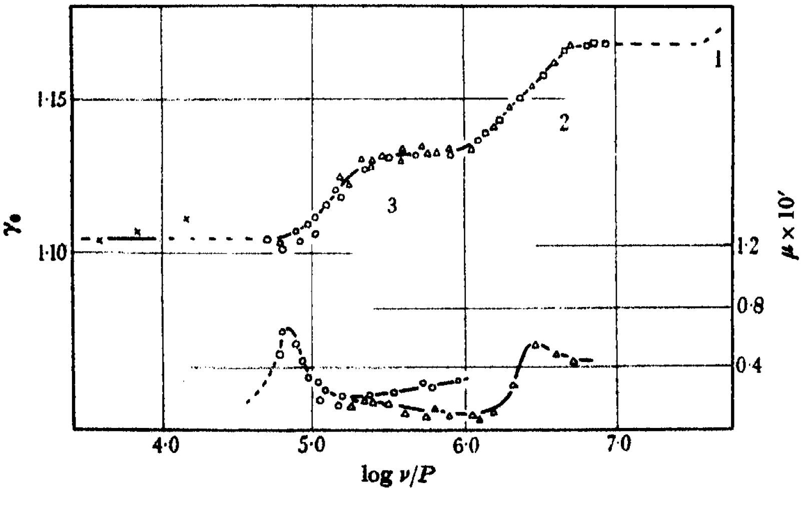

FIGURE 3

□ 1269 kcyc./sec. △ 572·2 kcyc./sec.
○ 231·0 kcyc./sec. and 226·8 kcyc./sec. × 2·47 kcyc./sec.

Calculation of the period of relaxation (β)

The general equation for β is given by

$$\gamma_0 = 1 + R\frac{C_{v_0} + \omega^2\beta^2 C_{v_\infty}}{C_{v_0}^2 + \omega^2\beta^2 C_{v_\infty}^2},$$

where C_{v_0} and C_{v_∞} are the specific heats for the lower and upper limits respectively of the dispersion region and ω is $2\pi\nu$.

For the point of inflexion of the dispersion curve it follows that

$$\beta = \frac{P}{2\pi\nu}\frac{(\gamma_\infty - 1)}{(\gamma_0 - 1)},$$

and this expression is used for the calculations from the dispersion results.

The period of relaxation may also be calculated from the absorption measurements, the general equation is

$$\mu = \frac{2\pi C_\infty \omega\beta}{C_0} \cdot \frac{V_\infty^2/V_0^2 - 1}{(V_\infty^2/V_0^2)(C_\infty\omega\beta/C_0)^2 + 1},$$

where V_0 and V_∞ are the velocities of sound at the lower and upper limits respectively of the dispersion region.

For the point of maximum absorption, it follows that

$$\beta = \frac{P_{\text{max.}}}{2\pi\nu}\frac{(\gamma_\infty - 1)}{(\gamma_0 - 1)}\sqrt{\frac{\gamma_0}{\gamma_\infty}},$$

where $P_{\text{max.}}$ is the pressure at which maximum absorption occurs. This expression is used for the calculations, as it is independent of the actual magnitude of the absorption coefficient.

The average values of the period of relaxation from both methods, where possible, are given in table 3. The γ_0 limits and the sizes in calories, of the dispersion regions are also included. The accuracy of β is of the order of ± 10 %.

TABLE 3

region	limits	sizes (cal.)	β
		at room temperature	
1	1·242–1·185	2·5	$1{\cdot}3 \times 10^{-8}$
2	1·185–1·152	2·6	$4{\cdot}63 \times 10^{-7}$
3	1·152–1·135 (± 0·005)	1·6 ± 0·5	$3{\cdot}7 \times 10^{-6}$
		at 110° C	
1	1·242–1·169	3·5	2×10^{-9} (estimate)
2	1·169–1·133	3·2	$8{\cdot}14 \times 10^{-8}$
3	1·133–1·105 (± 0·005)	4·8 ± 0·9	$2{\cdot}1 \times 10^{-6}$

DISCUSSION

The dispersion regions

The measurements at room temperature show the existence of three distinct dispersion regions (figure 2). *Dispersion region* (1) cannot be fully investigated as it lies mainly outside the range of the piezoelectric interferometer measurements. The lower limit is well defined, and a value of the upper limit is calculated from the theoretical specific heats of the molecule when deprived of all vibrational energy and by assuming that the contribution due to restricted rotation within the molecule is the same as in ethane. Independent evidence of the existence of this dispersion region is given by the absorption measurements. *Dispersion region* (2) is well defined and confirmed by absorption measurements. *Dispersion region* (3) is not completely defined, as it lies mainly outside the range of the magnetostriction interferometer measurements and its lower limit depends solely on the somewhat inaccurate Kundt's tube interferometer measurements.

The measurements at 110° C show two clearly defined dispersion regions (figure 3). The lower of these has as a lower limit the normal value of γ_0 for acetaldehyde at 110° C and corresponds to dispersion region (3), figure 2. The dispersion region is shifted to higher frequencies as the temperature rises. The other dispersion region will correspond to (2), figure 2. It is necessary to assume the existence of a third dispersion region corresponding to (1), figure 2, at a frequency too high to measure.

Dimerization dispersion

A dimerization dispersion is to be expected with any partially dimerized gas. The size of a pure dimerization dispersion region for acetaldehyde, from the degree of dimerization (Alexander and Lambert 1941), would be 0·45 and 0·30 cal. at room temperature and 110° C respectively. Considering the sizes of the dispersion regions given in table 3, it is evident that none of the three dispersion regions could possibly be due to a pure dimerization dispersion.

It is not possible to state whether any of the dispersion regions includes the dimerization dispersion, but it is just possible that it may be region (2). The absorption curves at both temperatures are not symmetrical, there is still a fair amount of absorption after the absorption maxima have been passed by increasing log ν/P (figures 2 and 3).

The significance of the dispersion regions

Acetaldehyde appears to be the first substance with which multiple dispersion regions have been observed. But, on the other hand, this is apparently the first attempt of a complete investigation of a complex substance. It may well be that multiple dispersion regions are a general characteristic of complex molecules. The fact that acetaldehyde has at least three dispersion regions means that the ease of excitation is different for at least three separate vibrations in the molecule and that they are independently activated. The other vibrations are subsequently activated by the higher states of these fundamental vibrations.

Acetaldehyde has essentially three different kinds of bonds, namely a C—C, a C—H and a C=O whose strengths are 81·2, 98·6 (Baughan 1941) and 149 (Pauling 1939) cal./mol. respectively. The C—C bond is most probably the one which is chiefly responsible for the chemical transformation of the molecule. The transformation in question may be a chain reaction thus:

$$\mathrm{CH_3{-}CHO \longrightarrow CH_3 + CHO}$$

in which the C—C bond has actually been ruptured, or it may be a molecular rearrangement, thus:

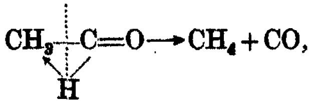

$$\mathrm{\underset{H}{CH_3{-}C}{=}O \longrightarrow CH_4 + CO,}$$

in which the C—C bond is only weakened. This does not affect the issue. If the energy must concentrate principally in a certain bond to cause the chemical transformation of the molecule, then it is *possible* that the probability of its concentrating in this bond will depend upon its mode of entry into the molecule, in which case the molecule will be associated with three distinct probabilities of chemical transformation.

According to one particular view the complex nature of the thermal decomposition of acetaldehyde suggests the existence of different types of activated molecules, which undergo independent unimolecular reactions, changing from the first to the second order at different pressures (Hinshelwood and Fletcher 1933). The pressures at which these hypothetical unimolecular reactions change their order are 1·25, 40 and 290 mm. respectively. Now in the second order region of one of these reactions, the pressure (P_0) determines the number of collisions which are necessary to activate the molecule. This is true right up to the point at which the reaction changes its order. Also at this point P_0 is closely related to the number of collisions which are necessary to deactivate the molecule. Hence it is reasonable to compare P_0 with the number of collisions which are necessary for the loss or gain of a quantum of vibrational energy (Z_{10} and Z_{01}) determined from the supersonic data. It is not possible to calculate Z_{10} and Z_{01} without knowing the frequency, as well as the period of relaxation, of the fundamental vibration which controls each dispersion region (Eucken and Becker 1934). The spectroscopic data are not certain and cannot at present supply the necessary information. It is possible to make a rough comparison by assuming that Z_{10} is proportional to β. Actually Z_{10} is proportional to $\beta(1+e^{-h\nu'/kT})$, but $e^{-h\nu'/kT}$ is small compared with unity for the probable values of the fundamental vibration frequency (ν') and its effect is within the experimental error. On the other hand, Z_{01} is proportional to $\beta(1+e^{+h\nu'/kT})$ and is therefore largely dependent upon the value of ν'. The values of the ratios of β at room temperature to P_0 are $1{\cdot}04\times10^{-8}$, $1{\cdot}15\times10^{-8}$ and $1{\cdot}28\times10^{-8}$ for dispersion regions (1), (2) and (3) respectively.

The above correlation should not be regarded as anything more than qualitative. The existence of the three dispersion regions, however, is definite and signifies that certain intramolecular vibrations are activated independently. Consequently there is a *possibility* of acetaldehyde possessing more than one type of activated molecule.

The authors are very grateful to Professor C. N. Hinshelwood and Dr B. Lambert for their keen interest and valuable assistance in the course of this investigation. Also to Dr T. Iredale who took part in preliminary experiments.

REFERENCES

Alexander, E. A. and Lambert, J. D. 1941 *Trans. Faraday Soc.* **37**, 421.
Baughan, E. G. 1941 *Nature, Lond.*, **147**, 542.
Eucken, A. and Becker, R. 1934 *Z. phys. Chem.* B, **27**, 235.
Eucken, A. and Nümann, E. 1937 *Z. phys. Chem.* B, **36**, 163.
Hinshelwood, C. N. and Fletcher, C. J. M. 1933 *Proc. Roy. Soc.* A, **141**, 41.
Kneser, H. O. 1931 *Ann. Phys., Lpz.*, **11**, 761.
Pauling, L. 1939 *The nature of the chemical bond.* Cornell Univ. Press.
Pierce, G. W. 1925 *Proc. Amer. Acad. Arts Sci.* **60**, 271.
Pierce, G. W. 1928 *Proc. Amer. Acad. Arts Sci.* **63**, 1.

INDEX TO VOLUME 179 (A)

Absorption spectra of the cyclic dienes in the vacuum ultra-violet (Price & Walsh), 201.
Adsorbed substances and insoluble monolayers, interaction (Pankhurst), 393.
Alexander, A. E. The role of hydrogen bonds in condensed monolayers, 470.
Alexander, A. E. A proposed general structure for condensed monomolecular films, 486.
Alexander, E. A. & Lambert, J. D. Supersonic dispersion in gases. The activation of the acetaldehyde molecule, 499.
Anniversary Address (Dale), 233.

Born, M. & Sarginson, K. The effect of thermal vibrations on the scattering of X-rays, 69.
Bragg, Sir William. The diffuse spots in X-ray photographs, 51.
Bragg, Sir William. The diffuse spots in X-ray crystal photographs, 94.
Bragg, Sir W. Lawrence. Diffraction of monochromatic X-rays by crystals at high temperature, 61.
Broda, E. E. & Goodeve, C. F. The behaviour of visual purple at low temperature, 151.
Buckingham, R. A., Hamilton, J. & Massey, H. S. W. The low-temperature properties of gaseous helium, II, 103.
Buckingham, R. A. & Massey, H. S. W. The scattering of neutrons by deuterons and the nature of nuclear forces, 123.

Carbon, heat of sublimation (Kynch & Penney), 214.
Chapman, S. & Cowling, T. G. The velocity of diffusion in a mixed gas; the second approximation, 159.
Cosmic-ray showers, penetrating (Jánossy), 361.
Cowling, T. G. *See* Chapman & Cowling.

Dale, Sir Henry. Anniversary Address, 233.
Danby, C. J. & Hinshelwood, C. N. The polymerization of olefines induced by free radicals, 169.
Darwin, C. G. Diffuse reflexions of X-rays by crystals, 65.
Diffuse reflexions of X-rays by crystals. *See* Discussion.
Discussion on diffuse reflexions of X-rays by crystals, 1, 289. *See* Born & Sarginson, Bragg, Bragg, Darwin, Finch, Jahn, Lonsdale, Lonsdale & Smith, Preston, Raman.

Equilibrium constant of ammonia, pressure dependence (Fuchs), 433.

Finch, G. I. Diffuse reflexions of X-rays by crystals, 67.
Fuchs, K. The vapour-pressure curve, 194.
Fuchs, K. Statistical mechanics of binary systems, 340.
Fuchs, K. The statistical mechanics of many component gases, 408.
Fuchs, K. Pressure dependence of the equilibrium constant of ammonia, 433.
Fürth, R. An elementary theory of thermal diffusion, 461.

Gaseous helium, low temperature properties (Buckingham, Hamilton & Massey), 103.
Gaydon, A. G. The spectra of chilled hydrocarbon flames, 439.
Goodeve, C. F. *See* Broda & Goodeve.

Hamilton, J. *See* Buckingham, Hamilton & Massey.
Hinshelwood, C. N. *See* Danby & Hinshelwood.

Isotope effects in some acid phosphates (Ubbelohde & Woodward), 399.

Jahn, H. A. The Faxén-Waller theory and the surfaces of isodiffusion for cubic crystals, 320.
Jánossy, L. Penetrating cosmic-ray showers, 361.

Kynch, G. J. & Penney, W. G. On the heat of sublimation of carbon and on some absorption bands of three mesomeric hydrocarbons, 214.

Lambert, J. D. *See* Alexander & Lambert.
Laplace's differential equations for tides (Proudman), 261.
Lonsdale, K. Extra reflexions from the two types of diamond, 315.
Lonsdale, K. & Smith, H. An experimental study of diffuse X-ray reflexion by single crystals, 8.

Massey, H. S. W. *See* Buckingham, Hamilton & Massey, *and* Buckingham & Massey.
Monolayers, condensed, hydrogen bonds in (Alexander), 470.
Monomolecular films, condensed, structure (Alexander), 486.

Olefines, polymerization induced by free radicals (Danby & Hinshelwood), 169.

Pallasites, structure and mode of formation (Rayleigh), 386.
Pankhurst, K. G. A. Interaction between adsorbed substances of simple constitution and insoluble monolayers, II, 393.
Penney, W. G. *See* Kynch & Penney.
Preston, G. D. Anomalous reflexions in X-ray patterns, 1.
Price, W. C. & Walsh, A. D. The absorption spectra of the cyclic dienes in the vacuum ultra-violet, 201.
Proudman, J. On Laplace's differential equations for the tides, 261.

Raman, Sir C. Venkata. Reflexion and scattering of X-rays with change of frequency, 289, 302.
Rayleigh, Lord. The stone-iron meteorites called pallasites: a synthetic study of their structure and probable mode of formation, 386.

Sarginson, K. *See* Born & Sarginson.
Scattering of neutrons by deuterons and the nature of nuclear forces (Buckingham & Massey), 123.
Smith, H. *See* Lonsdale & Smith.

Smith, S. L. & Wood, W. A. A stress-strain curve for the atomic lattice of mild steel, and the physical significance of the yield point of a metal, 450.
Soddy, F. The summation of infinite harmonic series, 377.
Spectra of chilled hydrocarbon flames (Gaydon), 439.
Statistical mechanics of binary systems (Fuchs), 340.
Statistical mechanics of many component gases (Fuchs), 408.
Steel, mild, atomic lattice (Smith & Wood), 450.
Summation of infinite harmonic series (Soddy), 377.
Supersonic dispersion in gases (Alexander & Lambert), 499.

Thermal diffusion theory (Fürth), 461.
Tides, Laplace's differential equations (Proudman), 261.

Ubbelohde, A. R. & Woodward, I. Structure and thermal properties associated with some hydrogen bonds in crystals, IV, 399.

Vapour-pressure curve (Fuchs), 194.
Velocity of diffusion in a mixed gas (Chapman & Cowling), 159.
Visual purple, behaviour at low temperature (Broda & Goodeve), 151.

Walsh, A. D. *See* Price & Walsh.
Wood, W. A. *See* Smith & Wood.
Woodward, I. *See* Ubbelohde & Woodward.

X-rays, diffuse reflexions by crystals. *See* Discussion.

Yield point of metal, significance (Smith & Wood), 450.

END OF THE ONE HUNDRED AND SEVENTY-NINTH VOLUME (SERIES A)

I.A.R.I. 75

INDIAN AGRICULTURAL RESEARCH
INSTITUTE LIBRARY, NEW DELHI.

Date of Issue	Date of Issue	Date of Issue
25.5.61		
[illegible]		
24.1.64		
18.3.64		
5.1.66		
26 APR 1969		
- 6 FEB 1970		
7.10.77		
17 OCT 1977		

GIPNLK—H-40 I.A.R.I.—29-4-55—15,000